frontiers | Research Topics

Impacts of climate change on seaweeds

Edited by
Christopher Edward Cornwall, Samuel Starko,
Caitlin Blain and Maggie D. Johnson

Coordinated by
Denisa Maria Berbece

Published in
Frontiers in Marine Science

ISSN 1664-8714
ISBN 978-2-8325-7006-7
DOI 10.3389/978-2-8325-7006-7

Generative AI statement
Any alternative text (Alt text) provided alongside figures in the articles in this ebook has been generated by Frontiers with the support of artificial intelligence and reasonable efforts have been made to ensure accuracy, including review by the authors wherever possible. If you identify any issues, please contact us.

About Frontiers

Frontiers is more than just an open access publisher of scholarly articles: it is a pioneering approach to the world of academia, radically improving the way scholarly research is managed. The grand vision of Frontiers is a world where all people have an equal opportunity to seek, share and generate knowledge. Frontiers provides immediate and permanent online open access to all its publications, but this alone is not enough to realize our grand goals.

Frontiers journal series

The Frontiers journal series is a multi-tier and interdisciplinary set of open-access, online journals, promising a paradigm shift from the current review, selection and dissemination processes in academic publishing. All Frontiers journals are driven by researchers for researchers; therefore, they constitute a service to the scholarly community. At the same time, the *Frontiers journal series* operates on a revolutionary invention, the tiered publishing system, initially addressing specific communities of scholars, and gradually climbing up to broader public understanding, thus serving the interests of the lay society, too.

Dedication to quality

Each Frontiers article is a landmark of the highest quality, thanks to genuinely collaborative interactions between authors and review editors, who include some of the world's best academicians. Research must be certified by peers before entering a stream of knowledge that may eventually reach the public - and shape society; therefore, Frontiers only applies the most rigorous and unbiased reviews. Frontiers revolutionizes research publishing by freely delivering the most outstanding research, evaluated with no bias from both the academic and social point of view. By applying the most advanced information technologies, Frontiers is catapulting scholarly publishing into a new generation.

What are Frontiers Research Topics?

Frontiers Research Topics are very popular trademarks of the *Frontiers journals series*: they are collections of at least ten articles, all centered on a particular subject. With their unique mix of varied contributions from Original Research to Review Articles, Frontiers Research Topics unify the most influential researchers, the latest key findings and historical advances in a hot research area.

Find out more on how to host your own Frontiers Research Topic or contribute to one as an author by contacting the Frontiers editorial office: frontiersin.org/about/contact

Impacts of climate change on seaweeds

Topic editors
Christopher Edward Cornwall — Victoria University of Wellington, New Zealand
Samuel Starko — The University of Western Australia, Australia
Caitlin Blain — The University of Auckland, New Zealand
Maggie D. Johnson — King Abdullah University of Science and Technology, Saudi Arabia

Topic coordinator
Denisa Maria Berbece — Victoria University of Wellington, New Zealand

Citation
Cornwall, C. E., Starko, S., Blain, C., Johnson, M. D., Berbece, D. M., eds. (2025). *Impacts of climate change on seaweeds*. Lausanne: Frontiers Media SA.
doi: 10.3389/978-2-8325-7006-7

Table of contents

frontiers | Frontiers in Marine Science

TYPE Editorial
PUBLISHED 02 October 2025
DOI 10.3389/fmars.2025.1702410

OPEN ACCESS

EDITED AND REVIEWED BY
Nuria Marba,
Spanish National Research Council (CSIC), Spain

*CORRESPONDENCE
Christopher E. Cornwall
christopher.cornwall@vuw.ac.nz

RECEIVED 09 September 2025
ACCEPTED 18 September 2025
PUBLISHED 02 October 2025

CITATION
Cornwall CE, Berbece DM, Blain CO, Johnson MD and Starko S (2025) Editorial: Impacts of climate change on seaweeds.
Front. Mar. Sci. 12:1702410.
doi: 10.3389/fmars.2025.1702410

Editorial: Impacts of climate change on seaweeds

Christopher E. Cornwall[1]*, Denisa M. Berbece[1], Caitlin O. Blain[2], Maggie D. Johnson[3] and Samuel Starko[4]

[1]School of Biological Sciences and Coastal People Southern Skies Centre of Research Excellence, Victoria University of Wellington, Wellington, New Zealand, [2]Institute of Marine Science and Coastal People Southern Skies Centre of Research Excellence, University of Auckland, Auckland, New Zealand, [3]Division of Biological and Environmental Science and Engineering, King Abdullah University of Science and Technology, Thuwal, Saudi Arabia, [4]Oceans Institute & School of Biological Sciences, University of Western Australia, Crawley, WA, Australia

KEYWORDS

seaweed, macroalgae, ocean warming, marine heatwaves, coral reefs, aquaculture, kelp forests

Editorial on the Research Topic
Impacts of climate change on seaweeds

Climate change is drastically altering the composition and abundance of seaweed-dominated ecosystems throughout our oceans. Ocean warming and associated intensifying marine heatwaves (Wernberg et al., 2016; Bunting et al., Trautmann et al., Gendall et al., Khen et al.), ocean acidification (Koch et al., 2013; Comeau and Cornwall, 2016), and deoxygenation (Altieri et al., 2021) can all impact the physiology of seaweeds and the ecological roles that they play. Ocean warming can cause long-term shifts in the ranges of seaweed species, usually in the form of range retractions at warm edges and expansions at cool edges (Straub et al., 2016). Marine heatwaves can elicit acute heat stress in seaweeds, drive subsequent mortality, and result in phase shifts from one ecosystem type to another (Wernberg et al., 2016, 2024). Ocean acidification causes the slow transformation of ecosystems from those dominated by coralline algal substrate to those characterised by a variety of turfing seaweeds or microalgae (Cornwall et al., 2024). Increasing intensity of ocean deoxygenation and frequency of acute localized events will likely exacerbate the effects of localized threats, but the effects of deoxygenation on seaweed communities remain poorly understood compared to other climate change-linked stressors (Altieri et al., 2021). Additionally, increased sedimentation caused by land use changes and increased storm frequencies brought on by climate change (termed 'coastal darkening'), is also an important stressor of seaweed communities (Blain et al., 2021). Increased sedimentation can interact with other stressors (e.g., temperature) or act on its own to alter the composition and function of seaweed-dominated ecosystems (Wernberg et al., 2024). To better predict and project how seaweed-dominated ecosystems will fare in the future, we require extensive further evidence regarding how the effects of climate change will manifest on seaweeds of all types across temperate, tropical, and polar regions.

Ocean warming is likely to have extensive impacts on the physiology and ecology of seaweeds. Trautmann et al. examine the impacts of ocean warming on the kelp *Laminaria digitata* in the Arctic during the winter months. They test the hypothesis that ocean warming during the Polar Night would reduce survivability due to increased metabolism

and resource consumption under a period of complete darkness. They found a reduction in energy stores, an increase in metabolic rates, and a decline in various biochemical compounds under winter warming. Despite a reduction in physiological health, specimens that underwent warming remained in relatively healthy condition, indicating that winter warming may not necessarily cause a significant decline in *L. digitata* populations in the High Arctic, at least in the near future.

Wu et al. investigated the combined effects of ocean warming and eutrophication on the competition dynamics between two bloom-forming seaweed species, *Ulva prolifera* (green tide) and *Sargassum horneri* (golden tide). The results show that while both seaweeds thrive with increasing temperatures and nutrients up to 25 °C, both had rapid declines in growth, pigment concentration, and photosynthetic activity at 30 °C. Furthermore, under eutrophic conditions, *Ulva prolifera* outcompeted *Sargassum horneri*, particularly at higher temperatures. Collectively, these results suggest that ocean warming and eutrophication, associated with climate change, will facilitate the dominance of green tide blooms.

Zhang et al. assessed the photosynthetic growth response of the rhodophyte *Gracilariopsis lemaneiformis* when exposed to four different nutrient conditions (full factorial high and low N and P) and two temperatures (20 and 23 °C). They found photosynthetic and growth rates of this species generally only increased by higher levels of both nutrients (N+P), but that there were minimal effects of temperature.

Bunting et al. assessed how marine heatwaves of differing intensities and durations impacted sporophytes of the giant kelp *Macrocystis pyrifera* in a laboratory experiment in Aotearoa New Zealand. They find that increasing both the duration (from 3 to 6 weeks) and intensity (from 18 °C to 20 or 22 °C) of marine heatwaves act to reduce the growth of *M. pyrifera*. Moreover, temperatures over 22 °C were found to have particularly strong negative impacts on growth, as this was the only temperature treatment to cause mortality, especially in the 6-week duration treatment. This indicates marine heatwaves above 20 °C will be especially problematic for this species *in situ*.

Understanding the drivers of kelp forest stability under ocean warming requires long-term, spatially explicit datasets. Multiple papers in this Research Topic develop such datasets using satellite-based remote sensing and uncover patterns of change in kelp forests across Western Canada. Despite its extensive ~26,000 km coastline, the trajectories of Western Canada's kelp forests have remained largely unknown until recently, even with clear evidence of localised climate impacts (Schroeder et al., 2020; Watson et al., 2021; Mora-Soto et al., Starko et al., 2024; Wernberg et al., 2024).

Gendall et al. combined archival charts with satellite imagery to reveal century-scale changes in *Macrocystis* forests of Haida Gwaii, including a persistent loss in the early 1970s likely driven by ocean warming. This is one of the earliest examples of climate-driven kelp loss globally (Wernberg et al., 2024). These declines were isolated to the warmest parts of the region, with nearby areas remaining stable. Mora-Soto et al. extend this perspective to bull kelp (*Nereocystis luetkeana*) in the Salish Sea, demonstrating that recent warming caused major kelp losses in the warmer, inner parts of the region. Notably, these declines occurred during the 2014–2016 marine heatwave, which had extensive impacts on kelp along the west coast of North America (Starko et al., 2025). However, cooler areas were much more stable and did not experience these same declines, similar to the findings of Gendall et al. Finally, Man et al. focus on kelp forest dynamics in the Broughton Archipelago and report high persistence of canopy kelps from 1984–2023, suggesting this cool region may serve as a climate refuge.

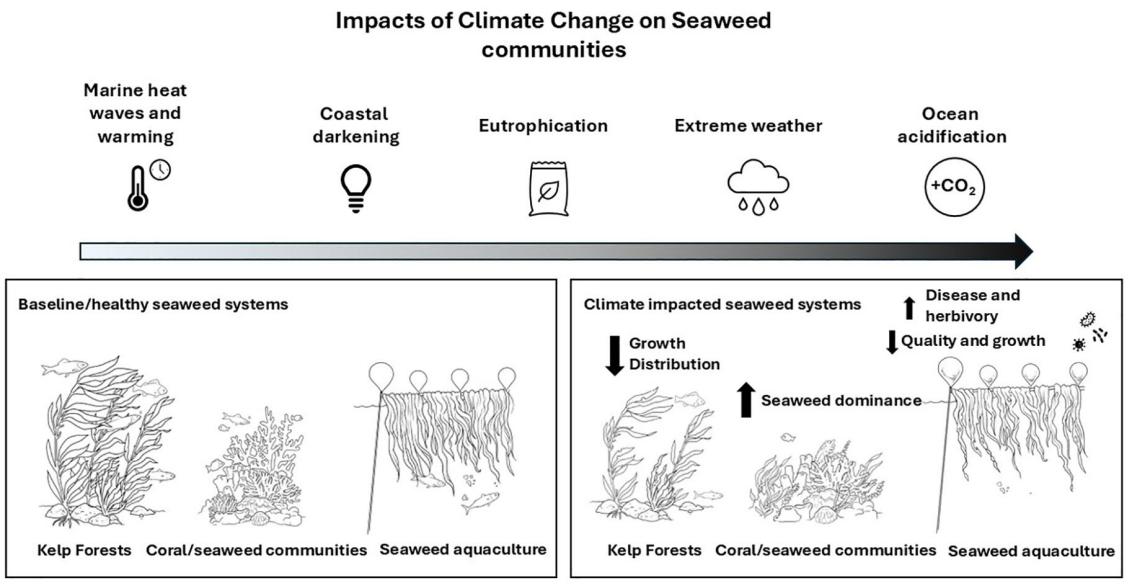

FIGURE 1
Impacts of climate change on seaweed ecosystems reviewed in this Research Topic. Importantly, ocean warming and marine heatwaves will have large consequences for kelp forest and coral/seaweed ecosystems, as well as seaweed aquaculture. The effects of temperature will also be highly modified by local contexts and drivers, such as nutrient and sediment levels.

Khen et al. assessed 11 years of benthic seaweed cover on the coral reefs of Palmyra Atoll in the tropical central Pacific. In addition to identifying that seaweed communities were dominated by calcareous taxa on the fore reef and by fleshy taxa on the reef terrace, they also found that marine heatwaves associated with El Niño years (2009, 2015) dramatically altered seaweed abundances. Fleshy seaweed tended to dominate reef communities after these periods of warming, while calcifying green seaweeds in the genus *Halimeda* declined. Palmyra Atoll's relatively pristine reefs, provide an opportunity to understand long-term patterns in seaweed community dynamics in the absence of direct local human impacts.

Climate change will not only impact seaweed ecology, but also impact their utility in aquaculture. Veenhof et al. provide a summary of climate change related challenges to this industry, contrasted by the various opportunities that seaweed aquaculture presents to enhance ecosystem resilience. The primary challenges experienced are those caused by changes to physical factors (such as ocean warming and acidification), an increase in extreme weather events, and a heightened prevalence of disease and herbivory (particularly by invasive species). To overcome these challenges, Veenhof et al. present the following recommendations: a) by selecting for restoration and aquaculture sites that balance climate change impacts and species responses; b) utilising genetic advancements to inform selective breeding and hybridization, microbiome manipulation, and priming strategies; and c) progressing aquaculture towards approaches that maximize both restoration and cultivation.

Liu et al. examines challenges in *Neopyropia yezoensis* (laver) cultivation in Jiangsu Province, China, focusing on the challenges it faces due to climate change. Warming sea temperatures, extreme weather, and high-density cultivation lead to crop failures, diseases, intra-specific competition and economic losses. The paper proposes strategies for sustainable, climate-resilient development, such as cultivating heat-resistant alternatives like *N. haitanensis*, relocating cultivation to cooler regions, integrating multi-trophic aquaculture systems (IMTA), and aligning the industry with carbon credit markets to improve future ecological and economic outcomes. These measures aim to ensure long-term productivity while mitigating environmental impacts.

Collectively, these studies emphasise the importance of local environmental conditions in mediating seaweed responses to ocean warming (Figure 1). This underscores the need for locally tailored conservation and management strategies to protect these vital ecosystems. Local variability in temperature extremes, ocean acidification, nutrient concentrations, and seasonality will all influence the response of seaweeds to ocean warming and marine heatwaves. This editorial highlights an urgent need for more experimental and observational work that tests the role of multiple environmental drivers on seaweed ecology and physiology.

Author contributions

CEC: Conceptualization, Investigation, Supervision, Visualization, Writing – original draft, Writing – review & editing. DMB: Conceptualization, Investigation, Writing – original draft, Writing – review & editing. COB: Conceptualization, Investigation, Visualization, Writing – original draft, Writing – review & editing. MDJ: Conceptualization, Investigation, Writing – original draft, Writing – review & editing. SS: Conceptualization, Investigation, Visualization, Writing – original draft, Writing – review & editing.

Funding

The author(s) declare that financial support was received for the research and/or publication of this article. CEC and DMB were funded by Coastal People Southern Skies Centre of Research Excellence, COB was funded by the Live Ocean Foundation. SS was funded by the Forrest Research Foundation.

Conflict of interest

The authors declare that the research was conducted in the absence of any commercial or financial relationships that could be construed as a potential conflict of interest.

The author(s) declared that they were an editorial board member of Frontiers, at the time of submission. This had no impact on the peer review process and the final decision.

Generative AI statement

The author(s) declare that no Generative AI was used in the creation of this manuscript.

Any alternative text (alt text) provided alongside figures in this article has been generated by Frontiers with the support of artificial intelligence and reasonable efforts have been made to ensure accuracy, including review by the authors wherever possible. If you identify any issues, please contact us.

Publisher's note

References

Altieri, A. H., Johnson, M. D., Swaminathan, S. D., Nelson, H. R., and Gedan, K. B. (2021). Resilience of tropical ecosystems to ocean deoxygenation. *Trends Ecol. Evol.* 36, 227–238. doi: 10.1016/j.tree.2020.11.003

Blain, C. O., Hansen, S. C., and Shears, N. T. (2021). Coastal darkening substantially limits the contribution of kelp to coastal carbon cycles. *Global Change Biol.* 27, 5547–5563. doi: 10.1111/gcb.15837

Comeau, S., and Cornwall, C. E. (2016). "Contrasting effects of ocean acidification on coral reef "Animal forests" versus seaweed "Kelp forests," in *Marine Animal Forests*. Ed. S. Rosi (Springer, Switzerland), 1–25.

Cornwall, C. E., Comeau, S., and Harvey, B. P. (2024). Are physiological and ecosystem-level tipping points caused by ocean acidification? A critical evaluation. *Earth Syst. Dynam.* 15, 671–687. doi: 10.5194/esd-15-671-2024

Koch, M., Bowes, G., Ross, C., and Zhang, X. H. (2013). Climate change and ocean acidification effects on seagrasses and marine macroalgae. *Global Change Biol.* 19, 103–132. doi: 10.1111/j.1365-2486.2012.02791.x

Schroeder, S. B., Boyer, L., Juanes, F., and Costa, M. (2020). Spatial and temporal persistence of nearshore kelp beds on the west coast of British Columbia, Canada using satellite remote sensing. *Remote Sens. Ecol. Conserv.* 6, 327–343. doi: 10.1002/rse2.142

Starko, S., Epstein, G., Chalifour, L., Bruce, K., Buzzoni, D., Csordas, M., et al. (2025). Ecological responses to extreme climatic events: a systematic review of the 2014–2016 Northeast Pacific marine heatwave. *Oceanogr. Mar. Biol. Annu. Rev.* 63, 42–96. doi: 10.1201/9781003589600-2

Starko, S., Timmer, B., Reshitnyk, L., Csordas, M., McHenry, J., Schroeder, S., et al. (2024). Local and regional variation in kelp loss and stability across coastal British Columbia. *Mar. Ecol. Prog. Ser.* 733, 1–26. doi: 10.3354/meps14548

Straub, S. C., Thomsen, M. S., and Wernberg, T. (2016). "The dynamic biogeography of the Anthropocene: the speed of recent range shifts in seaweeds," in *Seaweed phylogeography: Adaptation and evolution of seaweeds under environmental change* (Springer), 63–93. doi: 10.1007/978-94-017-7534-2

Watson, J. C., Hawkes, M. W., Lee, L. C., and Lamb, A. (2021). The dynamics and geographic disjunction of the kelp Eisenia arborea along the west coast of Canada. *Botanica Marina* 64, 395–406. doi: 10.1515/bot-2021-0040

Wernberg, T., Bennett, S., Babcock, R. C., de Bettignies, T., Cure, K., Depczynski, M., et al. (2016). Climate-driven regime shift of a temperate marine ecosystem. *Science* 353, 169–172. doi: 10.1126/science.aad8745

Wernberg, T., Thomsen, M. S., Baum, J. K., Bishop, M. J., Bruno, J. F., Coleman, M. A., et al. (2024). Impacts of climate change on marine foundation species. *Annu. Rev. Mar. Sci.* 16, 247–282. doi: 10.1146/annurev-marine-042023-093037

frontiers | Frontiers in Marine Science

TYPE Original Research
PUBLISHED 22 August 2024
DOI 10.3389/fmars.2024.1432937

OPEN ACCESS

EDITED BY
Christopher Edward Cornwall,
Victoria University of Wellington,
New Zealand

REVIEWED BY
Wei Liu,
Shanghai University, China
Fangfang Yang,
Chinese Academy of Sciences (CAS), China
Ralf Rautenberger,
Norwegian Institute of Bioeconomy Research (NIBIO), Norway

*CORRESPONDENCE
Di Zhang
zhangdi@ytu.edu.cn

RECEIVED 15 May 2024
ACCEPTED 26 July 2024
PUBLISHED 22 August 2024

CITATION
Zhang D, Sun J-Z, Fu M-H and Li C-J (2024) Photosynthetic performance and antioxidant activity of *Gracilariopsis lemaneiformis* are sensitive to phosphorus deficiency in elevated temperatures.
Front. Mar. Sci. 11:1432937.
doi: 10.3389/fmars.2024.1432937

Photosynthetic performance and antioxidant activity of *Gracilariopsis lemaneiformis* are sensitive to phosphorus deficiency in elevated temperatures

Di Zhang[1]*, Jia-Zhen Sun[2], Ming-Hui Fu[1] and Chang-Jun Li[1]

[1]School of Ocean, Yantai University, Yantai, China, [2]National Biopesticide Engineering Research Centre, Hubei Biopesticide Engineering Research Centre, Hubei Academy of Agricultural Sciences, Wuhan, China

Due to anthropogenic input of nutrients and emissions of greenhouse gases, macroalgae inhabiting coastal areas often experience drastic fluctuations in nutrients and seawater warming. In this work, we investigated the photosynthetic performance and antioxidant response of the commercially important red macroalgae *Gracilariopsis lemaneiformis* under four different nutrient conditions at 20°C and 23°C. Our results showed that the enrichment of NO_3^- and PO_4^{3-} (high concentrations of nitrogen (N) and phosphorus (P), denoted as HNHP) significantly enhanced photosynthesis and growth by up to 42% and 66% for net photosynthesis rate and 83% and 134% for relative growth rate (RGR) under 20°C and 23°C, respectively, compared with natural seawater (low concentrations of N and P, denoted as LNLP). However, enriching only with PO_4^{3-} (low concentration of N and high concentration of P, denoted as LNHP) or NO_3^- (high concentration of N and low concentration of P, denoted as HNLP) brought no significant change in RGR. A two-way ANOVA analysis revealed an interaction between nutrient variations and temperature, with elevated temperature intensifying the inhibition observed under HNLP conditions. To further elucidate this interaction, we assessed the damage and recovery processes of the photosynthetic apparatus, along with the antioxidant activities. The increased damage (*k*) and reduced recovery (*r*) rates of photosystem II (PSII) in both LNLP and HNLP conditions indicated a heightened susceptibility to photoinhibition in *G. lemaneiformis*, leading to reactive oxygen species (ROS) accumulation and exacerbated oxidative stress, culminating in decreased photosynthesis and growth rates. At higher temperatures, these phosphorus deficiency-induced inhibitions were amplified, as evidenced by increases in *k* values and ROS contents, coupled with a decrease

in *r* values. In summary, our data suggest that the photosynthetic performance and growth of *G. lemaneiformis* are vulnerable to phosphorus deficiency, particularly in the context of future ocean warming. Consequently, phosphorus fertilization during cultivation warrants more attention.

KEYWORDS

antioxidant enzymes, *Gracilariopsis lemaneiformis*, nutrient variations, ocean warming, photosynthesis

Introduction

The growth of macroalgae is highly sensitive to variable environmental changes, such as light fluctuations, temperature, and nutrients (Zhang et al., 2020a, b; Cohen et al., 2022; Jiang et al., 2022; Li et al., 2022). In coastal ecosystems, the levels of key nutrients, primarily nitrogen (N) and phosphorus (P), undergo dramatic shifts due to human activities. As an essential component, N is involved in the formation of proteins, chlorophyll, enzymes, nucleic acids, etc., and its availability significantly influences the physiological performance of algae (Roleda and Hurd, 2019). A number of studies have shown that a high nitrogen concentration could significantly prompt photosynthesis and growth of macroalgae, including *Gracilariopsis lemaneiformis* (Chen et al., 2018; Jiang et al., 2020), *Ulva* sp (Gao et al., 2018; Traugott et al., 2020). Similarly, phosphorus, another vital macronutrient, also influences photosynthetic productivity and biomass in the ocean (Karl, 2000; Kipp and Stüeken, 2017), with its enrichment shown to enhance photosynthesis in species such as *G. lemaneiformis* (Xu et al., 2010), *Sargassum muticum* (Xu et al., 2017) and *Pyropia yezoensis* (Kim et al., 2019). Conversely, nutrient limitations often decrease primary production by affecting carbon flux redirection and cellular energy (Falkowski and Raven, 2007; Lin et al., 2016; Brembu et al., 2017). In coastal areas, a previous investigation showed that N concentrations ranged from 10 to 17 μmol L^{-1} and the P concentration ranged from 0.2 to 1 μmol L^{-1} (Li et al., 2022). Another report also demonstrated that the lowest P concentration in core areas of large-scale macroalgae cultivation was only 0.08 μmol L^{-1} (Zhou et al., 2022). Such a dramatic fluctuation result in the N:P ratio, from 17:1 to 50:1, which exceeds the Redfield ratio of 16:1, suggests that P availability may be a limiting factor controlling algal photosynthesis and growth.

Temperature is considered to be another crucial factor that affects the photosynthesis and growth of macroalgae (Ji and Gao, 2021). Anthropogenic activities have increased atmospheric carbon dioxide (CO_2) from roughly 280 ppm in pre-industrial times to over 410 ppm today. Under the SSP5-8.5 emissions scenario, the greenhouse gas is expected to cause an increase in global mean temperature of 4.3°C by the end of this century (Masson-Delmotte et al., 2021), with ocean surface temperature potentially rising by 2.34-2.82°C (Pörtner et al., 2019). Previous studies have shown that ocean warming can have varied effects on algae—positive, negative, or neutral—likely due to species-specific optimal growth temperatures (Liu et al., 2020; Ji and Gao, 2021). For example, a ~3°C rise in eastern Tasmania led to a >90% decline in *Macrocystis pyrifera* forests (Johnson et al., 2011). In Japan, a ~1°C temperature increase favored warm-temperate species such as *Ecklonia cava*, *Ecklonia stolonifera*, and *Undaria peterseniana*, while reducing cold-temperate species such as *Laminaria japonica*, *Kjellmaniella crassifolia*, and *Costaria costata* (Serisawa et al., 2004; Kirihara et al., 2006). Another example in northern Spain, the decrease of *Fucus serratus* and *Himanthalia elongata* was linked to a 1.5°C–2°C rise in coastal seawaters (Duarte et al., 2013). These findings imply that macroalgae are highly sensitive to changes in temperature associated with global climate change despite being adapted to natural variations in temperature.

Gracilariopsis lemaneiformis (Gracilariaceae, Rhodophyta), an economically important marine crop, is the second largest cultivated macroalga after *Saccharina japonica* in China (Zhou et al., 2024). By using floating longlines and vegetative propagation methods, *G. lemaneiformis* has been seasonally cultivated from northern to southern China (Pang et al., 2017; Xue et al., 2022). As reported, the cultivation area of *G. lemaneiformis* in China is 13,924 hm^2 and its annual output reached 610,824 t (dry weight) in 2022 (Compiled by Fisheries Bureau of Ministry of Agriculture, 2023). Such high production of *G. lemaneiformis* not only provides food or industry resources but also contributes to mitigating climate change through the assimilation of inorganic carbon. Photosynthesis, the most general and sensitive physiological response, is pivotal for understanding how macroalgae adapt to varying temperatures and nutrient conditions (Ye et al., 2013). Currently, a number of studies have investigated the effect of nutrients or warming on photosynthesis and growth of *G. lemaneiformis* (Yang et al., 2021; Li et al, 2022; Zhou et al., 2024), while interaction between these factors has received less attention. Moreover, those published papers tend to focus on the reduction in photosynthetic efficiency, leaving the mechanisms of photoinhibition and their impact on cellular activities less explored. In our present study, changes in both photosynthesis performance and antioxidant enzyme activity were measured, aiming to characterize the different physiological

responses of *G. lemaneiformis* subjected to nutrient variations and ocean warming under natural sunlight.

Materials and methods

Experimental treatments

Thalli of *Gracilariopsis lemaneiformis* were collected from farmed rafts offshore of Ningde, Fujian province of China (119.31°E, 26.39°N), in December 2023, and transferred to the laboratory in a cooled Styrofoam box. Following rinsing, weighted thalli of ~0.5 g fresh weight (FW) were grown for 10 days in 1.5 L open-ended tubes filled with artificial seawater, which was continuously aerated and renewed every 2 days. According to previous studies (Jiang et al., 2022; Zhou et al., 2022, 2024), as well as *in-situ* measurement of seawater temperature (19.6°C), the ambient temperature was set as 20°C. The warming treatment (23°C) was set following the prediction of SSP5-8.5 (Pörtner et al., 2019; Masson-Delmotte et al., 2021), where the ocean surface temperature would increase by ~3°C. Under each temperature, four nutrient levels were set as low concentrations of N and P (LNLP) (N: 8 μmol L^{-1}, P: 0.5 μmol L^{-1}), low concentration of N and high concentration of P (LNHP) (N: 8 μmol L^{-1}, P: 10 μmol L^{-1}), high concentration of N and low concentration of P (HNLP) (N: 160 μmol L^{-1}, P: 0.5 μmol L^{-1}), and high concentrations of N and P (HNHP) (N: 160 μmol L^{-1}, P: 10 μmol L^{-1}). The artificial seawater used in this study was prepared according to Berges et al. (2001) without the addition of major nutrients and elements. The tubes were partly immersed in two water baths, where the ambient water temperature, 20°C and 23°C, were controlled by two heaters (SunSun, AR-450, SunSun Group Co., Ltd, China). Four nutrient levels were adjusted by adding NO_3^- and PO_4^{3-} into artificial seawater. Three independent replicate cultures were used for each treatment (n=3). The experiment set-up graphic is shown in Figure 1.

Determination of relative growth rate and contents of Chl *a*

Relative growth rate (RGR) was determined by measuring the changes in FW of the thalli after 10 days and was calculated by using the following equation RGR (% d^{-1}) = 100×(lnN_{10}-lnN_0)/10, where N_{10} and N_0 represented fresh weights of the thalli at day 10 and 0, respectively.

Approximately 0.05 g (FW) thalli was ground and extracted in 5 mL absolute methanol at 4°C in darkness for 12 h. After centrifugation at 4°C, 5000g for 15 min, the absorbance of the supernatant was measured from 400 nm – 700 nm using a scanning spectrophotometer (752N, INESA Co. Ltd., Shanghai, China). The contents of chlorophyll *a* (Chl *a*, mg/g FW) were calculated according to Porra (2002),

$$\text{Chl } a \text{ (mg/gFW)} = \frac{[16.29 \times (A_{665} - A_{750}) - 8.54 \times (A_{652} - A_{750})] \times V_E}{m}$$

where A_x is the absorbance under the x-wavelength, V_E is the volume of the methanol extraction, and m is the weight of the algae.

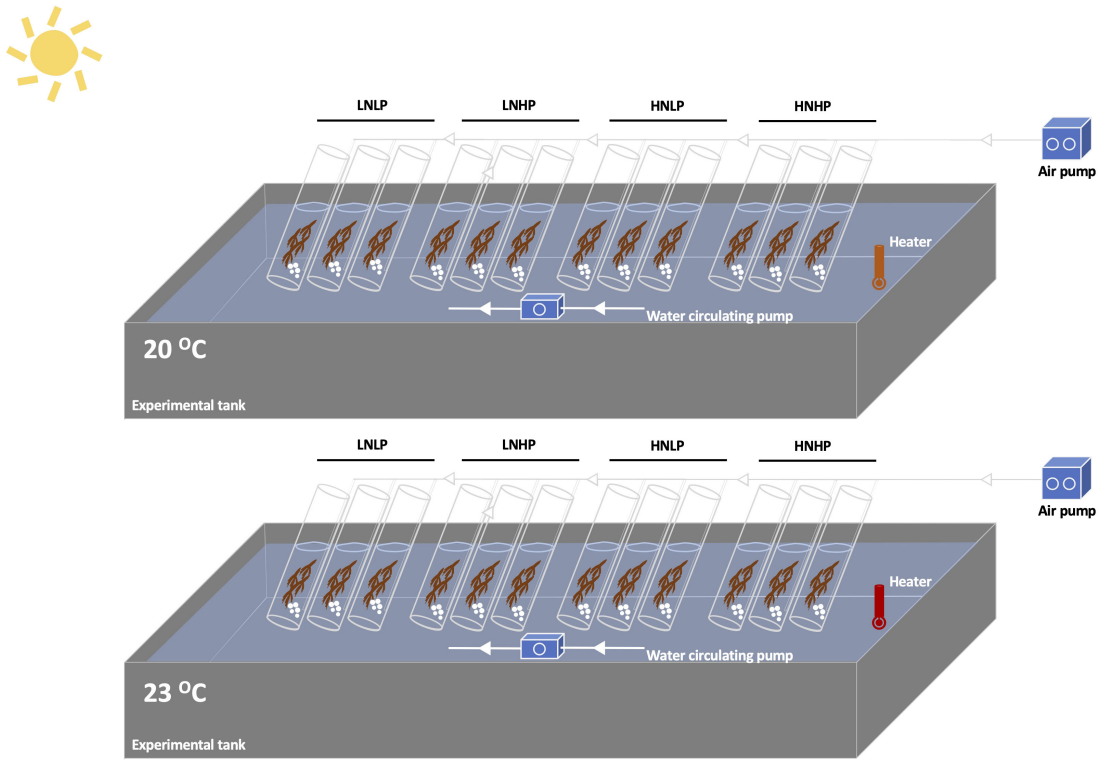

FIGURE 1
The graphic experiment set-up.

Measurement and analysis of chlorophyll fluorescence

A portable fluorimeter (AquaPen AP110, Photon Systems Instruments, Brno, Czech Republic) was employed to measure the photosynthetic performance of photosystem II (PSII). During the measurements, a blue LED emitter with excitation light at 455 nm was used to eliminate the effect of phycobiliproteins on chlorophyll fluorescence. The minimal fluorescence (F_o) for 30 min dark-adapted thalli was induced by a low irradiance (~0.15 µmol photons m^{-2} s^{-1}), and the maximum fluorescence (F_m) was obtained during a saturating flash (4000 µmol photons m^{-2} s^{-1}). Following that, an actinic light with an intensity of 400 µmol photons m^{-2} s^{-1} was employed to induce a steady state of photosynthesis. The stable fluorescence (F) and the corresponding maximum steady fluorescence (F_m') during the saturating flash were monitored. The maximum photochemical quantum yield of PSII (F_v/F_m), the non-photochemical quenching (NPQ), and the effective photochemical quantum yield of PSII (YII) were calculated as $F_v/F_m = (F_m - F_o)/F_m$; $NPQ = (F_m - F_m')/F_m'$; and $YII = (F_m' - F)/F_m'$, respectively.

According to Miao et al. (2018) and Heraud and Beardall (2000), the damage and recovery processes of the photosynthetic apparatus were obtained by periodically measuring the YII during photoinhibitory exposure (~1000 µmol photons m^{-2} s^{-1}). The damage (k, min^{-1}) and repair (r, min^{-1}) rates were estimated using the Kok model and calculated with the following equation:

$$\frac{Yn}{Yo} = \frac{r}{k+r} + \frac{k}{k+r} \times e^{-(k+r)/t}$$

where Y_n and Y_o are YII at time t_n and t_o, respectively.

Measurement of net photosynthesis and respiration rates

Net photosynthesis and dark respiration rates were measured with optical dissolved oxygen (DO) sensors (ProODO-BOD, YSI, USA). Approximately 0.2 g FW of *G. lemaneiformis* from each treatment was placed in a 100 mL BOD bottle containing cultivation artificial seawater, which was stirred continuously during the measurement. Temperature was maintained at either 20°C or 23°C, corresponding to the cultivation temperatures. The net photosynthesis and dark respiration rates (µmol O_2 h^{-1} g^{-1} FW) were determined as the variations of DO content during light (400 µmol photons m^{-2} s^{-1}) and dark conditions, respectively.

Measurement of reactive oxygen species content and antioxidant enzyme activity

Fresh samples were ground with liquid nitrogen and the tissue homogenates were used to analyze the ROS (mainly referred to as hydrogen peroxide, H_2O_2) content and enzyme (mainly referred to as superoxide dismutase (SOD) and catalase (CAT)) activity of *G. lemaneiformis* with a commercial assay kit (Jiancheng, Nanjing, China) following the manufacturer's protocols.

Statistical analyses

Statistical analyses were performed using SPSS 19.0 (SPSS Inc., Chicago, USA). The homogeneity of variance was examined using Levene's test before all statistical analyses. One-way ANOVA and t-test were used to establish differences among treatments. A two-way ANOVA was used to identify the effects of warming, nutrients, and their interactions. As shown in Figure 1, warming treatments were achieved by heating the water in the tank, therefore, all ANOVA analyses regarding warming in this study should be temperature and tank effects. Differences were considered to be statistically significant at $p<0.05$.

Results

Relative growth rate and Chl *a* content

As shown in Figure 2A, the RGR of *Gracilariopsis lemaneiformis* displayed a significant difference among the treatments. Compared with LNLP treatment (natural seawater), the enrichment with NO_3^- and PO_4^{3-} (HNHP) significantly increased RGR by up to 83% and 134% in 20°C and 23°C, respectively, reaching 3.2% and 3.5% per day. However, enrichment with only PO_4^{3-} concentration (LNHP), and enrichment with only NO_3^- concentration (HNLP) showed no significant effects on RGR. In terms of temperature variations, i.e., the temperature and tank effects, the higher temperature significantly increased the RGR in the HNHP condition but decreased in HNLP. A two-way ANOVA showed that both temperature, nutrient variations, and their interaction significantly affected RGR (Table 1). Considering the fact that both NO_3^- and PO_4^{3-} are essential for pigment formation, a significant increase of Chl *a* content was observed in HNHP treatment, but not for LNHP and HNLP treatments (Figure 2B). In contrast to higher values of RGR under 23°C, the elevated temperature did not enhance the contents of Chl *a* (Figure 2B).

Chlorophyll fluorescence, photosynthesis, and respiration

The maximum quantum yield of PSII (F_v/F_m) showed the highest values in the HNHP treatment, with an average value of ~0.54 at both 20°C and 23°C, and the lowest values in the HNLP treatment (Figure 3A). In terms of temperature, the values of F_v/F_m in 23°C in the LNHP and HNLP treatments were significantly higher than that in 20°C (t-test, $p<0.05$, $p<0.05$), while in the LNLP and HNHP treatments, the values of F_v/F_m showed no significant difference between 20°C and 23°C (Figure 3A, t-test, $p=0.243$, $p=0.197$). In contrast, the NPQ was significantly upregulated in the LNHP and HNLP treatment, with an average value of 0.39 and

10.3389/fmars.2024.1432937

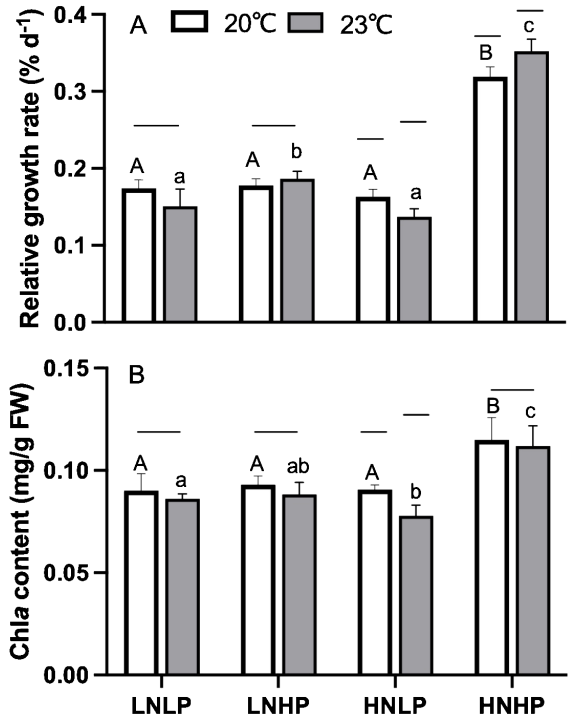

FIGURE 2
Relative growth rate[%d^{-1}, panel **(A)**] and Chl *a* content [mg/g FW, panel **(B)**] of *Gracilariopsis lemaneiformis* after growing for 10 days at four nutrients levels (LNLP, LNHP, HNLP and HNHP) and two temperature (20°C, open bars, 23°C, grey bars). Each data point is means ± SD (n=3). Different upper and lower letters above the bars indicate significant differences between nutrients levels under 20°C and 23°C, respectively (p<0.05, One-way ANOVA). Unconnected line above the bars indicate significant differences between temperature under each nutrients level (p<0.05, One-way ANOVA). LNLP, low nitrogen and low phosphorus concentrations (N: 8μmol/L, P: 0.5 μmol/L); LNHP, low nitrogen and high phosphorus concentrations (N: 8μmol/L, P: 10 μmol/L); HNLP, high nitrogen and low phosphorus concentrations (N: 160μmol/L, P: 0.5 μmol/L); HNHP, high nitrogen and high phosphorus concentrations (N: 160μmol/L, P: 10 μmol/L); FW, fresh weight; SD, standard deviation.

0.42 at 20°C and 23°C, respectively. The elevated temperature did not affect the NPQ, except for the HNLP treatment (Figure 3B).

Similar to RGR, the net photosynthesis rate of *G. lemaneiformis* showed the highest values in the HNHP treatment, with an average value of 40.38 μmol O_2 h^{-1} g^{-1} FW and 45.81 μmol O_2 h^{-1} g^{-1} FW at 20°C and 23°C, respectively (Figure 4A). The LNHP treatment brought no significant change to net photosynthesis rate (t-test, p=0.189), and the HNLP treatment significantly decreased the net photosynthesis rate (t-test, p<0.05). The elevated temperature significantly increased the net photosynthesis rate in the HNHP treatment (t-test, p<0.05), but this decreased in the HNLP treatment (Figure 4A, t-test, p<0.05). Changes in respiration rate are shown in Figure 4B; the highest values were observed in the HNHP treatment and the lowest values were observed in the HNLP treatment (Figure 4B). The elevated temperature showed no significant effect on respiration rate, except for the HNHP treatment (Figure 4B, t-test, p=0.176, p=0.237, p=0.467 for LNLP, LNHP, and HNLP, respectively, and p<0.05 for HNHP).

TABLE 1 Two-way ANOVA for the effects of temperature (20°C and 23°C) and nutrients variations (LNLP, LNHP, HNLP, HNHP) on the relative growth rate (RGR), the damage (*k*) and repair (*r*) rate.

Parameters	Source of variation	df	Mean square	F	*p*
RGR	Temperature	1	<0.001	5.645	0.03
	Nutrients variations	3	<0.001	273.413	<0.001
	Temperature× Nutrients variations	3	<0.001	7.612	0.002
	Error	16	<0.001		
k	Temperature	1	0.005	70.080	<0.001
	Nutrients variations	3	0.011	154.024	<0.001
	Temperature× Nutrients variations	3	0.001	9.236	0.001
	Error	16	<0.001		
r	Temperature	1	0.008	117.308	<0.001
	Nutrients variations	3	0.002	1.786	<0.001
	Temperature× Nutrients variations	3	<0.001	0.715	0.424
	Error	16	<0.001		

LNLP, low nitrogen and low phosphorus concentrations (N: 8μmol/L, P: 0.5 μmol/L); LNHP, low nitrogen and high phosphorus concentrations (N: 8μmol/L, P: 10 μmol/L); HNLP, high nitrogen and low phosphorus concentrations (N: 160μmol/L, P: 0.5 μmol/L); HNHP, high nitrogen and high phosphorus concentrations (N: 160μmol/L, P: 10 μmol/L).

Damage and repair rates of photosystem II

The rates of damage and repair of PSII during photoinhibitory exposure were estimated from the changes in the effective photochemical quantum yield of PSII (YII). The damage rate showed significantly higher values in low PO_4^{3-} concentrations, i.e., the LNLP and HNLP treatments, especially under the elevated temperature (Figure 5A). The elevated temperature showed no significant effects on the values of *k* in both the LNHP and HNHP treatments (Figure 5A, t-test, p=0.105, p=0.217 for LNHP and HNHP, respectively). By contrast, the repair rate showed significantly higher values in high PO_4^{3-} concentration, i.e., the LNHP and HNHP treatments (Figure 5A). The elevated temperature significantly decreased the repair rate by up to 8.5%, 3.4%, 16.1%, and 5.5% for LNLP, LNHP, HNLP, and HNHP, respectively. Accordingly, the ratio between *r* and *k* also showed significantly higher values in LNHP and HNHP treatments, and the elevated temperature significantly decreased the *r*/*k* (Figure 5C). A two-way ANOVA showed that temperature, nutrient variations, and their interaction, significantly affected the value of *k* (t-test, p<0.05, p<0.05, p<0.05) and *r* (Table 1, t-test, p<0.05, p<0.05), except for the interaction with *r* (t-test, p=0.424).

10.3389/fmars.2024.1432937

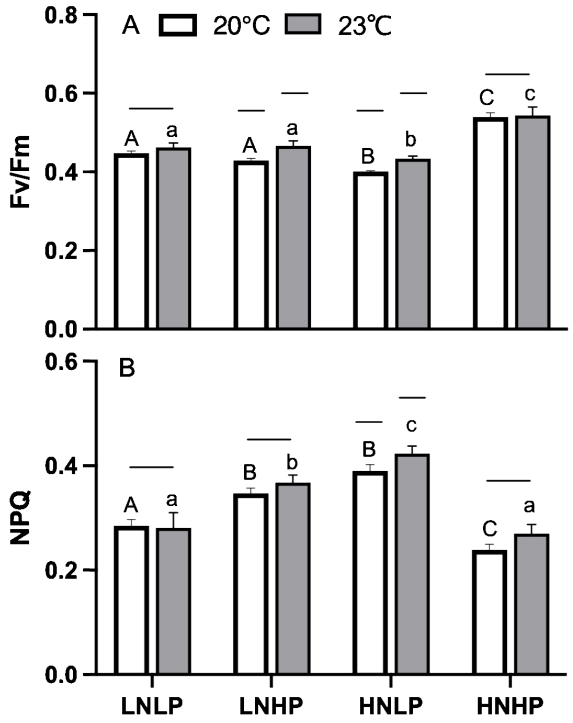

FIGURE 3
The maximum photochemical quantum yield of photosystem II [F_v/F_m, panel **(A)**] and non-photochemical quenching [NPQ, panel **(B)**] of *Gracilariopsis lemaneiformis* after growing for 10 days at four nutrients levels (LNLP, LNHP, HNLP and HNHP) and two temperature (20°C, open bars, 23°C, grey bars). Each data point is means ± SD (n=3). Different upper and lower letters above the bars indicate significant differences between nutrients levels under 20°C and 23°C, respectively (p<0.05, One-way ANOVA). Unconnected line above the bars indicate significant differences between temperature under each nutrients level (p<0.05, One-way ANOVA). LNLP, low nitrogen and low phosphorus concentrations (N: 8μmol/L, P: 0.5 μmol/L); LNHP, low nitrogen and high phosphorus concentrations (N: 8μmol/L, P: 10 μmol/L); HNLP, high nitrogen and low phosphorus concentrations (N: 160μmol/L, P: 0.5 μmol/L); HNHP, high nitrogen and high phosphorus concentrations (N: 160μmol/L, P: 10 μmol/L); SD, standard deviation.

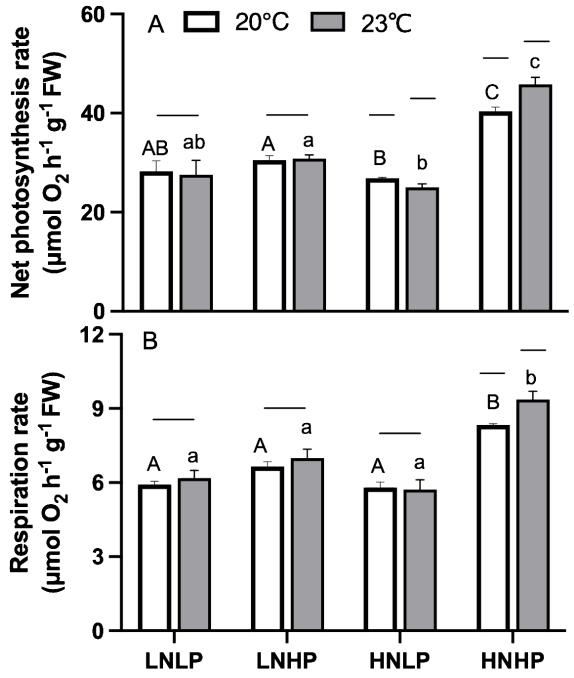

FIGURE 4
Net photosynthesis rate [μmol O_2 h^{-1} g^{-1} FW, panel **(A)**] and respiration rate 9μmol O_2 h^{-1} g^{-1} FW, panel **(B)**] of *Gracilariopsis lemaneiformis* after growing for 10 days at four nutrients levels (LNLP, LNHP, HNLP and HNHP) and two temperature (20°C, open bars, 23°C, grey bars). Each data point is means ± SD (n=3). Different upper and lower letters above the bars indicate significant differences between nutrients levels under 20°C and 23°C, respectively (p<0.05, One-way ANOVA). Unconnected line above the bars indicate significant differences between temperature under each nutrients level (p<0.05, One-way ANOVA). LNLP, low nitrogen and low phosphorus concentrations (N: 8μmol/L, P: 0.5 μmol/L); LNHP, low nitrogen and high phosphorus concentrations (N: 8μmol/L, P: 10 μmol/L); HNLP, high nitrogen and low phosphorus concentrations (N: 160μmol/L, P: 0.5 μmol/L); HNHP, high nitrogen and high phosphorus concentrations (N: 160μmol/L, P: 10 μmol/L); FW, fresh weight; SD, standard deviation.

Reactive oxygen species content and antioxidant enzyme activity

The ROS content was estimated by quantifying the production of H_2O_2 to assess the redox state of *G. lemaneiformis* under different treatments. As shown in Figure 6, the ROS content showed significantly higher values under the LNLP and HNLP treatments, while the enrichment of PO_4^{3-} significantly alleviated the production of ROS. The elevated temperature increased the production of ROS in low PO_4^{3-} concentrations (t-test, p<0.05 for both LNLP and HNLP treatments), but showed no significant effects on the LNHP and HNHP treatments (t-test, p=0.382, p=0.417 for LNHP and HNHP, respectively).

In turn, changes in antioxidant enzyme activity showed similar patterns. As shown in Figure 7, both SOD and CAT showed significantly higher activities under both LNLP and HNLP treatments, while decreased by the enrichment of PO_4^{3-}. The elevated temperature could further active the SOD and CAT activities in both LNLP and HNLP treatments, but not for LNHP and HNHP treatments.

Discussion

Effects of nutrients variations on *Gracilariopsis lemaneiformis*

Nitrogen and phosphorus are both involved the synthesis of amino acids and phycobilins, the transformation of enzymes, and the formation of germ cells in macroalgae, which are all necessary for growth (Zhou et al., 2024). In coastal areas, the drastic fluctuations of nutrients induced by human activities often expose macroalgae to an imbalance between nitrogen and phosphorus, which affects their growth and survival (Chu et al., 2019). In the present study, the enrichment of both PO_4^{3-} and NO_3^- prompted the synthesis of Chl *a* and active photochemical efficiency, which led to an increase in the net photosynthesis rate of *Gracilariopsis lemaneiformis* and further resulted in a parallel increase in RGR. However, enrichment of either PO_4^{3-} or NO_3^- alone did not enhance photosynthesis or growth. In the case of disturbed N:P,

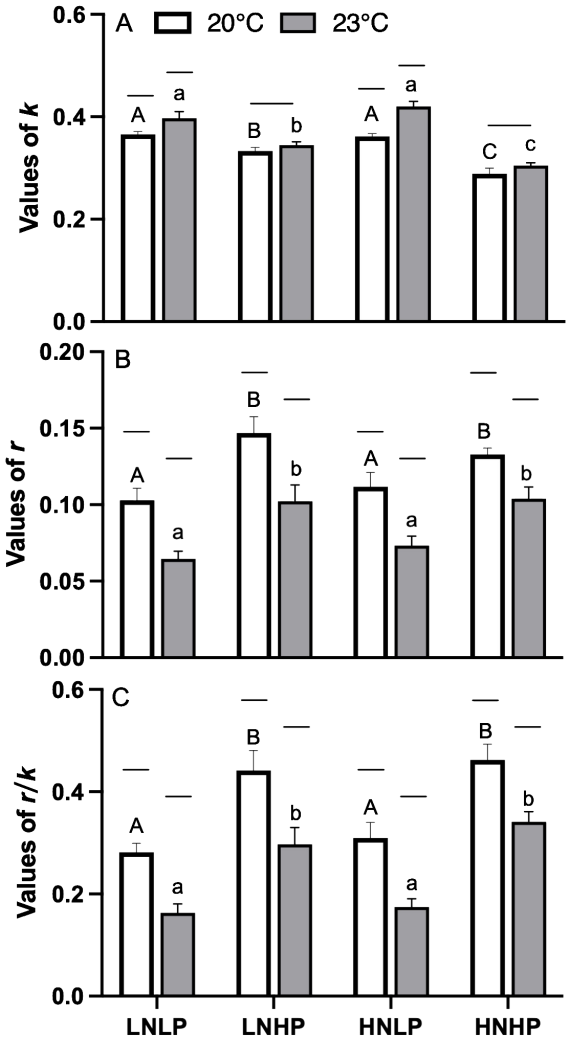

FIGURE 5
The damage [*k*, panel **(A)**], recovery [*r*, panel **(B)**] rates and the ratio between *r* and *k* [*r*/*k*, panel **(C)**] of *Gracilariopsis lemaneiformis* after growing for 10 days at four nutrients levels (LNLP, LNHP, HNLP and HNHP) and two temperature (20°C, open bars, 23°C, grey bars). Each data point is means ± SD (n=3). Different upper and lower letters above the bars indicate significant differences between nutrients levels under 20°C and 23°C, respectively ($p<0.05$, One-way ANOVA). Unconnected line above the bars indicate significant differences between temperature under each nutrients level ($p<0.05$, One-way ANOVA). LNLP, low nitrogen and low phosphorus concentrations (N: 8μmol/L, P: 0.5 μmol/L); LNHP, low nitrogen and high phosphorus concentrations (N: 8μmol/L, P: 10 μmol/L); HNLP, high nitrogen and low phosphorus concentrations (N: 160μmol/L, P: 0.5 μmol/L); HNHP, high nitrogen and high phosphorus concentrations (N: 160μmol/L, P: 10 μmol/L); SD, standard deviation.

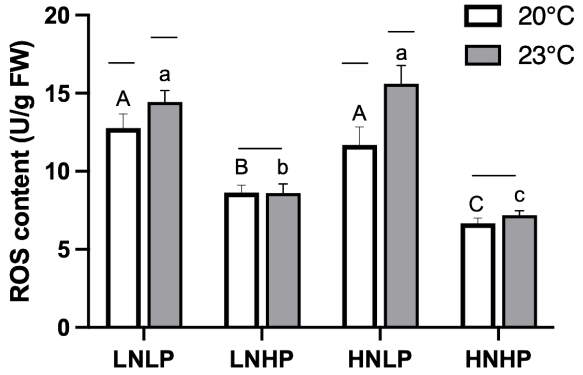

FIGURE 6
The reactive oxygen species content (U/g FW) of *Gracilariopsis lemaneiformis* after growing for 10 days at four nutrients levels (LNLP, LNHP, HNLP and HNHP) and two temperature (20°C, open bars, 23°C, grey bars). Each data point is means ± SD (n=3). Different upper and lower letters above the bars indicate significant differences between nutrients levels under 20°C and 23°C, respectively ($p<0.05$, One-way ANOVA). Unconnected line above the bars indicate significant differences between temperature under each nutrients level ($p<0.05$, One-way ANOVA). LNLP, low nitrogen and low phosphorus concentrations (N: 8μmol/L, P: 0.5 μmol/L); LNHP, low nitrogen and high phosphorus concentrations (N: 8μmol/L, P: 10 μmol/L); HNLP, high nitrogen and low phosphorus concentrations (N: 160μmol/L, P: 0.5 μmol/L); HNHP, high nitrogen and high phosphorus concentrations (N: 160μmol/L, P: 10 μmol/L); FW, fresh weight; SD, standard deviation.

the lower phosphorus treatment (HNLP) exhibited a worse effect, showing lower values of RGR and net photosynthesis rate.

As essential nutrients, both nitrogen and phosphorus are not only involved in the formation of chloroplast DNA and RNA, but also highly necessary for the generation of ATP, the synthesis of phospholipids, and the phosphorylation of photosynthesis proteins (Scheerer et al., 2019). In our present study, the significant increase of F_v/F_m under the HNHP condition indicated efficient conversion of absorbed light into chemical energy, as shown by higher net photosynthesis rates. Conversely, the significant decline of F_v/F_m under the HNLP condition suggested an inhibition of photosynthesis, which could further lead to reduced production of ATP and NADPH. As two essential molecules that fuel the Calvin cycle, the diminished ability to fix carbon would naturally result in a lower net photosynthesis rate and RGR. Similar results were also reported in several other macroalgae (e.g. *Sargassum muticum* in Xu et al., 2017; *Ulva linza* in Gao et al., 2018; and *Pyropia yezoensis* in Kim et al., 2019). In addition to the limitation of carbon fixation, photoinhibition-induced lower generation of ATP would also inhibit the high turnover rate of D1 protein [the core protein of photosystem II (PSII)], which is the prerequisite for PSII to flexibly respond to environmental fluctuations (Powles, 1984; Long et al., 1994). To clarify the occurrence of P deficiency-induced photoinhibition, non-photochemical quenching, the most common and quickest photoprotection mechanism (Adams and Demmig-Adams, 1994; Ruban, 2016), and the rates of damage and repair of PSII, were measured. In *G. lemaneiformis*, a decrease in F_v/F_m was always accompanied by an increase in NPQ (Figure 3), indicating an increase in energy dissipation, especially under the HNLP condition. Specifically, the required light energy for *G. lemaneiformis* cultured in the HNLP condition should be much less than that of other treatments, which easily suffer from photoinhibition. In terms of the rates of damage and repair of PSII during photoinhibitory exposure, the higher value of *k* and the

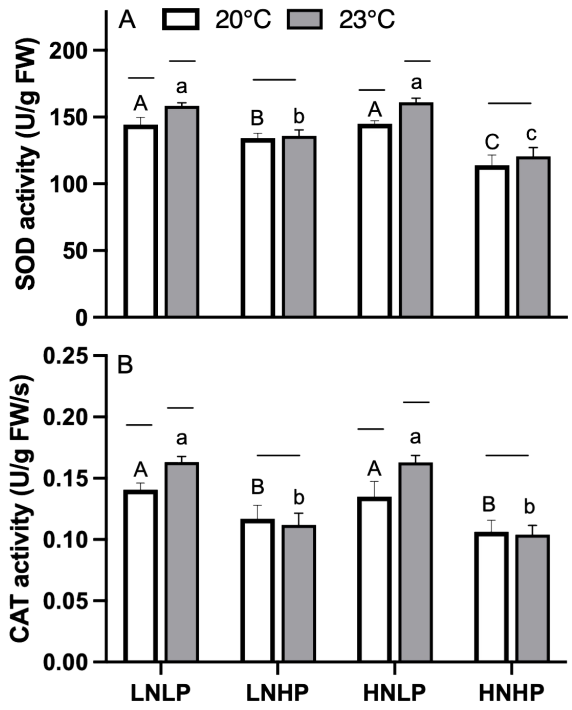

FIGURE 7
The SOD [U/g FW, panel **(A)**] and CAT [U/g FW, panel **(B)**] activities of *Gracilariopsis lemaneiformis* after growing for 10 days at four nutrients levels (LNLP, LNHP, HNLP and HNHP) and two temperature (20°C, open bars, 23°C, grey bars). Each data point is means ± SD (n=3). Different upper and lower letters above the bars indicate significant differences between nutrients levels under 20°C and 23°C, respectively (p<0.05, One-way ANOVA). Unconnected line above the bars indicate significant differences between temperature under each nutrients level (p<0.05, One-way ANOVA). SOD, superoxide dismutase; CAT, catalase; LNLP, low nitrogen and low phosphorus concentrations (N: 8μmol/L, P: 0.5 μmol/L); LNHP, low nitrogen and high phosphorus concentrations (N: 8μmol/L, P: 10 μmol/L); HNLP, high nitrogen and low phosphorus concentrations (N: 160μmol/L, P: 0.5 μmol/L); HNHP, high nitrogen and high phosphorus concentrations (N: 160μmol/L, P: 10 μmol/L); FW, fresh weight; SD, standard deviation.

lower value of r suggested severe photoinhibition of PSII occurred in P deficiency treatments (Figure 5). These results confirmed that *G. lemaneiformis* was sensitive to P deficiency, which could induce significant photoinhibition by decreasing the P utilization in photophosphorylation (Scheerer et al., 2019; Zhou et al., 2024) and retarding the repair of D1 protein.

Once the thermal energy dissipation could not satisfy the energy balance between absorption and utilization, the excess excitation energy would result in the accumulation of ROS (Logan et al., 1998, 2006), which is known to induce oxidative stress and damage biomolecules such as pigments, proteins, and lipids in plants and algae (Miller et al., 2010; Suzuki et al., 2012; Nahar et al., 2015; Barati et al., 2019). In the present study, the production of ROS was highly consistent with the damage and repair rates of the PSII, with high content in P deficiency conditions (Figure 6). The antioxidant system that scavenges ROS has been previously reported as a second line of defense against photoinhibition-induced oxidative stress (Logan et al., 2006). Here, SOD and CAT, which are responsible for turning O_2^- into H_2O_2, and turning H_2O_2 to H_2O, respectively, show similar trends to the production of ROS, with higher values in the P deficiency conditions. These results also confirmed that *G. lemaneiformis* was sensitive to P deficiency, which could induce severe oxidative stress by increasing photoinhibition risk.

Effects of warming on Gracilariopsis lemaneiformis

Generally, the elevated temperature could accelerate the growth of phytoplankton and macroalgae via upregulating the metabolic activity (Lund, 1949; Charan et al., 2017; Schaum et al., 2017; Wu et al., 2019). As mentioned above, the elevated temperature in this study was achieved by heating the water in the tank; therefore, the warming effect should be attributed to temperature and the tank. In *G. lemaneiformis*, both the net photosynthesis rate and growth under the HNHP treatment were increased by the elevated temperature. Similar results were also observed in *Chaetomorpha linum* and *Gracilaria blodgettii*, where their growth increased when the temperature rose from 20°C to 35°C within a phosphorus repletion condition (Zeng et al., 2020). In contrast, under P deficiency conditions, the higher temperature negatively affected both the net photosynthesis rate and growth in *G. lemaneiformis*. A plausible explanation for this is that the limited available P is prioritized for maintaining the basic functions of the cells and the high requirement of P (a high P uptake rate) induced by the high temperature could not be satisfied, resulting in a decrease in algal biomass (Talbot and De la Noüe, 1993; Mandal et al., 2015; Zhou et al., 2024). Additionally, the significant enhancement of k and decline of r at 23°C also implied that the elevated temperature increased the photoinhibition of *G. lemaneiformis* under P deficiency conditions. Together with the increase in ROS production (Figure 6) and antioxidant enzyme activity (Figure 7), our data demonstrated that future warming would exacerbate P deficiency-induced photoinhibition and oxidative stress.

Conclusion

Found in coastal areas, macroalgae are often exposed to drastic environmental fluctuations due to anthropogenic activities, including nutrient variations and seawater warming. The present study indicates that *G. lemaneiformis* is particularly susceptible to P deficiency, leading to significant photoinhibition and increased oxidative stress, ultimately reducing growth. Furthermore, projected seawater warming is likely to exacerbate the negative impacts of P deficiency, amplifying photoinhibition and oxidative stress.

Data availability statement

The raw data supporting the conclusions of this article will be made available by the authors, without undue reservation.

Author contributions

DZ: Conceptualization, Data curation, Formal analysis, Funding acquisition, Investigation, Methodology, Project administration, Writing – original draft, Writing – review & editing. J-ZS: Methodology, Writing – review & editing. M-HF: Investigation, Writing – review & editing. C-JL: Investigation, Writing – review & editing.

Funding

The author(s) declare financial support was received for the research, authorship, and/or publication of this article. This study was supported by the National Natural Science Youth Foundation (42306139) and the Natural Science Youth Foundation of Shandong Province (ZR2022QD134).

Conflict of interest

The authors declare that the research was conducted in the absence of any commercial or financial relationships that could be construed as a potential conflict of interest.

Publisher's note

References

Adams, W. W. III, and Demmig-Adams, B. (1994). Carotenoid composition and down regulation of photosystem II in three conifer species during the winter. *Physiol. Plant.* 92, 451–458. doi: 10.1111/j.1399-3054.1994.tb08835.x

Barati, B., Gan, S. Y., Lim, P. E., Beardall, J., and Phang, S. M. (2019). Green algal molecular responses to temperature stress. *Acta Physiol. Plant.* 41, 1–19. doi: 10.1007/s11738-019-2813-1

Berges, J. A., Franklin, D. J., and Harrison, P. J. (2001). Evolution of an artificial seawater medium: improvements in enriched seawater, artificial water over the last two decades. *J. phycol.* 37, 1138–1145. doi: 10.1046/j.1529-8817.2001.01052.x

Brembu, T., Mühlroth, A., Alipanah, L., and Bones, A. M. (2017). The effects of phosphorus limitation on carbon metabolism in diatoms. *Philos. Trans. R. Soc. B: Biol. Sci.* 372, 20160406.

Charan, H., N'Yeurt, A. D. R., Iese, V., and Chopin, T. (2017). "The effect of temperature on the growth of two pest seaweeds in Fiji," in *2nd International Conference on Energy, Environment and Climate-ICEECC*, University of Mauritius, Jan 2017, Moka, Mauritius. hal-04581450

Chen, B., Zou, D., Du, H., and Ji, Z. (2018). Carbon and nitrogen accumulation in the economic seaweed *Gracilaria lemaneiformis* affected by ocean acidification and increasing temperature. *Aquaculture* 482, 176–182. doi: 10.1016/j.aquaculture.2017.09.042

Chu, Y. Y., Liu, Y., Li, J., and Gong, Q. (2019). Effects of elevated pCO_2 and nutrient enrichment on the growth, photosynthesis, and biochemical compositions of the brown alga *Saccharina japonica* (Laminariaceae, Phaeophyta). *PeerJ* 7, e8040. doi: 10.7717/peerj.8040

Cohen, F. P. A., Faria, A. V. F., Braga, E. S., Chiozzini, V. G., and Plastino, E. M. (2022). Gracilarioid algae (Rhodophyta) cultured in eutrophic synthetic seawater: potential for growth and preliminary bioremediation assessment. *J. Appl. Phycol.* 34, 2783–2791. doi: 10.1007/s10811-022-02728-9

Compiled by Fisheries Bureau of Ministry of Agriculture. (2023). China Fishery Statistical Yearbook. China Agriculture, Beijing in Chinese.

Duarte, L., Viejo, R. M., Martínez, B., deCastro, M., Gómez-Gesteira, M., and Gallardo, T. (2013). Recent and historical range shifts of two canopy-forming seaweeds in North Spain and the link with trends in sea surface temperature. *Acta Oecol.* 51, 1–10. doi: 10.1016/j.actao.2013.05.002

Falkowski, P. G., and Raven, J. A. (2007). *Aquatic Photosynthesis* (Princeton, NJ: Princeton University Press).

Gao, G., Beardall, J., Bao, M., Wang, C., Ren, W., and Xu, J. (2018). Ocean acidification and nutrient limitation synergistically reduce growth and photosynthetic performances of a green tide alga *Ulva linza*. *Biogeosciences* 15, 3409–3420. doi: 10.5194/bg-15-3409-2018

Heraud, P., and Beardall, J. (2000). Changes in chlorophyll fluorescence during exposure of *Dunaliella tertiolecta* to UV radiation indicate a dynamic interaction between damage and repair processes. *Photosynth. Res.* 63, 123–134. doi: 10.1023/A:1006319802047

Ji, Y., and Gao, K. (2021). Effects of climate change factors on marine macroalgae: A review. *Adv. Mar. Biol.* 88, 91–136. doi: 10.1016/bs.amb.2020.11.001

Jiang, H., Liao, X., Zou, D., Huang, B., and Liu, Z. (2020). The regulations of varied carbon-nitrogen supplies to physiology and amino acid contents in *Gracilariopsis lemaneiformis* (Gracilariales, Rhodophyta). *Algal Res.* 47, 101818. doi: 10.1016/j.algal.2020.101818

Jiang, M., Gao, L., Huang, R., Lin, X., and Gao, G. (2022). Differential responses of bloom-forming *Ulva intestinalis* and economically important *Gracilariopsis lemaneiformis* to marine heatwaves under changing nitrate conditions. *Sci. Total Environ.* 840, 156591. doi: 10.1016/j.scitotenv.2022.156591

Johnson, C. R., Banks, S. C., Barrett, N. S., Cazassus, F., Dunstan, P. K., Edgar, G. J., et al. (2011). Climate change cascades: Shifts in oceanography, species' ranges and subtidal marine community dynamics in eastern Tasmania. *J. Exp. Mar. Biol. Ecol.* 400, 17–32. doi: 10.1016/j.jembe.2011.02.032

Karl, D. M. (2000). Phosphorus, the staff of life. *Nature* 406, 31–33. doi: 10.1038/35017683

Kim, S., Yoon, S. C., Yoo, M. H., Park, K. W., Park, S. R., and Youn, S. H. (2019). Physiological responses of cultured seaweed *Pyropia yezoensis* to phosphorous limitation in the Nakdong river estuary, Korea. *Ocean Sci. J.* 54, 129–139. doi: 10.1007/s12601-018-0065-4

Kipp, M. A., and Stüeken, E. E. (2017). Biomass recycling and Earth's early phosphorus cycle. *Sci. Adv.* 3, eaao4795. doi: 10.1126/sciadv.aao4795

Kirihara, S., Nakamura, T., Kon, N., Fujita, D., and Notoya, M. (2006). Recent fluctuations in distribution and biomass of cold and warm temperature species of Laminarialean algae at Cape Ohma, northern Honshu, Japan. *J. Appl. phycol.* 18, 521–527. doi: 10.1007/s10811-006-9057-3

Li, T., Wu, J., Du, H., Pei, P., Yang, C., Huang, J., et al. (2022). Environmental nitrogen and phosphorus nutrient variability triggers intracellular resource reallocation in *Gracilariopsis lemaneiformis* (Rhodophyta). *Algal Res.* 66, 102778. doi: 10.1016/j.algal.2022.102778

Lin, S., Litaker, R. W., and Sunda, W. G. (2016). Phosphorus physiological ecology and molecular mechanisms in marine phytoplankton. *J. Phycol.* 52, 10–36. doi: 10.1111/jpy.12365

Liu, C., Zou, D., Liu, Z., and Ye, C. (2020). Ocean warming alters the responses to eutrophication in a commercially farmed seaweed, *Gracilariopsis lemaneiformis*. *Hydrobiologia* 847, 879–893. doi: 10.1007/s10750-019-04148-2

Logan, B. A., Demmig-Adams, B., Adams, W. W. III, and Grace, S. C. (1998). Antioxidants and xanthophyll cycle-dependent energy dissipation in *Cucurbita pepo* L. and *Vinca major* L. acclimated to four growth PPFDs in the field. *J. Exp. Bot.* 49, 1869–1879. doi: 10.1093/jxb/49.328.1869

Logan, B. A., Kornyeyev, D., Hardison, J., and Holaday, A. S. (2006). The role of antioxidant enzymes in photoprotection. *Photosynth. Res.* 88, 119–132. doi: 10.1007/s11120-006-9043-2

Long, S. P., Humphries, S., and Falkowski, P. G. (1994). Photoinhibition of photosynthesis in nature. *Annu. Rev. Plant Biol.* 45, 633–662. doi: 10.1146/annurev.pp.45.060194.003221

Lund, J. W. G. (1949). Studies on asterionella: I. @ the origin and nature of the cells producing seasonal maxima. *J. Ecol.* 37 (2), 389–419.

Mandal, S. K., Ajay, G., Monisha, N., Malarvizhi, J., Temkar, G., and Mantri, V. A. (2015). Differential response of varying temperature and salinity regimes on nutrient uptake of drifting fragments of *Kappaphycus alvarezii*: implication on survival and growth. *J. Appl. Phycol.* 27, 1571–1581. doi: 10.1007/s10811-014-0469-1

Masson-Delmotte, V., Zhai, P., Pirani, A., Connors, S. L., Péan, C., Chen, Y., et al. (2021). *IPCC 2021: climate change 2021: the physical science basis. contribution of working group I to the sixth assessment report of the intergovernmental panel on climate change* (Cambridge: Cambridge University Press).

Miao, H., Beardall, J., and Gao, K. (2018). Calcification moderates the increased susceptibility to UV radiation of the coccolithophorid *Gephryocapsa oceanica* grown under elevated CO_2 concentration: evidence based on calcified and non-calcified cells. *Photochem. Photobiol.* 94, 994–1002. doi: 10.1111/php.12928

Miller, G. A. D., Suzuki, N., Ciftci-Yilmaz, S., and Mittler, R. O. N. (2010). Reactive oxygen species homeostasis and signalling during drought and salinity stresses. *Plant Cell Environ.* 33, 453–467. doi: 10.1111/j.1365-3040.2009.02041.x

Nahar, K., Hasanuzzaman, M., Alam, M. M., and Fujita, M. (2015). Exogenous glutathione confers high temperature stress tolerance in mung bean (*Vigna radiata* L.) by modulating antioxidant defense and methylglyoxal detoxification system. *Environ. Exp. Bot.* 112, 44–54. doi: 10.1016/j.envexpbot.2014.12.001

Pang, T., Li, X., Liu, J., Bian, D., Li, Y., and Guo, W. (2017). Chinese Patent CN201610811729.6. CNKI.

Porra, R. J. (2002). The chequered history of the development and use of simultaneous equations for the accurate determination of chlorophylls a and b. *Photosynth. Res.* 73, 149–156. doi: 10.1023/A:1020470224740

Pörtner, H.-O., Roberts, D. C., Masson-Delmotte, V., Zhai, P., Tignor, M., Poloczanska, E., et al. (2019). "IPCC special report on the ocean and cryosphere in a changing climate," in *IPCC intergovernmental panel on climate change*, vol. 1. (Cambridge University Press, Cambridge, UK and New York, NY, USA).

Powles, S. B. (1984). Photoinhibition of photosynthesis induced by visible light. *Annu. Rev. Plant Physiol.* 35, 15–44. doi: 10.1146/annurev.pp.35.060184.000311

Roleda, M. Y., and Hurd, C. L. (2019). Seaweed nutrient physiology: application of concepts to aquaculture and bioremediation. *Phycologia* 58, 552–562. doi: 10.1080/00318884.2019.1622920

Ruban, A. V. (2016). Nonphotochemical chlorophyll fluorescence quenching: mechanism and effectiveness in protecting plants from photodamage. *Plant Physiol.* 170, 1903–1916. doi: 10.1104/pp.15.01935

Schaum, C. E., Barton, S., Bestion, E., Buckling, A., Garcia-Carreras, B., Lopez, P., et al. (2017). Adaptation of phytoplankton to a decade of experimental warming linked to increased photosynthesis. *Nat. Ecol. Evol.* 1, 0094. doi: 10.1038/s41559-017-0094

Scheerer, U., Trube, N., Netzer, F., Rennenberg, H., and Herschbach, C. (2019). ATP as phosphorus and nitrogen source for nutrient uptake by *Fagus sylvatica* and *Populus x canescens* roots. *Front. Plant Sci.* 10, 416196. doi: 10.3389/fpls.2019.00378

Serisawa, Y., Imoto, Z., Ishikawa, T., and Ohno, M. (2004). Decline of the *Ecklonia cava* population associated with increased seawater temperatures in Tosa Bay, southern Japan. *Fish. Sci.* 70, 189–191. doi: 10.1111/j.0919-9268.2004.00788.x

Suzuki, N., Koussevitzky, S. H. A. I., Mittler, R. O. N., and Miller, G. A. D. (2012). ROS and redox signalling in the response of plants to abiotic stress. *Plant Cell Environ.* 35, 259–270. doi: 10.1111/j.1365-3040.2011.02336.x

Talbot, P., and De la Noüe, J. (1993). Tertiary treatment of wastewater with *Phormidium bohneri* (Schmidle) under various light and temperature conditions. *Water Res.* 27, 153–159. doi: 10.1016/0043-1354(93)90206-W

Traugott, H., Zollmann, M., Cohen, H., Chemodanov, A., Liberzon, A., and Golberg, A. (2020). Aeration and nitrogen modulated growth rate and chemical composition of green macroalgae Ulva sp. cultured in a photobioreactor. *Algal Res.* 47, 101808. doi: 10.1016/j.algal.2020.101808

Wu, H., Feng, J., Li, X., Zhao, C., Liu, Y., Yu, J., et al. (2019). Effects of increased CO2 and temperature on the physiological characteristics of the golden tide blooming macroalgae *Sargassum horneri* in the Yellow Sea, China. *Mar. pollut. Bull.* 146, 639–644. doi: 10.1016/j.marpolbul.2019.07.025

Xu, Z., Gao, G., Xu, J., and Wu, H. (2017). Physiological response of a golden tide alga (*Sargassum muticum*) to the interaction of ocean acidification and phosphorus enrichment. *Biogeosciences* 14, 671–681. doi: 10.5194/bg-14-671-2017

Xu, Z. G., Zou, D. H., and Gao, K. S. (2010). Effects of elevated CO_2 and phosphorus supply on growth, photosynthesis and nutrient uptake in the marine macroalga *Gracilaria lemaneiformis* (Rhodophyta). *Botanica Marina* 53, 123–129. doi: 10.1515/BOT.2010.012

Xue, J., Pang, T., and Liu, J. (2022). Changes in the temperature tolerance profile of *Gracilariopsis lemaneiformis* from the perspective of photosynthesis, respiration, and biochemical markers after many years of vegetative propagation. *J. Appl. Phycol.* 34, 1045–1058. doi: 10.1007/s10811-022-02687-1

Yang, Y., Li, W., Li, Y., and Xu, N. (2021). Photophysiological responses of the marine macroalga *Gracilariopsis lemaneiformis* to ocean acidification and warming. *Mar. Environ. Res.* 163, 105204. doi: 10.1016/j.marenvres.2020.105204

Ye, C. P., Zhang, M. C., Zhao, J. G., Yang, Y. F., and Zuo, Y. (2013). Photosynthetic response of the macroalga, *Gracilaria lemaneiformis* (Rhodophyta), to various N and P levels at different temperatures. *Int. Rev. hydrobiol.* 98, 245–252. doi: 10.1002/iroh.201301435

Zeng, J., Wu, X., Liao, X., Yang, S., Huang, M., and Tang, X. (2020). Effect of temperature on the uptake capacities of five large seaweeds for nitrogen and phosphorus. *Chin. Fish Qual Standards* 10, 31–37.

Zhang, D., Beer, S., Li, H., and Gao, K. (2020a). Photosystems I and II in *Ulva lactuca* are well protected from high incident sunlight. *Algal Res.* 52, 102094. doi: 10.1016/j.algal.2020.102094

Zhang, D., Xu, J., Bao, M., Yan, D., Beer, S., Beardall, J., et al. (2020b). Elevated CO_2 concentration alleviates UVR-induced inhibition of photosynthetic light reactions and growth in an intertidal red macroalga. *J. Photochem. Photobiol. B: Biol.* 213, 112074. doi: 10.1016/j.jphotobiol.2020.112074

Zhou, W., Wu, H., Huang, J., Wang, J., Zhen, W., Wang, J., et al. (2022). Elevated-CO_2 and nutrient limitation synergistically reduce the growth and photosynthetic performances of a commercial macroalga *Gracilariopsis lemaneiformis*. *Aquaculture* 550, 737878. doi: 10.1016/j.aquaculture.2021.737878

Zhou, W., Wu, H., Shi, M., Chen, Z., Wang, J., and Xu, J. (2024). Phosphorus deficiency regulates the growth and photophysiology responses of an economic macroalga *Gracilariopsis lemaneiformis* to ocean acidification and warming. *J. Appl. Phycol.* 36, 1–14. doi: 10.1007/s10811-024-03187-0

frontiers | Frontiers in Marine Science

TYPE Original Research
PUBLISHED 23 August 2024
DOI 10.3389/fmars.2024.1423595

OPEN ACCESS

EDITED BY
Thomas Wernberg,
University of Western Australia, Australia

REVIEWED BY
Jinlin Liu,
Tongji University, China
Kathryn Schoenrock,
University of Galway, Ireland

*CORRESPONDENCE
Imogen Bunting
imogen.bunting@vuw.ac.nz

RECEIVED 26 April 2024
ACCEPTED 29 July 2024
PUBLISHED 23 August 2024

CITATION
Bunting I, Kok YY, Krieger EC, Bury SJ, D'Archino R and Cornwall CE (2024) Marine heatwave intensity and duration negatively affect growth in young sporophytes of the giant kelp *Macrocystis pyrifera*. *Front. Mar. Sci.* 11:1423595. doi: 10.3389/fmars.2024.1423595

Marine heatwave intensity and duration negatively affect growth in young sporophytes of the giant kelp *Macrocystis pyrifera*

Imogen Bunting[1]*, Yun Yi Kok[2], Erik C. Krieger[1,3], Sarah J. Bury[2], Roberta D'Archino[2] and Christopher E. Cornwall[1]

[1]School of Biological Sciences, and Coastal People Southern Skies Centre of Research Excellence, Victoria University of Wellington Te Herenga Waka, Wellington, New Zealand, [2]Oceans Science Centre, National Institute of Water and Atmosphere Research Taihoro Nukurangi, Evans Bay, Wellington, New Zealand, [3]Red Sea Research Centre, King Abdullah University of Science and Technology, Thuwal, Saudi Arabia

Kelp forests are productive and biodiverse ecosystems with high ecological, cultural, and economic importance. However, the high sensitivity of kelp to water temperature means that these ecosystems are vulnerable to marine heatwaves (MHWs), especially at the equatorward edge of their range. To date, few laboratory studies have compared the effects of MHWs of different durations or intensities on kelp, and it is difficult to determine these effects from naturally occurring MHWs in the field. We exposed juvenile sporophytes of the giant kelp *Macrocystis pyrifera* from Wellington, Aotearoa New Zealand to simulated MHWs three or six weeks in duration, at temperatures of 18°C, 20°C, and 22°C, corresponding to 2, 4, and 6°C above local mean summer temperatures. While all MHW treatments reduced mean kelp growth rates by over 30% relative to 16°C controls, the 22°C treatments had much more severe and wide-ranging effects, including rapid blade erosion, reduced chlorophyll fluorescence, tissue bleaching, increased $\delta^{13}C$ values, and mortality. Nonetheless, sporophytes had some ability to recover from heat stress; within the 18°C treatment, mean relative growth rates neared or exceeded those within the control treatment within three weeks after MHWs concluded. These results support the findings of previous studies which indicate that *M. pyrifera* sporophytes experience a key physiological tipping point around 20°C. Additionally, our findings suggest that juvenile *M. pyrifera* from the Wellington population could be relatively resilient to MHWs if temperatures remain at sub-lethal levels. However, if average MHW intensities and durations continue to increase over time, survival and recruitment of juvenile kelp could be adversely affected, thus threatening the long-term persistence of giant kelp forests near the warm edge of their range in New Zealand.

KEYWORDS

kelp, climate change, marine heatwaves, macroalgae, thermal stress, resilience

Abbreviations: CCM, Carbon dioxide concentrating mechanism; DIC, Dissolved inorganic carbon; DMSO, Dimethyl sulfoxide; MHW, Marine heatwave; RGR, Relative growth rate; TA, Total alkalinity; $\delta^{13}C$ Ratio of ^{13}C to ^{12}C, expressed in ‰ units; $\delta^{15}N$ Ratio of ^{15}N to ^{14}N, expressed in ‰ units.

1 Introduction

Kelp forests are highly productive and biodiverse temperate marine ecosystems which occupy around a quarter of the world's coastlines (Wernberg et al., 2019). Kelps are ecosystem engineers that modify their physical environment through shading (Arkema et al., 2009) and alteration of current velocities (Gaylord et al., 2007), as well as altering their chemical environment by increasing oxygen concentrations and pH (Britton et al., 2016; Traiger et al., 2022). Kelp sporophytes create complex three-dimensional structures that serve as an important habitat for highly diverse biotic assemblages (Teagle et al., 2017), especially of sessile invertebrates (Graham, 2004; Arkema et al., 2009; Miller et al., 2015) and fish (Villegas et al., 2019). The loss of kelp canopies can cause severe declines in biomass and diversity within these communities, including the complete loss of commercially important species such as abalone (Graham, 2004; Vanella et al., 2007; O'Connor and Anderson, 2010; Johnson et al., 2011; Arafeh-Dalmau et al., 2019). Moreover, kelp forests contribute to many ecosystem services, including carbon sequestration (Filbee-Dexter and Wernberg, 2020), nutrient cycling (Wernberg et al., 2019), and reduction of coastal erosion (Løvås and Tørum, 2001). Kelp also holds cultural value and serves as food for some communities, and has a broad variety of commercial uses, including biofuel and production of pharmaceuticals (Wernberg et al., 2019; Li et al., 2023). The economic value of the ecosystem services provided by kelp forests globally is estimated to be as high as US$500 billion (Eger et al., 2023).

Anthropogenic stressors currently threaten the persistence of kelp forests and the biotic communities that they support. Kelps and other macroalgae are thought to be particularly susceptible to the impacts of ocean warming, as their large surface area to volume ratio makes them highly responsive to changes in environmental conditions (Smale, 2020). In kelps, thermal stress can cause thinning of cellular structures, leading to reduced tissue strength and rapid erosion (Simonson et al., 2015). Declines in abundance and range shifts or contractions have been reported for numerous kelp species within the past decade (Straub et al., 2016; Smale, 2020), and the total extent of kelp forests is declining at a global scale (Krumhansl et al., 2016). Climate change is thought to be one of the key drivers of these changes, along with pollution and overgrazing due to overexploitation of predators that consume grazers (Steneck et al., 2002; Wernberg et al., 2019). Climate change can also have indirect negative impacts on kelp, such as promoting range expansion by herbivores (Ling et al., 2009; Vergés et al., 2014; Provost et al., 2017) and increased competition between cold-temperate kelps and eurythermal algae (Filbee-Dexter and Wernberg, 2018) or heat-tolerant invasive kelps (Edwards and Hernández-Carmona, 2005; Smale et al., 2015; James and Shears, 2016; Lebrun et al., 2022; Wright et al., 2022).

The increasing frequency of marine heatwaves (MHWs) is an important consequence of climate change that threatens kelp forest ecosystems (Wernberg et al., 2023). MHWs are defined as anomalously warm events in which sea surface temperatures within a specified area exceed the 90th percentile, based on 30 years of historical baseline data, for at least five days (Hobday et al., 2016). They are often driven by interactions between local weather and oceanographic conditions and increasing greenhouse gas emissions (Salinger et al., 2019; de Burgh-Day et al., 2022; Kerry et al., 2022). The increasing frequency of MHWs means that local sea temperatures may exceed lethal thresholds for some species much earlier than predicted by some models of future climate scenarios that simply assess means changes in temperature (Harvey et al., 2022). MHWs have been linked to severe declines in kelp canopy cover (Wernberg et al., 2016, 2018; McPherson et al., 2021; Tolimieri et al., 2023) and regime shifts from kelp forests to less productive, turf algae-dominated ecosystems (Wernberg et al., 2016). More broadly, MHWs can cause local extinctions of sensitive macroalgal species (Smale and Wernberg, 2013; Thomsen et al., 2019).

The giant kelp *Macrocystis pyrifera* is an abundant and ecologically vital species, but its potential vulnerability to climate change and MHWs is concerning. *M. pyrifera* is the world's most widely distributed kelp species and is spread throughout temperate coastal regions of the Pacific basin, including the west coast of the Americas, southeastern Australia, and central and southern Aotearoa New Zealand (Mora-Soto et al., 2020). *M. pyrifera* is also the world's largest kelp species, reaching lengths of up to 60 meters (Schiel and Foster, 2015). MHWs and other extreme warming events have been linked to declines in *M. pyrifera* canopy cover (Dayton et al., 1992; Arafeh-Dalmau et al., 2019; Tait et al., 2021; Tolimieri et al., 2023). Laboratory studies have found that exposure to elevated temperatures can have a variety of adverse impacts on both microscopic stages (gametophytes) and diploid, macroscopic sporophytes of *M. pyrifera*, with gametophytes often having greater thermal resilience than sporophytes (Ladah, 2000; Hollarsmith et al., 2020; Le et al., 2024). The effects of increased temperatures can include increased mortality (e.g., Ladah and Zertuche-González, 2007; Fernández et al., 2020; Purcell et al., 2024), reduced reproductive success (Muth et al., 2019; Hollarsmith et al., 2020; Le et al., 2022; Fernández et al., 2023), lower growth rates (Brown et al., 2014; Fernández et al., 2020, 2021), photosynthetic impairment (Umanzor et al., 2021), and reduced pigmentation (Sánchez-Barredo et al., 2020; Umanzor et al., 2021). Increasing the duration of exposure to elevated temperatures can also increase the severity of these negative effects on kelps (Leathers et al., 2023).

M. pyrifera grows throughout the South Island and at the southern tip of the North Island of New Zealand, with its range limited mostly by temperature (Hay, 1990). Three genetic clusters have been identified for *M. pyrifera* diversity within New Zealand; gametophytes from the northernmost populations have a higher temperature threshold for successful fertilisation than those from southern regions, perhaps indicating higher thermal tolerance (Le, 2022). MHWs have become increasingly severe within New Zealand waters during the past three decades (Montie et al., 2023). Modelling suggests that mean MHW intensities could increase by up to 1.75°C by 2100 under a high greenhouse gas emissions scenario (SSP3–7.0) (Behrens et al., 2022). MHWs have been

linked to declines in *M. pyrifera* canopy cover throughout New Zealand (Tait et al., 2021), and there is anecdotal evidence of losses of *M. pyrifera* abundance throughout the Wellington region (authors, pers. obs), near the northern distribution limit described by Hay (1990). *M. pyrifera* abundance is predicted to decline near the northern edge of its distribution in New Zealand in the near future due to ongoing warming and MHWs (Cornwall et al., 2023).

Field studies of the impacts on MHWs on macroalgae must rely on naturally occurring events and cannot easily separate the effects of MHWs from other environmental stressors, nor determine the relative importance of MHW duration and intensity, thus limiting our ability to use past events to forecast future change. Manipulative experiments which simulate the impacts of MHWs are a useful tool to predict how wild populations might respond to MHWs of a specified duration or intensity. Previous laboratory studies on the effects of simulated MHWs on *M. pyrifera* sporophytes have typically focused on relatively short, intense heatwaves (up to 7 days, with temperature increases of 6–8°C relative to local mean temperatures), which led to severe reductions in growth and photosynthetic performance (see Sánchez-Barredo et al., 2020; Umanzor et al., 2021). In this study, we used a laboratory experiment to simulate longer heatwave periods (21 or 42 days) at several different temperatures (ranging from 2–6°C above local summer mean temperatures) to assess the impacts of heatwave duration and intensity on juvenile *M. pyrifera* sporophytes. Our aim was to investigate how *M. pyrifera* populations near their warm distribution limit in New Zealand might respond to a broad range of present-day and future MHW scenarios. We hypothesised that the severity of any negative physiological impacts of the heatwave would be positively correlated with both the temperature and duration of the heatwave.

2 Materials and methods

2.1 Spore collection and culture

Macrocystis pyrifera sori were collected by snorkelling at low tide, at depths of 1–2 meters, at Kau Bay in Wellington Harbour (41.29°S, 174.83°E) in the North Island of New Zealand in July 2022. Sori from several individuals were kept chilled and taken immediately to the National Institute of Water and Atmosphere Research's (NIWA) experimental facility. These sori were rinsed with freshwater and patted dry, then refrigerated overnight at 4°C. The next day, sori were cut into 1–2 cm^2 fragments, then immersed in F/2 nutrient-enriched filtered seawater (Guillard, 1975; AusAqua, Wallaroo, South Australia) for about an hour to stimulate spore release. The seawater slurry containing spores was then poured over sheets of plastic mesh immersed in 400 mL glass jars. This mesh was left undisturbed at 15°C for a few days to allow the spores to settle.

After settlement, the mesh sheets were transferred to tanks in a temperature-controlled room set at 15°C. Light panels provided steady illumination of around 30 µmol photons m^{-2} s^{-1} during a 12-hour photoperiod, giving a total daily dose of 1.3 mol photons m^{-2}. Seawater was sterilised using a 30 W UV steriliser (Trevoli, Auckland, New Zealand) and recirculated in a 295 L capacity system, which included a 250 L sump and seaweed growth tanks with an internal volume of 45 L. Water temperature was maintained using a 500 W drop-in aquarium element (EHEIM, Deizisau, Germany) located in the sump, which was controlled by a CN74 temperature controller (Omega Engineering, Norwalk, Connecticut, USA) and an electronic relay coupled to a PT100 temperature probe (Omega Engineering, Norwalk, Connecticut, USA), also located in the sump. Tank temperature was monitored using HOBO Pendant MX Data Loggers (Onset, Bourne, Massachusetts, USA).

Sporophytes with a blade length of at least 20 mm were removed from their original mesh sheets and re-attached to separate pieces of mesh. Sinkers were tied to these mesh parcels to keep the sporophytes submerged. The sporophytes were left for two weeks to re-attach and were then transferred to the experimental tanks at Victoria University of Wellington Coastal Ecology Laboratory on 4 October 2022.

2.2 Experimental conditions

The experimental setup consisted of eight 70 L (250 × 470 × 610 mm) water baths, each connected to a separate header tank. Each water bath contained four separate 4 L (155 × 235 × 105 mm) experimental tanks. Seawater was pumped continuously into the header tanks from the nearby Taputeranga Marine Reserve, on the south coast of Wellington. To stabilise pH, air was bubbled constantly through the header tanks via air stones (Aqua One, Ingleburn, Australia) connected to an LP-100 aerator pump (Resun, Shenzhen, China). Seawater flowed from the headers into the experimental tanks, then out into the water baths, at a rate of approximately 120 mL per minute. Each tank contained a 2 W, 150 L h^{-1} HL-BT100B immersible pump (Hailea, Guangdong, China) to maintain water motion. Tanks were scrubbed weekly to remove epiphytic algae.

The tanks were illuminated on a daily 12:12 light/dark cycle, with customised Zeus 70 LED panels (Ledzeal, Shenzhen, China). These turned on at 08:00, increased steadily in intensity to a peak at 13:00 of around 65 µmol m^{-2} s^{-1} of photons of photosynthetically active radiation (PAR), remained at that peak value for two hours, then steadily decreased in intensity until they turned off at 20:00. The LED panels predominantly emitted light in the blue and green regions of the visible light spectrum, to mimic the light spectrum available in subtidal habitats approximately 2 m deep along Wellington's south coast (see Krieger et al., 2023a). The tanks received a total daily irradiance dose of approximately 1.6 mol m^{-2} d^{-1}. The water baths were surrounded by a mesh curtain to limit exposure to external light sources.

Apex temperature probes (Neptune Systems, Morgan Hill, California, USA) were placed in one tank within each water bath. Probes were calibrated weekly against a reference thermometer (FisherBrand, Waltham, Massachusetts, USA). The temperature probes were connected via an Apex Classic programmable control unit (Neptune Systems, Morgan Hill, California, USA) to 300 W submersible heaters (Weipro, Zhongshan, China) within the water baths, and to Hailea 300A 1/4HP external chillers (Hailea,

Guangdong, China) connected to the header tanks. Heaters or chillers were automatically switched on if the temperature in the tanks exceeded 0.1°C below or 0.2°C above the target temperature.

To ensure consistency, temperature and pH were measured weekly in the experimental tanks, water baths, and header tanks. Temperature was measured using a Fisherbrand Traceable Kangaroo Thermometer (FisherBrand, Waltham, Massachusetts, USA) and pH was determined potentiometrically using an IntelliCAL PHC101 glass electrode (Hach New Zealand, Auckland, New Zealand). This electrode was calibrated weekly against artificial seawater with Tris buffer added (Dickson et al., 2007). The R package "seacarb" (Gattuso et al., 2021) was used to convert the tank pH readings from millivolts to the total scale. Water samples for nitrogen analysis were collected at two-week intervals during the heatwave period, using methods derived from Pritchard et al. (2015). Samples were taken using a 50 mL syringe and passed through a 0.45 µm filter into a labelled 50 mL plastic storage vial, then frozen at −20°C. A separate syringe and filter were used for each sample. The seawater samples were later analysed at the University of Otago's Portobello Marine Laboratory. A Lachat QuikChem 8500 Series 2 FIA auto analyser (Hach New Zealand, Auckland, New Zealand) was used to calculate the concentrations of NO_x ions and ammonia using methods derived from Strickland and Parsons (1972).

Two sporophytes were allocated to each experimental tank, giving a total of eight for each experimental treatment and 16 controls. The largest and smallest individuals were apportioned as evenly as possible between treatments. Sporophytes were scrubbed gently with a toothbrush once a week to remove epiphytic algae and dead tissue. Sporophytes were marked as dead if the blade completely eroded or detached from the meristem. The initial lengths of the sporophytes ranged from 20 to 95 mm, with an arithmetic mean value of 50.5 ± 2.2 mm (mean ± standard error).

2.3 Heatwave simulations

Initially, all tanks were kept at a stable temperature of 16°C for three weeks to allow the sporophytes to acclimate to laboratory conditions. The 16°C treatment was chosen to approximate the historical mean summer (i.e., December to February) sea surface temperature throughout the Wellington region (Booth, 1975; Krieger et al., 2023b; Supplementary Figure S1). Six different heatwave scenarios were simulated. Three of the water baths were subjected to three-week heatwaves, at temperatures of 18°C, 20°C, and 22°C respectively. Another three water baths were subjected to six-week heatwaves at the same temperatures. The remaining two water baths were kept at 16°C to act as controls. The experimental treatments were interspersed systematically to minimise the impact of any non-treatment effects (i.e., A-3 from Hurlbert, 1984). At the start of the simulated heatwaves, temperatures were increased by increments of 2°C day^{-1}, after Sánchez-Barredo et al. (2020) and Umanzor et al. (2021), in order to simulate a rapid onset MHW; temperatures were then lowered by 2°C daily increments at the end of each heatwave period. After the three-week heatwave period, the sporophytes were left in the tanks for another three weeks to examine whether they showed signs of recovery.

To compare the experimental scenarios to real-world MHWs, daily sea surface temperature data for the greater Wellington region were obtained from the National Oceanic and Atmospheric Administration's "Optimum Interpolation Sea Surface Temperature V2.1" dataset (Reynolds and Banzon, 2008). A baseline seasonal climatology from 1982 to 2011 was constructed for the greater Wellington region using the R package "heatwaveR" (Schlegel and Smit, 2021) to detect and analyse MHWs that occurred within the region between 1982 and 2023. These data are summarised in the Supplementary Material (Supplementary Figures S1–S3). Throughout the last three decades, there has been an average of 3.2 MHW events per year throughout the greater Wellington region, with a mean duration of 16 days and a mean temperature anomaly of 1.27°C (Supplementary Figures S1–S3). The 18°C treatment, or a temperature anomaly of approximately 2°C, is most similar to the mean temperatures during previous summer MHW events within the Wellington region (Supplementary Figures S1, S2). The 20°C treatment is more representative of maximum temperature anomalies of 3–4°C during more recent, strong heatwaves (Supplementary Figures S1, S2). The 22°C treatment, corresponding to a 6°C temperature anomaly, represents a worst-case scenario that has not yet occurred in this region, but could become more plausible under the most severe greenhouse gas emissions scenarios modelled by Behrens et al. (2022). Numerous MHWs within the Wellington region have lasted longer than three weeks, while a few events have surpassed six weeks (Supplementary Figure S3).

2.4 Kelp performance

2.4.1 Growth

Sporophyte length measurements were taken weekly during the acclimation and experimental phases. Length was measured to the nearest millimetre using a ruler, from the base of the blade to the apex. Relative growth rates (RGR; Kain and Jones, 1976) were calculated on a week-to-week basis, and for the duration of the acclimation and heatwave phases.

2.4.2 Chlorophyll fluorescence

Chlorophyll fluorescence was measured the day before the heatwaves began, and on the days that the three- and six-week heatwaves ended, using a Diving-PAM blue light fluorometer (Walz, Effeltrich, Germany). The effective quantum efficiency of photosystem II electron transport ($F_{v'}/F_{m'}$) was calculated by measuring the ratio of variable fluorescence to maximum fluorescence in the low-light adapted state. The fluorometer was held near the base of the blade to ensure consistent assessment of the youngest tissue.

2.4.3 Dissolved inorganic carbon uptake

Incubations were carried out during weeks two and five of the heatwave period. Four sporophytes from each heatwave treatment

and eight from the control treatment were assessed; one individual was chosen at random from each experimental tank. For each incubation, a 500 mL transparent plastic incubation chamber was filled with water from an experimental tank, then one of the sporophytes from that tank was placed into the chamber. A stirrer bar was placed in the chamber's lid, separated from the sporophyte by a mesh grid. The chamber was then sealed underwater to minimise the intrusion of air bubbles. The pH within the tank was measured in millivolts using an IntelliCAL PHC101 glass pH electrode (Hach New Zealand, Auckland, New Zealand), and its temperature was recorded in °C using a Fisherbrand Kangaroo Traceable Thermometer (FisherBrand, Waltham, Massachusetts, USA). The chamber was then placed upside-down on a 2mag MIXdrive 6 magnetic stirrer plate (2mag AG, Munich, Germany) set to 200 revolutions per minute, within a water bath set to the same temperature as the experimental tank, under illumination of 70 µmol photons m^{-2} s^{-1}. After half an hour, the chamber was taken out and the temperature and mV of the water in the chamber were measured. The R package "seacarb" (Gattuso et al., 2021) was later used to convert the pH readings to the total scale using mV calibration in Tris buffer, following Dickson et al. (2007).

A 150 mL water sample was taken from one of the header tanks on each day that incubations were carried out, and salinity was measured within that tank using an IntelliCAL CDC401 conductivity probe (Hach New Zealand, Auckland, New Zealand). These water samples were filtered through 0.45 µm glass microfiber discs (Whatman, Chalfont St. Giles, UK) and refrigerated in airtight containers, then total alkalinity (TA) was determined through titration and addition of 0.1 mol m^{-3} hydrochloric acid, according to the methodology described in Huang et al. (2012), using an AS-ALK2 titrator (Apollo SciTech, Newark, Delaware, USA). Titrations were carried out on at least three 25 mL subsamples from each water sample. During each titration, the weight of water used was measured, and the R package "seacarb" (Gattuso et al., 2021) was used to account for the mass and salinity of the water sample and to increase the accuracy of the calculated TA value. To assess the accuracy of these results, titrations were also regularly carried out on Certified Reference Material (University of California, San Diego, California, USA) with a known TA value; the final calculated TA values for the reference material remained within 95% confidence intervals.

The temperature, pH, and TA data were used to estimate the change in total dissolved inorganic carbon (DIC) during each incubation, using the CO2SYS Microsoft Office Excel program (Pierrot et al., 2011). DIC uptake rates were then standardised against the surface area of the sporophytes. This was estimated by taking a photograph of each sporophyte with a 1 cm grid in the background and counting the number of grid squares fully or partially covered by each specimen.

2.4.4 Pigment content

After three weeks in heatwave conditions, tissue sub-samples were taken from half of the sporophytes in the control and three-week heatwave treatments. Four individuals were sampled from each heatwave treatment, as well as eight from the control. Sub-samples were not taken from the sporophytes on which incubations were carried out, to avoid placing additional stress on these individuals. One small sporophyte was sacrificed at this timepoint; the other sporophytes were returned to their tanks. After the six-week heatwave ended, all surviving sporophytes were sampled. Sub-samples were taken using a scalpel blade, which was rinsed with ethanol between sampling to prevent cross-contamination. These sub-samples were patted dry, then sealed in Eppendorf tubes, which were wrapped in aluminium foil and frozen at −20°C.

Chlorophyll *a*, chlorophyll *c*, and fucoxanthin were extracted from these tissue samples using methods adapted from Seely et al. (1972). Each sub-sample was patted dry, and around 0.05 g of tissue was weighed out, then subsequently crushed in a mortar and pestle with a known volume of dimethyl sulfoxide (DMSO). More DMSO was used to wash the ground algal tissue into a 1.5 mL Eppendorf tube, which was put on ice for at least 10 minutes, then centrifuged at 13200 RPM for 10 minutes in a 5145 D centrifuge (Eppendorf, Hamburg, Germany). After centrifuging, the supernatant was transferred to a quartz cuvette (Starna Scientific, Hainault, UK). More DMSO was added to fill the cuvette if necessary; the total volume of DMSO used was in proportion to the mass of tissue used, and did not exceed 1.5 mL per sample. A UV-1900i spectrophotometer (Shimadzu, Kyoto, Japan) was used to measure the absorbance of each sample between 400 and 700 nm and to generate a spectrogram. Before running the algal samples, a "blank" cuvette containing DMSO only was run to correct for the absorbance of DMSO alone. Cuvettes were rinsed with DMSO between samples to avoid cross-contamination.

Acetone was then added to the pellets. The volume of acetone added to each sample was equal to the volume of DMSO used for the same sample. The Eppendorf tubes were shaken for 1 minute, then left on ice. After 1.5–3 hours, the Eppendorf tubes were centrifuged at 13200 rpm for 10 minutes. The supernatant was then transferred to a quartz cuvette, and spectrophotometry was carried out. Another "blank" sample was run to account for the absorbance of acetone, and cuvettes were rinsed with acetone between samples. Peak and trough values from the spectrograms were used to calculate the amount of chlorophyll *a* (Equation 1), chlorophyll *c* (Equation 2), and fucoxanthin (Equation 3) per gram of tissue in each sample.

Equation 1:

$$\text{Chlorophyll } a = \frac{\left(\frac{P_{1A}}{72.8} + \frac{P_{1D}}{73.6}\right) \times V}{m} \quad (1)$$

Equation 2:

$$\text{Chlorophyll } c = \frac{\left(\frac{T_{1D}+T_{2D}-0.297\times P_{1D}}{61.8} + \frac{T_{1A}+T_{2A}-0.3\times P_{1A}}{62.2}\right) \times V}{m} \quad (2)$$

Equation 3:

$$\text{Fucoxanthin} = \frac{\left(\frac{P_{2D}-0.722(T_{1D}+T_{2D}-0.297\times P_{1D})+0.049\times P_{1D}}{130} + \frac{P_{2A}-1.239(T_{1A}+T_{2A}-0.3\times P_{1A})+0.027\times P_{1A}}{141}\right) \times V}{m} \quad (3)$$

Where m is the wet weight of the tissue sample in grams, V is the total volume of DMSO or acetone used in litres, P_1 is the maximum absorbance value at the long-wavelength peak of the

spectrograph (around 660 nm) in DMSO (P_{1D}) or acetone (P_{1A}), P_2 is the maximum absorbance value at the short-wavelength peak (around 450 nm), T_1 is the minimum absorbance value at the trough nearest the long-wavelength peak, and T_2 is the minimum absorbance value at the trough nearest the short-wavelength peak.

2.4.5 Total % carbon, % nitrogen, and stable isotope values

Tissue samples were collected for stable isotope analysis from all surviving sporophytes after the conclusion of the six-week experimental period. These samples were wrapped in aluminium foil and left overnight in an Isotherm convection oven (Esco Lifesciences Group, Singapore) at 75°C. The dried samples were then homogenised by grinding into powder with a mortar and pestle, and were then sealed in Eppendorf tubes. The mortar and pestle were rinsed with water and dried between samples to avoid cross-contamination. Six additional sporophytes were sampled from the culture facility at NIWA to obtain baseline values and evaluate whether the different seawater sources utilised by NIWA and the Coastal Ecology Laboratory could have contributed to any differences in stable isotope ratios.

Stable isotope analyses were carried out at the NIWA Environmental and Ecological Stable Isotope Analytical Facility in Wellington. Dried algal samples were weighed to the nearest microgram. Samples were analysed for total carbon content (%), total nitrogen content (%), $\delta^{13}C$, and $\delta^{15}N$ values using a DELTA V Plus continuous flow isotope ratio mass spectrometer, linked to a Flash 2000 elemental analyser using a MAS200R autosampler (Thermo Fisher Scientific, Bremen, Germany). International reference materials were used to normalise the stable isotope values, after Paul et al. (2007). Sample $\delta^{15}N$ values were two-point normalised using stable isotope data from the daily analysis of National Institute of Standards and Technology (NIST)8573 USGS40 L-glutamic acid and NIST8548 International Atomic Energy Agency (IAEA)-N2 ammonium sulfate. Sample $\delta^{13}C$ values were two-point normalised using stable isotope data from the daily analysis of NIST8573 USGS40 L-Glutamic acid and USGS74 L-Valine #2. Data from the daily analysis of the following materials were used to check accuracy and precision: USGS65 Glycine (values of both $\delta^{15}N$ and $\delta^{13}C$) and L-Valine #2 USGS74 (value of $\delta^{15}N$ only). Precision was determined by the repeat analysis of a working laboratory standard DL-Leucine (DL-2-Amino-4-methylpentanoic acid, C6H13NO2, Lot 127H1084, Sigma, Australia). Repeat analysis of international reference standards produced data accurate to within 0.5% for % carbon and % nitrogen, and 0.2 ‰ for $\delta^{13}C$ and $\delta^{15}N$ values; and a precision of better than 0.2% for % carbon and % nitrogen, and 0.1 ‰ for $\delta^{13}C$ and $\delta^{15}N$ values.

2.5 Statistical analysis

The Shapiro-Wilk test (Shapiro and Wilk, 1965) was used to determine that the datasets from this experiment were normally distributed. The R package "lme4" (Bates et al., 2023) was then used to fit linear mixed-effects models to the data for growth rates, $F_{v'}/F_{m'}$, DIC uptake, pigment content, total % carbon and nitrogen, and $\delta^{15}N$ and $\delta^{13}C$ values. Temperature and heatwave duration were treated as fixed effects, while water bath was treated as a random effect. Only the effects of temperature were assessed for the data collected during the first three-week heatwave phase. The effects of temperature, duration, and their interaction were assessed for the data collected during the latter phase of the experiment, when the three-week heatwaves had concluded while the six-week heatwaves continued. Analysis of Variance (ANOVA) was then run on these models, and p-values were generated using the R package "car" (Fox et al., 2023). The R package "multcomp" (Hothorn et al., 2023) was used to run pairwise Tukey's tests (Tukey, 1949) on the models to assess significant differences between individual treatments.

3 Results

Raw experimental data is accessible in the Supplementary Material ("Supplementary Data", Sheet 1–5). Temperature, pH, and nitrogen availability data are available in the Supplementary Material ("Supplementary Figures and Tables", Supplementary Tables S1, S2).

3.1 Survival and physical appearance

By the third week in heatwave conditions, several of the sporophytes within the 22°C treatments were visibly bleached, and their blades were eroding rapidly (Supplementary Material, Images S1A–D). Bleaching was also visible after five weeks at 20°C. Five sporophytes died during the experiment. All deaths occurred in the 22°C treatments, during the second half of the heatwave period; two during week 4, and three during week 6. Four of the sporophytes within the 22°C, six-week heatwave treatment died in total, giving a mortality rate of 50%, while one sporophyte died within the 22°C, three-week treatment, with a mortality rate of 12.5%.2

3.2 Growth

There was no consistent variation in mean RGR between treatments during the acclimation period (Figure 1; $p = 0.847$). Heatwave temperature had a significant negative relationship with RGR during the three-week heatwave period (Figure 2; $p< 0.001$, Table 1). This effect was noticeable after just one week in heatwave conditions (Figure 1). By the end of the three-week heatwave, many of the sporophytes in heatwave conditions were eroding faster than they grew, including almost all of the sporophytes at 22°C. Mean RGR over the three-week heatwave period were 1.46 ± 0.28 in the control treatment, 0.17 ± 0.54 at 18°C, 0.50 ± 0.33 at 20°C, and −1.06 ± 0.23 at 22°C (mean ± SE) (Figure 2). The 22°C treatment was the only treatment with a significantly lower mean RGR than the control treatment over the three-week heatwave period ($p< 0.001$, Figure 2).

Heatwave temperature continued to have a significant negative effect on RGR during the last three weeks of the experimental period ($p< 0.001$, Table 1). Heatwave duration also had a significant effect on long-term RGR during this period ($p< 0.001$, Table 1), as the sporophytes which remained in heatwave conditions for six weeks

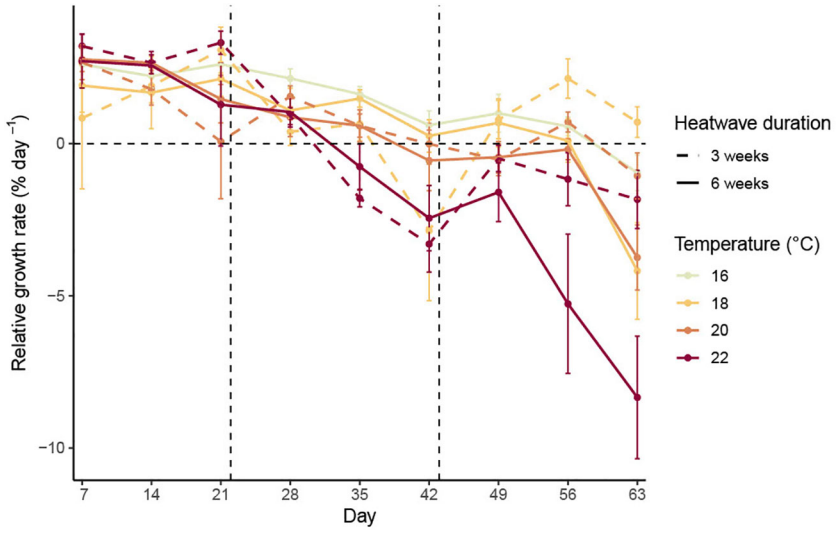

FIGURE 1
Mean relative growth rates (with standard error) of *Macrocystis pyrifera* sporophytes measured weekly over the experimental period.

continued to decline in length at a more rapid rate than those which were returned to 16°C after three weeks. The sporophytes returned to 16°C had some signs of recovery, with their mean RGR becoming more positive during weeks four and five (Figure 1; day 49–56). The sporophytes from the 18°C, three-week heatwave treatment had a particularly high mean RGR during this period (Figure 2). Conversely, many of the sporophytes that had been kept at 20°C and 22°C continued to erode, although less rapidly than those that remained in heatwave conditions (Figure 2). There was no evidence for an interactive effect of heatwave temperature and duration. Over the final three weeks of the experimental period, the sporophytes in the 22°C, six-week heatwave treatment had a significantly lower mean RGR than the control treatment (p = 0.001), as well as the three-week heatwave treatments at 18°C and 20°C (p< 0.001 and p = 0.029, respectively, Figure 2).

3.3 Chlorophyll fluorescence

Overall, there was little variation in mean F_v/F_m values between treatments, except for the 22°C heatwave treatment, which had a significantly lower mean (0.704 ± 0.012) than any of the other treatments after three weeks in heatwave conditions (p = 0.001, Figure 3). This difference decreased by the end of the six-week

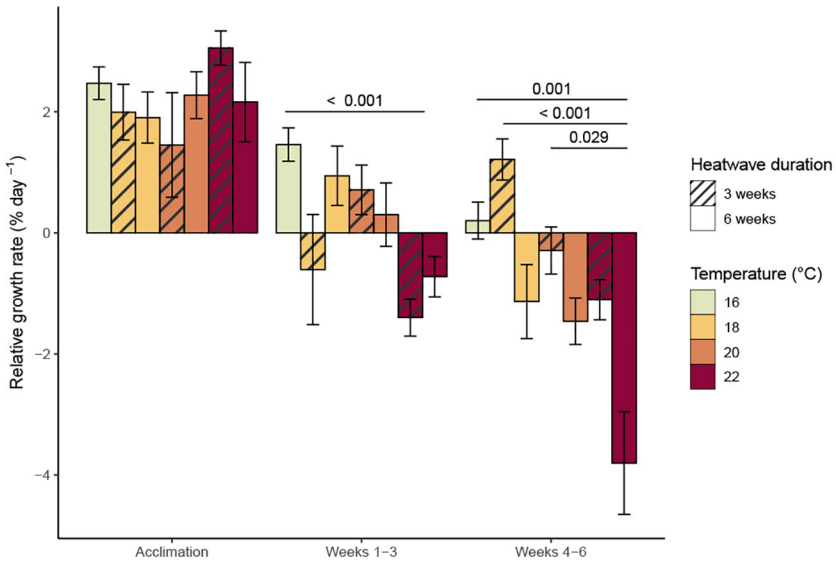

FIGURE 2
Mean relative growth rates (with standard error) of *Macrocystis pyrifera* sporophytes over each three-week experimental phase. Significant (p< 0.05) differences between treatments are indicated by bars, with p-values provided.

TABLE 1 Predicted effects of heatwave temperature, duration, and their interaction on *Macrocystis pyrifera* sporophyte relative growth rates (RGR), chlorophyll fluorescence (F_v/F_m), and pigment content, obtained by fitting linear mixed-effects models to the data collected during the heatwave experiment.

	Week 3		Week 6					
Response variable	*T (°C)*		*T (°C)*		*D*		*T:D*	
	Response	*p*-value	Response	*p*-value	Response	*p*-value	Response	*p*-value
RGR	**−0.361**	**0.001**	**−0.580**	**< 0.001**	**−0.992**	**< 0.001**	−0.052	0.879
F_v/F_m	**−0.005**	**0.004**	0.002	0.706	0.124	0.964	−0.006	0.259
Chlorophyll *a* (g kg^{-1} wet blade)	−0.008	0.465	**−0.048**	**0.020**	−0.866	0.129	0.042	0.094
Chlorophyll *c* (g kg^{-1} wet blade)	0.002	0.198	0.004	0.500	0.092	0.984	-0.005	0.427
Fucoxanthin (g kg^{-1} wet blade)	−0.012	0.337	−0.018	0.656	-0.620	0.570	0.031	0.136

RGR were calculated for each three-week experimental phase. Effects are expressed as the predicted change in each response variable resulting from a °C increase in temperature (T), the predicted difference in each response variable for the sporophytes exposed to a six-week heatwave relative to those exposed to a three-week heatwave (D), and the predicted effects of T and D in combination. Water bath was treated as a random effect. The p-values are provided and highlighted in grey, and statistically significant effects (p< 0.05) are indicated in **bold**.

heatwave; at that point, the mean F_v/F_m value of the surviving sporophytes in the 22°C, six-week treatment was 0.731 ± 0.010, which was noticeably, but not significantly, lower than the other treatments (Figure 3). Overall, temperature had a significant impact on F_v/F_m during the first three weeks of heatwave conditions (p = 0.004, Table 1), but not the latter half of the experiment (p = 0.706, Table 1).

3.4 Dissolved inorganic carbon uptake

DIC uptake rates were extremely variable within treatments; the sporophytes with the highest uptake rates tended to be those kept at 18°C and 20°C (Figure 4). Mean DIC uptake rates remained relatively stable between the heatwave and recovery periods in the 20°C and 22°C, three-week heatwave treatments. However, there was a noticeable, but non-significant, decline in mean DIC uptake rates within the 18°C, three-week treatment, from 2.50 ± 0.40 µmol hr^{-1} cm^{-2} during the heatwave to 1.99 ± 0.79 µmol hr^{-1} cm^{-2} during the recovery period. Conversely, mean DIC uptake rates increased non-significantly between week two and week five among the sporophytes subjected to six-week heatwaves (Figure 4). There was no relationship between temperature and DIC uptake (p = 0.642, Table 2); however, heatwave duration did have a significant impact on temperature, due to the increase in average DIC uptake rates within the heatwave treatments during the second half of the

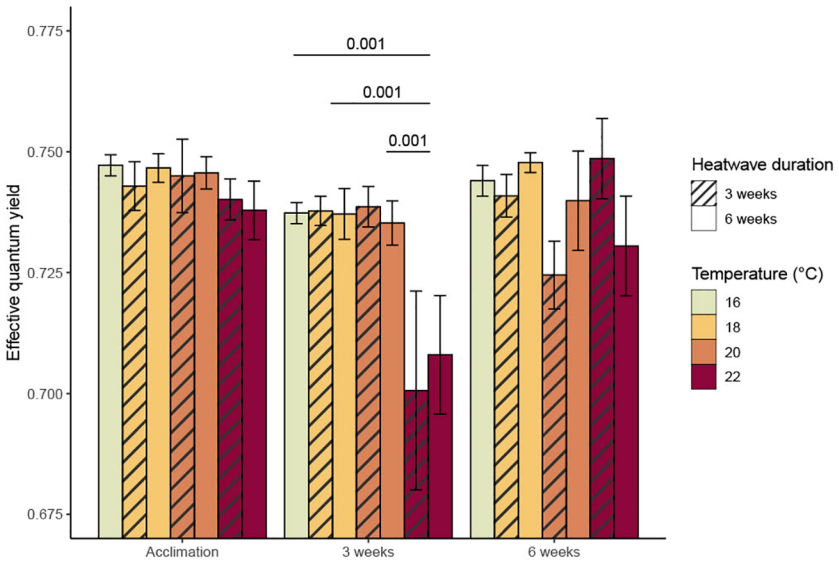

FIGURE 3
Mean effective quantum yield of photochemical energy conversion (F_v/F_m) (with standard error) of *Macrocystis pyrifera* sporophytes at the end of each experimental phase. Significant (p< 0.05) differences between treatments are indicated by bars, with p-values provided.

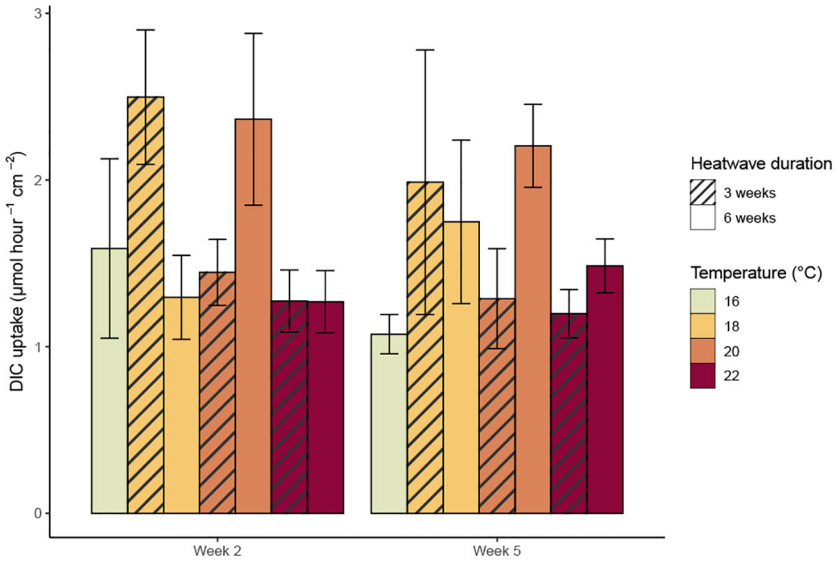

FIGURE 4
Mean dissolved inorganic carbon (DIC) uptake rates (with standard error) of *Macrocystis pyrifera* sporophytes at the mid-point of each heatwave phase.

six-week heatwave (p = 0.039, Table 2). There were no statistically significant differences between individual treatments.

3.5 Pigment content

After three weeks in heatwave conditions, the sporophytes kept at 22°C had relatively low mean chlorophyll *a* (0.123 ± 0.031 g kg^{-1}) and fucoxanthin (0.095 ± 0.025 g kg^{-1}) content when compared to the other temperature treatments (Figures 5A, C). Chlorophyll *a* and fucoxanthin content were also slightly lower (chlorophyll *a*: 0.173 ± 0.051 g kg^{-1}; fucoxanthin: 0.193 ± 0.027 g kg^{-1}) at 18°C and higher (chlorophyll *a*: 0.233 ± 0.010 g kg^{-1}; fucoxanthin: 0.252 ± 0.010 g kg^{-1}) at 20°C when compared to the control treatment (chlorophyll *a*: 0.204 ± 0.028 g kg^{-1}; fucoxanthin: 0.211 ± 0.027 g kg^{-1}). However, these differences were not statistically significant (Figures 5A, C; Table 1). Temperature had no effect on chlorophyll *c* content (Figure 5B; Table 1).

The mean pigment content of the tissue samples taken at week six was about twice as high as the week three samples. This trend was consistent across all treatments, including controls, and all three pigments analysed. The week six samples generally showed less variation in pigmentation between treatments when compared to the week three samples (Figures 5D–F). However, the sporophytes from the 18°C, three-week heatwave treatment had noticeably higher mean chlorophyll *a* (0.524 ± 0.028 g kg^{-1}) and fucoxanthin (0.443 ± 0.092 g kg^{-1}) content than the control treatment (chlorophyll *a*: 0.398 ± 0.026 g kg^{-1}; fucoxanthin: 0.353 ± 0.019 g kg^{-1}). The sporophytes from the 22°C treatments generally had low chlorophyll *a* content when compared to the other treatments, but this was not statistically significant. Overall, there was statistical support for a decrease in chlorophyll *a* content with increasing temperature at the six-week mark (p = 0.020, Table 1), but not at the three-week mark (p = 0.465, Table 1). No statistically significant relationships were found between heatwave temperature or duration and chlorophyll *c* or fucoxanthin content (Table 1).

3.6 Total % carbon, % nitrogen, and stable isotope values

There was a significant relationship between temperature and total % carbon content (p = 0.009, Table 3), with mean values of %

TABLE 2 Predicted effects of heatwave temperature, duration, and their interaction on dissolved inorganic carbon (DIC) uptake rates of *Macrocystis pyrifera* sporophytes, obtained by fitting linear mixed-effects models to the data collected during the heatwave experiment.

	Week 2		Week 5					
	T (°C)		*T* (°C)		*D*		*T:D*	
	Response	*p*-value	Response	*p*-value	Response	*p*-value	Response	*p*-value
DIC uptake (µmol hour^{-1} cm^{-2})	−0.047	0.642	−0.197	0.155	**2.301**	**0.039**	0.131	0.478

Effects are expressed as the predicted change in DIC uptake (µmol cm^{-2} hour^{-1}) resulting from a 1°C increase in temperature (T), the predicted difference in DIC uptake for the sporophytes exposed to a six-week heatwave relative to those exposed to a three-week heatwave (D), and the predicted effects of T and D in combination. Water bath was treated as a random effect. The p-values are provided and highlighted in grey, and statistically significant effects (p< 0.05) are indicated in **bold**.

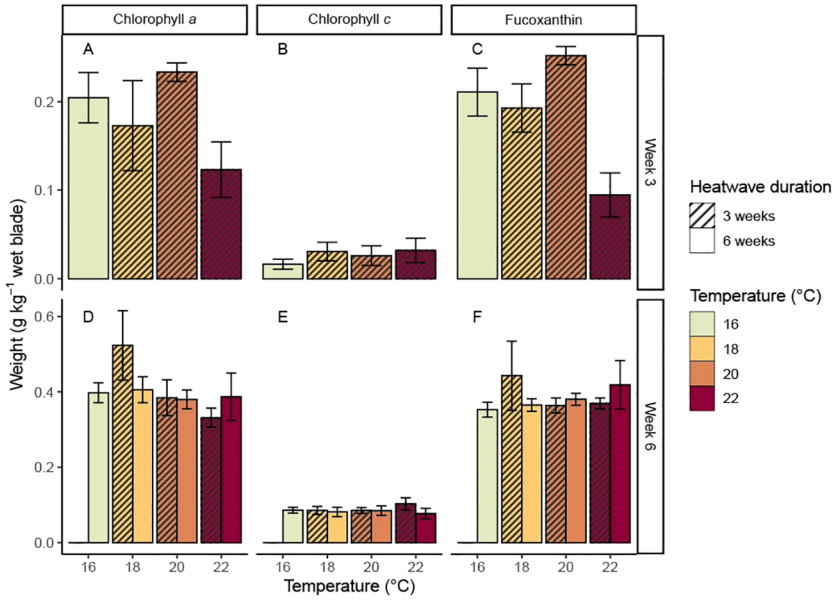

FIGURE 5
Mean concentrations of **(A)** chlorophyll a, **(B)** chlorophyll c, and **(C)** fucoxanthin (with standard error) in *Macrocystis pyrifera* blade tissue after three weeks in heatwave conditions, and mean concentrations of **(D)** chlorophyll a, **(E)** chlorophyll c, and **(F)** fucoxanthin (with standard error) in blade tissue at the end of the experiment.

carbon increasing consistently with temperature (Figure 6). The 20°C and 22°C, six-week treatments both had significantly higher mean % carbon values than the control treatment ($p = 0.031$ and $p < 0.001$, respectively). No significant relationship was found between temperature and % nitrogen content ($p = 0.350$, Table 3); however, the 22°C, six-week treatment had significantly higher mean % nitrogen (1.68 ± 0.12%) than the control and both 20°C treatments (Figure 7). There was no consistent relationship between temperature and mass carbon: nitrogen (C:N) ratios; the highest values were found in the 20°C, six-week treatment (Figure 8; $p = 0.720$, Table 3). Stable isotope ratios were also affected significantly by temperature, with both mean $\delta^{13}C$ values (Figure 9; $p < 0.001$, Table 3) and $\delta^{15}N$ values (Figure 10; $p = 0.043$, Table 3) increasing consistently with temperature among the sporophytes exposed to six-week heatwaves. There were no significant differences in $\delta^{15}N$ values between individual treatments, but the 22°C, six-week heatwave treatment had significantly higher $\delta^{13}C$ values than the control or 18°C treatments (Figure 9).

The sporophytes that had been kept in heatwave conditions for three weeks still showed some treatment effects at the end of their recovery period, with elevated carbon content, $\delta^{13}C$, and $\delta^{15}N$ values relative to the control treatment. The 18°C, three-week treatment was somewhat of an exception, as the sporophytes in this treatment had slightly lower mean values of $\delta^{13}C$ (−25.25 ± 0.33‰) and $\delta^{15}N$ (5.08 ± 0.31‰) relative to the control treatment (−24.90 ± 0.31‰ and 5.28 ± 0.18‰, respectively), however, these differences are within the range of analytical precision of the stable isotope measurements. Overall, total % carbon content and $\delta^{13}C$ values followed similar trends with temperature (Figures 6, 9), and subsequent modelling found evidence of a linear relationship between the two variables ($p = 0.009$). Conversely, there was no strong evidence of a relationship between total % nitrogen content

TABLE 3 Predicted effects of heatwave temperature, duration, and their interaction on % carbon and nitrogen content and $\delta^{13}C$ and $\delta^{15}N$ values, obtained by fitting linear mixed-effects models to the data obtained from stable isotope analysis of *Macrocystis pyrifera* blade tissue samples taken at the conclusion of the experiment.

Response variable	*T* (°C)		*D*		*T*:*D*	
	Response	*p*-value	Response	*p*-value	Response	*p*-value
Total carbon (%)	**0.196**	**0.009**	−10.328	0.226	0.571	0.116
Total nitrogen (%)	−0.002	0.350	−1.157	0.991	0.058	0.307
Mass C:N ratio	0.182	0.720	4.524	0.622	−0.188	0.704
$\delta^{13}C$ (‰)	**0.304**	**< 0.001**	−1.490	0.158	0.075	0.678
$\delta^{15}N$ (‰)	**0.146**	**0.043**	0.792	0.241	−0.024	0.858

Effects are expressed as the predicted change in each response variable resulting from a 1°C increase in temperature (T), the predicted difference in each response variable for the sporophytes exposed to a six-week heatwave relative to those exposed to a three-week heatwave (D), and the predicted effects of T and D in combination. Water bath was treated as a random effect. The p-values are provided and highlighted in grey, and statistically significant effects ($p < 0.05$) are indicated in **bold**.

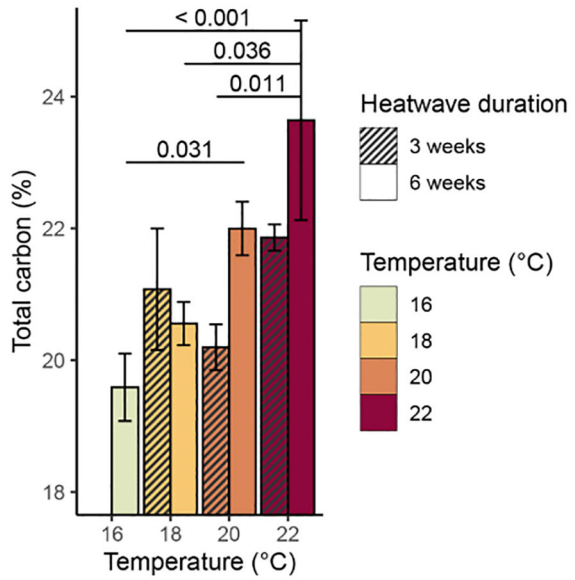

FIGURE 6
Mean % carbon content (with standard error) of *Macrocystis pyrifera* blade tissue at the end of the experiment. Significant ($p < 0.05$) differences between treatments are indicated by bars, with p-values provided.

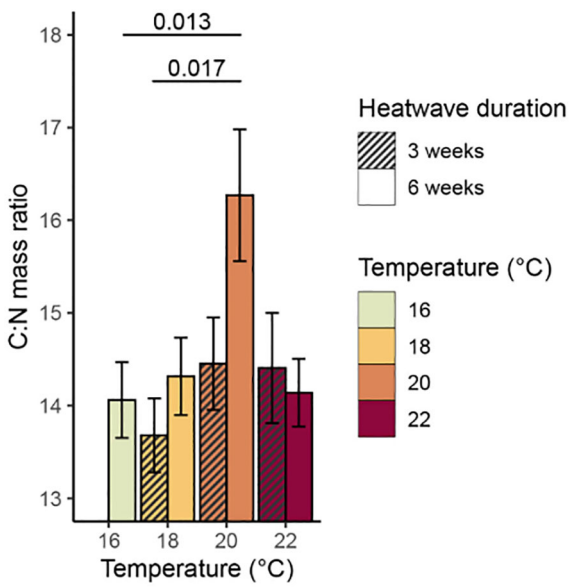

FIGURE 8
Mean mass carbon:nitrogen (C:N) ratio, with standard error, of *Macrocystis pyrifera* blade tissue at the end of the experiment. Significant ($p < 0.05$) differences between treatments are indicated by bars, with p-values provided.

and $\delta^{15}N$ values ($p = 0.074$). There was no evidence that heatwave duration had any significant effects on total % carbon, total % nitrogen, $\delta^{13}C$, or $\delta^{15}N$ values (Table 3).

The % carbon and % nitrogen content and carbon and nitrogen stable isotope ratios of the sporophytes sampled directly from the culture tanks at NIWA are summarized in the Supplementary Material (Supplementary Table S3). These sporophytes had a mean $\delta^{13}C$ value of −29.94 ± 0.33‰, and a mean $\delta^{15}N$ value of −3.22 ± 0.21‰; both values were much lower than any of the experimental treatments. Conversely, the sporophytes in the culture tanks had a mean % nitrogen content of 2.06 ± 0.05%, which was much higher than any of the experimental treatments.

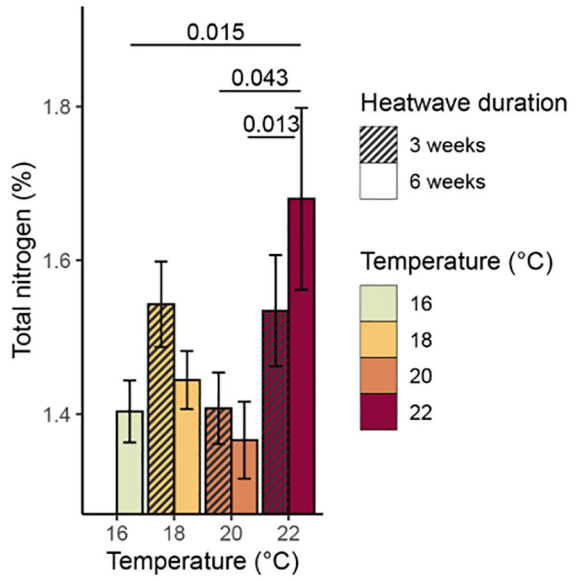

FIGURE 7
Mean % nitrogen content (with standard error) of *Macrocystis pyrifera* blade tissue at the end of the experiment. Significant ($p < 0.05$) differences between treatments are indicated by bars, with p-values provided.

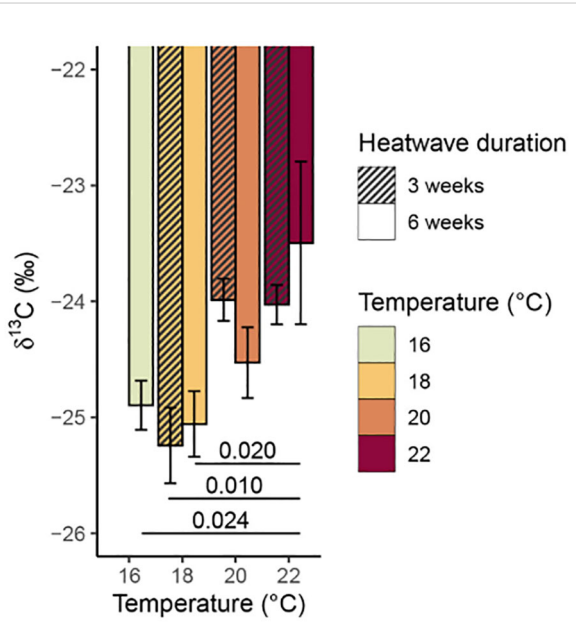

FIGURE 9
Mean $\delta^{13}C$ values (with standard error) of *Macrocystis pyrifera* blade tissue at the end of the experiment. Significant ($p < 0.05$) differences between treatments are indicated by bars, with p-values provided.

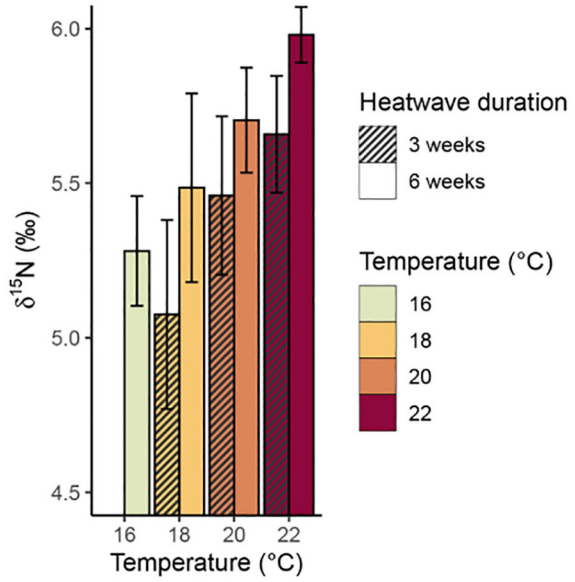

FIGURE 10
Mean $\delta^{15}N$ values (with standard error) of *Macrocystis pyrifera* blade tissue at the end of the experiment.

4 Discussion

4.1 Impacts of heatwave intensity and duration

Increasing both the duration and intensity of marine heatwave treatments used in this experiment had significant negative impacts on the growth of *Macrocystis pyrifera* sporophytes. The 22°C heatwave treatments, representing a 6°C temperature anomaly relative to summer average temperatures, had larger impacts on growth than any of the other treatments, and were the only treatments with consistent negative impacts on survival, photosynthetic performance, or pigmentation. These findings suggest that local *M. pyrifera* populations experience a tipping point near 22°C, beyond which significant physiological impacts, including photosynthetic impairment and death, become much more probable.

The longer heatwave had significantly greater impacts on blade growth rates than the shorter heatwave; however, the impacts of elevated temperatures on $F_{v'}/F_{m'}$ and pigmentation became less pronounced over time. In the case of the 22°C treatment, this may have been the result of the less thermally resistant sporophytes dying over the course of the longer heatwave, rather than a sign of acclimatisation to the increased temperature. We were unable to assess the recovery rates of the sporophytes exposed to six-week heatwaves due to time constraints; it would be worthwhile for future studies to further investigate the capacity for *M. pyrifera* sporophytes to recover from the effects of long-lasting heatwaves.

The *M. pyrifera* sporophytes used in this experiment were able to recover from thermal stress to some extent. The sporophytes exposed to an 18°C heatwave for three weeks appeared to be in good health by the end of the recovery period, growing more rapidly than the control treatment. The DIC uptake rates from this experiment, as well as previous studies (Fernández et al., 2020), suggest that *M. pyrifera* sporophytes have higher thermal optima for photosynthesis, at water temperatures between 17–20°C, than for growth. Therefore, the sporophytes in the 18°C treatments may have been able to photosynthesise more rapidly and accumulate greater quantities of stored carbohydrates during the heatwave. Since they were less severely affected by thermal stress than the higher temperature treatments, they may have been better able to direct these reserves towards growth and pigment production during their recovery period.

4.2 Trends and comparisons to previous findings

The consistent negative relationship between heatwave temperature and *M. pyrifera* growth rates that was observed during this study supports trends found in previous laboratory experiments. Temperatures higher than 14°C are consistently associated with reduced blade growth in *M. pyrifera* (Mabin et al., 2019; Fernández et al., 2020; Umanzor et al., 2021); our results mirror this trend, though we did not use a 14°C treatment here, as our experiment was designed to assess responses to MHWs at local summer temperatures. Our findings also support field observations which linked a MHW event, with widespread temperature anomalies of 1–4°C (equivalent to our 18°C and 20°C treatments), to declines in *M. pyrifera* canopy cover throughout southern New Zealand (Tait et al., 2021). Negative impacts on survival, chlorophyll fluorescence, and photosynthetic performance are often only observed at or above 20°C (Mabin et al., 2019; Fernández et al., 2020; Sánchez-Barredo et al., 2020; Fernández et al., 2021; Umanzor et al., 2021), as was the case in our experiment, although they have sometimes been reported at lower temperatures (Brown et al., 2014; Fernández et al., 2020). The threshold for 100% mortality in young *M. pyrifera* blades from Tasmania, Australia was between 24°C and 27°C (Fernández et al., 2020). The Wellington population could have a similar survival threshold; the study site used by Fernández et al. (2020) had a mean summer sea surface temperature of around 16°C between 1980 and 2010 (Butler et al., 2020), which is similar to Wellington's mean summer sea surface temperatures. Around 30% of *M. pyrifera* gametophytes from New Zealand survived at 23.6°C (Le et al., 2024). Further studies would be required to confirm where the survival threshold lies for sporophytes from the Wellington *M. pyrifera* population. The effect of temperature on pigmentation in *M. pyrifera* is variable (e.g., Mabin et al., 2019; Fernández et al., 2020; Sánchez-Barredo et al., 2020; Umanzor et al., 2021); it has been suggested that related stressors, such as nutrient depletion, could be a more important driver of tissue bleaching in *M. pyrifera* than temperature itself (Sánchez-Barredo et al., 2020).

The increased uptake of the heavier isotopes ^{13}C and ^{15}N by *M. pyrifera* sporophytes at elevated temperatures in this study is unusual when compared to previous studies (e.g., Fernández et al., 2020). We considered the alternative hypothesis that the seawater source used by NIWA, where the sporophytes were

originally cultured, might have had higher concentrations of these heavy isotopes than the source used by the Wellington University Coastal Ecology Laboratory, and the heat-stressed sporophytes might have preferentially retained these heavier isotopes due to their reduced growth and tissue turnover rates. However, the sporophytes grown under pre-experimental conditions at NIWA had much lower mean $\delta^{13}C$ and $\delta^{15}N$ values than the sporophytes used in the experiment. Hence, the increases in $\delta^{13}C$ and $\delta^{15}N$ values with temperature within our experiment are likely a direct response to the simulated heatwaves.

Macroalgal $\delta^{13}C$ values between -30 and -10 ‰ theoretically indicate the use of both bicarbonate and carbon dioxide (CO_2) as carbon sources (Raven et al., 2002). In macroalgae, an increase in photosynthetic rates can drive increased bicarbonate uptake to satisfy the carbon requirements of photosynthesis (Cornelisen et al., 2007). Direct uptake of bicarbonate is achieved by using CO_2-concentrating mechanisms (CCMs) (Raven et al., 2002; Meyer and Griffiths, 2013; Sun et al., 2023), which are present in *M. pyrifera* (Hepburn et al., 2011; Fernández et al., 2014). Although CCMs allow macroalgae to take up and store more carbon, they are energetically and nutrient costly, and these demands can limit the growth of CCM-using species in unfavourable environmental conditions (Hepburn et al., 2011). The correlation between total % carbon content and $\delta^{13}C$ values within our samples suggests that the relationship between temperature and carbon content may have been driven by increased bicarbonate uptake at higher temperatures. Thermal stress could perhaps have driven these kelp sporophytes to respond by actively taking up and storing more DIC. Since kelp blade tissue strength is compromised at high temperatures (Simonson et al., 2015), perhaps the sporophytes exposed to simulated MHWs in our experiment prioritised storage of carbohydrates instead of blade growth. These stored reserves could theoretically have been used to increase blade elongation rates if temperatures reduced, to compensate for reduced growth during the heatwave. The strategy of directing more energy towards DIC uptake and carbon storage could be disadvantageous in the long term, as the high energetic costs associated with CCM operation might limit the energy available for other necessary processes such as photosystem operation and pigment synthesis. Follow-up studies would be necessary to confirm whether, and how, this *M. pyrifera* population is capable of upregulating carbon storage in response to thermal stress. Perhaps this could be examined by measuring the uptake rates of different carbon species by kelp sporophytes, or by assessing the expression of genes related to carbon acquisition and storage. In other kelp species, some transcripts related to cell division and photosynthesis can be downregulated under thermal stress (Hara et al., 2022; Liesner et al., 2022), perhaps indicating a trade-off between acclimatisation to heat stress and the efficiency of some biological processes.

4.3 Wider context

Some *M. pyrifera* populations are relatively resistant to MHWs in the field, even when temperature anomalies exceed 4°C (Reed et al., 2016). Even when severe canopy losses occur, *M. pyrifera* stands can recover to their original canopy area and stem density within several months to two years after disturbance (Dayton et al., 1992; Edwards, 2004; Edwards and Hernández-Carmona, 2005; O'Connor and Anderson, 2010; Tolimieri et al., 2023). Juvenile recruitment plays a central role in this recovery process (Graham et al., 1997); recruitment success can also serve as an indicator of the overall health and resilience of kelp forests (Barrientos et al., 2024). Therefore, the ability of juveniles to survive MHWs, as demonstrated by this study, is likely a key contributing factor to the rapid recovery rates of *M. pyrifera* stands. However, kelp population dynamics are affected by more traits than survivorship rates alone. Larger *M. pyrifera* juveniles are much more likely to survive, potentially because they are better able to compete for light and less vulnerable to density-dependent mortality (Dean et al., 1989). Our findings suggest that long-lasting MHWs could limit the growth rates of new recruits. This means that even if they survive the direct effects of thermal stress, these sporophytes may be more susceptible to mortality due to other stressors, such as competition for light (Dean et al., 1989). Thus, reduced growth, and increased susceptibility to other stressors, could ultimately delay or prevent canopy recovery. In the field, kelp population recovery can be suppressed by long-lasting heatwaves (Arafeh-Dalmau et al., 2019), as well as other stressors including grazing (Dayton et al., 1992; Edwards, 2019) and wave exposure (Graham et al., 1997). MHWs can also create more favourable conditions for more heat-tolerant algal species, leading to increased competition (Wernberg et al., 2016; Atkinson et al., 2020), which would likely place additional pressure on thermally-stressed kelp recruits. In New Zealand, for instance, MHWs could allow the invasive kelp *Undaria pinnatifida* to outcompete native species (James and Shears, 2016). Additionally, the deaths of less heat-tolerant individuals during MHWs can lead to reductions in genetic diversity within kelp populations. While this process of "genetic tropicalisation" may lead to greater thermal tolerance at a population level, it also increases the risk of inbreeding depression, and may cause a reduction in overall adaptive capacity (Coleman et al., 2020). This could ultimately limit the ability of kelp populations to adapt to other threats, such as novel diseases or pollutants.

A 2°C anomaly relative to mean sea surface temperatures (i.e., the 18°C treatment) is the most representative of a typical MHW event in the Wellington region (Supplementary Figures S1, S2), as well as MHW events throughout New Zealand as a whole (Behrens et al., 2022; MetOcean Solutions, 2023). However, mean and maximum MHW intensities have been trending upwards within New Zealand for the past two decades (Montie et al., 2023), and are predicted to continue increasing (Behrens et al., 2022). The Wellington region has already experienced temperature spikes higher than 20°C during MHWs (Supplementary Figure S1), with some sites within the region experiencing temperatures of up to 21.5°C (Krieger et al., 2023c). Modelling suggests that long-lasting MHWs exceeding 22°C are presently unlikely to occur in the regions where *M. pyrifera* grows within New Zealand, but these could become more likely within the next century if global greenhouse gas emissions continue to increase (Behrens et al., 2022). Additionally, most models of historical and future occurrence of MHWs in New Zealand rely on satellite data

collected over broad spatial scales. The shallow coastal environments where kelp grows are highly dynamic; temperatures within these habitats could exceed MHW thresholds without being recognised as a regional MHW. Therefore, it is valuable to understand how *M. pyrifera* would respond to temperatures higher than those recorded during contemporary MHW events.

Temperature anomalies greater than 4°C have been recorded during MHWs in New Zealand, mostly in southern regions (MetOcean Solutions, 2023). There is some evidence that warm-edge kelp populations may be more resilient to increased temperatures than higher-latitude populations (Ladah, 2000; Muth et al., 2019; Hollarsmith et al., 2020; King et al., 2019; Liesner et al., 2020), though there are exceptions (Cavanaugh et al., 2019). Therefore, populations from New Zealand's South Island, where *M. pyrifera* is most widespread (Shaffer and Rovellini, 2020), could theoretically be less heat-tolerant than the warm-edge population studied here. Assessing the vulnerability of *M. pyrifera* populations from southern New Zealand to MHWs would be a worthwhile direction for further research.

4.4 Conclusion

This work demonstrates that marine heatwaves can reduce the growth rates of juvenile *M. pyrifera* sporophytes in New Zealand, while heatwaves surpassing 22°C have far more severe impacts, including potentially reducing the photosynthetic efficiency and survivorship of juveniles. Long-lasting heatwaves could suppress recruitment and growth of juvenile kelp, potentially jeopardising the long-term stability of local populations. However, the kelp studied here demonstrated a high capacity for recovery after heatwaves, suggesting that populations can persist if key temperature thresholds are not exceeded. If sea surface temperatures around New Zealand continue to rise, and temperature anomalies exceeding 6°C become more prevalent throughout central and southern New Zealand, *M. pyrifera* could face a greater risk of population collapse and local extinction.

Data availability statement

The original contributions presented in the study are included in the article/Supplementary Material. Further inquiries can be directed to the corresponding author.

Author contributions

IB: Conceptualization, Data curation, Formal analysis, Investigation, Methodology, Visualization, Writing – original draft. YK: Methodology, Writing – review & editing. EK: Conceptualization, Methodology, Supervision, Writing – review & editing. SB: Investigation, Methodology, Writing – review & editing. RD: Conceptualization, Funding acquisition, Methodology, Project administration, Resources, Supervision, Writing – review & editing. CC: Conceptualization, Funding acquisition, Methodology, Project administration, Resources, Supervision, Writing – review & editing.

Funding

The author(s) declare financial support was received for the research, authorship, and/or publication of this article. This research was supported by funding from the Coastal People, Southern Skies Centre for Research Excellence project to CEC (E4280), a Rutherford Discovery Fellowship to CEC (VUW 1701), the Wellington Community Fund, the Eurofins Foundation, and the Clare Foundation.

Acknowledgments

The authors would like to thank Neill Barr, Denisa Berbece, Imke Böök, Laura Bornemann Santamaría, Katie Fenton, Ashtyn Isaak, Holly Koch, Maya Korth, Journey Luond, Daniel McNaughtan, Alexandra Northmore, Ohad Peleg, Siddharth Ravishankar, Aleluia Taise, and John van der Sman for their help with kelp culture, data collection, maintaining the experiment, and feedback. Thanks also to Kat Siegers and Arlo McMahon for their assistance with experimental setup. Our thanks also go to Josette Delgado, Oliver Kerr-Hislop, Graeme Moss, and Julie Brown for their help with stable isotope analysis, and to Linda Groenewegen for her work on nutrient sample analysis.

Conflict of interest

The authors declare that the research was conducted in the absence of any commercial or financial relationships that could be construed as a potential conflict of interest.

The author(s) declared that they were an editorial board member of Frontiers, at the time of submission. This had no impact on the peer review process and the final decision.

Publisher's note

Supplementary material

The Supplementary Material for this article can be found online at: https://www.frontiersin.org/articles/10.3389/fmars.2024.1423595/full#supplementary-material

References

Arafeh-Dalmau, N., Montaño-Moctezuma, G., Martínez, J. A., Beas-Luna, R., Schoeman, D. S., and Torres-Moye, G. (2019). Extreme marine heatwaves alter kelp forest community near its equatorward distribution limit. *Front. Mar. Sci.* 6. doi: 10.3389/fmars.2019.00499

Arkema, K. K., Reed, D. C., and Schroeter, S. C. (2009). Direct and indirect effects of giant kelp determine benthic community structure and dynamics. *Ecology* 90, 3126–3137. doi: 10.1890/08-1213.1

Atkinson, J., King, N. G., Wilmes, S. B., and Moore, P. J. (2020). Summer and winter marine heatwaves favor an invasive over native seaweeds. *J. Phycol.* 56, 1591–1600. doi: 10.1111/jpy.13051

Barrientos, S., Piñeiro-Corbeira, C., Díaz-Tapia, P., García, M. E., and Barreiro, R. (2024). Recruitment as a possible indicator of declining resilience in degraded kelp forests. *Ecol. Indic.* 160, 111917. doi: 10.1016/j.ecolind.2024.111917

Bates, D., Maechler, M., Bolker, B., and Walker, S. (2023). *lme4: Linear Mixed-Effects Models using 'Eigen' and S4. R package version 1.1-33*. Available online at: https://cran.r-project.org/web/packages/lme4/index.html.

Behrens, E., Rickard, G., Rosier, S., Williams, J., Morgenstern, O., and Stone, D. (2022). Projections of future marine heatwaves for the oceans around New Zealand using New Zealand's Earth System Model. *Front. Climate* 4. doi: 10.3389/fclim.2022.798287

Booth, J. D. (1975). Seasonal and tidal variations in the hydrology of Wellington harbour. *New Z. J. Mar. Freshw. Res.* 9, 333–354. doi: 10.1080/00288330.1975.9515572

Britton, D., Cornwall, C. E., Revill, A. T., Hurd, C. L., and Johnson, C. R. (2016). Ocean acidification reverses the positive effects of seawater pH fluctuations on growth and photosynthesis of the habitat forming kelp, *Ecklonia radiata*. *Nat. Sci. Rep.* 6, 26036. doi: 10.1038/srep26036

Brown, M. B., Edwards, M. S., and Kim, K. Y. (2014). Effects of climate change on the physiology of giant kelp, *Macrocystis pyrifera*, and grazing by purple urchin, *Strongylocentrotus purpuratus*. *Algae* 29, 203–215. doi: 10.4490/algae.2014.29.3.203

Butler, C. L., Lucieer, V. L., Wotherspoon, S. J., and Johnson, C. R. (2020). Multi-decadal decline in cover of giant kelp *Macrocystis pyrifera* at the southern limit of its Australian range. *Mar. Ecol. Prog. Ser.* 653, 1–18. doi: 10.3354/meps13510

Cavanaugh, K. C., Reed, D. C., Bell, T. W., Castorani, M. C. N., and Beas-Luna, R. (2019). Spatial variability in the resistance and resilience of giant kelp in Southern and Baja California to a multiyear heatwave. *Front. Mar. Sci.* 6. doi: 10.3389/fmars.2019.00413

Coleman, M. A., Minne, A. J. P., Vranken, S., and Wernberg, T. (2020). Genetic tropicalisation following a marine heatwave. *Nat. Sci. Rep.* 10, 12726. doi: 10.1038/s41598-020-69665-w

Cornelisen, C. D., Wing, S. R., Clark, K. L., Bowman, M. H., Frew, R. D., and Hurd, C. L. (2007). Patterns in the $\delta^{13}C$ and $\delta^{15}N$ signature of *Ulva pertusa*: Interaction between physical gradients and nutrient source pools. *Limnol. Oceanogr.* 52, 820–832. doi: 10.4319/lo.2007.52.2.0820

Cornwall, C. E., Nelson, W. A., Aguirre, J. D., Blain, C. O., Coyle, L., D'Archino, R., et al. (2023). Predicting the impacts of climate change on New Zealand's seaweed-based ecosystems. *New Z. J. Bot.* doi: 10.1080/0028825X.2023.2245786

Dayton, P. K., Tegner, M. J., Parnell, P. E., and Edwards, P. B. (1992). Temporal and spatial patterns of disturbance and recovery in a kelp forest community. *Ecol. Monogr.* 62, 421–445. doi: 10.2307/2937118

Dean, T. A., Thies, K., and Lagos, S. L. (1989). Survival of juvenile giant kelp: the effects of demographic factors, competitors, and grazers. *Ecology* 70, 483–495. doi: 10.2307/1937552

de Burgh-Day, C. O., Spillman, C. M., Smith, G., and Stevens, C. L. (2022). Forecasting extreme marine heat events in key aquaculture regions around New Zealand. *J. South. Hemis. Earth Syst. Sci.* 72, 58–72. doi: 10.1071/ES21012

A. G. Dickson, C. L. Sabine and J. R. Christian (Eds.) (2007). *Guide to best practices for ocean CO_2 measurements* (PICES Special Publication 3. North Pacific Marine Science Organization: Sidney, BC, Canada).

Edwards, M. S. (2004). Estimating scale-dependency in disturbance impacts: El Niños and giant kelp forests in the northeast Pacific. *Oecologia* 138, 436–447. doi: 10.1007/s00442-003-1452-8

Edwards, M. S. (2019). Comparing the impacts of four ENSO events on giant kelp (*Macrocystis pyrifera*) in the northeast Pacific Ocean. *Algae* 34, 141–151. doi: 10.4490/algae.2019.34.5.4

Edwards, M. S., and Hernández-Carmona, G. (2005). Delayed recovery of giant kelp near its southern range limit in the North Pacific following El Niño. *Mar. Biol.* 147, 273–279. doi: 10.1007/s00227-004-1548-7

Eger, A. M., Marzinelli, E. M., Beas-Luna, R., Blain, C. O., Blamey, L. K., Byrnes, J. E. K., et al. (2023). The value of ecosystem services in global marine kelp forests. *Nat. Commun.* 14, 1894. doi: 10.1038/s41467-023-37385-0

Fernández, P. A., Gaitán-Espitia, J. D., Leal, P. P., Schmid, M., Revill, A. T., and Hurd, C. L. (2020). Nitrogen sufficiency enhances thermal tolerance in habitat-forming kelp: implications for acclimation under thermal stress. *Nat. Sci. Rep.* 10, 3186. doi: 10.1038/s41598-020-60104-4

Fernández, P. A., Hurd, C. L., and Roleda, M. Y. (2014). Bicarbonate uptake via an anion exchange protein is the main mechanism of inorganic carbon acquisition by the giant kelp *Macrocystis pyrifera* (Laminariales, Phaeophyceae) under variable pH. *J. Phycol.* 50, 998–1008. doi: 10.1111/jpy.12247

Fernández, P. A., Labbé, B., Gaitán-Espitia, J. D., Hurd, C. L., Paine, E. R., Willis, A., et al. (2023). The influence of ammonium to nitrate ratio on the thermal responses of early life stages of the giant kelp *Macrocystis pyrifera*. *Algal Res.* 72, 103114. doi: 10.1016/j.algal.2023.103114

Fernández, P. A., Navarro, J. M., Camus, C., Torres, R., and Buschmann, A. H. (2021). Effect of environmental history on the habitat–forming kelp *Macrocystis pyrifera* responses to ocean acidification and warming: a physiological and molecular approach. *Nat. Sci. Rep.* 11, 2510. doi: 10.1038/s41598-021-82094-7

Filbee-Dexter, K., and Wernberg, T. (2018). Rise of turfs: a new battlefront for globally declining kelp forests. *BioScience* 68, 64–76. doi: 10.1093/biosci/bix147

Filbee-Dexter, K., and Wernberg, T. (2020). Substantial blue carbon in overlooked Australian kelp forests. *Nat. Sci. Rep.* 10, 12341. doi: 10.1038/s41598-020-69258-7

Fox, J., Weisberg, S., and Price, B. (2023). *car: Companion to Applied Regression. R package version 3.1-2*. Available online at: https://cran.r-project.org/web/packages/car/index.html.

Gattuso, J.-P., Epitalon, J.-M., Lavigne, H., and Orr, J. (2021). *seacarb: Seawater Carbonate Chemistry. R package version 3.3.2*. Available online at: https://cran.r-project.org/web/packages/seacarb/index.html.

Gaylord, B., Rosman, J. H., Reed, D. C., Koseff, J. R., Fram, J., SacIntyre, S., et al. (2007). Spatial patterns of flow and their modification within and around a giant kelp forest. *Limnol. Oceanogr.* 52, 1838–1852. doi: 10.4319/lo.2007.52.5.1838

Graham, M. H. (2004). Effects of local deforestation on the diversity and structure of Southern California giant kelp forest food webs. *Ecosystems* 7, 341–357. doi: 10.1007/s10021-003-0245-6

Graham, M. H., Harrold, C., Lisin, S., Light, K., Watanabe, J. M., and Foster, M. S. (1997). Population dynamics of giant kelp *Macrocystis pyrifera* along a wave exposure gradient. *Mar. Ecol. Prog. Ser.* 148, 269–279. doi: 10.3354/meps148269

Guillard, R. R. L. (1975). "Culture of phytoplankton for feeding marine invertebrates," in *Culture of Marine Invertebrate Animals*. Eds. W. L. Smith and M. H. Chanley (Springer, Boston, MA). doi: 10.1007/978-1-4615-8714-9_3

Hara, Y., Otake, Y., Akita, S., Yamazaki, T., Takahashi, F., Yoshikawa, S., et al. (2022). Gene expression of a canopy-forming kelp, *Eisenia bicyclis* (Laminariales, Phaeophyceae), under high temperature stress. *Phycol. Res.* 70, 203–211. doi: 10.1111/pre.12497

Harvey, B. P., Marshall, K. E., Harley, C. D. G., and Russell, B. D. (2022). Predicting responses to marine heatwaves using functional traits. *Trends Ecol. Evol.* 37, 20–29. doi: 10.1016/j.tree.2021.09.003

Hay, C. H. (1990). The distribution of *Macrocystis* (Phaeophyta: Laminariales) as a biological indicator of cool sea surface temperature, with special reference to New Zealand waters. *J. R. Soc. New Z.* 20, 313–336. doi: 10.1080/03036758.1990.10426716

Hepburn, C. D., Pritchard, D. W., Cornwall, C. E., McLeod, R. J., Beardall, J., Raven, J. A., et al. (2011). Diversity of carbon use strategies in a kelp forest community: implications for a high CO_2 ocean. *Global Change Biol.* 17, 2488–2497. doi: 10.1111/j.1365-2486.2011.02411.x

Hobday, A. J., Alexander, L. V., Perkins, S. E., Smale, D. A., Straub, S. C., Oliver, E. C. J., et al. (2016). A hierarchical approach to defining marine heatwaves. *Prog. Oceanogr.* 141, 227–238. doi: 10.1016/j.pocean.2015.12.014

Hollarsmith, J. A., Buschmann, A. H., Camus, C., and Grosholz, E. D. (2020). Varying reproductive success under ocean warming and acidification across giant kelp (*Macrocystis pyrifera*) populations. *J. Exp. Mar. Biol. Ecol.* 522, 151247. doi: 10.1016/j.jembe.2019.151247

Hothorn, T., Bretz, F., Westfall, P., Heiberger, R. M., Schuetzenmeister, A., and Scheibe, S. (2023). *multcomp: Simultaneous Inference in General Parametric Models. R package version 1.4-25*. Available online at: https://cran.r-project.org/web/packages/multcomp/multcomp.pdf. (Accessed June 15, 2024)

Huang, W.-J., Wang, Y., and Cai, W.-J. (2012). Assessment of sample storage techniques for total alkalinity and dissolved inorganic carbon in seawater. *Limnol. Oceanogr.: Methods* 10, 711–717. doi: 10.4319/lom.2012.10.711

Hurlbert, S. H. (1984). Pseudoreplication and the design of ecological field experiments. *Ecol. Monogr.* 54, 187–211. doi: 10.2307/1942661

James, K., and Shears, N. T. (2016). Population ecology of the invasive kelp *Undaria pinnatifida* towards the upper extreme of its temperature range. *Mar. Biol.* 163, 225. doi: 10.1007/s00227-016-2993-9

Johnson, C. R., Banks, S. C., Barrett, N. S., Cazassus, F., Dunstan, P. K., Edgar, G. J., et al. (2011). Climate change cascades: Shifts in oceanography, species' ranges and subtidal marine community dynamics in eastern Tasmania. *J. Exp. Mar. Biol. Ecol.* 400, 17–32. doi: 10.1016/j.jembe.2011.02.032

Kain, J. M., and Jones, N. S. (1976). The biology of *Laminaria hyperborea*. VIII. Growth on cleared areas. *J. Mar. Biol. Assoc. United Kingdom* 56, 267–290. doi: 10.1017/S0025315400018907

Kerry, C., Roughan, M., and Azevedo Correia de Souza, J. M. (2022). Drivers of upper ocean heat content extremes around New Zealand revealed by Adjoint Sensitivity Analysis. *Front. Climate* 4. doi: 10.3389/fclim.2022.980990

King, N. G., McKeown, N. J., Smale, D. A., Wilcockson, D. C., Hoelters, L., Groves, E. A., et al. (2019). Evidence for different thermal ecotypes in range centre and trailing edge kelp populations. *J. Exp. Mar. Biol. Ecol.* 514–515, 10–17. doi: 10.1016/j.jembe.2019.03.004

Krieger, E. C., Nelson, W. A., Grand, J., Le Ru, E. C., Bury, S. J., Cossais, A., et al. (2023a). The role of irradiance in controlling coralline algal calcification. *Limnol. Oceanogr.* 68, 1269–1284. doi: 10.1002/lno.12345

Krieger, E. C., Sarid-Segal, Y., Böök, I. M., Taise, A., Berbece, D., and Cornwall, C. E. (2023b). Tolerance of three temperate macroalgal taxa to marine heatwaves of differing durations and intensities is not modulated by irradiance. *Phycologia* 62, 627–636. doi: 10.1080/00318884.2023.2267411

Krieger, E. C., Taise, A., Nelson, W. A., Grand, J., Le Ru, E., Davy, S. K., et al. (2023c). Tolerance of coralline algae to ocean warming and marine heatwaves. *PloS Climate* 2, e0000092. doi: 10.1371/journal.pclm.0000092

Krumhansl, K. A., Okamoto, D. K., Rassweller, A., and Byrnes, J. E. K. (2016). Global patterns of kelp forest change over the past half-century. *Proc. Natl. Acad. Sci.* 113, 13785–13790. doi: 10.1073/pnas.1606102113

Ladah, L. B. (2000). Life on the edge: Stress survival adaptations in southern limit *Macrocystis pyrifera* populations. *J. Phycol.* 36, 40–41. doi: 10.1046/j.1529-8817.1999.00001-120.x

Ladah, L. B., and Zertuche-González, J. A. (2007). Survival of microscopic stages of a perennial kelp (*Macrocystis pyrifera)* from the center and the southern extreme of its range in the Northern Hemisphere after exposure to simulated El Niño stress. *Mar. Biol.* 152, 677–686. doi: 10.1007/s00227-007-0723-z

Le, D. M. (2022). Thermal tolerance of the giant kelp *Macrocystis pyrifera*. University of Otago, Dunedin, New Zealand. Available at: http://hdl.handle.net/10523/13600.

Le, D. M., Desmond, M. J., Pritchard, D. W., and Hepburn, C. D. (2022). Effect of temperature on sporulation and spore development of giant kelp (*Macrocystis pyrifera*). *PloS One* 17, e0278268. doi: 10.1371/journal.pone.0278268

Le, D. M., Desmond, M. J., Pritchard, D. W., and Hepburn, C. D. (2024). Thermal threshold for fertilisation and gametophyte survivorship of the giant kelp *Macrocystis pyrifera*. *Mar. Ecol. Prog. Ser.* 734, 23–33. doi: 10.3354/meps14559

Leathers, T., King, N. G., Foggo, A., and Smale, D. A. (2023). Marine heatwave duration and intensity interact to reduce physiological tipping points of kelp species with contrasting thermal affinities. *Ann. Bot.* 133 (1), 51–60. doi: 10.1093/aob/mcad172

Lebrun, A., Comeau, S., Gazeau, F., and Gattuso, J.-P. (2022). Impact of climate change on Arctic macroalgal communities. *Global Planet. Change* 219, 103980. doi: 10.1016/j.gloplacha.2022.103980

Li, J., Bergman, K., Thomas, J.-B. E., Gao, Y., and Gröndahl, F. (2023). Life Cycle Assessment of a large commercial kelp farm in Shandong, China. *Sci. Total Environ.* 903, 166861. doi: 10.1016/j.scitotenv.2023.166861

Liesner, D., Fouqueau, L., Valero, M., Roleda, M. Y., Pearson, G. A., Bischof, K., et al. (2020). Heat stress responses and population genetics of the kelp Laminaria digitata (Phaeophyceae) across latitudes reveal differentiation among North Atlantic populations. *Ecol. Evol.* 10, 9144–9177. doi: 10.1002/ece3.6569

Liesner, D., Pearson, G. A., Bartsch, I., Rana, S., Harms, L., Heinrich, S., et al. (2022). Increased heat resilience of intraspecific outbred compared to inbred lineages in the kelp *Laminaria digitata*: physiology and transcriptomics. *Front. Mar. Sci.* 9. doi: 10.3389/fmars.2022.838793

Ling, S. D., Johnson, C. R., Frusher, S. D., and Ridgway, K. R. (2009). Overfishing reduces resilience of kelp beds to climate-driven catastrophic phase shift. *Proc. Natl. Acad. Sci.* 106, 22341–22345. doi: 10.1073/pnas.0907529106

Løvås, S. M., and Tørum, A. (2001). Effect of the kelp *Laminaria hyperborea* upon sand dune erosion and water particle velocities. *Coast. Eng.* 44, 37–63. doi: 10.1016/S0378-3839(01)00021-7

Mabin, C. J. T., Johnson, C. R., and Wright, J. T. (2019). Physiological response to temperature, light, and nitrates in the giant kelp *Macrocystis pyrifera* from Tasmania, Australia. *Mar. Ecol. Prog. Ser.* 614, 1–19. doi: 10.3354/meps12900

McPherson, M. L., Finger, D. J. I., Housekeeper, H. F., Bell, T. W., Carr, M. H., Rogers-Bennett, L., et al. (2021). Large-scale shift in the structure of a kelp forest ecosystem co-occurs with an epizootic and marine heatwave. *Commun. Biol.* 4, 298. doi: 10.1038/s42003-021-01827-6

MetOcean Solutions (2023). *Recent marine heatwaves in Aotearoa New Zealand* (Wellington, New Zealand: Meteorological Service of New Zealand Ltd). Available at: https://www.moanaproject.org/recent-marine-heatwaves.

Meyer, M., and Griffiths, H. (2013). Origins and diversity of eukaryotic CO_2-concentrating mechanisms: lessons for the future. *J. Exp. Bot.* 64, 769–786. doi: 10.1093/jxb/ers390

Miller, R. J., Page, H. M., and Reed, D. C. (2015). Trophic versus structural effects of a marine foundation species, giant kelp (*Macrocystis pyrifera*). *Oecologia* 179, 1199–1209. doi: 10.1007/s00442-015-3441-0

Montie, S., Thoral, F., Smith, R. O., Cook, F., Tait, L. W., Pinkerton, M. H., et al. (2023). Seasonal trends in marine heatwaves highlight vulnerable coastal ecoregions and historic change points in New Zealand. *New Z. J. Mar. Freshw. Res.* 58 (2), 274–299. doi: 10.1080/00288330.2023.2218102

Mora-Soto, A., Palacios, M., Macaya, E. C., Gómez, I., Huovinen, P., Pérez-Matus, A., et al. (2020). A high-resolution global map of giant kelp (*Macrocystis pyrifera*) forests and intertidal green algae (Ulvophyceae) with Sentinel-2 imagery. *Remote Sens.* 12, 694. doi: 10.3390/rs12040694

Muth, A. F., Graham, M. H., Lane, C. E., and Harley, C. D. G. (2019). Recruitment tolerance to increased temperature present across multiple kelp clades. *Ecology* 100, e02594. doi: 10.1002/ecy.2594

O'Connor, K. C., and Anderson, T. W. (2010). Consequences of habitat disturbance and recovery to recruitment and the abundance of kelp forest fishes. *J. Exp. Mar. Biol. Ecol.* 386, 1–10. doi: 10.1016/j.jembe.2010.01.016

Paul, D., Skrzypek, G., and Fórizs, I. (2007). Normalization of measured stable isotopic compositions to isotope reference scales - a review. *Rapid Commun. Mass Spectrom.* 21, 3006–3014. doi: 10.1002/rcm.3185

Pierrot, D. E., Wallace, D. W. R., and Lewis, E. (2011). *MS Excel Program Developed for CO2 System Calculations* (Bethel, PA: Carbon Dioxide Information Analysis Center, Oak Ridge National Laboratory). doi: 10.3334/cdiac/otg.co2sys_xls_cdiac105a

Pritchard, D. W., Hurd, C. L., Beardall, J., and Hepburn, C. D. (2015). Restricted use of nitrate and a strong preference for ammonium reflects the nitrogen ecophysiology of a light-limited red alga. *J. Phycol.* 51, 277–287. doi: 10.1111/jpy.12272

Provost, E. J., Kelaher, B. P., Dworjanyn, S. A., Russell, B. D., Connell, S. D., Ghedini, G., et al. (2017). Climate-driven disparities among ecological interactions threaten kelp forest persistence. *Global Change Biol.* 23, 353–361. doi: 10.1111/gcb.13414

Purcell, D., Wheeler, T. T., Hayes, M., and Packer, M. A. (2024). Effect of photoperiod and temperature on bioproduct production from juvenile sporophytes of *Macrocystis pyrifera*. *Front. Mar. Sci.* 11. doi: 10.3389/fmars.2024.1410877

Raven, J. A., Johnston, A. M., Kübler, J. E., Korb, R., McInroy, S. G., Handley, L. L., et al. (2002). Mechanistic interpretation of carbon isotope discrimination by marine macroalgae and seagrasses. *Funct. Plant Biol.* 29, 355–378. doi: 10.1071/PP01201

Reed, D., Washburn, L., Rassweiler, A., Miller, R., Bell, T., and Harrer, S. (2016). Extreme warming challenges sentinel status of kelp forests as indicators of climate change. *Nat. Commun.* 7, 13757. doi: 10.1038/ncomms13757

Reynolds, R. W., and Banzon, V. F. (2008). "NOAA Optimum Interpolation 1/4 Degree Daily Sea Surface Temperature (OISST) Analysis, Version 2," in *NOAA National Centers for Environmental Information* (NOAA, Washington, DC), V5SQ8XB5. doi: 10.1175/jcli-d-21-0001.1

Salinger, M. J., Renwick, J., Behrens, E., Mullan, A. B., Diamond, H. J., Sirguey, P., et al. (2019). The unprecedented coupled ocean-atmosphere summer heatwave in the New Zealand region 2017/18: drivers, mechanisms and impacts. *Environ. Res. Lett.* 14, 044023. doi: 10.1088/1748-9326/ab012a

Sánchez-Barredo, M., Sandoval-Gil, J. M., Zertuche-González, J. A., Ladah, L. B., Belando-Torrentes, M. D., Beas-Luna, R., et al. (2020). Effects of heat waves and light deprivation on giant kelp juveniles (*Macrocystis pyrifera*, Laminariales, Phaeophyceae). *J. Phycol.* 56, 880–894. doi: 10.1111/jpy.13000

Schiel, D. R., and Foster, M. S. (2015). *The biology and ecology of giant kelp forests* (Oakland: University of California Press). Available at: https://books.google.co.nz/books?id=dO_LBwAAQBAJ&printsec=frontcover#v=onepage&q&f=false.

Schlegel, R. W., and Smit, A. J. (2021). *heatwaveR: Detect Heatwaves and Cold-Spells. R package version 0.4.6.* Available online at: https://cran.r-project.org/web/packages/heatwaveR/index.html. (Accessed July 15, 2022)

Seely, G. R., Duncan, M. J., and Vidaver, W. E. (1972). Preparative and analytical extraction of pigments from brown algae with dimethyl sulfoxide. *Mar. Biol.* 12, 184–188. doi: 10.1007/BF00350754

Shaffer, M. R., and Rovellini, A. (2020). *A review of habitat use, home range size and connectivity for selected New Zealand species* (Department of Conservation, New Zealand). Available at: https://dxcprod.doc.govt.nz/globalassets/documents/conservation/marine-and-coastal/marine-protected-areas/mpa-publications/habitat-use-and-movement-patterns-2020.pdf.

Shapiro, S. S., and Wilk, M. B. (1965). An analysis of variance test for normality. *Biometrika* 52, 591–611. doi: 10.2307/2333709

Simonson, E. J., Scheibling, R. E., and Metaxas, A. (2015). Kelp in hot water: I. Warming seawater temperature induces weakening and loss of kelp tissue. *Mar. Ecol. Prog. Ser.* 537, 89–104. doi: 10.3354/meps11438

Smale, D. A. (2020). Impacts of ocean warming on kelp forest ecosystems. *New Phytol.* 225, 1447–1454. doi: 10.1111/nph.16107

Smale, D. A., and Wernberg, T. (2013). Extreme climatic event drives range contraction of a habitat-forming species. *Proc. R. Soc. B* 280, 20122829. doi: 10.1098/rspb.2012.2829

Smale, D. A., Wernberg, T., Yunnie, A. L. E., and Vance, T. (2015). The rise of Laminaria ochroleuca in the Western English Channel (UK) and comparisons with its competitor and assemblage dominant Laminaria hyperborea. *Mar. Ecol.* 36, 1033–1044. doi: 10.1111/maec.12199

Steneck, R. S., Graham, M. H., Bourque, B. J., Corbett, D., Erlandson, J. M., Estes, J. A., et al. (2002). Kelp forest ecosystems: biodiversity, stability, resilience and future. *Environ. Conserv.* 29, 436–459. doi: 10.1017/S0376892902000322

Straub, S. C., Thomsen, M. S., and Wernberg, T. (2016). "The dynamic biogeography of the anthropocene: the speed of recent range shifts in seaweeds," in *Seaweed Phylogeography*. Eds. Z. M. Hu and C. Fraser (Dordrecht, Springer). doi: 10.1007/978-94-017-7534-2_3

Strickland, J. D. H., and Parsons, T. R. (1972). *A Practical Handbook of Seawater Analysis. 2nd edition* (Ottawa, Canada: Fisheries Research Board of Canada). (Bulletin Fisheries Research Board of Canada, Nr. 167 (2nd ed)). doi: 10.25607/OBP-1791

Sun, J., Zhao, C., Zhao, S., Dai, W., Liu, J., Zhang, J., et al. (2023). Diversity of CO_2 concentrating mechanisms in macroalgae photosynthesis: a case study of Ulva sp. *J. Mar. Sci. Eng.* 11, 1911. doi: 10.3390/jmse11101911

Tait, L. W., Thoral, F., Pinkerton, M. H., Thomsen, M. S., and Schiel, D. R. (2021). Loss of giant kelp, *Macrocystis pyrifera*, driven by marine heatwaves and exacerbated by poor water quality in New Zealand. *Front. Mar. Sci.* 8. doi: 10.3389/fmars.2021.721087

Teagle, H., Hawkins, S. J., Moore, P. J., and Smale, D. A. (2017). The role of kelp species as biogenic habitat formers in coastal marine ecosystems. *J. Exp. Mar. Biol. Ecol.* 492, 81–98. doi: 10.1016/j.jembe.2017.01.017

Thomsen, M. S., Mondardini, L., Alestra, T., Gerrity, S., Tait, L., South, P. M., et al. (2019). Local extinction of bull kelp (*Durvillaea* spp.) due to a marine heatwave. *Front. Mar. Sci.* 6. doi: 10.3389/fmars.2019.00084

Tolimieri, N., Andrew O. Shelton, A. O., Samhouri, J. F., Harvey, C. J., Feist, B. E., Williams, G. D., et al. (2023). Changes in kelp forest communities off Washington, USA, during and after the 2014–2016 marine heatwave and sea star wasting syndrome. *Mar. Ecol. Prog. Ser.* 703, 47–66. doi: 10.3354/meps14220

Traiger, S. B., Cohn, B., Panos, D., Daly, M., Hirsh, H. K., Martone, M., et al. (2022). Limited biogeochemical modification of surface waters by kelp forest canopies: Influence of kelp metabolism and site-specific hydrodynamics. *Limnol. Oceanogr.* 67, 392–403. doi: 10.1002/lno.11999

Tukey, J. (1949). Comparing individual means in the analysis of variance. *Biometrics* 5, 99–114. doi: 10.2307/3001913

Umanzor, S., Sandoval-Gil, J., Sánchez-Barredo, M., Ladah, L. B., Ramírez-García, M., and Zertuche-González, J. A. (2021). Short-term stress responses and recovery of giant kelp (*Macrocystis pyrifera*, Laminariales, Phaeophyceae) juvenile sporophytes to a simulated marine heatwave and nitrate scarcity. *J. Phycol.* 57, 1604–1618. doi: 10.1111/jpy.13189

Vanella, F. A., Fernández, D. A., Carolina Romero, M., and Calvo, J. (2007). Changes in the fish fauna associated with a sub-Antarctic *Macrocystis pyrifera* kelp forest in response to canopy removal. *Polar Biol.* 30, 449–457. doi: 10.1007/s00300-006-0202-x

Vergés, A., Steinberg, P. D., Hay, M. E., Poore, A. G. B., Campbell, A. H., Ballesteros, E., et al. (2014). The tropicalization of temperate marine ecosystems: climate-mediated changes in herbivory and community phase shifts. *Proc. R. Soc. B* 281, 20140846. doi: 10.1098/rspb.2014.0846

Villegas, M., Laudien, J., Sielfeld, W., and Arntz, W. (2019). Effect of foresting barren ground with *Macrocystis pyrifera* (Linnaeus) C. Agardh on the occurrence of coastal fishes off northern Chile. *J. Appl. Phycol.* 31, 2145–2157. doi: 10.1007/s10811-018-1657-1

Wernberg, T., Bennett, S., Babcock, R. C., de Bettignies, T., Cure, K., Depczynski, M., et al. (2016). Climate-driven regime shift of a temperate marine ecosystem. *Science* 353, 169–172. doi: 10.1126/science.aad8745

Wernberg, T., Coleman, M. A., Bennett, S., Thomsen, M. S., Tuya, F., and Kelaher, B. P. (2018). Genetic diversity and kelp forest vulnerability to climatic stress. *Nat. Sci. Rep.* 8, 1–8. doi: 10.1038/s41598-018-20009-9

Wernberg, T., Krumhansl, K., Filbee-Dexter, K., and Pedersen, M. F. (2019). "Status and trends for the world's kelp forests," in *World Seas: An Environmental Evaluation, 2nd ed*. Ed. C Sheppard. (London, UK: Academic Press). doi: 10.1016/C2015-0-04336-2

Wernberg, T., Thomsen, M. S., Baum, J. K., Bishop, M. S., Bruno, J. F., Coleman, M. A., et al. (2023). Impacts of climate change on marine foundation species. *Annu. Rev. Mar. Sci.* 16, 247–282. doi: 10.1146/annurev-marine-042023-093037

Wright, L. S., Pessarrodona, A., and Foggo, A. (2022). Climate-driven shifts in kelp forest composition reduce carbon sequestration potential. *Global Change Biol.* 28, 5514–5531. doi: 10.1111/gcb.16299

frontiers | Frontiers in Marine Science

TYPE Original Research
PUBLISHED 17 September 2024
DOI 10.3389/fmars.2024.1446380

OPEN ACCESS

EDITED BY
Christopher Edward Cornwall,
Victoria University of Wellington,
New Zealand

REVIEWED BY
Kathryn Schoenrock,
University of Galway, Ireland
Jinlin Liu,
Tongji University, China

*CORRESPONDENCE
Alejandra Mora-Soto
alemoras@uvic.ca
Maycira Costa
maycira@uvic.ca

RECEIVED 09 June 2024
ACCEPTED 17 July 2024
PUBLISHED 17 September 2024

CITATION
Mora-Soto A, Schroeder S, Gendall L, Wachmann A, Narayan G, Read S, Pearsall I, Rubidge E, Lessard J, Martell K and Costa M (2024) Back to the past: long-term persistence of bull kelp forests in the Strait of Georgia, Salish Sea, Canada. *Front. Mar. Sci.* 11:1446380. doi: 10.3389/fmars.2024.1446380

Back to the past: long-term persistence of bull kelp forests in the Strait of Georgia, Salish Sea, Canada

Alejandra Mora-Soto[1*], Sarah Schroeder[1], Lianna Gendall[1,2], Alena Wachmann[1], Gita Narayan[3], Silven Read[1], Isobel Pearsall[4], Emily Rubidge[5], Joanne Lessard[6], Kathryn Martell[7] and Maycira Costa[1*]

[1]Spectral Lab, Department of Geography, University of Victoria, Victoria, BC, Canada, [2]School of Biological Sciences and Oceans Institute, University of Western Australia, Perth, WA, Australia, [3]Fisheries and Aquaculture Department, Vancouver Island University, Nanaimo, BC, Canada, [4]Marine Science Program, Pacific Salmon Foundation, Vancouver, BC, Canada, [5]Institute of Ocean Sciences, Fisheries and Oceans Canada, Sidney, BC, Canada, [6]Pacific Biological Station, Fisheries and Oceans Canada, Nanaimo, BC, Canada, [7]Islands Trust Conservancy, Victoria, BC, Canada

The Salish Sea, a dynamic system of straits, fjords, and channels in southwestern British Columbia, is home to ecologically and culturally important bull kelp (*Nereocystis luetkeana*) forests. Yet the long-term fluctuations in the area and the persistence of this pivotal coastal marine habitat are unknown. Using very high-resolution satellite imagery to map kelp forests over two decades, we present the spatial changes in kelp forest area within the Salish Sea, before (2002 to 2013) and after (2014 to 2022) the 'Blob,' an anomalously warm period in the Northeast Pacific. This analysis was spatially constrained by local environmental conditions. Based on nearshore sea surface temperatures (SSTs) from four decades (1984–2022), we found two periods of distinct increases in SST, one starting in 2000 and another in 2014. Further, the highest SST anomalies occurred on warmer coastlines in the enclosed inlets and the Strait of Georgia, while smaller anomalies were found on colder coastlines near the Strait of Juan de Fuca and the Discovery Passage. The total area of bull kelp forests from 2014 to 2022 has decreased compared to 2002 to 2013, particularly in the northern sector of the Salish Sea. Using the satellite-derived kelp data, we also present an analysis of kelp persistence compared with historical distribution of kelp forests depicted on British Admiralty Nautical Charts from 1858 to 1956. This analysis shows that warm, sheltered areas experienced a considerable decrease in persistence of kelp beds when compared to satellite-derived distribution of modern kelp, confirming a century-scale loss. In particular, the presence of kelp forests in the Strait of Georgia and on the warmest coasts has decreased considerably over the century, likely due to warming temperatures. While the

coldest coasts to the south have maintained their centennial persistence, the northern Salish Sea requires further research to understand its current dynamics. This research contributes to a wider understanding of temporal and spatial factors for kelp from the regional perspective of the Salish Sea.

KEYWORDS

Nereocystis luetkeana, bull kelp, persistence, Salish Sea, Blob, satellite imagery

1 Introduction

In natural history, persistence is understood as a population or species that did not become locally extinct during a given period of time, or if it did, it recolonized the area within certain reference bounds (Connell and Sousa, 1983). This definition recognizes the inherent variability of ecosystems in the real world, which can be particularly extreme in marine environments (Dayton et al., 1998). Abiotic factors such as patch size, rocky substrate, or wave velocity can increase the overall persistence of foundation species like kelp forests (Young et al., 2016). However, the lack of long-term, continuous surveys may underestimate the roles that biological and physical interactions plus anthropogenic impacts have exerted on them (Dayton et al., 1998). Paleoecological, archaeological, and historical proxies can provide some clues about kelp forest presence in the past (Jackson et al., 2001), allowing for the creation of accurate baselines of ecological persistence and informed perspectives toward effective management and conservation of this crucial habitat.

Monitoring kelp forests is becoming crucial for several reasons, such as their role as habitats for a multiplicity of organisms, including some of economic importance like salmon (Shaffer, 2003). They also play an important role in atmospheric carbon removal and sequestration (Pedersen et al., 2021) and have critical value to local and indigenous communities (Turner, 2001; United Nations Environment Programme, 2023; Wernberg et al., 2019), among other existential values (United Nations Environment Programme, 2023). Therefore, monitoring efforts have been conducted to estimate their trends globally (Krumhansl et al., 2016) and, specifically in British Columbia, kelps are conservation priorities for informing the development of a regional marine protected area (MPA) network (Gale et al., 2019; MPA Network BC Northern Shelf Initiative, 2023), currently under development.

In order to create a kelp monitoring framework, it is important to define the spatial and temporal bounds of the targeted kelp habitat. For example, choosing to study when kelp forests changed from a non-intervened starting point is challenging to achieve since the coast has seen continuous human occupation for more than 20,000 years in the North American Pacific region (Erlandson et al., 2007). However, there is an overall consensus that during the industrial era, several types of disturbances—such as overfishing, mechanical destruction of habitats, and climate change—have altered these ecosystems deeply (Dayton et al., 1998; Jackson et al., 2001; Steneck et al., 2002).

For a broader perspective to determine a starting point before the effects of the industrial era, important information sources are the traditional knowledge of local First Nations (Kobluk et al., 2021) and archaeological records (Dillehay et al., 2008; Erlandson et al., 2007). Historical records can also be used to document kelp distribution and help establish a baseline that goes back to the times of European exploration. This is the case for historical floating kelp records based on 1850s British Admiralty Charts in British Columbia (Costa et al., 2020) and Washington State (Berry et al., 2021; Pfister et al., 2017).

For the most recent past in the Northeast Pacific, satellite imagery has provided estimations of change from the decade of 1970s (Gendall et al., in prep.; Mora-Soto et al., 2024), 1980s (Bell et al., 2015, 2020, 2023; Cavanaugh et al., 2011; Hamilton et al., 2020; Man et al., in prep; McPherson et al., 2021; Nijland et al., 2019), and from the decade of 2000s on (Cavanaugh et al., 2019; Mora-Soto et al., 2024; Schroeder et al., 2020). The gap between the historical and the contemporary (satellite-derived) kelp records in British Columbia has not been filled yet.

A recent paper by Mora-Soto et al. (2024) analyzed the resilience of bull kelp (*Nereocystis luetkeana*) forests from 2005 to 2022 in the southern Salish Sea of British Columbia, including a sentinel site at the southern end of Vancouver Island with data spanning back to 1972. There, kelp forests generally showed signs of resilience to increased temperatures, probably due to a combination of fewer marine heatwaves and a higher frequency of extreme wind-wave motion during the growth season from 2020 to 2022 (Mora-Soto et al., 2024). This study, nevertheless, lacks perspective on the long-term trends in the greater Salish Sea ecosystem. Century-old kelp records from an adjacent region, the Strait of Juan de Fuca, confirmed that kelp forests have generally persisted, although they have diminished in the eastern limit (Pfister et al., 2017). In southern Puget Sound, bull kelp distribution has shown losses of up to 96% compared to an 1878 baseline (Berry et al., 2021). Sea surface temperature in the Salish Sea has shown an increase over the century (Pfister et al., 2017) by 0.57°C per decade (Amos et al., 2014), with an even warmer anomaly event in the North Pacific called the 'Blob' of 2014–2019 (Bond et al., 2015) and analogous

events (Chen et al., 2021) that maintained lingering effects even in deep water (Jackson et al., 2018). As ocean warming is a clear threat to kelp forest persistence globally (Schiel et al., 2004; Smale, 2020), increasing nearshore temperatures may result in limited kelp presence in the Salish Sea over a longer time frame.

Here, we complement the resilience work by Mora-Soto et al. (2024) by analyzing the long-term persistence of floating kelp canopies of *Nereocystis luetkeana* (kelp hereafter) in the Salish Sea of British Columbia. The objectives of this research are twofold: to determine the change in areal extent in modern kelp during the period called the Blob and the years after (2014–2022) compared with previously mapped kelp areas from 2002 to 2013; and to define the long-term persistence of kelp over the century. For this analysis, we used high-resolution satellite-derived kelp areal extent to determine modern changes. Our long-term baseline is the oldest published records of kelp presence based on British Admiralty Nautical Charts from the late 19th to the early 20th centuries (Costa et al., 2020). In order to facilitate comparisons within this geographical area, the coastline was divided into clusters of similar environmental conditions. Additionally, spring and summer sea surface temperatures (SSTs) from 1984 to 2022 were used to characterize nearshore SST trends along this extensive coastline. This research adds crucial temporal and spatial data for a more comprehensive understanding of the Salish Sea nearshore ecosystem. Additionally, it brings a wider perspective about the geographical diversity of nearshore ecosystems located along temperate coastlines.

2 Methods

2.1 Environmental clusters

The study area spanned the British Columbian section of the Salish Sea, from the southern limit of the Johnstone Strait (50.37° N) to the Strait of Juan de Fuca (48.25°N) (Figure 1). In this research, the northern Gulf lslands are Denman, Hornby, Lasqueti, and Texada, whereas the southern Gulf Islands are Pender, Mayne, Salt Spring, Galiano, Penelakut, Thetis, and Gabriola, among others not mentioned in the text. The coastline of the study area was classified by environmental clusters (clusters hereafter), defined by the spatial distribution of abiotic factors, following a method developed by Mora-Soto et al. (2024). The variables used in this study were: nearshore Landsat-derived SST (Wachmann et al., 2024); climatology in spring and summer (see section 2.2); fetch or distance to the closest shore, measured as the linear distance in a 360° radius (Gregr et al., 2019); modelled wind speed at 10 m height, expressed as m/seg, obtained from the Global Wind Atlas version 3.3 (Davis et al., 2023); modelled tidal current in m/s (Foreman et al., 2004); and satellite-derived total suspended matter (TSM) for spring and summer (mg/L) (Giannini et al., 2021). These variables were sampled by alongshore points located 1000 m apart and 300 m away from the coastline. Each variable was summarized by the mean of values falling within a 100 m buffer around each point using zonal statistics. This dataset was clustered using K-means (Hartigan and Wong, 1979) in R (R Core Team, 2024).

The environmental partition of the coastline resulted in five clusters encompassing the main characteristics of the study area (Figures 1, 2). Cluster 1 is the coldest coast, with a mean SST climatology in spring and summer of 10.6°C and 12.0°C, respectively. This cluster has the longest tidal amplitude current, with a mean of 0.49 m/s. Cluster 2 is a moderately sheltered coast with a mean fetch of 178 km and a slightly higher temperature, with mean values of 12.2°C and 14.0°C for spring and summer, respectively. Cluster 3, in the Strait of Georgia, has higher temperatures (mean of 15.4°C and 18.3°C for spring and summer) and is particularly exposed, resulting in higher fetch (mean of 716 km) and wind speed (mean of 4.5 m/s). The highest mean temperatures are found in Cluster 4 (15.8°C and 18.8°C for spring and summer), as the most sheltered coast with a mean wind speed of 2.5 m/s and fetch of 157 km. Cluster 5 is characterized for having the highest TSM of the Salish Sea (mean of 15 mg/L), mainly due to the plume of sediments from the Fraser River, thus preventing this area from having any kelp presence. Lacking kelp beds, Cluster 5 is not considered in the rest of the kelp analysis.

2.2 Nearshore SST

Nearshore sea surface temperature records for four decades (1984–2022) were seasonally selected by spring and summer values to characterize thermal conditions during the growth season for bull kelp (Springer et al., 2010). Nearshore SST was obtained from thermal bands from the Landsat constellation (courtesy of the U.S. Geological Survey), available in Google Earth Engine (Gorelick et al., 2017) and validated as a reliable source to obtain nearshore temperature data (Wachmann et al., 2024). The temporal coverage for each satellite was 1984–2011 for Landsat 5, 1999–2002 for Landsat 7, 2013–2022 for Landsat 8, and 2022 for Landsat 9. SST was extracted from an algorithm designed to integrate different sensors and spatially overlapping imagery into a seasonal mosaic. For every spring (May, June) and summer (July, August) season, the image collection was filtered by selecting images of 50% or less cloud coverage. The thermal pixel values from the filtered collection were scaled, cloud-masked, and transformed from Kelvin to Celsius, according to Wachmann et al. (2024). Two additional filters of temperatures <7.0°C and the 30th percentile of the lowest values were applied to discard any possible fog contamination on the image. If the average value of the SST collection was within 1.5 standard deviations, it was considered a valid pixel to represent the seasonal temperature; if not, the value was discarded.

The resultant seasonal mosaic was spatially joined to the sampling points that were used as input for the cluster analysis (see section 2.1) using the Spatial Join tool, whereas missing values were interpolated using the Kriging tool in ArcGIS 10.8.1. As a result, seasonal temperature per year from 1984 to 2022 was added to the table of attributes of the points. The mean of this dataset was the seasonal climatology used in the environmental cluster definition (see section 2.1).

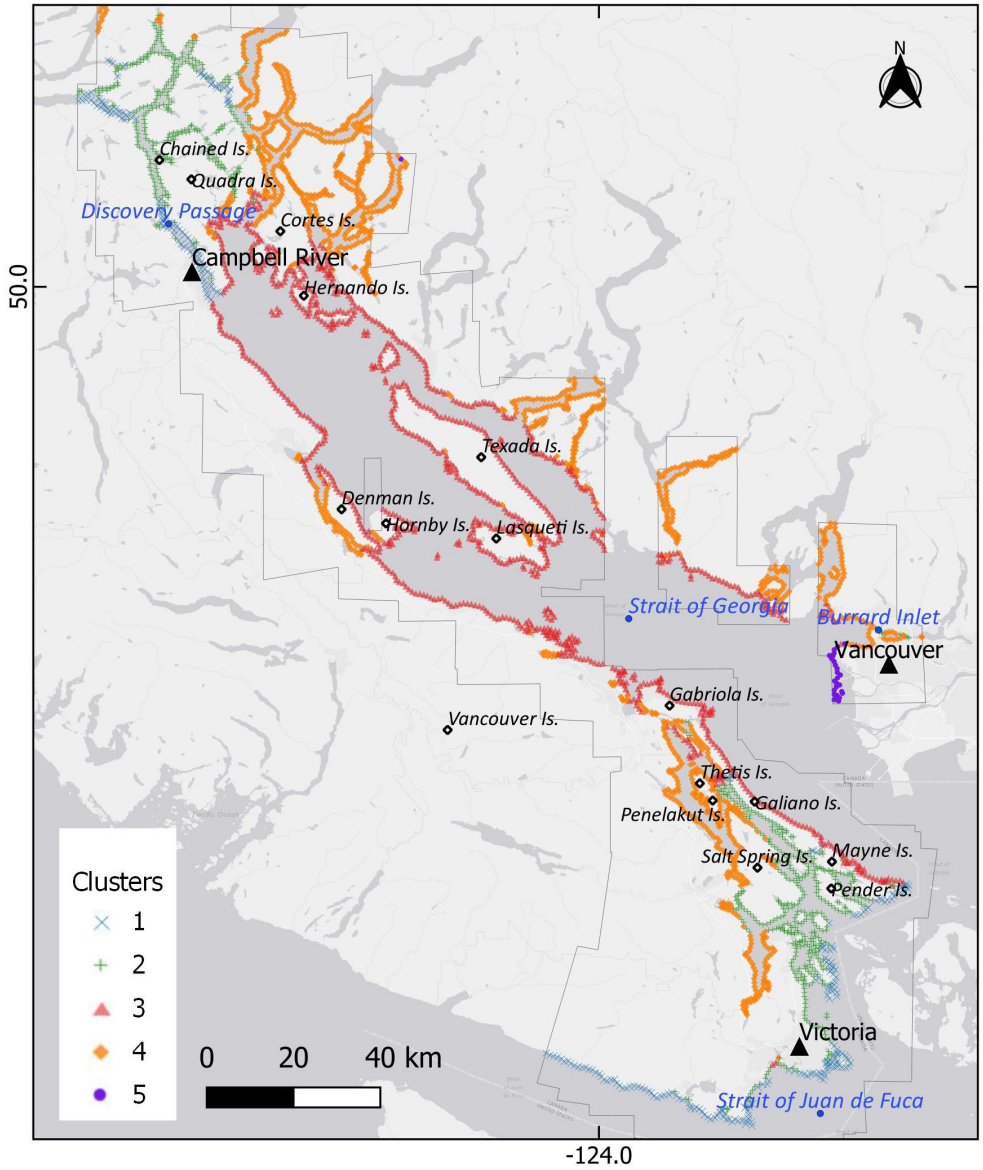

FIGURE 1
Map of the study area, including the toponyms mentioned in this research. The coastline is classified into clusters defined by similar environmental conditions, represented by points. The main polygons represent the total coverage of the high-resolution imagery available from 2002 to 2022.

2.3 High-resolution satellite maps of kelp

Modern-day kelp, from 2002 to 2022 (modern kelp hereafter), was mapped with archived high-resolution imagery of <6 m of spatial resolution, which had a modest coverage for the northern sector of the Salish Sea due to cloud cover and imagery quality (see annual coverage in Supplementary Figures S1, S2). This dataset was grouped into two main periods: 1) the years before the Blob (2002–2013), hereafter called PreBlob, and 2) the period encompassing the Blob and subsequent years (2014–2022), Blob+Post hereafter. Kelp was mapped by classifying high-resolution remote sensing imagery from the summer peak (July or August) at the lowest tide. The procedure follows previous research (Cavanaugh et al., 2021; Gendall et al., 2023; Mora-Soto et al., 2024; Schroeder et al., 2019) and is summarized as follows: the corrected and georeferenced image was masked from the lowest tide mark to 40 m depth (low tide mask hereafter). Normalized Difference Vegetation Index (NDVI; Kriegler et al., 1969), Green Normalized Difference Vegetation Index (GNDVI; Gitelson et al., 1996), near-infrared bands, and visible enhanced bands were segmented using the multi-resolution segmentation tool and classified into kelp and no-kelp classes in the eCognition software (Trimble Germany GmbH, 2021) using expert knowledge. The outputs were maps of the maximum kelp extent observed per year. These classifications were compared with Google Earth imagery, ancillary data, and anecdotal observations. Additional validation was conducted with *in-situ* mapping surveys from different years, resulting in an accuracy of 70%.

10.3389/fmars.2024.1446380

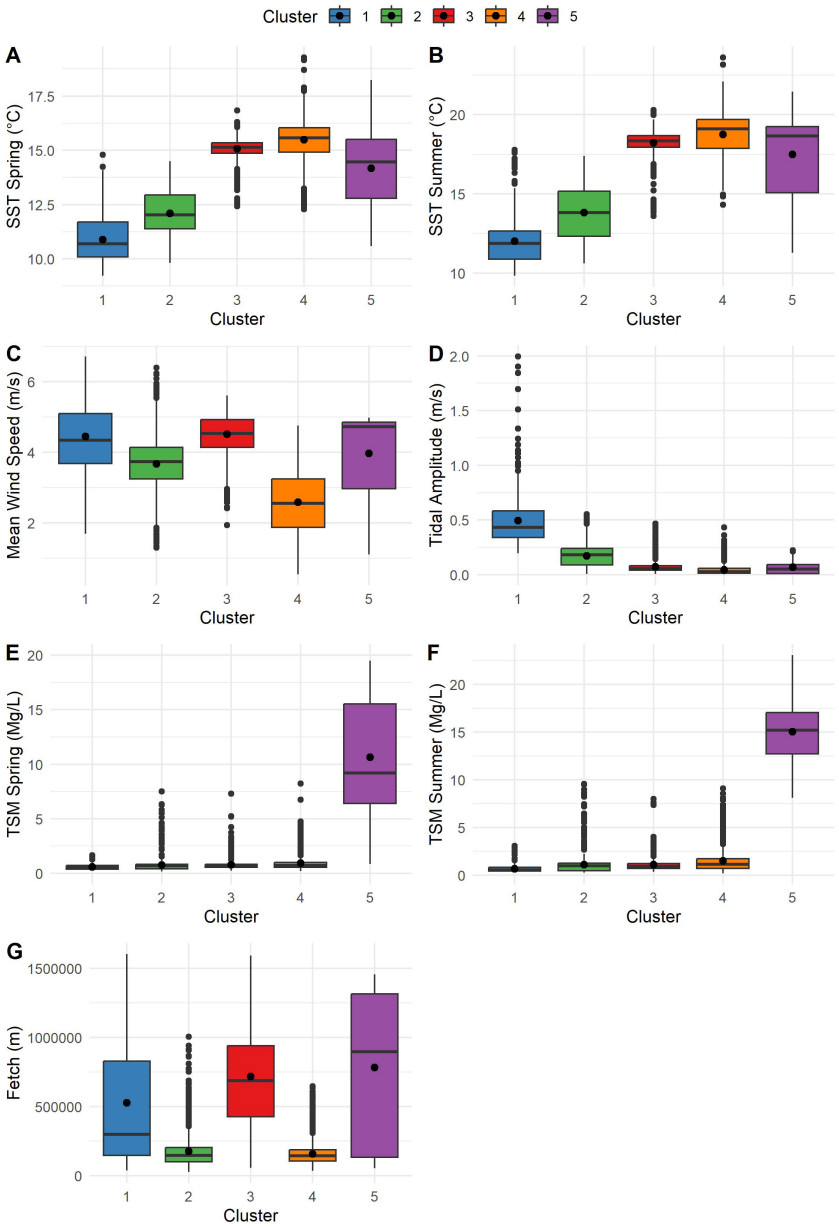

FIGURE 2
Box and whisker plots characterizing the clusters by variables; the point in the center denotes the mean. SST, Sea Surface Temperature; TSM, Total Suspended Matter. **(A)** SST climatology in spring (°C). **(B)** SST climatology in summer (°C). **(C)** Mean wind speed (m/s). **(D)** Tidal amplitude (m/s). **(E)** TSM spring (mg/L). **(F)** TSM summer (mg/L). **(G)** Fetch (m). Cluster 1 represents the coldest areas with the highest current; Cluster 2 is moderately cold and semi-sheltered; Cluster 3 is the exposed coast in the Strait of Georgia; and Cluster 4 is the most sheltered and warmest coast. Cluster 5 is the coastline with the highest total suspended matter in the Salish Sea.

2.4 Historical kelp surveys from the 19th and 20th centuries

The earliest written historical source of kelp distribution in British Columbia comes from the British Admiralty Nautical Charts (historical kelp hereafter), published from 1858 with successive updates until 1956 (Costa et al., 2020). Kelp canopies were often depicted as dendritic features, particularly in detailed, fine-scale charts (<1:10,000), as they posed dangers to navigation (Imray, 1870). Costa et al. (2020) georeferenced the complete dataset of nautical charts of the province, and kelp features were digitized as a multi-polygon shapefile layer. The reliability of those locations was then calculated by comparing them within a bathymetry range of 40 m, resulting in 99% reliability. However, given the diversity of scales and accuracies of the depicted kelp, our analyses relied on their distributions instead of areal extents. Non-kelp in the nautical charts may either represent a generalized representation of coastlines or the actual absence of kelp. For this reason, we only used the mapped historical kelp records for this analysis.

2.5 Spatial and statistical analysis

Our spatial analysis was conducted by kelp area comparisons between PreBlob and Blob+Post periods, nearshore SST anomalies per cluster, and kelp persistence of historical versus modern distributions (PreBlob and Blob+Post). To compare PreBlob with Blob+Post periods, the intersecting kelp area between the PreBlob and Blob+Post imagery coverages was chosen for analysis. The kelp layers from both periods were spatially analyzed within the scale of segments per cluster, as defined in section 2.1. The segments were defined by the Voronoi distance among the alongshore points that intersected with the low tide mask, consisting of polygons of ~1000 m in length. Mapped kelp layers were spatially merged to the segments, adding kelp area per segment (m^2) as a variable. The non-parametric Kruskal-Wallis chi-square test (Kruskal and Wallis, 1952) was used to identify significant changes in kelp area per period (PreBlob and Blob+Post) and cluster. Further, the study area was divided into a northern sector and a southern sector to avoid underrepresentation of the generally smaller northern kelp area.

The climatological baseline was defined by extracting the averages of nearshore SSTs from 1984–2022 per cluster and season (spring and summer) for the entire study area. The data was compared with the seasonal nearshore SSTs per cluster by calculating their anomalies as the difference between the nearshore SST per cluster (by season and year) and their averages. The Kruskal-Wallis test was used to examine temporal patterns that could constitute specific periods of anomalies. For each period, the difference in positive and negative values was used to describe significant anomaly patterns and to identify differences among clusters.

Lastly, the analysis was restricted to the historical distribution of kelp beds from nautical charts to identify kelp persistence. If historical kelp presence matched PreBlob or Blob+Post kelp presence at the same segment, the segment was classified as containing persistent kelp from historical to modern times. If not, the segment was classified as non-persistent kelp.

3 Results

3.1 Nearshore SST anomalies and trends

Thermal anomalies of nearshore SST show three main periods within the 1984–2022 baseline (Figures 3A, B). First, there was an initial period of predominantly colder anomalies (0.0 to -3.0°C in spring and summer) from 1984 until 1999. A second period, starting in 2000, varied within a range of -3.0 to +3.0°C in spring and -2.0 to +2.0°C in summer. Finally, a third period, starting in 2014, had a predominance of warmer anomalies in both the spring and summer seasons.

Mean SSTs for Cluster 1, representing the coasts with the coldest waters (see the temperatures in Table 1) and the highest tidal currents, increased by 1.0°C for the spring and summer seasons over four decades. Cluster 2, representing slightly warmer and semi-sheltered coasts, expressed a mean increase of 1.6°C in the spring and 2.0°C in the summer. Cluster 3 had an average increase of around 2.0°C for both seasons in the Strait of Georgia. Finally, Cluster 4, representing the warmest and most sheltered coastlines, showed an increase higher than 2.0°C in SSTs for both seasons. The nearshore SST per cluster and season did not change significantly from the northern to the southern sectors. All of the temporal changes across periods were statistically significant (Kruskal-Wallis test p-value <0.005).

3.2 High-resolution mapped kelp changes

The total kelp area mapped from 2002 to 2022 with high-resolution imagery in the study area was 2,086 hectares. Kelp forests largely dominated the southern sector from Burrard Inlet to southern Vancouver Island (Figure 1). The northern sector had more narrow kelp forests—smaller than one hectare per segment—along the coastline of islands and channels (Figures 4A, B).

Specifically, the PreBlob distribution (Figure 4A) spanned the complete Salish Sea; the larger areas in the southern sector (>6 ha) were located along the coasts in the Strait of Juan de Fuca (Cluster 1 south), some semi-sheltered coasts in the southern Gulf Islands (Cluster 2 south), and Burrard Inlet (Clusters 1 and 2 south). In the northern sector, relatively small and narrow but continuous kelp forests (between 1.5 to 6.0 ha) were present at Discovery Passage and Quadra Island (Clusters 1 and 2 north). Small (<1.5 ha) and relatively continuous forests were in the Strait of Georgia, particularly at Galiano, Lasqueti, Texada, and Hornby Islands (Cluster 3 north), while sparse kelps were found in more sheltered inlets (Cluster 4 north). The Blob+Post map (Figure 4B) showed a smaller and more scattered distribution of kelp, with an absence of kelp in the central Salish Sea (Strait of Georgia, Cluster 3 north), particularly around the northern Gulf Islands, as well as the Discovery Passage and Quadra Island (Clusters 1 and 2 north). In contrast, small but continuous kelp beds were mapped in the southern Gulf Islands (Clusters 2 and 4 south). The distribution of kelp beds in Cluster 1 south in the Strait of Juan de Fuca matched the PreBlob period, although the sizes of the beds were relatively smaller.

Changes in kelp abundance were evident per cluster and sector (north and south), either in the total area per cluster (Figure 5A) or as area per segment (Figure 5B). The majority of the small kelp beds mapped in the northern sector in the PreBlob period were not detected in the Blob+Post period, meaning that kelp was not present or the density of the canopies was too negligible to be detected with the high-resolution remote sensing imagery. At the cluster level (Figures 5A, B), the northern sector showed large and significant declines in area per segment (Kruskal-Wallis test p-value <0.05), in Cluster 1, Cluster 2, and Cluster 4 (1.8 ha PreBlob to 0.4 ha in Blob+Post). Despite having less kelp presence in the northern Gulf Islands, the total area in Cluster 3 remained relatively constant. In the southern sector, Cluster 1 in the Strait of Juan de Fuca and Cluster 3 in the southern part of the Strait of Georgia had reductions in total area from PreBlob to Blob+Post. In contrast, the semi-sheltered and sheltered coasts of Clusters 2 and 4 in the interior of the Gulf Islands showed significant increases in total area of kelp.

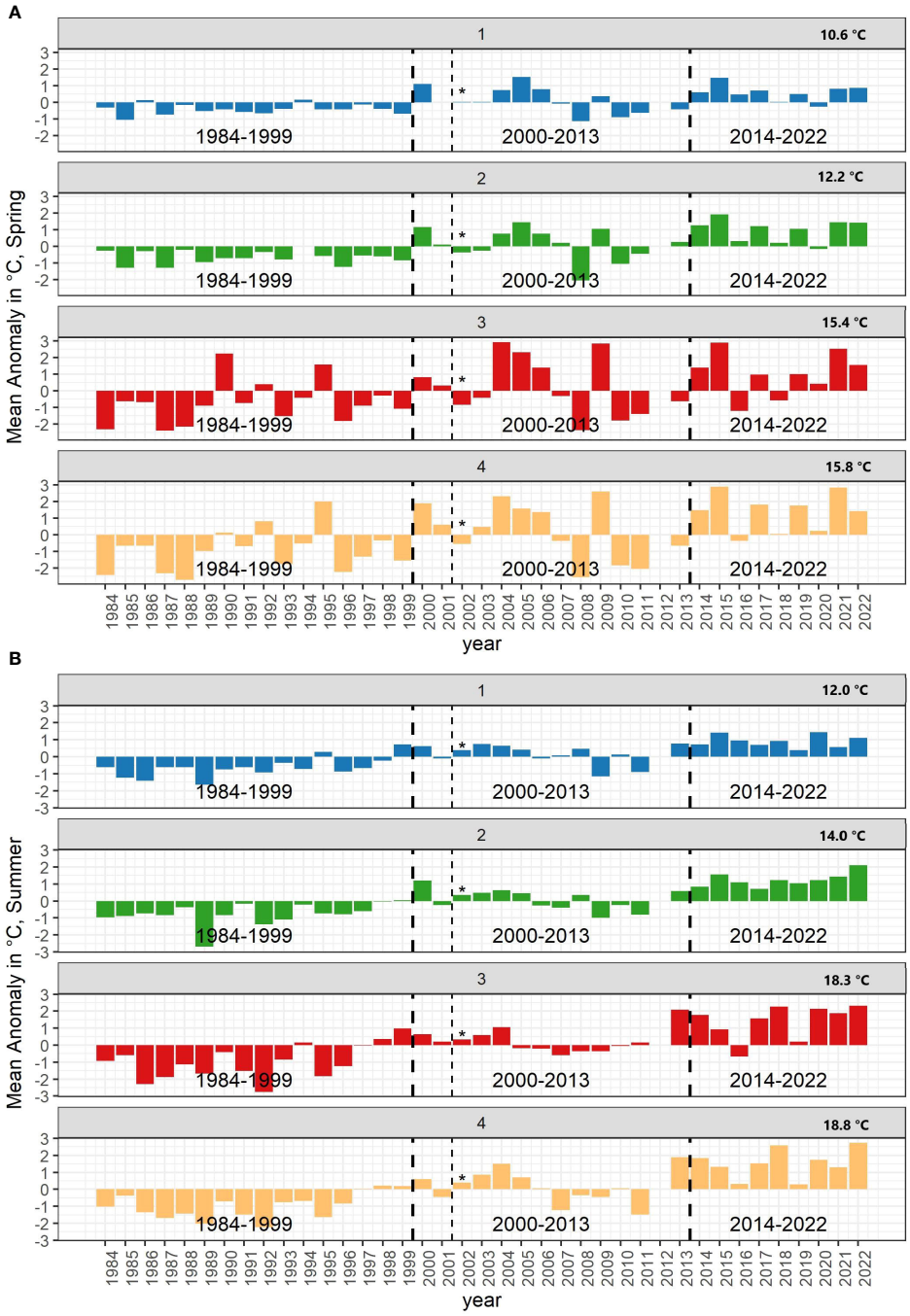

FIGURE 3
Nearshore sea surface temperature anomalies per cluster in **(A)** spring and **(B)** summer; the values in the right corner show the total average from 1984 to 2022. Bold-dashed lines indicate the periods 1984–1999, 2000–2013 (PreBlob), and 2014–2022 (Blob+Post). The vertical line with * in 2002 indicates the initial year of the high-resolution mapping classification.

3.3 Historical assessment of kelp persistence

Historical kelp was compared to PreBlob and Blob+Post periods to identify their persistence within a century time scale. The historical kelp forests compared to the PreBlob distribution (Figure 6A) showed a relatively high persistence of continuous kelp beds in the extreme north (Discovery Passage and around Quadra Island, Clusters 1 and 2), the southern sector (Strait of Juan de Fuca and southern Gulf Islands, Burrard Inlet), and some groups of persistent kelp near Texada and Lasqueti Islands. Non-persistent kelp areas dominated the central part of the Strait of Georgia (Cluster 3). On the other hand, the historical distribution compared to the Blob+Post period (Figure 6B) showed that non-persistent kelp dominated the Strait of Georgia from the southern Gulf Islands (Galiano, Penelakut, and Thetis Islands) to Quadra

TABLE 1 Descriptive statistics of nearshore SST (°C) per season and cluster.

Season	Cluster	Period	Min	1st Q.	Median	Mean	3rd Q.	Max	Diff with 1984–1999
Spring	1	1984–1999	9.6	10.0	10.2	10.2	10.3	10.8	
		2000–2013	9.5	10.2	10.6	10.7	11.4	12.1	0.5
		2014–2022	10.3	11.1	11.2	11.2	11.4	12.1	1.0
	2	1984–1999	10.9	11.3	11.5	11.5	11.9	12.2	
		2000–2013	10.1	11.8	12.4	12.3	13.0	13.6	0.8
		2014–2022	12.0	12.5	13.4	13.2	13.6	14.1	1.6
	3	1984–1999	12.9	13.8	14.5	14.6	15.0	17.6	
		2000–2013	13.0	14.5	15.0	15.6	16.8	18.3	1.0
		2014–2022	14.1	15.8	16.4	16.4	16.9	18.2	1.7
	4	1984–1999	13.1	13.9	15.0	14.8	15.3	17.8	
		2000–2013	13.2	15.1	16.3	16.0	17.4	18.4	1.2
		2014–2022	15.4	16.0	17.3	17.1	17.6	18.7	2.3
Summer	1	1984–1999	10.3	11.1	11.3	11.3	11.4	12.7	
		2000–2013	10.8	11.9	12.4	12.1	12.6	12.8	0.8
		2014–2022	12.4	12.7	12.9	12.9	13.1	13.4	1.6
	2	1984–1999	11.3	13.1	13.3	13.3	13.7	14.1	
		2000–2013	13.1	13.8	14.4	14.1	14.5	15.2	0.9
		2014–2022	14.8	15.1	15.3	15.3	15.5	16.2	2.0
	3	1984–1999	15.5	16.6	17.3	17.3	18.0	19.3	
		2000–2013	17.7	18.1	18.4	18.5	18.9	20.4	1.2
		2014–2022	17.6	19.2	20.1	19.7	20.4	20.6	2.4
	4	1984–1999	16.6	17.3	17.9	17.8	18.2	19.0	
		2000–2013	17.3	18.4	18.9	19.0	19.5	20.7	1.2
		2014–2022	19.1	20.1	20.3	20.3	20.6	21.5	2.5

Periods in this table are from 1984 to 1999; from 2000 to 2013; and from 2014 to 2022. The last column refers to the mean differences (°C) of 2000–2013 and 2014–2022 compared with 1984–1999.

Island in the northern extreme of the Salish Sea. Kelp persistence remained in Burrard Inlet, southern Vancouver Island, and the southern Gulf Islands.

Summarizing these changes at the Cluster and sector level (Figure 6 and Table 2), the northern sector had a historical kelp baseline presence of 179 segments. Among them, 45% were non-persistent in the PreBlob period and 79% in the Blob+Post period. The most exposed coastlines to high tidal current and colder temperatures (Cluster 1), as well as more sheltered areas (Cluster 2), show a moderate reduction in the PreBlob period that increased sharply in Blob+Post, suggesting that an important reduction occurred in recent years. On the exposed coasts in the Strait of Georgia (Cluster 3), a small fraction of historical kelp persisted in the PreBlob period, which also decreased for the Blob+Post. The warmest and most sheltered areas (Cluster 4) had a small record of historical kelp that was reduced to two and one segments in the PreBlob and Blob+Post periods, respectively.

In the southern sector (Figure 6 and Table 2), the coldest coastlines show a noticeable long-term persistence among the 474 segments with historical kelp records. In general, 30% of the historical kelp were non-persistent in the PreBlob and Blob+Post periods. Most of the change occurred in the warmest and most sheltered areas of the southern sector (Cluster 4) and some reductions in Clusters 2 and 3; Cluster 1 remained stable in PreBlob and Blob+Post periods.

4 Discussion

4.1 General overview of kelp trends in the Salish Sea

Nearshore ecosystems are spatially and temporally variable, therefore, studies considering large spatial and temporal scales can more accurately identify patterns of change in presence and

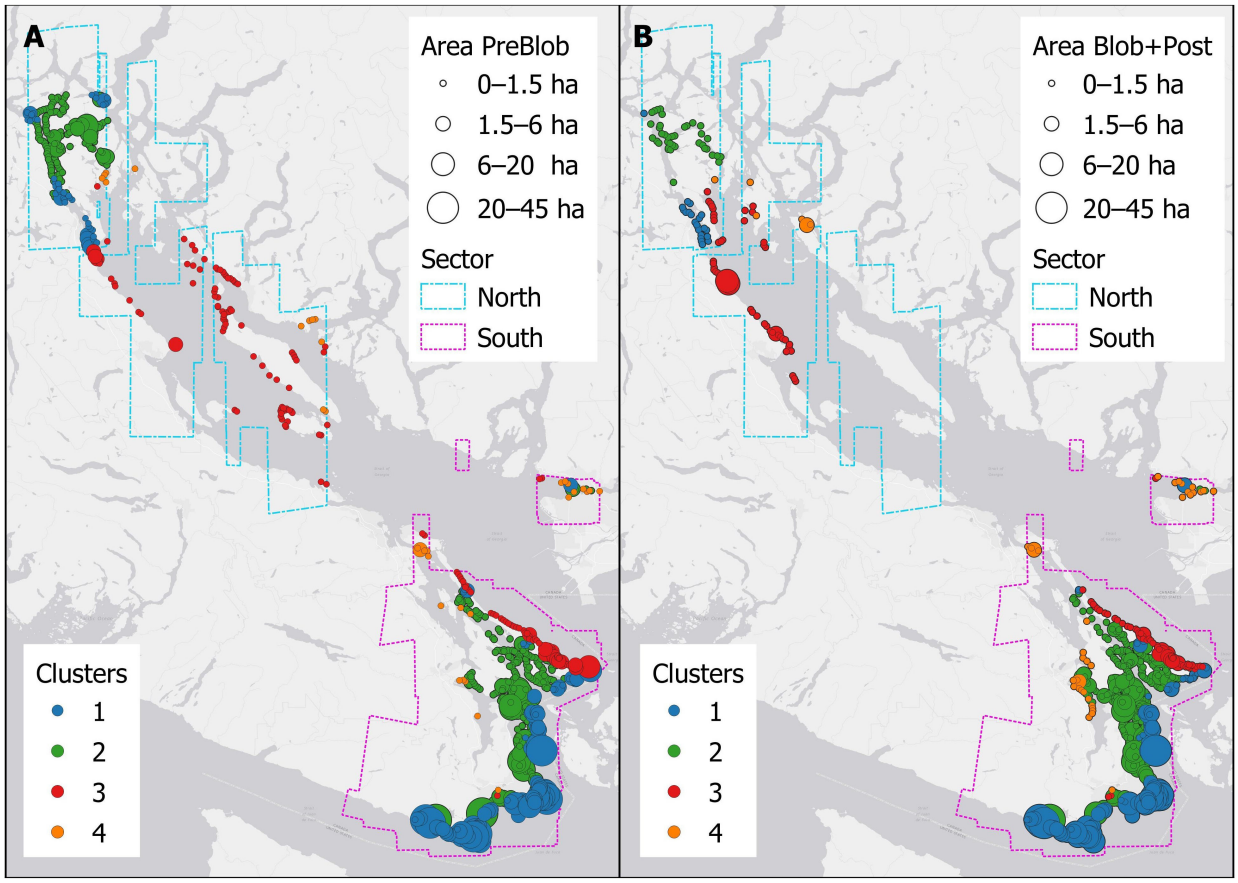

FIGURE 4
Kelp area during: **(A)** PreBlob (2002–2013), and **(B)** Blob+Post (2014–2022). In **(A, B)**, the size of the circles represents area per segment.

persistence (Steneck et al., 2002). In that regard, a dataset with long enough time frame and/or broad enough area can help to provide an understanding of kelp persistence beyond what is available to monitor with satellite imagery. This study used high spatial resolution satellite-derived kelp maps to compare areas and presence of kelp in PreBlob versus Blob+Post periods, and it also compared these periods with a baseline of historical nautical charts and nearshore SST. Our aim was to provide the first large spatial and temporal analysis of the long-term persistence of kelp in relation to the most recent effects of the Blob in the Salish Sea, an enclosed sea representing 3300 km of coastline of British Columbia, Canada. In the last two decades, the PreBlob and Blob+Post periods show a general decline in kelp area in the northern sector and stability in the south. However, century-old records bring a new perspective on these observations.

The comparison of the PreBlob with the Blob+Post period shows that kelp in the northern section of the Salish Sea decreased considerably in terms of area and distribution. A possible explanation for these results is the magnitude of nearshore SST anomalies using a baseline of four decades (1984–2022). Our nearshore SST records display an acute span of higher temperatures during and after the Blob anomaly of 2014–2019 (Blob +Post period). However, this increase was already preceded by an anomaly period of higher SST that started in 2000, which is in line with earlier studies (Amos et al., 2014). In the warmest coasts (Clusters 3 and 4), the Blob+Post spring and summer temperatures are 2.0°C higher than in the 1984–1999 period. For these regions, these anomalies represent temperatures near the lethal limit for gametophytes and blade tissue (20.0°C), especially during long periods (Supratya et al., 2020; Weigel et al., 2023). Consequently, we infer that the total area and likely density of kelp canopies were negatively impacted, making them less functional as forests.

To a certain extent, the local decrease of kelp in the warmer coastlines of the Salish Sea can be related to similar events affecting the broader Northeast Pacific region, including the Blob of 2014–2019. Prolonged and extreme marine heatwaves exerted devastating changes on kelp forests, shifting large areas of kelp habitat from previously healthy ecosystems to infertile urchin barrens (Arafeh-Dalmau et al., 2019; Cavanaugh et al., 2019; Rogers-Bennett and Catton, 2019). Previous anomalous warming events combined with intense storm activity and dampened nutrient levels meant a reduction in kelp growth and life span (Dayton and Tegner, 1984; Tegner et al., 1997). Although the nature and extent of kelp fluctuations have shown to be variable at the local level (Cavanaugh et al., 2019; Mora-Soto et al., 2024; Starko et al., 2022, 2024), absolute and relative high temperatures beyond a stressing level are frequently associated with devastating kelp loss and co-occurrence of cascading effects in the associated ecosystem (Cavanaugh et al., 2019; McPherson et al., 2021).

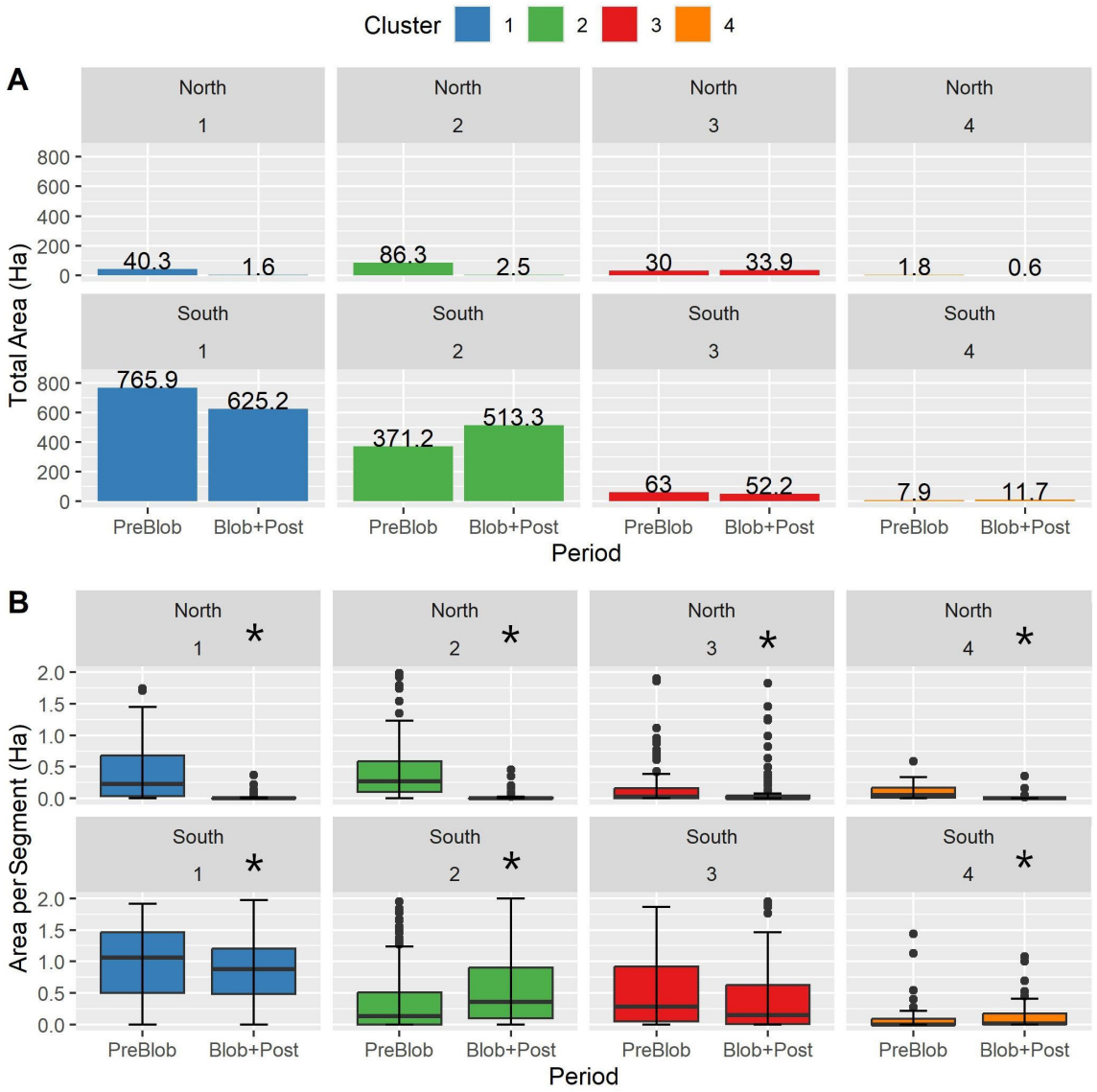

FIGURE 5
(A) Kelp total area by cluster corresponding to the northern and southern sectors of the Salish Sea during PreBlob (2002–2013) and Blob+Post (2014–2022) periods. **(B)** Kelp area per coastal segment by period, cluster, and sector. The asterisks indicate significant differences (Kruskal-Wallis test p-value <0.005).

In contrast, the coldest coasts in the northern sector, represented by Clusters 1 and 2, were warmer by 1.0°C in spring and summer compared to the 1984–1999 baseline but remained within the thermal tolerance limit (<17.0°C) (Springer et al., 2010; Supratya et al., 2020). The reasons for the kelp decrease in these clusters remain unclear and require further studies. The southern section of the Salish Sea remained relatively stable compared with the northern section. Kelp beds changed in area from PreBlob to Blob+Post (-140.7 ha in Cluster 1, +142.1 ha in Cluster 2, -10.8 ha in Cluster 3, +3.8 ha in Cluster 4), but their distributions remained at similar locations, suggesting that area fluctuations do not necessarily mean strong drops in presence. This affirmation is supported by earlier research on kelp resilience in this area (Mora-Soto et al., 2024).

Our data indicates that persistent kelp happens in Clusters 1 and 2 in the southern sector. This result could be explained by local variables, such as nutrient availability and currents. Nutrient availability driven by freshwater inputs from the Fraser River (Khangaonkar et al., 2021) and others could support kelp presence, given that increased nitrogen positively increases the density and size of sporophytes within the thermal tolerance limit of 20.0°C (Weigel et al., 2023). In previous research, Berry et al. (2021) have indicated that currents, either by superficial wave velocity or deep-water mixing, play an important role in kelp persistence in the Puget Sound region of the Salish Sea because high hydrodynamic flows can bring nitrogen and other nutrients to the kelp. As Clusters 1 and 2 south are represented by high tidal amplitude current (m/s), high fetch, and lower SSTs, their behavior support Berry et al. (2021)'s observations of kelp persistence at highly dynamic and enhanced nutrient areas. In that case, high fetch could be a complementary factor that helps sustain kelp

10.3389/fmars.2024.1446380

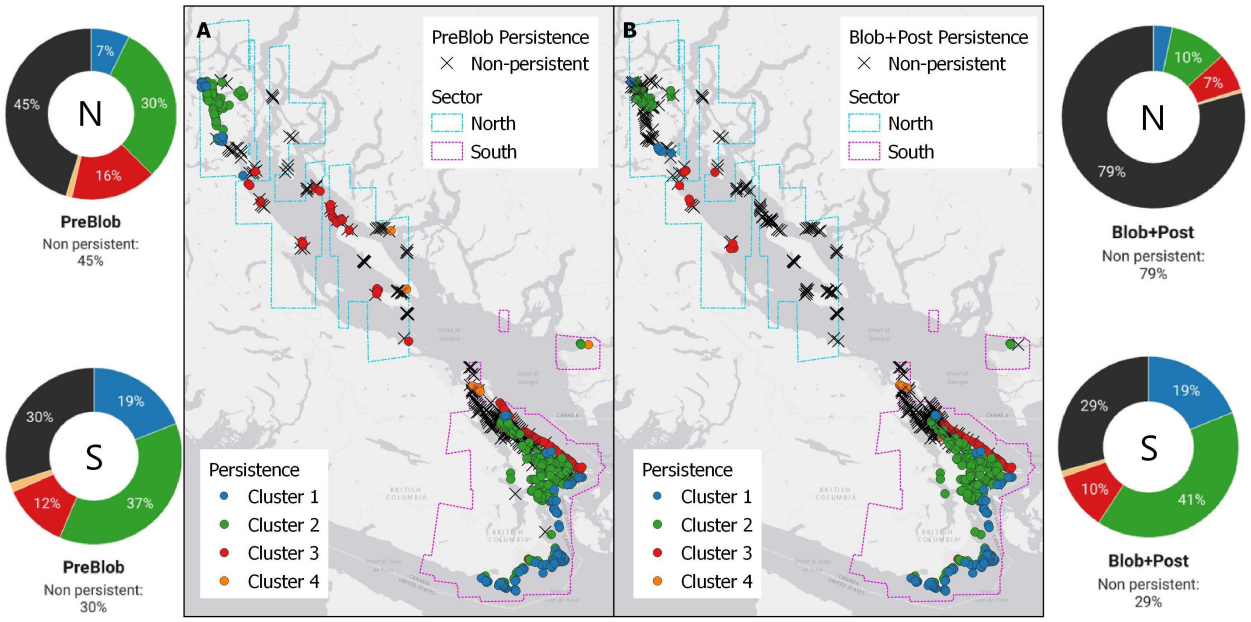

FIGURE 6
Comparison of historical long-term persistence of kelp from historical records with the **(A)** PreBlob period (2002–2013) and **(B)** the Blob+Post period (2014–2022). In **(A, B)**, crosses represent non-persistence and circles represent persistence classified by cluster, compared with the historical nautical charts (1858–1956) from Costa et al., 2020. Donut charts at both sides summarize the persistence of the clusters in the northern (N) and southern (S) sectors of the Salish Sea.

resilience under thermal stress and contributes to long-term persistence (Mora-Soto et al., 2024; Pfister et al., 2017), as well as the wind-motion regime that could potentially increase kelp resilience (Mora-Soto et al., 2024). Lacking high fetch or large freshwater inputs, Clusters 1 and 2 in the northern sector show less resilient kelp than in the south.

4.2 Historical and ecological perspectives of the Salish Sea kelp ecosystem

The persistence assessment, comparing PreBlob and Blob+Post periods with the historical baseline, reveals that kelp beds in the northern sector of the Salish Sea are present in a minor portion of the places where they existed in the late 19th and early 20th centuries (55% and 21% of persistent kelp, respectively). Most of the decreases in the northern sector occurred before the PreBlob times in the warmest coastlines and the Strait of Georgia, while a recent drop occurred in the Blob+Post times in the coldest and semi-sheltered coastlines. On the other hand, the coldest coasts in the southern sector, in the Strait of Juan de Fuca, show a constant 30% loss compared to the historical kelp baseline, implying that the fluctuations of the last decades do not reflect significant changes in long-term persistence. This result aligns with previous regional research in Washington State (Berry et al., 2021; Pfister et al., 2017).

TABLE 2 Summary of the long-term persistence of segments in the northern and southern sectors of the Salish Sea (illustrated in Figure 6).

Sector	Cluster	Nautical Charts	PreBlob	Blob+Post
North = 179 segments	Cluster 1	22 (12%)	13 (7%)	6 (3%)
	Cluster 2	61 (34%)	54 (30%)	18 (10%)
	Cluster 3	85 (47%)	29 (16%)	12 (7%)
	Cluster 4	11 (6%)	2 (1%)	1 (1%)
	Non-persistent		81 (45%)	142 (79%)
South = 474 segments	Cluster 1	90 (19%)	90 (19%)	89 (19%)
	Cluster 2	234 (49%)	177 (37%)	192 (41%)
	Cluster 3	81 (17%)	57 (12%)	49 (10%)
	Cluster 4	69 (15%)	8 (2%)	5 (1%)
	Non-persistent		142 (30%)	139 (29%)

The numbers in PreBlob and Blob+Post refer to segments (%) compared to the Nautical Charts baseline.

In previous research, Mora-Soto et al. (2024) showed that kelp located around southern Vancouver Island and the southern Gulf Islands (southern sector in this research) were resilient to marine heatwaves that occurred between 2014 to 2019. In this study, we show that in warmer locations like Cluster 4, a small fraction of kelp had persisted compared to a century ago, indicating that the decline happened before the decade of 2010. This finding largely agrees with previous research spanning 145 years in the southern Puget Sound, in the southern Salish Sea (Berry et al., 2021).

Other factors not analyzed in this research that may have played a role in long-term trends of kelp persistence include the presence (or lack) of nutrients (Weigel et al., 2023), plus effects of herbivory from urchins (Estes et al., 2016; Estes and Duggins, 1995; Wilmers et al., 2012) and kelp crabs (Dobkowski, 2017), with limited presence of predators like sea otters (*Enhydra lutris*). Century-long assessments have demonstrated that sea otters are drivers of kelp recovery and area increases (Hollarsmith et al., 2024; Nicholson et al., 2024). However, archaeological records show that sea otters have been nearly absent in the Salish Sea for the past 8,000 years (McKechnie and Wigen, 2011), contrary to the Strait of Juan de Fuca and the western side of Vancouver Island (Klinkenberg, 2012; Nichol et al., 2020). In contrast, spatial distribution models of green, red, and purple urchins in the Salish Sea built from species occurrence records from 2005–2021 (Nephin et al., 2020), provided in the Supplementary Material, show a high likelihood for the occurrence of red (Supplementary Figure S5) and green (Supplementary Figure S6) urchins in both the northern and the southern borders of the Salish Sea, matching kelp distribution patterns. The urchin-kelp-sea otter link is a well-known factor contributing to kelp persistence in the Northeast Pacific due to the key ecological role of sea otters in exerting top-down control on kelp herbivory (Estes et al., 2016; Estes and Duggins, 1995; Wilmers et al., 2012). Since there is a relative lack of sea otters in the Salish Sea, there may be more impact from urchins driving declines or preventing recovery of kelp after stressing periods like the Blob, but comparisons of past versus modern records to support that correlation are missing. Further studies that take these dynamics into account will need to be undertaken.

Another important factor to consider in future research is the role of anthropogenic disturbances (Dayton et al., 1998; Steneck et al., 2002) that could add more pressure on kelp already stressed by ocean warming. Our data show that relatively century-persistent kelp areas remain in highly populated areas like Burrard Inlet in Vancouver (Cluster 2) and around the Greater Victoria area (Clusters 1 and 2). However, a recent drop in kelp persistence occurred near Quadra Island and the Discovery Passage (Clusters 1 and 2), which is a narrow pass within the Salish Sea extending to the north of Vancouver Island, with relatively low levels of modern human occupation. Still, there are visible effects of land use changes, including logging, major shipping traffic routes, and industrial activities, among others (Hollarsmith et al., 2022). This area (Clusters 1 and 2 north) is characterized by the coldest clusters in which, for the period of analysis, temperatures did not reach sub-lethal levels for kelp growth (beyond 20.0°C; Supratya et al., 2020). Evaluating the effects of mechanical removal of fronds, pollution, or other types of disturbances could give more clues on the reasons for the decrease in remote and less populated areas, considering that urbanization and other economic activities such as lumber production and fishing have largely degraded ecosystems on the eastern border of the Strait of Juan de Fuca and Puget Sound (Berry et al., 2021; Pfister et al., 2017).

4.3 Use of remote sensing data to determine long-term changes of kelp in the study area

We acknowledge both the strengths and limitations of our remote sensing approach. In the northern section, our modest imagery coverage (limited by cloud cover and archived data availability) for modern kelp was mainly represented by narrow kelp beds along the coastline, while the more comprehensive available imagery for the southern section showed more extensive kelp beds. Narrow kelp beds are prevalent on the coastlines of British Columbia, characterized by high-slope bathymetries and a complex geography of islands and channels (Cavanaugh et al., 2021; Gendall et al., 2023). In these areas, kelp beds are prone to more uncertainties when mapped with medium-resolution (~30 m) satellite imagery versus areas of low-slope bathymetries where kelp areas are generally larger (Gendall et al., 2023; Mora-Soto et al., 2021; Nijland et al., 2019). For this reason, this research used only high-resolution imagery, which is limited in frequency but brings the best results at detecting kelp in this region. In the northern sector, the lack of modern kelp does not necessarily mean that kelps have vanished completely; currents, tidal fluctuations, water mixing, and the frequency of available imagery could have played a role in reducing their detectability (Cavanaugh et al., 2021; Gendall et al., 2023). Additionally, the semi-stochastic nature of *Nereocystis* (Springer et al., 2010) can cause significant variability in detecting kelp at the segment level (Mora-Soto et al., 2024). Nevertheless, our protocol, which used very high-resolution imagery compilation and a detailed mapping process, was designed to detect and map conspicuous canopies. Therefore, our results suggest that the northern canopies are not large or dense enough to form functional underwater forests as found in the more extensive kelp beds in the southern section of the study area. Our assemblage of several coastline segments at the cluster level suggests that even with very high-resolution imagery, there are fewer chances to detect fringing kelp beds in modern records.

4.4 Management implications

The results of this study can inform present and future management needs, such as managing kelp harvesting, identifying potential marine protected areas, and prioritizing kelp restoration projects in British Columbia and the Northeast Pacific (Cavanaugh et al., 2021). Specifically, this research emphasizes that realistic expectations for future restoration projects will be better informed by considering both the historical baseline and local environmental conditions. As the Strait of Georgia coastline and most sheltered coastlines (Clusters 3 and 4) predominantly show

non-persistent kelp in modern times compared to historical kelp, restoring these habitats to reach the historical baseline may be a difficult task, considering the present environmental conditions. The recent kelp decrease in the northern area could be the focus of more urgent attention, while the extreme southern reaches of the study area do not seem to be of immediate concern unless environmental conditions change. Further studies are recommended to understand the causes of losses in remote areas, while more experimental *in-situ* data could lead to a new chapter on the conservation and restoration of coastal ecosystems in the Salish Sea.

5 Conclusion

This research explored the long-term persistence of kelp forests in the Salish Sea of British Columbia, Canada, by comparing remote sensing-derived modern snapshots (2002–2013 and 2014–2022), representing PreBlob and Blob+Post conditions, respectively, and contrasting them with historical kelp from the late 19th to early 20th centuries. These data were complemented with nearshore SST from a baseline of four decades (1984–2022). Nearshore temperatures showed a warming trend, with two anomaly periods starting in 2000 and 2014. Further, higher temperature anomalies occurred in warmer areas than in colder areas. The colder coasts in the southern section, from southern Vancouver Island to the Gulf Islands, fluctuated in kelp area but remained persistent in comparison with the historical record. Kelp area also fluctuated along the coasts of the Strait of Georgia and the most sheltered coastlines, but kelp beds only persisted in small fractions compared to their historical distributions. On the coldest coasts of the northern section, kelp was seldom found in the 2014–2022 period, suggesting that more studies are required to understand the underlying reasons for the area decrease along these coastlines. Overall, given the clear evidence of increasing temperatures and previous literature showing the adverse effects of temperature on *Nereocystis*, further studies should consider nearshore SST among the root causes that negatively impact kelp persistence. These data could help to determine the best strategies for conserving and restoring this ecosystem in present and future times.

Data availability statement

The raw data supporting the conclusions of this article will be made available on request to MC (maycira@uvic.ca), without undue reservation.

Author contributions

AM-S: Conceptualization, Data curation, Formal analysis, Investigation, Methodology, Software, Validation, Visualization, Writing – original draft, Writing – review & editing. SS: Conceptualization, Data curation, Investigation, Methodology, Software, Validation, Visualization, Writing – review & editing. LG: Conceptualization, Data curation, Investigation, Methodology, Software, Validation, Writing – review & editing. AW: Investigation, Methodology, Validation, Writing – review & editing. GN: Data curation, Formal analysis, Investigation, Writing – review & editing. SR: Writing – review & editing. IP: Funding acquisition, Project administration, Resources, Writing – review & editing. ER: Funding acquisition, Resources, Writing – review & editing. JL: Funding acquisition, Resources, Writing – review & editing. KM: Funding acquisition, Resources, Writing – review & editing. MC: Conceptualization, Funding acquisition, Methodology, Project administration, Resources, Supervision, Writing – review & editing.

Funding

The author(s) declare financial support was received for the research, authorship, and/or publication of this article. This work was supported by Fisheries and Oceans Canada and the Canadian Hydrographic Service to obtain the high-resolution satellite imagery, the Capital Regional District of Victoria for providing high-resolution aerial photos, and the Island Trust Conservancy for providing *in-situ* kelp observation for validation of classified kelp. Funds were available from the Pacific Salmon Foundation through a Mitacs Accelerate grant awarded to AM-S and technician salary to process digital images. Funds were also available from the Natural Sciences and Engineering Research Council of Canada Alliance grant awarded to MC (Ref. number: ALLRP 566735 - 21).

Acknowledgments

We thank the collaboration from local partners (Hakai Institute, MaPP, Mayne Island Conservancy, Parks Canada) at different stages of this project.

Conflict of interest

The authors declare that the research was conducted in the absence of any commercial or financial relationships that could be construed as a potential conflict of interest.

Publisher's note

Supplementary material

The Supplementary Material for this article can be found online at: https://www.frontiersin.org/articles/10.3389/fmars.2024.1446380/full#supplementary-material

References

Amos, C. L., Martino, S., Sutherland, T. F., and Al Rashidi, T. (2014). Sea surface temperature trends in the coastal zone of British Columbia, Canada. *J. Coast. Res.* 31, 434–446. doi: 10.2112/JCOASTRES-D-14-00114.1

Arafeh-Dalmau, N., Montaño-Moctezuma, G., Martínez, J. A., Beas-Luna, R., Schoeman, D. S., and Torres-Moye, G. (2019). Extreme marine heatwaves alter kelp forest community near its equatorward distribution limit. *Front. Mar. Sci.* 6. doi: 10.3389/fmars.2019.00499

Bell, T. W., Allen, J. G., Cavanaugh, K. C., and Siegel, D. A. (2020). Three decades of variability in California's giant kelp forests from the Landsat satellites. *Remote Sens. Environ.* 238, 110811. doi: 10.1016/j.rse.2018.06.039

Bell, T. W., Cavanaugh, K. C., Reed, D. C., and Siegel, D. A. (2015). Geographical variability in the controls of giant kelp biomass dynamics. *J. Biogeogr.* 42, 2010–2021. doi: 10.1111/jbi.12550

Bell, T. W., Cavanaugh, K. C., Saccomanno, V. R., Cavanaugh, K. C., Houskeeper, H. F., Eddy, N., et al. (2023). Kelpwatch: a new visualization and analysis tool to explore kelp canopy dynamics reveals variable response to and recovery from marine heatwaves. *PLoS One* 18, e0271477. doi: 10.1371/journal.pone.0271477

Berry, H. D., Mumford, T. F., Christiaen, B., Dowty, P., Calloway, M., Ferrier, L., et al. (2021). Long-term changes in kelp forests in an inner basin of the Salish Sea. *PLoS One* 16, e0229703. doi: 10.1371/journal.pone.0229703

Bond, N. A., Cronin, M. F., Freeland, H., and Mantua, N. (2015). Causes and impacts of the 2014 warm anomaly in the NE Pacific. *Geophys. Res. Lett.* 42, 3414–3420. doi: 10.1002/2015GL063306

Cavanaugh, K. C., Bell, T., Costa, M., Eddy, N. E., Gendall, L., Gleason, M. G., et al. (2021). A review of the opportunities and challenges for using remote sensing for management of surface-canopy forming kelps. *Front. Mar. Sci.* 8. doi: 10.3389/fmars.2021.753531

Cavanaugh, K. C., Reed, D. C., Bell, T. W., Castorani, M. C. N., and Beas-Luna, R. (2019). Spatial variability in the resistance and resilience of giant kelp in southern and Baja California to a multiyear heatwave. *Front. Mar. Sci.* 6. doi: 10.3389/fmars.2019.00413

Cavanaugh, K. C., Siegel, D. A., Reed, D. C., and Dennison, P. E. (2011). Environmental controls of giant-kelp biomass in the Santa Barbara Channel, California. *Mar. Ecol. Prog. Ser.* 429, 1–17. doi: 10.3354/meps09141

Chen, Z., Shi, J., Liu, Q., Chen, H., and Li, C. (2021). A persistent and intense marine heatwave in the Northeast Pacific during 2019–2020. *Geophys. Res. Lett.* 48, e2021GL093239. doi: 10.1029/2021GL093239

Connell, J. H., and Sousa, W. P. (1983). On the evidence needed to judge ecological stability or persistence. *Am. Nat.* 121, 789–824. doi: 10.1086/284105

Costa, M., Le Baron, N., Tenhunen, K., Nephin, J., Willis, P., Mortimor, J. P., et al. (2020). Historical distribution of kelp forests on the coast of British Columbia: 1858–1956. *Appl. Geogr.* 120, 102230. doi: 10.1016/j.apgeog.2020.102230

Davis, N. N., Badger, J., Hahmann, A. N., Hansen, B. O., Mortensen, N. G., Kelly, M., et al. (2023). The Global Wind Atlas: a high-resolution dataset of climatologies and associated web-based application. *Bull. Am. Meteorol. Soc.* 104, E1507–E1525. doi: 10.1175/BAMS-D-21-0075.1

Dayton, P. K., and Tegner, M. J. (1984). Catastrophic storms, El Niño, and patch stability in a southern California kelp community. *Science* 224, 283–285. doi: 10.1126/science.224.4646.283

Dayton, P. K., Tegner, M. J., Edwards, P. B., and Riser, K. L. (1998). Sliding baselines, ghosts, and reduced expectations in kelp forest communities. *Ecol. Appl.* 8, 309–322. doi: 10.1890/1051-0761(1998)008[0309:SBGARE]2.0.CO;2

Dillehay, T. D., Ramírez, C., Pino, M., Collins, M. B., Rossen, J., and Pino-Navarro, J. D. (2008). Monte Verde: seaweed, food, medicine, and the peopling of South America. *Science* 320, 784–786. doi: 10.1126/science.1156533

Dobkowski, K. (2017). The role of kelp crabs as consumers in bull kelp forests—evidence from laboratory feeding trials and field enclosures. *PeerJ* 5, e3372. doi: 10.7717/peerj.3372

Erlandson, J. M., Graham, M. H., Bourque, B. J., Corbett, D., Estes, J. A., and Steneck, R. S. (2007). The kelp highway hypothesis: marine ecology, the coastal migration theory, and the peopling of the Americas. *J. Island Coast. Archaeol.* 2, 161–174. doi: 10.1080/15564890701628612

Estes, J. A., Burdin, A., and Doak, D. F. (2016). Sea otters, kelp forests, and the extinction of Steller's sea cow. *Proc. Natl. Acad. Sci.* 113, 880–885. doi: 10.1073/pnas.1502552112

Estes, J. A., and Duggins, D. O. (1995). Sea otters and kelp forests in Alaska: generality and variation in a community ecological paradigm. *Ecol. Monogr.* 65, 75–100. doi: 10.2307/2937159

Foreman, M. G. G., Sutherland, G., and Cummins, P. F. (2004). M2 tidal dissipation around Vancouver Island: an inverse approach. *Continental Shelf Res.* 24, 2167–2185. doi: 10.1016/j.csr.2004.07.008

Gale, K. S. P., Frid, A., Lee, L., McCarthy, J.-B., Robb, C., Rubidge, E., et al. (2019). *A framework for identification of ecological conservation priorities for marine protected area network design and its application in the Northern Shelf Bioregion* (Nanaimo, BC Canada: Canadian Science Advisory Secretariat). Available at: https://publications.gc.ca/site/eng/9.871144/publication.html

Gendall, L., Schroeder, S. B., Wills, P., Hessing-Lewis, M., and Costa, M. (2023). A multi-satellite mapping framework for floating kelp forests. *Remote Sens.* 15, 1276. doi: 10.3390/rs15051276

Giannini, F., Hunt, B. P. V., Jacoby, D., and Costa, M. (2021). Performance of OLCI Sentinel-3A satellite in the Northeast Pacific coastal waters. *Remote Sens. Environ.* 256, 112317. doi: 10.1016/j.rse.2021.112317

Gitelson, A. A., Kaufman, Y. J., and Merzlyak, M. N. (1996). Use of a green channel in remote sensing of global vegetation from EOS-MODIS. *Remote Sens. Environ.* 58, 289–298. doi: 10.1016/S0034-4257(96)00072-7

Gorelick, N., Hancher, M., Dixon, M., Ilyushchenko, S., Thau, D., and Moore, R. (2017). Google Earth Engine: planetary-scale geospatial analysis for everyone. *Remote Sens. Environ.* 202, 18–27. doi: 10.1016/j.rse.2017.06.031

Gregr, E. J., Palacios, D. M., Thompson, A., and Chan, K. M. A. (2019). Why less complexity produces better forecasts: an independent data evaluation of kelp habitat models. *Ecography* 42, 428–443. doi: 10.1111/ecog.03470

Hamilton, S. L., Bell, T. W., Watson, J. R., Grorud-Colvert, K. A., and Menge, B. A. (2020). Remote sensing: generation of long-term kelp bed data sets for evaluation of impacts of climatic variation. *Ecology* 101, e03031. doi: 10.1002/ecy.3031

Hartigan, J. A., and Wong, M. A. (1979). Algorithm AS 136: a K-Means clustering algorithm. *J. R. Stat. Soc. Ser. C Appl. Stat.* 28, 100–108. doi: 10.2307/2346830

Hollarsmith, J. A., Andrews, K., Naar, N., Starko, S., Calloway, M., Obaza, A., et al. (2022). Toward a conceptual framework for managing and conserving marine habitats: a case study of kelp forests in the Salish Sea. *Ecol. Evol.* 12, e8510. doi: 10.1002/ece3.8510

Hollarsmith, J. A., Cornett, J. C., Evenson, E., and Tugaw, A. (2024). A century of canopy kelp persistence and recovery in the Gulf of Alaska. *Ann. Bot.* 133, 105–116. doi: 10.1093/aob/mcad149

Imray, J. F. (1870). *North pacific pilot, part 1: sailing directions for the west coast of North America* (London: James Imray & Son).

Jackson, J. B. C., Kirby, M. X., Berger, W. H., Bjorndal, K. A., Botsford, L. W., Bourque, B. J., et al. (2001). Historical overfishing and the recent collapse of coastal ecosystems. *Science* 293, 629–637. doi: 10.1126/science.1059199

Jackson, J. M., Johnson, G. C., Dosser, H. V., and Ross, T. (2018). Warming from recent marine heatwave lingers in deep British Columbia fjord. *Geophys. Res. Lett.* 45, 9757–9764. doi: 10.1029/2018GL078971

Khangaonkar, T., Nugraha, A., Yun, S. K., Premathilake, L., Keister, J. E., and Bos, J. (2021). Propagation of the 2014–2016 Northeast Pacific marine heatwave through the Salish Sea. *Front. Mar. Sci.* 8. doi: 10.3389/fmars.2021.787604

Klinkenberg, B. (2012). *E-Fauna BC: electronic atlas of the fauna of British Columbia*. Available online at: https://ibis.geog.ubc.ca/biodiversity/efauna/indexoneword.shtml.

Kobluk, H. M., Gladstone, K., Reid, M., Brown, K., Krumhansl, K. A., and Salomon, A. K. (2021). Indigenous knowledge of key ecological processes confers resilience to a small-scale kelp fishery. *People Nat.* 3, 723–739. doi: 10.1002/pan3.10211

Kriegler, F. J., Malila, W. A., Nalepka, R. F., and Richardson, W. (1969). Preprocessing transformations and their effects on multispectral recognition. *Remote Sens. Environ. VI* 97–131.

Krumhansl, K. A., Okamoto, D. K., Rassweiler, A., Novak, M., Bolton, J. J., Cavanaugh, K. C., et al. (2016). Global patterns of kelp forest change over the past half-century. *Proc. Natl. Acad. Sci.* 113, 13785–13790. doi: 10.1073/pnas.1606102113

Kruskal, W. H., and Wallis, W. A. (1952). Use of ranks in one-criterion variance analysis. *J. Am. Stat. Assoc.* 47, 583–621. doi: 10.1080/01621459.1952.10483441

McKechnie, I., and Wigen, R. J. (2011). "Toward a historical ecology of pinniped and sea otter hunting traditions on the coast of Southern British Columbia," in *Human impacts on seals, sea lions, and sea otters: integrating archaeology and ecology in the Northeast Pacific, 1st ed.* Eds. T. J. Braje and T. C. Rick (Oakland, CA: University of California Press), 129–166. doi: 10.1525/j.ctt1pntkp.10

McPherson, M. L., Finger, D. J. I., Houskeeper, H. F., Bell, T. W., Carr, M. H., Rogers-Bennett, L., et al. (2021). Large-scale shift in the structure of a kelp forest ecosystem co-occurs with an epizootic and marine heatwave. *Commun. Biol.* 4, 298. doi: 10.1038/s42003-021-01827-6

Mora-Soto, A., Capsey, A., Friedlander, A. M., Palacios, M., Brewin, P. E., Golding, N., et al. (2021). One of the least disturbed marine coastal ecosystems on Earth: spatial and temporal persistence of Darwin's sub-Antarctic giant kelp forests. *J. Biogeogr.* 48, 2562–2577. doi: 10.1111/jbi.14221

Mora-Soto, A., Schroeder, S., Gendall, L., Wachmann, A., Narayan, G. R., Read, S., et al. (2024). Kelp dynamics and environmental drivers in the southern Salish Sea, British Columbia, Canada. *Front. Mar. Sci.* 11. doi: 10.3389/fmars.2024.1323448

MPA Network BC Northern Shelf Initiative (2023). *Network action plan – A summary*. Available online at: https://www.dfo-mpo.gc.ca/oceans/publications/nsb-mpan-ramp-bpn/index-eng.html (Accessed 03 July, 2024).

Nephin, J., Gregr, E. J., St. Germain, C., Fields, C., and Finney, J. L. (2020). *Development of a species distribution modelling framework and its application to twelve species on Canada's pacific coast.* (Ottawa ON, Canada: DFO Can. Sci. Advis. Sec. Res. Doc). xii + 107 p.

Nichol, L. M., Doniol-Valcroze, T., Watson, J. C., and Foster, E. U. (2020). Trends in growth of the sea otter (*Enhydra lutris*) population in British Columbia 1977 to 2017 (Nanaimo, BC Canada: DFO Can. Sci. Advis. Sec. Res. Doc). vii + 29 p.

Nicholson, T. E., McClenachan, L., Tanaka, K. R., and Van Houtan, K. S. (2024). Sea otter recovery buffers century-scale declines in California kelp forests. *PLoS Climate* 3, e0000290. doi: 10.1371/journal.pclm.0000290

Nijland, W., Reshitnyk, L., and Rubidge, E. (2019). Satellite remote sensing of canopy-forming kelp on a complex coastline: a novel procedure using the Landsat image archive. *Remote Sens. Environ.* 220, 41–50. doi: 10.1016/j.rse.2018.10.032

Pedersen, M. F., Filbee-Dexter, K., Frisk, N. L., Sárossy, Z., and Wernberg, T. (2021). Carbon sequestration potential increased by incomplete anaerobic decomposition of kelp detritus. *Mar. Ecol. Prog. Ser.* 660, 53–67. doi: 10.3354/meps13613

Pfister, C. A., Berry, H. D., and Mumford, T. (2017). The dynamics of Kelp Forests in the Northeast Pacific Ocean and the relationship with environmental drivers. *J. Ecol.* 106, 1520–1533. doi: 10.1111/1365-2745.12908

R Core Team (2024). *R: A language and environment for statistical computing* (Vienna, Austria: R Foundation for Statistical Computing). Available at: https://www.r-project.org/.

Rogers-Bennett, L., and Catton, C. A. (2019). Marine heat wave and multiple stressors tip bull kelp forest to sea urchin barrens. *Sci. Rep.* 9, 15050. doi: 10.1038/s41598-019-51114-y

Schiel, D. R., Steinbeck, J. R., and Foster, M. S. (2004). Ten years of induced ocean warming causes comprehensive changes in marine benthic communities. *Ecology* 85, 1833–1839. doi: 10.1890/03-3107

Schroeder, S. B., Boyer, L., Juanes, F., and Costa, M. (2020). Spatial and temporal persistence of nearshore kelp beds on the west coast of British Columbia, Canada using satellite remote sensing. *Remote Sens. Ecol. Conserv.* 6, 327–343. doi: 10.1002/rse2.142

Schroeder, S. B., Dupont, C., Boyer, L., Juanes, F., and Costa, M. (2019). Passive remote sensing technology for mapping bull kelp (*Nereocystis luetkeana*): a review of techniques and regional case study. *Global Ecol. Conserv.* 19, e00683. doi: 10.1016/j.gecco.2019.e00683

Shaffer, A. (2003). "Preferential use of nearshore kelp habitats by juvenile salmon and forage fish," in *Proceedings of the 2003 Georgia Basin/Puget Sound Research Conference*. (Vancouver, Canada: Puget Sound Action Team), 1–11.

Smale, D. A. (2020). Impacts of ocean warming on kelp forest ecosystems. *New Phytol.* 225, 1447–1454. doi: 10.1111/nph.16107

Springer, Y. P., Hays, C. G., Carr, M. H., and Mackey, M. R. (2010). Toward ecosystem-based management of marine macroalgae—the bull kelp, *Nereocystis luetkeana*. *Oceanogr. Mar. Biol.* 48, 1. doi: 10.1201/EBK1439821169-c1

Starko, S., Neufeld, C. J., Gendall, L., Timmer, B., Campbell, L., Yakimishyn, J., et al. (2022). Microclimate predicts kelp forest extinction in the face of direct and indirect marine heatwave effects. *Ecol. Appl.* 32, e2673. doi: 10.1002/eap.2673

Starko, S., Timmer, B., Reshitnyk, L., Csordas, M., McHenry, J., Schroeder, S., et al. (2024). Local and regional variation in kelp loss and stability across coastal British Columbia. *Mar. Ecol. Prog. Ser.* 733, 1–26. doi: 10.3354/meps14548

Steneck, R. S., Graham, M. H., Bourque, B. J., Corbett, D., Erlandson, J. M., Estes, J. A., et al. (2002). Kelp forest ecosystems: biodiversity, stability, resilience and future. *Environ. Conserv.* 29, 436–459. doi: 10.1017/S0376892902000322

Supratya, V. P., Coleman, L. J. M., and Martone, P. T. (2020). Elevated temperature affects phenotypic plasticity in the bull kelp (*Nereocystis luetkeana*, Phaeophyceae). *J. Phycol.* 56, 1534–1541. doi: 10.1111/jpy.13049

Tegner, M. J., Dayton, P. K., Edwards, P. B., and Riser, K. L. (1997). Large-scale, low-frequency oceanographic effects on kelp forest succession: a tale of two cohorts. *Mar. Ecol. Prog. Ser.* 146, 117–134. doi: 10.3354/meps146117

Trimble Germany GmbH (2021). *Trimble documentation eCognition developer 10.1 user guide* (Munich, Germany: Trimble Germany GmbH).

Turner, N. J. (2001). "Coastal peoples and marine plants on the Northwest Coast," in *Proceedings of the International Association of Aquatic and Marine Science Libraries and Information Centers*, Victoria, British Columbia.

United Nations Environment Programme (2023). *Into the blue: securing a sustainable future for kelp forests* (Nairobi: GRID-Arendal).

Wachmann, A., Starko, S., Neufeld, C. J., and Costa, M. (2024). Validating Landsat analysis ready data for nearshore sea surface temperature monitoring in the Northeast Pacific. *Remote Sens.* 16, 920. doi: 10.3390/rs16050920

Weigel, B. L., Small, S. L., Berry, H. D., and Dethier, M. N. (2023). Effects of temperature and nutrients on microscopic stages of the bull kelp (*Nereocystis luetkeana*, Phaeophyceae). *J. Phycol.* 59, 893–907. doi: 10.1111/jpy.13366

Wernberg, T., Krumhansl, K., Filbee-Dexter, K., and Pedersen, M. F. (2019). "Status and trends for the world's kelp forests," in *World seas: an environmental evaluation* (London: Academic Press, Elsevier Inc.), 57–78. doi: 10.1016/B978-0-12-805052-1.00003-6

Wilmers, C. C., Estes, J. A., Edwards, M., Laidre, K. L., and Konar, B. (2012). Do trophic cascades affect the storage and flux of atmospheric carbon? An analysis of sea otters and kelp forests. *Front. Ecol. Environ.* 10, 409–415. doi: 10.1890/110176

Young, M., Cavanaugh, K., Bell, T., Raimondi, P., Edwards, C. A., Drake, P. T., et al. (2016). Environmental controls on spatial patterns in the long-term persistence of giant kelp in central California. *Ecol. Monogr.* 86, 45–60. doi: 10.1890/15-0267.1

frontiers | Frontiers in Marine Science

TYPE Original Research
PUBLISHED 01 October 2024
DOI 10.3389/fmars.2024.1464511

OPEN ACCESS

EDITED BY
Christopher Edward Cornwall,
Victoria University of Wellington,
New Zealand

REVIEWED BY
Shigeki Wada,
University of Tsukuba, Japan
Jinlin Liu,
Tongji University, China

*CORRESPONDENCE
Hailong Wu
hlwu@jou.edu.cn

RECEIVED 14 July 2024
ACCEPTED 06 September 2024
PUBLISHED 01 October 2024

CITATION
Wu H, Zhang J, Li H, Li S, Pan C, Yi L, Xu J and He P (2024) Ocean warming enhances the competitive advantage of *Ulva prolifera* over a golden tide alga, *Sargassum horneri* under eutrophication.
Front. Mar. Sci. 11:1464511.
doi: 10.3389/fmars.2024.1464511

Ocean warming enhances the competitive advantage of *Ulva prolifera* over a golden tide alga, *Sargassum horneri* under eutrophication

Hailong Wu[1,2]*, Jiankai Zhang[1,2], He Li[1,2], Sufang Li[1,2], Chen Pan[1,2], Lefei Yi[1,2], Juntian Xu[1,2] and Peimin He[2,3]

[1]Jiangsu Key Laboratory of Marine Bioresources and Environment, Jiangsu Ocean University, Lianyungang, China, [2]Co-Innovation Center of Jiangsu Marine Bio-industry Technology, Jiangsu Ocean University, Lianyungang, China, [3]College of Marine Ecology and Environment, Shanghai Ocean University, Shanghai, China

Recent years have seen the *Ulva* green tide and *Sargassum* golden tide become commonplace in the coastal waters of China. However, little is known on how the combination of ocean warming and eutrophication would affect the interaction of green and golden tides. In this study, we cultured the green tide alga *Ulva prolifera* and the golden tide alga *Sargassum horneri* under different temperatures (5, 10, 15, 20, 25, and 30°C) and two nutrient concentrations (Low nutrient, LN: 5 μM-nitrate and 0.5 μM-phosphate; High nutrient, HN: 500 μM-N and 50 μM-P) in both monoculture and coculture systems to investigate the physiological responses and their competitive relationships. In monocultures, the growth of *U. prolifera* and *S. horneri*, along with pigment concentrations and photosynthesis, increased with rising temperature, reaching a plateau at 15 - 25°C. However, when the temperature increased to 30°C, the growth of *U. prolifera* and *S. horneri* decreased abruptly, with *S. horneri* even suffering death. In coculture, the growth of both *U. prolifera* and *S. horneri* was inhibited compared to the monoculture, with the greatest decline observed in *S. horneri* at 25°C under two nutrient conditions. Our results show that *U. prolifera* would outcompete *S. horneri* under high temperature in coculture, suggesting that ocean warming would enhance the competitive advantage of green tide over golden tide under eutrophication in the future.

KEYWORDS

competition, eutrophication, *Sargassum horneri*, temperature, *Ulva prolifera*

1 Introduction

Macroalgae, as important primary producers in the coastal zone, contribute about 1521 Tg C yr^{-1} of the global net primary production (Krause-Jensen and Duarte, 2016). Through carbon fixation, sequestration and habitat provision, they often play significantly structural roles in coastal ecosystems (Machado and Oliveira, 2024). Due to continued anthropogenic pressure on marine systems, many macroalgae species have been harmed by environmental changes and face an uncertain future, jeopardizing their important contributions to global productivity and ecosystem service (Hanley et al., 2024).

It is widely recognized that human-induced greenhouse gas emissions (CO_2, methane, etc.) have been the primary driver of global warming since the industrial revolution (IPCC, 2019). Over 90% of the anthropogenic increase in heat is absorbed by the global ocean, leading to ocean warming (Durack et al., 2014). The average sea surface temperature has risen by 1.1°C up to now, and is predicted to further increase 1.9 – 5.8°C by the end of the century based on Representative Concentration Pathway (RCP) 8.5 (Gattuso et al., 2015; IPCC, 2019). In addition, macroalgae also experience diurnal and seasonal temperature variations in the nature (Martin and Gattuso, 2009). It is well established that temperature directly influences intracellular biochemical reactions and metabolic activities, thereby affecting their survival and growth (Zou and Gao, 2014b; Chen et al., 2018). In a suitable range, increased temperature is beneficial for the photosynthesis and growth of macroalgae (Fan et al., 2014; Zou and Gao, 2014a). However, temperatures below or above this range can slow down growth or even cause cellular damage and mortality. High temperatures could trigger the *Ulva* to generate more reactive oxygen species (ROS), resulting in oxidative damage to proteins, lipids, DNA within cells (Apel and Hirt, 2004). Macroalgae have also evolved ROS scavenging mechanisms to cope with the potential damage from ROS, such as superoxide dismutase (SOD), ascorbate peroxidase (APX), glutathione peroxidase (GPX) and catalase (CAT) (Apel and Hirt, 2004). A previous report found that temperatures exceed 35°C inhibit the photosynthetic performance of *Ulva conglobate* (Zou and Gao, 2014a). Moreover, tropical seaweeds such as *Wurdemannia miniata* and *Valonia utricularis* were found to be induced to death under extreme high temperatures (Pakker and Breeman, 1996). Moreover, ocean warming will expand the distribution of tropical and temperate species towards the poles (Díez et al., 2012), which was supported by a model prediction (Jueterbock et al., 2013).

Under the influence of prevalently industrial and agricultural activities, the anthropogenic input of nutrients (e. g. nitrogen and phosphorus) into coastal waters has continuously increased, leading to eutrophication, a trend that threatens the health of coastal ecosystems worldwide (Paerl et al., 2014; Malone and Newton, 2020). It has been shown that elevated nutrient concentrations reduce biodiversity, impact marine habitats, and alter ecosystem functions (Yang et al., 2005; Liu et al., 2009; Mineur et al., 2015). Nitrogen is a crucial component of many compounds, such as the photosynthetic enzyme, Rubisco (Dawes and Koch, 1990); and phosphorus is also an essential element in macroalgal cells for genetic replication, energy supply, and growth metabolism (Zer and Ohad, 2003). The increase in nitrogen and phosphorus concentrations could enhance the growth and biomass of macroalgae (Li et al., 2016). Moreover, temperature also influences algal growth rates by affecting nutrient uptake rates through the nitrate reductase activity (NRA) (Granbom et al., 2004). Feng et al. (2021) also reported that NRA of *Ulva prolifera*, associated with growth, decreased with the rising temperature while exceeded 15°C.

Macroalgae have competitive advantages due to its higher affinity with nutrients, leading to frequently outbreaks of macroalgae blooms (Luo et al., 2012). As an opportunistically growing macroalgal genera, *Ulva* is strongly adaptable to environment which has high tolerance for variable temperature, salinity, irradiance and nutrient concentrations (Taylor et al., 2001; Xiao et al., 2016). At optimal temperature conditions from April to June, detached green patches of *Ulva* species had grown rapidly and accumulated to form green tides, transporting northward into the Yellow Sea of China by monsoon winds and ocean currents (Sun et al., 2008; Liu et al., 2010, 2021b; Xia et al., 2024). Meanwhile, Large-scale drifting biomass of *Sargassum horneri*, known as golden tides, has been reported in the Yellow Sea since 2010 (Liu et al., 2018; Su et al., 2018; Wang et al., 2023). These drifting macroalgae originally grew on the rocky bottom. In spring, the increased buoyancy provided by their numerous sporophyte vesicles could keep the plants floating after detachment, forming the drifting biomass on the sea surface (Yoshida, 1963). *Sargassum* from the coastal region of Shandong Peninsula drifted southwards in winter months, while *Sargassum* along the coast of Zhejiang Province drifted northwards in summer, eventually reaching the largest *Pyropia* aquaculture area of China (Xing et al., 2017; Zhang et al., 2019; Liu et al., 2021a). In recent years, green and golden tides have frequently occurred simultaneously due to excessive nutrient inputs, resulting in a severely economic and ecological disaster in China's coastal waters (Su et al., 2018; Xiao et al., 2020b).

Under the complex context of global climate changes coupled with regional eutrophication, harmful algal blooms are gradually increasing. In particular, the frequency of green and gold tides caused by *Ulva* and *Sargassum* has increased by years, replacing red tides as the main disasters in the coastal waters of China (Feng et al., 2024). However, few studies have been conducted to investigate the competition between *Ulva* and *Sargassum* under the combined effects of local stressor of eutrophication and global stressor of ocean warming. In this study, *U. prolifera* and *S. horneri* were selected and treated to explore the physiological responses and their competitive relationships of the typical harmful algae to high nutrients availability and temperature change scenarios in the Yellow Sea of China. Our results are expected to provide helpful insights into understanding the adaption mechanism and competitive relationships of two macroalgae species under ocean warming and eutrophication in the future.

2 Materials and methods

2.1 Sample collection and experiment design

Floating samples of *U. prolifera* and *S. horneri* were collected from Gaogong island, Lianyungang city, Jiangsu province (119.53°E;

34.91°N) and the nearshore sea of Dongtai, Yancheng city, Jiangsu province of China (121.33°E; 33.02°N) in early June of 2020, respectively. The *in situ* nutrient levels were 10.72 μmol L^{-1} nitrate and 0.42 μmol L^{-1} phosphate in coastal area of north Jiangsu in early summer (Wang et al., 2022). Considering that June is the end of the life cycle in *S. horneri*, the thalli should be a bit senescent. The thalli were transferred to the laboratory under low temperature conditions in a cool container within 2 hours. After removing the sediments and impurities using filtered and autoclaved seawater, healthy thalli were selected and pre-cultured in 1 L balloon flasks containing sterile seawater enriched with von Stosch's enrichment (VSE) Medium (Ott, 1965), which was aerated continuously and changed every 2 days. The cultures were kept in an intelligent illumination incubator (Jiangnan GXZ-300C, Ningbo, China) at 20°C with a 12 h: 12 h (light/dark) photoperiod under 100 μmol photons m^{-2} s^{-1} light intensity.

After the pre-culture of one week, thalli samples with similar length and shape were chose and divided randomly to different treatments. Approximately 0.10 g (fresh weight, FW) thalli were cultured in 500 mL sterile seawater enriched with VSE medium. Six temperature treatments (5, 10, 15, 20, 25, and 30°C) were obtained using different incubators (same brand model to avoid the influence of light), while two levels of nutrient [Low nutrient, LN: 5 μmol L^{-1} N (nitrate) and 0.5 μmol L^{-1} P (phosphate); High nutrient, HN: 500 μmol L^{-1} N and 50 μmol L^{-1} P] were set based on VSE medium. The LN condition represented the low nutrient levels and HN condition was set as eutrophication (Wang et al., 2022). At the same time, we also selected three temperatures (15, 20, and 25°C) to study the competition between *U. prolifera* and *S. horneri* under eutrophication conditions. The initial biomass of *U. prolifera* and *S. horneri* were about 0.05 g (FW) in coculture, respectively. The medium was renewed every 3 d to maintain the abundance of nutrients. Triplicate cultures were conducted for two weeks and all the parameters were measured at the end of culture period.

2.2 Measurement of growth

The relative growth rates (RGR) of *U. prolifera* and *S. horneri* were estimated by changes in biomass (FW), which were performed according to the following formula:

$$RGR(\%\,d^{-1}) = \ln(W_t/W_0)/t \times 100\,\% \quad (1)$$

where the W_0 and W_t are the initial and final fresh weight of thalli after t days culture, respectively.

2.3 Measurement of photosynthetic pigments and soluble protein

To determine pigments content, about 0.02 g FW per sample were cut into pieces and extracted in absolute methanol and kept at 4°C for 24 h in darkness (Porra et al., 1989). The value of Chl *a* and Car might be low due to the incomplete extraction without grinding. After centrifugation (Centrifuge 5407, Eppondorf, Germany) at 5000×g for 10 min, the supernatant was scanned by a spectrophotometer (UV-1800, Shimadzu, Japan) at 470, 652, and 665 nm, respectively. The concentrations of Chlorophyll *a* (Chl *a*) and carotenoids (Car) were determined according to the methods of Wellburn (1994):

$$\text{Chl } a\ (\text{mg g FW}^{-1}) = (15.65 \times A_{665} - 7.53 \times A_{652}) \times V/FW \quad (2)$$

$$\text{Car}\ (\text{mg g FW}^{-1}) = (1000 \times A_{470} + 1403.57 \times A_{665} - 3473.87 \times A_{652})/221 \times V/FW \quad (3)$$

where the A_{470}, A_{652}, and A_{665} were the absorbance of samples at respective wavelength, V is the volume of methanol, and FW is the fresh weight of samples.

Soluble protein contents were measured according to the methods of Bradford (1976). Briefly, about 0.02 g FW thalli was homogenized in phosphate buffer (0.1 M, pH 6.8) and then centrifuged at 5000× g for 15 min at 4°C. The supernatant was mixed with Coomassie brilliant blue G-250 dye solution and scanned at 595 nm by spectrophotometer to calculate the soluble protein contents (SP, mg g FW^{-1}) based on the standard curve of bovine serum albumin.

2.4 Measurement of photosynthesis and respiration

The photosynthetic oxygen evolution and respiration of these two species were measured with a Clark-type electrode (Oxygraph, Hansatech, UK) at the end of experiments. Samples of thalli were cut into 0.5 cm length segments and placed in culture conditions for about 2 h to alleviate cutting damage (Xu and Gao, 2012). During the middle light period (10:00–16:00), about 0.02 g FW thalli were transferred into the reaction chamber containing 5 ml fresh growth medium. The light (100 μmol photons m^{-2} s^{-1}) and temperature condition were set at the same with every culture condition, and seawater in the chamber was stirred during the measurement to keep the oxygen signal steady. The decreased rate (in dark condition) and increased rate (in light condition) of oxygen concentrations were defined as net photosynthetic rate and dark respiration, respectively.

2.5 Assessment of superoxide dismutase activity

Superoxide dismutase (SOD) activity was were examined by using nitroblue tetrazolium (NBT) method (Merzbach and Obedeanu, 1975). Approximately 0.05 g of samples was homogenized in 4 mL phosphate buffer (0.05 M, pH 7.8) and then centrifuged at 5000× g for 10 min at 4°C. The supernatant of the crude extract of SOD was mixed with the NBT solution. After 20 min incubation under 80 μmol photons m^{-2} s^{-1} at 25°C, the absorbance at 560 nm was measured. The amount of SOD that reduces NBT by 50% is defined as the SOD activity.

$$\text{SOD activity (U g FW}^{-1}) = (\text{Ac}-\text{As}) \times \text{V}/(\text{Ac} \times 50\,\% \times \text{FW} \times \text{Vt}) \quad (4)$$

where the Ac and As represent the absorbance of mixed NBT solution (V) with distilled water and sample enzyme, respectively. Vt is the crude extract of fresh weight (FW) thalli samples.

2.6 Statistical analysis

All data were expressed as mean of triplicate analysis ± standard deviations. Before performing parametric tests, data were tested for homogeneity of variance (Levene test, see Supplementary Table S1 in Supplementary Materials) and normality (Shapiro-Wilk test, Supplementary Table S2). Two-way ANOVA was performed to assess the interactive effects of temperature and nutrient levels. Three-way ANOVA employed to determine the effects of temperature, nutrient and coculture. One-way ANOVA was applied to analyze the statistical differences among different temperature treatments under LN and HN conditions. An independent-samples t-test were used to compare the differences between LN and HN within the same temperature treatment and differences between monoculture and coculture under the same condition. Considering that temperature treatments were achieved by different incubators (same brand model) and one incubator per temperature, it should be noted that all ANOVA analyses assessing temperature in this study assess the temperature plus incubator effects. Tukey's honest significant difference (Tukey HSD) was used for ANOVA analysis and differences were termed significant when $p < 0.05$.

3 Results

3.1 Relative growth rate of *U. prolifera* and *S. horneri*

Two-way ANOVA analysis indicated that there were significant individual and interactive effects of temperature (i.e. the temperature and incubator effects) and nutrient on the relative growth rate (RGR) of *U. prolifera* (Table 1, $p < 0.001$, $p < 0.001$, $p = 0.009$),. The growth of thalli in both LN and HN conditions enhanced with the increased levels of temperature, peaking at 20°C (17.2 ± 1.0% for LN, 20.1 ± 3.0% for HN), and began decline at temperature above 25°C. RGR were significantly affected by HN at 5, 15, and 30°C (Figure 1A, $p < 0.001$, $p = 0.009$, $p = 0.039$). For *S. horneri*, temperature and the interaction with nutrient had significant effect on RGR of thalli (Table 1, $p < 0.001$, $p < 0.001$). In general, RGR of *S. horneri* showed an increased trend with temperatures (Figure 1B). Specially, RGR began to plunge at 30°C, and was even negative under HN condition.

In coculture, RGR of both *U. prolifera* and *S. horneri* were declined compared to those in monoculture (Supplementary Table S3, Figure 1C, $p = 0.002$, $p = 0.029$). RGR of *U. prolifera* were significantly enhanced by HN compared to LN at 15 and 20°C ($p = 0.029$, $p = 0.021$), and *S. horneri* showed the same trend ($p = 0.006$, $p = 0.005$). Coculture with *U. prolifera* led to the obvious decline in RGR of *S. horneri*, which were decreased by 61.2% and 49.7% compared to monoculture at 25°C under LN and HN, respectively ($p < 0.001$, $p = 0.002$). Meanwhile, even though the RGR of *U. prolifera* were reduced by 18.6% and 10.4% compared to monoculture at 25°C under LN and HN, respectively, it was still highest in the coculture.

TABLE 1 Statistical analyses (two-way ANOVA) of physiological traits of *Ulva prolifera* and *Sargassum horneri* grown under various temperature and nutrient conditions in the monoculture.

Trait	Temperature			Nutrient			T × N		
	df	F	Sig.	df	F	Sig.	df	F	Sig.
U. prolifera									
RGR	5	51.2	<0.001	1	21.2	<0.001	5	4.0	0.009
Chl *a*	5	29.5	<0.001	1	46.6	<0.001	5	9.3	<0.001
Car	5	15.2	<0.001	1	2.8	0.108	5	1.0	0.459
NPR	5	10.1	<0.001	1	473.6	<0.001	5	4.2	0.007
DR	5	19.8	<0.001	1	170.4	<0.001	5	18.1	<0.001
SP	5	54.3	<0.001	1	25.9	<0.001	5	3.7	0.013
SOD	5	293.7	<0.001	1	107.1	<0.001	5	13.4	<0.001
S. horneri									
RGR	5	157.9	<0.001	1	4.0	0.058	5	20.4	<0.001
Chl *a*	5	89.3	<0.001	1	12.8	0.002	5	5.4	0.002
Car.	5	237.5	<0.001	1	0.1	0.723	5	1.5	0.214
NPR	5	124.5	<0.001	1	8.7	0.007	5	3.6	0.015
DR	5	46.0	<0.001	1	4.5	0.045	5	0.8	0.560
SP	5	44.6	<0.001	1	3.1	0.091	5	0.1	0.986
SOD	5	224.9	<0.001	1	8.5	0.008	5	0.8	0.549

The physiological parameters include the relative growth rate (RGR), the pigment content of chlorophyll a (Chl a), carotenoid (Car), net photosynthetic rate (NPR), dark respiration (DR), soluble protein (SP), and superoxide dismutase activity (SOD). df means degree of freedom, F means the value of the F statistic, and Sig. indicates p-value.

3.2 Pigment contents of *U. prolifera* and *S. horneri*

The Chlorophyll *a* (Chl *a*) content of *U. prolifera* was significantly influenced by temperature, nutrient, and the interaction between them (Table 1, $p < 0.001$, $p < 0.001$, $p < 0.001$). Meanwhile, the carotenoids (Car) content was only significantly influenced by temperature ($p < 0.001$). The Chl *a* of thalli was increased with rising temperature at the range of 5-25°C, especially under HN condition, and reached a maximum 309.4 ± 52.8 μg g^{-1} under LN at 30°C and 520.8 ± 46.8 μg g^{-1} under HN at 25°C, respectively (Figure 2A). HN significantly promoted the Chl *a* content of *U. prolifera* at 15, 20, and 25°C ($p = 0.005$, $p = 0.018$, $p = 0.004$). Similarly, the Car content was increased with the temperature up to 20°C, and declined at higher temperatures (25 and 30°C), which was in line with growth (Figure 3A).

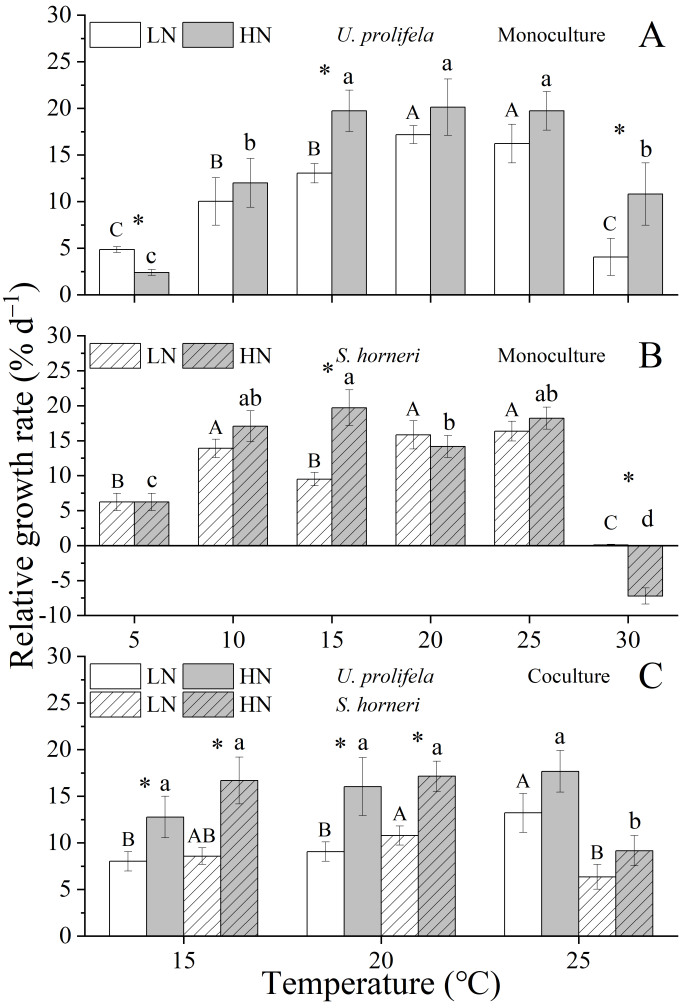

FIGURE 1
Relative growth rate (RGR) of *Ulva prolifera* and *Sargassum horneri* grown under various temperature and nutrient conditions in the monoculture **(A, B)** and coculture **(C)**. Different uppercase letters represent significant differences among different temperature treatment under LN ($p < 0.05$), and different lowercase letters represent significant differences among different temperature treatment under HN ($p < 0.05$). Asterisk indicates whether there was a significant difference between LN and HN under the same temperature conditions ($p < 0.05$).

Temperature and nutrient had individual and interactive effect on Chl *a* content of *S. horneri* ($p < 0.001$, $p < 0.002$, $p = 0.002$), and only temperature had an individual effect on Car content of thalli (Table 1, $p < 0.001$). The Chl *a* of *S. horneri* was enhanced with increased temperature but declined at 30°C under LN and HN conditions (Figure 2B). HN only increased significantly the Chl *a* at 10°C compared to LN ($p = 0.006$). Similarly, the Car of *S. horneri* was promoted slightly by temperature until up to 30°C, with a substantial decline (Figure 3B).

In coculture, both Chl *a* and Car contents of *U. prolifera* were decreased compared to those in monoculture (Supplementary Tables S4, S5, Figures 2C, 3C, $p < 0.001$, $p < 0.001$). Increased temperature only enhanced the Chl *a* of *U. prolifera* under HN condition. Meanwhile, HN promoted the Chl *a* of thalli at three temperatures compared to LN ($p = 0.007$, $p = 0.001$, $p < 0.001$). In addition, coculture with *U. prolifera* inhibited the Chl *a* of *S. horneri* at all treatments ($p = 0.006$, $p = 0.003$, $p = 0.012$ for 15, 20, 25 under LN and $p = 0.003$, $p = 0.020$, $p = 0.116$ for 15, 20, 25 under HN) but significantly enhanced the Car content of thalli by 10.3% at 15°C under LN ($p = 0.047$). HN only significantly enhanced the Chl *a* of *S. horneri* at 20 and 25°C ($p = 0.027$, $p = 0.023$).

3.3 Photosynthesis and respiration of *U. prolifera* and *S. horneri*

The net photosynthetic rate (NPR) and dark respiration rate (R_d) of *U. prolifera* were significantly influenced by temperature, nutrient and their interaction (Table 1, $p < 0.001$, $p < 0.001$, $p = 0.007$ for NPR, and $p < 0.001$, $p < 0.001$, $p < 0.001$ for R_d). NPR of *U. prolifera* thalli showed a relative stability regardless of temperature under LN and HN conditions (Figure 4A). However, the increased temperature enhanced the R_d of *U. prolifera* within a range of 5 - 25° C (Figure 5A). At the different temperatures, HN condition promoted both the NPR and R_d of thalli significantly except for the R_d under 5 and 10°C.

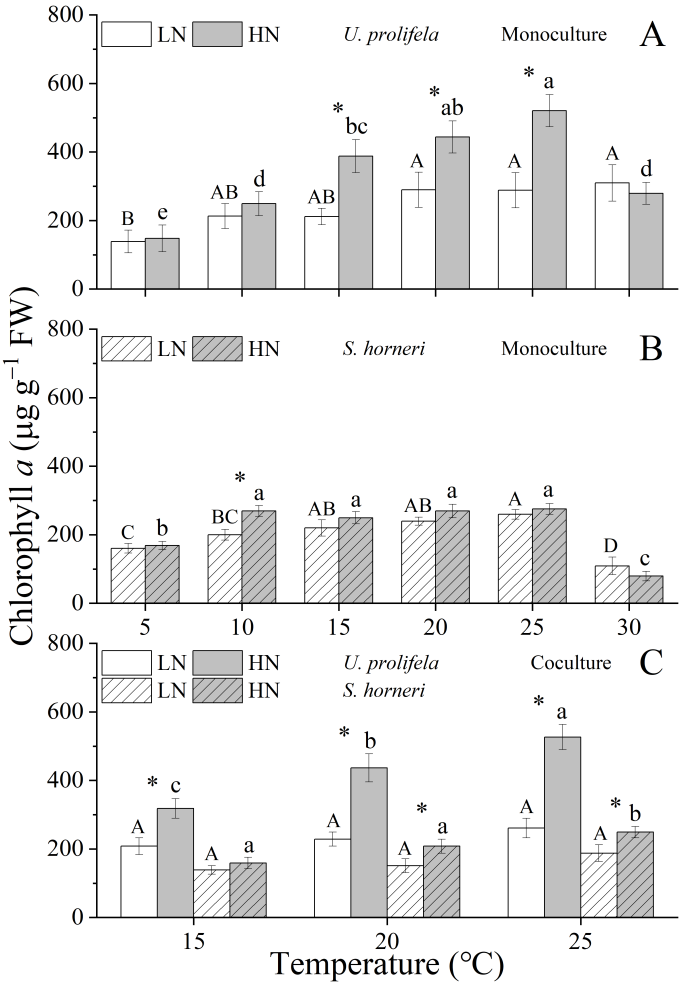

FIGURE 2
Content of Chlorophyll *a* in *Ulva prolifera* and *Sargassum horneri* grown under various temperature and nutrient conditions in the monoculture **(A, B)** and coculture **(C)**. Different uppercase letters represent significant differences among different temperature treatment under LN ($p < 0.05$), and different lowercase letters represent significant differences among different temperature treatment under HN ($p < 0.05$). Asterisk indicates whether there was a significant difference between LN and HN under the same temperature conditions ($p < 0.05$).

As for *S. horneri*, Temperature and nutrient had individual effects on NPR and R_d of thalli, and only had an interactive effect on NPR (Table 1, $p < 0.001$, $p = 0.007$, $p = 0.015$ for NPR, and $p < 0.001$, $p = 0.045$ for R_d). The NPR of *S. horneri* was enhanced with increased temperature within a range of 5-20°C, then decreased at temperature above 25 °C under LN and HN (Figure 4B). However, the R_d of *S. horneri* showed an increasing trend with the temperatures, and reached the highest value of 67.5 and 73.9 μmol O_2 g^{-1} FW h^{-1} at 30°C under LN and HN condition, respectively (Figure 5B).

In coculture, NPR and R_d of both *U. prolifera* and *S. horneri* were decreased significantly compared to those in monoculture (Supplementary Tables S6, S7, Figure 4C and 5C, $p < 0.001$, $p < 0.001$ for NPR and R_d in *U. prolifera*, and $p < 0.001$, $p < 0.001$ in *S. horneri*). However, compared to monoculture, the highest drop of NPR in *U. prolifera* was about 33.0% and 30.8% under LN and HN at 20°C ($p = 0.011$, $p = 0.002$), while the highest drop in *S. horneri* was about 79.78% and 67.0% at 25 °C ($p < 0.001$, $p < 0.001$), respectively. Moreover, HN enhanced the NPR of thalli under all treatments. Similarly to the trend of R_d in *U. prolifera* and *S. horneri* under monoculture, temperature enhanced the R_d of *U. prolifera* and *S. horneri* in coculture.

3.4 Soluble protein content of *U. prolifera* and *S. horneri*

Significant individual and interactive effects of temperature and nutrient were observed on soluble protein content (SP) of *U. prolifera* (Table 1, $p < 0.001$, $p < 0.001$, $p = 0.013$). In general, the SP of *U. prolifera* showed a rising trend with the increased temperature except under HN at 30 °C. Compared to LN, HN promotes SP at all temperatures, with significant differences at 20 and 25°C and a maximum value of 2.7 ± 0.2 mg g^{-1} at 25°C (Figure 6A, $p = 0.008$, $p = 0.010$).

As for *S. horneri*, only temperature had an individual effect on SP (Table 1, $p < 0.001$). The SP of thalli in both LN and HN treatments enhanced with the increased temperatures, peaking at 15 and 20°C, and thereafter declined at temperature above this optimal point.

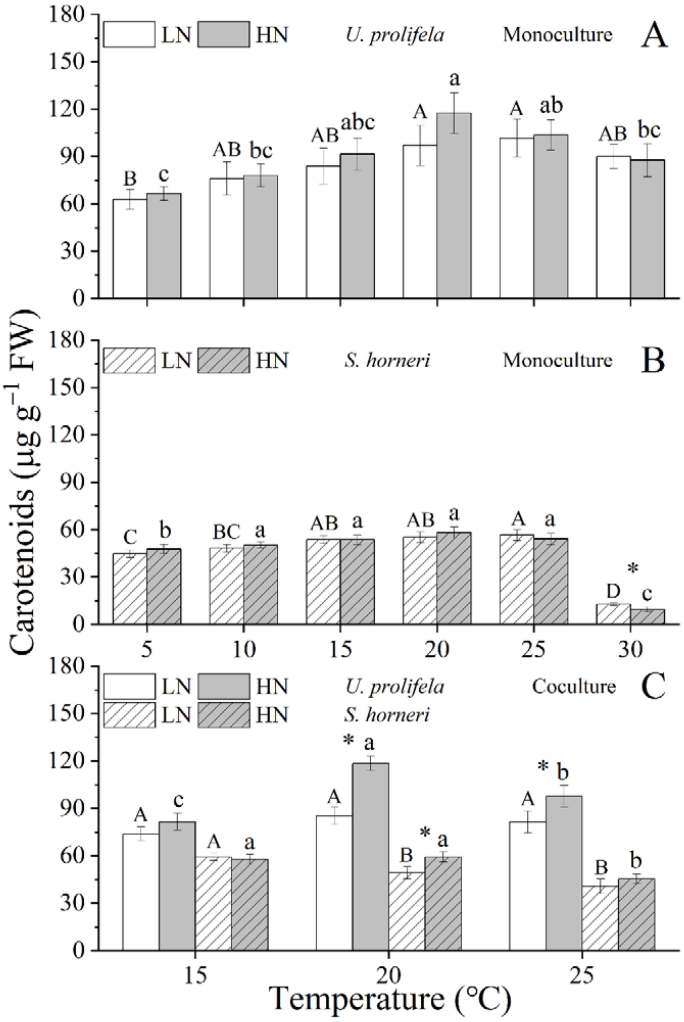

FIGURE 3
Content of Carotenoid in *Ulva prolifera* and *Sargassum horneri* grown under various temperature and nutrient conditions in the monoculture **(A, B)** and coculture **(C)**. Different uppercase letters represent significant differences among different temperature treatment under LN ($p < 0.05$), and different lowercase letters represent significant differences among different temperature treatment under HN ($p < 0.05$). Asterisk indicates whether there was a significant difference between LN and HN under the same temperature conditions ($p < 0.05$).

Compared to LN, HN enhanced SP, but there was no significant difference between them under all temperatures (Figure 6B).

3.5 Superoxide dismutase activity of *U. prolifera* and *S. horneri*

Temperature, nutrient, and the interaction between them had significant effect on SOD of *U. prolifera* (Table 1, $p < 0.001$, $p < 0.001$, $p < 0.001$). The SOD of thalli was enhanced with the temperature increased until 25°C, but decreased significantly at higher temperature (30°C) (Figure 7A). HN promotes SOD activity at all temperatures, but only was significant at 15, 20, and 25°C compared with LN condition ($p = 0.032$, $p = 0.005$, $p < 0.001$).

As for *S. horneri*, Temperature and nutrient had significant individual effect on SOD (Table 1, $p < 0.001$, $p = 0.008$). The SOD activity showed a significant increase by rising temperatures under both LN and HN conditions, with the maximum value of 987.8 ± 71.0 and 1021.8 ± 68.1 U g^{-1} FW at 30 °C, respectively (Figure 7B). HN enhanced the SOD significantly only at 15 °C compared with LN condition ($p = 0.023$).

4 Discussion

As main species of green and golden tides, *U. prolifera* and *S. horneri* both respond positively to temperature and eutrophication. In this study, the growth of *U. prolifera* and *S. horneri*, along with pigment concentrations and photosynthesis, increased with rising temperature, reaching a plateau at 15 – 25°C. However, when the temperature increased to 30°C, the growth of *U. prolifera* and *S. horneri* decreased abruptly, and the latter even suffered death. In cocultures, the growth of both *U. prolifera* and *S. horneri* was inhibited compared to the monocultures, with

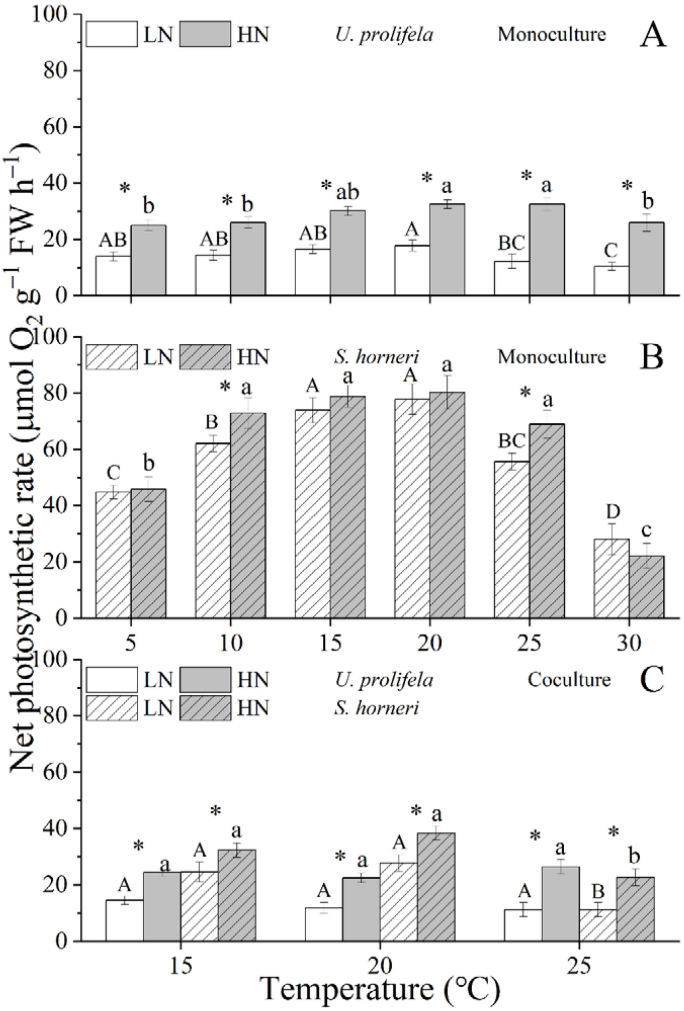

FIGURE 4
Net photosynthetic rate of *Ulva prolifera* and *Sargassum horneri* grown under various temperature and nutrient conditions in the monoculture **(A, B)** and coculture **(C)**. Different uppercase letters represent significant differences among different temperature treatment under LN ($p < 0.05$), and different lowercase letters represent significant differences among different temperature treatment under HN ($p < 0.05$). Asterisk indicates whether there was a significant difference between LN and HN under the same temperature conditions ($p < 0.05$).

the greatest decrease in *S. horneri* at 25°C under two nutrient conditions.

4.1 Response of *U. prolifera* and *S. horneri* to temperature

Temperature is an important factor that limits the cellular enzymatic activities (Raven and Geider, 1988). In this study, proper warming promoted pigments synthesis in both *U. prolifera* and *S. horneri* in monoculture, which was reported in other macroalgae (Figures 2, 3) (Wu et al., 2022). The enhancement of Chl *a* and carotenoids in the two macroalgal genera allow the algae to absorb more light energy and maintain higher photosynthetic rates (Figure 4) (Jiang et al., 2016). In addition to its light-capture role, carotenoids can also act as auxiliary antioxidant that reduces damage caused by high temperature (Yoshiki et al., 2009). The high photosynthetic rate in PSII system, which provides more ATP and NADPH for subsequent physiological processes, improved the growth ultimately (Figure 1) (Jiang et al., 2016). Moreover, the rising temperature increased the mitochondrial respiration (Zou and Gao, 2014a). This similar phenomenon was observed for both algae at temperature from 5 to 25°C in this experiment (Figure 5). The increased consumption of carbon compound by respiration in nighttime could provide more ATP and carbon skeletons for the synthesis of pigment and soluble protein contents (Figures 2, 3, 6) (Zou and Gao, 2014a). Warming would cause algal cells to produce ROS, and algae can scavenge the increased reactive oxygen species (ROS) by activating antioxidant systems, one of which is superoxide dismutase (SOD), to prevent organelles from oxidative damage (Liu et al., 2017). The SOD activity of *U. prolifera* and *S. horneri* increased with rising temperature from 5 to 25°C (Figure 7).

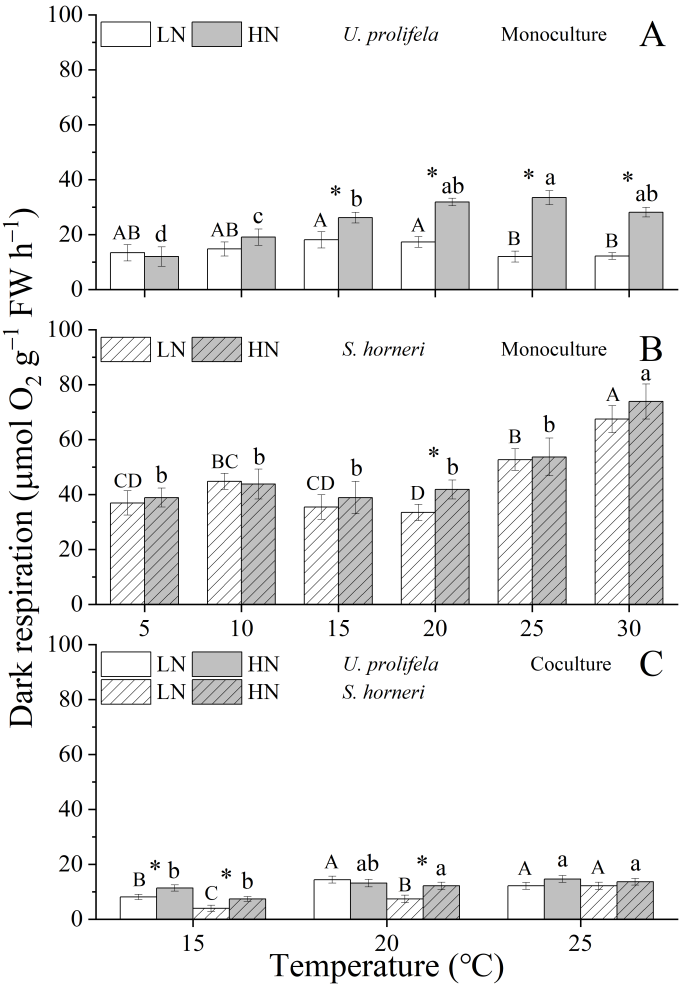

FIGURE 5
Dark respiration rate of *Ulva prolifera* and *Sargassum horneri* grown under various temperature and nutrient conditions in the monoculture **(A, B)** and coculture **(C)**. Different uppercase letters represent significant differences among different temperature treatment under LN ($p < 0.05$), and different lowercase letters represent significant differences among different temperature treatment under HN ($p < 0.05$). Asterisk indicates whether there was a significant difference between LN and HN under the same temperature conditions ($p < 0.05$).

However, when temperature was up to 30°C, the scavenging efficiency of ROS by antioxidant in thalli was reduced, which led to the inhibition of all physiological parameters in both genera in this experiment. Although the SOD activity of *U. prolifera* was reduced at 30°C, it was still able to maintain low growth due to the highly environmental adaptability (Xiao et al., 2016). For *S. horneri*, the SOD activity was still at a high level at 30°C, but the thalli still suffered leaf shedding, which ultimately led to negative algal growth (Liu and Pang, 2010).

4.2 Effects of eutrophication on *U. prolifera* and *S. horneri*

In natural waters, Nitrogen and phosphorus are essential components for cellular metabolic synthesis and critical factors limiting algal primary productivity. Therefore, nutrient enrichment often enhances the physiological performance of *Ulva* spp (Kang et al., 2016; Li et al., 2016; Kang and Chung, 2017). In this study, pigment synthesis, soluble proteins were increased in both *U. prolifera* and *S. horneri* due to higher availability of nutrients, which ultimately improved their photosynthesis and growth (Figures 1-5). Furthermore, the morphology of *Ulva* spp. could enhance the nutrient uptake rates at elevated nutrient concentrations, affecting the metabolism of macroalgae, which could produce more Rubisco using nitrogen (Zer and Ohad, 2003). This is also verified by our results that nutrient enrichment promotes pigmentation and photosynthesis of *U. prolifera* more than that in *S. horneri* (Figures 2-4). Temperature plays a crucial role in the nutrient uptake, nitrate reductase activity of algae (Cade-Menun and Paytan, 2010; Gao et al., 2018). Our results also showed inconsistent enhancement effects of nutrient enrichment on the two macroalgal genera under various temperature conditions, indicating different nutrient requirements of macroalgae at different temperatures (Fan et al., 2014).

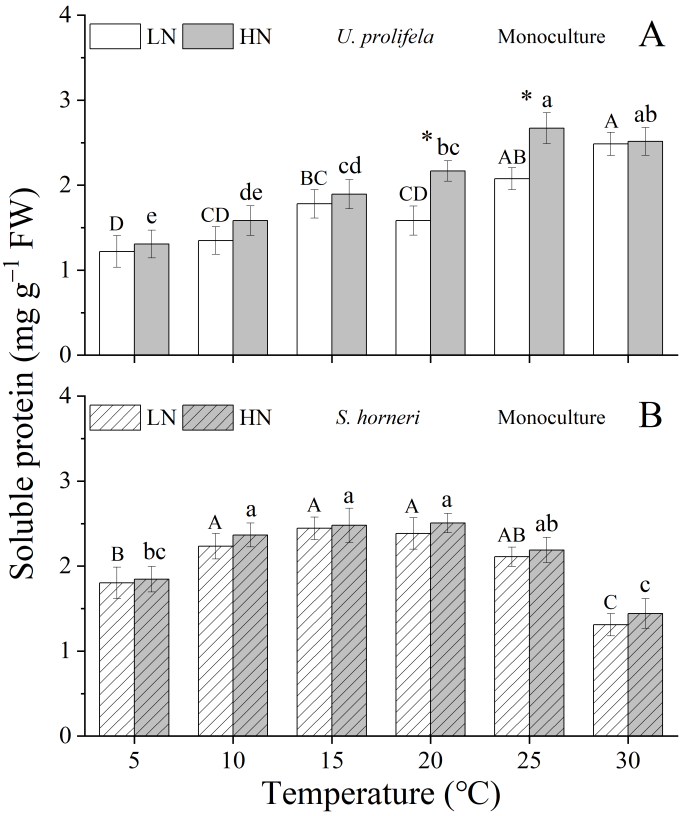

FIGURE 6
Content of soluble protein in *Ulva prolifera* **(A)** and *Sargassum horneri* **(B)** grown under various temperature and nutrient conditions in the monoculture. Different uppercase letters represent significant differences among different temperature treatment under LN ($p < 0.05$), and different lowercase letters represent significant differences among different temperature treatment under HN ($p < 0.05$). Asterisk indicates whether there was a significant difference between LN and HN under the same temperature conditions ($p < 0.05$).

4.3 Competition between *U. prolifera* and *S. horneri*

In recent years, coexisting outbreaks of green and golden tides in coastal waters have occurred, yet have been little studied in laboratory (Xiao et al., 2020a; Zhao et al., 2021). In the present study, three temperature and two nutrient levels were selected to investigate the competition between *U. prolifera* and *S. horneri*. The results showed that the photosynthesis and growth of both *U. prolifera* and *S. horneri* in coculture were decreased compared to monoculture, suggesting ecological niche competition between the two genera (Figures 1, 4). Moreover, the pigment contents of *U. prolifera* did not change significantly in coculture compared to monoculture under both LN and HN conditions. However, an interesting finding is that the pigment contents of *S. horneri* were dramatically reduced, especially under nutrient-rich conditions (Figures 2, 3). Many factors could affect the coculture experiment, including shading, competition of nutrients, and allelopathy. The decline may be attributed to allelopathic effects from *U. prolifera*, as the abundant nutrients under HN condition are unlikely to be depleted given that the medium was renewed every 3 d to maintain nutrient levels. Additionally, the initial biomass of the thalli was consistent, with approximately 0.10 g FW for each species in monoculture and 0.05 + 0.05 g FW for both species in coculture. Furthermore, photosynthesis of both genera was declined compared to monoculture (Figure 4), suggesting that the allelopathic compounds may initially damage the photosynthetic apparatus, thereby inhibiting growth, as observed in other cocultures of macroalgae and microalgae (Ye and Zhang, 2013; Gao et al., 2019). Although the pigment contents of *S. horneri* was lower than those of *U. prolifera*, its photosynthesis was maintained at a higher level. Under these three temperature conditions, *U. prolifera* maintained a relatively stable photosynthetic rate, showing its stronger adaptability (Xiao et al., 2016). Meanwhile, at 15 and 20° C, *S. horneri* exhibited higher photosynthetic rates and lower respiration rates, resulted in more carbon accumulation for higher growth compared to *U. prolifera* under HN condition, suggesting that it was more competitive below 20°C (Figures 1, 4, 5). At 25°C, photosynthesis of *S. horneri* decreased and respiration increased dramatically, ultimately leading to a reduction in growth that was much lower than in monoculture (Figures 1, 3, 4). One reason for this phenomenon might be that temperature changes alter allelopathic efficiency and/or sensitivity (Semmouri et al., 2024). This suggests that coculture with *U. prolifera* weakened the resistance of *S. horneri* to high temperatures and exacerbated its apoptosis eventually. Further studies are required to confirm this conclusion, as allelopathic compounds were not directly measured in this study.

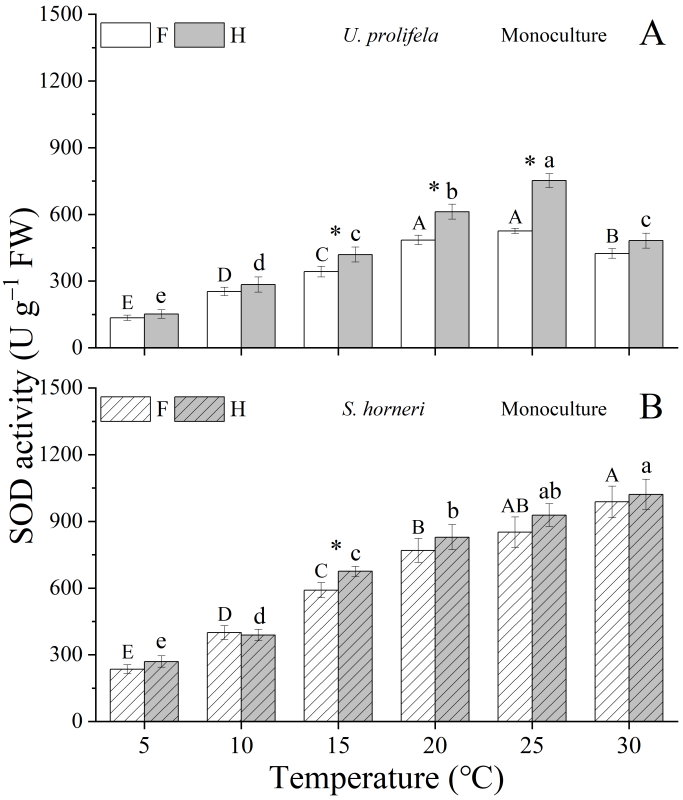

FIGURE 7
SOD activity of *Ulva prolifera* **(A)** and *Sargassum horneri* **(B)** grown under various temperature and nutrient conditions in the monoculture. Different uppercase letters represent significant differences among different temperature treatment under LN ($p < 0.05$), and different lowercase letters represent significant differences among different temperature treatment under HN ($p < 0.05$). Asterisk indicates whether there was a significant difference between LN and HN under the same temperature conditions ($p < 0.05$).

5 Conclusion

Our study investigated the combined impacts of ocean warming and eutrophication on the green tides and golden tides macroalgae and the interaction between them for the first time. As mentioned above, the temperatures in this study were achieved by different incubators, but one per temperature; therefore, the temperature effect is a combined temperature plus incubator effect. In conclusion, the findings demonstrate that the appropriate or seasonal temperature increases can promote the photosynthesis of *U. prolifera* and *S. horneri*. This effect is further exacerbated by eutrophication, which lead to the rapid blooms of *Ulva* and *Sargassum* and subsequently result in frequent outbreaks of green and golden tides. When green and gold tides occur simultaneously, the high environmental adaptivity of *Ulva* enables it to exacerbate the decline of *Sargassum* during periods of high temperatures. This suggests that green tides would outcompete golden tides in coastal waters under seasonal transition from spring to summer and even in future scenarios of ocean warming.

Data availability statement

The raw data supporting the conclusions of this article will be made available by the authors, without undue reservation.

Author contributions

HW: Conceptualization, Funding acquisition, Project administration, Supervision, Writing – original draft. JZ: Data curation, Formal analysis, Investigation, Methodology, Writing – original draft. HL: Writing – original draft, Writing – review & editing. SL: Formal analysis, Writing – original draft. CP: Data curation, Formal analysis, Investigation, Writing – original draft. LY: Formal analysis, Writing – review & editing. JX: Writing – review & editing. PH: Writing – review & editing.

Funding

The author(s) declare financial support was received for the research, authorship, and/or publication of this article. This study was supported by the Natural Science Foundation of Jiangsu Province (grant number BK20221398), National Natural Science Foundation of China (grant number 41706141), “333” project of Jiangsu Province, the Jiangsu Planned Projects for Postdoctoral Research Funds (grant number 2018K025A), “521 project” of Lianyungang city (grant number LYG06521202169), Open project of Jiangsu Institute of Marine Resources Development (grant number SH20231211), “Haiyan project” of Lianyungang city (grant number 2018-ZD-005).

Conflict of interest

The authors declare that the research was conducted in the absence of any commercial or financial relationships that could be construed as a potential conflict of interest.

Publisher's note

All claims expressed in this article are solely those of the authors and do not necessarily represent those of their affiliated organizations, or those of the publisher, the editors and the reviewers. Any product that may be evaluated in this article, or claim that may be made by its manufacturer, is not guaranteed or endorsed by the publisher.

Supplementary material

The Supplementary Material for this article can be found online at: https://www.frontiersin.org/articles/10.3389/fmars.2024.1464511/full#supplementary-material

References

Apel, K., and Hirt, H. (2004). Reactive oxygen species: metabolism, oxidative stress, and signal transduction. *Annu. Rev. Plant Biol.* 55, 373–399. doi: 10.1146/annurev.arplant.55.031903.141701

Bradford, M. M. (1976). A rapid and sensitive method for the quantitation of microgram quantities of protein utilizing the principle of protein-dye binding. *Anal. Biochem.* 72, 248–254. doi: 10.1016/0003-2697(76)90527-3

Cade-Menun, B. J., and Paytan, A. (2010). Nutrient temperature and light stress alter phosphorus and carbon forms in culture-grown algae. *Mar. Chem.* 121, 27–36. doi: 10.1016/j.marchem.2010.03.002

Chen, B., Zou, D., Du, H., and Ji, Z. (2018). Carbon and nitrogen accumulation in the economic seaweed *Gracilaria lemaneiformis* affected by ocean acidification and increasing temperature. *Aquaculture* 482, 176–182. doi: 10.1016/j.aquaculture.2017.09.042

Dawes, C. J., and Koch, E. W. (1990). Physiological responses of the red algae *Gracllarla Verrucosa* and *G. Tikvahiae* before and after nutrient enrichment. *B. Mar. Sci.* 46, 335–344.

Díez, I., Muguerza, N., Santolaria, A., Ganzedo, U., and Gorostiaga, J. (2012). Seaweed assemblage changes in the eastern Cantabrian Sea and their potential relationship to climate change. *Estuar. Coast. Shelf S.* 99, 108–120. doi: 10.1016/j.ecss.2011.12.027

Durack, P. J., Gleckler, P. J., Landerer, F. W., and Taylor, K. E. (2014). Quantifying underestimates of long-term upper-ocean warming. *Nat. Clim. Change* 4, 999–1005. doi: 10.1038/nclimate2389

Fan, X., Xu, D., Wang, Y., Zhang, X., Cao, S., Mou, S., et al. (2014). The effect of nutrient concentrations, nutrient ratios and temperature on photosynthesis and nutrient uptake by *Ulva prolifera*: implications for the explosion in green tides. *J. Appl. Phycol.* 26, 537–544. doi: 10.1007/s10811-013-0054-z

Feng, L., Shi, X., Chen, Y., Tang, H., and Wang, L. (2021). Effects of temperature on the nitrate reductase activity and growth of *Ulva prolifera*. *J. Phycol.* 57, 955–966. doi: 10.1111/jpy.13141

Feng, Y., Xiong, Y., Hall-Spencer, J. M., Liu, K., Beardall, J., Gao, K., et al. (2024). Shift in algal blooms from micro-to macroalgae around China with increasing eutrophication and climate change. *Global Change Biol.* 30, e17018. doi: 10.1111/gcb.17018

Gao, G., Clare, A. S., Rose, C., and Caldwell, G. S. (2018). *Ulva rigida* in the future ocean: potential for carbon capture, bioremediation and biomethane production. *Gcb. Bioenergy* 10, 39–51. doi: 10.1111/gcbb.12465

Gao, G., Fu, Q., Beardall, J., Wu, M., and Xu, J. (2019). Combination of ocean acidification and warming enhances the competitive advantage of *Skeletonema costatum* over a green tide alga, *Ulva linza*. *Harmful Algae* 85, 101698. doi: 10.1016/j.hal.2019.101698

Gattuso, J.-P., Magnan, A., Billé, R., Cheung, W. W., Howes, E. L., Joos, F., et al. (2015). Contrasting futures for ocean and society from different anthropogenic CO_2 emissions scenarios. *Science* 349, aac4722. doi: 10.1126/science.aac4722

Granbom, M., Chow, F., De Oliveira, M. C., Colepicolo, P., De Paula, E. J., et al. (2004). Characterisation of nitrate reductase in the marine macroalga *Kappaphycus alvarezii* (Rhodophyta). *Aquat. Bot.* 78, 295–305. doi: 10.1016/j.aquabot.2003.11.001

Hanley, M. E., Firth, L. B., and Foggo, A. (2024). Victim of changes? Marine macroalgae in a changing world. *Ann. Bot-London* 133, 1–16. doi: 10.1093/aob/mcad185

IPCC (2019). *Special Report on the Ocean and Cryosphere in a Changing Climate*. Eds. H.-O. Pörtner, D. C. Roberts, V. Masson-Delmotte, P. Zhai, M. Tignor, E. Poloczanska, K. Mintenbeck, A. Alegría, M. Nicolai, A. Okem, J. Petzold, B. Rama and N. M. Weyer (UK and New York, NY, USA: Cambridge).

Jiang, H., Zou, D., and Li, X. (2016). Growth, photosynthesis and nutrient uptake by *Grateloupia livida* (Halymeniales, Rhodophyta) in response to different carbon levels. *Phycologia* 55, 462–468. doi: 10.2216/16-11.1

Jueterbock, A., Tyberghein, L., Verbruggen, H., Coyer, J. A., Olsen, J. L., and Hoarau, G. (2013). Climate change impact on seaweed meadow distribution in the North Atlantic rocky intertidal. *Ecol. Evol.* 3, 1356–1373. doi: 10.1002/ece3.541

Kang, J. W., and Chung, I. K. (2017). The effects of eutrophication and acidification on the ecophysiology of *Ulva pertusa* Kjellman. *J. Appl. Phycol.* 29, 2675–2683. doi: 10.1007/s10811-017-1087-5

Kang, E. J., Kim, J.-H., Kim, K., and Kim, K. Y. (2016). Adaptations of a green tide forming *Ulva linza* (Ulvophyceae, Chlorophyta) to selected salinity and nutrients conditions mimicking representative environments in the Yellow Sea. *Phycologia* 55, 210–218. doi: 10.2216/15-67.1

Krause-Jensen, D., and Duarte, C. M. (2016). Substantial role of macroalgae in marine carbon sequestration. *Nat. Geosci.* 9, 737–742. doi: 10.1038/ngeo2790

Li, S., Yu, K., Huo, Y., Zhang, J., Wu, H., Cai, C.e., et al. (2016). Effects of nitrogen and phosphorus enrichment on growth and photosynthetic assimilation of carbon in a green tide-forming species (*Ulva prolifera*) in the Yellow Sea. *Hydrobiologia* 776, 161–171. doi: 10.1007/s10750-016-2749-z

Liu, D., Keesing, J. K., Xing, Q., and Shi, P. (2009). World's largest macroalgal bloom caused by expansion of seaweed aquaculture in China. *Mar. pollut. Bull.* 58, 888–895. doi: 10.1016/j.marpolbul.2009.01.013

Liu, F., Liu, X., Wang, Y., Jin, Z., Moejes, F. W., and Sun, S. (2018). Insights on the *Sargassum horneri* golden tides in the Yellow Sea inferred from morphological and molecular data. *Limnol. Oceanogr.* 63, 1762–1773. doi: 10.1002/lno.10806

Liu, F., and Pang, S. J. (2010). Stress tolerance and antioxidant enzymatic activities in the metabolisms of the reactive oxygen species in two intertidal red algae *Grateloupia turuturu* and *Palmaria palmata*. *J. Exp. Mar. Biol. Ecol.* 382, 82–87. doi: 10.1016/j.jembe.2009.11.005

Liu, F., Pang, S. J., Xu, N., Shan, T. F., Sun, S., Hu, X., et al. (2010). *Ulva* diversity in the Yellow Sea during the large-scale green algal blooms in 2008–2009. *Phycol. Res.* 58, 270–279. doi: 10.1111/j.1440-1835.2010.00586.x

Liu, J., Xia, J., Zhuang, M., Zhang, J., Sun, Y., Tong, Y., et al. (2021a). Golden seaweed tides accumulated in *Pyropia* aquaculture areas are becoming a normal phenomenon in the Yellow Sea of China. *Sci. Total Environ.* 774, 145726. doi: 10.1016/j.scitotenv.2021.145726

Liu, J., Xia, J., Zhuang, M., Zhang, J., Yu, K., Zhao, S., et al. (2021b). Controlling the source of green tides in the Yellow Sea: NaClO treatment of *Ulva* attached on *Pyropia* aquaculture rafts. *Aquaculture* 535, 736378. doi: 10.1016/j.aquaculture.2021.736378

Liu, C., Zou, D., Yang, Y., Chen, B., and Jiang, H. (2017). Temperature responses of pigment contents, chlorophyll fluorescence characteristics, and antioxidant defenses in *Gracilariopsis lemaneiformis* (Gracilariales, Rhodophyta) under different CO_2 levels. *J. Appl. Phycol.* 29, 983–991. doi: 10.1007/s10811-016-0971-8

Luo, M. B., Liu, F., and Xu, Z. L. (2012). Growth and nutrient uptake capacity of two co-occurring species, *Ulva prolifera* and *Ulva linza*. *Aquat. Bot.* 100, 18–24. doi: 10.1016/j.aquabot.2012.03.006

Machado, J. P., and Oliveira, V. P. (2024). Seaweed functional ecology models: a comprehensive review of theory and applications. *J. Appl. Phycol.*, 1–16. doi: 10.1007/s10811-024-03293-z

Malone, T. C., and Newton, A. (2020). The globalization of cultural eutrophication in the coastal ocean: causes and consequences. *Front. Mar. Sci.* 7. doi: 10.3389/fmars.2020.00670

Martin, S., and Gattuso, J. P. (2009). Response of Mediterranean coralline algae to ocean acidification and elevated temperature. *Global Change Biol.* 15, 2089–2100. doi: 10.1111/j.1365-2486.2009.01874.x

Merzbach, D., and Obedeanu, N. (1975). Standardisation of the nitroblue-tetrazolium test. *J. Med. Microbiol.* 8, 375–384. doi: 10.1099/00222615-8-2-375

Mineur, F., Arenas, F., Assis, J., Davies, A. J., Engelen, A. H., Fernandes, F., et al. (2015). European seaweeds under pressure: Consequences for communities and ecosystem functioning. *J. Sea Res.* 98, 91–108. doi: 10.1016/j.seares.2014.11.004

Ott, F. D. (1965). Synthetic media and techniques for the xenic cultivation of marine algae and flagellate. *Va. J. Sci.* 16, 205–218.

Paerl, H. W., Hall, N. S., Peierls, B. L., and Rossignol, K. L. (2014). Evolving paradigms and challenges in estuarine and coastal eutrophication dynamics in a culturally and climatically stressed world. *Estuar. Coast.* 37, 243–258. doi: 10.1007/s12237-014-9773-x

Pakker, H., and Breeman, A. (1996). Temperature responses of tropical to warm-temperate Atlantic seaweeds. II. Evidence for ecotypic differentiation in amphi-Atlantic tropical-Mediterranean species. *Eur. J. Phycol.* 31, 133–141. doi: 10.1080/09670269600651301

Porra, R. J., Thompson, W. A., and Kriedemann, P. E. (1989). Determination of accurate extinction coefficients and simultaneous equations for assaying chlorophylls a and *b* extracted with four different solvents: verification of the concentration of chlorophyll standards by atomic absorption spectroscopy. *BBA-Bioenergetics* 975, 384–394. doi: 10.1016/S0005-2728(89)80347-0

Raven, J. A., and Geider, R. J. (1988). Temperature and algal growth. *New Phytol.* 110, 441–461. doi: 10.1111/j.1469-8137.1988.tb00282.x

Semmouri, I., Janssen, C. R., and Asselman, J. (2024). Allelopathy in macroalgae: Ecological principles, research opportunities and pitfalls reviewed. *J. Appl. Phycol.* 36, 441–458. doi: 10.1007/s10811-023-03110-z

Su, L., Shan, T., Pang, S., and Li, J. (2018). Analyses of the genetic structure of *Sargassum horneri* in the Yellow Sea: implications of the temporal and spatial relations among floating and benthic populations. *J. Appl. Phycol.* 30, 1417–1424. doi: 10.1007/s10811-017-1296-y

Sun, S., Wang, F., Li, C., Qin, S., Zhou, M., Ding, L., et al. (2008). Emerging challenges: Massive green algae blooms in the Yellow Sea. *Nat. Precedings*, 1–1. doi: 10.1038/npre.2008.2266.1

Taylor, R., Fletcher, R., and Raven, J. (2001). Preliminary studies on the growth of selected 'green tide'algae in laboratory culture: effects of irradiance, temperature, salinity and nutrients on growth rate. *Bot. Mar.* 44, 327–336. doi: 10.1515/BOT.2001.042

Wang, Z., Yuan, C., Zhang, X., Liu, Y., Fu, M., and Xiao, J. (2023). Interannual variations of *Sargassum* blooms in the Yellow Sea and East China Sea during 2017–2021. *Harmful Algae* 126, 102451. doi: 10.1016/j.hal.2023.102451

Wang, Y., Zhang, J., Wu, W., Liu, J., Ran, X., Zhang, A., et al. (2022). Variations in the marine seawater environment and the dominant factors in the Lianyungang coastal area. *Reg. Stud. Mar. Sci.* 52, 102276. doi: 10.1016/j.rsma.2022.102276

Wellburn, A. R. (1994). The spectral determination of chlorophylls a and *b*, as well as total carotenoids, using various solvents with spectrophotometers of different resolution. *J. Plant Physiol.* 144, 307–313. doi: 10.1016/S0176-1617(11)81192-2

Wu, H., Chen, J., Feng, J., Liu, Y., Li, X., Chen, R., et al. (2022). Thermal fluctuations and nitrogen enrichment synergistically accelerate biomass yield of *Pyropia haitanensis*. *Aquat. Bot.* 179, 103501. doi: 10.1016/j.aquabot.2022.103501

Xia, Z., Liu, J., Zhao, S., Sun, Y., Cui, Q., Wu, L., et al. (2024). Review of the development of the green tide and the process of control in the southern Yellow Sea in 2022. *Estuar. Coast. Shelf S.* 30, 108772. doi: 10.1016/j.ecss.2024.108772

Xiao, J., Fan, S., Wang, Z., Fu, M., Song, H., Wang, X., et al. (2020a). Decadal characteristics of the floating *Ulva* and *Sargassum* in the Subei Shoal, Yellow Sea. *Acta Oceanol. Sin.* 39, 1–10. doi: 10.1007/s13131-020-1655-4

Xiao, J., Wang, Z., Song, H., Fan, S., Yuan, C., Fu, M., et al. (2020b). An anomalous bi-macroalgal bloom caused by *Ulva* and Sargassum seaweeds during spring to summer of 2017 in the western Yellow Sea, China. *Harmful Algae* 93, 101760. doi: 10.1016/j.hal.2020.101760

Xiao, J., Zhang, X., Gao, C., Jiang, M., Li, R., Wang, Z., et al. (2016). Effect of temperature, salinity and irradiance on growth and photosynthesis of *Ulva prolifera*. *Acta Oceanol. Sin.* 35, 114–121. doi: 10.1007/s13131-016-0891-0

Xing, Q., Guo, R., Wu, L., An, D., Cong, M., Qin, S., et al. (2017). High-resolution satellite observations of a new hazard of golden tides caused by floating *Sargassum* in winter in the Yellow Sea. *IEEE Geosci. Remote S.* 14, 1815–1819. doi: 10.1109/LGRS.2017.2737079

Xu, J., and Gao, K. (2012). Future CO_2-induced ocean acidification mediates the physiological performance of a green tide alga. *Plant Physiol.* 160, 1762–1769. doi: 10.1104/pp.112.206961

Yang, H., Zhou, Y., Mao, Y., Li, X., Liu, Y., and Zhang, F. (2005). Growth characters and photosynthetic capacity of *Gracilaria lemaneiformis* as a biofilter in a shellfish farming area in Sanggou Bay, China. *J. Appl.Phycol.* 17, 199–206. doi: 10.1007/s10811-005-6419-1

Ye, C. P., and Zhang, M. C. (2013). Allelopathic inhibitory effects of the dried macroalga *Ulva pertusa* on the photosynthetic activities of red tide-causing microalga *Skeletonema costatum*. *Adv. Mater. Res.* 726, 29–34. doi: 10.4028/www.scientific.net/AMR.726-731.29

Yoshida, T. (1963). Studies on the distribution and drift of the floating seaweeds. *Bull. Tohoku Reg. Fish. Res. Lab.* 23, 141–186.

Yoshiki, M., Tsuge, K., Tsuruta, Y., Yoshimura, T., Koganemaru, K., Sumi, T., et al. (2009). Production of new antioxidant compound from mycosporine-like amino acid, porphyra-334 by heat treatment. *Food Chem.* 113, 1127–1132. doi: 10.1016/j.foodchem.2008.08.087

Zer, H., and Ohad, I. (2003). Light, redox state, thylakoid-protein phosphorylation and signaling gene expression. *Trends Biochem. Sci.* 28, 467–470. doi: 10.1016/S0968-0004(03)00173-7

Zhang, J., Ding, X., Zhuang, M., Wang, S., Chen, L., Shen, H., et al. (2019). An increase in new *Sargassum* (Phaeophyceae) blooms along the coast of the East China Sea and Yellow Sea. *Phycologia* 58, 374–381. doi: 10.1080/00318884.2019.1585722

Zhao, X., Zhong, Y., Zhang, H., Qu, T., Hou, C., Guan, C., et al. (2021). Comparison of environmental responding strategies between *Ulva prolifera* and *Sargassum horneri*: an *in-situ* study during the co-occurrence of green tides and golden tides in the Yellow Sea, China in 2017. *J. Oceanol. Limnol.* 39, 2252–2266. doi: 10.1007/s00343-021-0397-2

Zou, D., and Gao, K. (2014a). The photosynthetic and respiratory responses to temperature and nitrogen supply in the marine green macroalga *Ulva conglobata* (Chlorophyta). *Phycologia* 53, 86–94. doi: 10.2216/13-189.1

Zou, D., and Gao, K. (2014b). Temperature response of photosynthetic light-and carbon-use characteristics in the red seaweed *Gracilariopsis lemaneiformis* (Gracilariales, Rhodophyta). *J. Phycol.* 50, 366–375. doi: 10.1111/jpy.12171

frontiers | Frontiers in Marine Science

TYPE Review
PUBLISHED 22 October 2024
DOI 10.3389/fmars.2024.1483330

OPEN ACCESS

EDITED BY
Samuel Starko,
University of Victoria, Canada

REVIEWED BY
Jinlin Liu,
Tongji University, China
Wei Liu,
Shanghai University, China

*CORRESPONDENCE
Reina J. Veenhof
reina.veenhof@sams.ac.uk

RECEIVED 19 August 2024
ACCEPTED 01 October 2024
PUBLISHED 22 October 2024

CITATION
Veenhof RJ, Burrows MT, Hughes AD, Michalek K, Ross ME, Thomson AI, Fedenko J and Stanley MS (2024) Sustainable seaweed aquaculture and climate change in the North Atlantic: challenges and opportunities. *Front. Mar. Sci.* 11:1483330. doi: 10.3389/fmars.2024.1483330

Sustainable seaweed aquaculture and climate change in the North Atlantic: challenges and opportunities

Reina J. Veenhof[1*], Michael T. Burrows[1], Adam D. Hughes[1], Kati Michalek[1], Michael E. Ross[1,2], Alex I. Thomson[1], Jeffrey Fedenko[3] and Michele S. Stanley[1]

[1]Scottish Association for Marine Science, Argyll, Oban, United Kingdom, [2]Culture Collection of Algae and Protozoa (CCAP), Argyll, Oban, United Kingdom, [3]Shell Technology Center, Shell Exploration and Production Inc., Houston, TX, United States

Seaweed aquaculture is gaining traction globally as a solution to many climate issues. However, seaweeds themselves are also under threat of anthropogenically driven climate change. Here, we summarize climate-related challenges to the seaweed aquaculture industry, with a focus on the developing trade in the North Atlantic. Specifically, we summarize three main challenges: i) abiotic change; ii) extreme events; and iii) disease & herbivory. Abiotic change includes negative effects of ocean warming and acidification, as well as altered seasonality due to ocean warming. This can lower biomass yield and change biochemical composition of the seaweeds. Extreme events can cause considerable damage and loss to seaweed farms, particularly due to marine heatwaves, storms and freshwater inputs. Seaweed diseases have a higher chance of proliferating under environmentally stressful conditions such as ocean warming and decreased salinity. Herbivory causes loss of biomass but is not well researched in relation to seaweed aquaculture in the North Atlantic. Despite challenges, opportunities exist to improve resilience to climate change, summarized in three sections: i) future proof site selection; ii) advances in breeding and microbiome manipulation; and iii) restorative aquaculture. We present a case study where we use predictive modelling to illustrate suitable habitat for seaweed cultivation in the North Atlantic under future ocean warming. Notably, there was a large loss of suitable habitat for cultivating *Alaria esculenta* and *Laminaria digitata*. We show how selection and priming and microbe inoculates may be a cost-effective and scalable solution to improve disease- and thermal tolerance. Co-cultivation of seaweeds may increase both yield and biodiversity co-benefits. Finally, we show that aquaculture and restoration can benefit from collaborating on nursery techniques and push for improved legislation.

KEYWORDS

seaweed aquaculture, climate change, breeding, ocean warming, salinity, restorative aquaculture, site selection, omics

1 Introduction

Climate change is putting increased pressure on food production, creating a rising demand for sustainable aquaculture solutions (Subasinghe et al., 2009). Among the different avenues of aquaculture, seaweeds are a promising candidate. Seaweeds are capable of growing without the addition of nutrients or fertilizers and can be used in a multitude of downstream applications (Buschmann et al., 2017). In addition, seaweeds have great potential to increase sustainability of mariculture projects, such as in restorative aquaculture or integrated multitrophic aquaculture (IMTA; Duarte et al., 2022). Currently, almost all (97%) commercially grown seaweeds come from Asia, with China, Indonesia, and South Korea being the top three global producers (Sultana et al., 2023; Khan et al., 2024). However, the seaweed cultivation industry is growing in other parts of the world, including the North Atlantic (Figure 1). In 2024, a total of 1,240.86 KT wet weight of seaweed was produced annually by 139 companies, with the main species for cultivation being *Saccharina latissima*, *Ulva* sp. and *Alaria esculenta* (Figure 1, data sourced from www.phyconomy.net).

For seaweed aquaculture to expand in the North Atlantic, there are still many challenges that need to be addressed. Despite recognition as an emerging industry, there is a significant lack of seaweed policy and regulation in countries bordering the North Atlantic (Campbell et al., 2020; Naylor et al., 2021). Largely, seaweed policy is based on existing shellfish regulation, with some nations, such as Scotland and Norway, having started to develop independent seaweed aquaculture policies (Alexander et al., 2015; Wood et al., 2017). Seaweed cultivation requires large spatial areas for operations to be economically feasible, which is largely due to current market values for seaweeds and the costs associated with small-scale farming (Hughes and Black, 2016). Available space in the marine environment is highly contested, with potential solutions for avoiding conflict including the combination of seaweed with other aquaculture or marine-related industries, or offshore operations (Hughes and Black, 2016; Kim et al., 2017; Duarte et al., 2017). In addition, social licensing to build large scale seaweed farms in the North Atlantic may not yet be on par with other parts of the world (Billing et al., 2021), and the nursery phase of seaweed farming is still labor intensive and therefore costly.

Next to the economic, social, environmental and policy challenges of seaweed aquaculture (reviewed in for example Alexander et al., 2015; Campbell et al., 2019; Kerrison et al., 2015; Wood et al., 2017; Visch et al., 2023), there are concerns regarding seaweed aquaculture viability in relation to climate change threats. Climate stressors have long been recognized to affect natural seaweed habitats (e.g. Harley et al., 2012; Wernberg et al., 2023; Steneck et al., 2002; Schiel et al., 2004). At the same time, the commercial growth of seaweeds has been suggested as a solution to certain climate stressors, through carbon capture, pH buffering, waste-water remediation and offering a low-carbon alternative to certain products (reviewed in for example Yong et al., 2022; Sultana et al., 2023; Ross et al., 2023; Duarte et al., 2022). However, climate change stress will also have a profound effect on the seaweed growing industry (Chung et al., 2017). Climate change effects on the seaweed aquaculture industry have been reviewed for specific locations such as California (Kübler et al., 2021), the UK and Ireland (Callaway et al., 2012), the Gulf of Maine (Bricknell et al., 2021), Korea (Kim et al., 2019) and Norway (Stévant et al., 2017), as well as focusing on specific species such as tropical red seaweeds (Largo et al., 2017). This review focuses on the seaweed aquaculture species relevant to the North Atlantic (Figure 1). The species

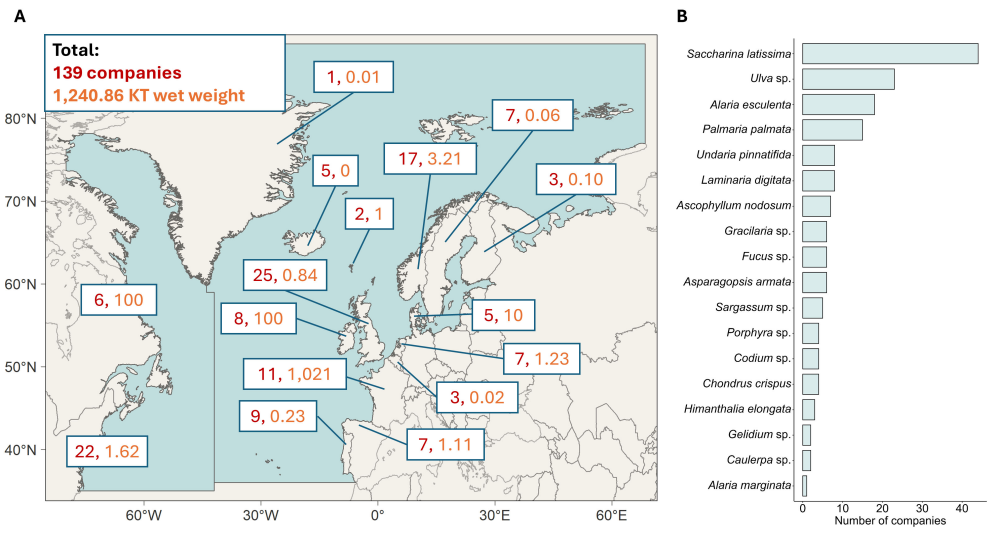

FIGURE 1
Production numbers and main species of seaweed cultivated in the North Atlantic seaweed industry. Data were taken from www.phyconomy.net in August 2024 and collated for visual presentation. Companies were only included if active seaweed growing took place in the North Atlantic (i.e. excluding any Pacific companies from Canada and the USA, and companies only practicing wild harvesting. Onshore cultivation and companies practicing both wild-harvesting and cultivation were included). **(A)** Map of the North Atlantic defined as area 21 and 27 of the FAO Major Fishing Areas, depicted by the two blue areas. In red is the number of seaweed cultivation companies per country, as well as the metric KT (kilo ton) of wet weight produced annually. **(B)** Main species grown in the North Atlantic seaweed industry, ordered by number of companies cultivating these species.

cultivated span across all three domains of seaweeds, therefore responses to climate change will differ. We summarize the main climate change challenges facing the seaweed aquaculture industry. At the same time, we address emerging opportunities and potential solutions to some of the challenges. As the focus is on the North Atlantic, most species discussed are of a temperate distribution. However, where relevant, examples might be provided from tropical seaweed aquaculture, particularly if the research is innovative and paves the way for technological improvements from which the temperate aquaculture industry may learn.

2 Challenges

Climate change is driving profound changes in seaweed ecosystems globally (Wernberg et al., 2023; Filbee-Dexter and Wernberg, 2018; Smale, 2020). Anthropogenic CO_2 has been steadily rising since the start of the industrial era, which has driven multiple changes in the environment affecting marine ecosystems (Allen et al., 2009). The acceleration of carbon emissions has caused global atmospheric temperatures to rise, and a large proportion of that temperature increase is absorbed by the ocean, causing ocean temperatures to increase (Reichert et al., 2002; Bronselaer and Zanna, 2020; Goodwin et al., 2015). Ocean systems are also becoming more acidic due to increased absorption of atmospheric CO_2 (Doney et al., 2009; Iida et al., 2021; Ma et al., 2023a). Through increased temperatures, weather patterns are shifting globally resulting in increased rainfall, which in turn can change salinity levels in coastal areas (Marsooli et al., 2019). Extreme events such as storms and marine heatwaves are also increasing in frequency and intensity (Coumou and Rahmstorf, 2012; Smale et al., 2019). The direct effects of ocean warming have other indirect consequences upon seaweed ecology and aquaculture, such as altered herbivory rates, species range shifts and the prevalence of disease (Vergés et al., 2014; Krumhansl et al., 2016; Gachon et al., 2010). All these ocean change factors represent risk and may influence seaweed aquaculture endeavors. The challenges they present are discussed here.

2.1 Challenge 1: abiotic change

2.1.1 Ocean warming

Increasing ocean temperatures have been identified as a major challenge to seaweed aquaculture industries, though it also may increase areas available for aquaculture (Largo et al., 2017; Chung et al., 2017). Global climate change is predicted to increase sea surface temperatures from an average 1.5°C to 3.5°C under low- and high-emission CMIP6 models, respectively (Kwiatkowski et al., 2020; IPCC, 2023). Since the latitudinal distribution of seaweed is largely constrained by temperature (Smale, 2020; Jayathilake and Costello, 2020), this could have a profound impact upon ecosystem ecology, as well as existing and future seaweed and IMTA enterprises (Chung et al., 2017). Temperature stress has effects on both the individual level, altering a seaweed's morphology and biochemical profile (Eggert, 2012), and population level, including range shifts, genetic shifts, and decreased productivity of the whole ecosystem (Harley et al., 2012; Wernberg et al., 2023; Coleman et al., 2020a). However, how this may impact seaweed aquaculture remains uncertain and requires more detailed study and models to predict impacts.

Seaweeds have a multitude of mechanisms to acclimate, protect, or repair in response to temperature stress, among them adjusting cell membrane fluidity and production of a suite of enzymes to protect against intracellular reactive oxygen species (ROS) which may be formed in response to temperature stress (e.g. Eggert, 2012; Choo et al., 2004; Britton et al., 2020; Hammann et al., 2016) However, their upregulation will come at a metabolic cost. which reduces growth and net primary productivity (NPP) as temperature increases (Harley et al., 2012; Eggert, 2012). This has been observed in the northeast Atlantic, where net primary productivity (NPP) and biomass standing stock of *Laminaria hyperborea* was respectively 1.5 and 2.5 times greater in northern sites compared to the southernmost sites in the UK, across a temperature gradient of ~2.5°C (Smale et al., 2020). Overall trends show that NPP of seaweed systems is highest in temperate regions, where ocean temperatures are between 10-18°C (Pessarrodona et al., 2022). This indicates that ocean warming may shift areas of greatest NPP from temperate to arctic regions, which currently represent lower NPP rates. For higher NPP in seaweed farming, farms may thus be best placed in cooler thermal regions, or use species that have a higher NPP under increased temperatures. For example, the pseudo-kelp *Saccorhiza polyschides* has a higher mean NPP and a larger capacity to respond to thermal stress compared to *Laminaria ochroleuca*, in part due to its annual life cycle (Biskup et al., 2014). However, this does not take into account that NPP can become temperature acclimated (Davison et al., 1991; Kübler and Davison, 1995), or that photosynthetic rates may be adapted to local temperatures (King et al., 2020; Smolina et al., 2016). In addition, NPP can be influenced by other abiotic factors, e.g. light regimes or CO_2, and biotic factors, e.g. life history stage or tissue type, which adds extra caution to extrapolating NPP measurements from limited data points (Franke et al., 2023; Veenhof et al., 2024).

Increased temperature can also alter the biochemical composition of seaweeds. As a majority of seaweeds are processed downstream for their primary and secondary metabolites (Buschmann et al., 2017), this can have a large impact on marketable products for the seaweed aquaculture industry. The effects of climate change on seaweed metabolites have recently been reviewed, and we refer to this body of work for further reading (Park et al., 2023). Briefly, the composition of carbohydrates, amino acids, and other metabolites can change under temperature stress potentially altering the overall nutritional composition of the seaweed (Park et al., 2023), which will likely have knock-on effects for human consumption (Shalders et al., 2022). Mixed reports show both no effect of temperature stress on the nutritional quality of seaweeds (*Ecklonia radiata* and *Sargassum* sp.; Shalders et al., 2023) or a decrease in nutritional quality with increased temperatures (*Macrocystis pyrifera, Derbesia tenuissima;* Lowman et al., 2022; Gosch et al., 2015), which could be due to

separate stress tolerances between species. Research should address the changes in nutritional quality of seaweeds commonly grown for commercial aquaculture. This is particularly important as consistent biochemical composition of the seaweeds is key for delivering products to end-users such as the food- and feed industry (Park et al., 2023).

Range shifts of seaweeds induced by warming may change the species composition of natural seaweed populations, which may affect the total nutritional value of those seaweed environments (Shalders et al., 2023). Similarly, in the context of seaweed aquaculture, the species that are viable for culture and their nutritional content at one specific site may change with ocean warming. Or, the time of harvest may be shortened to earlier in the season from current operational farms. As such, projections of seaweed species' distributions in a future ocean are crucial for marking locations suitable for seaweed aquaculture. Climate change has already resulted in the range shift of commercially important populations of seaweed. For instance, in North America, there has been a decline in *S. latissima* and *Laminaria digitata* populations on the southern range edge and in warming hotspots (Feehan et al., 2019; Filbee-Dexter et al., 2016). In Europe, shifts in seaweed distributions have also been reported, including poleward shifts in the cold-water species *S. latissima* and *A. esculenta* from Northern Europe (Moy and Christie, 2012; Simkanin et al., 2005). Warmer water affiliated *L. ochroleuca* and *L. hyperborea* have been reported to decline in Southern Europe (Piñeiro-Corbeira et al., 2018; Casado-Amezúa et al., 2019), but are expanding into Northern Europe (Schoenrock et al., 2019; Rinde et al., 2014). These examples indicate that site-specific consideration should be given to which species are currently suitable for aquaculture, and which species might offer more appropriate candidates for cultivation under future warming scenarios and predicted species range shifts.

2.1.2 Ocean acidification

An increase in atmospheric CO_2 leads not only to ocean warming, but also to ocean acidification (OA). Rising atmospheric CO_2 levels are tempered by oceanic uptake, removing approximately one third of all anthropogenic released carbon (Iida et al., 2021). Yet this uptake causes a shift in ocean carbonate chemistry (Doney et al., 2009; Kwiatkowski et al., 2020). As CO_2 is absorbed by the oceans, it reacts with seawater to create carbonic acid, causing pH levels to decrease and thus making seawater overall more acidic (Raven et al., 2005). On average, anthropogenic emissions of greenhouse gases have caused pH to decrease in ocean surface seawater by around 0.1 since the beginning of the industrial era (Iida et al., 2021). Future estimates predict that oceanic pH could drop by another 0.2 - 0.3 units by the end of this century (IPCC, 2023). Coastal seas, where most seaweed aquaculture currently takes place, are more at risk of acidification than the open ocean. This is due to the multiple sources of CO_2 and acidic sources that coastal seas are exposed to (such as river inputs, discharge, erosion runoff, etc.), compared with the well-buffered open ocean that is only significantly affected by atmospheric CO_2 (Chan et al., 2017; Clements and Chopin, 2017).

Seaweeds are predicted to have a mixed response to OA as concentrations of dissolved CO_2 increase (Roleda and Hurd, 2012). Calcifying seaweeds are expected to have a negative response toward acidification, yet few studies have examined the response of non-calcifying seaweeds dominating the aquaculture trade (Buschmann et al., 2017; Kim et al., 2017). For non-calcifying seaweeds, it is hypothesized that increased acidification may either have a neutral or a beneficial effect, especially if the seaweed does not use carbon concentrating mechanisms (CCM) as an active carbon uptake strategy (Kübler and Dudgeon, 2015). Britton et al. (2019) studied the effect of diel fluctuating pH levels (representative of coastal environments) on two seaweed species without CCMs. Effects were species-specific, where diel pH fluctuation reduced photosynthesis in the red seaweed *Callophyllis lambertii*, but increased OA benefited physiological rates. Conversely, another rhodophyte, *Plocamium dilatum*, showed no effects of pH fluctuations or OA. Other studies support the findings of species-specific responses to OA (Paine et al., 2023; Ho et al., 2021; Taise et al., 2023; van der Loos et al., 2019b) suggesting that its effects are not just dependent on the method of carbon acquisition, but also species-specific enzyme activity and natural pH fluctuations (Britton et al., 2019; van der Loos et al., 2019b).

In addition, some degree of pH fluctuation happens naturally in many seaweed environments, caused by carbon cycling of the seaweeds. Dissolved inorganic carbon is taken up during the day, increasing the surrounding water pH, and decreases pH during the night as they release CO_2 through respiration (Noisette et al., 2022). Organisms (including seaweeds themselves) which reside in these diel cycle systems are subjected to highly variable pH and CO_2 concentrations that can be of a similar or larger magnitude to the near-future changes expected to occur due to OA (Frieder et al., 2012; Krause-Jensen et al., 2015). As such, these species may be less susceptible and more resilient toward ocean acidification.

2.1.3 Altered seasonality

Both growth and biochemical composition of seaweed species vary temporally. Growth is often determined according to season, such that it is mostly related to available daylight hours independent of other abiotic factors (Lüning, 1994, 1993). On the other hand, processes such as nutrient accumulation in seaweeds may be influenced by temperature, the type and concentration of water nutrient and other abiotic factors that vary seasonally (Rioux et al., 2009; Suresh Kumar et al., 2015). As such, ocean change may cause a mismatch between the optimal environmental conditions for biomass acquisition and intended biochemical composition at harvest time. For example, in cold-water species, such as kelps and fucoids, highest growth is achieved over winter and/or spring when daylight and SST increase, while growth diminishes in summer (Lüning, 1993). While daylength dictates growth, seasonal temperature influences lipid and fatty acid composition (Britton et al., 2021). Elevated water temperatures earlier in the season may thus shift the biochemical composition of harvested species, which will affect end-consumers if harvest time is kept similar, but may also influence the broader fisheries industry

through trophic interactions (Shalders et al., 2022). This may be mitigated by shifting of harvest season to earlier in the season, which may offer a potential opportunity for a second harvest later in the season. Seasonal mismatches may also occur between spore production and the ideal conditions for microscopic life phases of seaweed to grow and recruit (Martins et al., 2017; Bartsch et al., 2013). While the commercial culture of gametophytes is generally achieved under controlled lab conditions, spores are often sourced from wild populations. Tracking optimum time frames for spore harvesting as seasons shift may thus be of relevance to future aquaculture projects (Veenhof et al., 2023).

The seasonal effects of temperature may also interact with effects from ocean acidification. OA can stimulate growth and nitrogen accumulation during warmer seasons in *Gracilaria lemaneiformis* and thus a shift of harvest period to later in the season may be beneficial in an acidifying ocean (Chen et al., 2018). Season can also determine whether OA exacerbates or mitigates the negative effect of ocean warming, which may have knock-on effects for time of harvest. For example, in *Fucus vesiculosus*, OA mitigate the effects of warming in spring and early summer, but the mitigating effect of OA on temperature stress ceased in high summer (Graiff et al., 2015). The results suggest that ocean acidification may impart benefits to temperature resilience in some seaweeds, but that these benefits are limited beyond certain temperature thresholds (24°C, *F. vesiculosus*), and at certain seasonal time-points (spring, *F. vesiculosus*).

Iodine is one of many biochemical components of seaweeds that can vary seasonally and with environmental conditions. Iodine is a key food supplement derived from seaweeds, but can be harmful to for example thyroid function when consumed in excess through seaweed consumption by both humans and animals (Farebrother et al., 2019). Iodine from seaweeds can also bio-accumulate in higher trophic levels, for instance in abalones in integrated aquaculture systems, leading to a risk of excess consumption (Xu et al., 2019). Increased temperature can increase iodine concentration in *Ecklonia cava* (Satoh et al., 2019). In contrast, iodine content increased in winter during colder conditions for *L. digitata* (Nitschke et al., 2018). Iodine content also significantly increased in monocultures of cultivated kelp as compared to wild stands of *S. latissima* (Roleda et al., 2018). In cultivation trials for *S. latissima*, early deployment (October) decreased iodine content as compared to late (January) deployment, demonstrating the clear influence of seasonality on iodine accumulation (Arlov et al., 2024). Currently, many available seaweed food products already contain more iodine per serving portion than is recommended by the Scientific Committee on Food (Aakre et al., 2021; Redway and Combet, 2023). As such, increased iodine content from shifts in season or time of harvest may cause increased risk of excess iodine intake. In addition, increased iodine may be excreted as volatile halocarbon compounds particularly under ocean warming scenarios, which can increase radiative forcing if released in large quantities (Keng et al., 2020). However, at current scale, Atlantic aquaculture is unlikely to pose a significant effect on global radiative forcing (Duarte et al., 2022).

2.2 Challenge 2: extreme events

2.2.1 Storms

Ocean warming has been linked to an increase in storm events and other extreme weather events (Meehl et al., 2000). There is evidence for the enhanced poleward movement of storms in the mid-latitudes due to the increase in atmospheric water vapor and strengthening of upper-level wind velocities (Tamarin-Brodsky and Kaspi, 2017; Wolf et al., 2020). This could increase the risk of severe winter storms over the mid-latitudes in Europe resulting in intense rainfall and stronger winds (Wolf et al., 2020). Changes in the strength of the North Atlantic Oscillation (NAO) towards the end of the 21st century may lead to regional differences in the frequency and intensity of storms. Storms and wind speeds over Central and Western Europe may increase in prevalence and strength, which have the potential to be more destructive to coastal systems (Wolf et al., 2020; Woollings et al., 2012). The North Atlantic coast of North America is also expected to see an increase in tropical storms and hurricanes due to increasing SSTs in the North Atlantic (Marsooli et al., 2019; Villarini and Vecchi, 2012). Increased storms can damage seaweed aquaculture infrastructure, which are often submerged floating longlines (Figure 2), resulting in economic losses and potential risk of marine pollution, affecting overall sustainability of a seaweed farm (Campbell et al., 2019).

The biology of the seaweeds themselves can also be affected by increased storminess. The morphology of cultivated seaweed species (e.g. frond length and width) and the ability of their holdfast to stay secured may be affected by increased hydrodynamic forcing caused by the increase in storm frequency and strength. For example, the cultivated kelp species *S. latissima* generally grows longer and thinner in higher energy, exposed environments where stronger wave action and current strength occur (Peteiro and Freire, 2013). Deploying morphologically plastic crops in increasingly storm-affected environments could result in the direct loss of biomass, as well as compositional changes, due to 'skinnier' growth forms, generally better adapted to high wave energy (Koehl et al., 2008). It may be more desirable to cultivate

FIGURE 2
Harvest of sugar kelp (*Saccharina latissima*) at an experimental seaweed farm, Scotland. This farm utilizes the traditional submerged longline design. Photo credit: A. O'Dell (Scottish Association for Marine Science).

species that are able to adapt to grow in high energy environments and maintain high biomass, such as the kelp species *L. hyperborea* and *A. esculenta* (Pedersen et al., 2012; Stamp, 2015; Smale and Vance, 2015).

Seasonal variations in the individual kelp biomass and surface area can decrease effects of wave action, whereby a loss in kelp tissue due to erosion or spore production results in less storm-generated drag so that the kelp is less prone to detachment and better able to withstand peak water velocities (de Bettignies et al., 2013, 2015). Peak water velocities and minimum individual biomass both occur over the autumn-winter season. This reflects the kelps adaptive response to severe hydrological impact. Kelp survival is also enhanced by a strong holdfast attachment to the substrate, although holdfast fatigue can occur over time with maturity (de Bettignies et al., 2015). Indeed, resilience to high wave-energy environments can change with life stage, where young plants and old plants are both at higher risk of dislodgement (Thomsen et al., 2004). Increased storms can thereby influence choice of deployment times, as optimal nutrient and light conditions for holdfast development in autumn in the Atlantic region coincide with periods of increased storms during which early life stages may become easily dislodged (Kerrison et al., 2015). Despite the increased risk of breakage through entanglement and drag, high wave-energy can increase NPP in certain species of kelps (Smale et al., 2016; Pedersen et al., 2012), though high energy storms in coastal areas can also reduce light availability through sediment turbidity, decreasing NPP (Franke et al., 2023).

2.2.2 Freshwater input and flooding

With increasing incidence of storms and cyclones also comes the increased risk of flooding and freshwater input to surface waters (Marsooli et al., 2019). Freshwater runoff from terrestrial systems can temporarily decrease the salinity in near-coastal waters and impact biodiversity (Gillanders and Kingsford, 2002). In polar regions, seasonal increase of ice melting may also contribute to freshwater influxes (IPCC, 2023; Timmermans and Marshall, 2020). Riverine runoff can also cause nutrient influxes as well as decreased light availability due to increased turbidity (Gillanders and Kingsford, 2002). All these factors may influence growth and performance of seaweeds and are thus relevant for seaweed aquaculture.

Lowered salinity can cause considerable damage to a seaweed crop, depending on the severity of the salinity fluctuation and the species involved. Euryhaline species with high tolerance for salinity changes such as *Ulva* sp. and red seaweeds including *Gracilaria* sp. could be good candidates for aquaculture near major river mouths (Glauco et al., 2024; Yu et al., 2013). However, many of the species currently targeted for aquaculture in the Atlantic, for instance many Laminarian species, have a lower tolerance for reduced salinity. For example, *E. radiata* kelp forests have been reported to decline as a result of increased rainfall and flooding off the Australian coast (Davis et al., 2022b). Adverse effects of reduced salinity can also be compounded by temperature or light stress (Monteiro et al., 2021; Diehl et al., 2020; Spurkland and Iken, 2011). Some kelp sporophytes endemic to the Arctic display a tolerance to low salinity (5-33 ppt) offering potential candidates for aquaculture in low salinity environments (Muth et al., 2021). Whilst under osmotic stress, brown algae can synthesize mannitol, a low molecular weight carbohydrate, which acts as an osmolyte and prevents damage from low salinities (Iwamoto and Shiraiwa, 2005; Diehl et al., 2023). Other compositional changes observed in brown seaweeds include a higher percentage of fermentable sugars (glucose and mannitol) due to low salinity in *S. latissima* and *L. digitata* as opposed to higher biomass and protein content at high salinity (Nielsen et al., 2016). The effect of salinity on biochemical composition varies with species and populations (Diehl et al., 2023), highlighting the need for further research in this area on aquaculture species.

Increase in frequency and severity of extreme weather is also predicted to cause deterioration in water quality in coastal areas, through enhanced runoff, flooding events and upwelling (Nazari-Sharabian et al., 2018). Though seaweeds can mitigate nutrient and pollutant increase through absorption, the increased variability in nutrient loading in coastal waters has also been directly linked to the establishment of invasive algal species in new areas (Incera et al., 2009; Bermejo et al., 2020). Nutrient loading can increase growth of faster growing invasive species on and near slow-growing cultivated species. This in turn leads to a reduced quantity of the biomass produced and a competition for nutrients, light and space (Pedersen and Borum, 1996). Flooding can cause epiphytes and diseases to decrease crop yields, which makes them unsuitable for harvest and consumption and may have consequences for food security (Behera et al., 2022; Ward et al., 2020). In addition to nutrient runoff and eutrophication, decreased clarity of seawater due to sediment discharge may majorly impact upon the production of seaweed farms, as it does in natural seaweed beds (Tait et al., 2021). This is especially relevant in more urbanized areas, where many river-linked systems have already experienced a lowering in water clarity, also called coastal darkening, such as the North Sea. Coastal darkening can reduce carbon acquisition up to 95% in kelps, which has major consequences for kelp farming in coastal areas (Blain et al., 2021). Research shows that despite a decrease in light availability, good crop yields may still be obtained in certain seaweed species due to greater nutrient availability (van der Molen et al., 2018).

2.2.3 Marine heatwaves

As well as driving an increase in average SST, climate change also contributes significantly to the increased frequency and intensity of marine heatwave events (defined as spikes of anomalous temperatures lasting at least five consecutive days) (IPCC, 2023; Sen Gupta et al., 2020). In the last century, marine heatwaves have doubled in intensity and duration (Oliver et al., 2018). These heatwaves can cause direct mortality of seaweeds and can favor the establishment of non-native or invasive species (Atkinson et al., 2020). Marine heatwaves have been directly linked to increased incidence and susceptibility to algal diseases, pests, and epiphytes, including the tropical bacterial disease 'ice-ice' in *Kappaphycus* sp. and *Eucheuma* spp (Largo et al., 2017). Ice-ice is a major disease of *Kappaphycus* and has been reported to have

caused local losses on farms in Indonesia of up to $17,300–18,500 USD, and amounting to an estimated $100 million USD losses annually in the Philippines (Ward et al., 2020, 2022).

Short-term thermal stress may alter both productivity and biochemical composition of cultivated seaweeds. Short-term temperature stresses have been linked to reduced product quality in *K. alvarezii*, in particular in terms of the yield and characteristics of extracted carrageenan (Kumar et al., 2020). Likewise, brown seaweeds can reduce photosynthesis, protein and total fatty acid content in response to heatwaves (Britton et al., 2023; Nepper-Davidsen et al., 2019). On the other hand, certain species have shown no change in their biochemical composition in reaction to marine heatwaves (Shalders et al., 2023). Most research on marine heatwaves to-date has focused on the effects on natural seaweed populations (Smith et al., 2024, 2023; Smale et al., 2019), pointing to a knowledge gap on how marine heatwaves will affect chemical composition and productivity of farmed seaweed. These studies often mark warm-edge populations as most vulnerable to marine heatwaves, indicating that site selection should ideally be in the center range of the species of interest. Sudden loss of crops or disease outbreaks may be linked to marine heatwaves, but further evidence is required. In addition, seaweed farms are often located in sheltered areas which may be more exposed to localized surface warming, especially in areas of reduced tidal exchange. More fundamental and applied research is essential to enable technical and strategic mitigation strategies, such as lowering growing lines to cooler waters, to be proactively employed before marine heatwaves occur, thereby minimizing damage and economical loss to seaweed farms.

2.3 Challenge 3: disease and herbivory

2.3.1 Disease

Physiological impacts from the changes in temperature, salinity, and CO_2 on seaweeds are often compounded by increased disease and pest susceptibility due to cumulative physiological stresses and reduced fitness (Largo et al., 2017; Qiu et al., 2019). Increased disease susceptibility can also be caused by environmental factors that disturb the microbiota that naturally occur on the seaweed, termed 'dysbiosis', which then leaves the seaweed vulnerable to invasion of pathogenic microbes (Egan and Gardiner, 2016). For example, decreased survival in the seaweed *Delisea pulchra* was caused by warmer waters, inducing stress and increasing its susceptibility to bacterial infection. This then led to an increased occurrence of bleaching events, which in turn further damaged and stressed the seaweed (Campbell et al., 2011).

Research on diseases in seaweed species has so far focused on species of aquaculture interest (Gachon et al., 2010; Ward et al., 2020). Of these, there is more research available on tropical species, such as *Kappaphycus* and *Eucheuma* species, including the widespread infection that commonly afflicts them, 'ice-ice' (Behera et al., 2022). Ice-ice presents a clear example of ocean-warming induced disease spread, as stock is more susceptible to infection with ice-ice during spikes of warming or heatwave events (Largo et al., 2017). For example, a significantly higher susceptibility to ice-ice (from 0 to 100% infection) following just one week of >30°C water temperatures was shown in lab studies of *K. alvarezii* (Largo et al., 1995). Similar patterns of association between disease outbreaks in *Kappaphycus* and *Eucheuma* sp. and heatwave events or spikes of low salinity have also been observed in natural populations and on cultivation lines (Pang et al., 2015; Ndawala et al., 2022).

There is less available knowledge on prevalent diseases and their interactions with environmental factors in temperate species currently used in Atlantic aquaculture (but see Ward et al., 2020). White spot disease in *S. japonica* causes blisters and white spots on the front, and can decrease iodine and crude protein content by ~20%, as well as lower photosynthetic pigment concentrations and daily growth rates (Wang et al., 2021). Green rotten disease meanwhile strikes early, mostly affecting *S. japonica* juveniles (Li et al., 2020). Cataloguing different pathogens has mainly focused on bacteria and fungi. Epiphytes and viruses may also cause considerable damage and need further research attention (Behera et al., 2022; Matsson et al., 2019). Creative solutions need to be developed to minimize the threat of crop diseases under ocean change and foster collaboration. A fantastic, albeit short-lived, example of this was the web-portal where farmers can report seaweed disease and send samples found on their farms (Strittmatter et al., 2022). Lessons can be learned from some of the problems encountered with tropical seaweed aquaculture, where the extensive use of cloning has reduced the gene pool and is thought to have lowered disease resistance (Valero et al., 2017). However, solutions can also be found in tropical aquaculture, for example, usage of mixed crops which can enhance resilience to diseases (Pang et al., 2015).

2.3.2 Herbivory

Grazing is a well-known mechanism controlling the range and productivity of natural seaweed beds (Ling et al., 2015; Vergés et al., 2016; Dayton et al., 1984). Despite extensive attention on the effects of grazing on wild seaweed populations, little is known about the effects of herbivory on commercially grown seaweeds in the North Atlantic (Behera et al., 2022). As with diseases, most of the knowledge is concentrated around the tropical species *Kappaphycus* and *Eucheuma*. Grazing of these cultivated species can lead to tissue damage, and thus crop loss (Mantri et al., 2017), but also an increased risk of further infection (Tan et al., 2020). Grazing can trigger the seaweeds defense mechanisms, which in turn can change the biochemical composition of the crop and may lower the nutritional or palatable quality of the products (Cruz-Rivera and Villareal, 2006; Toth et al., 2007). As an example, many brown seaweeds increase phlorotannin content as a reaction to grazing (Pavia and Toth, 2000; Taylor et al., 2002).

In the context of climate change, there are certain factors which may exacerbate grazing activity on commercial farms. Topicalization is the movement of tropical species into temperate habitats, where they can cause substantial damage to seaweed beds (Vergés et al., 2016). Tropical fish can cause more extensive damage than native species, as they are adapted to feed continuously and are able to remove large portions (60 - 97%) from seaweed systems daily (Hay and Fenical, 1988). In tropical reef systems, this

maintains a balance between coral and seaweed abundance (Bellwood and Fulton, 2008). However, in temperate reef environments, this mode of grazing can often be unsustainable and detrimental to seaweed populations (Vergés et al., 2016; Bennett et al., 2015). Atlantic fish assemblages are shifting towards more warm water affiliated species (Chust et al., 2024; Horta e Costa et al., 2014). The inclusion of large-scale farms in these temperate environments may allow tropical grazers to flourish in these regions under ocean warming, potentially acting as initial foothold habitats for invasive species and resulting in spillover to natural seaweed populations. In addition, metabolic theory predicts that increased temperature increases oxygen consumption (Gillooly et al., 2001), which can lead to increased consumption in some grazers (Leung et al., 2021; O'Connor, 2009; Carey et al., 2016). Chemical defense mechanisms against grazers may also be reduced under warming and acidified conditions (Kinnby et al., 2021). Compounding factors such as these may exacerbate grazing impact on seaweed farms under ocean change.

Grazing by herbivorous fish in temperate aquaculture systems has already been observed on *S. latissima* and *U. pinnatifida* (Peteiro and Freire, 2012). The types of grazers that may affect seaweed farms will depend on the location of the farm. With inshore farms, it is expected that similar grazers to those of natural seaweed beds will interact with the farmed seaweed, both macrograzers (e.g. fish and sea urchins) and mesograzers (small crustaceans and gastropods). However, with the introduction of open ocean seaweed farming, novel interactions between grazers, epifauna and the farmed seaweed may occur. Currently, there are very few offshore, open ocean farms in operation but there is considerable interest given the spatial scale needed to make seaweed farming more economically viable (Visch et al., 2023; Bak et al., 2020). It will be vital to thoroughly research any potential interactions harmful for either the farmed seaweed or the environment at large before open ocean aquaculture ventures are carried out at scale.

3 Opportunities

As the effects of climate change become more severe, there is a greater drive for researching potential solutions and adaptations in seaweeds to changing climate conditions. With increasingly sophisticated oceanographic and climate modelling, future conditions at potential cultivation sites may be more accurately predicted to assist in the selection of seaweed aquaculture sites and species with changing oceans in mind. In the era of 'omics' approaches, there are opportunities in breeding and trait selection for climate resilience, as well as enhancing performance through targeted microbe treatments (Li et al., 2023; Kim et al., 2017). And finally, the capacity and motivation to restore natural seaweed habitats has increased with the public awareness that many seaweed ecosystems are under threat from climate change (Eger et al., 2023). Many individual restoration projects have sprung up worldwide in recent years, however technical challenges remain in terms of scale and feasibility (Coleman et al., 2020b). Here we highlight the benefits from closer collaboration between restoration and aquaculture ventures and investigate the use of restorative approaches in aquaculture beneficial to both industry and the environment it depends on.

3.1 Opportunity 1: 'future-proof' site selection

Site selection is the first barrier to overcome when starting a new seaweed cultivation operation. The environmental conditions of the site must include the suitable range for the chosen species over the cultivation cycle in order to ensure adequate crop quantity and quality (Kerrison et al., 2015). This will include seawater temperature, salinity, nutrient and light levels, as well as prevalent current and wave regime. However, environmental conditions are set to shift in response to climate change, which will affect not only existing aquaculture operations, but also the siting of future developments. With careful consideration, sites and species can be selected with an eye on future climate conditions.

3.1.1 Site considerations in a changing climate

Current cultivation sites in the North Atlantic are often positioned in naturally sheltered, coastal and estuarine environments to facilitate operations and minimize wave and storm damage. The physical resilience of aquaculture infrastructure and gear (such as anchored lines or mooring systems) must be modified to withstand increased loading and mechanical failure due to storm surge damage such as increased wave current velocities, high winds and large waves (Bricknell et al., 2021). For example, infrastructure designs may be optimized to dissipate wave energy and take into consideration local geomorphology and hydrology to select sheltered sites at peak storm surge timings. As such, a farm site can even protect the shoreline from damaging wave action and increase coastal resilience (Zhu et al., 2021). However, the selection of such sites is not straightforward. With increased storms, increased flooding is expected to affect tide-surges in estuarine and coastal systems, for which there is currently a lack of accurate modelling capacity (Bricknell et al., 2021). Resolving these issues through improved modelling may greatly improve spatial planning of seaweed farms with consideration given to future storm and flooding events.

Another important consideration with regard to increased flooding is the increased influx of freshwater and decreased salinity, which can have detrimental effects on seaweed beds (Davis et al., 2022b). Choosing sites with higher vertical mixing and/or upwelling may better help mitigate against the impact of osmotic stress, as they restore salinity to ambient levels. Alternatively, cultivation of seaweed at greater depths, with adjustable depth control, or on offshore sites may resolve some of these issues as salinity is more stable at greater depths and offshore (Stammer et al., 2021). Light may become limited at greater depths, though successful cultivation and greater depths have been reported from pilot off-shore farms as water clarity often improves offshore (Bak et al., 2020).

Increasing average SST, as well as increased occurrences of marine heatwaves, may make sites unsuitable for the cultivation of

certain species in the near future. However, suitable management plans can help to mitigate negative outcomes. Marine heatwaves can be forecast with reasonable accuracy up to one year in advance (Jacox et al., 2022). Digital resources, such as www.marineheatwaves.org, which can be used for real-time monitoring and future prediction of marine heatwaves, are becoming an increasingly powerful tool for preventative strategies and policies. For example, both the United States and Australia recently implemented nationwide marine heatwave briefings designed to aid the shellfish aquaculture industry in mitigating damage (Hobday et al., 2023). As the seaweed aquaculture industry uses controlled environment nursery systems for seed-line production, operations may choose to deploy later in the season if heatwaves are predicted to occur at the time of deployment. This delayed deployment however comes at the cost of greater risks of autumn storms and increased light limitation during the critical early grow-out stage.

3.1.2 Future range shifts of Atlantic commercial species

With increasingly sophisticated models of historic and future natural kelp distributions, a clearer picture emerges of where net gain/loss in kelp biomass will occur under long-term ocean warming (e.g. Krumhansl et al., 2016; Davis et al., 2022a; Goldsmit et al., 2021; Gouvêa et al., 2024; Assis et al., 2024, 2022). However, analysis of range shifts that focus specifically on commercially important species in the context of seaweed aquaculture remain scarce (but see Assis et al., 2018; Wilson et al., 2019). We, therefore, present a case study where we project future distributions based on thermal niche of five commercially important species in the North Atlantic; *L. digitata*, *A. esculenta*, *S. latissima*, *L. hyperborea* and *Palmaria palmata*. Projections use the ssp370 medium-high warming scenario and project to a near-future of 2070 (methods fully described in García Molinos et al. (2016); see also Supplementary Material for clarification).

Climate velocity trajectory (CVTs, Figure 3) models show projected losses at warm edges of species ranges and gains at cold edges. Together, these approximate the simple predictions of shifts in the isotherms corresponding to thermal limits. Losses at warm edges were projected to be severe for some species. They include a complete loss by 2070 of *L. hyperborea* and *S. latissima* from northern Spain (Figures 3C, E), reduction in range in the same area for *P. palmata* (Figure 3D), and extensive loss of range in southwest Britain, Ireland, and France for *A. esculenta* and *L. digitata* (Figures 3A, B). Importantly, the projected distributions indicate that large parts of the UK, Ireland and North America will be unsuitable for growing *A. esculenta* by 2070, and parts of Spain and France unsuitable for *S. latissima*, both species being currently favored in Atlantic aquaculture (Figure 1). A shift in the species considered for aquaculture to more thermally tolerant species, for example *L. ochroleuca* and *S. polyschides*, may mitigate some of these losses (Casado-Amezúa et al., 2019).

CVT models suggest that all species examined would have newly suitable areas for growth at the cold edges of their distributions. Range expansions in the sugar kelp *S. latissima* and winged kelp *A. esculenta* may occur in the Russian Arctic, but less area appears suitable in Greenland and the Canadian Arctic. Aquaculture activity will not be limited by considerations of population connectivity and available rocky substrate, although use of species in newly thermally suitable areas may be limited by other factors. Most importantly among these are water clarity, salinity fluxes and the extreme seasonality of light availability, which may be a constraint for poleward expansion of cold-temperate species of seaweed (Filbee-Dexter et al., 2019) and thus cultivation of seaweed in these regions. For example, *Laminaria solidungula* is endemic to the Arctic, though kelps common in the Atlantic and suited for aquaculture such as *S. latissima, A. esculenta*, and *L. digitata* grow in the Arctic as well (Wiencke and Amsler, 2012; Filbee-Dexter et al., 2019). Generally, if a kelp is a seasonal anticipator (starting growth and reproduction under short-day conditions in winter and early spring, anticipating summer conditions) they may fare well under Arctic conditions, where long daylight coincides with low nutrient conditions (Wiencke and Amsler, 2012; Kain, 1989). This growth under suboptimal light conditions is facilitated by the storing of carbon acquired during summer periods, in the form of laminarian and/or lipids, thus potentially changing biochemical composition compared to temperate kelps (Scheschonk et al., 2019; Olischläger et al., 2014). Many kelps growing in the North Atlantic originated in the Pacific with multiple crossings of the Arctic occurring in their evolutionary past (Starko et al., 2019), while recent genomic data shows that kelps persisted through several periods of glaciation (Bringloe et al., 2022). This indicates that North Atlantic kelps may already be adapted to grow under future polar conditions. Trials with commonly cultured species under darkness would be beneficial to understand the constraints of expanding seaweed aquaculture into the Arctic as more areas become continuously free of sea ice.

3.2 Opportunity 2: advances in breeding & microbiome manipulation

3.2.1 Breeding and hybridization

Advances in genomic research on seaweeds has greatly expanded the toolkit available for breeding desirable traits in seaweeds. So far, many of the breeding efforts in seaweeds have been focused on increased biomass and growth, and most available knowledge is on the few species grown in large quantities in Asia, predominantly of the genera *Gracilaria, Porphyra, Saccharina, Undaria* and *Ulva* (Patwary et al., 2021). Through a mixture of self-fertilization, cross breeding between populations, and selection of well-performing offspring, strains of *S. japonica* and *U. pinnatifida* now exist in China and Korea that yield far higher growth and dry biomass weights than in early cultivar lines (Li et al., 2016a; Shan et al., 2016; Li et al., 2016b). The number of available seaweed genomes for commercially grown species has also increased rapidly in the past decade offering platforms for further genetic breeding programs (Wang et al., 2020; Nelson et al., 2024). A recent leap in sequencing effort has made a further 110 seaweed genomes publicly available, spanning 105 different species (Nelson et al., 2024). Among cultivated seaweeds, several have been successfully genetically modified to express recombinant proteins, including *S. japonica, U. pinnatifida, K. alvarezii, Porphyra*

10.3389/fmars.2024.1483330

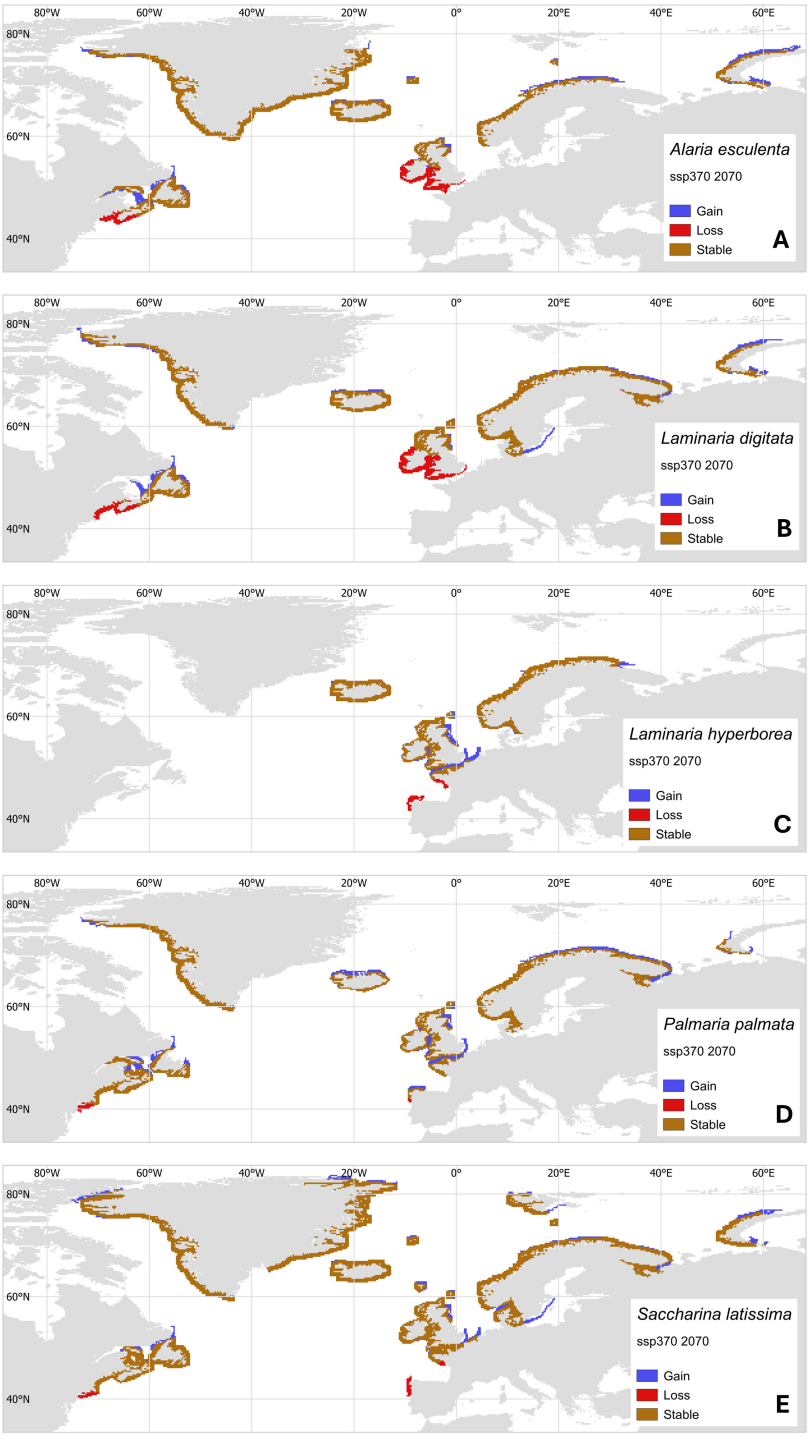

FIGURE 3
Projected geographical distributions of North Atlantic aquaculture species by 2070 under the medium-high ssp370 warming scenario from shifts in isotherms from present-day range locations. Maps show projected changes for **(A)** *Alaria esculenta*, **(B)** *Laminaria digitata*, **(C)** *Laminaria hyperborea*, **(D)** *Palmaria palmata*, and **(E)** *Saccharina latissima*. New areas of habitat (Gain, blue) are where conditions become climatically suitable, while habitats lost (Loss, red) are where future temperatures are likely to exceed maximum baseline temperatures within the distribution range. Stability (brown) is indicated where populations persist.

yezoensis and *Ulva lactuca* (Trujillo et al., 2024). Recently, CRISPR-Cas9 has been used to successfully gene edit *Ectocarpus* and *S. japonica* gametophytes which were able to produce sporophytes, paving the way for further gene-editing studies (Shen et al., 2023; Badis et al., 2021). The use of transcriptomics, metabolomics and proteomics are still in their early stages for most seaweeds compared to terrestrial crop species (Patwary et al., 2021). However, exciting advances have been made in recent years

which offer potential solutions to the challenges presented by climate change, which are discussed below.

With increasing pressure from climate change, there has been an increased effort to discover and characterize environmentally resilient strains of seaweeds for cultivation. One major advance in this area has been the identification of the molecular basis of stress responses in several species of seaweed, such as heat shock proteins (HSPs) (Hammann et al., 2016; Eggert, 2012; Smolina et al., 2016). HSPs are key players in stress response in land plants and protect cells from damage due to heat (and other) stress (Timperio et al., 2008). Stress-related transcriptomic studies have mostly been carried out on red seaweeds, paving the way to understanding the molecular basis for stress resilience in algae more widely. For example, *P. yezoensis* displays upregulation of HSP under increased temperature stress (Sun et al., 2015). More recently, transcriptomic analysis showed that thermal resilience is higher among outbred crosses of *L. digitata*, which was underpinned by differentially expressed genes (Liesner et al., 2022). Interestingly, whilst inbred and outbred crosses performed similarly physiologically, the underlying protein expressions were different, indicating a divergent metabolic pathway to cope with temperature stress (Liesner et al., 2022). Such use of transcriptomics in breeding experiments under heat stress provides invaluable data that may be further used in targeted molecular breeding.

Huang et al. (2022) trialed genomic selection in kelp breeding in *S. latissima*, where genotyped gametophytes were used to grow sporophytes, which were then evaluated for desirable traits such as increased wet and dry weight. The next breeding cycle used genetic selection to perform optimal crosses with gametophytes containing beneficial traits as defined by genotyping. Genetic selection at the gametophyte stage was successful which resulted in higher yields (weight, length) in farmed sporophytes, the effects of which increased over several breeding cycles, indicating genetic gain (Huang et al., 2023). Some roadblocks to successful use of genetic selection in seaweed breeding still remain, e.g. difficulties in upscaling bulk cultures of gametophytes, improving spore survival, and in inducing spore release of desirable sporophytes to start the next breeding cycle (Huang et al., 2022). If these roadblocks can be overcome, genetic selection may be useful in the selection of climate stress resilient strains for future deployment. Furthermore, legislation around breeding and genetic modification in kelps is not yet well-defined in many countries, and should be underpinned by knowledge on genetic variety in local populations, as well as the scale of genetic impact from farm to wild populations (Goecke et al., 2020).

Whilst many of these advances can help make seaweed farms more resilient to ocean change, care should be taken to not negatively impact genetic diversity in natural seaweed beds (Campbell et al., 2019; Hu et al., 2023). The widespread use of clonal monocultures, as well as threats from climate change, can result in the loss of wild genetic resources that underpin climate resilience (Goecke et al., 2020; Coleman et al., 2020a; Valero et al., 2017). Efforts to map wild genetic diversity in seaweed species of cultivation interest are improving (e.g. Fouqueau et al., 2024), alongside efforts to biobank and preserve wild genetic resources for future use (Wade et al., 2020; Brakel et al., 2021). Taking note of genetic diversity within farms may not only help in preserving genetic diversity of wild populations but can also enhance resilience of the farmed species to climate change. Through hybridization, which may preserve genetic diversity, physiological performance under stress can be increased (Goecke et al., 2020; Hu et al., 2023). This has been shown in multiple kelp species (e.g. Martins et al., 2019; Murúa et al., 2021; Hara and Akiyama, 1985) and *Porphyra* (Kim, 2011). Interestingly, fecundity in *M. pyrifera* gametophytes appears influenced by the degree of relatedness, as well as population of origin (Camus et al., 2021; Solas et al., 2024). This indicates that interpopulation breeding may also benefit productivity at the nursery stage, depending on the population of origin.

3.2.2 Priming of early life history stages

Another promising avenue for advancing stress tolerance of broodstock is through priming the early life history stages of seaweed with sublethal levels of stress, so that the subsequent adult generation is more resilient to that stressor (Jueterbock et al., 2021). As this can be done without the need for inbreeding or performing outcrosses, this does not increase risk of genetic depression in either farmed or natural populations. The molecular basis for priming is relatively well established in agriculture practices, where this technique is routinely used to enhance crop stress resilience (Liu et al., 2022a). Exposure to heat stress, for example, triggers certain genes to switch on, which is retained in later life stages through epigenetic modification such as methylation (Liu et al., 2022a). However, as seaweeds often have several life history phases, the basis of passing on 'stress memory' diverges from that of land plants. Recently, cold-priming of *L. digitata* gametophytes was shown to improve thermal resilience in the sporophyte generation, which is thought to be a result of epigenetic modification (Gauci et al., 2022). Increased methylation under both cold and warm temperature stress has been found in *G. lemaneiformis* (Peng et al., 2018). In *S. latissima*, methylation patterns were associated with culturing conditions, and differed significantly from field samples, as well as differing between populations of origin, showing the importance of environment in determining methylation patterns (Scheschonk et al., 2023). In *S. japonica*, heat stress caused an increase of methylation, which in turn regulated genes connected to heat stress response such as the production of HSPs (Liu et al., 2023a). Cross-stressor use of priming has also proven effective in *A. esculenta*, where high light doses during early cultivation decreased the thermal stress response of sporophytes (Martins et al., 2022). These results indicate that priming may be an effective and relatively easy to achieve method of increasing thermal resilience in seaweed stocks used for aquaculture. However, the effect of priming has only been tested in gametophytes and juvenile sporophytes. Whether the increased resilience to temperature stress from priming carries over into adult cultivated sporophytes remains to be tested.

3.2.3 Microbiome manipulation in the nursery stage

There is increasing research interest in the role of microbiota on the physiology and ecology of the seaweed host. The microbial community and the host, together termed the holobiont, can be considered as one functional entity responding and adapting to environmental change (Egan et al., 2013; van der Loos et al.,

2019a). As microbes have short generation spans, they can be of use in accelerating adaptation to environmental change in the host organism and, as such, have received attention in the context of climate change adaptability of seaweeds (Eger et al., 2022; Wood et al., 2019). As early as the 1980s, research on *Ulva* sp. showed abnormal development of morphological characteristics when changing the epibiotic community associated with the *Ulva* host (Provasoli and Pintner, 1980). Since then, research has expanded to characterize, identify and isolate beneficial strains of microorganisms involved in seaweed growth and disease resistance. A recent review by Li et al. (2023) outlines a pathway for using microbiota manipulation for improving the seaweed aquaculture industry. Here, we focus on some studies that have the potential to increase climate change resilience of cultivated species.

Disease resistance is one major pathway in which microbiota can be exploited to increase climate change resilience of cultivated seaweed species. For example, identification of a bacterial strain (*Phaeobacter* sp. BS52) that protects against opportunistic harmful microbial invasion causing bleaching in *Delisea pulchra* (using the model pathogen *Aquimarina* sp. AD1) shows a potential pathway of enhancing disease resistance through manipulation of microbial communities (Li et al., 2022a). As *D. pulchra* is more susceptible to pathogens under elevated temperature, the addition of BS52 may enhance its resilience to ocean warming. Moreover, the beneficial effects of BS52 were applicable to a non-native host, *Agarophyton vermiculophyllum*, where inoculation worked better in reducing harmful effects of a bleaching disease as compared to its native microbiota (Li et al., 2022b). In *S. japonica*, differences in associated microbiota between healthy and infected juvenile sporophytes offer the potential for developing microbial inoculates to enhance resistance against white bleaching disease, which has a damaging effect on the nursery stages of this cultivated kelp (Ling et al., 2022). Based on this, a beneficial strain of bacteria was isolated (*Vibrio alginolyticus* X-2) which increased *S. japonica*'s immune response and disease resistance via changing the transcriptome and metabolome of inoculated juvenile sporophytes (Ma et al., 2023b).

Inoculation of early life history stages may be an effective way of improving overall disease and climate resilience in cultivated species, as this can be done *in vivo* in nursery facilities, and whole broodstocks can be treated at once. There are, however, some significant knowledge gaps in how effectively the microbiota transfer from one life stage to the next. Recently, some indication was found that the parent microbiota transfers to the gametophyte in *M. pyrifera*, as there was a significant effect of population of origin on the microbiome of gametophyte cultures (Osborne et al., 2023). In addition, strains were identified (within the *Mesorhizobium* genus) that were associated with increased biomass acquisition in the sporophyte stage (Osborne et al., 2023). Contrastingly, Davis et al. (2023) found little to no transference of nursery gametophyte microbes to the out-planted sporophytes of *A. marginata* and *S. latissima*. Instead, species, time of year and source microbiota influenced the associated microbiota on cultivated sporophytes (Davis et al., 2023). Recruitment of microbial communities in cultivated *Sargassum fusiforme* seedlings was also mostly governed by stochastic processes (Liu et al., 2023b).

There is increased evidence that the microbiota of the seaweed holobiont plays a role in the response of the host to thermal stress. The ability to maintain stable microbiota through host selection under thermal stress was linked to invasiveness in *G. vermiculophylla* (Bonthond et al., 2023). Thermal stress also changes the microbiota of *Cystoceira compressa* and *E. radiata*, among other species, which subsequently affects both growth and photosynthetic capability (Qiu et al., 2019; Mancuso et al., 2023). However, direct evidence for microbial inoculation increasing thermal resilience is still lacking. Juveniles of *Dictyota dichotoma* did not perform better when inoculated with a mix of naturally occurring microbiota, neither did the inoculum affect the epibiota (Delva et al., 2023). However, this may have been due to the sourcing of the inoculum, which was taken from seawater at the same temperature as the lower thermal treatment. This shows that ample opportunity still exists to examine the potential of enhanced stress tolerance in seaweeds via microbiota manipulation, and conflicting results point to knowledge gaps defining the underlying mechanisms of the role of microbiota in seaweed stress resilience.

3.3 Opportunity 3: restorative aquaculture

While seaweed aquaculture production continues to accelerate, there is an increasing awareness of the simultaneous threat to natural seaweed beds from changing climate. Initiatives to restore natural seaweed ecosystems have developed worldwide in the last few decades (e.g. Eger et al., 2023; Vergés et al., 2020; Chung et al., 2013). However, large-scale restoration projects are still rare. There are some success stories, for example active restoration of 500-800 hectare of seaweed habitat in Korea and Japan (Eger et al., 2020), 8500 hectares of macrophyte habitat (also including seagrass) in China (Liu et al., 2022b) and the protection of 30,000 hectares of kelp habitat for rewilding in the English Channel (Williams et al., 2022). While these are all steps in the right direction, large scale restoration will need significant investment of both time and monetary funds, as well as technological advances in growing and breeding seaweeds (Eger et al., 2020). There is an opportunity for collaboration between aquaculture and restoration projects, as investment and technical advances will be more likely to develop in the aquaculture sector. This synergy is required so that maximum benefits can be derived from restorative approaches to seaweed aquaculture, which will be discussed in this section.

3.3.1 Co-culture

Improving resilience in both aquaculture and restoration projects may be boosted by using co-culture techniques rather than growing one target species for restoration and cultivation. There are not many studies available yet which examine a more ecosystem-based approach to growing seaweed, such as is being trialed in agriculture with the use of restorative and permaculture practices (Corrigan et al., 2022). However, there are some studies that indicate that diversifying crops grown in aquaculture facilities can increase yield. For example, co-culture of *Kappaphycus* sp. with *Euchema denticulatum* increased resistance against ice-ice during the summer months, when chances of infection rise with ocean temperatures (Pang et al., 2015). In their study, co-culturing was

achieved by alternating longlines growing one species each, and infection rates of ice-ice and the epiphyte *Neosiphonia savatieri* were reduced from ~80% in individually cultured species, to ~14% in co-culture (Pang et al., 2015). Furthermore, the co-culture of cultivated seaweeds with species that are non-palatable to grazers such as *Caulerpa* and *Halimeda* spp. also decreased grazing of *Gracilaria* sp. by herbivores (Ganesan et al., 2006). Co-culture may thus increase resilience to ocean-warming induced disease, while also increasing the potential increasing derived biodiversity benefits of a seaweed farm by increasing macroalgal diversity.

This concept may be extended to co-culture with species of shellfish or finfish, which has been more widely researched. Integrated multitrophic aquaculture (IMTA) may have further knock-on benefits for the local system it is placed in by absorbing nutrients and dissolved CO_2 (Duarte et al., 2022; Kim et al., 2017; Ross et al., 2023). This lowers pH locally and provides a chemical refuge for marine calcifiers such as shellfish, limiting low saturation levels of aragonite (Ω_{Arag}) and thus lowering the risk of shell dissolution (Fernández et al., 2019; Falkenberg et al., 2021). In turn, the shellfish provide additional nutrients (e.g. nitrate, urea, phosphate) for seaweed growth, thus increasing the potential for large-scale macroalgal cultivation and providing economic benefits for both the seaweed and shellfish farm. However, the pH-buffering capacity of seaweeds is highly species-specific and depends on the local community structure and prevailing hydrodynamic conditions (Ricart et al., 2023). Some studies show a significant increase in pH, O_2 and Ω_{Arag} in seaweed farms which can increase shellfish growth, as well as large fluctuations in pH hypothesized to help shellfish adapt to acidification (Xiao et al., 2021; Li et al., 2021; Young et al., 2022). Others have found no benefits derived from co-culturing shellfish with several species of seaweed (Leal et al., 2024). Overall, more research is required in this area, particularly regarding the cumulative effect of OA and warming on seaweed performances. Often the negative impact of ocean warming outweighs any beneficial effect of acidification (Graba-Landry et al., 2018; Britton et al., 2020; Wahl et al., 2020). In addition, a better understanding is needed for the co-culture of shellfish and seaweeds regarding target species and productivity rates and their interactions with local environmental factors.

3.3.2 Restoration and cultivation co-benefits

Besides bio-buffering in a commercial IMTA context, seaweed farms may also be used as a pH buffering strategy in naturally occurring ecosystems which rely on calcifying species (e.g. coral reefs, maerl beds, oyster reefs). These species are most vulnerable to OA as their structural integrity is threatened by lowered oceanic pH (Doney et al., 2009). For example, seaweed farming partially mitigated OA in a coral reef ecosystem, but mitigation success (in terms of maximum increase in pH and Ω_{Arag}) depended on the optimum location, size, seaweed density and harvesting strategy of the farm (Mongin et al., 2016). To the best of our knowledge, this is the only study that has investigated benefits of acidification in the context of coral reefs, but the projected co-benefits certainly warrant further research.

Other ways in which restoration and aquaculture industries can benefit from collaboration is through knowledge sharing and generating funds to achieve successful restoration. Certainly, one of the main roadblocks to many restoration initiatives is lack of funding, as well as technical knowledge and facilities for cultivating seaweeds on a large scale (Eger et al., 2020). The aims of aquaculture and restoration industries are distinct: where aquaculture may be concerned mostly with increasing biomass and composition of the product, restoration is interested in successful transference of ecosystem-wide benefits. There are, however, some areas in which these two industries overlap. For example, both industries will benefit from climate-proof solutions to cultivation, maintaining genetic variety in

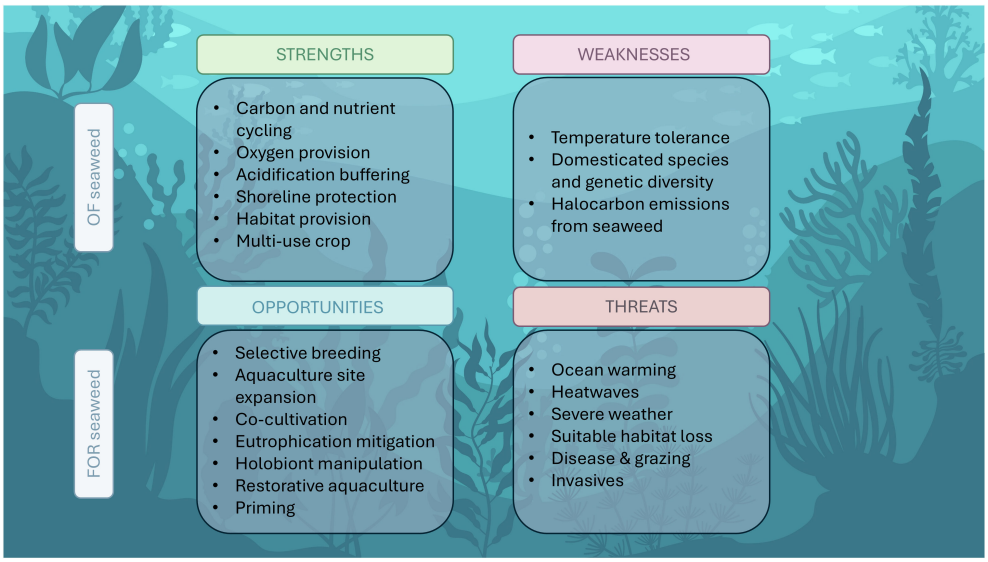

FIGURE 4
Summary of strengths and weaknesses of seaweed cultivation in the context of climate change, and the opportunities and challenges facing the seaweed industry.

biobanks and cost-effective technologies for large-scale deployment. In particular, the maintenance and provision of seedstock by commercial scale nurseries to support restoration has the potential to accelerate restoration scale and success (Filbee-Dexter et al., 2022). Currently, many restoration projects propagate their own seedstock derived from small source populations or transplanted adult individuals, which is both costly and diminishes the chances of success through lack of genetic resilience (Eger et al., 2022). Commercial scale nurseries have the knowledge and skills to increase resilience and genetic diversity in their broodstock, which will benefit restoration by increasing robustness to climate change. Recent biobanking initiatives focusing on Atlantic species are paving the way for preserving genetically diverse broodstock (e.g. the SeaStrains initiative by the Global Seaweed Coalition, and several biobanks like Biobancos (Portugal), the Seaweed Nursery at the Scottish Association for Marine Science (UK), and CCAP (UK)). Another factor that can hinder both aquaculture and restoration initiatives is permitting, social license and legislation (Eger et al., 2022; Wood et al., 2017). A more integrated push from both restoration and aquaculture industries may increase the speed and efficacy in which the necessary legislative changes for both coastal cultivation and restoration are achieved.

4 Conclusion

Globally, seaweed aquaculture is currently a major contributor (~50%) to ocean-based aquaculture production and has the potential to expand further as the need for sustainable food and materials increases (FAO, 2022). The seaweed industry, however, faces key challenges from ongoing climate change. In this review we have summarized some of the major challenges that the industry is facing through climate change stressors. On the other hand, we have highlighted opportunities for increasing resilience and sustainable development. These findings are summarized in Figure 4. Whilst some of the challenges are considerable, the strengths and opportunities highlighted in this review outnumber the weaknesses and threats, emphasizing the great potential of the seaweed industry as a sustainable industry. In recent years, there has been a lot of media attention on seaweed as a solution to many climate issues, creating a 'seaweed hype'. To deliver on its promise however, technological difficulties and practical challenges pertaining to thermal tolerance, genetic diversity, scalability and disease resistance must be overcome. Here we have summarized research efforts that can provide a solution to some of these hurdles, and we hope to inspire further research in the three areas of opportunity: 'Future-proof' site selection, development of selective breeding and microbe inoculations for increased resilience, and taking a restorative or ecosystem approach to seaweed aquaculture. In the face of climate change, seaweed aquaculture offers a globally sustainable solution to some of the most pressing challenges related to food security and environmental stress.

Author contributions

RV: Conceptualization, Visualization, Writing – original draft, Writing – review & editing. MB: Conceptualization, Data curation, Formal analysis, Writing – review & editing, Visualization. AH: Conceptualization, Funding acquisition, Writing – review & editing. KM: Conceptualization, Writing – review & editing. MR: Conceptualization, Writing – review & editing. AT: Conceptualization, Writing – review & editing. JF: Conceptualization, Writing – review & editing. MS: Conceptualization, Funding acquisition, Supervision, Writing – review & editing.

Funding

The author(s) declare financial support was received for the research, authorship, and/or publication of this article. This review was funded by Shell Global Solutions International BV and the EU H2020 project ASTRAL [grant agreement No. 863034].

Conflict of interest

Author JF was employed by the company Shell Exploration and Production Inc.

The remaining authors declare that the research was conducted in the absence of any commercial or financial relationships that could be construed as a potential conflict of interest.

The authors declare that this study received funding from Shell Global Solutions International BV. The funder had the following involvement in the study: review of the article and the decision to submit it for publication.

Publisher's note

Supplementary material

The Supplementary Material for this article can be found online at: https://www.frontiersin.org/articles/10.3389/fmars.2024.1483330/full#supplementary-material

References

Aakre, I., Solli, D. D., Markhus, M. W., Mæhre, H. K., Dahl, L., Henjum, S., et al. (2021). Commercially available kelp and seaweed products–valuable iodine source or risk of excess intake? *Food Nutr. Res.* 65, 7584. doi: 10.29219/fnr.v65.7584

Alexander, K. A., Potts, T. P., Freeman, S., Israel, D., Johansen, J., Kletou, D., et al. (2015). The implications of aquaculture policy and regulation for the development of integrated multi-trophic aquaculture in Europe. *Aquaculture* 443, 16–23. doi: 10.1016/j.aquaculture.2015.03.005

Allen, M. R., Frame, D. J., Huntingford, C., Jones, C. D., Lowe, J. A., Meinshausen, M., et al. (2009). Warming caused by cumulative carbon emissions towards the trillionth tonne. *Nature* 458, 1163–1166. doi: 10.1038/nature08019

Arlov, Ø, Nøkling-Eide, K., Aarstad, O. A., Jacobsen, S. S., Langeng, A.-M., Borrero-Santiago, A. R., et al. (2024). Variations in the chemical composition of Norwegian cultivated brown algae *Saccharina latissima* and *Alaria esculenta* based on deployment and harvest times. *Algal. Res.* 78, 103421. doi: 10.1016/j.algal.2024.103421

Assis, J., Araújo, M. B., and Serrão, E. A. (2018). Projected climate changes threaten ancient refugia of kelp forests in the North Atlantic. *Global Change Biol.* 24, e55–e66. doi: 10.1111/gcb.2018.24.issue-1

Assis, J., Fragkopoulou, E., Gouvêa, L., Araújo, M. B., and Serrão, E. A. (2024). Kelp forest diversity under projected end-of-century climate change. *Diversity Distrib.* 30, e13837. doi: 10.1111/ddi.13837

Assis, J., Serrão, E. A., Duarte, C. M., Fragkopoulou, E., and Krause-Jensen, D. (2022). Major expansion of marine forests in a warmer arctic. *Front. Mar. Sci.* 9, 850368. doi: 10.3389/fmars.2022.850368

Atkinson, J., King, N. G., Wilmes, S. B., and Moore, P. J. (2020). Summer and winter marine heatwaves favor an invasive over native seaweeds. *J. Phycol.* 56, 1591–1600. doi: 10.1111/jpy.13051

Badis, Y., Scornet, D., Harada, M., Caillard, C., Godfroy, O., Raphalen, M., et al. (2021). Targeted CRISPR-Cas9-based gene knockouts in the model brown alga *Ectocarpus*. *New Phytol.* 231, 2077–2091. doi: 10.1111/nph.v231.5

Bak, U. G., Gregersen, Ó, and Infante, J. (2020). Technical challenges for offshore cultivation of kelp species: lessons learned and future directions. *Botanica Marina.* 63, 341–353. doi: 10.1515/bot-2019-0005

Bartsch, I., Vogt, J., Pehlke, C., and Hanelt, D. (2013). Prevailing sea surface temperatures inhibit summer reproduction of the kelp *Laminaria digitata* at Helgoland (North Sea). *J. Phycol.* 49, 1061–1073. doi: 10.1111/jpy.2013.49.issue-6

Behera, D. P., Ingle, K. N., Mathew, D. E., Dhimmar, A., Sahastrabudhe, H., Sahu, S. K., et al. (2022). Epiphytism, diseases and grazing in seaweed aquaculture: A comprehensive review. *Rev. Aquacult.* 14, 1345–1370. doi: 10.1111/raq.12653

Bellwood, D. R., and Fulton, C. J. (2008). Sediment-mediated suppression of herbivory on coral reefs: Decreasing resilience to rising sea-levels and climate change? *Limnol. Oceanogr.* 53, 2695–2701. doi: 10.4319/lo.2008.53.6.2695

Bennett, S., Wernberg, T., Harvey, E. S., Santana-Garcon, J., and Saunders, B. J. (2015). Tropical herbivores provide resilience to a climate-mediated phase shift on temperate reefs. *Ecol. Lett.* 18, 714–723. doi: 10.1111/ele.2015.18.issue-7

Bermejo, R., Macmonagail, M., Heesch, S., Mendes, A., Edwards, M., Fenton, O., et al. (2020). The arrival of a red invasive seaweed to a nutrient over-enriched estuary increases the spatial extent of macroalgal blooms. *Mar. Environ. Res.* 158, 104944. doi: 10.1016/j.marenvres.2020.104944

Billing, S.-L., Rostan, J., Tett, P., and Macleod, A. (2021). Is social license to operate relevant for seaweed cultivation in Europe? *Aquaculture* 534, 736203. doi: 10.1016/j.aquaculture.2020.736203

Biskup, S., Bertocci, I., Arenas, F., and Tuya, F. (2014). Functional responses of juvenile kelps, *Laminaria ochroleuca* and *Saccorhiza polyschides*, to increasing temperatures. *Aquat. Bot.* 113, 117–122. doi: 10.1016/j.aquabot.2013.10.003

Blain, C. O., Hansen, S. C., and Shears, N. T. (2021). Coastal darkening substantially limits the contribution of kelp to coastal carbon cycles. *Global Change Biol.* 27, 5547–5563. doi: 10.1111/gcb.v27.21

Bonthond, G., Neu, A.-K., Bayer, T., Krueger-Hadfield, S. A., Künzel, S., and Weinberger, F. (2023). Non-native hosts of an invasive seaweed holobiont have more stable microbial communities compared to native hosts in response to thermal stress. *Ecol. Evol.* 13, e9753. doi: 10.1002/ece3.v13.1

Brakel, J., Sibonga, R. C., Dumilag, R. V., Montalescot, V., Campbell, I., Cottier-Cook, E. J., et al. (2021). Exploring, harnessing and conserving marine genetic resources towards a sustainable seaweed aquaculture. *Plants. People. Planet.* 3, 337–349. doi: 10.1002/ppp3.10190

Bricknell, I. R., Birkel, S. D., Brawley, S. H., Van Kirk, T., Hamlin, H. J., Capistrant-Fossa, K., et al. (2021). Resilience of cold water aquaculture: a review of likely scenarios as climate changes in the Gulf of Maine. *Rev. Aquacult.* 13, 460–503. doi: 10.1111/raq.12483

Bringloe, T. T., Fort, A., Inaba, M., Sulpice, R., Ghriofa, C. N., Mols-Mortensen, A., et al. (2022). Whole genome population structure of North Atlantic kelp confirms high-latitude glacial refugia. *Mol. Ecol.* 31, 6473–6488. doi: 10.1111/mec.v31.24

Britton, D., Craig Mundy, C. J., and Mcallister, J. (2023). "Nutritional quality of kelp as a key driver of commercial abalone productivity," in *Technical report series* (Hobart, Tasmania: University of Tasmania: Institute for Marine and Antarctic Studies).

Britton, D., Mundy, C. N., Mcgraw, C. M., Revill, A. T., and Hurd, C. L. (2019). Responses of seaweeds that use CO_2 as their sole inorganic carbon source to ocean acidification: differential effects of fluctuating pH but little benefit of CO_2 enrichment. *ICES. J. Mar. Sci.* 76, 1860–1870. doi: 10.1093/icesjms/fsz070

Britton, D., Schmid, M., Noisette, F., Havenhand, J. N., Paine, E. R., Mcgraw, C. M., et al. (2020). Adjustments in fatty acid composition is a mechanism that can explain resilience to marine heatwaves and future ocean conditions in the habitat-forming seaweed *Phyllospora comosa* (Labillardière) C.Agardh. *Global Change Biol.* 26, 3512–3524. doi: 10.1111/gcb.15052

Britton, D., Schmid, M., Revill, A. T., Virtue, P., Nichols, P. D., Hurd, C. L., et al. (2021). Seasonal and site-specific variation in the nutritional quality of temperate seaweed assemblages: implications for grazing invertebrates and the commercial exploitation of seaweeds. *J. Appl. Phycol.* 33, 603–616. doi: 10.1007/s10811-020-02302-1

Bronselaer, B., and Zanna, L. (2020). Heat and carbon coupling reveals ocean warming due to circulation changes. *Nature* 584, 227–233. doi: 10.1038/s41586-020-2573-5

Buschmann, A. H., Camus, C., Infante, J., Neori, A., Israel, Á., Hernández-González, M. C., et al. (2017). Seaweed production: overview of the global state of exploitation, farming and emerging research activity. *Eur. J. Phycol.* 52, 391–406. doi: 10.1080/09670262.2017.1365175

Callaway, R., Shinn, A. P., Grenfell, S. E., Bron, J. E., Burnell, G., Cook, E. J., et al. (2012). Review of climate change impacts on marine aquaculture in the UK and Ireland. *Aquat. Conserv.: Mar. Freshw. Ecosyst.* 22, 389–421. doi: 10.1002/aqc.2247

Campbell, A. H., Harder, T., Nielsen, S., Kjelleberg, S., and Steinberg, P. D. (2011). Climate change and disease: bleaching of a chemically defended seaweed. *Global Change Biol.* 17, 2958–2970. doi: 10.1111/j.1365-2486.2011.02456.x

Campbell, I., Kambey, C. S. B., Mateo, J. P., Rusekwa, S. B., Hurtado, A. Q., Msuya, F. E., et al. (2020). Biosecurity policy and legislation for the global seaweed aquaculture industry. *J. Appl. Phycol.* 32, 2133–2146. doi: 10.1007/s10811-019-02010-5

Campbell, I., Macleod, A., Sahlmann, C., Neves, L., Funderud, J., Øverland, M., et al. (2019). The environmental risks associated with the development of seaweed farming in Europe - Prioritizing key knowledge gaps. *Front. Mar. Sci.* 6. doi: 10.3389/fmars.2019.00107

Camus, C., Solas, M., Martínez, C., Vargas, J., Garcés, C., Gil-Kodaka, P., et al. (2021). Mates matter: Gametophyte kinship recognition and inbreeding in the giant kelp, *Macrocystis pyrifera* (Laminariales, Phaeophyceae). *J. Phycol.* 57, 711–725. doi: 10.1111/jpy.13146

Carey, N., Harianto, J., and Byrne, M. (2016). Sea urchins in a high-CO_2 world: partitioned effects of body size, ocean warming and acidification on metabolic rate. *J. Exp. Biol.* 219, 1178–1186. doi: 10.1242/jeb.136101

Casado-Amezúa, P., Araújo, R., Bárbara, I., Bermejo, R., Borja, Á., Díez, I., et al. (2019). Distributional shifts of canopy-forming seaweeds from the Atlantic coast of Southern Europe. *Biodivers. Conserv.* 28, 1151–1172. doi: 10.1007/s10531-019-01716-9

Chan, F., Barth, J. A., Blanchette, C. A., Byrne, R. H., Chavez, F., Cheriton, O., et al. (2017). Persistent spatial structuring of coastal ocean acidification in the California Current System. *Sci. Rep.* 7, 2526. doi: 10.1038/s41598-017-02777-y

Chen, B., Zou, D., Du, H., and Ji, Z. (2018). Carbon and nitrogen accumulation in the economic seaweed *Gracilaria lemaneiformis* affected by ocean acidification and increasing temperature. *Aquaculture* 482, 176–182. doi: 10.1016/j.aquaculture.2017.09.042

Choo, K.-S., Snoeijs, P., and Pedersén, M. (2004). Oxidative stress tolerance in the filamentous green algae *Cladophora glomerata* and *Enteromorpha ahlneriana*. *J. Exp. Mar. Biol. Ecol.* 298, 111–123. doi: 10.1016/j.jembe.2003.08.007

Chung, I. K., Oak, J. H., Lee, J. A., Shin, J. A., Kim, J. G., and Park, K.-S. (2013). Installing kelp forests/seaweed beds for mitigation and adaptation against global warming: Korean Project Overview. *ICES. J. Mar. Sci.* 70, 1038–1044. doi: 10.1093/icesjms/fss206

Chung, I. K., Sondak, C. F. A., and Beardall, J. (2017). The future of seaweed aquaculture in a rapidly changing world. *Eur. J. Phycol.* 52, 495–505. doi: 10.1080/09670262.2017.1359678

Chust, G., Villarino, E., Mclean, M., Mieszkowska, N., Benedetti-Cecchi, L., Bulleri, F., et al. (2024). Cross-basin and cross-taxa patterns of marine community tropicalization and deborealization in warming European seas. *Nat. Commun.* 15, 2126. doi: 10.1038/s41467-024-46526-y

Clements, J. C., and Chopin, T. (2017). Ocean acidification and marine aquaculture in North America: potential impacts and mitigation strategies. *Rev. Aquacult.* 9, 326–341. doi: 10.1111/raq.2017.9.issue-4

Coleman, M. A., Minne, A. J. P., Vranken, S., and Wernberg, T. (2020a). Genetic tropicalisation following a marine heatwave. *Sci. Rep.* 10, 12726. doi: 10.1038/s41598-020-69665-w

Coleman, M. A., Wood, G., Filbee-Dexter, K., Minne, A. J. P., Goold, H. D., Vergés, A., et al. (2020b). Restore or redefine: Future trajectories for restoration. *Front. Mar. Sci.* 7, 237. doi: 10.3389/fmars.2020.00237

Corrigan, S., Brown, A. R., Ashton, I. G. C., Smale, D. A., and Tyler, C. R. (2022). Quantifying habitat provisioning at macroalgal cultivation sites. *Rev. Aquacult.* 14, 1671–1694. doi: 10.1111/raq.12669

Coumou, D., and Rahmstorf, S. (2012). A decade of weather extremes. *Nat. Climate Change* 2, 491–496. doi: 10.1038/nclimate1452

Cruz-Rivera, E., and Villareal, T. A. (2006). Macroalgal palatability and the flux of ciguatera toxins through marine food webs. *Harmful. Algae.* 5, 497–525. doi: 10.1016/j.hal.2005.09.003

Davis, K. M., Zeinert, L., Byrne, A., Davis, J., Roemer, C., Wright, M., et al. (2023). Successional dynamics of the cultivated kelp microbiome. *J. Phycol.* 59, 538–551. doi: 10.1111/jpy.13329

Davis, T. R., Champion, C., and Coleman, M. A. (2022a). Ecological interactions mediate projected loss of kelp biomass under climate change. *Diversity Distrib.* 28, 306–317. doi: 10.1111/ddi.13462

Davis, T. R., Larkin, M. F., Forbes, A., Veenhof, R. J., Scott, A., and Coleman, M. A. (2022b). Extreme flooding and reduced salinity causes mass mortality of nearshore kelp forests. *Estuarine. Coast. Shelf. Sci.* 275, 107960. doi: 10.1016/j.ecss.2022.107960

Davison, I. R., Greene, R. M., and Podolak, E. J. (1991). Temperature acclimation of respiration and photosynthesis in the brown alga *Laminaria saccharina*. *Mar. Biol.* 110, 449–454. doi: 10.1007/BF01344363

Dayton, P. K., Currie, V., Gerrodette, T., Keller, B. D., Rosenthal, R., and Tresca, D. V. (1984). Patch dynamics and stability of some California kelp communities. *Ecol. Monogr.* 54, 253–289. doi: 10.2307/1942498

de Bettignies, T., Wernberg, T., Lavery, P. S., Vanderklift, M. A., Gunson, J. R., Symonds, G., et al. (2015). Phenological decoupling of mortality from wave forcing in kelp beds. *Ecology* 96, 850–861. doi: 10.1890/13-2365.1

de Bettignies, T., Wernberg, T., Lavery, P. S., Vanderklift, M. A., and Mohring, M. B. (2013). Contrasting mechanisms of dislodgement and erosion contribute to production of kelp detritus. *Limnol. Oceanogr.* 58, 1680–1688. doi: 10.4319/lo.2013.58.5.1680

Delva, S., De Baets, B., Baetens, J. M., De Clerck, O., and Stock, W. (2023). No bacterial-mediated alleviation of thermal stress in a brown seaweed suggests the absence of ecological bacterial rescue effects. *Sci. Total. Environ.* 876, 162532. doi: 10.1016/j.scitotenv.2023.162532

Diehl, N., Karsten, U., and Bischof, K. (2020). Impacts of combined temperature and salinity stress on the endemic Arctic brown seaweed *Laminaria solidungula* J. Agardh. *Polar. Biol.* 43, 647–656. doi: 10.1007/s00300-020-02668-5

Diehl, N., Steiner, N., Bischof, K., Karsten, U., and Heesch, S. (2023). Exploring intraspecific variability – biochemical and morphological traits of the sugar kelp *Saccharina latissima* along latitudinal and salinity gradients in Europe. *Front. Mar. Sci.* 10, 995982. doi: 10.3389/fmars.2023.995982

Doney, S. C., Fabry, V. J., Feely, R. A., and Kleypas, J. A. (2009). Ocean acidification: The other CO_2 problem. *Annu. Rev. Mar. Sci.* 1, 169–192. doi: 10.1146/annurev.marine.010908.163834

Duarte, C. M., Bruhn, A., and Krause-Jensen, D. (2022). A seaweed aquaculture imperative to meet global sustainability targets. *Nat. Sustainabil.* 5, 185–193. doi: 10.1038/s41893-021-00773-9

Duarte, C. M., Wu, J., Xiao, X., Bruhn, A., and Krause-Jensen, D. (2017). Can seaweed farming play a role in climate change mitigation and adaptation? *Front. Mar. Sci.* 4, 100. doi: 10.3389/fmars.2017.00100

Egan, S., and Gardiner, M. (2016). Microbial dysbiosis: Rethinking disease in marine ecosystems. *Front. Microbiol.* 7, 00991. doi: 10.3389/fmicb.2016.00991

Egan, S., Harder, T., Burke, C., Steinberg, P., Kjelleberg, S., and Thomas, T. (2013). The seaweed holobiont: understanding seaweed–bacteria interactions. *FEMS Microbiol. Rev.* 37, 462–476. doi: 10.1111/1574-6976.12011

Eger, A. M., Aguirre, J. D., Altamirano, M., Arafeh-Dalmau, N., Arroyo, N. L., Bauer-Civiello, A. M., et al. (2023). The Kelp Forest Challenge: A collaborative global movement to protect and restore 4 million hectares of kelp forests. *J. Appl. Phycol.* 36, 951–964. doi: 10.1007/s10811-023-03103-y

Eger, A. M., Marzinelli, E. M., Christie, H., Fagerli, C. W., Fujita, D., Gonzalez, A. P., et al. (2022). Global kelp forest restoration: past lessons, present status, and future directions. *Biol. Rev.* 97, 1449–1475. doi: 10.1111/brv.12850

Eger, A. M., Vergés, A., Choi, C. G., Christie, H., Coleman, M. A., Fagerli, C. W., et al. (2020). Financial and institutional support are important for large-scale kelp forest restoration. *Front. Mar. Sci.* 7, 811. doi: 10.3389/fmars.2020.535277

Eggert, A. (2012). "Seaweed responses to temperature," in *Seaweed Biology: Novel Insights into Ecophysiology, Ecology and Utilization*. Eds. C. Wiencke and K. Bischof (Springer Berlin Heidelberg, Berlin, Heidelberg).

Falkenberg, L. J., Scanes, E., Ducker, J., and Ross, P. M. (2021). Biotic habitats as refugia under ocean acidification. *Conserv. Physiol.* 9, coab077. doi: 10.1093/conphys/coab077

FAO (2022). *The state of world fisheries and aquaculture 2022. Towards Blue Transformation* (Rome: FAO).

Farebrother, J., Zimmermann, M. B., and Andersson, M. (2019). Excess iodine intake: sources, assessment, and effects on thyroid function. *Ann. New York. Acad. Sci.* 1446, 44–65. doi: 10.1111/nyas.2019.1446.issue-1

Feehan, C. J., Grace, S. P., and Narvaez, C. A. (2019). Ecological feedbacks stabilize a turf-dominated ecosystem at the southern extent of kelp forests in the Northwest Atlantic. *Sci. Rep.* 9, 7078. doi: 10.1038/s41598-019-43536-5

Fernández, P. A., Leal, P. P., and Henríquez, L. A. (2019). Co-culture in marine farms: macroalgae can act as chemical refuge for shell-forming molluscs under an ocean acidification scenario. *Phycologia* 58, 542–551. doi: 10.1080/00318884.2019.1628576

Filbee-Dexter, K., Feehan, C. J., and Scheibling, R. E. (2016). Large-scale degradation of a kelp ecosystem in an ocean warming hotspot. *Mar. Ecol. Prog. Ser.* 543, 141–152. doi: 10.3354/meps11554

Filbee-Dexter, K., and Wernberg, T. (2018). Rise of turfs: a new battlefront for globally declining kelp forests. *BioScience* 68, 64–76. doi: 10.1093/biosci/bix147

Filbee-Dexter, K., Wernberg, T., Barreiro, R., Coleman, M. A., De Bettignies, T., Feehan, C. J., et al. (2022). Leveraging the blue economy to transform marine forest restoration. *J. Phycol.* 58, 198–207. doi: 10.1111/jpy.13239

Filbee-Dexter, K., Wernberg, T., Fredriksen, S., Norderhaug, K. M., and Pedersen, M. F. (2019). Arctic kelp forests: Diversity, resilience and future. *Global Planet. Change* 172, 1–14. doi: 10.1016/j.gloplacha.2018.09.005

Fouqueau, L., Reynes, L., Blanfuné, A., Mauger, S., and Assis, J. (2024). Seascape genetic study on *Laminaria digitata* underscores the critical role of sampling schemes. *Mar. Ecol. Prog. Ser.* 740, 23–42. doi: 10.3354/meps14640

Franke, K., Matthes, L. C., Graiff, A., Karsten, U., and Bartsch, I. (2023). The challenge of estimating kelp production in a turbid marine environment. *J. Phycol.* 59, 518–537. doi: 10.1111/jpy.13327

Frieder, C. A., Nam, S. H., Martz, T. R., and Levin, L. A. (2012). High temporal and spatial variability of dissolved oxygen and pH in a nearshore California kelp forest. *Biogeosciences* 9, 3917–3930. doi: 10.5194/bg-9-3917-2012

Gachon, C. M., Sime-Ngando, T., Strittmatter, M., Chambouvet, A., and Kim, G. H. (2010). Algal diseases: spotlight on a black box. *Trends Plant Sci.* 15, 633–640. doi: 10.1016/j.tplants.2010.08.005

Ganesan, M., Thiruppathi, S., Sahu, N., Rengarajan, N., Veeragurunathan, V., and Jha, B. (2006). In situ observations on preferential grazing of seaweeds by some herbivores. *Current Science*, 1256-1260.

García Molinos, J., Halpern, B. S., Schoeman, D. S., Brown, C. J., Kiessling, W., Moore, P. J., et al. (2016). Climate velocity and the future global redistribution of marine biodiversity. *Nat. Climate Change* 6, 83–88. doi: 10.1038/nclimate2769

Gauci, C., Bartsch, I., Martins, N., and Liesner, D. (2022). Cold thermal priming of *Laminaria digitata* (Laminariales, Phaeophyceae) gametophytes enhances gametogenesis and thermal performance of sporophytes. *Front. Mar. Sci.* 9, 862923. doi: 10.3389/fmars.2022.862923

Gillanders, B. M., and Kingsford, M. J. (2002). Impact of changes in flow of freshwater on estuarine and open coastal habitats and the associated organisms. *Oceanogr. Mar. Biol.: Annu. Rev.* 40, 233–309.

Gillooly, J. F., Brown, J. H., West, G. B., Savage, V. M., and Charnov, E. L. (2001). Effects of size and temperature on metabolic rate. *Science* 293, 2248–2251. doi: 10.1126/science.1061967

Glauco, F., He, P., and Chen, Z. (2024). Combine effects of multiple environmental factors on growth and nutrient uptake of euryhaline seaweed growth in integrated multitrophic aquaculture systems. *Algal. Res.* 77, 103347. doi: 10.1016/j.algal.2023.103347

Goecke, F., Klemetsdal, G., and Ergon, Å. (2020). Cultivar development of kelps for commercial cultivation—Past lessons and future prospects. *Front. Mar. Sci.* 7, 110. doi: 10.3389/fmars.2020.00110

Goldsmit, J., Schlegel, R. W., Filbee-Dexter, K., Macgregor, K. A., Johnson, L. E., Mundy, C. J., et al. (2021). Kelp in the Eastern Canadian Arctic: Current and future predictions of habitat suitability and cover. *Front. Mar. Sci.* 8, 742209. doi: 10.3389/fmars.2021.742209

Goodwin, P., Williams, R. G., and Ridgwell, A. (2015). Sensitivity of climate to cumulative carbon emissions due to compensation of ocean heat and carbon uptake. *Nat. Geosci.* 8, 29–34. doi: 10.1038/ngeo2304

Gosch, B. J., Lawton, R. J., Paul, N. A., De Nys, R., and Magnusson, M. (2015). Environmental effects on growth and fatty acids in three isolates of *Derbesia tenuissima* (Bryopsidales, Chlorophyta). *Algal. Res.* 9, 82–93. doi: 10.1016/j.algal.2015.02.022

Gouvêa, L., Fragkopoulou, E., Legrand, T., Serrão, E. A., and Assis, J. (2024). Range map data of marine ecosystem structuring species under global climate change. *Data Brief* 52, 110023. doi: 10.1016/j.dib.2023.110023

Graba-Landry, A., Hoey, A. S., Matley, J. K., Sheppard-Brennand, H., Poore, A. G. B., Byrne, M., et al. (2018). Ocean warming has greater and more consistent negative effects than ocean acidification on the growth and health of subtropical macroalgae. *Mar. Ecol. Prog. Ser.* 595, 55–69. doi: 10.3354/meps12552

Graiff, A., Bartsch, I., Ruth, W., Wahl, M., and Karsten, U. (2015). Season exerts differential effects of ocean acidification and warming on growth and carbon metabolism of the seaweed *Fucus vesiculosus* in the Western Baltic Sea. *Front. Mar. Sci.* 2, 00112. doi: 10.3389/fmars.2015.00112

Hammann, M., Wang, G., Boo, S. M., Aguilar-Rosas, L. E., and Weinberger, F. (2016). Selection of heat-shock resistance traits during the invasion of the seaweed *Gracilaria vermiculophylla*. *Mar. Biol.* 163, 104. doi: 10.1007/s00227-016-2881-3

Hara, M., and Akiyama, K. (1985). Heterosis in growth of *Undaria pinnatifida* (Harvey) Suringar. *Bull. Tohoku. Regional. Fisheries. Res. Lab.* 47, 47–50.

Harley, C. D. G., Anderson, K. M., Demes, K. W., Jorve, J. P., Kordas, R. L., Coyle, T. A., et al. (2012). Effects of climate change on global seaweed communities. *J. Phycol.* 48, 1064–1078. doi: 10.1111/j.1529-8817.2012.01224.x

Hay, M. E., and Fenical, W. (1988). Marine plant-herbivore interactions: The ecology of chemical defense. *Annu. Rev. Ecol. Syst.* 19, 111–145. doi: 10.1146/annurev.es.19.110188.000551

Ho, M., Mcbroom, J., Bergstrom, E., and Diaz-Pulido, G. (2021). Physiological responses to temperature and ocean acidification in tropical fleshy macroalgae with varying affinities for inorganic carbon. *ICES. J. Mar. Sci.* 78, 89–100. doi: 10.1093/icesjms/fsaa195

Hobday, A. J., Burrows, M. T., Filbee-Dexter, K., Holbrook, N. J., Sen Gupta, A., Smale, D. A., et al. (2023). With the arrival of El Niño, prepare for stronger marine heatwaves. *Nature* 621, 38–41. doi: 10.1038/d41586-023-02730-2

Horta e Costa, B., Assis, J., Franco, G., Erzini, K., Henriques, M., Gonçalves, E. J., et al. (2014). Tropicalization of fish assemblages in temperate biogeographic transition zones. *Mar. Ecol. Prog. Ser.* 504, 241–252. doi: 10.3354/meps10749

Hu, Z.-M., Shan, T.-F., Zhang, Q.-S., Liu, F.-L., Jueterbock, A., Wang, G., et al. (2023). Kelp breeding in China: Challenges and opportunities for solutions. *Rev. Aquacult.* 16, 855–871. doi: 10.1111/raq.12871

Huang, M., Robbins, K. R., Li, Y., Umanzor, S., Marty-Rivera, M., Bailey, D., et al. (2023). Genomic selection in algae with biphasic lifecycles: A *Saccharina latissima* (sugar kelp) case study. *Front. Mar. Sci.* 10, 1040979. doi: 10.3389/fmars.2023.1040979

Huang, M., Robbins, K. R., Li, Y., Umanzor, S., Marty-Rivera, M., Bailey, D., et al. (2022). Simulation of sugar kelp (*Saccharina latissima*) breeding guided by practices to accelerate genetic gains. *G3 Genes|Genomes|Genetics.* 12, jkac003. doi: 10.1093/g3journal/jkac003

Hughes, A. D., and Black, K. D. (2016). Going beyond the search for solutions: understanding trade-offs in European integrated multi-trophic aquaculture development. *Aquacult. Environ. Interact.* 8, 191–199. doi: 10.3354/aei00174

Iida, Y., Takatani, Y., Kojima, A., and Ishii, M. (2021). Global trends of ocean CO_2 sink and ocean acidification: an observation-based reconstruction of surface ocean inorganic carbon variables. *J. Oceanogr.* 77, 323–358. doi: 10.1007/s10872-020-00571-5

Incera, M., Olabarria, C., Troncoso, J. S., and López, J. (2009). Response of the invader *Sargassum muticum* to variability in nutrient supply. *Mar. Ecol. Prog. Ser.* 377, 91–101. doi: 10.3354/meps07866

IPCC (2023). *Climate Change 2023: Synthesis Report. Contribution of Working Groups I, II and III to the Sixth Assessment Report of the Intergovernmental Panel on Climate Change* (Geneva, Switzerland: IPCC).

Iwamoto, K., and Shiraiwa, Y. (2005). Salt-regulated mannitol metabolism in algae. *Mar. Biotechnol.* 7, 407–415. doi: 10.1007/s10126-005-0029-4

Jacox, M. G., Alexander, M. A., Amaya, D., Becker, E., Bograd, S. J., Brodie, S., et al. (2022). Global seasonal forecasts of marine heatwaves. *Nature* 604, 486–490. doi: 10.1038/s41586-022-04573-9

Jayathilake, D. R. M., and Costello, M. J. (2020). A modelled global distribution of the kelp biome. *Biol. Conserv.* 252, 108815. doi: 10.1016/j.biocon.2020.108815

Jueterbock, A., Minne, A. J. P., Cock, J. M., Coleman, M. A., Wernberg, T., Scheschonk, L., et al. (2021). Priming of marine macrophytes for enhanced restoration success and food security in future oceans. *Front. Mar. Sci.* 8, 658485. doi: 10.3389/fmars.2021.658485

Kain, J. M. (1989). The seasons in the subtidal. *Br. Phycol. J.* 24, 203–215. doi: 10.1080/00071618900650221

Keng, F. S.-L., Phang, S.-M., Abd Rahman, N., Leedham Elvidge, E. C., Malin, G., and Sturges, W. T. (2020). The emission of volatile halocarbons by seaweeds and their response towards environmental changes. *J. Appl. Phycol.* 32, 1377–1394. doi: 10.1007/s10811-019-02026-x

Kerrison, P. D., Stanley, M. S., Edwards, M. D., Black, K. D., and Hughes, A. D. (2015). The cultivation of European kelp for bioenergy: Site and species selection. *Biomass Bioenergy* 80, 229–242. doi: 10.1016/j.biombioe.2015.04.035

Khan, N., Sudhakar, K., and Mamat, R. (2024). Macroalgae farming for sustainable future: Navigating opportunities and driving innovation. *Heliyon* 10, e28208. doi: 10.1016/j.heliyon.2024.e28208

Kim, N.-G. (2011). Culture study on the hybrid by interspecific crossing between *Porphyra pseudolinearis* and *P. dentata* (Bangiales, Rhodophyta), two dioecious species in culture. *Algae* 26, 79–86. doi: 10.4490/algae.2011.26.1.079

Kim, B.-T., Brown, C. L., and Kim, D.-H. (2019). Assessment on the vulnerability of Korean aquaculture to climate change. *Mar. Policy* 99, 111–122. doi: 10.1016/j.marpol.2018.10.009

Kim, J. K., Yarish, C., Hwang, E. K., Park, M., and Kim, Y. (2017). Seaweed aquaculture: cultivation technologies, challenges and its ecosystem services. *Algae* 32, 1–13. doi: 10.4490/algae.2017.32.3.3

King, N. G., Moore, P. J., Pessarrodona, A., Burrows, M. T., Porter, J., Bue, M., et al. (2020). Ecological performance differs between range centre and trailing edge populations of a cold-water kelp: implications for estimating net primary productivity. *Mar. Biol.* 167, 1–12. doi: 10.1007/s00227-020-03743-5

Kinnby, A., Toth, G. B., and Pavia, H. (2021). Climate change increases susceptibility to grazers in a foundation seaweed. *Front. Mar. Sci.* 8, 688406. doi: 10.3389/fmars.2021.688406

Koehl, M. A. R., Silk, W. K., Liang, H., and Mahadevan, L. (2008). How kelp produce blade shapes suited to different flow regimes: A new wrinkle. *Integr. Comp. Biol.* 48, 834–851. doi: 10.1093/icb/icn069

Krause-Jensen, D., Duarte, C. M., Hendriks, I. E., Meire, L., Blicher, M. E., Marbà, N., et al. (2015). Macroalgae contribute to nested mosaics of pH variability in a subarctic fjord. *Biogeosciences* 12, 4895–4911. doi: 10.5194/bg-12-4895-2015

Krumhansl, K. A., Okamoto, D. K., Rassweiler, A., Novak, M., Bolton, J. J., Cavanaugh, K. C., et al. (2016). Global patterns of kelp forest change over the past half-century. *Proc. Natl. Acad. Sci.* 113, 13785–13790. doi: 10.1073/pnas.1606102113

Kübler, J. E., and Davison, I. R. (1995). Thermal acclimation of light-use characteristics of *Chondrus crispus* (Rhodophyta). *Eur. J. Phycol.* 30, 189–195. doi: 10.1080/09670269500650971

Kübler, J. E., and Dudgeon, S. R. (2015). Predicting effects of ocean acidification and warming on algae lacking carbon concentrating mechanisms. *PloS One* 10, e0132806. doi: 10.1371/journal.pone.0132806

Kübler, J. E., Dudgeon, S. R., and Bush, D. (2021). Climate change challenges and opportunities for seaweed aquaculture in California, the United States. *J. World Aquacult. Soc.* 52, 1069–1080. doi: 10.1111/jwas.12794

Kumar, Y. N., Poong, S.-W., Gachon, C., Brodie, J., Sade, A., and Lim, P.-E. (2020). Impact of elevated temperature on the physiological and biochemical responses of *Kappaphycus alvarezii* (Rhodophyta). *PloS One* 15, e0239097. doi: 10.1371/journal.pone.0239097

Kwiatkowski, L., Torres, O., Bopp, L., Aumont, O., Chamberlain, M., Christian, J. R., et al. (2020). Twenty-first century ocean warming, acidification, deoxygenation, and upper-ocean nutrient and primary production decline from CMIP6 model projections. *Biogeosciences* 17, 3439–3470. doi: 10.5194/bg-17-3439-2020

Largo, D. B., Chung, I. K., Phang, S.-M., Gerung, G. S., and Sondak, C. F. A. (2017). "Impacts of climate change on *Eucheuma-Kappaphycus* Farming," in *Tropical Seaweed Farming Trends, Problems and Opportunities. Developments in Applied Phycology*. Eds. A. Q. Hurtado, A. T. Critchley and I. C. Neish (Springer International Publishing, Cham).

Largo, D. B., Fukami, K., Nishijima, T., and Ohno, M. (1995). Laboratory-induced development of the ice-ice disease of the farmed red algae *Kappaphycus alvarezi*i and *Eucheuma denticulatum* (Solieriaceae, Gigartinales, Rhodophyta). *J. Appl. Phycol.* 7, 539–543. doi: 10.1007/BF00003940

Leal, P. P., Uribe, D., Henríquez-Antipa, L. A., Jiménez, C., Hormazábal, L., and Cascales, E.-K. (2024). Evaluating the ability of macroalgae to create a chemical refuge for bivalves under ocean acidification conditions in closed-environment experiments. *J. Appl. Phycol.* 36, 1561–1575. doi: 10.1007/s10811-023-03163-0

Leung, J. Y. S., Russell, B. D., Coleman, M. A., Kelaher, B. P., and Connell, S. D. (2021). Long-term thermal acclimation drives adaptive physiological adjustments of a marine gastropod to reduce sensitivity to climate change. *Sci. Total. Environ.* 771, 145208. doi: 10.1016/j.scitotenv.2021.145208

Li, J., Majzoub, M. E., Marzinelli, E. M., Dai, Z., Thomas, T., and Egan, S. (2022a). Bacterial controlled mitigation of dysbiosis in a seaweed disease. *ISME. J.* 16, 378–387. doi: 10.1038/s41396-021-01070-1

Li, J., Pang, S., Shan, T., and Su, L. (2020). Changes of microbial community structures associated with seedlings of *Saccharina japonica* at early stage of outbreak of green rotten disease. *J. Appl. Phycol.* 32, 1323–1327. doi: 10.1007/s10811-019-01975-7

Li, J., Weinberger, F., De Nys, R., Thomas, T., and Egan, S. (2023). A pathway to improve seaweed aquaculture through microbiota manipulation. *Trends Biotechnol.* 41, 545–556. doi: 10.1016/j.tibtech.2022.08.003

Li, J., Weinberger, F., Saha, M., Majzoub, M. E., and Egan, S. (2022b). Cross-host protection of marine bacteria against macroalgal disease. *Microbial. Ecol.* 84, 1288–1293. doi: 10.1007/s00248-021-01909-2

Li, J., Zhang, W., Ding, J., Xue, S., Huo, E., Ma, Z., et al. (2021). Effect of large-scale kelp and bivalve farming on seawater carbonate system variations in the semi-enclosed Sanggou Bay. *Sci. Total. Environ.* 753, 142065. doi: 10.1016/j.scitotenv.2020.142065

Li, X., Zhang, Z., Qu, S., Liang, G., Sun, J., Zhao, N., et al. (2016a). Improving seedless kelp (*Saccharina japonica*) during its domestication by hybridizing gametophytes and seedling-raising from sporophytes. *Sci. Rep.* 6, 21255. doi: 10.1038/srep21255

Li, X. J., Zhang, Z. Z., Qu, S. C., Liang, G. J., Zhao, N., Sun, J., et al. (2016b). Breeding of an intraspecific kelp hybrid Dongfang no. 6 (*Saccharina japonica*, Phaeophyceae, Laminariales) for suitable processing products and evaluation of its culture performance. *J. Appl. Phycol.* 28, 439–447. doi: 10.1007/s10811-015-0562-0

Liesner, D., Pearson, G. A., Bartsch, I., Rana, S., Harms, L., Heinrich, S., et al. (2022). Increased heat resilience of intraspecific outbred compared to inbred lineages in the kelp laminaria digitata: physiology and transcriptomics. *Front. Mar. Sci.* 9, 838793. doi: 10.3389/fmars.2022.838793

Ling, F., Egan, S., Zhuang, Y., Chang, L., Xiao, L., Yang, Q., et al. (2022). Epimicrobiome shifts with bleaching disease progression in the brown seaweed *Saccharina japonica*. *Front. Mar. Sci.* 9, 865224. doi: 10.3389/fmars.2022.865224

Ling, S., Scheibling, R., Rassweiler, A., Johnson, C., Shears, N., Connell, S., et al. (2015). Global regime shift dynamics of catastrophic sea urchin overgrazing. *Philos. Trans. R. Soc. B.*, 370, 20130269. doi: 10.1098/rstb.2013.0269

Liu, H., Able, A. J., and Able, J. A. (2022a). Priming crops for the future: rewiring stress memory. *Trends Plant Sci.* 27, 699–716. doi: 10.1016/j.tplants.2021.11.015

Liu, F., Zhang, P., Liang, Z., Yuan, Y., Liu, Y., and Wu, Y. (2023a). The global dynamic of DNA methylation in response to heat stress revealed epigenetic mechanism of heat acclimation in *Saccharina japonica*. *J. Phycol.* 59, 249–263. doi: 10.1111/jpy.13305

Liu, S., Zhou, X., Zeng, C., Frankstone, T., and Cao, L. (2022b). Characterizing the development of Sea ranching in China. *Rev. Fish. Biol. Fisheries*. 32, 783–803. doi: 10.1007/s11160-022-09709-8

Liu, W., Zou, H., Wu, S., Li, N., Pang, Q., and Yan, X. (2023b). Growth promotion of *Sargassum fusiforme* by epiphytic microbes is dependent on the extent of interspecific interactions of the microbial community. *Sci. Total. Environ.* 897, 165449. doi: 10.1016/j.scitotenv.2023.165449

Lowman, H. E., Emery, K. A., Dugan, J. E., and Miller, R. J. (2022). Nutritional quality of giant kelp declines due to warming ocean temperatures. *Oikos* 2022, e08619. doi: 10.1111/oik.v2022.i7

Lüning, K. (1993). Environmental and internal control of seasonal growth in seaweeds. *Hydrobiologia* 260, 1–14. doi: 10.1007/BF00048997

Lüning, K. (1994). When do algae grow? The third Founders' lecture. *Eur. J. Phycol.* 29, 61–67. doi: 10.1080/09670269400650501

Ma, D., Gregor, L., and Gruber, N. (2023a). Four decades of trends and drivers of global surface ocean acidification. *Global Biogeochem. Cycles.* 37, e2023GB007765. doi: 10.1029/2023GB007765

Ma, M., Zhuang, Y., Chang, L., Xiao, L., Lin, Q., Qiu, Q., et al. (2023b). Naturally occurring beneficial bacteria *Vibrio alginolyticus* X-2 protects seaweed from bleaching disease. *mBio* 14, e00065–e00023. doi: 10.1128/mbio.00065-23

Mancuso, F. P., Morrissey, K. L., De Clerck, O., and Airoldi, L. (2023). Warming and nutrient enrichment can trigger seaweed loss by dysregulation of the microbiome structure and predicted function. *Sci. Total. Environ.* 879, 162919. doi: 10.1016/j.scitotenv.2023.162919

Mantri, V. A., Eswaran, K., Shanmugam, M., Ganesan, M., Veeragurunathan, V., Thiruppathi, S., et al. (2017). An appraisal on commercial farming of *Kappaphycus alvarezii* in India: success in diversification of livelihood and prospects. *J. Appl. Phycol.* 29, 335–357. doi: 10.1007/s10811-016-0948-7

Marsooli, R., Lin, N., Emanuel, K., and Feng, K. (2019). Climate change exacerbates hurricane flood hazards along US Atlantic and Gulf Coasts in spatially varying patterns. *Nat. Commun.* 10, 3785. doi: 10.1038/s41467-019-11755-z

Martins, N., Barreto, L., Bartsch, I., Bernard, J., Serrão, E. A., and Pearson, G. A. (2022). Daylength influences reproductive success and sporophyte growth in the Arctic kelp species *Alaria esculenta*. *Mar. Ecol. Prog. Ser.* 683, 37–52. doi: 10.3354/meps13950

Martins, N., Pearson, G. A., Gouveia, L., Tavares, A. I., Serrao, E. A., and Bartsch, I. (2019). Hybrid vigour for thermal tolerance in hybrids between the allopatric kelps *Laminaria digitata* and *L. pallida* (Laminariales, Phaeophyceae) with contrasting thermal affinities. *Eur. J. Phycol.* 54, 548–561. doi: 10.1080/09670262.2019.1613571

Martins, N., Tanttu, H., Pearson, G. A., Serrão, E. A., and Bartsch, I. (2017). Interactions of daylength, temperature and nutrients affect thresholds for life stage transitions in the kelp *Laminaria digitata* (Phaeophyceae). *Botanica Marina.* 60, 109–121. doi: 10.1515/bot-2016-0094

Matsson, S., Christie, H., and Fieler, R. (2019). Variation in biomass and biofouling of kelp, *Saccharina latissima*, cultivated in the Arctic, Norway. *Aquaculture* 506, 445–452. doi: 10.1016/j.aquaculture.2019.03.068

Meehl, G. A., Zwiers, F., Evans, J., Knutson, T., Mearns, L., and Whetton, P. (2000). Trends in extreme weather and climate events: Issues related to modeling extremes in projections of future climate change. *Bull. Am. Meteorol. Soc.* 81, 427–436. doi: 10.1175/1520-0477(2000)081<0427:TIEWAC>2.3.CO;2

Mongin, M., Baird, M. E., Hadley, S., and Lenton, A. (2016). Optimising reef-scale CO_2 removal by seaweed to buffer ocean acidification. *Environ. Res. Lett.* 11, 034023. doi: 10.1088/1748-9326/11/3/034023

Monteiro, C., Li, H., Diehl, N., Collén, J., Heinrich, S., Bischof, K., et al. (2021). Modulation of physiological performance by temperature and salinity in the sugar kelp *Saccharina latissima*. *Phycol. Res.* 69, 48–57. doi: 10.1111/pre.12443

Moy, F. E., and Christie, H. (2012). Large-scale shift from sugar kelp (*Saccharina latissima*) to ephemeral algae along the south and west coast of Norway. *Mar. Biol. Res.* 8, 309–321. doi: 10.1080/17451000.2011.637561

Murúa, P., Patiño, D. J., Müller, D. G., and Westermeier, R. (2021). Sexual compatibility in giant kelp gametophytes: inter-cultivar hybridization is average between parents but excels under harsher conditions. *J. Appl. Phycol.* 33, 3261–3275. doi: 10.1007/s10811-021-02506-z

Muth, A. F., Bonsell, C., and Dunton, K. H. (2021). Inherent tolerance of extreme seasonal variability in light and salinity in an Arctic endemic kelp (*Laminaria solidungula*). *J. Phycol.* 57, 1554–1562. doi: 10.1111/jpy.13187

Naylor, R. L., Hardy, R. W., Buschmann, A. H., Bush, S. R., Cao, L., Klinger, D. H., et al. (2021). A 20-year retrospective review of global aquaculture. *Nature* 591, 551–563. doi: 10.1038/s41586-021-03308-6

Nazari-Sharabian, M., Ahmad, S., and Karakouzian, M. (2018). Climate change and eutrophication: a short review. *Engineering. Technol. Appl. Sci. Res.* 8, 3668–3672. doi: 10.48084/etasr.2392

Ndawala, M. A., Msuya, F. E., Cabarubias, J. P., Kambey, C. S. B., Buriyo, A. S., Mvungi, E. F., et al. (2022). Effect of biosecurity practices and diseases on growth and carrageenan properties of *Kappaphycus alvarezii* and *Eucheuma denticulatum* cultivated in Zanzibar, Tanzania. *J. Appl. Phycol.* 34, 3069–3085. doi: 10.1007/s10811-022-02835-7

Nelson, D. R., Mystikou, A., Jaiswal, A., Rad-Menendez, C., Preston, M. J., De Boever, F., et al. (2024). Macroalgal deep genomics illuminate multiple paths to aquatic, photosynthetic multicellularity. *Mol. Plant* 17, 747–771. doi: 10.1016/j.molp.2024.03.011

Nepper-Davidsen, J., Andersen, D. T., and Pedersen, M. F. (2019). Exposure to simulated heatwave scenarios causes long-term reductions in performance in *Saccharina latissima*. *Mar. Ecol. Prog. Ser.* 630, 25–39. doi: 10.3354/meps13133

Nielsen, M. M., Manns, D., D'este, M., Krause-Jensen, D., Rasmussen, M. B., Larsen, M. M., et al. (2016). Variation in biochemical composition of *Saccharina latissima* and *Laminaria digitata* along an estuarine salinity gradient in inner Danish waters. *Algal. Res.* 13, 235–245. doi: 10.1016/j.algal.2015.12.003

Nitschke, U., Walsh, P., Mcdaid, J., and Stengel, D. B. (2018). Variability in iodine in temperate seaweeds and iodine accumulation kinetics of *Fucus vesiculosus* and *Laminaria digitata* (Phaeophyceae, Ochrophyta). *J. Phycol.* 54, 114–125. doi: 10.1111/jpy.2018.54.issue-1

Noisette, F., Pansch, C., Wall, M., Wahl, M., and Hurd, C. L. (2022). Role of hydrodynamics in shaping chemical habitats and modulating the responses of coastal benthic systems to ocean global change. *Global Change Biol.* 28, 3812–3829. doi: 10.1111/gcb.v28.12

O'Connor, M. I. (2009). Warming strengthens an herbivore–plant interaction. *Ecology* 90, 388–398. doi: 10.1890/08-0034.1

Olischläger, M., Iñiguez, C., Gordillo, F. J. L., and Wiencke, C. (2014). Biochemical composition of temperate and Arctic populations of Saccharina latissima after exposure to increased pCO2 and temperature reveals ecotypic variation. *Planta* 240, 1213–1224. doi: 10.1007/s00425-014-2143-x

Oliver, E. C. J., Donat, M. G., Burrows, M. T., Moore, P. J., Smale, D. A., Alexander, L. V., et al. (2018). Longer and more frequent marine heatwaves over the past century. *Nat. Commun.* 9, 1324. doi: 10.1038/s41467-018-03732-9

Osborne, M. G., Molano, G., Simons, A. L., Dao, V., Ong, B., Vong, B., et al. (2023). Natural variation of *Macrocystis pyrifera* gametophyte germplasm culture microbiomes and applications for improving yield in offshore farms. *J. Phycol.* 00, 1–16. doi: 10.1111/jpy.13320

Paine, E. R., Britton, D., Schmid, M., Brewer, E. A., Diaz-Pulido, G., Boyd, P. W., et al. (2023). No effect of ocean acidification on growth, photosynthesis, or dissolved organic carbon release by three temperate seaweeds with different dissolved inorganic carbon uptake strategies. *ICES. J. Mar. Sci.* 80, 272–281. doi: 10.1093/icesjms/fsac221

Pang, T., Liu, J., Liu, Q., Li, H., and Li, J. (2015). Observations on pests and diseases affecting a eucheumatoid farm in China. *J. Appl. Phycol.* 27, 1975–1984. doi: 10.1007/s10811-014-0507-z

Park, E., Yu, H., Lim, J.-H., Hee Choi, J., Park, K.-J., and Lee, J. (2023). Seaweed metabolomics: A review on its nutrients, bioactive compounds and changes in climate change. *Food Res. Int.* 163, 112221. doi: 10.1016/j.foodres.2022.112221

Patwary, Z. P., Paul, N. A., Nishitsuji, K., Campbell, A. H., Shoguchi, E., Zhao, M., et al. (2021). Application of omics research in seaweeds with a focus on red seaweeds. *Briefings Funct. Genomics* 20, 148–161. doi: 10.1093/bfgp/elab023

Pavia, H., and Toth, G. B. (2000). Inducible chemical resistance to herbivory in the brown seaweed *Ascophyllum nodosum*. *Ecology* 81, 3212–3225. doi: 10.1890/0012-9658(2000)081[3212:ICRTHI]2.0.CO;2

Pedersen, M. F., and Borum, J. (1996). Nutrient control of algal growth in estuarine waters. Nutrient limitation and the importance of nitrogen requirements and nitrogen storage among phytoplankton and species of macroalgae. *Mar. Ecol. Prog. Ser.* 142, 261–272. doi: 10.3354/meps142261

Pedersen, M. F., Nejrup, L. B., Fredriksen, S., Christie, H., and Norderhaug, K. M. (2012). Effects of wave exposure on population structure, demography, biomass and productivity of the kelp *Laminaria hyperborea*. *Mar. Ecol. Prog. Ser.* 451, 45–60. doi: 10.3354/meps09594

Peng, C., Sui, Z., Zhou, W., Hu, Y., Mi, P., Jiang, M., et al. (2018). Analysis of DNA methylation of *Gracilariopsis lemaneiformis* under temperature stress using the methylation sensitive amplification polymorphism (MSAP) technique. *J. Ocean. Univ. China* 17, 623–631. doi: 10.1007/s11802-018-3426-9

Pessarrodona, A., Assis, J., Filbee-Dexter, K., Burrows, M. T., Gattuso, J.-P., Duarte, C. M., et al. (2022). Global seaweed productivity. *Sci. Adv.* 8, eabn2465. doi: 10.1126/sciadv.abn2465

Peteiro, C., and Freire, Ó. (2012). Observations on fish grazing of the cultured kelps *Undaria pinnatifida* and *Saccharina latissima* (Phaeophyceae, Laminariales) in Spanish Atlantic waters. *Aquacult. Aquarium. Conserv. Legislation.* 5, 189–196.

Peteiro, C., and Freire, Ó. (2013). Biomass yield and morphological features of the seaweed *Saccharina latissima* cultivated at two different sites in a coastal bay in the Atlantic coast of Spain. *J. Appl. Phycol.* 25, 205–213. doi: 10.1007/s10811-012-9854-9

Piñeiro-Corbeira, C., Barreiro, R., Cremades, J., and Arenas, F. (2018). Seaweed assemblages under a climate change scenario: Functional responses to temperature of eight intertidal seaweeds match recent abundance shifts. *Sci. Rep.* 8, 12978. doi: 10.1038/s41598-018-31357-x

Provasoli, L., and Pintner, I. J. (1980). Bacteria induced polymorphism in an axenic laboratory strain of *Ulva lactuca* (chlorophyceae)1. *J. Phycol.* 16, 196–201. doi: 10.1111/j.1529-8817.1980.tb03019.x

Qiu, Z., Coleman, M. A., Provost, E., Campbell, A. H., Kelaher, B. P., Dalton, S. J., et al. (2019). Future climate change is predicted to affect the microbiome and condition of habitat-forming kelp. *Proc. R. Soc. B.* 286, 20181887. doi: 10.1098/rspb.2018.1887

Raven, J., Caldeira, K., Elderfield, H., Hoegh-Guldberg, O., Liss, P., Riebesell, U., et al. (2005). *Ocean acidification due to increasing atmospheric carbon dioxide* (London: The Royal Society).

Redway, M. L., and Combet, E. (2023). Seaweed as food: survey of the UK market and appraisal of opportunities and risks in the context of iodine nutrition. *Br. Food J.* 125, 3601–3622. doi: 10.1108/BFJ-01-2023-0024

Reichert, B. K., Schnur, R., and Bengtsson, L. (2002). Global ocean warming tied to anthropogenic forcing. *Geophys. Res. Lett.* 29, 20–1-20-4. doi: 10.1029/2001GL013954

Ricart, A. M., Honisch, B., Fachon, E., Hunt, C. W., Salisbury, J., Arnold, S. N., et al. (2023). Optimizing marine macrophyte capacity to locally ameliorate ocean acidification under variable light and flow regimes: Insights from an experimental approach. *PloS One* 18, e0288548. doi: 10.1371/journal.pone.0288548

Rinde, E., Christie, H., Fagerli, C. W., Bekkby, T., Gundersen, H., Norderhaug, K. M., et al. (2014). The influence of physical factors on kelp and sea urchin distribution in previously and still grazed areas in the NE Atlantic. *PloS One* 9, e100222. doi: 10.1371/journal.pone.0100222

Rioux, L.-E., Turgeon, S. L., and Beaulieu, M. (2009). Effect of season on the composition of bioactive polysaccharides from the brown seaweed *Saccharina longicruris*. *Phytochemistry* 70, 1069–1075. doi: 10.1016/j.phytochem.2009.04.020

Roleda, M. Y., and Hurd, C. L. (2012). "Seaweed responses to ocean acidification," in *Seaweed Biology*. Eds. C. Wiencke and K. Bischof (Springer, Berlin, Heidelberg).

Roleda, M. Y., Skjermo, J., Marfaing, H., Jónsdóttir, R., Rebours, C., Gietl, A., et al. (2018). Iodine content in bulk biomass of wild-harvested and cultivated edible seaweeds: Inherent variations determine species-specific daily allowable consumption. *Food Chem.* 254, 333–339. doi: 10.1016/j.foodchem.2018.02.024

Ross, F. W. R., Boyd, P. W., Filbee-Dexter, K., Watanabe, K., Ortega, A., Krause-Jensen, D., et al. (2023). Potential role of seaweeds in climate change mitigation. *Sci. Total. Environ.* 885, 163699. doi: 10.1016/j.scitotenv.2023.163699

Satoh, Y., Wada, S., and Hisamatsu, S. I. (2019). Seasonal variations in iodine concentrations in a brown alga (*Ecklonia cava* Kjellman) and a seagrass (*Zostera marina* L.) in the northwestern Pacific coast of central Japan. *J. Oceanogr.* 75, 111–117. doi: 10.1007/s10872-018-0479-8

Scheschonk, L., Becker, S., Hehemann, J. H., Diehl, N., Karsten, U., and Bischof, K. (2019). Arctic kelp eco-physiology during the polar night in the face of global warming: a crucial role for laminarin. *Mar. Ecol. Prog. Ser.* 611, 59–74. doi: 10.3354/meps12860

Scheschonk, L., Bischof, K., Kopp, M. E. L., and Jueterbock, A. (2023). Differences by origin in methylome suggest eco-phenotypes in the kelp *Saccharina latissima*. *Evol. Appl.* 16, 262–278. doi: 10.1111/eva.13382

Schiel, D. R., Steinbeck, J. R., and Foster, M. S. (2004). Ten years of induced ocean warming causes comprehensive changes in marine benthic communities. *Ecology* 85, 1833–1839. doi: 10.1890/03-3107

Schoenrock, K. M., O'callaghan, T., O'callaghan, R., and Krueger-Hadfield, S. A. (2019). First record of *Laminaria ochroleuca* Bachelot de la Pylaie in Ireland in Béal an Mhuirthead, county Mayo. *Mar. Biodivers. Records.* 12, 9. doi: 10.1186/s41200-019-0168-3

Sen Gupta, A., Thomsen, M., Benthuysen, J. A., Hobday, A. J., Oliver, E., Alexander, L. V., et al. (2020). Drivers and impacts of the most extreme marine heatwaves events. *Sci. Rep.* 10, 19359. doi: 10.1038/s41598-020-75445-3

Shalders, T. C., Champion, C., Benkendorff, K., Davis, T., Wernberg, T., Morris, S., et al. (2023). Changing nutritional seascapes of kelp forests. *Front. Mar. Sci.* 10, 1197468. doi: 10.3389/fmars.2023.1197468

Shalders, T. C., Champion, C., Coleman, M. A., and Benkendorff, K. (2022). The nutritional and sensory quality of seafood in a changing climate. *Mar. Environ. Res.* 176, 105590. doi: 10.1016/j.marenvres.2022.105590

Shan, T. F., Pang, S. J., Li, J., and Gao, S. Q. (2016). Breeding of an elite cultivar Haibao No. 1 of Undaria pinnatifida (Phaeophyceae) through gametophyte clone crossing and consecutive selection. *J. Appl. Phycol.* 28, 2419–2426. doi: 10.1007/s10811-015-0748-5

Shen, Y., Motomura, T., Ichihara, K., Matsuda, Y., Yoshimura, K., Kosugi, C., et al. (2023). Application of CRISPR-Cas9 genome editing by microinjection of gametophytes of *Saccharina japonica* (Laminariales, Phaeophyceae). *J. Appl. Phycol.* 35, 1431–1441. doi: 10.1007/s10811-023-02940-1

Simkanin, C., Power, A. M., Myers, A., Mcgrath, D., Southward, A., Mieszkowska, N., et al. (2005). Using historical data to detect temporal changes in the abundances of intertidal species on Irish shores. *J. Mar. Biol. Assoc. United. Kingdom.* 85, 1329–1340. doi: 10.1017/S0025315405012506

Smale, D. A. (2020). Impacts of ocean warming on kelp forest ecosystems. *New Phytol.* 225, 1447–1454. doi: 10.1111/nph.v225.4

Smale, D. A., Burrows, M. T., Evans, A. J., King, N., Sayer, M. D. J., Yunnie, A. L. E., et al. (2016). Linking environmental variables with regional-scale variability in ecological structure and standing stock of carbon within UK kelp forests. *Mar. Ecol. Prog. Ser.* 542, 79–95. doi: 10.3354/meps11544

Smale, D. A., Pessarrodona, A., King, N., Burrows, M. T., Yunnie, A., Vance, T., et al. (2020). Environmental factors influencing primary productivity of the forest-forming kelp *Laminaria hyperborea* in the northeast Atlantic. *Sci. Rep.* 10, 12161. doi: 10.1038/s41598-020-69238-x

Smale, D. A., and Vance, T. (2015). Climate-driven shifts in species' distributions may exacerbate the impacts of storm disturbances on North-east Atlantic kelp forests. *Mar. Freshw. Res.* 67, 65–74. doi: 10.1071/MF14155

Smale, D. A., Wernberg, T., Oliver, E. C. J., Thomsen, M., Harvey, B. P., Straub, S. C., et al. (2019). Marine heatwaves threaten global biodiversity and the provision of ecosystem services. *Nat. Climate Change* 9, 306–312. doi: 10.1038/s41558-019-0412-1

Smith, K. E., Aubin, M., Burrows, M. T., Filbee-Dexter, K., Hobday, A. J., Holbrook, N. J., et al. (2024). Global impacts of marine heatwaves on coastal foundation species. *Nat. Commun.* 15, 5052. doi: 10.1038/s41467-024-49307-9

Smith, K. E., Burrows, M. T., Hobday, A. J., King, N. G., Moore, P. J., Sen Gupta, A., et al. (2023). Biological impacts of marine heatwaves. *Annu. Rev. Mar. Sci.* 15, 119–145. doi: 10.1146/annurev-marine-032122-121437

Smolina, I., Kollias, S., Jueterbock, A., Coyer, J. A., and Hoarau, G. (2016). Variation in thermal stress response in two populations of the brown seaweed, *Fucus distichus*, from the Arctic and subarctic intertidal. *R. Soc. Open Sci.* 3, 150429. doi: 10.1098/rsos.150429

Solas, M., Correa, R. A., Barría, F., Garcés, C., Camus, C., and Faugeron, S. (2024). Assessment of local adaptation and outbreeding risks in contrasting thermal environments of the giant kelp, Macrocystis pyrifera. *J. Appl. Phycol.* 36, 471–483. doi: 10.1007/s10811-023-03119-4

Spurkland, T., and Iken, K. (2011). Salinity and irradiance effects on growth and maximum photosynthetic quantum yield in subarctic *Saccharina latissima* (Laminariales, Laminariaceae). *Botanica Marina.* 54, 355–365. doi: 10.1515/bot.2011.042

Stammer, D., Martins, M. S., Köhler, J., and Köhl, A. (2021). How well do we know ocean salinity and its changes? *Prog. Oceanogr.* 190, 102478. doi: 10.1016/j.pocean.2020.102478

Stamp, T. (2015). "*Alaria esculenta* forest with dense anemones and crustose sponges on extremely exposed infralittoral bedrock," in *Marine life Information Network: Biology and Sensitivity Key Information Reviews*. Eds. H. Tyler-Walters and K. Hiscock (Marine Biological Association of the United Kingdom, Plymouth).

Starko, S., Soto Gomez, M., Darby, H., Demes, K. W., Kawai, H., Yotsukura, N., et al. (2019). A comprehensive kelp phylogeny sheds light on the evolution of an ecosystem. *Mol. Phylogenet. Evol.* 136, 138–150. doi: 10.1016/j.ympev.2019.04.012

Steneck, R. S., Graham, M. H., Bourque, B. J., Corbett, D., Erlandson, J. M., Estes, J. A., et al. (2002). Kelp forest ecosystems: biodiversity, stability, resilience and future. *Environ. Conserv.* 29, 436–459. doi: 10.1017/S0376892902000322

Stévant, P., Rebours, C., and Chapman, A. (2017). Seaweed aquaculture in Norway: recent industrial developments and future perspectives. *Aquacult. Int.* 25, 1373–1390. doi: 10.1007/s10499-017-0120-7

Strittmatter, M., Murúa, P., Arce, P., Perrineau, M.-M., and Gachon, C. (2022). My seaweed looks weird: a community web portal to accelerate pathogen discovery in seaweeds. *Appl. Phycol.* 3, 300–305. doi: 10.1080/26388081.2022.2059783

Subasinghe, R., Soto, D., and Jia, J. (2009). Global aquaculture and its role in sustainable development. *Rev. Aquacult.* 1, 2–9. doi: 10.1111/j.1753-5131.2008.01002.x

Sultana, F., Wahab, M. A., Nahiduzzaman, M., Mohiuddin, M., Iqbal, M. Z., Shakil, A., et al. (2023). Seaweed farming for food and nutritional security, climate change mitigation and adaptation, and women empowerment: A review. *Aquacult. Fisheries.* 8, 463–480. doi: 10.1016/j.aaf.2022.09.001

Sun, P., Mao, Y., Li, G., Cao, M., Kong, F., Wang, L., et al. (2015). Comparative transcriptome profiling of *Pyropia yezoensis* (Ueda) M.S. Hwang & H.G. Choi in response to temperature stresses. *BMC Genomics* 16, 463. doi: 10.1186/s12864-015-1586-1

Suresh Kumar, K., Ganesan, K., and Subba Rao, P. V. (2015). Seasonal variation in nutritional composition of *Kappaphycus alvarezii* (Doty) Doty—an edible seaweed. *J. Food Sci. Technol.* 52, 2751–2760. doi: 10.1007/s13197-014-1372-0

Taise, A., Krieger, E., Bury, S. J., and Cornwall, C. E. (2023). Physiological responses of Caulerpa spp. (with different dissolved inorganic carbon physiologies) to ocean acidification. *New Z. J. Bot.* 19, 1–25. doi: 10.1080/0028825X.2023.2289432

Tait, L. W., Thoral, F., Pinkerton, M. H., Thomsen, M. S., and Schiel, D. R. (2021). Loss of Giant Kelp, *Macrocystis pyrifera*, driven by marine heatwaves and exacerbated by poor water clarity in New Zealand. *Front. Mar. Sci.* 8, 721087. doi: 10.3389/fmars.2021.721087

Tamarin-Brodsky, T., and Kaspi, Y. (2017). Enhanced poleward propagation of storms under climate change. *Nat. Geosci.* 10, 908–913. doi: 10.1038/s41561-017-0001-8

Tan, T.-T., Song, S.-L., Poong, S.-W., Ward, G. M., Brodie, J., and Lim, P.-E. (2020). The effect of grazing on the microbiome of two commercially important agarophytes, *Gracilaria firma* and *G. salicornia* (Gracilariaceae, Rhodophyta). *J. Appl. Phycol.* 32, 2549–2559. doi: 10.1007/s10811-020-02062-y

Taylor, R. B., Sotka, E., and Hay, M. E. (2002). Tissue-specific induction of herbivore resistance: seaweed response to amphipod grazing. *Oecologia* 132, 68–76. doi: 10.1007/s00442-002-0944-2

Thomsen, M. S., Wernberg, T., and Kendrick, G. A. (2004). The effect of thallus size, life stage, aggregation, wave exposure and substratum conditions on the forces required to break or dislodge the small kelp *Ecklonia radiata*. *Botanica Marina*. 47, 454–460. doi: 10.1515/BOT.2004.068

Timmermans, M.-L., and Marshall, J. (2020). Understanding Arctic Ocean circulation: A review of ocean dynamics in a changing climate. *J. Geophys. Res.: Oceans.* 125, e2018JC014378. doi: 10.1029/2018JC014378

Timperio, A. M., Egidi, M. G., and Zolla, L. (2008). Proteomics applied on plant abiotic stresses: Role of heat shock proteins (HSP). *J. Proteomics* 71, 391–411. doi: 10.1016/j.jprot.2008.07.005

Toth, G. B., Karlsson, M., and Pavia, H. (2007). Mesoherbivores reduce net growth and induce chemical resistance in natural seaweed populations. *Oecologia* 152, 245–255. doi: 10.1007/s00442-006-0643-5

Trujillo, E., Monreal-Escalante, E., Ramos-Vega, A., and Angulo, C. (2024). Macroalgae: Marine players in vaccinology. *Algal. Res.* 78, 103392. doi: 10.1016/j.algal.2024.103392

Valero, M., Guillemin, M.-L., Destombe, C., Jacquemin, B., Gachon, C. M., Badis, Y., et al. (2017). Perspectives on domestication research for sustainable seaweed aquaculture. *Perspect. Phycol.* 4, 33–46. doi: 10.1127/pip/2017/0066

van der Loos, L. M., Eriksson, B. K., and Falcão Salles, J. (2019a). The macroalgal holobiont in a changing sea. *Trends Microbiol.* 27, 635–650. doi: 10.1016/j.tim.2019.03.002

van der Loos, L. M., Schmid, M., Leal, P. P., Mcgraw, C. M., Britton, D., Revill, A. T., et al. (2019b). Responses of macroalgae to CO_2 enrichment cannot be inferred solely from their inorganic carbon uptake strategy. *Ecol. Evol.* 9, 125–140. doi: 10.1002/ece3.2019.9.issue-1

van der Molen, J., Ruardij, P., Mooney, K., Kerrison, P., O'connor, N. E., Gorman, E., et al. (2018). Modelling potential production of macroalgae farms in UK and Dutch coastal waters. *Biogeosciences* 15, 1123–1147. doi: 10.5194/bg-15-1123-2018

Veenhof, R. J., Champion, C., Dworjanyn, S. A., Shalders, T. C., and Coleman, M. A. (2023). Reproductive phenology of the kelp *Ecklonia radiata* at its Australian warm range edge and the influence of environmental factors. *Mar. Freshw. Res.* 74, 928–940. doi: 10.1071/MF22259

Veenhof, R. J., Coleman, M. A., Champion, C., Dworjanyn, S. A., Venhuizen, R., Kearns, L., et al. (2024). Novel high-throughput oxygen saturation measurements for quantifying the physiological performance of macroalgal early life stages. *J. Phycol*, 1–12 doi: 10.1111/jpy.13489

Vergés, A., Campbell, A. H., Wood, G., Kajlich, L., Eger, A. M., Cruz, D., et al. (2020). Operation Crayweed: Ecological and sociocultural aspects of restoring Sydney's underwater forests. *Ecol. Manage. Restor.* 21, 74–85. doi: 10.1111/emr.12413

Vergés, A., Doropoulos, C., Malcolm, H. A., Skye, M., Garcia-Pizá, M., Marzinelli, E. M., et al. (2016). Long-term empirical evidence of ocean warming leading to tropicalization of fish communities, increased herbivory, and loss of kelp. *Proc. Natl. Acad. Sci.* 113, 13791–13796. doi: 10.1073/pnas.1610725113

Vergés, A., Steinberg, P. D., Hay, M. E., Poore, A. G. B., Campbell, A. H., Ballesteros, E., et al. (2014). The tropicalization of temperate marine ecosystems: climate-mediated changes in herbivory and community phase shifts. *Proc. R. Soc. B.* 281, 20140846. doi: 10.1098/rspb.2014.0846

Villarini, G., and Vecchi, G. A. (2012). Twenty-first-century projections of North Atlantic tropical storms from CMIP5 models. *Nat. Climate Change* 2, 604–607. doi: 10.1038/nclimate1530

Visch, W., Layton, C., Hurd, C. L., Macleod, C., and Wright, J. T. (2023). A strategic review and research roadmap for offshore seaweed aquaculture—A case study from southern Australia. *Rev. Aquacult.* 15, 1467–1479. doi: 10.1111/raq.12788

Wade, R., Augyte, S., Harden, M., Nuzhdin, S., Yarish, C., and Alberto, F. (2020). Macroalgal germplasm banking for conservation, food security, and industry. *PloS Biol.* 18, e3000641. doi: 10.1371/journal.pbio.3000641

Wahl, M., Werner, F. J., Buchholz, B., Raddatz, S., Graiff, A., Matthiessen, B., et al. (2020). Season affects strength and direction of the interactive impacts of ocean warming and biotic stress in a coastal seaweed ecosystem. *Limnol. Oceanogr.* 65, 807–827. doi: 10.1002/lno.11350

Wang, W., Li, X., Liang, G., Zhao, N., Shi, L., and Yang, G. (2021). Description of a white spot disease of field cultivated kelp (*Saccharina japonica*) and evaluation of its influences on the growth and phytochemical contents. *Aquat. Bot.* 173, 103414. doi: 10.1016/j.aquabot.2021.103414

Wang, X., Yao, J., Zhang, J., and Duan, D. (2020). Status of genetic studies and breeding of *Saccharina japonica* in China. *J. Oceanol. Limnol.* 38, 1064–1079. doi: 10.1007/s00343-020-0070-1

Ward, G. M., Faisan, J. P. Jr., Cottier-Cook, E. J., Gachon, C., Hurtado, A. Q., Lim, P. E., et al. (2020). A review of reported seaweed diseases and pests in aquaculture in Asia. *J. World Aquacult. Soc.* 51, 815–828. doi: 10.1111/jwas.12649

Ward, G. M., Kambey, C. S. B., Faisan, J. P. Jr., Tan, P.-L., Daumich, C. C., Matoju, I., et al. (2022). Ice-Ice disease: An environmentally and microbiologically driven syndrome in tropical seaweed aquaculture. *Rev. Aquacult.* 14, 414–439. doi: 10.1111/raq.12606

Wernberg, T., Thomsen, M. S., Baum, J. K., Bishop, M. J., Bruno, J. F., Coleman, M. A., et al. (2023). Impacts of climate change on marine foundation species. *Annu. Rev. Mar. Sci.* 16, 13–59. doi: 10.1146/annurev-marine-042023-093037

Wiencke, C., and Amsler, C. D. (2012). "Seaweeds and their communities in polar regions," in *Seaweed Biology: Novel Insights into Ecophysiology, Ecology and Utilization*. Eds. C. Wiencke and K. Bischof (Springer Berlin Heidelberg, Berlin, Heidelberg).

Williams, C., Rees, S., Sheehan, E. V., Ashley, M., and Davies, W. (2022). Rewilding the sea? A rapid, low cost model for valuing the ecosystem service benefits of kelp forest recovery based on existing valuations and benefit transfers. *Front. Ecol. Evol.* 10, 642775. doi: 10.3389/fevo.2022.642775

Wilson, K. L., Skinner, M. A., and Lotze, H. K. (2019). Projected 21st-century distribution of canopy-forming seaweeds in the Northwest Atlantic with climate change. *Diversity Distrib.* 25, 582–602. doi: 10.1111/ddi.2019.25.issue-4

Wolf, J., Woolf, D., and Bricheno, L. (2020). Impacts of climate change on storms and waves relevant to the coastal and marine environment around the UK. *MCCIP. Sci. Rev.* 2020, 132–157. doi: 10.14465/2020.arc07.saw

Wood, D., Capuzzo, E., Kirby, D., Mooney-Mcauley, K., and Kerrison, P. (2017). UK macroalgae aquaculture: What are the key environmental and licensing considerations? *Mar. Policy* 83, 29–39. doi: 10.1016/j.marpol.2017.05.021

Wood, G., Marzinelli, E. M., Coleman, M. A., Campbell, A. H., Santini, N. S., Kajlich, L., et al. (2019). Restoring subtidal marine macrophytes in the Anthropocene: trajectories and future-proofing. *Mar. Freshw. Res.* 70, 936–951. doi: 10.1071/MF18226

Woollings, T., Gregory, J. M., Pinto, J. G., Reyers, M., and Brayshaw, D. J. (2012). Response of the North Atlantic storm track to climate change shaped by ocean–atmosphere coupling. *Nat. Geosci.* 5, 313–317. doi: 10.1038/ngeo1438

Xiao, X., Agustí, S., Yu, Y., Huang, Y., Chen, W., Hu, J., et al. (2021). Seaweed farms provide refugia from ocean acidification. *Sci. Total. Environ.* 776, 145192. doi: 10.1016/j.scitotenv.2021.145192

Xu, D., Brennan, G., Xu, L., Zhang, X. W., Fan, X., Han, W. T., et al. (2019). Ocean acidification increases iodine accumulation in kelp-based coastal food webs. *Global Change Biol.* 25, 629–639. doi: 10.1111/gcb.2019.25.issue-2

Yong, W. T. L., Thien, V. Y., Rupert, R., and Rodrigues, K. F. (2022). Seaweed: A potential climate change solution. *Renewable Sustain. Energy Rev.* 159, 112222. doi: 10.1016/j.rser.2022.112222

Young, C. S., Sylvers, L. H., Tomasetti, S. J., Lundstrom, A., Schenone, C., Doall, M. H., et al. (2022). Kelp (*Saccharina latissima*) mitigates coastal ocean acidification and increases the growth of North Atlantic bivalves in lab experiments and on an oyster farm. *Front. Mar. Sci.* 9, 881254. doi: 10.3389/fmars.2022.881254

Yu, C.-H., Lim, P.-E., and Phang, S.-M. (2013). Effects of irradiance and salinity on the growth of carpospore-derived tetrasporophytes of *Gracilaria edulis* and *Gracilaria tenuistipitata* var liui (Rhodophyta). *J. Appl. Phycol.* 25, 787–794. doi: 10.1007/s10811-012-9960-8

Zhu, L., Lei, J., Huguenard, K., and Fredriksson, D. W. (2021). Wave attenuation by suspended canopies with cultivated kelp (*Saccharina latissima*). *Coast. Eng.* 168, 103947. doi: 10.1016/j.coastaleng.2021.103947

frontiers | Frontiers in Marine Science

TYPE Original Research
PUBLISHED 08 November 2024
DOI 10.3389/fmars.2024.1478238

OPEN ACCESS

EDITED BY
Christopher Edward Cornwall,
Victoria University of Wellington,
New Zealand

REVIEWED BY
Wei Liu,
Shanghai University, China
Matthew Desmond,
University of Otago, New Zealand

*CORRESPONDENCE
Nora Diehl
ndiehl@uni-bremen.de

RECEIVED 09 August 2024
ACCEPTED 30 September 2024
PUBLISHED 08 November 2024

CITATION
Trautmann M, Bartsch I, Bligh M, Buck-Wiese H, Hehemann J-H, Niedzwiedz S, Plag N, Shan T, Bischof K and Diehl N (2024) Impact of climate change on the kelp *Laminaria digitata* – simulated Arctic winter warming. *Front. Mar. Sci.* 11:1478238. doi: 10.3389/fmars.2024.1478238

Impact of climate change on the kelp *Laminaria digitata* – simulated Arctic winter warming

Moritz Trautmann[1], Inka Bartsch[2], Margot Bligh[1,3], Hagen Buck-Wiese[3], Jan-Hendrik Hehemann[1,3], Sarina Niedzwiedz[1], Niklas Plag[4,5], Tifeng Shan[6], Kai Bischof[1] and Nora Diehl[1,2]*

[1]Faculty of Biology and Chemistry & Center for Marine Environmental Sciences (MARUM), University of Bremen, Bremen, Germany, [2]Alfred Wegener Institute, Helmholtz Centre for Polar and Marine Research, Bremerhaven, Germany, [3]Max-Planck-Institute for Marine Microbiology, Bremen, Germany, [4]Institute of Biological Sciences, University of Rostock, Rostock, Germany, [5]Julius Kühn-Institute (JKI) – Federal Research Centre for Cultivated Plants, Brunswick, Germany, [6]Institute of Oceanology, Chinese Academy of Sciences, Qingdao, China

The Arctic is seasonally exposed to long periods of low temperatures and complete darkness. Consequently, perennial primary producers have to apply strategies to maximize energy efficiency. Global warming is occurring in the Arctic faster than the rest of the globe. The highest amplitude of temperature rise occurs during Polar Night. To determine the stress resistance of the ecosystem-engineering kelp *Laminaria digitata* against Arctic winter warming, non-meristematic discs of adult sporophytes from Porsangerfjorden (Finnmark, Norway) were kept in total darkness at 0°C and 5°C over a period of three months. Physiological variables, namely maximum quantum yield of photosynthesis (F_v/F_m) and dry weight, as well as underlying biochemical variables including pigments, storage carbohydrates, total carbon and total nitrogen were monitored throughout the experiment. Although all samples remained in generally good condition with F_v/F_m values above 0.6, *L. digitata* performed better at 0°C than at 5°C. Depletion of metabolic products resulted in a constant decrease of dry weight over time. A strong decrease in mannitol and laminarin was observed, with greater reductions at 5°C than at 0°C. However, the total carbon content did not change, indicating that the sporophytes were not suffering from "starvation stress" during the long period of darkness. A decline was also observed in the accessory pigments and the pool of xanthophyll cycle pigments, particularly at 5°C. Our results indicate that *L. digitata* has a more active metabolism, but a lower physiological and biochemical performance at higher temperatures in the Arctic winter. Obviously, *L. digitata* is well adapted to Arctic Polar Night conditions, regardless of having its distributional center at lower latitudes. Despite a reduced vitality at higher temperatures, a serious decline in Arctic populations of *L. digitata* due to winter warming is not expected for the near future.

KEYWORDS

Arctic amplification, C:N, F_v/F_m, laminarin, mannitol, pigments, Polar Night

1 Introduction

The Arctic is one of the regions that is changing most rapidly due to climate factors, feedback mechanisms and changes in energy transport towards the poles (Richter-Menge et al., 2017; Previdi et al., 2021). This results in 3.8 times faster warming in the Arctic than the global average (Rantanen et al., 2022), with the strongest temperature rise detected during the winter months (Wang et al., 2017; Maturilli et al., 2019). Generally, organisms populating the Arctic must have the ability to survive extreme abiotic conditions due to the strong seasonality (Zacher et al., 2009). For instance, Arctic kelps have to endure extreme photoperiodic conditions (Gattuso et al., 2020). In winter, they are exposed to very low temperatures and months-long complete darkness (Polar Night). Due to climate change, however, strong fluctuations in sea surface temperature (SST) have occurred in recent decades. For example, in Kongsfjorden, Svalbard, winter SST minima of −1.8°C were measured, while the maximum SST reached ~5°C (Huang et al., 2021; see Supplementary Material; Diehl et al., 2024).

Kelp forests are among the largest biogenic structures of marine benthic habitats and are highly productive ecosystems with structural complexity and phyletic diversity (Steneck et al., 2002; Wernberg et al., 2019). By definition, they are formed by brown algae of the order Laminariales, which dominate shallow rocky shores of temperate and Arctic regions. As sedentary organisms, kelps are particularly affected by changes in their environment and rising temperatures result in shifts in distribution and abundance of many species (Smale et al., 2019). On the one hand, new suitable and ice-free habitats are expected to increasingly appear in the future (Krause-Jensen et al., 2020; Castro de la Guardia et al., 2023). Changes in kelp abundance have already been observed in High Arctic regions (Bartsch et al., 2016; Düsedau et al., 2024). On the other hand, elevated temperatures generally stimulate the metabolic activity of organisms (Pörtner et al., 2005), and may therefore have a negative impact on the dark survival of kelps (Gordillo et al., 2022). Yet, the mechanisms of winter survival are still poorly understood and only a few studies have investigated acclimation of kelps to the Polar Night (Scheschonk et al., 2019; Gordillo et al., 2022; Summers et al., 2023; Diehl et al., 2024).

Kelps have evolved various mechanisms to acclimatize to abiotic variations in the environment (Hurd et al., 2014). Due to the seasonal photoperiods in the Arctic, growth and reproduction of most kelps species is limited to a short time in spring and summer, while in winter they undergo a "starvation mode" due to the lack of light for photosynthesis (Wiencke et al., 2009; Gordillo et al., 2022).

The vitality of kelps can be determined via fluorescence-based measurements of the maximum quantum yield of photosystem II (F_v/F_m), a common parameter for assessing the health and stress level of photosynthetic organisms, including macroalgae (Dring et al., 1996; Dring, 2006). As they are part of the cellular machinery for photosynthesis, pigment contents in some seaweeds decrease during Polar Night, when the metabolism of the organisms slows down to survive this period of total darkness (Wiencke et al., 2009). Moreover, the de-epoxidation state of the xanthophyll cycle pigments (DPS), an intracellular stress response, is affected by light and low temperatures (Fernández-Marín et al., 2011; Li et al., 2020; Monteiro et al., 2021). The carbohydrates mannitol and laminarin play a crucial role in surviving the Polar Night. Mannitol is the primary photosynthesis product and an important short-term storage carbohydrate in brown algae (Yamaguchi et al., 1966). In summer, when photosynthesis rates are high, mannitol is converted into the polysaccharide laminarin, the long-term storage carbohydrate (Johnston et al., 1977). In periods of darkness, laminarin can be reconverted into mannitol to maintain important metabolic functions (Yamaguchi et al., 1966; Johnston et al., 1977; Küppers and Kremer, 1978). We hypothesize that winter warming could accelerate the use of carbon reserves and increase the decomposition of the biomass. Monitoring dry weight and the total carbon content alongside quantifying mannitol and laminarin provides information on the consumption of carbon-containing metabolites as well as the storage carbohydrates.

Laminaria digitata (Hudson) J.V. Lamouroux is a broadly distributed cold–temperate to Arctic North Atlantic kelp growing on hard substrates in the sublittoral zone. In the East Atlantic, it is present from Southern Brittany to Spitsbergen (Lüning, 1990), where it survives up to four months of Polar Night. The species is described to survive and grow at temperatures as low as 0°C, with a temperature optimum at 10°C (Bolton and Lüning, 1982; tom Dieck (Bartsch), 1992). Recent studies showed a distinct decrease in digitate kelps (including *L. digitata*) in Arctic fjords (Düsedau et al., 2024), potentially in response to changes in the underwater light climate as a consequence of increased meltwater run-off (Schlegel et al., 2024). Liesner et al. (2020) showed that lower temperatures (5 vs. 15°C) led to a higher phenotypic plasticity, as well as higher growth rates of juvenile sporophytes, highlighting the importance of cold seasons for the survival of *L. digitata* and potential threats of climate change. Exposing *L. digitata* gametophytes to low temperatures (5 vs. 15°C) also facilitated a positive growth response from subsequent juvenile sporophytes at sub-optimal low (0°C) and warm (20°C) conditions (Gauci et al., 2022).

The aim of this study was to determine the resistance of *L. digitata* sporophytes to simulated temperature increases during the Polar Night in the High Arctic. Therefore, we kept discs from *L. digitata* sporophytes at temperatures of 0°C and 5°C in total darkness for three months. Various physiological and biochemical variables were monitored during the experiment. We hypothesized that higher temperatures during Polar Night would lead to an increased metabolism and therefore a reduced survival capacity of *L. digitata*.

2 Material and methods

2.1 Sampling and experimental design

Twenty adult sporophytes (~75–200 cm) of *Laminaria digitata* (Hudson) J.V. Lamouroux were collected at Porsangerfjorden (N 70°24', E 25°32'; N 70°29', E 25°39'; N 70°30', E 25°42'), Finnmark in Northern Norway (Figure 1A). Individuals were sampled on July 12, 2022 at depths of 3–5 m, and stored in running seawater until July 20. Between 20 and 50 discs (ø 2.8 cm) per sporophyte were cut 10–40 cm above the meristem and

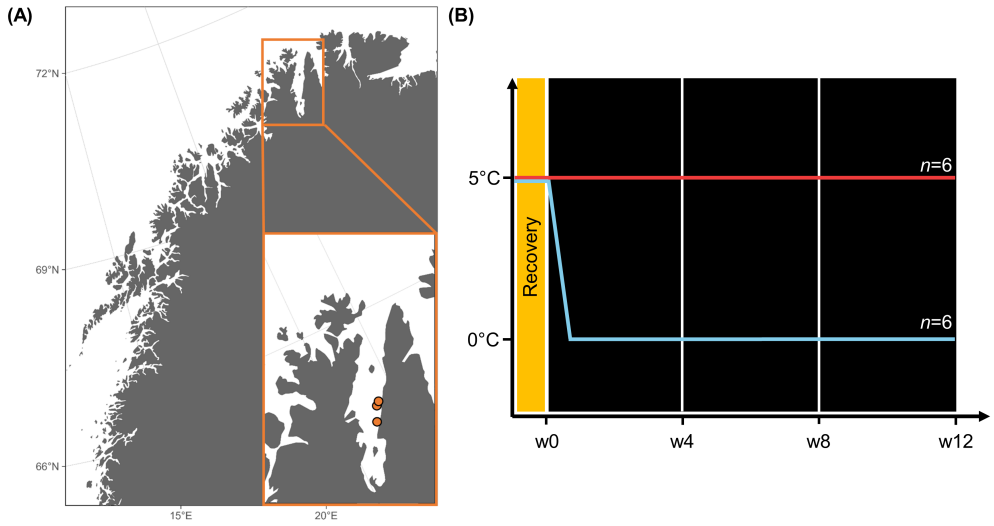

FIGURE 1
(A) Map of Northern Norway and Porsangerfjorden (Finnmark). The orange dots mark the sampling locations of *Laminaria digitata*. **(B)** Experimental setup. Week 0 (w0), w4, w8, and w12: Biochemical sampling during the experiment. Map was created with ggOceanMaps (Vihtakari, 2024).

kept moist, cool, and dark during transport. The experiment was conducted at the Alfred Wegener Institute in Bremerhaven, Germany. The samples arrived on July 22. After arrival, the discs were cultivated in a climate chamber at 5°C (± 0.5°C) and constant light (30 µmol photons m^{-2} s^{-1}, λ ~380–700 nm, ProfiLux 3 with LED Mitras daylight 150, GHL Advanced Technology, Kaiserslautern, Germany) over three days for recovery (Figure 1B). After the recovery period, the subsamples from 12 sporophytes were distributed across the replicates, treatments and time points. To do so, 20 healthy discs (Dring et al., 1996; F_v/F_m >0.6 data not shown) from one individual each were used per replicate and treatment (n = 6), e.g. 0°C Replicate A. First biochemical sampling was conducted on August 01 (week 0 = "w0"). Therefore, five discs per replicate were randomly selected before the acclimation began, shock-frozen in liquid N_2 and stored at −80°C until further processing. Then, the samples were maintained in two separate climate chambers (0°C and 5°C; ± 0.5°C) in the dark and the 0°C replicates were stepwise acclimated from 5°C to 0°C. Over a period of three months, three more biochemical samplings were conducted in the same way (September 02: "w4", September 30: "w8", October 27: "w12"). During the experiment, each replicate was kept in an aerated 2 L clear plastic bottle containing 1/40 Provasoli-enriched seawater [1/40 PES, 13.7 µmol NO_3^- L^{-1}; 0.55 µmol PO_4^{3-} L^{-1}] in total darkness (0 µmol photons m^{-2} s^{-1}), simulating Polar Night conditions in this High Arctic fjord Kongsfjorden, Svalbard (Bischof et al., 2019). Water was exchanged twice a week.

2.2 Species identification

As discrimination between digitate *Laminaria digitata*, *Hedophyllum nigripes* and *Laminaria hyperborea* is difficult based on morphology alone (Longtin and Saunders, 2015; Dankworth et al., 2020), we genetically identified the collected specimens. Genomic DNA was extracted from subsamples, which were stored in silica gel, using a plant genomic DNA extraction kit (DP305, Tiangen Biotech, China) following the manufacturer's instructions. Species were identified according to the method of Mauger et al. (2021), which involves amplifying a fragment of the mitochondrial COI gene (COI-5P). In short, two PCR reactions (PCR1 and PCR2) were conducted using a Taq Master Mix kit (Accurate Biology, China) and a T-gradient thermocycler (Biometra, Germany), with the primers and programs outlined in Mauger et al. (2021). PCR products were separated by electrophoresis, and then stained with GelRed and visualized under UV light. The amplified fragment patterns were compared with Mauger et al. (2021) to identify species.

2.3 Physiological response variables

Maximum *in vivo* chlorophyll-fluorescence of photosystem II (F_v/F_m) was measured weekly, using a pulse-amplitude-modulated fluorometer (Imaging-PAM, Walz GmbH Mess- und Regeltechnik, Effeltrich, Germany) to assess algal vitality. The I-PAM was set up to determine the initial amplitude of the fluorescence signal (Ft) between 0.15 and 0.2 (Int. 4, Gain 4, Damp. 4, SP 8, Width 0.8 s).

Pictures of the samples were taken every two weeks against a white background to exclude potential effects of the discs' size on dry weight (DW). A ruler was included in the pictures for reference. Areas of the discs (cm^2) were determined using ImageJ (Version 1.54d, Java 1.8.0_345, Wayne Rasband, National Institute of Health, USA). For monitoring the DW (w0, w4, w8, w12), samples were freeze-dried (Alpha 1–4 LO plus, Martin Christ Gefriertrocknungsanlagen GmbH, Osterode am Harz, Germany) and then weighed.

2.4 Biochemical response variables

Total carbon (Total C) and nitrogen (Total N) were analyzed following the protocol of Graiff et al. (2015). 2–3 mg of freeze-dried samples were weighed into tin cartridges and incinerated at 950°C in an elemental analyzer (Vario EL III, Elementar). Acetanilide was used as a standard (Verardo et al., 1990).

Mannitol content was determined following the methods of Diehl et al. (2020). In short, 1 mL of 70% ethanol was added to 10–15 mg of freeze-dried samples and incubated at 70°C for three to four hours in a water bath. The samples were then centrifuged for 5 min at 13,000 rpm. 800 µL of the supernatant was transferred and evaporated to dryness. The pellets were re-dissolved in ultrapure water (0.055 µS/cm) by vortexing and ultrasonication. Resuspended samples were then centrifuged for 5 min at 13,000 rpm. Mannitol content in the supernatants was determined following the protocol of Karsten et al. (1991). A High Performance Liquid Chromatography system (HPLC; Agilent Technologies 1200 series, Santa Clara, California, USA) was used with a guard cartridge (Phenomenex, Carbo-Pb^{2+} 4 x 3.00 mm I.D.) and an analytical Aminex Fast Carbohydrate Analysis Column (100 x 7.8 mm, 9 µm, BioRad, Munich, Germany) using ultrapure water as mobile phase. Calibration standards contained 0.5, 1.0, 2.5, 5.0 and 10.0 mM mannitol. Initial (w0) values were set to 100% and other samples to percentage of the initial.

Laminarin content was quantified following the methods of Becker et al. (2017) and Becker and Hehemann (2018). Laminarin was first extracted from 35–65 mg of freeze-dried material with 50 mM 3-(N-morpholino)propanesulfonic acid (MOPS) buffer (pH 7.0) at 4°C for 5 h (Scheschonk et al., 2019). Three recombinantly expressed laminarinases (FbGH30, FaGH17A and FbGH17A) were used to specifically hydrolyze laminarin to glucose (Becker et al., 2017). The reducing ends of sugars were quantified via the PAHBAH assay (Lever, 1972). The concentration of laminarin in each sample was calculated by comparison to non-hydrolyzed samples and calibration against a standard curve of *Laminaria digitata* laminarin (Sigma-Aldrich) processed in the same way as the extracts. Calibration concentrations were 7.8125, 15.625, 31.25, 62.5, 125, 250 and 500 µg mL^{-1}. Concentrations were converted to mg of laminarin per mg DW.

Pigments were analyzed following the methods of Koch et al. (2015). 45–55 mg of freeze-dried samples were extracted in 1 mL 90% fridge-cold acetone at 4°C in darkness for 24 h. The filtered supernatant was analyzed by HPLC (LaChromElite® system, L-2200 cooled autosampler, DA-detector L-2450; VWR Hitachi International). Pigments were separated on a Spherisorb® ODS-2 (250 × 4.6 mm, 5 µm; Waters) column following the gradient from Wright et al. (1991). Reference standards were laboratory standard solutions (DHI Lab Products) of chlorophyll *a* (Chl *a*), chlorophyll c2 (Chl c2), fucoxanthin (Fuco), violaxanthin (V), antheraxanthin (A) and zeaxanthin (Z). The accessory pigment pool (Acc; Chl c2 + Fuco) as well as the pool size of the xanthophyll cycle pigments (VAZ; V+A+Z) were determined in µg g^{-1} DW. The ratios of VAZ:Chl*a* and Acc:Chl*a* were calculated to detect modulations in the photosynthetic apparatus. In addition, the de-epoxidation-state of the xanthophyll cycle (DPS), describing the process of converting V via A to Z, which reduces intracellular stress by dissipating excess energy (Wiencke and Bischof, 2012), was calculated after Colombo-Pallotta et al. (2006).

2.4 Statistics

As initial F_v/F_m values (w0) differed significantly between 0°C and 5°C, F_v/F_m and all other variables were displayed as "% of w0".

"R" version 4.2.2 (R Core Team, 2022) was used for statistical evaluation. First, extreme outliers (Bonferroni, $p < 0.05$) were excluded. Normal distribution and homogeneity of variances were checked for all datasets using a Shapiro-Wilk test ($p > 0.05$) and Levene's test ($p > 0.05$) respectively (Zuur et al., 2013). Data were also checked visually for normal distribution. If data appeared normally distributed, they were not transformed, regardless of the Shapiro-Wilk test statistic. The F-statistic for small sampling sizes is robust to a moderate deviation from the normal distribution (Blanca et al., 2017). Variation in F_v/F_m and area of all discs were examined using repeated unifactorial ANOVAs followed by *post hoc* Tukey tests. All other variables measured for the subsampled discs were assessed with two-factorial ANOVAs followed by *post hoc* Sidak tests, due to multiple pairwise comparison. When interpreting the data, it must be taken into account that the samples were cultivated in two different climate chambers, so that the temperature treatments contain a certain chamber effect. All statistical evaluations of the physiological and biochemical response variables are summarized in Supplementary Table S2.

3 Results

3.1 Species identification

Based on genetic data, the collected specimens were confirmed to be *Laminaria digitata* (Hudson) J.V. Lamouroux (Supplementary Figure S1).

3.2 Physiological response variables

The physiological vitality of *Laminaria digitata*, measured as the maximum quantum yield of photosystem II (F_v/F_m as % of w0; Figure 2 was strongly affected by the temperature treatments (0°C > 5°C, $p < 0.001$). Within each temperature treatment there were no significant changes over time. F_v/F_m was similar at both temperature treatments up to w6. From w8 onwards vitality of samples at 0°C increased slightly, while a trend toward decreasing vitality was observed for samples at 5°C. Throughout the entire experiment, F_v/F_m (raw data as "absolute values") in both treatments remained above 0.6 (Supplementary Table S1).

Although dry weight (DW as % of w0; Figure 3A) of the freeze-dried samples decreased significantly between w0 and w12 for pooled 0°C and 5°C ($p < 0.01$), no significant weight loss over time was

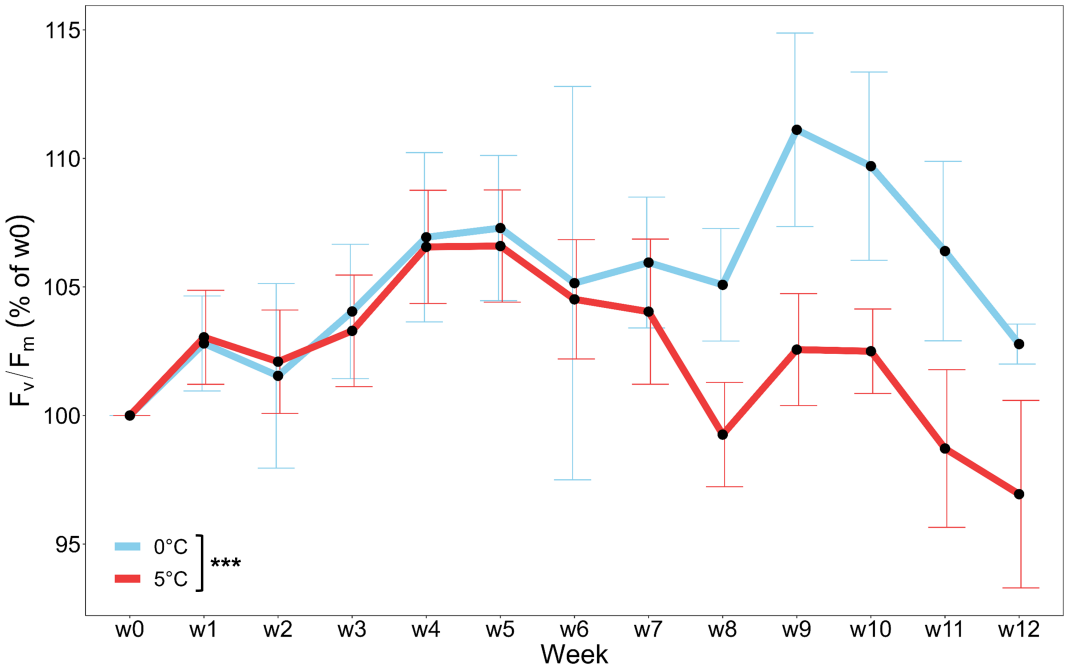

FIGURE 2
Vitality (maximum quantum yield of photosystem II; F_v/F_m) of *Laminaria digitata*, monitored weekly over three months under Polar Night conditions at 0°C (blue) and 5°C (red). Values are given as % of week 0 (w0) and means ± SD (n = 6). Significances between temperatures are indicated by black asterisks (p < 0.001***).

determined for 0°C and 5°C when considered individually. Time-integrated DW did not differ between the temperature treatments.

3.3 Biochemical response variables

The ratio between carbon and nitrogen (C:N as % of w0; Table 1) in the samples was affected by the temperature treatments ($p < 0.05$), decreasing significantly from w0 to w12 in samples at 5°C ($p < 0.01$) but not in samples at 0°C. These changes reflect higher total nitrogen contents (Total N) toward the end of the experiment. Total N (% of w0; Table 1) increased significantly over time at 5°C ($p < 0.01$), whereas no significant differences were measured for total carbon content (Total C; Figure 3B) of the samples at both temperature treatments. While not statistically significant, trend towards decreasing Total C over time were observed for both temperature treatments. Comparison of the raw data (absolute values) of C:N (Supplementary Table S1) revealed that ratios were slightly above 20 at the beginning of the experiment and declined to 17.9 ± 1.9 (0°C, $p = 0.29$) and 13.4 ± 0.6 (5°C, $p < 0.01$) at w12.

Mannitol content (% of w0; Figure 3C) decreased significantly over time (0°C: $p < 0.01$; 5°C: $p < 0.001$) in both treatments. While there was no significant difference between the two temperature treatments, a trend was observed to lower mannitol concentrations at 5°C compared to 0°C. Laminarin content (% of w0; Figure 3D) differed significantly between the temperature treatments ($p < 0.05$), with lower concentrations measured in samples at 5°C than at 0°C. Significant changes over time were only found for samples at 5°C (w0 > w12; $p < 0.05$).

Content of Chl*a*, Acc and VAZ (% of w0; Figures 4A–C) in samples decreased over time. Trends to higher concentrations in samples at 0°C than in samples at 5°C were observed for all pigments. Chl*a*, depleted significantly from w0 to w12 of the experiment when treatments were pooled ($p < 0.05$; Figure 4A). when considering treatments individually there was no significant decrease in Chl*a* over time for either 0°C or 5°C. for a significant reduction in Acc content (% of w0; Figure 4B) was only measured at 5°C ($p < 0.05$), resulting in significant differences between the temperature treatments ($p < 0.05$). The greatest effects of sampling time and temperature were detected for VAZ, which was significantly depleted in samples from w0 to w12 at both temperatures ($p < 0.001$; Figure 4C) and was significantly higher in samples at 0°C than in samples at 5°C ($p < 0.01$). No significant changes between w0 and w12 were observed in the relative (% of w0; Figure 4D) or absolute (Supplementary Table S1) values of DPS. While temperature had no significant effect on relative DPS, absolute DPS values were significantly higher at 0°C than at 5°C ($p < 0.001$) at the end of the experiment. Acc:Chl*a* (% of w0; Table 1) increased over time ($p < 0.05$) at 0°C, while VAZ:Chl*a* (% of w0; Table 1) decreased over time at both temperature treatments ($p < 0.001$), with lower values at 5°C ($p < 0.01$).

4 Discussion

This study determined the impact of Arctic winter warming on *Laminaria digitata* sporophytes in a simulation of High Arctic Polar Nights. Over a period of three months in darkness, physiological

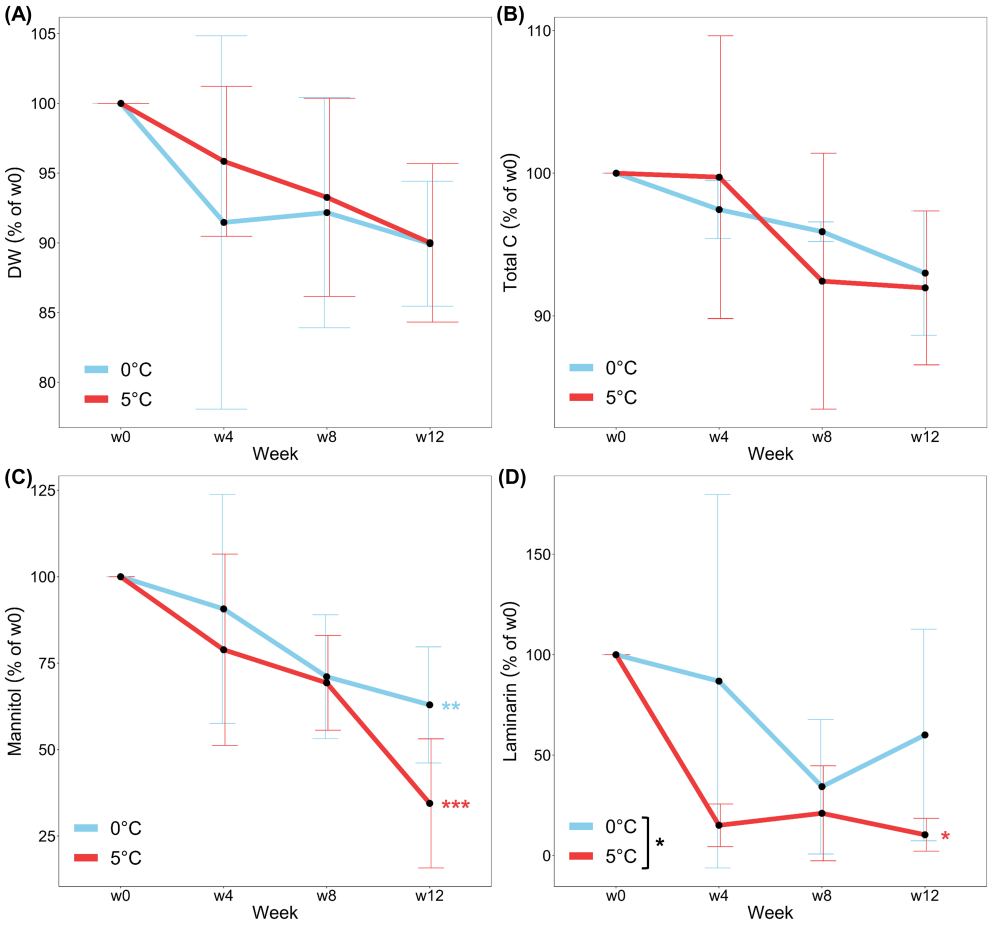

FIGURE 3
(A) Dry weight (DW) **(B)** Total carbon (Total C), **(C)** Mannitol and **(D)** Laminarin of *Laminaria digitata*, monitored every four weeks over three months under Polar Night conditions at 0°C (blue) and 5°C (red). Values are given as % of week 0 (w0) and means ± SD (n = 6). Significances between temperatures are indicated by black asterisks ($p < 0.05$*). Time-integrated significances between w0 and w12 within each temperature are marked by blue and red asterisks ($p < 0.01$**, $p < 0.001$***).

variables and underlying biochemical metabolites were monitored in samples maintained at 0°C and 5°C. The two temperature treatments represented the mean and the maximum winter temperatures that have already been measured in the High Arctic, for example in Kongsfjorden, Svalbard (Huang et al., 2021; see Supplementary Material; Diehl et al., 2024). From our results (Figure 5), it can be deduced that *L. digitata* sporophytes from Arctic regions are well adapted to prolonged darkness regardless of temperature and do not reach the end of Polar Night with a considerable lack of storage reserves and pigments.

Relative changes in vitality indicated that *L. digitata* performed better at 0°C compared to 5°C. Yet, a certain chamber effect in combination with the temperature treatments cannot be ruled out as the samples were maintained in two different climate chambers. Relative F_v/F_m values increased for samples at 0°C and decreased for samples at 5°C from week 8 onwards. However, absolute F_v/F_m values were never below 0.6, so all samples could be considered vital for the duration of the experiment (Dring et al., 1996). Laminariales have been observed to maintain a good vitality after long periods of darkness before (Scheschonk et al., 2019; Gordillo et al., 2022; Summers et al., 2023; Diehl et al., 2024).

The degradation of metabolites during prolonged darkness was reflected in a continuous loss in DW over time, as has also been observed for other kelps (Gordillo et al., 2022). However, contrary to previous data on *Saccharina latissima* and *Alaria esculenta*, weight loss in *L. digitata* did not increase at enhanced temperatures (3°C vs. 8°C; Gordillo et al., 2022). By visually observing the discs and monitoring disc area every two weeks, we were able to exclude any impact of decomposition on the DW (Supplementary Table S1; Supplementary Figure S2).

During polar winter kelps rely on accumulated energy stores, and must therefore be particularly energy efficient (Wiencke et al., 2009). In times of prolonged darkness, kelp derive mannitol from stocks of laminarin that they replenished during summer (Johnston et al., 1977; Küppers and Kremer, 1978). Accordingly, mannitol can be considered the main metabolite for respiration during the Polar Night. It must be taken into account that the storage carbohydrate content varies between the meristem and the distal part of the sporophyte (Scheschonk et al., 2019). By conducting the experiment with subsamples taken from the central part of the phylloid, we aimed to eliminate any impact of these variations. Mannitol content of *L. digitata* decreased by 37% (0°C) and 65% (5°C) over the three-

10.3389/fmars.2024.1478238

TABLE 1 Biochemical variables of *Laminaria digitata* monitored over three months under Polar Night conditions at 0°C and 5°C.

Variable	Temperature	Week	% of w0	Statistical comparison	
C:N	0°C	w0	100 ± 0	0°C > 5°C*	w0 = w12
		w4	87.3 ± 12.9		
		w8	90.9 ± 23.0		
		w12	84.6 ± 21.4		
	5°C	w0	100 ± 0		w0 > w12**
		w4	88.1 ± 20.8		
		w8	66.8 ± 11.7		
		w12	67.4 ± 17.0		
Total N	0°C	w0	100 ± 0	0°C < 5°C*	w0 = w12
		w4	102.3 ± 14.5		
		w8	111.9 ± 29.9		
		w12	115.1 ± 25.5		
	5°C	w0	100 ± 0		w0 < w12**
		w4	108.5 ± 9.8		
		w8	131.9 ± 6.3		
		w12	143.1 ± 33.8		
Acc:Chl*a*	0°C	w0	100 ± 0	0°C > 5°C**	w0 < w12*
		w4	102.8 ± 5.3		
		w8	105.1 ± 4.4		
		w12	108.0 ± 5.0		
	5°C	w0	100 ± 0		w0 = w12
		w4	100.2 ± 3.0		
		w8	104.5 ± 4.2		
		w12	96.2 ± 4.7		
VAZ:Chl*a*	0°C	w0	100 ± 0	0°C > 5°C**	w0 > w12***
		w4	84.8 ± 10.9		
		w8	69.0 ± 19.1		
		w12	68.0 ± 21.4		
	5°C	w0	100 ± 0		w0 > w12***
		w4	75.6 ± 8.3		
		w8	52.9 ± 7.4		
		w12	50.9 ± 8.6		

C:N, carbon to nitrogen ratio; Total N, total nitrogen; VAZ:Chl*a*, ratio of xanthophyll cycle pigment pool to chlorophyll *a*; Acc:Chl*a*:, ratio of accessory pigments to chlorophyll *a*. Values are given as % of week 0 (w0) and means ± SD (n = 6). Significances are indicated by asterisks: $p < 0.05$*, $p < 0.01$**, $p < 0.001$***.

month experiment, while laminarin decreased by 40% and 90% respectively. When comparing energy stocks in the cold–temperate kelp *S. latissima* from Kongsfjorden (Svalbard), Scheschonk et al. (2019) measured comparably high declines of mannitol and laminarin between October and February. They concluded that the strong reduction (>90%) of laminarin over the Polar Night maintains the metabolic functions of the kelp in that period. Additionally, lower laminarin concentrations were measured in *L. digitata* at higher temperatures during an experimental Polar Night treatment, as also observed in *S. latissima* (Scheschonk et al., 2019). The faster consumption of storage carbohydrates at higher temperatures suggests an increased energy requirement of *L. digitata* at 5°C. An

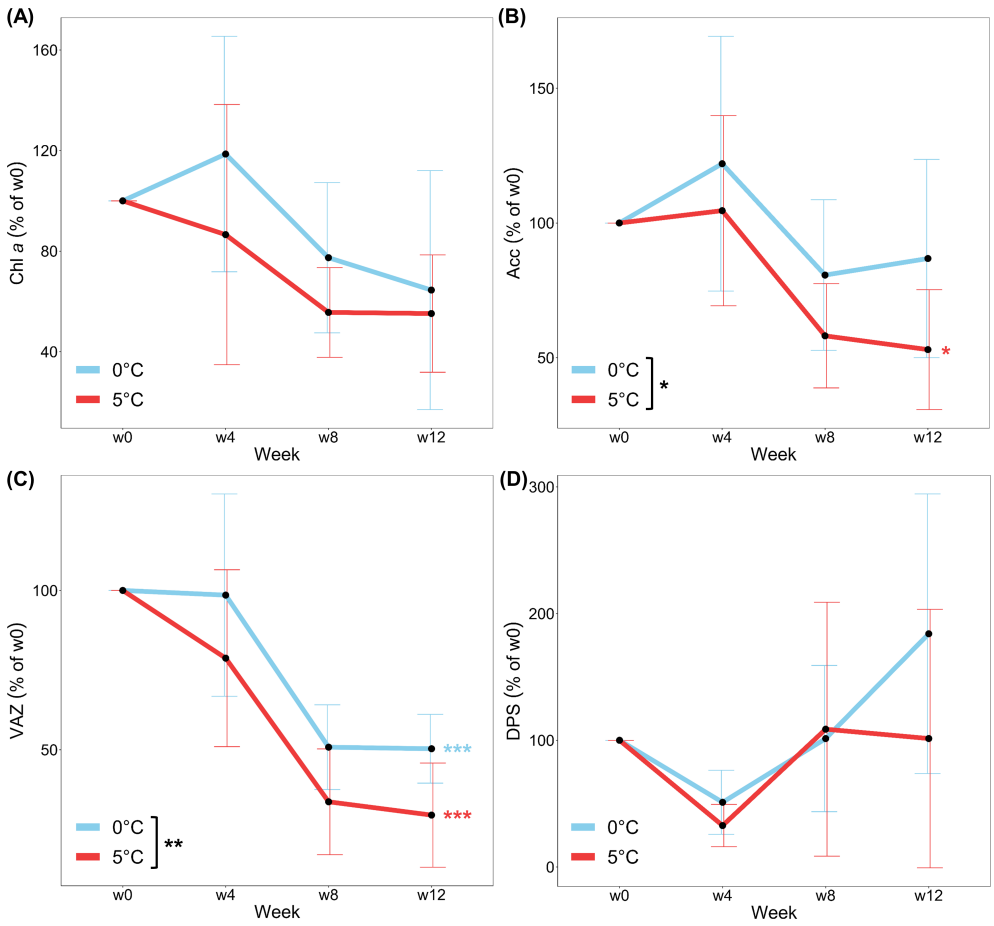

FIGURE 4
(A) Chlorophyll *a* (Chl *a*) **(B)** Accessory pigments (Acc) **(C)** Pool of xanthophyll cycle pigments (VAZ) and **(D)** De-epoxidation state of the xanthophyll cycle pigments (DPS) of *Laminaria digitata*, monitored every four weeks over three months under Polar Night conditions at 0°C (blue) and 5°C (red). Values are given as % of week 0 (w0) and means ± SD (n = 6). Significances between temperatures are indicated by black asterisks ($p < 0.05$*, $p < 0.01$**). Time-integrated significances between w0 and w12 within each temperature are marked by blue and red asterisks ($p < 0.05$*, $p < 0.001$***).

even stronger rise in winter temperatures in the future could completely deplete L. digitata energy stocks before the end of the Polar Night and thus might lead to starvation or extensive stress. A faster consumption of storage carbohydrates with increasing temperatures during Polar Night was not observed for *Laminaria hyperborea* (Diehl et al., 2024). The different responses of Laminariales to winter warming will presumably have an impact on seaweed diversity and species abundance in the High Arctic in the future.

Nonetheless, despite the almost complete depletion of laminarin stocks at 5°C, *L. digitata* was not exposed to a "starvation stress" during three months of total darkness, as seen in stable total carbon content (Total C) over the three-month experiment. Although tendencies towards decreasing Total C content were observed in the samples, the degradation was less than 10% and independent from temperature. Consequently, *L. digitata* must have developed a strategy to preserve C during the Polar Night period. For *S. latissima*, also no changes in Total C were measured after four months of darkness (Gordillo et al., 2022). We assume that at complete darkness similar processes take place in *L. digitata* as have been described for the growth phase, when Laminariales remobilize and utilize their storage carbohydrates for energy generation (Gómez and Huovinen, 2012). Laminarin is first transformed into mannitol. Subsequently, mannitol is degraded stepwise to generate cellular energy, releasing CO_2 which can be directly recovered by the enzyme phosphoenolpyruvate carboxykinase (PEP-CK) (Gómez and Huovinen, 2012). Comparable to the mechanism of dark carbon fixation (Wiencke et al., 2009), this allows an efficient recycling of every available C molecule to the kelp. Since we worked with non-meristematic tissues of *L. digitata* and the total C content was unaffected throughout the experiment, we assume that *L. digitata* uses the same strategy employed to restore C in times when photosynthesis is not possible. Our samples were taken in July during Polar Day, hence with almost "full carbohydrate stores" (Singh et al., 2024). We conclude that the carbohydrate reserves accumulated over the summer are sufficient to maintain the physiological functions of *L. digitata* during Polar Nights in future warming scenarios, as reflected in high F_v/F_m values at enhanced temperatures.

This conclusion is further supported by an observed increase in total nitrogen content (Total N) during the experiment. High environmental N availability in winter, which exceeds the N demand for protein and amino acid synthesis, enables and regulates the

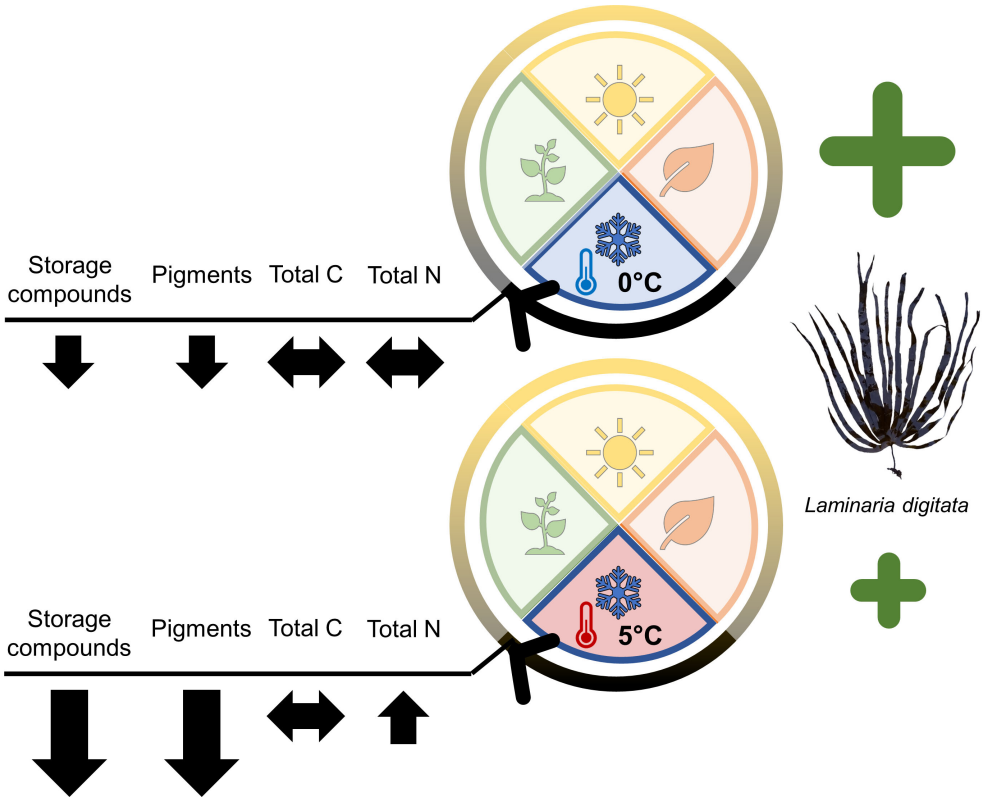

FIGURE 5
Summary of the biochemical acclimation strategies by *Laminaria digitata* sporophytes to Arctic winter warming during three months of Polar Night. Picture of *L. digitata* by D. Liesner.

remobilization of carbon stocks in Laminariales (Gómez and Huovinen, 2012). We kept our samples under realistic Arctic winter nutrient conditions (~14 µmol NO_3^- L^{-1}; Rokkan Iversen and Seuthe, 2011) and observed an increase in Total N over time, with significant increases at 5°C of about 40%. Potentially, a higher metabolic and enzymatic activity at 5°C enabled enhanced N uptake (Harrison and Hurd, 2001). The stable Total C and increased Total N contents led to C:N ratios below 20 towards the end of the experiment, showing that the samples were not N-limited at both temperatures (Atkinson and Smith, 1983).

The pigment content of seaweeds responds to metabolic processes and light availability (Blain and Shears, 2019), while metabolism and enzyme activity are in turn dependent on temperature (Daniel et al., 2008). Polar red algae are known to strongly adjust their pigments concentrations during the seasonal cycle, degrading pigments during long dark exposure (Wiencke et al., 2009). Pigment degradation during extended darkness is not yet confirmed for kelps, e.g., in Arctic *S. latissima* populations (Scheschonk et al., 2019; Gordillo et al., 2022). We observed that all pigments in *L. digitata* tend to deplete over three months in the dark, decreasing more at 5°C than at 0°C. Strongest reductions were measured in the xanthophyll cycle pool (VAZ). Chl*a* remained almost stable and Acc only decreased significantly at 5°C. While Chl*a* is the main photosynthetic pigment and Acc are important antenna pigments, VAZ are not directly involved in the process of photon harvesting, but act as photo-protective pigments (Falkowski and Raven, 2007). Though VAZ content was highly depleted during the experiment, the protective mechanism of the xanthophyll cycle (DPS) was still active and slightly increased over time. DPS increases during stress, such as dehydration or high and low temperatures, and is known to be active in the dark (Fernández-Marín et al., 2019; Li et al., 2020; Monteiro et al., 2021). We assume that the pigments in *L. digitata* were degraded to save energy or function as an additional energy source to outlast the long period of the Polar Night, while still keeping the photosynthetic machinery and photo-protective mechanisms intact, as was shown by Summers et al. (2023). Pigment reduction was enhanced at 5°C compared to 0°C, which aligns with higher physiological activity in *L. digitata* at 5°C.

In summary, our study has shown that the cold–temperate to Arctic kelp *L. digitata* is well adapted to Polar Night conditions in the Arctic. Although it has a lower performance and reveals higher biochemical activity levels at 5°C than at 0°C, our results indicate that Arctic winter warming alone will not result in a serious decline of Arctic *L. digitata* populations in the near future. Nevertheless, interactions between warming and changing light conditions, e.g. due to terrestrial or glacial run-off, have to be considered in studies

on the prospective distribution of *L. digitata* in High Arctic regions (Niedzwiedz and Bischof, 2023; Düsedau et al., 2024).

Data availability statement

All raw data analyzed for this study can be found in the PANGAEA Database: https://doi.org/10.1594/PANGAEA.972789.

Author contributions

MT: Data curation, Formal analysis, Methodology, Visualization, Writing – original draft, Writing – review & editing. IB: Conceptualization, Methodology, Resources, Supervision, Writing – review & editing. MB: Data curation, Methodology, Writing – review & editing. HB: Data curation, Methodology, Writing – review & editing. JH: Methodology, Resources, Writing – review & editing. SN: Data curation, Methodology, Writing – review & editing. NP: Data curation, Methodology, Writing – review & editing. TS: Data curation, Methodology, Writing – review & editing. KB: Funding acquisition, Project administration, Resources, Supervision, Writing – review & editing. ND: Conceptualization, Data curation, Methodology, Supervision, Visualization, Writing – original draft, Writing – review & editing.

Funding

The author(s) declare financial support was received for the research, authorship, and/or publication of this article. This study was conducted in the frame of the project FACE-IT (The Future of Arctic Coastal Ecosystems – Identifying Transitions in Fjord Systems and Adjacent Coastal Areas). FACE-IT has received funding from the European Union's Horizon 2020 research and innovation program under grant agreement No. 869154.

Acknowledgments

The authors are grateful to H-K Strand from the Holmfjorden Research Station of the Norwegian Institute for Marine Research for the sampling support and logistics. ND thanks S Jungblut and M Koch for their support in sample preparation and U Karsten for the opportunity to measure mannitol at the University of Rostock. The experiment has been conducted at the Alfred Wegener Institute for Polar and Marine Research (AWI), Bremerhaven. The authors thank A Wagner (AWI) for his support in the set-up of the experiment, and B Iken (University of Bremen) for supporting the pigment and C:N analyses.

Conflict of interest

The authors declare that the research was conducted in the absence of any commercial or financial relationships that could be construed as a potential conflict of interest.

Publisher's note

Supplementary material

The Supplementary Material for this article can be found online at: https://www.frontiersin.org/articles/10.3389/fmars.2024.1478238/full#supplementary-material

References

Atkinson, M. J., and Smith, S. V. (1983). C:N:P ratios of benthic marine plants. *Limnol. Oceanogr.* 28, 568–574. doi: 10.4319/lo.1983.28.3.0568

Bartsch, I., Paar, M., Fredriksen, S., Schwanitz, M., Daniel, C., Hop, H., et al. (2016). Changes in kelp forest biomass and depth distribution in Kongsfjorden, Svalbard, between 1996–1998 and 2012–2014 reflect Arctic warming. *Polar Biol.* 39, 2021–2036. doi: 10.1007/s00300-015-1870-1

Becker, S., and Hehemann, J.-H. (2018). Laminarin quantification in microalgae with enzymes from marine microbes. *Bio-Protocol* 8, e2666. doi: 10.21769/bioprotoc.2666

Becker, S., Scheffel, A., Polz, M. F., and Hehemann, J. H. (2017). Accurate quantification of laminarin in marine organic matter with enzymes from marine microbes. *Appl. Environ. Microbiol.* 83, 1–14. doi: 10.1128/AEM.03389-16

Bischof, K., Buschbaum, C., Fredriksen, S., Gordillo, F. J. L., Heinrich, S., Jiménez, C., et al. (2019). "Kelps and environmental changes in kongsfjorden: stress perception and responses," in *The Ecosystem of Kongsfjorden*. Eds. H. Hop and C. Wiencke (Springer, Cham), 373–422. doi: 10.1007/978-3-319-46425-1_10

Blain, C. O., and Shears, N. T. (2019). Seasonal and spatial variation in photosynthetic response of the kelp *Ecklonia radiata* across a turbidity gradient. *Photosynth. Res.* 140, 21–38. doi: 10.1007/s11120-019-00636-7

Blanca, M. J., Alarcón, R., Arnau, J., Bono, R., and Bendayan, R. (2017). Datos no normales: ¿es el ANOVA una opción válida? *Psicothema* 29, 552–557. doi: 10.7334/psicothema2016.383

Bolton, J. J., and Lüning, K. (1982). Optimal growth and maximal survival temperatures of Atlantic *Laminaria* species (Phaeophyta) in culture. *Mar. Biol.* 66, 89–94. doi: 10.1007/BF00397259

Castro de la Guardia, L., Filbee-Dexter, K., Reimer, J., MacGregor, K. A., Garrido, I., Singh, R. K., et al. (2023). Increasing depth distribution of Arctic kelp with increasing number of open water days with light. *Elem. Sci. Anthr.* 11, 51. doi: 10.1525/elementa.2022.00051

Colombo-Pallotta, M. F., García-Mendoza, E., and Ladah, L. B. (2006). Photosynthetic performance, light absorption, and pigment composition of *Macrocystis pyrifera* (Laminariales, Phaeophyceae) blade from different depths. *J. Phycol.* 42, 1225–1234. doi: 10.1111/j.1529-8817.2006.00287.x

Daniel, R. M., Danson, M. J., Eisenthal, R., Lee, C. K., and Peterson, M. E. (2008). The effect of temperature on enzyme activity: New insights and their implications. *Extremophiles* 12, 51–59. doi: 10.1007/s00792-007-0089-7

Dankworth, M., Heinrich, S., Fredriksen, S., and Bartsch, I. (2020). DNA barcoding and mucilage ducts in the stipe reveal the presence of *Hedophyllum nigripes* (Laminariales, Phaeophyceae) in Kongsfjorden (Spitsbergen). *J. Phycol.* 56, 1245–1254. doi: 10.1111/jpy.13012

Diehl, N., Karsten, U., and Bischof, K. (2020). Impacts of combined temperature and salinity stress on the endemic Arctic brown seaweed *Laminaria solidungula* J. Agardh. *Polar Biol.* 43, 647–656. doi: 10.1007/s00300-020-02668-5

Diehl, N., Laeseke, P., Bartsch, I., Bligh, M., Buck-Wiese, H., Hehemann, J.-H., et al. (2024). Photoperiod and temperature interactions drive the latitudinal distribution of kelps under climate change. *J. Phycol.* 00, 1–19. doi: 10.1111/jpy.13497

Dring, M. J. (2006). Stress resistance and disease resistance in seaweeds: the role of reactive oxygen metabolism. *Adv. Bot. Res.* 43, 175–207. doi: 10.1016/S0065-2296(05)43004-9

Dring, M. J., Makarov, V., SchosChina, E., Lorenz, M., and Lüning, K. (1996). Influence of ultraviolet-radiation on chlorophyll fluorescence and growth in different life-history stages of three species of *Laminaria* (Phaeophyta). *Mar. Biol.* 126, 183–191. doi: 10.1007/BF00347443

Düsedau, L., Fredriksen, S., Brand, M., Fischer, P., Karsten, U., Bischof, K., et al. (2024). Kelp forest community structure and demography in Kongsfjorden (Svalbard) across 25 years of Arctic warming. *Ecol. Evol.* 14, e11606. doi: 10.1002/ece3.11606

Falkowski, P. G., and Raven, J. A. (2007). *Aquatic Photosynthesis. 2nd ed* (Princeton and Oxford: Princeton University Press).

Fernández-Marín, B., Gago, J., Clemente-Moreno, M. J., Flexas, J., Gulías, J., and García-Plazaola, J. I. (2019). Plant pigment cycles in the high-Arctic Spitsbergen. *Polar Biol.* 42, 675–684. doi: 10.1007/s00300-019-02463-x

Fernández-Marín, B., Míguez, F., Becerril, J. M., and García-Plazaola, J. I. (2011). Activation of violaxanthin cycle in darkness is a common response to different abiotic stresses: A case study in Pelvetia canaliculata. *BMC Plant Biol.* 11, 181. doi: 10.1186/1471-2229-11-181

Gattuso, J. P., Gentili, B., Antoine, D., and Doxaran, D. (2020). Global distribution of photosynthetically available radiation on the seafloor. *Earth Syst. Sci. Data* 12, 1697–1709. doi: 10.5194/essd-12-1697-2020

Gauci, C., Bartsch, I., Martins, N., and Liesner, D. (2022). Cold thermal priming of *Laminaria digitata* (Laminariales, Phaeophyceae) gametophytes enhances gametogenesis and thermal performance of sporophytes. *Front. Mar. Sci.* 9. doi: 10.3389/fmars.2022.862923

Gómez, I., and Huovinen, P. (2012). "Morpho-functionality of carbon metabolism in seaweeds," in *Seaweed Biology: Novel Insights into Ecophysiology, Ecology and Utilization*. Eds. C. Wiencke and K. Bischof (Berlin Heidelberg: Springer), 25–46.

Gordillo, F. J. L., Carmona, R., and Jiménez, C. (2022). A warmer Arctic compromises winter survival of habitat-forming seaweeds. *Front. Mar. Sci.* 8. doi: 10.3389/fmars.2021.750209

Graiff, A., Bartsch, I., Ruth, W., Wahl, M., and Karsten, U. (2015). Season exerts differential effects of ocean acidification and warming on growth and carbon metabolism of the seaweed *Fucus vesiculosus* in the western Baltic Sea. *Front. Mar. Sci.* 2. doi: 10.3389/fmars.2015.00112

Harrison, P. J., and Hurd, C. L. (2001). Nutrient physiology of seaweeds: Application of concepts to aquaculture. *Cah. Biol. Mar.* 42, 71–82. doi: 10.1080/00318884.2019.1622920

Huang, B., Liu, C., Banzon, V., Freeman, E., Graham, G., Hankins, B., et al. (2021). Improvements of the daily optimum interpolation sea surface temperature (DOISST) version 2.1. *J. Clim.* 34, 2923–2939. doi: 10.1175/JCLI-D-20-0166.1

Hurd, C. L., Harrison, P. J., Bischof, K., and Lobban, C. S. (2014). *Seaweed Ecology and Physiology. 2nd ed.* (Cambridge: Cambridge University Press).

Johnston, C. S., Jones, R. G., and Hunt, R. D. (1977). A seasonal carbon budget for a laminarian population in a Scottish sea-loch. *Helgoländer wissenschaftliche Meeresuntersuchungen* 30, 527–545. doi: 10.1007/BF02207859

Karsten, U., Thomas, D. N., Weykam, G., Daniel, C., and Kirst, G. O. (1991). A simple and rapid method for extraction and separation of low molecular weight carbohydrates from macroalgae using high-performance liquid chromatography, II. Intracellular inorganic ions and organic compounds. *Plant Physiol. Biochem.* 29, 373–378. Available online at: https://epic.awi.de/id/eprint/1579/.

Koch, K., Thiel, M., Tellier, F., Hagen, W., Graeve, M., Tala, F., et al. (2015). Species separation within the *Lessonia nigrescens* complex (Phaeophyceae, Laminariales) is mirrored by ecophysiological traits. *Bot. Mar.* 58, 81–92. doi: 10.1515/bot-2014-0086

Krause-Jensen, D., Archambault, P., Assis, J., Bartsch, I., Bischof, K., Filbee-Dexter, K., et al. (2020). Imprint of climate change on Pan-Arctic marine vegetation. *Front. Mar. Sci.* 7. doi: 10.3389/fmars.2020.617324

Küppers, U., and Kremer, B. P. (1978). Longitudinal profiles of carbon dioxide fixation capacities in marine macroalgae. *Plant Physiol.* 62, 49–53. doi: 10.1104/pp.62.1.49

Lever, M. (1972). A new reaction for colorimetric determination of carbohydrates. *Anal. Biochem.* 47, 273–279. doi: 10.1016/0003-2697(72)90301-6

Li, H., Monteiro, C., Heinrich, S., Bartsch, I., Valentin, K., Harms, L., et al. (2020). Responses of the kelp *Saccharina latissima* (Phaeophyceae) to the warming Arctic: From physiology to transcriptomics. *Physiol. Plant* 168, 5–26. doi: 10.1111/ppl.13009

Liesner, D., Shama, L. N. S., Diehl, N., Valentin, K., and Bartsch, I. (2020). Thermal plasticity of the kelp *Laminaria digitata* (Phaeophyceae) across life cycle stages reveals the importance of cold seasons for marine forests. *Front. Mar. Sci.* 7. doi: 10.3389/fmars.2020.00456

Longtin, C. M., and Saunders, G. W. (2015). On the utility of mucilage ducts as a taxonomic character in *Laminaria* and *Saccharina* (Phaeophyceae) - The conundrum of *S. groenlandica*. *Phycologia* 54, 440–450. doi: 10.2216/15-19.1

Lüning, K. (1990). *Seaweeds - Their environment, biogeography, and ecophysiology*. Eds. C. Yarish and H. Kirkman (Stuttgart: John Wiley & Sons, Inc).

Maturilli, M., Hanssen-Bauer, I., Neuber, R., Rex, M., and Edvardsen, K. (2019). "The atmosphere above Ny-Ålesund: Climate and global warming, ozone and surface UV radiation," in *The ecosystem of Kongsfjorden, Svalbard*. Eds. H. Hop and C. Wiencke (Springer Nature Switzerland AG, Cham).

Mauger, S., Fouqueau, L., Avia, K., Reynes, L., Serrao, E. A., Neiva, J., et al. (2021). Development of tools to rapidly identify cryptic species and characterize their genetic diversity in different European kelp species. *J. Appl. Phycol.* 33, 4169–4186. doi: 10.1007/s10811-021-02613-x

Monteiro, C., Li, H., Diehl, N., Collén, J., Heinrich, S., Bischof, K., et al. (2021). Modulation of physiological performance by temperature and salinity in the sugar kelp Saccharina latissima. *Phycol. Res.* 69, 48–57. doi: 10.1111/pre.12443

Niedzwiedz, S., and Bischof, K. (2023). Glacial retreat and rising temperatures are limiting the expansion of temperate kelp species in the future Arctic. *Limnol. Oceanogr.* 68, 816–830. doi: 10.1002/lno.12312

Pörtner, H., Lucassen, M., and Storch, D. (2005). Metabolic biochemistry: Its role in thermal tolerance and in the capacities of physiological and ecological gunction. *Fish Physiol.* 22, 79–154. doi: 10.1016/S1546-5098(04)22003-9

Previdi, M., Smith, K. L., and Polvani, L. M. (2021). Arctic amplification of climate change: A review of underlying mechanisms. *Environ. Res. Lett.* 16, 093003. doi: 10.1088/1748-9326/ac1c29

Rantanen, M., Karpechko, A. Y., Lipponen, A., Nordling, K., Hyvärinen, O., Ruosteenoja, K., et al. (2022). The Arctic has warmed nearly four times faster than the globe since 1979. *Commun. Earth Environ.* 3, 168. doi: 10.1038/s43247-022-00498-3

R Core Team, R. (2022). *R: A language and environment for statistical computing*. (Vienna, Austria: R Foundation for Statistical Computing).

Richter-Menge, J., Overland, J. E., Mathis, J. T., and Osborne, E. E. (2017). *Arctic report card 2017*. Available online at: www.arctic.noaa.gov/Report-Card (Accessed December, 2023).

Rokkan Iversen, K., and Seuthe, L. (2011). Seasonal microbial processes in a high-latitude fjord (Kongsfjorden, Svalbard): I. Heterotrophic bacteria, picoplankton and nanoflagellates. *Polar Biol.* 34, 731–749. doi: 10.1007/s00300-010-0929-2

Scheschonk, L., Becker, S., Hehemann, J.-H., Diehl, N., Karsten, U., and Bischof, K. (2019). Arctic kelp eco-physiology during the polar night in the face of global warming: A crucial role for laminarin. *Mar. Ecol. Prog. Ser.* 611, 59–74. doi: 10.3354/meps12860

Schlegel, R. W., Singh, R. K., Gentili, B., Bélanger, S., Castro de la Guardia, L., Krause-Jensen, D., et al. (2024). Underwater light environment in Arctic fjords. *Earth Syst. Sci. Data* 16, 2773–2788. doi: 10.5194/essd-16-2773-2024

Singh, A., Pal, B., and Singh, K. S. (2024). Carbohydrate and pigment composition of macroalgae in a kelp-dominated Arctic fjord. *Reg. Stud. Mar. Sci.* 77, 103644. doi: 10.1016/j.rsma.2024.103644

Smale, D. A., Wernberg, T., Oliver, E. C. J., Thomsen, M., Harvey, B. P., Straub, S. C., et al. (2019). Marine heatwaves threaten global biodiversity and the provision of ecosystem services. *Nat. Clim. Change* 9, 306–312. doi: 10.1038/s41558-019-0412-1

Steneck, R. S., Graham, M. H., Bourque, B. J., Corbett, D., Erlandson, J. M., Estes, J. A., et al. (2002). Kelp forest ecosystems: Biodiversity, stability, resilience and future. *Environ. Conserv.* 29, 436–459. doi: 10.1017/S0376892902000322

Summers, N., Fragoso, G. M., and Johnsen, G. (2023). Photophysiologically active green, red, and brown macroalgae living in the Arctic Polar Night. *Sci. Rep.* 13, 17971. doi: 10.1038/s41598-023-44026-5

tom Dieck (Bartsch), I. (1992). North Pacific and North Atlantic digitate *Laminaria* species (Phaeophyta): hybridization experiments and temperature responses. *Phycologia* 31, 147–163. doi: 10.2216/i0031-8884-31-2-147.1

Verardo, D. J., Froelich, P. N., and McIntyre, A. (1990). Determination of organic carbon and nitrogen in marine sediments using the Carlo Erba NA-1500 Analyzer. *Deep. Res.* 37, 157–165. doi: 10.1016/0198-0149(90)90034-S

Vihtakari, M. (2024). ggOceanMaps: Plot Data on Oceanographic Maps using 'ggplot2'. *R package version 2.2.0*. Available online at: https://CRAN.R-project.org/package=ggOceanMaps.

Wang, Y., Huang, F., and Fan, T. (2017). Spatio-temporal variations of Arctic amplification and their linkage with the Arctic oscillation. *Acta Oceanol. Sin.* 36, 42–51. doi: 10.1007/s13131-017-1025-z

Wernberg, T., Krumhansl, K., Filbee-Dexter, K., and Pedersen, M. F. (2019). "Status and trends for the world's kelp forests," in *World Seas: An environmental evaluation* (Cambridge, Massachusetts: Academic Press), 57–78. doi: 10.1016/b978-0-12-805052-1.00003-6

Wiencke, C., and Bischof, K. (2012). *Seaweed Biology - Novel insights into ecophysiology, ecology and utilization* (Heidelberg New York Dodrecht London: Springer).

Wiencke, C., Gómez, I., and Dunton, K. (2009). Phenology and seasonal physiological performance of polar seaweeds. *Bot. Mar.* 52, 585–592. doi: 10.1515/BOT.2009.078

Wright, S. W., Jeffrey, S. W., Mantoura, R. F. C., Llewelly, C. A., Bjørnland, T., Repeta, D., et al. (1991). Improved HPLC method for the analysis of chlorophylls and carotenoids from marine phytoplankton. *Mar. Ecol. Prog. Ser.* 77, 183–196. doi: 10.3354/meps077183

Yamaguchi, T., Ikawa, T., and Nisizawa, K. (1966). Incorporation of radioactive carbon from $H^{14}CO_3$- into sugar constituents by a brown alga, *Eisenia bicyclis*, during photosynthesis and its fate in the dark. *Plant Cell Physiol.* 7, 217–229. doi: 10.1093/oxfordjournals.pcp.a079175

Zacher, K., Rautenberger, R., Hanelt, D., Wulff, A., and Wiencke, C. (2009). The abiotic environment of polar marine benthic algae. *Bot. Mar.* 52, 483–490. doi: 10.1515/BOT.2009.082

Zuur, A. F., Hilbe, J., and Ieno, E. N. (2013). *A Beginner's Guide to GLM and GLMM with R: A frequentist and Bayesian perspective for ecologists* (Newburgh, United Kingdom: Highland Statistics Ltd).

frontiers | Frontiers in Marine Science

TYPE Opinion
PUBLISHED 15 January 2025
DOI 10.3389/fmars.2025.1526933

OPEN ACCESS

EDITED BY
Caitlin Blain,
The University of Auckland, New Zealand

REVIEWED BY
Hongtian Luo,
Hainan University, China
Lara Elisabeth Stuthmann,
Leibniz Centre for Tropical Marine Research (LG), Germany

*CORRESPONDENCE
Jinlin Liu
jlliu@tongji.edu.cn
Wei Liu
hsliuwei@shu.edu.cn
Jing Xia
xiajingsherry@sjtu.edu.cn

RECEIVED 12 November 2024
ACCEPTED 02 January 2025
PUBLISHED 15 January 2025

CITATION
Liu J, Liu W and Xia J (2025) Perplexity and choice: challenges and future development of laver cultivation in Jiangsu Province, China. *Front. Mar. Sci.* 12:1526933. doi: 10.3389/fmars.2025.1526933

Perplexity and choice: challenges and future development of laver cultivation in Jiangsu Province, China

Jinlin Liu[1,2]*, Wei Liu[3,4]* and Jing Xia[5]*

[1]State Key Laboratory of Marine Geology, Tongji University, Shanghai, China, [2]Project Management Office of China National Scientific Seafloor Observatory, Tongji University, Shanghai, China, [3]School of Environmental and Chemical Engineering, Shanghai University, Shanghai, China, [4]Department of Agriculture and Biotechnology, Wenzhou Vocational College of Science and Technology, Wenzhou, China, [5]School of Oceanography, Shanghai Jiao Tong University, Shanghai, China

KEYWORDS

seaweed cultivation, *Neopyropia yezoensis*, climate change, bio-disaster, sustainable development strategy

1 Introduction

Seaweed cultivation holds significant importance in addressing global challenges. On the one hand, it aids in alleviating the food crisis. On the other hand, it offers substantial ecological benefits, such as enhancing carbon sequestration, facilitating nitrogen cycling, and mitigating eutrophication (He et al., 2008; Wu et al., 2015; Mantri et al., 2023). Globally, the dominant cultivated economic seaweeds include *Laminaria* spp., *Kappaphycus* spp., *Gracilaria* spp., *Neopyropia* spp., and *Undaria* spp (Park et al., 2021; Khan et al., 2024). In 2022, the annual global production of seaweed is estimated to be approximately 36.4 million metric tons (live weight), with red algae accounting for about 55.8% and brown algae for approximately 43.8% (FAO, 2024). Asia constitutes the principal region for seaweed cultivation, representing over 97% of global production, with China (about 60%), Indonesia (about 25%), South Korea (about 5%), and the Philippines (about 4%) being the largest contributors to this industry (Khan et al., 2024; Liu et al., 2024).

Among them, the *Neopyropia* species, a type of high-end red algae, is highly favored among consumers (Li et al., 2023) and possesses rich edible and medicinal values (Subramaniyan et al., 2021; Zhao et al., 2023; Wu et al., 2024). It is frequently utilized for the production of foods such as laver sushi and laver pancakes. Consequently, the significance of laver cultivation is self-evident. China boasts the world's largest laver cultivation area, with total production reaching 209,939 metric tons (dry weight) in 2023 (Fishery Administration Bureau of Ministry of Agriculture and Rural Affairs et al., 2024). The main cultivated laver species include *Neopyropia haitanensis*, *Neopyropia yezoensis*, *Neopyropia acanthophora*, and *Neopyropia dentata* (Wang et al., 2020; Wu et al., 2024). Notably, Jiangsu Province, China, serves as the leading production area for the highly sought-after *N. yezoensis* (Figure 1).

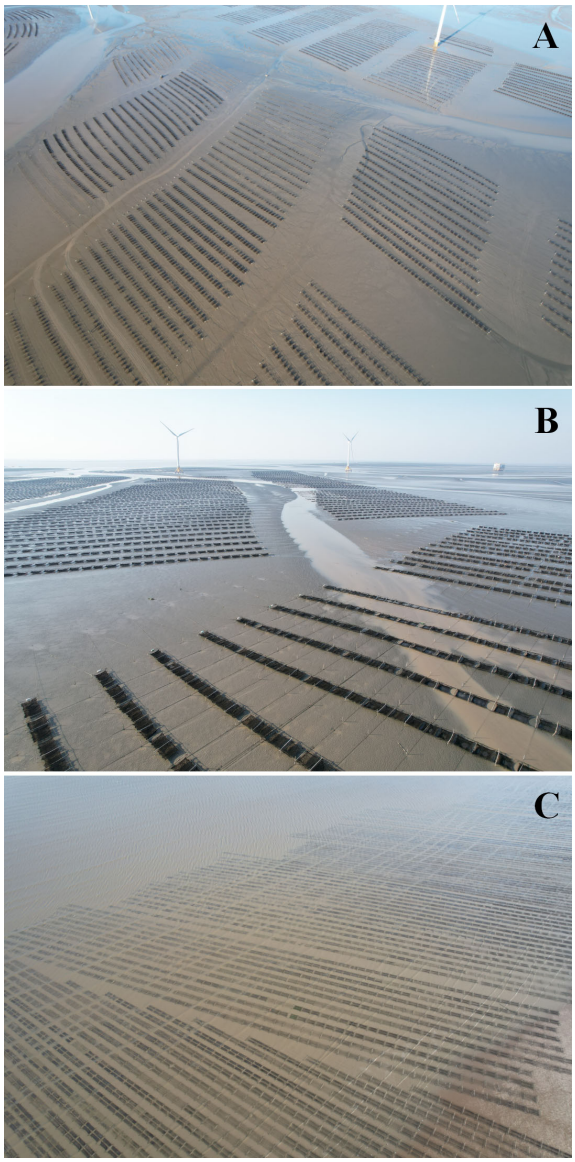

FIGURE 1
Laver cultivation areas in the coastal seawaters of Nantong **(A)**, Yancheng **(B)**, and Lianyungang **(C)** cities in Jiangsu Province.

The *N. yezoensis* aquaculture industry in the Subei intertidal zone of Jiangsu Province originated in the 1970s of the 20th century (Liu et al., 2021a). After more than 50 years of development, the intertidal zone in Jiangsu Province has become the largest global *N. yezoensis* aquaculture area, leading both nationally and globally. For instance, in 2023, the area of laver cultivation in Jiangsu Province reached 33,393 hectares, approximately 51.81% of the total national laver cultivation area. During the same year, the production of laver in Jiangsu Province reached 35,936 metric tons (dry weight), accounting for about 17.12% of the total national laver production (Fishery Administration Bureau of Ministry of Agriculture and Rural Affairs et al., 2024). The industry is of considerable scale and has comprehensively enhanced the coastal economic development and industrial reputation of Jiangsu Province. Furthermore, many impoverished individuals have achieved poverty alleviation and wealth accumulation through seaweed cultivation (Li et al., 2011).

Nevertheless, the laver cultivation industry in Jiangsu Province is progressively encountering certain challenges, such as extreme marine events and disasters. This opinion article aims to identify the key factors affecting laver cultivation in Jiangsu Province and proposes recommendations for its sustainable development.

2 The principal elements influencing the development of laver cultivation in Jiangsu Province

2.1 Climate change

For the growth stages of seaweed, extreme climate changes can lead to cellular and subcellular damage in the thalli, ultimately

affecting its growth, quality, and yield (Khan et al., 2024). Currently, the negative impact of climate change on seaweed aquaculture is a long-term and widespread issue encountered in global aquaculture processes (Veenhof et al., 2024), which is difficult to resolve effectively in the short term. Over the past six decades, the sea surface temperature in the Southern Yellow Sea (SYS) has generally shown an increasing trend, with a warming amplitude of approximately 0.61°C. This indicates that under the backdrop of global warming, the SYS region has exhibited a warming trend (Guo et al., 2024). Concurrently, the interannual and multidecadal variability of sea surface temperature in the SYS is also associated with large-scale climatic factors such as El Niño-Southern Oscillation (ENSO) and Pacific Decadal Oscillation (PDO) (Wang and Yu, 2014), leading to anomalous warming of regional seawater temperatures in certain years. Elevated seawater temperatures indirectly promote the frequent occurrence of diseases and other factors that hinder the growth of *N. yezoensis*. Currently, climate warming is leading to frequent occurrences of seedling rot, slow growth, and significant reductions in yield during the cultivation of *Neopyropia*, resulting in economic losses for the laver cultivation industry in the SYS region in recent years (Figure 2A). For instance, from late 2016 to mid-2017, influenced by factors such as abnormally high temperatures in the Haizhou Bay area, the production of *N. yezoensis* in Lianyun District, Lianyungang City, Jiangsu Province, was severely reduced, with a decrease of about 60% compared to the previous year (Lianyun District People's Government, 2017).

Extreme weather events triggered by climate change also warrant attention. At the end of April 2021, an infrequent event featuring extreme winds and thunderstorms occurred in the Subei intertidal zone of the SYS, with wind gusts reaching level 14. This event resulted in direct economic losses exceeding 140 million RMB Yuan in Nantong City, Jiangsu Province (Lu and Du, 2022), and the large-scale collapse of *Neopyropia* cultivation rafts (Lu and Du, 2022). Tens of thousands of raft components, including ropes and bamboo poles (Figure 2B), are being swept into the ocean (Sun et al., 2022a), causing economic losses to laver farmers. It affected the smooth progress of the *Neopyropia* raft recovery operations, and in addition, caused casualties, either directly or indirectly (CCTV, 2021). Similarly, in January 2016, Lianyungang City, Jiangsu Province experienced severe sea ice and strong winds caused by extremely cold weather. This affected over 7,000 hectares of *N. yezoensis* cultivation area, leading to incalculable economic losses for local farmers (Sohu, 2016).

In addition, rising global CO_2 concentrations contribute to ocean acidification, which can impact interspecific competition among seaweeds (Feng et al., 2024). Although the elevated CO_2 levels alleviate the competitive relationship between *N. yezoensis* and the harmful epiphyte *Ulva* species (e.g., *Ulva prolifera*), the long-term perspective indicates a growing competitive advantage for *Ulva* under this climate change scenario (Sun et al., 2021). Traditionally, *N. yezoensis* is considered a cold-tolerant seaweed, whereas *U. prolifera* exhibits a greater capacity to endure higher temperatures compared to *N. yezoensis*. Micropropagules of *U. prolifera* are persistently present in the SYS region (Cao et al., 2023; Xia et al., 2024a), and the areas on the raft components not colonized by laver are also conducive to the attachment of *U. prolifera*, leading to the subsequent occupation of ecological niches by *U. prolifera* on the raft structures (Zhang et al., 2019a). Concurrently, as *U. prolifera* matures, it demonstrates a stronger ability to absorb nutrients than *N. yezoensis*, thereby allowing the epiphytically growing *U. prolifera* to gradually establish a growth advantage (Shan, 2022). This results in *Ulva* species with an enhanced capability to occupy ecological niches, which subsequently impacts the normal growth of laver and affects the future development of *Neopyropia* aquaculture in the SYS region.

2.2 Diseases

Neopyropia yezoensis is susceptible to various diseases during cultivation and growth due to the impact of global climate change, harmful microbial infection, and overcrowding during cultivation (Kim et al., 2014). Common diseases include seedling rot, chytrid blight, green spot disease, and white rot (Qiu et al., 2019; Yang et al., 2020; Bae et al., 2024), which frequently lead to the genetic characterization decline of laver populations. In addition, the coastal waters of Jiangsu Province are severely eutrophic (Liu et al., 2013), and heavily polluted sea areas are particularly prone to harmful pathogens proliferation. These pathogens negatively impact seaweed growth, ultimately reducing laver yield and causing significant economic losses for local farmers. For instance, in 2004, approximately 5,000 hectares of *N. yezoensis* in the Nantong City maritime area suffered from severe rot, resulting in an estimated loss of 60 million RMB Yuan (Yangtze Evening Post, 2004). Similarly, in 2016, over 1,300 hectares of *N. yezoensis* in the Rudong County maritime area of Nantong City experienced rot, with cost losses alone amounting to around 40 million RMB Yuan, causing economic losses to more than 3,000 laver farmers (Wang, 2016). In January 2019, 134 hectares of *N. yezoensis* in the Yancheng City maritime area exhibited rot, which was caused by the pathogenic bacterium *Opliidopsis* sp (He et al., 2021).

It should be clarified that seaweed cultivation inevitably faces diseases to varying degrees (Khan et al., 2024). These diseases encountered during laver cultivation are not unique to China but represent a global issue (Yang et al., 2020). For example, between 2013 and 2014, an outbreak of green spot disease in the laver farms in Sunchon, South Korea, could cause complete rot of laver thalli within 1-2 days, resulting in a loss of 1.1 million USD, equivalent to 10.7% of total farm sales (Kim et al., 2014). The sudden onset of such diseases during *N. yezoensis* cultivation often prevents timely and effective mitigation measures to reduce disease damage, ultimately leading to substantial losses for laver farmers.

2.3 High-density cultivation

Neopyropia yezoensis cultivation demands high-quality seawater and thrives best in waters with moderate flow velocity and strong water exchange capacity (He et al., 2018). In Jiangsu Province, suitable cultivation areas have been largely exploited, limiting the potential for further expansion of the cultivation scale.

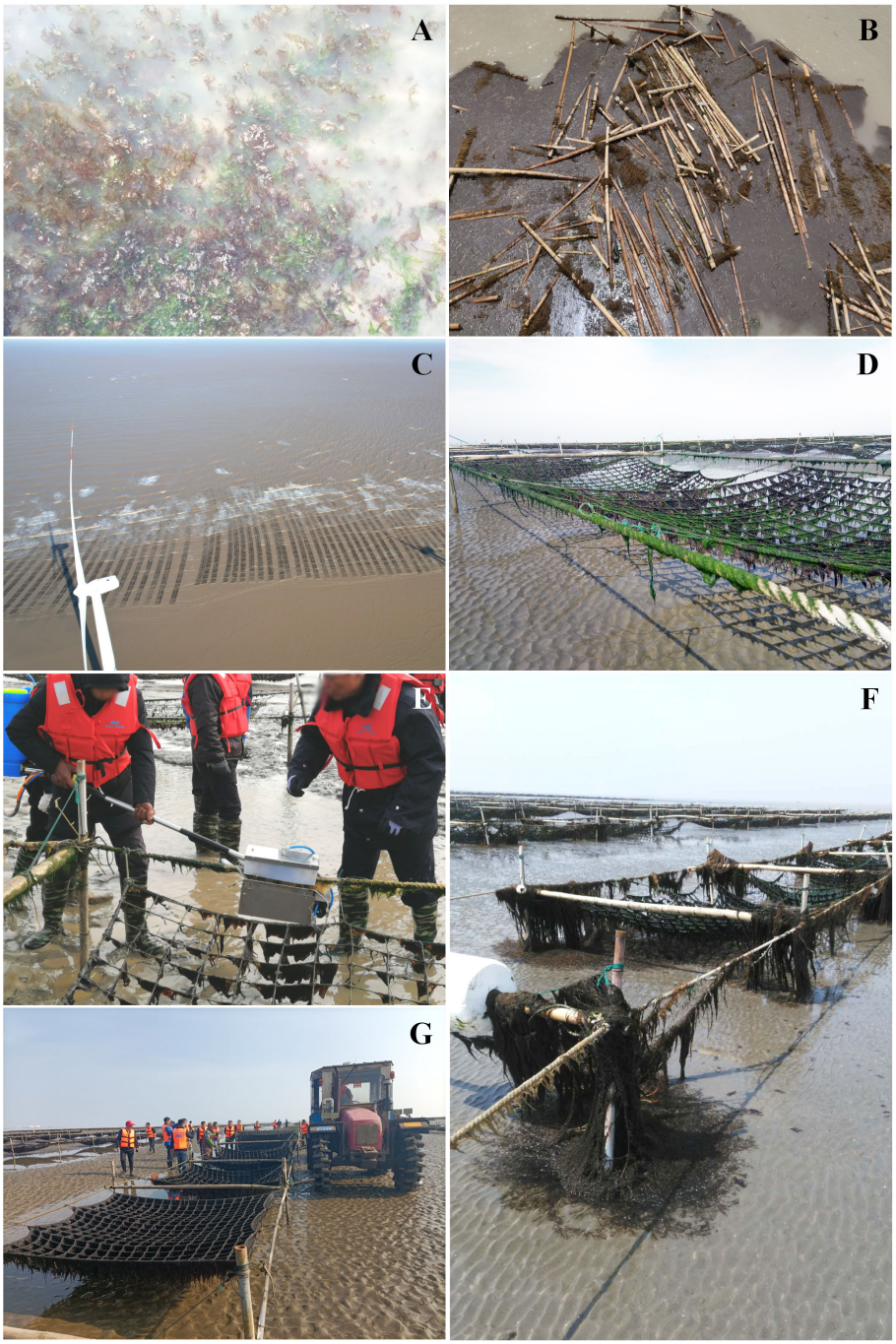

FIGURE 2
Death and detachment of *Neopyropia yezoensis* (indicated by brownish-red areas) on laver cultivation nets due to unusually high temperatures, along with *Ulva* species (green areas) remaining on the tidal flats after manual cleanup **(A)**; Damage to laver cultivation facilities caused by extreme wind events, leading to the drift of some raft components into open waters **(B)**; A laver cultivation area in Binhai County, Yancheng City, Jiangsu Province, which did not comply with the maritime usage standards, has subsequently been banned by the government **(C)**; *Ulva* species, which appear as green areas, are epiphytic on laver cultivation rafts **(D)**; Laver farmers are removing the green seaweed tide that is attached to the ropes **(E)**; The accumulation of invasive golden seaweed tide on laver cultivation rafts is damaging the raft facilities and affecting the normal growth of *N. yezoensis* **(F)**; Laver farmers in the coastal waters of Nantong City, Jiangsu Province, are beginning to experiment with the cultivation of *Neopyropia haitanensis* **(G)**.

Similarly, *N. yezoensis* struggles to grow in low-nutrient sea areas (Huang et al., 2023). Although the high levels of nitrogen and phosphorus in Jiangsu's coastal waters support the growth of *Neopyropia*, the extensive cultivation area and high cultivation density inevitably restrict growth due to the limited carrying capacity of the sea area (Shan, 2022). Taking the outer radial sandbars of Dafeng District in Yancheng City as an example, the laver cultivation scale once spanned a continuous distribution of

13,000 hectares. However, the excessive scale of cultivation adversely affected seawater exchange within the cultivation area (Shan, 2022). As a result, laver in the center parts of the cultivation zone could not receive sufficient nutrient replenishment, leading to deficiencies essential for growth (Shan, 2022). Additionally, the close proximity of cultivation facilities also facilitates the rapid spread of diseases, further reducing laver yields (Shan, 2022).

Concurrently, some marine areas in Jiangsu Province have been engaged in aquaculture activities that do not comply with regulations established by the Chinese government (Figure 2C). This noncompliance has exacerbated the scope and cultivation density of laver cultivation activities, creating additional challenges. Lin et al. (2021) identified two special utilization zones and six port shipping areas in Jiangsu Province where unreasonable or illegal laver cultivation activities occurred. These activities involved a total of 135.84 hectares, primarily concentrated in locations such as Tianwan Nuclear Power Plant Special Utilization Zone, Ganyu Port Special Utilization Zone, Shiqiao Port Shipping Area, Xuwei Port Shipping Area, Ganyu Port Shipping Area, Lvsi Port Shipping Area, Xiaomiao Hong Port Shipping Area, and Jinniu Port Shipping Area (Lin et al., 2021).

2.4 Impacts of green tides disaster

Green seaweed blooms have persisted in the SYS for eighteen consecutive years (Zhang et al., 2019b; Xia et al., 2024b), predominantly caused by *U. prolifera*, which has led to significant adverse effects on marine aquaculture and related fisheries industries (Cao et al., 2023; Yao et al., 2024). On the one hand, the attachment of various *Ulva* species to laver cultivation facilities (Han et al., 2013; Huo et al., 2015) competes with *Neopyropia* for ecological niches and nutrients (Figure 2D), thereby impeding laver growth. On the other hand, removing attached green seaweeds during production incurs substantial labor costs for laver farmers (Sun et al., 2022a). Notably, the outbreak of large-scale green tide disasters near laver cultivation areas is rarely observed globally, with no similar reports from other countries or regions' laver cultivation areas.

To effectively mitigate the scale of green tide outbreaks, the Ministry of Natural Resources of the People's Republic of China is currently focusing on reducing the biomass of *U. prolifera* attached to laver cultivation rafts in Jiangsu Province (Liu et al., 2021b; Xia et al., 2022; He et al., 2023; Sun et al., 2022b), and has taken measures to curb illegal occupation of marine areas for seaweed cultivation (Jiangsu Laver Association, 2020). Additionally, laver farmers are encouraged to proactively adjust their raft cultivation schedules, including withdrawing facilities in advance during the production cycle and conducting early cleanup of green seaweeds (Figure 2E). These measures are aimed at maximizing ecological benefits (Sun et al., 2022a). However, these actions also impacted seaweed yields in Jiangsu Province, posing challenges to the long-term formation of a "common interest group" that balances fishery production and green tide control. For instance, in 2021, Jiangsu Province collectively retired approximately 4,000 hectares of laver cultivation and reduced the area of sea used for laver cultivation by about 6,400 hectares. By May 8, 2021, all laver cultivation facilities were brought ashore, prematurely ending the laver production period spanned the late 2020 to mid-2021. This adjustment resulted in a revenue reduction of 1-1.2 billion RMB Yuan for the province's laver cultivation industry (Diao and Ma, 2021) and led to widespread dissatisfaction among regional laver farmers about the potential economic impacts of green tide disaster management. Furthermore, since 2023, the funds allocated for green tide disaster prevention have nearly approached the actual direct economic benefits of laver cultivation in Jiangsu Province. Taking 2024 as a case in point, the annual investment in green tide prevention special funds (including both central and local government financial allocations) has exceeded one billion RMB Yuan, underscoring the financial burden of addressing this ecological challenge.

2.5 Impacts of golden tides disaster

The phenomenon of golden tide disasters impacting the laver cultivation industry is currently observed only in the marine regions of Jiangsu Province. The proliferation of *Sargassum horneri*, the primary species responsible for golden tides, has posed significant challenges to laver cultivation activities in Jiangsu Province in recent years. Since 2016, large-scale gatherings of drifting *S. horneri* have been frequently observed in the coastal waters off Jiangsu during winter and spring (Wang et al., 2023). The arrival of the golden tide "algal mat" in the laver raft cultivation area (Figure 2F) led to the structural collapse of some rafts (Zhuang et al., 2020). Moreover, golden tide seaweed entangled in the laver cultivation nets hinders *Neopyropia* from conducting photosynthesis effectively, leading to damage during its growth stage. To address this issue, laver farmers are compelled to manually remove *S. horneri* tangled around the rafts, which not only increases labor costs but also causes the detachment of *Neopyropia* during this process. Such disruptions often result in significant financial losses, amounting to hundreds of millions of RMB Yuan for local laver farmers (Liu et al., 2021c). For instance, from the winter of 2016 to the spring of 2017, the golden tide disaster severely impacted the laver cultivation industry in Jiangsu Province, causing economic losses of up to 500 million RMB Yuan in the laver cultivation industries of Yancheng and Nantong cities (Liu et al., 2018). Currently, there is no effective method to mitigate the golden tide macroalgal biomass at their source, as the origin of recent golden tide outbreaks in China remains unclear (Wang et al., 2024). Therefore, when laver cultivation activities are affected by golden tide disasters, manual clearance remains the only viable approach to minimize economic losses.

3 Optional strategies for the sustainable development of laver cultivation in Jiangsu Province

3.1 Cultivating heat-resistant laver varieties

Given the current climate warming trend, effective alleviation measures are challenging (Liu et al., 2021b). In areas where *N.*

yezoensis is no longer suitable for growth, it could be worthwhile to gradually attempt the cultivation of heat-resistant strains, such as *N. haitanensis* (Zhou et al., 2023), which can contribute to the sustainable development of the laver cultivation industry in Jiangsu Province. Following the successful pilot cultivation of *N. haitanensis* in the SYS (Figure 2G), some laver farmers have opted to cease the cultivation of *N. yezoensis* in favor of *N. haitanensis*, while others have initiated experiments in the rotation planting of *N. yezoensis* and *N. haitanensis*. Taking 2024 as an example, Lianyun District People's Government of Lianyungang City has encouraged laver farmers to engage in the rotational cultivation of *N. haitanensis* and *N. yezoensis* (Liandao Subdistrict, 2024). Laver farmers in Liandao Subdistrict have collectively piloted the cultivation of *N. haitanensis* over an area of approximately 800 hectares, achieving a bountiful harvest in October 2024, with an estimated annual yield of 15 tons per hectare (live weight), resulting in an annual output value of up to 130 million RMB Yuan (Liandao Subdistrict, 2024). At present, the Jiangsu Provincial Government's promotion of the pilot rotational planting and cultivation scheme for *N. yezoensis* and *N. haitanensis* has achieved initial success and is deemed worthy of further promotion and application.

3.2 Promoting standardization and orderliness in laver cultivation

At present, the Chinese government has focused on addressing the illegal occupation of maritime areas for aquaculture, explicitly prohibiting the establishment of new aquaculture projects that occupy natural coastlines or fall within ecological protection red lines (Ministry of Natural Resources of the People's Republic of China, 2024). It has gradually cleared areas of illegal and unlicensed *Neopyropia* cultivation and withdrawn cultivation within the ecological red line areas (Figure 2C). Meanwhile, efforts are underway to optimize the spatial planning and layout of laver cultivation by adhering to principles of high-quality, ecological, and standardized development. These efforts gradually transferring laver cultivation rafts from nearshore tidal flats to deeper sea areas and strengthening the management and supervision of no-culture zones, limited-culture zones, and aquaculture zones (Jiangsu Laver Association, 2020; Lianyungang Municipal Bureau of Agriculture and Rural Affairs, 2021). In addition, research and promotion of technologies to prevent the attachment of *Ulva* on laver cultivation rafts are being carried out (Jiangsu Provincial Bureau of Geology, 2024). Efforts are also being made to strengthen the management of aquaculture waste, such as discarded *Ulva* species by promoting the centralized treatment and resource utilization of aquaculture production waste. These measures aim to reduce the initial biomass of *U. prolifera*, the dominant species in green tide outbreaks in the SYS, providing a scientific basis for the ecological cultivation of laver and green tide prevention.

Simultaneously, relevant government departments are researching the resource and environmental carrying capacities under the guidance of superior authorities to provide theoretical and scientific foundations for determining the appropriate cultivation scale of *Neopyropia* in Jiangsu Province. In response to excessive laver cultivation density, the government recommends reducing high-density cultivation and gradually guiding farmers and enterprises to control cultivation density within a reasonable range (Lianyungang Municipal Bureau of Agriculture and Rural Affairs, 2021). Appropriately reducing cultivation density also helps slow the spread of diseases during the cultivation process. To address these issues, Shan (2022) suggests controlling the continuous distribution scale of laver cultivation rafts and reducing the overall cultivation area. Furthermore, the government or industry associations could coordinate to divide the continuous distribution areas into several smaller zones, increasing the spacing between these zones to allow for sufficient seawater exchange. At the same time, individual farmers or aquaculture enterprises could reduce the density of raft arrangements, expanding the current spacing from approximately 4 meters to 6-7 meters (Shan, 2022). This approach will ensure seawater exchange, reduce disease incidence, and effectively increase the yield per unit area of laver cultivation.

3.3 The industrial chain could transition to regions at higher latitudes

There is a significant demand for *N. yezoensis* cultivated in China (Li et al., 2023) from countries including Japan, the United States, and South Korea. To meet this demand, it is crucial to maintain the cultivation scale of *N. yezoensis* in Jiangsu Province (Figure 1) and other regions of China. Yang et al. (2021) reported that in the lower-salinity marine waters of Nantong City, elevated ocean temperatures suppress the activity of antioxidant enzymes and the expression of related genes within *N. yezoensis*, rendering the seaweed more vulnerable to disease and decay. To address these issues, a progressive relocation of the *N. yezoensis* cultivation industry from the southern coastal waters of Jiangsu Province to the cities of Yancheng and Lianyungang is imperative. Notably, parts of this industry have already been transferred to the marine areas of Shandong and Liaoning provinces in China, where the colder seawater conditions during the same cultivation period are more conducive to *N. yezoensis* growth and can mitigate the risk of disease and decay (Yang et al., 2021). Moreover, it is anticipated that by 2050, the suitable growth range for *N. yezoensis* in the East Asian region will expand to include the Sea of Okhotsk in Russia (Zhou et al., 2023). Shifting the *N. yezoensis* industrial chain towards higher-latitude regions is expected to enhance both yield and quality.

Furthermore, considering the frequent outbreaks of green tides and other biological disasters in mid- and low-latitude regions (Yao et al., 2024), as well as the impact of ocean warming, algal bloom outbreaks, are expected to occur earlier and expand further (Qi et al., 2022). Gradually relocating the laver cultivation industry to higher-latitude regions may help reduce the impact of algal bloom disasters and ensure the sustainable development of the industry.

3.4 Transformation of the laver fishery economic model

The laver cultivation industry, characterized by its labor-intensive nature, requires substantial labor input throughout the

production cycle while typically yielding modest economic returns. In the future, integrating the laver cultivation cycle with Integrated Multi-Trophic Aquaculture (IMTA) models (Kang et al., 2013) may help mitigate significant monoculture risks and unlock considerable economic potential (Lianyungang Municipal Bureau of Agriculture and Rural Affairs, 2021). For example, in 2021, Lianyungang City established a new Integrated Multi-Trophic Aquaculture (IMTA) management model incorporating the co-cultivation of shellfish and seaweeds. Demonstration farming under this model produced positive results, achieving an economic benefit of 3.19 million RMB Yuan and generating significant carbon sequestration effects (Ministry of Education of the People's Republic of China, 2023). With the establishment of IMTA systems and supporting infrastructure, additional opportunities for developing recreational and ecotourism farms, such as "new energy+" marine farms (Yi and Li, 2024), can emerge. This synergy between agriculture and recreational fishing has the potential to maximize economic benefits and increase income for laver farmers. However, the adoption and refinement of such development models still require ongoing feasibility studies and remain highly dependent on the maturity of the service industry at the national level. Currently, local governments at various levels in China are gradually formulating relevant laws and regulations. For instance, from January 1, 2025, to December 31, 2029, the Shandong Provincial Government will permit recreational fishing activities within marine ranching areas (Shandong Provincial Department of Agriculture and Rural Affairs, 2024). This initiative is expected to promote the integration of marine aquaculture with recreational fishing, enhancing the overall income of farmers.

In addition, by further integrating laver cultivation into carbon emission trading markets and exploring blue carbon economic development pathways, future carbon sink revenues could support both the advancement of laver cultivation and the stabilization of marine ecosystems, thereby achieving mutually beneficial outcomes. For example, leveraging the blue carbon value of laver (Cangnan County People's Government, 2022), Yonggui Aquaculture Family Farm in Rudong County has secured a "laver carbon credit loan" valued at 1.75 million RMB Yuan, using future revenue rights from carbon reduction and sequestration generated by laver cultivation as collateral (The People's Government of Nantong Municipality, 2023). Notably, the Chinese government is actively promoting the regulation and orderly development of carbon sink trading. The "Interim Regulations on the Administration of Carbon Emission Rights Trading", effective May 1, 2024 (The State Council of the People's Republic of China, 2024), provide institutional guarantees for carbon emission rights trading at the national legislative level. However, the realization of specific economic, ecological, and social benefits still depends on the establishment of a comprehensive carbon sink trading accounting standard system. At present, the transformation of the laver fishery economic model is still in its early exploratory stage and requires further practical innovation and robust government policy support.

4 Conclusion

This opinion article systematically outlines the current state of the laver (*N. yezoensis*) cultivation industry in Jiangsu Province, the challenges it faces, and strategies for sustainable development. Jiangsu Province, as the world's largest cultivation area for *N. yezoensis*, plays a critical role in local economic development and provides a substantial supply of high-quality laver to the global market. However, factors such as climate change, diseases, high-density cultivation, green tides, and golden tide disasters pose severe threats to laver cultivation. To address these challenges, we propose key development strategies, including the cultivation of heat-resistant laver varieties, improving standardization and order in laver cultivation practices, relocating the industry chain to higher latitude regions, and transforming the laver fishery economic model. The implementation of these strategies will support the sustainable development and industrial upgrading of Jiangsu Province's laver cultivation industry, as well as the formulation of long-term aquaculture development strategies. Additionally, these measures will contribute to marine ecosystem protection, achieving a win-win situation for both economic and ecological benefits.

Author contributions

JL: Conceptualization, Formal analysis, Funding acquisition, Investigation, Methodology, Project administration, Resources, Supervision, Writing – original draft, Writing – review & editing. WL: Conceptualization, Formal analysis, Methodology, Resources, Supervision, Writing – original draft, Writing – review & editing. JX: Conceptualization, Formal analysis, Methodology, Resources, Supervision, Writing – original draft, Writing – review & editing.

Funding

The author(s) declare financial support was received for the research, authorship, and/or publication of this article. This work was supported by the Youth Development Fund Project of the State Key Laboratory of Marine Geology, the Shanghai Super Postdoctoral Incentive Plan, the National Key Research & Development Program of China (2022YFC3106001), and the Shanghai Ocean Bureau Project (Shanghai Ocean Science 2022-03).

Acknowledgments

Dr. Liu thanks the Ministry of Natural Resources of the People's Republic of China and the Ministry of Agriculture and Rural Affairs of the People's Republic of China for facilitating the progress of relevant scientific research endeavors. Meanwhile, Dr. Liu expresses gratitude to Professor Peimin He (Shanghai Ocean University) and

Associate Professor Jianheng Zhang (Shanghai Ocean University) for their educational guidance, and also to Professor Qunhui Yang for providing a suitable working environment (Project Management Office of China National Scientific Seafloor Observatory). Thank Dr. Zhangyi Xia (Xiamen University) for providing the image of laver cultivation in Yancheng City.

Conflict of interest

The authors declare that the research was conducted in the absence of any commercial or financial relationships that could be construed as a potential conflict of interest.

Generative AI statement

The author(s) declare that no Generative AI was used in the creation of this manuscript.

Publisher's note

References

Bae, H., Bang, Y., Jeong, J., Kim, W., Lee, H., Moon, S., et al. (2024). Differential surface microbial community and thalli metabolome as early indicators of disease in red algae *Pyropia yezoensis*. *Aquacult. Int.* 32, 8963–8980. doi: 10.1007/s10499-024-01600-6

Cangnan County People's Government (2022). *Cangnan Explores the Development of Marine Fishery Carbon Trading, Mariculture Earns "Ecological Income"* (Zhejiang Province: Cangnan County News Network). Available at: https://www.cncn.gov.cn/art/2022/10/24/art_1255449_59044206.html (Accessed December 19, 2024).

Cao, J., Liu, J., Zhao, S., Tong, Y., Li, S., Xia, Z., et al. (2023). Advances in the research on micropropagules and their role in green tide outbreaks in the Southern Yellow Sea. *Mar. pollut. Bull.* 188, 114710. doi: 10.1016/j.marpolbul.2023.114710

CCTV (2021). *Jiangsu faces severe convective weather on the evening of April 30, with maximum wind force reaching level 14* (Beijing Province: China Central Television). Available at: https://tv.cctv.com/2021/05/01/ARTIQxoVn7vV21FDIwLYRhmO210501.shtml (Accessed December 12, 2024).

Diao, F., and Ma, F. (2021). *Experts Discuss the Control of Green Tide: Coordinated Land-Sea Management, Reducing the Degree of Eutrophication in Seawater is Key* (The Paper). Available at: https://www.sohu.com/a/477265398_726570 (Accessed December 22, 2024).

FAO. (2024). "The state of world fisheries and aquaculture 2024," in *Blue Transformation in Action* (FAO, Rome), 1–232. Available at: https://openknowledge.fao.org/handle/20.500.14283/cd0683en (Accessed December 19, 2024).

Feng, Y., Xiong, Y., Hall-Spencer, J., Liu, K., Beardall, J., Gao, K., et al. (2024). Shift in algal blooms from micro– to macroalgae around China with increasing eutrophication and climate change. *GCB Bioenergy* 30, e17018. doi: 10.1111/gcb.17018

Fishery Administration Bureau of Ministry of Agriculture and Rural Affairs, National Fisheries Technology Extension Center and China Society of Fisheries (2024). *The China Fishery Statistical Yearbook 2024.* (Beijing: China Agriculture Press), 1–159.

Guo, S., Sun, X., Zhang, J., Yao, Q., Wei, C., and Wang, F. (2024). Unveiling the evolution of phytoplankton communities: Decades-long insights into the southern Yellow Sea, China, (1959[amp]]ndash;2023). *Mar. pollut. Bull.* 201, 116179. doi: 10.1016/j.marpolbul.2024.116179

Han, W., Chen, L., Zhang, J., Tian, X., Hua, L., He, Q., et al. (2013). Seasonal variation of dominant free-floating and attached *Ulva* species in Rudong coastal area, China. *Harmful Algae* 28, 46–54. doi: 10.1016/j.hal.2013.05.018

He, P., Xu, S., Zhang, H., Wen, S., Dai, Y., Lin, S., et al. (2008). Bioremediation efficiency in the removal of dissolved inorganic nutrients by the red seaweed, *Porphyra yezoensis*, cultivated in the open sea. *Water Res.* 42, 1281–1289. doi: 10.1016/j.watres.2007.09.023

He, L., Yang, H., Li, J., Tang, L., Liu, C., and Mo, Z. (2021). Diagnosis of Oplidiopsis disease in *Pyropia yezoensis*. *Prog. Fis.h Sci.* 42, 177–183. doi: 10.19663/j.issn2095-9869.20200225002

He, R., Zeng, Y., Zhao, S., Zhang, J., He, P., and Liu, J. (2023). Use of citric acid-activated chlorine dioxide to control *Ulva prolifera*. *Mar. pollut. Bull.* 194, 115357. doi: 10.1016/j.marpolbul.2023.115357

He, P., Zhang, Z., Zhang, X., and Ma, J. (2018). "Chapter 5: cultivation of *Neopyropia yezoensis*," in *The Cultivation of Seaweed*, (Beijing: Science Press). 1–442.

Huang, D., Sun, Z., Wang, L., Feng, Z., Niu, J., Ye, Q., et al. (2023). Analysis of environmental factors affecting the quality of *neopyropia yezoensis* cultivated in the yellow sea. *J. Mar. Sci. Eng.* 11, 428. doi: 10.3390/jmse11020428

Huo, Y., Han, H., Shi, H., Wu, H., Zhang, J., Yu, K., et al. (2015). Changes to the biomass and species composition of *Ulva* sp. on *Porphyra* aquaculture rafts, along the coastal radial sandbank of the Southern Yellow Sea. *Mar. pollut. Bull.* 93, 210–216. doi: 10.1016/j.marpolbul.2015.01.014

Jiangsu Laver Association. (2020). *Notice from the Department of Agriculture and Rural Affairs of Jiangsu Province on further strengthening the management of ecological and healthy laver cultivation* (Jiangsu Laver Association Fair Trade Workstation). Available at: http://www.jslaver.cn/Home/Index/views/aid/4068.html (Accessed December 15, 2024).

Jiangsu Provincial Bureau of Geology. (2024). *The 'Technical Guidelines for* Ulva *Prevention in Laver Farming on the Subei Shoal' compiled by the Marine Institute has passed the review* (Jiangsu Provincial Bureau of Geology). Available at: https://jsdk.Jiangsu.gov.cn/art/2024/4/17/art_3888_11220314.html (Accessed December 24, 2024).

Kang, Y., Hwang, J., Chung, I., and Park, S. (2013). Development of a seaweed species-selection index for successful culture in a seaweed-based integrated aquaculture system. *J. Ocean Univ. China* 12, 125–133. doi: 10.1007/s11802-013-1928-z

Khan, N., Sudhakar, K., and Mamat, R. (2024). Macroalgae farming for sustainable future: Navigating opportunities and driving innovation. *Heliyon* 10, e28208. doi: 10.1016/j.heliyon.2024.e28208

Kim, G., Moon, K., Kim, J., Shim, J., and Klochkova, T. (2014). A revaluation of algal diseases in Korean *Pyropia* (*Porphyra*) sea farms and their economic impact. *Algae* 29, 249–265. doi: 10.4490/algae.2014.29.4.249

Li, S., Hu, M., Tong, Y., Xia, Z., Tong, Y., Sun, Y., et al. (2023). A review of volatile compounds in edible macroalgae. *Food Res. Int.* 165, 112559. doi: 10.1016/j.foodres.2023.112559

Li, X., Yang, L., and He, M. (2011). Formation and growth of free-living conchosporangia of *Porphyra yezoensis*: Effects of photoperiod, temperature and light intensity. *Aquacult. Res.* 42, 1079–1086. doi: 10.1111/j.1365-2109.2010.02691.x

Liandao Subdistrict (2024). *First Harvest of* Neopyropia haitanensis *Ashore: Bustling "Marine Ranching" Harvest Season* (Lianyun District People's Government of Lianyungang City). Available at: http://www.lianyun.gov.cn/lyq/jrly/content/b4031e2f-64a8-4303-aa29-88e9d1ec61aa.shtml (Accessed December 23, 2024).

Lianyun District People's Government (2017). *Lianyun district holds symposium to discuss the development path of laver industry* (Lianyun District People's Government of Lianyungang City). Available at: http://www.lianyun.gov.cn/lygslyqlyhhyj/msgy/content/lyhyj_37260.html (Accessed December 20, 2024).

Lianyungang Municipal Bureau of Agriculture and Rural Affairs (2021). *Notice on the issuance of "Guiding opinions on accelerating the healthy development of the laver industry"* (Lianyungang Municipal Bureau of Agriculture and Rural Affairs). Available at: http://nync.lyg.gov.cn/lygnyxxw/ywwj/content/cd8b11eb-5b23-490b-9f29-a38bf1a369cf.html (Accessed December 23, 2024).

Lin, H., Lu, X., Wang, X., He, S., Li, S., Zheng, W., et al. (2021). Research on spatial expansion mode of laver farming area in Jiangsu Province. *Mar. Sci. Bull.* 40, 206–216. doi: 10.11840/j.issn.1001-6392.2021.02.010

Liu, J., Li, C., Xia, J., Sun, Y., Tong, Y., Zhang, J., et al. (2021a). Epizoic *Ulva* attached to intertidal animals in the Subei intertidal zone are not the additional source of the famed Yellow Sea green tides. *J. Sea Res.* 174, 102065. doi: 10.1016/j.seares.2021.102065

Liu, F., Liu, X., Wang, Y., Jin, Z., Moejes, F., and Sun, S. (2018). Insights on the *Sargassum horneri* golden tides in the Yellow Sea inferred from morphological and molecular data. *Limnol. Oceanogr.* 63, 1762–1773. doi: 10.1002/lno.10806

Liu, F., Pang, S., Chopin, T., Gao, S., Shan, T., Zhao, X., et al. (2013). Understanding the recurrent large-scale green tide in the Yellow Sea: Temporal and spatial correlations between multiple geographical, aquacultural and biological factors. *Mar. Environ. Res.* 83, 38–47. doi: 10.1016/j.marenvres.2012.10.007

Liu, J., Xia, J., Zhuang, M., Zhang, J., Sun, Y., Tong, Y., et al. (2021c). Golden seaweed tides accumulated in *Pyropia* aquaculture areas are becoming a normal phenomenon in the Yellow Sea of China. *Sci. Total Environ.* 774, 145726. doi: 10.1016/j.scitotenv.2021.145726

Liu, J., Xia, J., Zhuang, M., Zhang, J., Yu, K., Zhao, S., et al. (2021b). Controlling the source of green tides in the Yellow Sea: NaClO treatment of *Ulva* attached on *Pyropia* aquaculture rafts. *Aquaculture* 535, 736378. doi: 10.1016/j.aquaculture.2021.736378

Liu, J., Yuan, H., Xia, Z., and He, P. (2024). Paying attention to the safety of global edible seaweeds after the discharge of nuclear-contaminated water from Japan. *Algal Res.* 84, 103811. doi: 10.1016/j.algal.2024.103811

Lu, W., and Du, H. (2022). Retrospective and improvement measures of emergency disposal work for the "4·30" sudden large-scale convective weather disaster in Nantong City, Jiangsu Province. *Disaster Reduct. China* 24, 52–55. doi: 10.3969/j.issn.1002-4549.2022.24.021

Mantri, V., Kambey, C., Cottier-Cook, E., Usandizaga, S., Buschmann, A., Chung, I., et al. (2023). Overview of global *Gracilaria* production, the role of biosecurity policies and regulations in the sustainable development of this industry. *Rev. Aquacult.* 15, 801–819. doi: 10.1111/raq.12761

Ministry of Education of the People's Republic of China (2023). *Jiangsu ocean university: the transformation brought by the laver* (Beijing: Ministry of Education of the People's Republic of China Government Portal). Available at: http://www.moe.gov.cn/jyb_xwfb/xw_zt/moe_357/jjyzt_2022/2022_zt04/dianxing/xiangmu/shengshu/shengshu6th/202312/t20231212_1094291.html (Accessed December 24, 2024).

Ministry of Natural Resources of the People's Republic of China (2024). *Notice on issuing the "Guidance catalogue for high-quality development supported by natural resource elements, (2024 edition)"* (Beijing: Ministry of Natural Resources of the People's Republic of China, National Development and Reform Commission, National Forestry and Grassland Administration). Available at: https://gi.mnr.gov.cn/202412/t20241223_2878837.html (Accessed December 24, 2024).

Park, S., Shin, S., Wu, H., Yarish, C., Yoo, H., and Kim, J. (2021). Evaluation of nutrient bioextraction by seaweed and shellfish aquaculture in Korea. *J. World Aquacult. Soc* 52, 1118–1134. doi: 10.1111/jwas.12786

Qi, L., Hu, C., Barnes, B., Lapointe, B., Chen, Y., Xie, Y., et al. (2022). Climate and anthropogenic controls of seaweed expansions in the East China Sea and yellow sea. *Geophys. Res. Lett.* 49, e2022GL098185. doi: 10.1029/2022GL098185

Qiu, L., Mao, Y., Tang, L., Tang, X., and Mo, Z. (2019). Characterization of *Pythium chondricola* associated with red rot disease of *Pyropia yezoensis* (Ueda) (Bangiales, Rhodophyta) from Lianyungang, China. *J. Oceanol. Limnol.* 37, 1102–1112. doi: 10.1007/s00343-019-8075-3

Shan, C. (2022). The key technology affecting the production of *Neopyropia yezoensis* farming. *J. Aquacult.* 43, 57–58. doi: 10.3969/j.issn.1004-2091.2022.04.014

Shandong Provincial Department of Agriculture and Rural Affairs (2024). *Shandong Provincial Department of Agriculture and Rural Affairs issues the "Shandong Province Leisure Fisheries Management Measures"* (Shandong Province: Shandong Provincial Department of Agriculture and Rural Affairs). Available at: https://www.yyj.moa.gov.cn/dfqk/202411/t20241129_6467173.htm (Accessed December 24, 2024).

Sohu (2016). *110,000 Mu of Laver Severely Damaged by Extreme Cold* (Sohu News). Available at: https://www.sohu.com/a/57268342_114954 (Accessed December 24, 2024).

Subramaniyan, S., Begum, N., Kim, S., Choi, Y., and Nam, T. (2021). Biopeptides of *Pyropia yezoensis* and their potential health benefits: A review. *Asian Pac. J. Trop. Biomed.* 11, 375–384. doi: 10.4103/2221-1691.321127

Sun, J., Bao, M., Xu, T., Li, F., Wu, H., Li, X., et al. (2021). Elevated CO_2 influences competition for growth, photosynthetic performance and biochemical composition in *Neopyropia yezoensis* and *Ulva prolifera*. *Algal Res.* 56, 102313. doi: 10.1016/j.algal.2021.102313

Sun, Y., Xia, Z., Cao, X., Tong, Y., He, R., Fu, M., et al. (2022b). A mixed acid treatment for the prevention of *Ulva prolifera* attachment to *Neopyropia* aquaculture rafts: Laboratory experimentation. *Mar. Pollut. Bull.* 184, 114134. doi: 10.1016/j.marpolbul.2022.114134

Sun, Y., Yao, L., Liu, J., Tong, Y., Xia, J., Zhao, X., et al. (2022a). Prevention strategies for green tides at source in the Southern Yellow Sea. *Mar. Pollut. Bull.* 178, 113646. doi: 10.1016/j.marpolbul.2022.113646

The People's Government of Nantong Municipality (2023). *Jiangsu Province Manages "Two Sands" Marine Area, First Ocean Carbon Sink Loan Settles in Nantong City* (Jiangsu Province: Nantong Daily). Available at: https://www.nantong.gov.cn/ntsrmzf/ntxw/content/8e4db5d8-21af-4a6d-b7ce-cc1c1b985733.html (Accessed December 20, 2024).

The State Council of the People's Republic of China (2024). *Interim Regulations on the Administration of Carbon Emission Rights Trading* (Beijing: China Government Network). Available at: https://www.gov.cn/zhengce/zhengceku/202402/content_6930138.htm (Accessed December 20, 2024).

Veenhof, R., Burrows, M., Hughes, A., Michalek, K., Ross, M., Thomson, A., et al. (2024). Sustainable seaweed aquaculture and climate change in the North Atlantic: Challenges and opportunities. *Front. Mar. Sci.* 11. doi: 10.3389/fmars.2024.1483330

Wang, J. (2016). *Over 20,000 mu of laver in Rudong, Jiangsu, suffer from disease and decay, and local investigation into the cause* (Dazhong Net). Available at: https://news.dzwww.com/guoneixinwen/201602/t20160226_13890966.htm (Accessed December 22, 2024).

Wang, X., He, L., Ma, Y., Huan, L., Wang, Y., Xia, B., et al. (2020). Economically important red algae resources along the Chinese coast: History, status, and prospects for their utilization. *Algal Res.* 46, 101817. doi: 10.1016/j.algal.2020.101817

Wang, R., and Yu, F. (2014). Impact of climatic change on sea surface temperature variation in Subei coastal waters, East China. *Chin. J. Ocean. Limnol.* 32, 1406–1413. doi: 10.1007/s00343-015-3336-2

Wang, Z., Yuan, C., Zhang, X., Liu, Y., Fu, M., and Xiao, J. (2023). Interannual variations of *Sargassum* blooms in the Yellow Sea and East China Sea during 2017–2021. *Harmful Algae* 126, 102451. doi: 10.1016/j.hal.2023.102451

Wang, X., Zhao, W., Zhuang, M., Wu, T., Zhao, C., Dai, W., et al. (2024). Population genetic structure of *Sargassum horneri*, the dominant species of golden tide in the Yellow Sea. *J. Mar. Sci. Eng.* 12, 900. doi: 10.3390/jmse12060900

Wu, H., Huo, Y., Zhang, J., Liu, Y., Zhao, Y., and He, P. (2015). Bioremediation efficiency of the largest scale artificial *Porphyra yezoensis* cultivation in the open sea in China. *Mar. pollut. Bull.* 95, 289–296. doi: 10.1016/j.marpolbul.2015.03.028

Wu, H., Wang, C., Li, H., Chen, J., Zhang, J., Luo, Z., et al. (2024). High light intensity and CO_2 enrichment synergistically mitigated the stress caused by low salinity in. *Pyropia yezoensis. J. Mar. Sci. Eng.* 11, 2193. doi: 10.3390/jmse11112193

Xia, Z., Liu, J., Zhao, S., Sun, Y., Cui, Q., Wu, L., et al. (2024b). Review of the development of the green tide and the process of control in the southern Yellow Sea in 2022. *Estuarine Coast. Shelf Sci.* 302, 108772. doi: 10.1016/j.ecss.2024.108772

Xia, Z., Yang, Y., Zeng, Y., Sun, Y., Cui, Q., Chen, Z., et al. (2024a). Temporal succession of micropropagules during accumulation and dissipation of green tide algae: A case study in Rudong coast, Jiangsu Province. *Mar. Environ. Res.* 202, 106719. doi: 10.1016/j.marenvres.2024.106719

Xia, Z., Yuan, H., Liu, J., Sun, Y., Tong, Y., Zhao, S., et al. (2022). A review of physical, chemical, and biological green tide prevention methods in the Southern Yellow Sea. *Mar. pollut. Bull.* 180, 113772. doi: 10.1016/j.marpolbul.2022.113772

Yang, J., Feng, Z., Niu, J., Gu, W., He, B., Liu, X., et al. (2021). Preliminary study on the mechanism of rotten diseases induced by low salinity and high temperature in *Pyropia yezoensis*. *Oceanol. Limnol. Sin.* 52, 1214–1223. doi: 10.11693/hyhz20210300057

Yang, H., Yan, Y., Li, J., Tang, L., Mao, Y., and Mo, Z. (2020). Development of a PCR method for detection of *Pseudoalteromonas marina* associated with green spot disease in *Pyropia yezoensis*. *J. Oceanol. Limnol.* 38, 168–176. doi: 10.1007/s00343-019-9045-5

Yangtze Evening Post (2004). *Large-scale Growth Disorders of Laver Along the Rudong Coastline* (Jiangsu Province: Yangtze Evening Post). Available at: http://finance.sina.com.cn/roll/20041025/10341104746.shtml (Accessed December 23, 2024).

Yao, L., He, P., Xia, Z., Li, J., and Liu, J. (2024). Typical marine ecological disasters in China attributed to marine organisms and their significant insights. *Biology* 13, 678. doi: 10.3390/biology13090678

Yi, W., and Li, S. (2024). Research on current situation and typical models of marine ranching development in China. *Chin. Fish. Econ.* 42, 51–60. doi: 10.3969/j.issn.1009-590X.2024.04.006

Zhang, Y., He, P., Li, H., Li, G., Liu, J., Jiao, F., et al. (2019a). *Ulva prolifera* green-tide outbreaks and their environmental impact in the Yellow Sea, China. *Natl. Sci. Rev.* 6, 825–838. doi: 10.1093/nsr/nwz026

Zhang, J., Shi, J., Gao, S., Huo, Y., Cui, J., Shen, H., et al. (2019b). Annual patterns of macroalgal blooms in the Yellow Sea during 2007–2017. *PLoS One* 14, e0210460. doi: 10.1371/journal.pone.0210460

Zhao, Y., Wu, J., Kang, X., Guo, Y., Wang, L., Sheng, X., et al. (2023). Elemental profiling of red seaweed *Neopyropia yezoensis* used in fast authenticating the geographical origin and food safety assessment. *J. Food Compos. Anal.* 125, 105839. doi: 10.1016/j.jfca.2023.105839

Zhou, W., Li, B., Xu, H., Liang, Z., Lu, X., Yang, L., et al. (2023). Potential distribution of two economic laver species-*Neoporphyra haitanensis* and *Neopyropia yezoensis* under climate change based on MaxEnt prediction and phylogeographic profiling. *Ecol. Indic.* 150, 110219. doi: 10.1016/j.ecolind.2023.110219

Zhuang, M., Liu, J., Ding, X., He, J., Zhao, S., Wu, L., et al. (2020). *Sargassum* blooms in the East China Sea and Yellow Sea: Formation and management. *Mar. pollut. Bull.* 162, 111845. doi: 10.1016/j.marpolbul.2020.111845

frontiers | Frontiers in Marine Science

TYPE Original Research
PUBLISHED 28 January 2025
DOI 10.3389/fmars.2025.1539865

OPEN ACCESS

EDITED BY
Guang Gao,
Xiamen University, China

REVIEWED BY
Jinlin Liu,
Tongji University, China
Robert Steneck,
University of Maine, United States

*CORRESPONDENCE
Adi Khen
akhen@ucsd.edu

RECEIVED 04 December 2024
ACCEPTED 13 January 2025
PUBLISHED 28 January 2025

CITATION
Khen A, Johnson MD, Fox MD and Smith JE (2025) Benthic algal community dynamics on Palmyra Atoll throughout a decade with two thermal anomalies.
Front. Mar. Sci. 12:1539865.
doi: 10.3389/fmars.2025.1539865

Benthic algal community dynamics on Palmyra Atoll throughout a decade with two thermal anomalies

Adi Khen[1]*, Maggie D. Johnson[2], Michael D. Fox[2] and Jennifer E. Smith[1]

[1]Center for Marine Biodiversity and Conservation, Scripps Institution of Oceanography, University of California, San Diego, La Jolla, CA, United States, [2]Biological and Environmental Sciences and Engineering Division, King Abdullah University of Science and Technology, Thuwal, Saudi Arabia

Coral reef algae serve many important ecological functions, from primary production to nutrient uptake and reef stabilization, but our knowledge of longer-term effects of thermal stress on algae *in situ* is limited. While ocean warming can facilitate proliferation of algae and potential phase shifts from coral to macroalgal-dominated states, algal responses may vary by species, genus, functional group, or type (e.g., calcareous vs. fleshy). We used 11 years of annual monitoring data (2009-2019) that spans two El Niño-associated heatwaves to examine benthic algal community dynamics on Palmyra Atoll in the central Pacific Ocean. We quantified the percent cover of algal taxa via image analysis of permanent benthic photoquadrats from two habitats on Palmyra: the deeper, wave-exposed fore reef (10 m depth) and the shallower, wave-sheltered reef terrace (5 m depth). Each habitat was characterized by distinct algal communities: predominantly calcareous taxa on the fore reef and predominantly fleshy taxa on the reef terrace. Patterns in abundance fluctuated over time and/or in response to thermal anomalies in 2009 and 2015. Fleshy algae generally increased in cover post-warming, which coincided with large declines of the calcified macroalgae, *Halimeda* spp. Long-term monitoring of coral reef algal communities is critical for understanding their differential responses to thermal stress and can improve projections of ecosystem functioning in the context of global change.

KEYWORDS

long-term monitoring, seaweed, macroalgae, *Halimeda*, community composition, thermal stress, coral reefs, climate change

1 Introduction

Benthic algae are key components of coral reef ecosystems, where they contribute to primary production and reef building as well as sand, sediment, and carbonate production. The dominance of one functional group or taxon over another has implications for coral reef functioning and the ecological services they provide (Woodhead et al., 2019). Although

many coral reefs across the globe are shifting from coral to algal dominance (Pandolfi et al., 2003; McManus and Polsenberg, 2004; Hughes et al., 2010, 2017), algae are inherently a natural component of healthy coral reefs. Despite their functional, morphological, and taxonomic diversity (Fong and Paul, 2011), reef algae remain understudied relative to other reef taxa. Aside from some short-term laboratory studies, little is known about how individual algal taxa or functional groups respond to a combination of stressors in nature (Wernberg et al., 2012). Thus, *in situ* studies integrating natural environmental conditions with longer-term benthic algal community dynamics are essential for revealing possible reef community trajectories in the coming decades.

Algae on coral reefs are often classified into functional groups (e.g., turf, crustose coralline algae, and macroalgae), based on the underlying assumption that shared traits correspond to similar ecological roles, functions, or processes. Algal functional groups have previously been defined by their susceptibility to herbivory (Steneck and Watling, 1982), their nutrient uptake, productivity, and turnover rates (Littler and Littler, 1980; Littler et al., 1983), or their morphology, internal anatomy (e.g., cortication), thallus structure, and branching pattern (Steneck and Dethier, 1994; Balata et al., 2011). However, there is still a potential for variable responses to environmental conditions within functional groups, particularly following disturbance events (Phillips et al., 1997). Moreover, calcareous algal taxa (in which photosynthesis is coupled with the deposition of calcium carbonate) and non-calcareous (i.e., fleshy) taxa are differentially affected by environmental stressors (Johnson et al., 2014). While the functional group approach (when based on morphological traits) can sometimes predict community assemblage (Stelling-Wood et al., 2020), these traits may not accurately represent functional identity (Mauffrey et al., 2020) and individual genus and/or species variability must be considered (Fong and Fong, 2014; Ryznar et al., 2021).

Two algal functional groups that are sometimes pooled in reef benthic studies, yet have distinct ecological roles, are the crustose coralline algae (CCA) and the algal turfs. CCA are encrusting, calcifying red algae that stabilize the reef framework and support structural complexity (Teichert et al., 2020; Littler and Littler, 2013; Steneck, 1986). They also contribute to carbonate production, possibly more so than reef-building corals (Cornwall et al., 2023). By releasing chemical cues that induce settlement in coral larvae (Harrington et al., 2004), CCA further promote reef growth and resilience. The ecological contributions of CCA on coral reefs are threatened by environmental change, as they are sensitive to thermal stress in both experimental and field settings (Martin and Gattuso, 2009; Short et al., 2015). "Turf algae" (algal turfs) refers to a mixed assemblage of largely fleshy filamentous algae, juvenile macroalgae, and/or cyanobacteria less than 2 cm tall (Adey and Steneck, 1985). Algal turfs are opportunistic and rapid colonizers of open space after coral bleaching or disease outbreaks (Diaz-Pulido and McCook, 2002). They are a main food source for herbivorous grazers (Carpenter, 1986), but can have negative effects on reefs by inhibiting coral recruitment (Birrell et al., 2008) or harboring pathogenic microbes that compromise coral health (Pratte et al., 2018). Despite occupying much of the benthos on today's reefs (Wismer et al., 2009), they are often miscategorized as "bare space" and, thus, grossly underestimated in surveys of benthic community coverage. Turfs thrive under conditions that threaten corals, including nutrient pollution (Smith et al., 2010), warming (Johnson et al., 2017), ocean acidification (Falkenberg et al., 2013), and sedimentation (Birrell et al., 2005), which suggests that their abundance on reefs will continue to increase with the progression of climate change (Harris et al., 2015; Tebbett and Bellwood, 2019).

Another distinction lost with the typical categorization of algae is the presence or absence of a calcium carbonate skeleton (i.e., calcification). The relative balance of fleshy to calcareous or reef-building taxa may be indicative of more degraded vs. "healthier" coral reefs (Smith et al., 2016), and thus tracking the abundance of calcareous and fleshy algal taxa is useful for assessing ecosystem status. Moreover, fleshy and calcareous taxa have different ecological functions, whether beneficial or detrimental. Fleshy macroalgae typically grow faster than calcareous macroalgae and are generally more edible to herbivores. However, fleshy macroalgae can harm corals directly through abrasion, or indirectly by releasing toxic allelochemicals (Rasher and Hay, 2010), causing hypoxia and physiological stress (Barott et al., 2012) by limiting photosynthetic activity and depleting the corals of energy (Titlyanov et al., 2007). Calcareous algae are generally more benign competitors with corals than fleshy algae (Barott et al., 2012; but see: Keats et al., 1997a and Longo and Hay, 2015, where corals frequently experienced damage from contact with calcareous algae), although their competitive ability may be influenced by seasonality (Brown et al., 2020). Therefore, to holistically evaluate the ecological implications of stressors such as warming, it is informative to look not only at variability across individual algal taxa or functional groups, but also between fleshy and calcareous algae.

For algae and other primary producers, temperature is expected to increase metabolic and photosynthetic rates until a thermal tolerance limit is exceeded (Davison, 1991). Calcification in calcareous algae may initially benefit from warmer temperatures until prolonged exposure leads to mortality or reduction in productivity, as seen in experimental studies (Martin and Gattuso, 2009; Page et al., 2021; but see: Krieger et al., 2023). In contrast, fleshy algae have been found to respond positively to thermal stress in field studies (McClanahan et al., 2001; Burt et al., 2013; Graham et al., 2015). The combined effects of temperature and other stressors can be synergistic (Ellis et al., 2019) or antagonistic (Darling et al., 2010). For example, ocean acidification has been found to cause net negative or species-specific effects on tropical calcareous algae while stimulating growth in some fleshy algae (Johnson et al., 2014), but when combined with warming, effects can be more complex or interactive (Diaz-Pulido et al., 2012; Kram et al., 2016; Johnson et al., 2017).

The calcareous macroalgal genus *Halimeda* is a group of siphonous green algae that contribute significantly to productivity and calcification on coral reefs (Hillis-Colinvaux, 1980), and can cover up to 20% of the benthos (Perry et al., 2020). *Halimeda* is one of the most ubiquitous tropical algal genera with representative species occurring on reefs around the world. Indeed, *Halimeda* spp. may contribute more to tropical carbonate budgets than corals (Rees et al., 2007) due to their fast growth and high turnover rates (Vroom et al., 2003; Smith et al., 2004). Most species of *Halimeda*

are holocarpic and as such, when they reproduce they die and their calcified segments break down into sand (Harney and Fletcher, 2003). *Halimeda* spp. are synchronous spawners that release all of their gametes simultaneously, leading to complete adult mortality (Hay, 1997), although the exact mechanisms that trigger their reproduction are unknown (Clifton and Clifton, 1999; Clifton, 2013). Considering the high abundance, cosmopolitan distribution, and ecological significance of *Halimeda* spp., it is important to monitor their cover on a consistent basis as well as before, during, and after thermal anomalies. Few studies have examined the long-term changes in cover of *Halimeda* spp. *in situ* (but see: Lambo and Ormond, 2006, where *Halimeda* cover decreased in Kenya at the time of the 1998 coral bleaching event but increased drastically by 2004).

Here, we measured benthic algal cover over an 11-year time series of permanent benthic photoquadrats from two reef habitats on Palmyra Atoll. Thermal anomalies occurred in both 2009 and 2015 (Williams et al., 2010; Fox et al., 2019), which allowed us to explore how temperature may influence algal community dynamics. Our objectives were to (i) describe benthic algal community composition on the fore reef and reef terrace habitats, (ii) quantify the abundance of individual algal taxa or functional groups, (iii) compare fleshy (turf and fleshy macroalgae) vs. calcareous (CCA and calcareous macroalgae) cover, and (iv) determine whether benthic algal cover varied over time, with temperature, and/or by habitat. Additionally, for the major calcareous macroalgal genus, *Halimeda*, we measured yearly changes in benthic cover by habitat and site to validate our hypothesis that *Halimeda* spp. may be temperature-sensitive and negatively affected by warm-water events.

2 Methods

2.1 Study site

Palmyra Atoll (5.89 °N, 162.08 °W), U.S. Minor Outlying Islands, is located in the Northern Line Islands, central Pacific. Palmyra was designated as a National Wildlife Refuge in 2001 and this protection was further expanded in 2009 as part of the Pacific Remote Islands Marine National Monument. The Atoll was temporarily occupied by the U.S. military during World War II but is currently uninhabited aside from a small field research station. Thus, its reefs are considered quasi-pristine (Sandin et al., 2008) and relatively undisturbed from localized human impacts such as fishing or pollution, yet are still susceptible to global climate change. Palmyra's benthic communities are dominated by reef-builders such as hard corals and CCA, with remaining surfaces covered by turf algae, macroalgae, soft corals, and other invertebrates (Braun et al., 2009; Williams et al., 2013; Khen et al., 2022).

2.2 Data collection

In September 2009, permanent monitoring plots were established in the two major reef habitats on Palmyra: the wave-exposed fore reef (FR) at 10 m depth and the wave-sheltered reef terrace (RT) at 5 m depth, with four sites per habitat and ten replicate plots (90 cm x 60 cm) per site (Supplementary Figure 1), for a total surveyed area of 21.6 m^2 at each habitat. Replicate plots were 5 m apart along a 50 m transect perpendicular to shore, marked by stainless steel eye bolts in opposing corners that were secured to the benthos with marine epoxy. At least once a year from 2009 to 2019, usually in the late summer or early fall, plots were photographed by SCUBA divers with a Canon G-series camera attached to a PVC frame that maintained a fixed distance from the substrate. All images were digitized (i.e., manually traced) in Adobe Photoshop (Creative Cloud) to quantify abundance of algal taxa in terms of planar areas or percent cover at the functional group level for CCA and turf, family-level for peyssonnelioids, and genus or species-level for other macroalgae. Algae were identified visually by morphology, and taxa were grouped as either calcareous (CCA, *Halimeda* spp., *Galaxaura rugosa*, and Peyssonneliaceae sp.) or fleshy (*Avrainvillea* sp., *Lobophora* sp., *Dictyosphaeria* spp., *Caulerpa serrulata*, and turf) based on the presence or absence of biogenic calcium carbonate structures. Palmyra's thermal history was obtained from a revised percentile-based method of estimating Degree Heating Weeks (DHW; Liu et al., 2006) developed by Mollica et al. (2019), which more accurately captures the degree of accumulated thermal stress experienced by central equatorial Pacific reefs than traditional DHW (Fox et al., 2021).

2.3 Statistical analyses

All analyses were conducted in R software version 3.6.3 (R Core Team, 2018). First, using only annual time points taken during the late summer or fall (excluding irregular time points to minimize the effect of seasonal variation), we constructed a non-metric multidimensional scaling (nMDS, via *metaMDS* in *vegan* for R; Oksanen et al., 2019) ordination plot visualizing the trajectory of algal community composition through time at each habitat. This nMDS was based on Bray-Curtis dissimilarity measures for square-root-transformed algal percent cover data (Anderson, 2001). We applied a square-root transformation to balance the effect of disproportionately-abundant taxa. We tested the effects of habitat, year, and/or their interaction by conducting a three-way permutational multivariate analysis of variance (PERMANOVA with 9999 permutations via *adonis* in *vegan*; Anderson, 2001; Oksanen et al., 2019) on the same Bray-Curtis distance matrix. We did not include site as a nested factor because not all algal taxa were present at each site within a habitat. To identify which algal taxa were the main contributors to differences among habitats, we ran a SIMPER or "similarity percentages" analysis (via *simper* in *vegan*; Clarke, 1993; Oksanen et al., 2019).

To test whether percent cover of fleshy or calcareous algae varied by habitat and/or over time (only for consistent annual time points), we ran two-way analyses of variance (ANOVAs) with Type-II sum of squares. Assumptions of normality and homogeneity of variance were checked through visual inspection of the residuals. We did not incorporate repeated measures and instead treated years independently because different algal

populations were sampled each year rather than the same individuals. *Post-hoc* letter groupings were assigned via Tukey's multiple comparisons using *multcomp* (Hothorn et al., 2008).

Next we explored possible effects of temperature on a single taxon of interest, *Halimeda*, through an analysis of covariance (ANCOVA) with Type-II sum of squares. Habitat was considered a fixed factor and temperature (in terms of percentile-based DHW values during the week of sampling) was considered a continuous factor. We also examined the relationship between accumulated thermal stress and *Halimeda* cover using Pearson's correlation. To further investigate patterns in abundance for this genus, we plotted its percent cover within each quadrat, by site, over time. Lines were smoothed by locally-weighted regression (i.e., LOESS in *ggplot2*; Wickham, 2016). Finally, we calculated the difference in mean percent cover of *Halimeda* by site (with quadrats as replicates) between consecutive years. Two-tailed t-tests were used to determine which sites experienced significant changes not overlapping zero (e.g., an increase or decrease in percent cover one year later).

3 Results

3.1 Algal community composition in each habitat over time

The benthic algal community on Palmyra's fore reef was calcifier-dominated compared to the fleshy-dominated reef terrace (Figure 1; Supplementary Figure 1). Certain taxa were only present in either habitat: *G. rugosa* on the reef terrace and *Avrainvillea* sp. on the fore reef. Across both habitats, the most abundant algal taxa or groups on Palmyra included CCA (exhibiting a percent cover range of 0 to 87.6% of the benthos within a single quadrat, average = 20.2 ± 17.4% SD), turf (percent cover = 0 to 88.3%, average = 16.7 ± 17.6%), and *Halimeda* (percent cover = 0 to 92.3%, average = 8.4 ± 12.4%). The least abundant algal genera were *Avrainvillea* (percent cover = 0 to 1.7%, average = 0 ± 0.1%), *Dictyosphaeria* (percent cover = 0 to 27.1%, average = 0.4 ± 1.7%), and *Caulerpa* (percent cover = 0 to 46.6%, average = 0.6 ± 3.3%). Distinct yearly trajectories of algal community composition were seen in each habitat (Figure 2).

Benthic algal community composition on Palmyra varied significantly by habitat ($p < 0.001$) and year ($p < 0.001$), with an interaction indicating that habitats changed differently across years ($p < 0.001$; Supplementary Table 1). There was more year-to-year variation in algal community composition on the fore reef compared to the reef terrace, particularly after the second thermal anomaly in 2015. However, habitat was a better predictor for algal community composition than year, explaining 11.6% of the variation ($R^2 = 0.116$; Supplementary Table 1) compared to 4.3%. A SIMPER analysis revealed that the taxa contributing most to habitat differences were CCA, turf algae, and *Halimeda* (Supplementary Table 2). Calcareous algae (particularly CCA, *Halimeda* spp., and Peyssonneliaceae sp.) were more abundant on the fore reef whereas fleshy algae (turf, *Lobophora* sp., *C. serrulata*, and *Dictyosphaeria* spp.) were more abundant on the reef terrace.

3.2 Cover of individual algal taxa by habitat and year

Overall, CCA were more abundant on the fore reef than the reef terrace, covering 25.3 ± 0.8% (mean ± SE) and 15.4 ± 0.8% of the total benthos, respectively (Figure 3B). In contrast, turf algae were more abundant on the reef terrace than the fore reef at 21.3 ± 1.0% and 11.5 ± 0.5% cover, respectively (Figure 3H). Between fall 2014 and fall 2015 on the reef terrace, there was a decline in CCA from 20.0 ± 3.2% to 12.7 ± 2.9% and a concomitant rise in turf algae from 19.6 ± 3.5% to 28.6 ± 3.7%; the increase in turf at the time of the

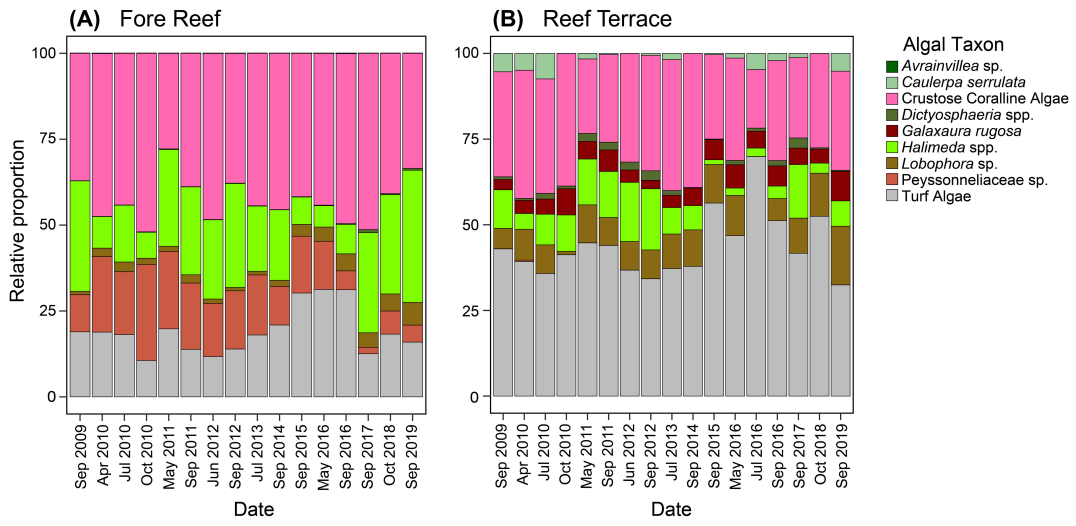

FIGURE 1
Benthic algal community composition over time on Palmyra from 2009 to 2019 at the **(A)** Fore Reef and **(B)** Reef Terrace habitats in terms of relative proportions of each taxon or functional group.

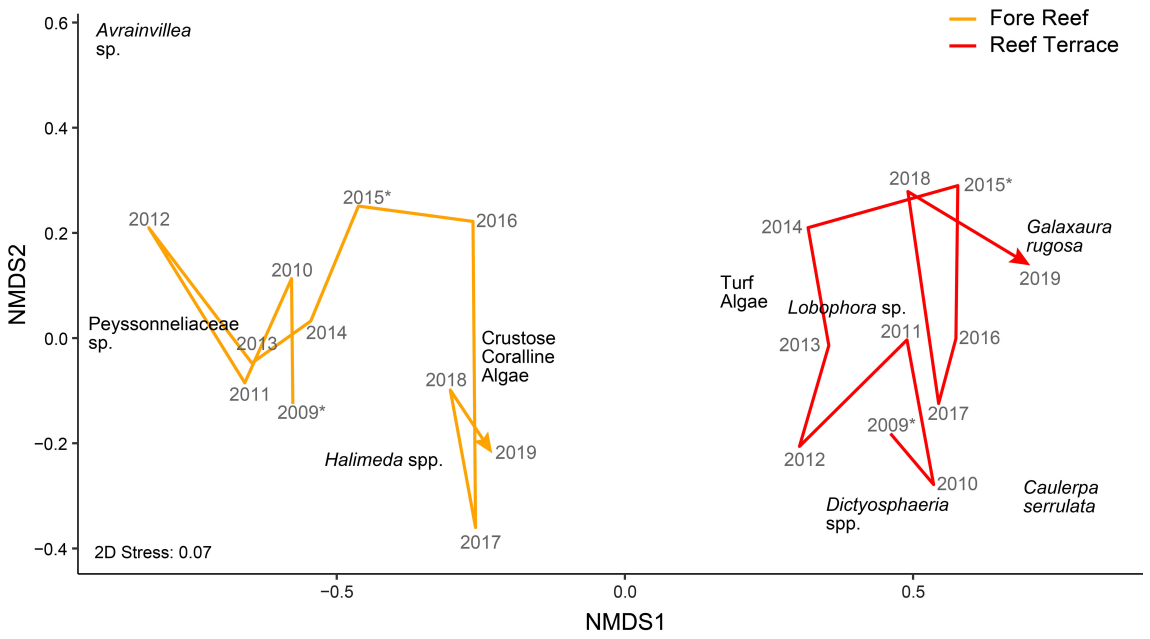

FIGURE 2
Non-metric multidimensional scaling (nMDS) based on Bray-Curtis dissimilarity measures of benthic algal community composition by taxon (in terms of square-root-transformed percent cover data). Lines terminating in an arrowhead represent the yearly trajectory of each habitat (Fore Reef in orange, Reef Terrace in red) from 2009 to 2019. Asterisks denote thermal anomalies in 2009 and 2015.

second thermal anomaly was seen to a lesser extent on the fore reef. However, by fall 2017, turf and CCA cover were restored to pre-disturbance levels in both habitats. Other algal groups were far less abundant than turf and CCA. Benthic cover of *C. serrulata*, found almost exclusively on the reef terrace, was highest in the fall of 2010 and 2019 at 3.6 ± 1.5%, but dropped to undetectable levels in fall 2012, 2014, and 2018 (Figure 3A). Similarly, also on the reef terrace, *Dictyosphaeria* spp. (*D. cavernosa* and *D. versluysii*) comprised up to 1.5% total cover but were nearly negligible in the fall of 2014, 2015, 2018, and 2019 (Figure 3C). The reef terrace had 4.3 ± 0.6% cover of *G. rugosa* in fall 2019 but was typically around 2.5% (Figure 3D). There was consistently higher cover of *Lobophora* sp. on the reef terrace (5.0 ± 0.5%) compared to the fore reef (1.9 ± 0.2%; Figure 3F). Cover of Peyssonneliaceae sp., found mainly at the fore reef, was lowest in the fall of 2017 at 1.2 ± 0.3% yet reached up to 10-15% of the benthos every fall between 2011 and 2014 (Figure 3G). *Avrainvillea* sp. was not plotted because it occupied less than 0.01% of the benthos. *Halimeda* spp. (primarily *H. opuntia* with minor coverage by *H. taenicola* and *H. fragilis*) were more abundant on the fore reef, at 14.2 ± 0.8% cover throughout the time series compared to 4.4 ± 0.3% on the reef terrace (Figure 3E).

3.3 Calcareous vs. fleshy algal trajectories by habitat

Throughout the time series, the fore reef had higher cover of calcareous algae than fleshy algae, at 46.5 ± 0.8% (mean ± SE) and 13.4 ± 0.5%, respectively (Figure 4A), whereas the reef terrace had similar cover of calcareous and fleshy algae, at 22.1 ± 0.8% and 28.0 ± 0.9%, respectively (Figure 4B). Percent cover of fleshy algae varied by habitat ($p < 0.001$) and year ($p < 0.001$) with no significant interaction (Supplementary Table 3). Percent cover of calcareous algae also varied by habitat ($p < 0.001$) and year ($p = 0.004$), with habitats changing differently over time ($p = 0.011$). On the reef terrace, the cover of calcareous algae remained consistent through time whereas on the fore reef, calcareous algae were replaced by fleshy algae at the time of the second thermal anomaly in 2015 but re-stabilized by fall 2017. A similar yet less pronounced response was observed on the reef terrace.

3.4 Abundance of *Halimeda* spp. with respect to temperature

Several months after the first thermal anomaly, *Halimeda* cover dropped from 18.8 ± 3.2% (mean ± SE) in fall 2009 to 5.8 ± 0.8% in spring 2010 on the fore reef and 5.4 ± 1.0% to 2.2 ± 0.4% on the reef terrace (Figure 3E). By late summer 2010, *Halimeda* cover had decreased significantly at four out of eight sites (Supplementary Table 5) but increased in subsequent years. Between fall 2014 and fall 2015, *Halimeda* cover decreased again at all sites; its cover during the second thermal anomaly was among its lowest throughout the time series, at 4.5 ± 0.9% on the fore reef and 0.7 ± 0.2% on the reef terrace. Regardless of the amount of *Halimeda* within each quadrat or site, its abundance followed a similar trajectory with sharp declines by 2015, and growth or no change thereafter (Supplementary Figure 2). Between fall 2016 and fall 2017, *Halimeda* cover increased significantly at six out of eight sites by up to 20% (Supplementary Table 5). Thus, in all cases where significant differences were detected,

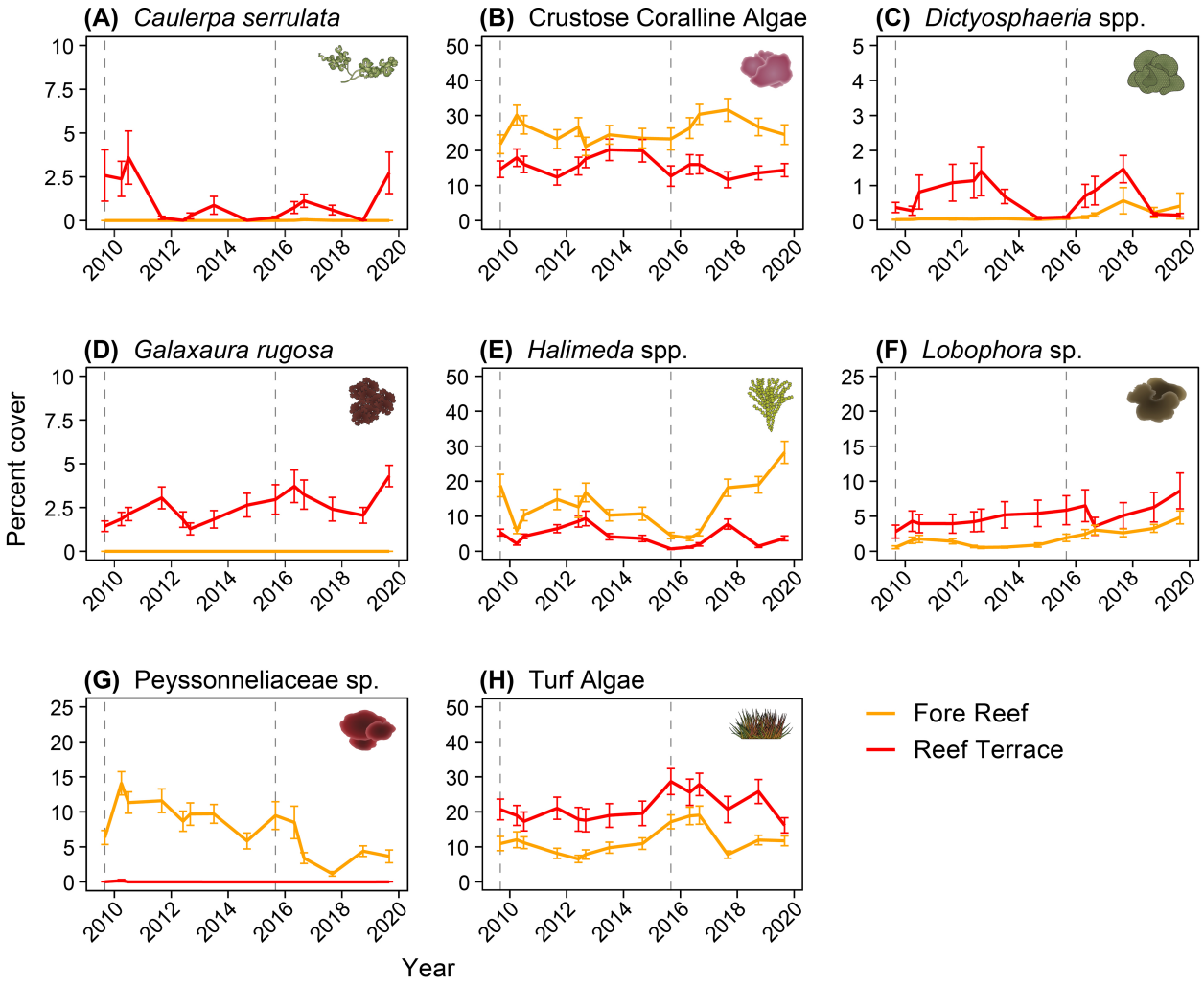

FIGURE 3
Percent cover (mean ± SE) of **(A)** *Caulerpa serrulata*, **(B)** Crustose Coralline Algae, **(C)** *Dictyosphaeria spp.*, **(D)** *Galaxaura rugosa*, **(E)** *Halimeda spp.*, **(F)** *Lobophora sp.*, **(G)** Peyssonneliaceae sp., and **(H)** Turf Algae, by habitat (Fore Reef in orange, Reef Terrace in red). Dashed vertical lines indicate thermal anomalies in 2009 and 2015.

the sites that changed did so in the same direction. There were significant effects of percentile-based DHW ($p = 0.023$) and habitat ($p < 0.001$) on *Halimeda* cover (Supplementary Table 4). A negative relationship between *Halimeda* cover and accumulated thermal stress was seen (Figure 5), with a linear correlation on the reef terrace (Pearson's $r = -0.65$, $p = 0.03$) but not on the fore reef (Pearson's $r = -0.03$, $p = 0.92$).

4 Discussion

As corals suffer widespread declines due to climate change, there has been a corresponding rise in the abundance of algae on reefs worldwide (Pandolfi et al., 2003; Hughes et al., 2017; Reverter et al., 2021). However, "algae" encompass a heterogenous group of functionally, phylogenetically, morphologically, and taxonomically distinct taxa (Fong and Paul, 2011). While short-term changes in macroalgal abundance on coral reefs, including seasonality, have been well-documented (Aguila Ramírez et al., 2003; Ateweberhan et al., 2006; Lefèvre and Bellwood, 2010), longer-term dynamics of benthic algae at the community, functional group, or species level remain poorly characterized. Here, we present results of an 11-year time series from Palmyra Atoll in the central Pacific Ocean. From 2009 to 2019, the cover of fleshy and calcareous algae was more stable at the reef terrace but fluctuated at the fore reef. At the time of the second, more-severe thermal anomaly in 2015, there was a general decrease in calcareous algae at both habitats accompanied by an increase in fleshy algae which was restored within two years. Given Palmyra's remote location and high level of federal protection, such data sets can provide baseline information on coral reef algal communities in the context of global stressors.

Long-term ecological monitoring is necessary for detecting trends in species abundance and distribution through time. Prior to this study, the latest comprehensive analysis of Palmyra's benthic algal community composition was based on summary data from surveys conducted sporadically between 2004 to 2008 (Braun et al., 2009). Before that, knowledge of algal diversity on Palmyra was limited to early explorers' species lists (Rock, 1916; Dawson et al.,

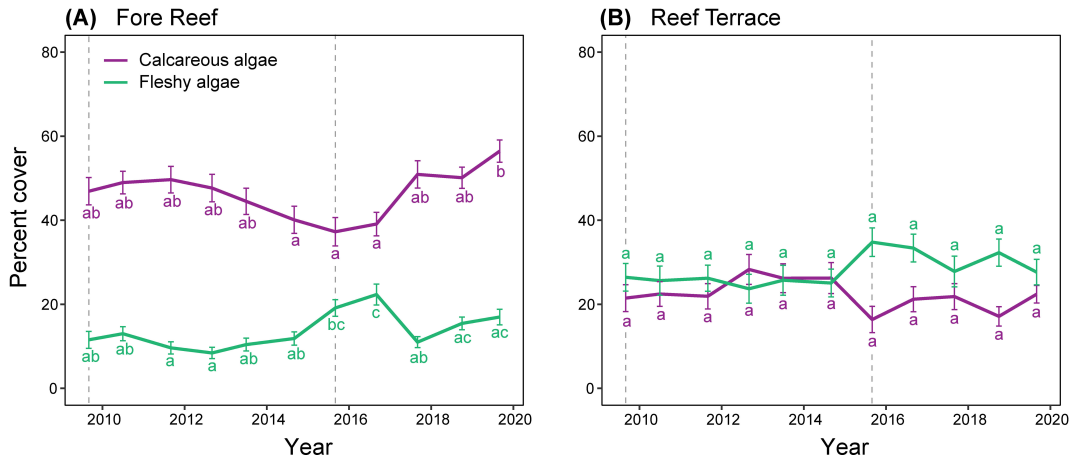

FIGURE 4
Percent cover (mean ± SE) of calcareous (in purple) and fleshy algae (in green) on Palmyra at the **(A)** Fore Reef and **(B)** Reef Terrace habitats, along with *post-hoc* letter groupings for significant (α = 0.01) differences among years. Dashed vertical lines indicate thermal anomalies in 2009 and 2015.

1955; Dawson, 1959). In 2008, the most abundant macroalgal genera on Palmyra were *Halimeda*, *Lobophora*, *Galaxaura*, and *Dictyosphaeria* (Braun et al., 2009). This remained consistent through 2019, although we also identified *C. serrulata* as a common macroalgal taxon on the reef terrace (Supplementary Table 2). Additionally, Braun et al. (2009) mentioned high cover of the red alga *Dichotomaria marginata* near a shipwrecked longliner vessel which was removed in 2013. *Dichotomaria* was absent from our analyses, although not all of the same reef habitats or sites were represented here, and our study involved small-scale photoquadrats as opposed to large spatial scale surveys. Braun et al. (2009) found algal communities to be relatively similar across sites from the reef terrace and fore reef habitats across the atoll, whereas in the present study, algal communities showed significant differences by habitat and time, with more overall stability at the reef terrace. Calcareous algal cover was consistently higher at the fore reef, although it is worthwhile to note that Palmyra's reef terrace is largely occupied (up to 50%) by hard corals (Fox et al., 2019; Khen et al., 2022, 2024). Overall, fleshy algal abundance on Palmyra (average percent cover = 20.8%) was low in comparison to

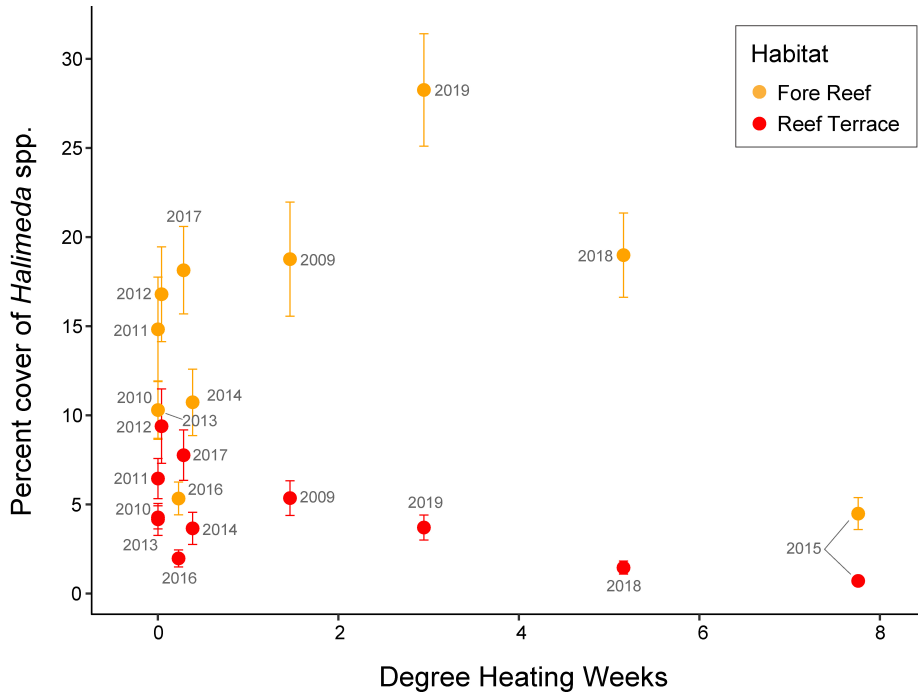

FIGURE 5
Percent cover of *Halimeda* spp. (mean ± SE) by habitat (Fore Reef in orange, Reef Terrace in red) corresponding to the percentile-based Degree Heating Weeks (DHW) at each observation time point, labeled by year.

reefs with local human populations (average percent cover = 59.3% according to Smith et al., 2016) whereas calcareous algal abundance (average percent cover = 34.4%) was much higher than that of inhabited islands (average percent cover = 16.9%; Smith et al., 2016).

4.1 Environmental drivers of algal community structure

Ecological succession and community structure can be shaped by physical forces such as light and sediment transport (Glynn, 1976), irradiance and water motion (Done, 1982), and wave energy (Dollar, 1982). On Palmyra, local environmental factors likely contributed to the spatial variability in benthic algal communities by habitat. The shallower, wave-sheltered reef terrace, which receives more light, solar irradiance (Hamilton et al., 2014), and an influx of nutrients and sediments from the nearby lagoon (Rogers et al., 2017), had a higher relative abundance of turf and other fleshy algae throughout the study (Figure 1; Supplementary Figure 1). The fore reef, which is subject to more wave action and water motion (Williams et al., 2013; Hamilton et al., 2014; Gove et al., 2015), had a higher relative abundance of calcareous algae. Calcified crusts such as CCA and peyssonnelioid taxa are resistant to high wave energy, which may explain their dominance at this habitat, as has been seen elsewhere in the tropical Pacific (Page-Albins et al., 2012). Coralline algae can also shed their epithallial cells to prevent fouling by fleshy organisms and reinforce their foundation in wave-exposed habitats (Keats et al., 1997b). Articulated algal morphologies such as *Halimeda* are more vulnerable to dislodgement by waves (Steneck and Dethier, 1994), but nutrients supplied from upwelling and internal tides on the fore reef (Williams et al., 2018) may have promoted their growth (Smith et al., 2004). While temperature could be expected to differ by habitat, our observations were limited to 10 m depth and upwelling-induced cooling on Palmyra has only been found to occur below 15 m (Fox et al., 2023).

4.2 Role of herbivory in benthic algal communities

Although we did not quantify herbivore abundance in this study, given that Palmyra has very high fish biomass (Williams et al., 2011; Edwards et al., 2014) and that grazing pressure drives algal succession (Carpenter, 1986; Hixon and Brostoff, 1996), biological factors such as grazing may have further contributed to differences in algal community structure. In our photoquadrat time series, algal turfs often appeared cropped (pers. obs.), indicative of grazing. Herbivores can help control fleshy algal cover (Littler et al., 2006; Burkepile and Hay, 2009) and their presence is associated with higher cover of corals and CCA (Smith et al., 2010). With herbivores now being used as a restoration tool to reverse coral-algal phase shifts on degraded reefs (Mumby, 2014; Ladd and Shantz, 2020), Palmyra exemplifies the role of herbivory in maintaining a "healthy" calcifier-dominated reef. Palmyra's reef system is dominated by top predators and larger-bodied grazers (e.g., parrotfish and surgeonfish) as opposed to small planktivores or echinoids (Sandin et al., 2008). Hamilton et al. (2014) found that Palmyra's reef terrace had a higher density of herbivorous fish and higher grazing intensity (in terms of bite rates) than the fore reef. Most herbivorous fish on Palmyra feed preferentially on algal turfs (Hamilton et al., 2014), which are more abundant on the reef terrace (although parrotfish bite scars are also seen frequently on CCA on the fore reef; see Charendoff et al., 2023), suggesting that habitat-specific differences in algal and herbivore assemblages are interrelated.

4.3 Evidence of thermal sensitivity in *Halimeda* spp.

Our study also provides observational evidence that the calcareous macroalgal genus, *Halimeda*, may be sensitive to warming. At both habitats on Palmyra, benthic cover of *Halimeda* was among its lowest in 2015 (Figure 5), when percentile-based DHWs reached a value of 7.76 (or a monthly mean sea surface temperature of 29.8 °C; National Oceanic and Atmospheric Administration's Coral Reef Watch). Perhaps if temperatures on Palmyra had reached a more extreme upper limit, this would have had a more measurable impact on *Halimeda* cover across the atoll. It has previously been proposed that *Halimeda* growth and calcification could benefit from seawater temperatures ranging from 24 to 32 °C, but that temperatures above 34 °C will have consequences that may become lethal at 36 °C (Wei et al., 2020). Other experimental studies have shown that exposure to elevated temperatures can either inhibit (Sinutok et al., 2011) or enhance (Campbell et al., 2016) photosynthetic efficiency, calcification, and growth in *Halimeda* spp., indicating that results may be context-dependent or species-specific (Schubert et al., 2023). Given their role in both primary and calcium carbonate production on reefs (Rees et al., 2007), and as a preferred food source to many reef fishes (Mantyka and Bellwood, 2007; Hamilton et al., 2014), refining the thermal sensitivity limits of *Halimeda* by species (while also taking into account accumulated thermal stress) and identifying the mechanisms behind this observed phenomenon will be ecologically relevant in the face of global climate change.

5 Conclusion

In conclusion, more species-specific studies on the thermal tolerance of benthic algae are needed in order to better understand current and potential impacts of climate change on coral reefs. Additionally, comparing calcareous vs. fleshy responses of benthic algae *in situ* will be useful for assessing ecosystem status in the context of rising seawater temperatures. Long-term monitoring in relatively unimpacted locations, such as Palmyra Atoll, allows us to track baseline algal community dynamics over time. To strengthen the value and resolution of these ecological data sets, future efforts should consider larger-scale surveys with higher sampling frequency. Although Palmyra's reefs have remained

calcifier-dominated as of 2019, successional trajectories from Palmyra could inform mitigation strategies at more degraded reefs shifting toward fleshy algal dominance.

Data availability statement

The datasets presented in this study can be found in online repositories. The names of the repository/repositories and accession number(s) can be found below: https://github.com/akhen1/palmyra-algae.

Author contributions

AK: Conceptualization, Data curation, Formal Analysis, Funding acquisition, Investigation, Visualization, Writing – original draft, Writing – review & editing, Methodology. MJ: Conceptualization, Investigation, Methodology, Writing – review & editing. MF: Conceptualization, Formal Analysis, Investigation, Methodology, Writing – review & editing. JS: Conceptualization, Funding acquisition, Investigation, Resources, Supervision, Writing – review & editing, Methodology, Project administration.

Funding

The author(s) declare that financial support was received for the research, authorship, and/or publication of this article. AK was supported by the National Science Foundation Graduate Research Fellowship (Award No. 1650112) and the Beyster Family Fellowship in Conservation and Biodiversity. Funding for this work was generously provided by the Scripps Family Foundation, the Bohn Family, and the Gordon and Betty Moore Foundation.

Acknowledgments

We thank the staff of The Nature Conservancy, U.S. Fish and Wildlife Service, and the Palmyra Atoll Research Consortium (PARC) for their logistical support and access to the refuge. This publication is PARC contribution #168. We thank Gareth Williams, Brian Zgliczynski, Clinton Edwards, Amanda Carter, Samantha Clements, and Stuart Sandin for their assistance with fieldwork. We thank Karina Arzuyan, Marie Diaz, Sarah Romero, Kyle Conner, Shelley Hazen, and Kailey Ramsing for their help with image digitization.

Conflict of interest

The authors declare that the research was conducted in the absence of any commercial or financial relationships that could be construed as a potential conflict of interest.

The author(s) declared that they were an editorial board member of Frontiers, at the time of submission. This had no impact on the peer review process and the final decision.

Generative AI statement

The author(s) declare that no Generative AI was used in the creation of this manuscript.

Publisher's note

Supplementary material

The Supplementary Material for this article can be found online at: https://www.frontiersin.org/articles/10.3389/fmars.2025.1539865/full#supplementary-material

References

Adey, W. H., and Steneck, R. S. (1985). Highly productive eastern Caribbean reefs: Synergistic effects of biological, chemical, physical, and geological factors. *Ecol. Coral Reefs* 3, 163–187.

Aguila Ramírez, R., Valdez, M. C., García, S. O., López, R. N., and Ayala, M. C. (2003). Spatial and seasonal variation of macroalgal biomass in Laguna Ojo de Liebre, Baja California Sur, Mexico. *Hydrobiologia* 501, 207–214. doi: 10.1023/A:1026210312362

Anderson, M. J. (2001). A new method for non-parametric multivariate analysis of variance. *Austral Ecol.* 26, 32–46. doi: 10.1111/j.1442-9993.2001.01070.pp.x

Ateweberhan, M., Bruggemann, J., and Breeman, A. (2006). Effects of extreme seasonality on community structure and functional group dynamics of coral reef algae in the southern Red Sea (Eritrea). *Coral Reefs* 25, 391–406. doi: 10.1007/s00338-006-0109-6

Balata, D., Piazzi, L., and Rindi, F. (2011). Testing a new classification of morphological functional groups of marine macroalgae for the detection of responses to stress. *Mar. Biol.* 158, 2459–2469. doi: 10.1007/s00227-011-1747-y

Barott, K. L., Williams, G. J., Vermeij, M. J., Harris, J., Smith, J. E., Rohwer, F. L., et al. (2012). Natural history of coral–algae competition across a gradient of human activity in the Line Islands. *Mar. Ecol. Prog. Ser.* 460, 1–12. doi: 10.3354/meps09874

Birrell, C. L., Mccook, L. J., and Willis, B. L. (2005). Effects of algal turfs and sediment on coral settlement. *Mar. pollut. Bull.* 51, 408–414. doi: 10.1016/j.marpolbul.2004.10.022

Birrell, C. L., Mccook, L. J., Willis, B. L., and Diaz-Pulido, G. A. (2008). Effects of benthic algae on the replenishment of corals and the implications for the resilience of coral reefs. *Oceanogr. Mar. Biol. Annu. Rev.* 46, 25–63. doi: 10.1201/9781420065756-4

Braun, C., Smith, J., and Vroom, P. (2009). "Examination of algal diversity and benthic community structure at Palmyra Atoll, US Line Islands," in *Proc 11th Coral Reef Symp*, Ft. Lauderdale, Florida. 865–869.

Brown, K. T., Bender-Champ, D., Hoegh-Guldberg, O., and Dove, S. (2020). Seasonal shifts in the competitive ability of macroalgae influence the outcomes of coral–algal competition. *R. Soc. Open Sci.* 7, 201797. doi: 10.1098/rsos.201797

Burkepile, D. E., and Hay, M. E. (2009). Nutrient versus herbivore control of macroalgal community development and coral growth on a Caribbean reef. *Mar. Ecol. Prog. Ser.* 389, 71–84. doi: 10.3354/meps08142

Burt, J. A., Al-Khalifa, K., Khalaf, E., Alshuwaikh, B., and Abdulwahab, A. (2013). The continuing decline of coral reefs in Bahrain. *Mar. pollut. Bull.* 72, 357–363. doi: 10.1016/j.marpolbul.2012.08.022

Campbell, J. E., Fisch, J., Langdon, C., and Paul, V. J. (2016). Increased temperature mitigates the effects of ocean acidification in calcified green algae (*Halimeda* spp.). *Coral Reefs* 35, 357–368. doi: 10.1007/s00338-015-1377-9

Carpenter, R. C. (1986). Partitioning herbivory and its effects on coral reef algal communities. *Ecol. Monogr.* 56, 345–364. doi: 10.2307/1942551

Charendoff, J. A., Edwards, C. B., Pedersen, N. E., Petrovic, V., Zgliczynski, B., Sandin, S. A., et al. (2023). Variability in composition of parrotfish bite scars across space and over time on a central Pacific atoll. *Coral Reefs* 42, 905–918. doi: 10.1007/s00338-023-02392-6

Clarke, K. R. (1993). Non-parametric multivariate analyses of changes in community structure. *Aust. J. Ecol.* 18, 117–143. doi: 10.1111/j.1442-9993.1993.tb00438.x

Clifton, K. E. (2013). The ecological significance of sexual reproduction by tropical green algae. *Smithsonian Contributions to the Marine Sciences* 39, 219–228.

Clifton, K. E., and Clifton, L. M. (1999). The phenology of sexual reproduction by green algae (Bryopsidales) on Caribbean coral reefs. *J. Phycol.* 35, 24–34. doi: 10.1046/j.1529-8817.1999.3510024.x

Cornwall, C. E., Carlot, J., Branson, O., Courtney, T. A., Harvey, B. P., Perry, C. T., et al. (2023). Crustose coralline algae can contribute more than corals to coral reef carbonate production. *Commun. Earth Environ.* 4, 105. doi: 10.1038/s43247-023-00766-w

Darling, E. S., McClanahan, T. R., and Côté, I. M. (2010). Combined effects of two stressors on Kenyan coral reefs are additive or antagonistic, not synergistic. *Conserv. Lett.* 3, 122–130. doi: 10.1111/j.1755-263X.2009.00089.x

Davison, I. R. (1991). Environmental effects on algal photosynthesis: Temperature. *J. Phycol.* 27, 2–8. doi: 10.1111/j.0022-3646.1991.00002.x

Dawson, E. (1959). Changes in Palmyra Atoll and its vegetation through the activities of man 1913-1958. *Pacif. Naturalist* 1, 1-51.

Dawson, E. Y., Aleem, A. A., and Halstead, B. W. (1955). Marine algae from Palmyra Island with special reference to the feeding habits and toxicology of reef fishes. *Occ. Pap. Allan Hancock Fdn.* 17, 1–39.

Diaz-Pulido, G., Anthony, K., Kline, D., Dove, S., and Hoegh-Guldberg, O. (2012). Interactions between ocean acidification and warming on the mortality and dissolution of coralline algae. *J. Phycol.* 48, 32–39. doi: 10.1111/j.1529-8817.2011.01084.x

Diaz-Pulido, G., and McCook, L. J. (2002). The fate of bleached corals: Patterns and dynamics of algal recruitment. *Mar. Ecol. Prog. Ser.* 232, 115–128. doi: 10.3354/meps232115

Dollar, S. (1982). Wave stress and coral community structure in Hawaii. *Coral Reefs* 1, 71–81. doi: 10.1007/BF00301688

Done, T. (1982). Patterns in the distribution of coral communities across the central Great Barrier Reef. *Coral Reefs* 1, 95–107. doi: 10.1007/BF00301691

Edwards, C. B., Friedlander, A., Green, A., Hardt, M., Sala, E., Sweatman, H., et al. (2014). Global assessment of the status of coral reef herbivorous fishes: Evidence for fishing effects. *Proc. R. Soc. B: Biol. Sci.* 281, 20131835. doi: 10.1098/rspb.2013.1835

Ellis, J. I., Jamil, T., Anlauf, H., Coker, D. J., Curdia, J., Hewitt, J., et al. (2019). Multiple stressor effects on coral reef ecosystems. *Global Change Biol.* 25, 4131–4146. doi: 10.1111/gcb.14819

Falkenberg, L. J., Russell, B. D., and Connell, S. D. (2013). Contrasting resource limitations of marine primary producers: Implications for competitive interactions under enriched CO_2 and nutrient regimes. *Oecologia* 172, 575–583. doi: 10.1007/s00442-012-2507-5

Fong, C. R., and Fong, P. (2014). Why species matter: an experimental assessment of assumptions and predictive ability of two functional-group models. *Ecology* 95, 2055–2061. doi: 10.1890/13-1557.1

Fong, P., and Paul, V. J. (2011). "Coral reef algae," in *Coral Reefs: An Ecosystem in Transition* (Dordrecht: Springer), 241–272.

Fox, M. D., Carter, A. L., Edwards, C. B., Takeshita, Y., Johnson, M. D., Petrovic, V., et al. (2019). Limited coral mortality following acute thermal stress and widespread bleaching on Palmyra Atoll, central Pacific. *Coral Reefs* 38, 701–712. doi: 10.1007/s00338-019-01796-7

Fox, M. D., Cohen, A. L., Rotjan, R. D., Mangubhai, S., Sandin, S. A., Smith, J. E., et al. (2021). Increasing coral reef resilience through successive marine heatwaves. *Geophysical Res. Lett.* 48, e2021GL094128. doi: 10.1029/2021GL094128

Fox, M. D., Guillaume-Castel, R., Edwards, C. B., Glanz, J., Gove, J. M., Green, J. M., et al. (2023). Ocean currents magnify upwelling and deliver nutritional subsidies to reef-building corals during El Niño heatwaves. *Sci. Adv.* 9, eadd5032. doi: 10.1126/sciadv.add5032

Glynn, P. W. (1976). Some physical and biological determinants of coral community structure in the eastern Pacific. *Ecol. Monogr.* 46, 431–456. doi: 10.2307/1942565

Gove, J. M., Williams, G. J., Mcmanus, M. A., Clark, S. J., Ehses, J. S., and Wedding, L. M. (2015). Coral reef benthic regimes exhibit non-linear threshold responses to natural physical drivers. *Mar. Ecol. Prog. Ser.* 522, 33–48. doi: 10.3354/meps11118

Graham, N. A., Jennings, S., Macneil, M. A., Mouillot, D., and Wilson, S. K. (2015). Predicting climate-driven regime shifts versus rebound potential in coral reefs. *Nature* 518, 94–97. doi: 10.1038/nature14140

Hamilton, S. L., Smith, J. E., Price, N. N., and Sandin, S. A. (2014). Quantifying patterns of fish herbivory on Palmyra Atoll (USA), an uninhabited predator-dominated central Pacific coral reef. *Mar. Ecol. Prog. Ser.* 501, 141–155. doi: 10.3354/meps10684

Harney, J., and Fletcher, C. III. (2003). A budget of carbonate framework and sediment production, Kailua Bay, Oahu, Hawaii. *J. Sedimentary Res.* 73, 856–868. doi: 10.1306/051503730856

Harrington, L., Fabricius, K., De'ath, G., and Negri, A. (2004). Recognition and selection of settlement substrata determine post-settlement survival in corals. *Ecology* 85, 3428–3437. doi: 10.1890/04-0298

Harris, J. L., Lewis, L., and Smith, J. (2015). Quantifying scales of spatial variability in algal turf assemblages on coral reefs. *Mar. Ecol. Prog. Ser.* 532, 41–57. doi: 10.3354/meps11344

Hay, M. (1997). Synchronous spawning—When timing is everything. *Science* 275, 1080–1081. doi: 10.1126/science.275.5303.1080

Hillis-Colinvaux, L. (1980). Ecology and taxonomy of *Halimeda*: Primary producer of coral reefs. *Adv. Mar. Biol.* 17, 1–327. doi: 10.1016/S0065-2881(08)60303-X

Hixon, M. A., and Brostoff, W. N. (1996). Succession and herbivory: Effects of differential fish grazing on Hawaiian coral-reef algae. *Ecol. Monogr.* 66, 67–90. doi: 10.2307/2963481

Hothorn, T., Bretz, F., and Westfall, P. (2008). Simultaneous inference in general parametric models. *Biometrical Journal: J. Math. Methods Biosci.* 50, 346–363. doi: 10.1002/bimj.200810425

Hughes, T. P., Barnes, M. L., Bellwood, D. R., Cinner, J. E., Cumming, G. S., Jackson, J. B., et al. (2017). Coral reefs in the anthropocene. *Nature* 546, 82–90. doi: 10.1111/1365-2435.13247

Hughes, T. P., Graham, N. A., Jackson, J. B., Mumby, P. J., and Steneck, R. S. (2010). Rising to the challenge of sustaining coral reef resilience. *Trends Ecol. Evol.* 25, 633–642. doi: 10.1016/j.tree.2010.07.011

Johnson, M. D., Comeau, S., Lantz, C. A., and Smith, J. E. (2017). Complex and interactive effects of ocean acidification and temperature on epilithic and endolithic coral-reef turf algal assemblages. *Coral Reefs* 36, 1059–1070. doi: 10.1007/s00338-017-1597-2

Johnson, M. D., Price, N. N., and Smith, J. E. (2014). Contrasting effects of ocean acidification on tropical fleshy and calcareous algae. *PeerJ* 2, e411. doi: 10.7717/peerj.411

Keats, D., Chamberlain, Y., and Baba, M. (1997a). *Pneophyllum conicum* (Dawson) comb. nov.(Rhodophyta, Corallinaceae), a widespread Indo-Pacific non-geniculate coralline alga that overgrows and kills live coral. *Botanica Marina* 40, 263–279. doi: 10.1515/botm.1997.40.1-6.263

Keats, D., Knight, M., and Pueschel, C. (1997b). Antifouling effects of epithallial shedding in three crustose coralline algae (Rhodophyta, Corallinales) on a coral reef. *J. Exp. Mar. Biol. Ecol.* 213, 281–293. doi: 10.1016/S0022-0981(96)02771-2

Khen, A., Fox, M. D., Johnson, M. D., Wall, C. B., and Smith, J. E. (2024). Inter-and intraspecific responses of coral colonies to thermal anomalies on Palmyra Atoll, central Pacific. *PloS One* 19, e0312409. doi: 10.1371/journal.pone.0312409

Khen, A., Johnson, M. D., Fox, M. D., Clements, S. M., Carter, A. L., and Smith, J. E. (2022). Decadal stability of coral reef benthic communities on Palmyra Atoll, central Pacific, through two bleaching events. *Coral Reefs* 41, 1–13. doi: 10.1007/s00338-022-02271-6

Kram, S., Price, N., Donham, E., Johnson, M., Kelly, E., Hamilton, S., et al. (2016). Variable responses of temperate calcified and fleshy macroalgae to elevated pCO_2 and warming. *ICES J. Mar. Sci.* 73, 693–703. doi: 10.1093/icesjms/fsv168

Krieger, E. C., Taise, A., Nelson, W. A., Grand, J., Le Ru, E., Davy, S. K., et al. (2023). Tolerance of coralline algae to ocean warming and marine heatwaves. *PloS Climate* 2, e0000092. doi: 10.1371/journal.pclm.0000092

Ladd, M. C., and Shantz, A. A. (2020). Trophic interactions in coral reef restoration: A review. *Food Webs* 24, e00149. doi: 10.1016/j.fooweb.2020.e00149

Lambo, A., and Ormond, R. (2006). Continued post-bleaching decline and changed benthic community of a Kenyan coral reef. *Mar. pollut. Bull.* 52, 1617–1624. doi: 10.1016/j.marpolbul.2006.05.028

Lefèvre, C. D., and Bellwood, D. R. (2010). Seasonality and dynamics in coral reef macroalgae: Variation in condition and susceptibility to herbivory. *Mar. Biol.* 157, 955–965. doi: 10.1007/s00227-009-1376-x

Littler, M. M., and Littler, D. S. (1980). The evolution of thallus form and survival strategies in benthic marine macroalgae: Field and laboratory tests of a functional form model. *Am. Nat.* 116, 25–44. doi: 10.1086/283610

Littler, M. M., and Littler, D. S. (2013). The nature of crustose coralline algae and their interactions on reefs. *Smithson. Contrib. Mar. Sci.* 39, 199–212.

Littler, M. M., Littler, D. S., and Brooks, B. L. (2006). Harmful algae on tropical coral reefs: Bottom-up eutrophication and top-down herbivory. *Harmful Algae* 5, 565–585. doi: 10.1016/j.hal.2005.11.003

Littler, M. M., Littler, D. S., and Taylor, P. R. (1983). Evolutionary strategies in a tropical barrier reef system: Functional-form groups of marine macroalgae. *J. Phycol.* 19, 229–237. doi: 10.1111/j.0022-3646.1983.00229.x

Liu, G., Strong, A. E., Skirving, W., and Arzayus, L. F. (2006). "Overview of NOAA coral reef watch program's near-real time satellite global coral bleaching monitoring activities," in *Proc 10th Int Coral Reef Symp*, Okinawa. 1783–1793.

Longo, G., and Hay, M. (2015). Does seaweed–coral competition make seaweeds more palatable? *Coral Reefs* 34, 87–96. doi: 10.1007/s00338-014-1230-6

Mantyka, C. S., and Bellwood, D. R. (2007). Macroalgal grazing selectivity among herbivorous coral reef fishes. *Mar. Ecol. Prog. Ser.* 352, 177–185. doi: 10.3354/meps07055

Martin, S., and Gattuso, J.-P. (2009). Response of Mediterranean coralline algae to ocean acidification and elevated temperature. *Global Change Biol.* 15, 2089–2100. doi: 10.1111/j.1365-2486.2009.01874.x

Mauffrey, A. R., Cappelatti, L., and Griffin, J. N. (2020). Seaweed functional diversity revisited: Confronting traditional groups with quantitative traits. *J. Ecol.* 108, 2390–2405. doi: 10.1111/1365-2745.13460

McClanahan, T., Muthiga, N., and Mangi, S. (2001). Coral and algal changes after the 1998 coral bleaching: Interaction with reef management and herbivores on Kenyan reefs. *Coral Reefs* 19, 380–391. doi: 10.1007/s003380000133

McManus, J. W., and Polsenberg, J. F. (2004). Coral–algal phase shifts on coral reefs: Ecological and environmental aspects. *Prog. Oceanogr.* 60, 263–279. doi: 10.1016/j.pocean.2004.02.014

Mollica, N. R., Cohen, A. L., Alpert, A. E., Barkley, H. C., Brainard, R. E., Carilli, J. E., et al. (2019). Skeletal records of bleaching reveal different thermal thresholds of Pacific coral reef assemblages. *Coral Reefs* 38, 743–757. doi: 10.1007/s00338-019-01803-x

Mumby, P. J. (2014). Stratifying herbivore fisheries by habitat to avoid ecosystem overfishing of coral reefs. *Fish Fisheries* 17, 266–278. doi: 10.1111/faf.12078

Oksanen, J., Blanchet, F. G., Friendly, M., Kindt, R., Legendre, P., Mcglinn, D., et al. (2019). *vegan: Community Ecology Package. R package version 2.5-6*. Available online at: https://CRAN.R-project.org/package=vegan.

Page, T. M., Bergstrom, E., and Diaz-Pulido, G. (2021). Acclimation history of elevated temperature reduces the tolerance of coralline algae to additional acute thermal stress. *Front. Mar. Sci.* 8. doi: 10.3389/fmars.2021.660196

Page-Albins, K. N., Vroom, P. S., Hoeke, R., Albins, M. A., and Smith, C. M. (2012). Patterns in Benthic Coral Reef Communities at Pearl and Hermes Atoll along a Wave-Exposure Gradient. *Pacific Sci.* 66, 481–496. doi: 10.2984/66.4.6

Pandolfi, J. M., Bradbury, R. H., Sala, E., Hughes, T. P., Bjorndal, K. A., Cooke, R. G., et al. (2003). Global trajectories of the long-term decline of coral reef ecosystems. *Science* 301, 955–958. doi: 10.1126/science.1085706

Perry, C. T., Morgan, K. M., Lange, I. D., and Yarlett, R. T. (2020). Bleaching-driven reef community shifts drive pulses of increased reef sediment generation. *R. Soc. Open Sci.* 7, 192153. doi: 10.1098/rsos.192153

Phillips, J., Kendrick, G., and Lavery, P. (1997). A test of a functional group approach to detecting shifts in macroalgal communities along a disturbance gradient. *Mar. Ecol. Prog. Ser.* 153, 125–138. doi: 10.3354/meps153125

Pratte, Z. A., Longo, G. O., Burns, A. S., Hay, M. E., and Stewart, F. J. (2018). Contact with turf algae alters the coral microbiome: Contact versus systemic impacts. *Coral Reefs* 37, 1–13. doi: 10.1007/s00338-017-1615-4

Rasher, D. B., and Hay, M. E. (2010). Chemically rich seaweeds poison corals when not controlled by herbivores. *Proc. Natl. Acad. Sci.* 107, 9683–9688. doi: 10.1073/pnas.0912095107

R Core Team (2018). *R: A language and environment for statistical computing* (Vienna, Austria: R Foundation for Statistical Computing). Available at: https://www.R-project.org/.

Rees, S., Opdyke, B., Wilson, P., and Henstock, T. (2007). Significance of *Halimeda* bioherms to the global carbonate budget based on a geological sediment budget for the Northern Great Barrier Reef, Australia. *Coral Reefs* 26, 177–188. doi: 10.1007/s00338-006-0166-x

Reverter, M., Helber, S. B., Rohde, S., De Goeij, J. M., and Schupp, P. J. (2021). Coral reef benthic community changes in the Anthropocene: Biogeographic heterogeneity, overlooked configurations, and methodology. *Global Change Biol.* 28, 1956–1971. doi: 10.1111/gcb.16034

Rock, J. F. (1916). "Palmyra Island: With a Description of Its Flora." *Bull. Coll. Hawaii Publ.* 4, 1–53.

Rogers, J. S., Monismith, S. G., Fringer, O. B., Koweek, D. A., and Dunbar, R. B. (2017). A coupled wave-hydrodynamic model of an atoll with high friction: Mechanisms for flow, connectivity, and ecological implications. *Ocean Model.* 110, 66–82. doi: 10.1016/j.ocemod.2016.12.012

Ryznar, E. R., Fong, P., and Fong, C. R. (2021). When form does not predict function: Empirical evidence violates functional form hypotheses for marine macroalgae. *J. Ecol.* 109, 833–846. doi: 10.1111/1365-2745.13509

Sandin, S. A., Smith, J. E., Demartini, E. E., Dinsdale, E. A., Donner, S. D., Friedlander, A. M., et al. (2008). Baselines and degradation of coral reefs in the Northern Line Islands. *PloS One* 3, e1548. doi: 10.1371/journal.pone.0001548

Schubert, N., Alvarez-Filip, L., and Hofmann, L. C. (2023). Systematic review and meta-analysis of ocean acidification effects in *Halimeda*: Implications for algal carbonate production. *Climate Change Ecol.* 4, 100059. doi: 10.1016/j.ecochg.2022.100059

Short, J., Foster, T., Falter, J., Kendrick, G. A., and Mcculloch, M. T. (2015). Crustose coralline algal growth, calcification and mortality following a marine heatwave in Western Australia. *Continental Shelf Res.* 106, 38–44. doi: 10.1016/j.csr.2015.07.003

Sinutok, S., Hill, R., Doblin, M. A., Wuhrer, R., and Ralph, P. J. (2011). Warmer more acidic conditions cause decreased productivity and calcification in subtropical coral reef sediment-dwelling calcifiers. *Limnol. Oceanogr.* 56, 1200–1212. doi: 10.4319/lo.2011.56.4.1200

Smith, J. E., Brainard, R., Carter, A., Grillo, S., Edwards, C., Harris, J., et al. (2016). Re-evaluating the health of coral reef communities: Baselines and evidence for human impacts across the central Pacific. *Proc. R. Soc. B: Biol. Sci.* 283, 20151985. doi: 10.1098/rspb.2015.1985

Smith, J. E., Hunter, C. L., and Smith, C. M. (2010). The effects of top–down versus bottom–up control on benthic coral reef community structure. *Oecologia* 163, 497–507. doi: 10.1007/s00442-009-1546-z

Smith, J. E., Smith, C. M., Vroom, P. S., Beach, K. L., and Miller, S. (2004). Nutrient and growth dynamics of *Halimeda tuna* on Conch Reef, Florida Keys: Possible influence of internal tides on nutrient status and physiology. *Limnol. Oceanogr.* 49, 1923–1936. doi: 10.4319/lo.2004.49.6.1923

Stelling-Wood, T. P., Gribben, P. E., and Poore, A. G. (2020). Habitat variability in an underwater forest: Using a trait-based approach to predict associated communities. *Funct. Ecol.* 34, 888–898. doi: 10.1111/1365-2435.13523

Steneck, R. S. (1986). The ecology of coralline algal crusts: convergent patterns and adaptative strategies. *Annu. Rev. Ecol. Systematics* 71, 273–303. doi: 10.1146/annurev.es.17.110186.001421

Steneck, R. S., and Dethier, M. N. (1994). A functional group approach to the structure of algal-dominated communities. *Oikos* 69, 476–498. doi: 10.2307/3545860

Steneck, R. S., and Watling, L. (1982). Feeding capabilities and limitation of herbivorous mollusks: A functional group approach. *Mar. Biol.* 68, 299–319. doi: 10.1007/BF00409596

Tebbett, S. B., and Bellwood, D. R. (2019). Algal turf sediments on coral reefs: What's known and what's next. *Mar. pollut. Bull.* 149, 110542. doi: 10.1016/j.marpolbul.2019.110542

Teichert, S., Steinbauer, M., and Kiessling, W. (2020). A possible link between coral reef success, crustose coralline algae and the evolution of herbivory. *Sci. Rep.* 10, 17748. doi: 10.1038/s41598-020-73900-9

Titlyanov, E., Yakovleva, I., and Titlyanova, T. (2007). Interaction between benthic algae (*Lyngbya bouillonii*, *Dictyota dichotoma*) and scleractinian coral *Porites lutea* in direct contact. *J. Exp. Mar. Biol. Ecol.* 342, 282–291. doi: 10.1007/bf00409596

Vroom, P. S., Smith, C. M., Coyer, J. A., Walters, L. J., Hunter, C. L., Beach, K. S., et al. (2003). Field biology of *Halimeda tuna* (Bryopsidales, Chlorophyta) across a depth gradient: Comparative growth, survivorship, recruitment, and reproduction. *Hydrobiologia* 501, 149–166. doi: 10.1023/A:1026287816324

Wei, Z., Mo, J., Huang, R., Hu, Q., Long, C., Ding, D., et al. (2020). Physiological performance of three calcifying green macroalgae *Halimeda* species in response to altered seawater temperatures. *Acta Oceanologica Sin.* 39, 89–100. doi: 10.1007/s13131-019-1471-3

Wernberg, T., Smale, D. A., and Thomsen, M. S. (2012). A decade of climate change experiments on marine organisms: Procedures, patterns and problems. *Global Change Biol.* 18, 1491–1498. doi: 10.1111/j.1365-2486.2012.02656.x

Wickham, H. (2016). *ggplot2:* Elegant Graphics for Data Analysis. New York: Springer-Verlag.

Williams, G. J., Knapp, I. S., Maragos, J. E., and Davy, S. K. (2010). Modeling patterns of coral bleaching at a remote Central Pacific atoll. *Mar. pollut. Bull.* 60, 1467–1476. doi: 10.1016/j.marpolbul.2010.05.009

Williams, I. D., Richards, B. L., Sandin, S. A., Baum, J. K., Schroeder, R. E., Nadon, M. O., et al. (2011). Differences in reef fish assemblages between populated and remote reefs spanning multiple archipelagos across the central and western Pacific. *J. Mar. Biol.* 2011, 1-14. doi: 10.1155/2011/826234

Williams, G. J., Sandin, S. A., Zgliczynski, B. J., Fox, M. D., Gove, J. M., Rogers, J. S., et al. (2018). Biophysical drivers of coral trophic depth zonation. *Mar. Biol.* 165, 1–15. doi: 10.1007/s00227-018-3314-2

Williams, G. J., Smith, J. E., Conklin, E. J., Gove, J. M., Sala, E., and Sandin, S. A. (2013). Benthic communities at two remote Pacific coral reefs: Effects of reef habitat, depth, and wave energy gradients on spatial patterns. *PeerJ* 1, e81. doi: 10.7717/peerj.81

Wismer, S., Hoey, A. S., and Bellwood, D. R. (2009). Cross-shelf benthic community structure on the Great Barrier Reef: Relationships between macroalgal cover and herbivore biomass. *Mar. Ecol. Prog. Ser.* 376, 45–54. doi: 10.3354/meps07790

Woodhead, A. J., Hicks, C. C., Norström, A. V., Williams, G. J., and Graham, N. A. (2019). Coral reef ecosystem services in the Anthropocene. *Funct. Ecol.* 33, 1023–1034. doi: 10.1111/1365-2435.13331

frontiers | Frontiers in Marine Science

TYPE Original Research
PUBLISHED 13 March 2025
DOI 10.3389/fmars.2025.1537498

OPEN ACCESS

EDITED BY
Caitlin Blain,
The University of Auckland, New Zealand

REVIEWED BY
Yuyuan Xie,
University of South Florida, United States
Matthew Desmond,
University of Otago, New Zealand

*CORRESPONDENCE
L. Man
longching.man@gmail.com

RECEIVED 01 December 2024
ACCEPTED 13 February 2025
PUBLISHED 13 March 2025

CITATION
Man L, Barbosa RV, Reshitnyk LY, Gendall L, Wachmann A, Dedeluk N, Kim U, Neufeld CJ and Costa M (2025) Canopy-forming kelp forests persist in the dynamic subregion of the Broughton Archipelago, British Columbia, Canada.
Front. Mar. Sci. 12:1537498.
doi: 10.3389/fmars.2025.1537498

Canopy-forming kelp forests persist in the dynamic subregion of the Broughton Archipelago, British Columbia, Canada

L. Man[1]*, R. V. Barbosa[1,2], L. Y. Reshitnyk[3], L. Gendall[1,4], A. Wachmann[1], N. Dedeluk[5], U. Kim[5], C. J. Neufeld[2,6,7] and M. Costa[1]

[1]Department of Geography, University of Victoria, Victoria, BC, Canada, [2]The Kelp Rescue Initiative, Bamfield Marine Sciences Centre, Bamfield, BC, Canada, [3]Hakai Institute, Victoria, BC, Canada, [4]UWA Oceans Institute, University of Western Australia, Crawley, WA, Australia, [5]Namgis First Nation, Alert Bay, BC, Canada, [6]Department of Biology, University of British Columbia, Okanagan Campus, Kelowna, BC, Canada, [7]LGL Limited Environmental Research Associates, Sidney, BC, Canada

Canopy-forming kelp forests act as foundation species that provide a wide range of ecosystem services along temperate coastlines. With climate change, these ecosystems are experiencing changing environmental and biotic conditions; however, the kelp distribution and drivers of change in British Columbia remain largely unexplored. This research aimed to use satellite imagery and environmental data to investigate the spatiotemporal persistence and resilience of kelp forests in a dynamic subregion of cool ocean temperatures and high kelp abundance in the Broughton Archipelago, British Columbia. The specific objectives were to identify: 1) long-term (1984 to 2023) and short-term (2016 to 2023) kelp responses to environmental changes; and 2) spatial patterns of kelp persistence. The long-term time series was divided into three climate periods: 1984 to 1998, 1999 to 2014, and 2014 to 2023. The first transition between these periods represented a shift into cooler regional sea-surface temperatures and a negative Pacific Decadal Oscillation in 1999. The second transition represented a change into warmer temperatures (with more marine heatwaves and El Niño conditions) after 2014. In the long-term time series (1984 to 2023), which covered a site with *Macrocystis pyrifera* beds, kelp area increased slightly after the start of the second climate period in 1999. For the short-term time series (2016 to 2023), which focused on eight sites with *Nereocystis luetkeana* beds, most sites either did not change significantly or expanded in kelp area. This suggests that kelp areas remained persistent across these periods despite showing interannual variability. Thus, the dynamic subregion of the Broughton Archipelago may be a climate refuge for kelps, likely due to cool water temperatures that remain below both species' upper thermal limits. Spatially, on a bed level, both species were more persistent in the center of the kelp beds, but across the subregion, *Macrocystis* had more persistent areas than *Nereocystis*, suggesting life history and/or other factors may be impacting

these kelp beds differently. These findings demonstrate the spatiotemporal persistence of kelp forests in the dynamic subregion of the Broughton Archipelago, informing the management of kelp forest ecosystems by First Nations and local communities.

KEYWORDS

kelp forests, remote sensing, *Macrocystis pyrifera*, *Nereocystis luetkeana*, persistence

1 Introduction

Canopy-forming kelp forests (order Laminariales) are key habitats in temperate marine regions globally (Jayathilake and Costello, 2021) and are vulnerable to climate change impacts (Reed et al., 2016; Smale, 2020; Wernberg et al., 2024), which can potentially disrupt ecosystem functions, such as habitat provision, fisheries production, nutrient cycling, carbon sequestration, and cultural value (Lamy et al., 2020; Eger et al., 2023; Turner, 2001). Kelp distribution and extent are affected by changes in environmental and biotic conditions, including ocean temperature, salinity, exposure, light, nutrient availability, and the abundance of kelp grazers and predators (Jayathilake and Costello, 2021; Springer et al., 2010; Druehl, 1977; Traiger and Konar, 2018; Hollarsmith et al., 2022; Starko et al., 2024a). These conditions are often closely related to temperature in region-specific ways; for example, in the Northeast Pacific Ocean, warmer waters can correlate with lower salinities (Druehl, 1977), poor nutrient availability (Lowman et al., 2022), and ecological regime shifts (Burt et al., 2018; Hamilton et al., 2021). Furthermore, studies have shown how ocean temperatures directly or indirectly drive kelp dynamics (e.g. Jayathilake and Costello, 2021; Gonzalez-Aragon et al., 2024; Hamilton et al., 2020; Bell et al., 2020; Starko et al., 2022; Mora-Soto et al., 2024a, 2024b).

In the Northeast Pacific Ocean, temperature changes can occur at variable time scales, from steady long-term trends or cyclic changes spanning decades or years, to short-term marine heatwaves, affecting the kelp dynamics differently (Cavanaugh et al., 2011; Krumhansl et al., 2016; Levitus et al., 2000; Mora-Soto et al., 2024a; Smith et al., 2024; Wernberg et al., 2024). Since the 1950s, long-term increases in ocean temperatures have primarily been driven by anthropogenic climate change (Cheng et al., 2022) and can drive changes in kelp distribution and area (Beas-Luna et al., 2020; Berry et al., 2021; Mora-Soto et al., 2024a). For instance, Berry et al. (2021) documented a shift in kelp distribution and a 63% decrease in its area coinciding with a 0.7°C sea-surface temperature (SST) increase throughout the 20th century in Puget Sound, Washington. Additionally, ocean temperatures are influenced by cyclic climatic oscillations (Di Lorenzo et al., 2008), such as the El Niño Southern Oscillation (ENSO) (quantified with the Oceanic Niño Index, ONI) and the Pacific Decadal Oscillation (PDO), which are multi-year and decadal modes of climate variability (Di Lorenzo et al., 2008). These oscillations often lead to warming in the Northeast Pacific Ocean when in a positive phase (Di Lorenzo and Mantua, 2016), with consequent changes in kelp responses. For instance, kelp areas decreased after shifting to positive PDO and ONI but rebounded after the oscillations shifted to negative phases in the Strait of Juan de Fuca (Pfister et al., 2018) and the Strait of Georgia (Mora-Soto et al., 2024a); conversely, kelp disappeared after a positive PDO shift in the 1970s and did not rebound afterward in Gray Bay, Haida Gwaii (Gendall et al., submitted).

Furthermore, ocean temperature change can also manifest in the form of short-term marine heat waves (MHWs), which are anomalously warm events (>5 days) with temperatures above the 90th percentile based on a 30-year climatological baseline (Hobday et al., 2016). A higher frequency and magnitude of MHWs have been observed due to climate change (Frölicher et al., 2018) and are generally associated with positive PDO and ONI years (Di Lorenzo and Mantua, 2016), resulting in prolonged, anomalously warm conditions (Bond et al., 2015). Such conditions were present during the Blob of 2014 to 2016, a prolonged MHW (Bond et al., 2015) that devastated kelp forests across the Northeast Pacific Ocean (Bell et al., 2023; Arafeh-Dalmau et al., 2019; Starko et al., 2024; Mora-Soto et al., 2024a, 2024b). Kelp was reduced after the Blob to 60% of its pre-Blob distribution in Barkley Sound (Starko et al., 2022), to 21% of its pre-Blob distribution in the Northern Salish Sea (Mora-Soto et al., 2024b), and to 13% of its historical area in Haida Gwaii (Gendall et al., submitted).

Kelp forest persistence and resilience to ocean warming and climatic oscillations can be characterized in temporal and spatial domains. In this context, persistence refers to the continued existence of kelp forests through time (Connell & Sousa, 1983), and resilience refers to kelps returning to a reference state after a disturbance, such as thermal stress periods (Holling, 1973). Some studies consider kelp persistence and resilience in the temporal domain, including increasing, decreasing, or no change in kelp areas within a specific study site or region (e.g. Cavanaugh et al., 2019; Mora-Soto et al., 2024a, 2024; etc.). Other studies investigate kelp persistence and resilience in the spatial domain, i.e., identifying areas where kelp is often present. (e.g. Schroeder et al., 2020; Hamilton et al., 2020; Cavanaugh et al., 2023; Arafeh-Dalmau et al., 2023). Currently, kelp forests are declining globally (Krumhansl et al., 2016), however, their persistence and resilience to climate change have been spatially variable, with decreases in 38% of the regions, increases in 27% of regions, and no change in 35% of regions (Krumhansl et al., 2016).

This variability in persistence and resilience is often due to spatially explicit patterns in environmental and biotic conditions (Smale, 2020; Bell et al., 2023; Starko et al., 2024a), which can influence the amount of stress the kelps directly experience, as well as have implications for adaptation and ecosystem-scale responses to stressors (Starko et al., 2024b). For instance, kelp areas are expanding in the Arctic due to the increase in ice-free areas (Filbee-Dexter et al., 2019), and conversely, are diminishing in subtropical latitudes such as in Baja California due to the increase in ocean temperatures (Cavanaugh et al., 2019; Beas-Luna et al., 2020; Bell et al., 2023). Beyond global-scale variability, this spatially driven variation in kelp persistence and resilience can be observed at a regional scale in British Columbia (BC), Canada. Kelp areas are increasing on the northwest coast of Vancouver Island where keystone predators (sea otters) have returned (Watson and Estes, 2011; Starko et al., 2024a), and displaying no change in area in the cooler waters of the Strait of Juan de Fuca (Mora-Soto et al., 2024a). Conversely, kelp areas decreased in the warmer waters of the central Gulf Islands and Northern Salish Sea (Mora-Soto et al., 2024a, 2024b). This spatial variation in kelp responses can also be found on local scales (a few kilometers or less), with kelps persisting on the cooler outer coasts and displaying loss in the warmer inlets, for instance, in Barkley Sound and around the Gray Bay and Cumshewa Inlet region of Haida Gwaii (Starko et al., 2022; Gendall et al., 2023). As such, local-scale studies are needed to understand the response of kelp to environmental conditions.

Canopy-forming kelp species such as *Macrocystis pyrifera* and *Nereocystis luetkeana* can be present at the ocean surface and have biomass that is detectable by optical remote sensing tools, equipping researchers with the ability to survey kelp across large spatial and temporal scales (Stekoll et al., 2006; Cavanaugh et al., 2011, 2019; Bell et al., 2015; Schroeder et al., 2019, 2020; Nijland et al., 2019; Mora-Soto et al., 2020, 2024a, 2024b; Gendall et al., 2023). Mid-resolution satellite imagery such as Landsat (spatial resolution: 30 to 80 m), available since 1972 (NASA, n.d.[1]), provides data to discern trends observed over multiple decades (Cavanaugh et al., 2011; Bell et al., 2020; Gendall et al., 2023; Mora-Soto et al., 2024a). This enables researchers to differentiate kelps' interannual variability from monotonic trends (Reed et al., 2015; Wernberg et al., 2019) and establish a more historical and accurate baseline of kelp areas (Bell et al., 2023; Mora Soto et al., 2024a). On the other hand, high-resolution satellite imagery such as Rapideye (5 m), Planetscope (3 m), and Quickbird-2 (1.84 m), allows for better accuracy when mapping fringing and smaller kelp beds (e.g., Gendall et al., 2023; Mora-Soto et al., 2024a), although their temporal coverage and resolution are more limited (Rapideye: 2009 to 2020, Planetscope: 2016 to present, Quickbird-2: 2001 to 2015) (Planet, 2024[2]; ESA, n.d, a[3].; ESA, n.d., b[4][5]). This difference in data sources results in a trade-off between spatial resolution, the ability to detect smaller kelp beds (Gendall et al., 2023), and the time series length. Due to the range of kelp bed sizes present on the BC coast, from large offshore beds to small fringing beds, utilizing satellite imagery of different spatial and temporal resolutions improves our ability to uncover temporal trends and identify areas of persistence and/or resilience in kelp beds of various sizes and distribution (e.g., Gendall et al., 2023; Mora-Soto et al., 2024a).

Here, we use satellite imagery to define the persistence and resilience of kelp forests to environmental changes in the dynamic subregion of the Broughton Archipelago, BC, Canada. The dynamic subregion is characterized by cool water temperatures, relatively flat bottom slopes, high seawater salinity, exposure, and tidal current speeds (Foreman et al., 2009; Brewer-Dalton et al., 2014; Lin and Bianucci, 2023). Specifically, this study addresses the following two objectives: 1) to identify the temporal responses of *Macrocystis pyrifera* and *Nereocystis luetkeana*, respectively, to changes in temperature and climatic oscillations, and 2) to identify spatial patterns of kelp persistence. We achieved these objectives by first characterizing environmental conditions in the Broughton Archipelago across various spatial scales with 1) local SST climatologies from temporally discontinuous Landsat data, 2) regional SST and MHW climatologies from temporally continuous *in-situ* measurements, and 3) global ONI and PDO indices. Next, we identified kelp persistence and resilience at one *Macrocystis* site (time series length: 1984 to 2023) and eight *Nereocystis* sites (time series length: 2016 to 2023) and compared them to the environmental changes. In this study, kelp persistence was quantified in two domains: (1) temporal persistence corresponding to an increase or no significant change in kelp area at the site level throughout the studied time series, and (2) spatial persistence corresponding to the existence of persistent areas inside each site where kelp was present >50% of the time series. Conversely, non-persistence is defined as (1) a temporal decrease in kelp and/or (2) spatially, the lack of any persistent area. Synthesizing both spatial and temporal domains, a kelp forest would be deemed resilient if the system experienced a disturbance and yet still displayed both temporal and spatial persistence. If the kelp forest displayed both spatial and temporal persistence but did not experience any disturbance, evaluating its resilience would not be possible. This study synthesizes both spatial and temporal domains to provide valuable information about the status of the kelp forests and their responses to environmental variability to the local First Nations and their monitoring efforts. At a broader spatial scale, this study also contributes to regional and global endeavors to understand the status and responses of kelp forests during an era of unprecedented climate change.

2 Methods

2.1 Study area

This study was conducted on the traditional and unceded territories of the Kwakwa̱ka̱'wakw peoples (Umista Cultural

1 https://landsat.gsfc.nasa.gov/satellites/timeline

2 https://developers.planet.com/docs/data/rapideye/

3 https://earth.esa.int/eogateway/missions/worldview

4 https://earth.esa.int/eogateway/missions/planetscope/description

5

Society, n.d.[6]) within the Broughton Archipelago. This region sits at the interface of two major bodies of water: the Johnstone Strait and Queen Charlotte Strait, near the northeast of Vancouver Island, BC, Canada (Figure 1). The Broughton Archipelago features many islands in the west and glacially carved fjords in the east (Shugar et al., 2014; Davies et al., 2018). Due to its strong environmental gradient in seawater temperature and clear differences in bathymetry, this region can be distinctly divided into two subregions: the cooler, dynamic western archipelago, and the warmer, sheltered, eastern fjords (Foreman et al., 2009; Brewer-Dalton et al., 2014; Lin and Bianucci, 2023). This environmental gradient and spatial differences in bathymetry drive kelp abundance, with the larger and denser kelp beds that can be detected with satellite imagery only located in the dynamic subregion, whereas the smaller, fringing beds that are challenging to detect with satellite imagery are in the fjord subregion (Man et al., in prep). We focused on the dynamic subregion due to the limited availability of high-resolution satellite imagery in the fjord subregion (Figure 1). This subregion is dominated by *Nereocystis* beds, except for on the north shore of Malcolm Island, which is lined with large, dense beds primarily composed of *Macrocystis* (Man et al., in prep; Sutherland, 1990). *Macrocystis* and *Nereocystis* are the only canopy-forming kelp species in the subregion, and "kelp" hereafter collectively refers to both species. *Nereocystis*, as an annual species, tends to display more interannual variability than *Macrocystis*, a perennial species (Dayton et al., 1984; Springer et al., 2010).

Local community members, including First Nations, have revealed that, generally, the kelp forests have declined in density and coverage in their territories (Broughton Aquaculture Transition Initiative (BATI), unpublished, 2021; Salmon Coast Field Station (SCFS), unpublished, 2023). Community members have also reported specific locations of kelp change in the region, including an increase around Malcolm Island, and decreases at an offshore kelp bed at the mouth of the Nimpkish River ("NR"), at a nearshore kelp bed off the shore of the Alert Bay Lighthouse ("ABL"), and along the salmon migration routes in the fjords near now-decommissioned open-net salmon farms (SCFS, 2023; Mountain, pers comm, 2023).

One *Macrocystis* site and eight smaller *Nereocystis* sites were selected to represent the temporal dynamics of kelp beds of different species and sizes exposed to different environmental conditions. The *Macrocystis* site encompasses the entire north shore of Malcolm Island (spanning 11.6 km^2), and the eight smaller *Nereocystis* sites (ranging from 0.03-1.45 km^2 per site) represent the portion of the eastern shore of Malcolm Island with high kelp abundance and the smaller islands east of Malcolm Island (Figure 1). Only one *Macrocystis* site was selected as this was the only area within the Broughton Archipelago where *Macrocystis* was present. The bottom substrate type at the *Macrocystis* site was primarily mixed rocky and sandy substrate, with kelp growing on the rocky areas (Haggarty et al., 2020; Man et al., in prep). The smaller site approach was chosen for the *Nereocystis* sites rather than mapping all of their coastlines due to the geomorphological complexity of the area, which imposed a challenge for the satellite remote sensing of kelp because of the increased land adjacency effects (Cavanaugh et al., 2021). The *Nereocystis* sites included the offshore kelp beds at the mouth of the Nimpkish River (NR), the nearshore kelp beds off the shore of the Alert Bay Lighthouse (ABL), the eastern coastline of Alert Bay (ABE), the eastern tip of Malcolm Island (MIE), Pearse Islands (PI), Bold Head (BH), Wedge Island (WI), and South Leading Islet (SLI) (Figure 1). PI, BH, and WI had primarily shallow (<20 m depth) rocky bottom substrate, surrounded by deeper (>20 m) areas where kelp cannot grow (Haggarty et al., 2020). ABL, ABE, and MIE had mixed rocky and sandy bottom substrates, and NR and SLI had mixed rocky and sandy bottom substrates surrounded by pure sandy substrates which cannot support kelp growth (Haggarty et al., 2020).

The locations of the *Macrocystis* and *Nereocystis* sites were selected opportunistically during a field visit and based on their importance to the Mamalilikulla First Nation, 'Namgis First Nation, and Kwikwasut'inuxw/Haxwa'mis First Nation. These three Nations formed the Broughton Aquaculture Transition Initiative (BATI), a coalition that emphasized the need to continue monitoring and protecting the Archipelago's kelp forests due to their importance as nearshore salmon habitat (BATI, unpublished, 2021). The *Macrocystis* and the *Nereocystis* sites experience slightly different environmental and topographical conditions from each other, with the *Macrocystis* site having flatter slopes and lower tidal current speeds than the *Nereocystis* sites (Davies et al., 2018; Foreman et al., 2009).

2.2 Data compilation and processing

The following data were compiled: (1) local, regional, and global-scale environmental conditions, (2) Landsat-derived canopy kelp area (1984 to 2023) at the *Macrocystis* site, and (3) Planetscope-derived kelp area (2016 to 2023) at the *Nereocystis* sites (both "kelp area" hereafter) (Figure 2). In addition, very high-resolution Worldview-2 and GeoEye-1 imagery was used to validate kelp classifications derived from Landsat and Planetscope imagery (Figure 2). The environmental variables were used to define climate periods (years with similar environmental conditions) (Figure 2). Objective 1 (identify the temporal responses of *Macrocystis pyrifera* and *Nereocystis luetkeana*, respectively, to changes in temperature and climatic oscillations) was achieved by analyzing both long-term and short-term kelp time series alongside environmental changes at local, regional, and global scales (Figure 2). Objective 2 (identifying spatial patterns of kelp persistence) was achieved by spatially combining yearly kelp areas (Figure 2).

2.2.1 Environmental conditions

The environmental conditions from the past four decades (1984 to 2023) were compiled to evaluate their roles as drivers of kelp area change. Environmental data was acquired to represent three different spatial scales: 1) Local: Summer climatologies compiled from temporally discontinuous Landsat-derived SST from the *Macrocystis* and *Nereocystis* sites; 2) Regional: spring, and

6 https://umistapotlatch.ca/notre_terre-our_land-eng.php

10.3389/fmars.2025.1537498

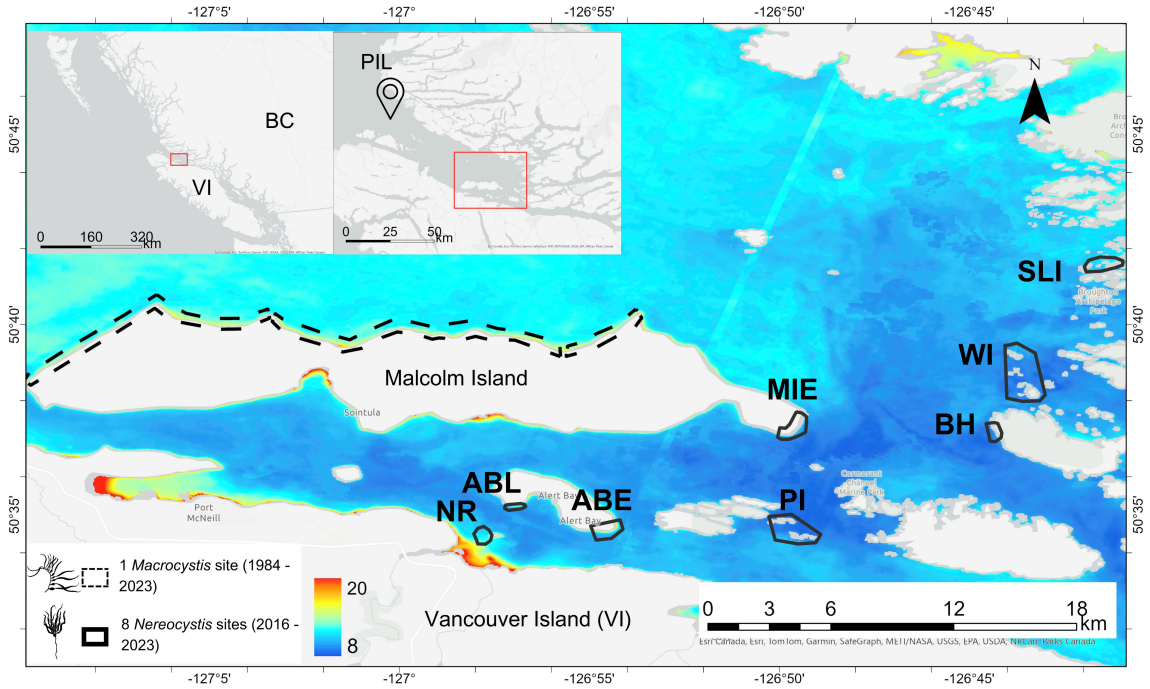

FIGURE 1
The main map shows the study area (the dynamic subregion of the Broughton Archipelago), with the *Macrocystis* site on the north shore of Malcolm Island marked in a dashed black outline and the eight *Nereocystis* sites marked in solid black outlines. The *Nereocystis* sites include kelp beds at Nimpkish River (NR), Alert Bay Lighthouse (ABL), Alert Bay East (ABE), Pearse Islands (PI), Bold Head (BH), Wedge Island (WI), and South Leading Islet (SLI). The background of the main map is the mean Landsat-derived SST from the summers (July and August) of 2016 to 2023. The left inset map shows the location of the study area at a provincial scale relative to Vancouver Island (VI) and mainland BC (BC). The right inset map shows the study area (marked by the red rectangle) situated within the Queen Charlotte Strait region, relative to the location of the Pine Island Lighthouse (PIL), from which the regional SST and MHW metrics were derived (see 2.2.1). *Macrocystis* and *Nereocystis* graphics were obtained from phylopic.org, with the former created by Harold N Eyster (CC BY 3.0, Attribution 3.0 Unported), and the latter created by Guillaume Dera (CC0 1.0 Universal Public Domain Dedication license.)

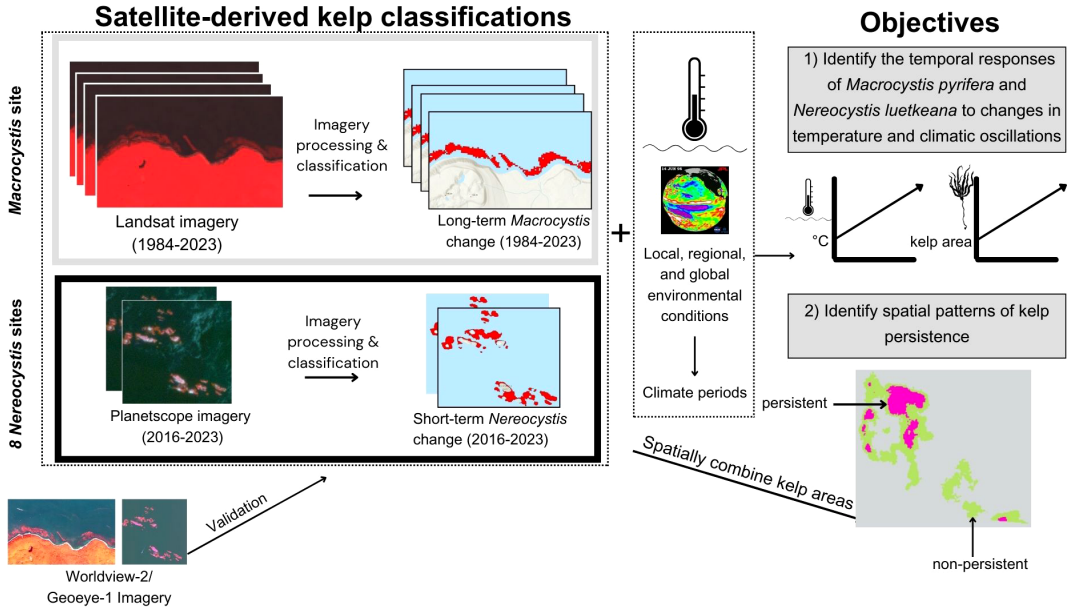

FIGURE 2
A flow chart representing the data compilation and processing, as well as the spatial and temporal dimensions of the study, and how satellite-derived kelp classifications and environmental data are combined to achieve the objectives of the study.

summer climatologies derived from temporally continuous (daily) *in-situ* SST measurements collected at Pine Island Lighthouse about 57 km north of the study area (Figure 1), representative of the Queen Charlotte Strait region; and 3) Global: annual ONI and PDO indices representing the climatic conditions of the broader Northeast Pacific Ocean.

Local SST

We characterized local SST changes in the study area by deriving mean summer (July-August) SST climatologies from the thermal infrared band of Landsat 5, 7, 8, and 9 imagery ("local SST" hereafter, spatial resolution: 30 m) for each year; note that this dataset was temporally discontinuous due to low availability of imagery related to frequent high cloud cover. Furthermore, only summer SST was considered for the local-level dataset due to the even more frequent high cloud cover present during spring in the Broughton Archipelago. To create the SST climatologies, we first compiled all cloud-free Landsat images captured during the summer months from 1984 to 2023, excluding years with only one cloud-free image to prevent skewing the summer mean with short-term extremes. As a result, only 13 years of mean local SST data were analyzed out of the total 40-year period for the *Macrocystis* site (Table 1). For each of the 13 years, mean local SST was calculated using zonal statistics in a polygon spanning the entirety of the *Macrocystis* site (Figure 1), buffered 300 m away from the shoreline. This reduced the interference of land temperature on the water pixels, producing accurate nearshore SST data (Wachmann et al., 2024). Mean local Landsat SST data for the *Nereocystis* sites were available for 26 out of the 39 years analyzed (Table 1). For each of these 26 years, local SST was calculated using zonal statistics in a 200-m radius buffer 300 m from any land (Wachmann et al., 2024). These annual mean summer SST

TABLE 1 The environmental variables at local, regional, and global scales.

Variable	Temporal availability	Temporal resolution	Explanation
Local (from the Macrocystis and Nereocystis sites, all derived from Landsat thermal bands)			
Local summer SST (°C)	*Macrocystis* site: 1985, 1990, 1995, 2003, 2005, 2006, 2008, 2009, 2010, 2013 to 2017, 2020, and 2023 *Nereocystis* site: 1984, 1985, 1990, 1993, 1995, 1997, 2003 to 2011, 2014 to 2018, and 2020 to 2023	Discontinuous	July & August mean calculated from available cloud-free Landsat images
Regional (all derived from the Pine Island Lighthouse in-situ daily measurements)			
Regional summer SST (°C)	July & August, 1984 to 2023	Continuous	July & August mean calculated from daily data
Regional spring SST (°C)	May & June, 1984 to 2023	Continuous	May & June mean calculated from daily data
Regional summer SST anomaly (°C)	July & August, 1984 to 2023	Continuous	The difference between the yearly summer mean (July-August) and the total summer (July-August) climatological mean calculated from daily values
Regional spring SST anomaly(°C)	May & June, 1984 to 2023	Continuous	The difference between the yearly spring (May-June) SST for that year and the total spring (May-June) climatological mean calculated from daily values
The 2-year mean of regional spring SST (°C)	May & June, 1983 to 2023	Continuous	For a year *n*, this is a 2-year moving mean of spring SST measurements from years n-1 to n
The 2-year mean of regional summer SST (°C)	July & August, 1983 to 2023	Continuous	For a year *n*, this is a 2-year moving mean of summer SST measurements from years n-1 to n
The 3-year mean of regional spring SST (°C)	May & June, 1984 to 2023	Continuous	For a year *n*, this is a 3-year moving mean of spring SST measurements from years n-2 to n
The 3-year mean of regional summer SST (°C)	July & August, 1984 to 2023	Continuous	For a year *n*, this is a 3-year moving mean of summer SST measurements from years n-2 to n
Pre-summer MHW (°C days)	September-June, 1983 to 2023	Continuous	For a year *n*, the sum of the total cumulative intensity of all MHWs from September of year n-1 to June of year n
Summer MHW (°C days)	July-August, 1984 to 2023	Continuous	For a year *n*, the sum of the total cumulative intensity of all MHWs from July to August.
Global (all derived from NOAA, 2024a, 2024b)			
ONI	May-August, 1984 to 2023	Continuous	Z-scored spring and summer ONI calculated from the mean spring and summer ONI for that year
PDO	May-August, 1984 to 2023	Continuous	Z-scored spring and summer PDO calculated from the mean spring and summer PDO for that year.

measurements were then compiled into site-specific climatologies. Note that although local SST measurements for the *Nereocystis* sites were acquired between 1984 and 2023, their kelp time series only ranged from 2016 to 2023 due to the limited availability of Planetscope imagery.

Regional SST and MHWs

We characterized the regional SST based on daily *in-situ* SST measurements collected at Pine Island Lighthouse ("regional SST" hereafter), compiled from 1982 to 2023 (Fisheries & Oceans Canada, 2024[7]) *(*Figure 1*)*. Pine Island Lighthouse is 57 km away from Malcolm Island, thus representing the general environmental conditions of the Queen Charlotte Strait region rather than the local conditions at the sites. However, its high temporal resolution allowed us to calculate MHW frequencies and magnitudes (Hobday et al., 2016, 2018).

The following metrics were calculated from the daily regional SST measurements: (i) spring (May-June), and summer (July-August) SST climatologies, (ii) mean yearly spring and summer SST anomalies, and (iii) two- and three-year mean climatologies of regional spring and summer SST. Spring and summer SST metrics represented the conditions during stages of high kelp growth and peak kelp biomass, respectively (Springer et al., 2010). Winter SST metrics, which would represent the environmental conditions present during the kelp gametophyte stages (Springer et al., 2010), were not included as there were a few winter months with no SST data collected (December 2018-January 2019, December 2019 to January 2020, and December 2020 to January 2021), compromising the continuity of the data. The two- and three-year SST means were computed for each season to evaluate the potential lagged effects of temperature changes on kelp (Pfister et al., 2018) *(*Table 1*)*.

Beyond the SST metrics above, MHWs were identified from the regional daily SST measurements, with an MHW defined as when the maximum observed day temperature surpasses the day's seasonal climatology and 90th percentile temperature threshold for more than five days, *sensu* Hobday et al. (2016). Following Hobday et al. (2016, 2018), we calculated four MHW categories (I - IV), corresponding to multiples of the seasonal difference between the climatological mean and the climatological 90th percentile. A Category I MHW surpasses the climatological 90th percentile once, and a Category II MHW twice, etc. Multiples of this difference vary by location and time of year; thus the category may not directly correspond to the maximum intensity. For example, a MHW on December 2, 2016, of maximum intensity 2.0°C, was classified as Category II because this event surpassed the climatological 90th percentile of this season twice, yet another MHW on September 24, 2019, of maximum intensity 2.5°C was only classified as Category I because this event surpassed the climatological 90th percentile of that season only once. After identifying the MHWs, the cumulative intensity of each MHW was calculated as the MHW's temperature anomaly (°C) multiplied by the number of heatwave days. For each year *n*, the following metrics were noted: (i) total pre-summer MHW cumulative intensity, which is the cumulative intensity of all MHWs that occurred from September 1st of year *n-1* to June 30th of year *n*, and (ii) total summer MHW cumulative intensity, which is the combined cumulative intensity of all MHWs between July and August of year *n*. The total pre-summer MHW cumulative intensity would represent the MHWs occurring in the fall and winter of year *n-1*, and in the spring of year *n*, which may affect the kelp spores and gametophytes that will eventually reach canopy height as sporophytes in year *n* (Springer et al., 2010), thus affecting the kelp area detected in year n. Although there were data gaps in the SST during the winter months from 2018 to 2020 (December 2018 - January 2019, December 2019 - January 2020, and November 2020 - Jan 2021), we determined that it was still suitable to use the pre-summer MHW metrics because some of these months were still represented, from September of year n-1 to June of year n. Regardless, this limitation should be kept in mind when interpreting the results for 2018-2020, where pre-summer MHW cumulative intensity may be underestimated.

Global: climatic oscillations

The global environmental conditions were characterized by the mean yearly ONI and PDO (NOAA, 2024a[8], 2024b[9]). Mean yearly ONI and PDO were calculated from spring and summer (May to August) values and were then rescaled using Z-scores to identify when each index was above or below their 40-year climatological mean, following the methods of Mora-Soto et al. (2024a). This resulted in an ONI and PDO Z-score for each year *(*Table 1*)*, with positive values indicating warmer years with less optimal conditions for kelp (Mora-Soto et al., 2024a)

2.2.2 Mapping canopy kelp area

Kelp area was quantified by classifying satellite imagery from 1984 to 2023. Higher-resolution satellite imagery was selected to map the floating kelp area in the *Nereocystis* sites than the *Macrocystis* sites, as higher-resolution imagery is more appropriate for mapping the fringing *Nereocystis* beds typical of this region (Cavanaugh et al., 2021; Gendall et al., 2023). Landsat imagery (spatial resolution: 30 m, 1984 to 2023) was selected to map the large kelp beds at the *Macrocystis* site, creating a longer time series. Planetscope imagery (spatial resolution: 3 m, 2016 to 2023) was used to represent kelp changes at the smaller *Nereocystis* sites after the Blob (Bond et al., 2015). Then, very-high-resolution Worldview-2 and GeoEye-1 imagery (spatial resolution: 0.46 and 1.84 m, respectively) obtained from 2017 and 2023 were used to validate the satellite-derived kelp area classifications.

Long-term *Macrocystis* time series

For the *Macrocystis* site, the kelp area was derived from Landsat imagery using two different classification approaches: Multiple Endmember Spectral Mixture Analysis (MESMA) (Cavanaugh

7 https://open.canada.ca/data/en/dataset/719955f2-bf8e-44f7-bc26-6bd623e82884

8 https://origin.cpc.ncep.noaa.gov/products/analysis_monitoring/ensostuff/ONI_v5.php

9 https://www.ncei.noaa.gov/access/monitoring/pdo/

et al., 2011; Bell et al., 2020) and Object-Based Image Analysis (OBIA) (e.g. Gendall et al., 2023; Mora Soto et al., 2024a). The mixture of approaches was used due to the availability of a pre-existing dataset from 1984 to 2020 (Reshitnyk, unpublished data, 2024) classified using MESMA. Additional classifications of kelp area using OBIA allowed us to expand the time series to include 2021 to 2023. For the 1984-2020 Landsat dataset, atmospherically corrected surface reflectance products (Landsat Collection 1 Level-2 reflectance data) were downloaded from the United States Geological Survey Earth Explorer website[10] for the sites for Landsat sensors TM, ETM+, and OLI for each year. To mask out intertidal areas, a land mask was derived for the region using a single Landsat scene collection at a 0.2 m tide (Mean Lower Low Water) to remove all land and intertidal pixels (mask creation details in Supplementary material S1). Classification of the kelp area followed methods described by Bell et al., 2020. Following cloud and land masking, for each scene, a binary classification decision tree was used to classify each pixel into one of four classes: seawater, cloud, land, and kelp. A Multiple Endmember Spectral Mixture Analysis (MESMA) (Bell et al., 2020; Roberts et al., 1998) was used to determine the kelp fraction contained in each kelp pixel. We converted the fractional cover dataset to a binary time series based on a fractional kelp cover threshold of 13% (Houskeeper et al., 2022: Cavanaugh et al., 2011). The final dataset represents the maximum kelp area for a given year. 1992 was excluded from this analysis as there was no available cloud-free imagery for the study area.

For the 2021-2023 Landsat dataset, we used one yearly cloud-free Landsat image acquired during low tide between spring and summer, thus representing the kelp area captured at peak biomass (Springer et al., 2010). For each image, the land was masked out, and a Normalized Difference Vegetation Index (NDVI) and linear enhancements were applied to increase the spectral separability between kelp and water (following the protocols in Gendall et al. (2023). Each image was classified using an OBIA approach (OBIA classification methods in Supplementary material S2). For the entire time series (1984 to 2023), the kelp area was normalized as a percentage of the maximum kelp area, i.e. aggregated area of all kelp detected for the entire time series.

Short-term *Nereocystis* time series

Planetscope imagery was used to derive kelp areas for the short-term time series (2016 to 2023) covering the eight *Nereocystis* sites (Table 2). One cloud-free summer image acquired at a tidal height less than 2.50 m above the chart datum was used to derive each year's kelp area. The processing and classification of the short-term time series followed the methods delineated in Gendall et al. (2023). Imagery from 2016 required atmospheric correction as only top-of-atmosphere reflectance products were available. Atmospheric correction was performed using a Rayleigh correction, with dark targets selected using the darkest pixel histogram adjustment method described in Hadjimitsis et al. (2004). Atmospheric correction was not conducted on imagery from 2017 to 2023, as surface reflectance products were available. In terms of geometry, georeferencing using a single-order polynomial transformation against the ArcGIS base map was conducted if an image was misaligned relative to the base map. Next, areas where kelp cannot grow (i.e. land, deep water (>20 m), and sandy and mud substrate) were masked from imagery to avoid false positives in kelp area classifications following the methods outlined in Gendall et al. (2023). The land mask was manually delineated based on the lowest tide Planetscope image (tidal height: 0.716 m) in this kelp time series, acquired on August 4, 2023; the sandy and mud substrate mask was created using the BC bottom patch model (Haggarty et al., 2020); and the deep water mask (depths >20.0 m) was created using a coastal digital elevation model for Pacific Canadian waters (Davies et al., 2018). Following the masking step, a Near-Infrared/Green (NIR/G) band ratio and linear enhancements were applied to the imagery before classification (Gendall et al., 2023). The images were subsequently classified using the aforementioned OBIA methods (see details in the classification methods in Appendix S2), resulting in yearly kelp area products from 2016 to 2023 for each *Nereocystis* site. Finally, yearly kelp areas were normalized into percent kelp area.

Methods comparison and validation of kelp area products

We ensured that the MESMA-based yearly kelp aggregate area classification method (as used in 1984 to 2020 *Macrocystis* site classifications) and OBIA-based non-aggregate kelp area classification method (as used in 2021 to 2023 *Macrocystis* site classifications and 2016 to 2023 *Nereocystis* site classifications) created comparable results by conducting a sensitivity analysis. Two Landsat summer images, from 1986 and 2015, covering part of the *Macrocystis* site already classified using MESMA, were additionally classified using OBIA. The percent kelp area derived from the OBIA classification was within a 1% difference from that of the MESMA classification; thus, the two classification methods were deemed comparable.

Moreover, we confirmed that there were no confounding effects of tidal height on the percent kelp area by fitting a linear mixed model for the short-term time series (tidal height range: 0.716-2.500 m), with percent kelp area as the dependent variable, tidal height as a fixed effect, and site as a random effect (R package "lme4", Bates et al., 2015). This analysis confirmed that the percent kelp area was not significantly affected by tidal height ($p=0.320$) and, therefore, suitable for use in subsequent data analysis. This test was not conducted for the long-term time series as the kelp area for each year was derived from multiple images of various tidal heights, minimizing the tidal height-induced variability associated with this dataset.

The satellite-derived kelp area products were validated by comparing the spatial overlap between the kelp classifications and very high-resolution satellite images (spatial resolution: 0.460-1.84 m). The very high-resolution satellite images provided more accurate representations of the kelp beds due to the reduced pixel mixing between kelp and water (Cavanaugh et al., 2021; Gendall et al., 2023). As the validation of all the yearly kelp classifications was challenging due to the lack of historical *in-situ* data and very high-resolution imagery, we selected one year to validate the kelp classification approach of each of the time series and assumed this

10 earthexplorer.usgs.gov

validation would be representative of the other years. For the long-term *Macrocystis* time series, a Worldview-2 image (spatial resolution: 1.84 m, acquired on August 1, 2017), was used to validate the Landsat-based classification of the *Macrocystis* site kelp beds from 2017. For the short-term *Nereocystis* time series, we validated the 2023 Planetscope-derived classifications of six *Nereocystis* sites' kelp beds by using a pan-sharpened Worldview-2 image (spatial resolution: 0.46 m, acquired on August 4, 2023) and a pan-sharpened GeoEye-1 image (spatial resolution: 0.46 m, acquired on August 6, 2023) *(*Table 2*)*. Overall accuracy of 89.7% and 89.1% were found for the long-term and the short-term time series, respectively *(Details on validation methods and results in* Supplementary Material S3, Supplementary Table S1*)*.

2.3 Data analysis

2.3.1 Identifying environmental trends at different spatial scales and climate periods

The Modified Mann-Kendall test (Hamed and Rao, 1998, R package: rtrend), a non-parametric test for monotonic trends adjusted for serial autocorrelation, was used to investigate significant temporal trends of local summer SST climatologies, regional spring and summer SST climatologies, and MHWs. Here, a significant and positive Z-statistic would indicate an increasing trend, a significant and negative Z-statistic would indicate a decreasing trend, and a non-significant test result would indicate no significant temporal trends. We did not test for trends in PDO and ONI as these climatic oscillations are inherently cyclical (Norel et al., 2021).

The time series of environmental variables were statistically organized into climate periods to define kelp area changes between these periods. This is because kelp can generally show lagged fluctuations for one to two years in response to environmental conditions due to the potential multi-year impacts of environmental changes (Pfister et al., 2018; Mora-Soto et al., 2024a). The climate periods were identified by defining changepoints, i.e., points in the time series where abrupt changes in temporal trends occur (Zhao et al., 2019), in the regional spring and summer SST. These datasets were selected to define the transitions between climate periods because of the *in-situ* nature and the continuity of the time series *(*Table 1*)*; the local satellite-derived SST data was not fit for this analysis due to its temporally discontinuous nature (see section 2.2.1). The changepoint analysis was conducted using the Bayesian Estimator of Abrupt change, Seasonal change, and Trend (BEAST) algorithm, an ensemble algorithm that leverages time series decomposition models using Bayesian model averaging (Zhao et al., 2019, R package: rBeast). We further conducted Kruskal-Wallis tests to define significant differences in each environmental variable *(*Table 1*)* between climate periods, and Dunn's tests with the Benjamani-Hochberg adjustment for multiple testing were used for *post hoc* comparisons (Kruskal and Wallis, 1952; Dunn, 1964; Benjamini & Hochberg, 1995).

2.3.2 Long-term (1984 to 2023) and short-term (2016 to 2023) kelp response to environmental changes

The modified Mann-Kendall test (Hamed and Rao, 1998) was used to define both long-term (1984 to 2023) and short-term (2016 to 2023) temporal trends in the kelp area at each site. Here, a significant and positive Mann Kendall's Z-statistic would indicate increasing kelp area, a significant and negative Z-statistic would indicate decreasing kelp area, and a non-significant test result would indicate no significant temporal trends. An increase or no significant change in the kelp area would indicate temporal persistence.

In addition, for the long-term *Macrocystis* time series, the Kruskal-Wallis test (Kruskal and Wallis, 1952) was conducted to identify potential differences in kelp area between the climate periods. Dunn's test was used for *post hoc* comparisons, with the Benjamini-Hochberg correction for multiple testing (Dunn, 1964; Benjamini & Hochberg, 1995). Furthermore, linear models with different combinations of regional and global environmental variables were tested to define the most significant environmental variables affecting changes in the kelp area. The tested variables (predictors) included yearly, two-year, and three-year average climatologies of spring and summer SST/SST anomalies, pre-summer and summer MHWs, PDO, and ONI. The Landsat-derived local SST climatologies were not used as predictors in this linear model due to the lack of data for several years of the time series. All the predictor variables were tested for collinearity using Kendall's correlation test and visual data exploration (Kendall, 1948). The Akaike Information Criteria (AIC) (Akaike, 1974) was used to determine the most suitable combination of predictors from

TABLE 2 Table detailing imagery used for the long-term and short-term time series, as well as imagery validation.

Spatial coverage	Temporal coverage	Data source	Classification method	Purpose
Macrocystis site	1984 to 2023	Landsat 5, 7, 8 9 (30 m)	1984 to 2020 (MESMA) 2021 to 2023 (OBIA)	Create long-term kelp time series
Eight *Nereocystis* sites	2016 to 2023	Planetscope (3 m)	OBIA	Create a short-term kelp time series
Macrocystis site	Aug 1, 2017	Worldview (1.84 m)	Not classified, a 30 m grid was overlaid and all grids with >50% kelp were visually identified as kelp	Validation of long-term kelp time series
Six *Nereocystis* sites	Aug 4, 2023, Aug 6, 2023	Worldview, GeoEye (0.46 m)	Not classified, a 10 m grid was overlaid and all grids with >50% kelp were visually identified as kelp	Validation of short-term kelp time series

the non-autocorrelated variables. The assumptions of the linear model were visually evaluated with histograms of the model residuals, residuals' quantile-quantile plots, plots of the fitted values vs residuals, and statistically evaluated for the normality assumption using Shapiro-Wilk tests (Shapiro and Wilk, 1965). A plot of the residuals vs the observed site numbers was used to identify patterns in the order of the data, which tests for the assumption of the independence of observations, whereas a plot of the models' fitted vs residuals values was used to test for the linearity and constant variance assumptions. All visualizations were consistent with the assumptions required by the model, and the result of the Shapiro-Wilk tests confirmed that the model residuals were normal.

A similar comparison of kelp area change across climate periods and linear model analysis of the effect of environmental conditions were not conducted for the *Nereocystis* sites due to the reduced time series. However, a descriptive characterization of the observed kelp percent area change and the local environmental conditions during and after the end of the Blob (2016 to 2023) was conducted. These included noting down the mean local summer SST at each site, identifying the hottest and coolest sites, as well as years of kelp loss.

2.3.3 Spatial patterns of kelp persistence

Persistent kelp areas within the maximum kelp area were defined as areas (m^2) where kelp was present for more than 50% of the time-series length (>19 years of presence for the long-term *Macrocystis* time series; >4 years for the short-term *Nereocystis* time series). Our definition of a persistent area was adapted from the "refugia" definition of Cavanaugh et al. (2023), who identified as refugia areas of kelp that occurred in 50% of the years in a Planetscope-derived time series (2016 to 2021 in their case). We simply defined these as "persistent" areas rather than "refugia", as the study area did not experience environmental conditions detrimental to kelps as the term "refugia" would imply (see results). We identified the spatial distribution of kelp persistence at each site using the 'Count overlapping features' tool in ArcGIS Pro 3.0 (ESRI, Redlands, United States), which indicated where and how many times the yearly kelp areas overlap, using the 'Count overlapping features' tool in ArcGIS Pro 3.0 (ESRI, Redlands, United States). Finally, the percent of the persistent kelp area $\left(\frac{persistent\ \ kelp\ \ area}{maximum\ \ kelp\ \ area}\right)$ was calculated for each site.

3 Results

3.1 Environmental conditions and their differences among climate periods at local, regional, and global scales

At the regional level, the mean spring SST ranged from 8.4°C to 11.1°C, and mean summer SST ranged from 9.6°C to 12.6°C (Figure 3, SST anomalies in Supplementary Figure S1), with no temporal trends in either regional spring or summer SST (modified Mann-Kendall's test: spring: Z-statistic = 0.187, p=0.0911; summer: Z-statistic = 0.195, p=0.0785; Table 3). Based on the mean summer and spring regional SST, the changepoints analysis (Supplementary Table S2) indicated three climate periods: Period 1 represents generally warmer ocean temperatures from 1984 to 1998, Period 2 represents cooler temperatures from 1999 to 2013, and Period 3 represents the highest temperatures of the time series from 2014 to 2023 (Figure 3). Accordingly, mean spring and summer regional SST were different across all periods (Figure 3, Table 3). For both spring and summer, Period 1 (spring SST: 9.8 ± 0.41°C, summer SST: 10.7 ± 0.31°C) had significantly warmer SST than Period 2 (spring SST: 9.2 ± 0.47°C, summer SST: 10.1 ± 0.41°C, Figure 3, Table 3). Furthermore, Period 3 (spring SST: 10.5 ± 0.37°C, summer SST: 11.6 ± 0.5°C, summer SST anomaly: 0.9 ± 0.53°C) had significantly warmer SST than both Periods 1 and 2 (Figure 3, Table 3).

At the local scale, the Landsat-derived SST showed some variability, with the *Macrocystis* site presenting warmer SST (11.5 ± 0.96°C) (climatological summer mean ± standard deviation) than the *Nereocystis* sites (10.1 ± 1.05°C). On average, the hottest *Nereocystis* sites were ABL, ABE, and SLI (~10.3°C), and the coolest *Nereocystis* site was BH (9.4 ± 0.72°C) (Figure 4A, Supplementary Table S3). Across the three identified climate periods, the mean local SST significantly increased for the *Macrocystis* site and six *Nereocystis* sites (ABL, ABE, MIE, BH, WI, PI) (Figure 4A, Table 3A), with ~1.4°C (Table 3A) higher SST in Period 3 (*Macrocystis* site: 12.5 ± 0.42°C, *Nereocystis* sites: 10.6 ± 0.71°C) than in Period 1 (*Macrocystis* site: 10.3 ± 0.20°C, *Nereocystis* sites: 9.2 ± 0.54°C). However, neither Periods 1 nor 3 had significant differences with Period 2 regarding the mean local SST (Figure 4B, Table 3A). For the other two *Nereocystis* sites (NR, SLI), local SST measurements were not significantly different among the periods (Figure 4B, Table 3A), although local SST peaked in 2004 in sites NR and SLI, reaching mean summer temperatures of 14.2 ± 1.50°C and 12.0 ± 0.31°C. respectively.

On the regional scale, 57 MHWs were identified between January 1983 and August 2023. Among these, 27 were in Category I, 23 in Category II, 6 in Category III, and 1 in Category IV (Figure 5A). The most intense (Category IV) MHW occurred on 30 July 2020, lasting six days and reaching a maximum temperature intensity of 15.4°C (a +4.7°C anomaly), with a total cumulative intensity (calculated as the mean temperature anomaly of the MHW multiplied by the number of heatwave days) of 18.2°C days. The most cumulatively intense MHW occurred at the beginning of 2016, starting on 20 January and lasting 98 days, resulting in a cumulative total of 146.0°C days, and reaching a maximum intensity of 10.8°C (a +2.2°C anomaly). Note that there were several winter months with no SST data available, namely December 2018 - January 2019, December 2019 - January 2020, and November 2020 - Jan 2021 (see section 2.2.1), thus the lack of MHWs detected during those periods may be attributed to this reason. Furthermore, the pre-summer cumulative MHW intensity may be underestimated as a result. The pre-summer MHW time series did not display any temporal trends, but the summer MHW time series exhibited a statistically significant increase (Table 3B). Pre-summer MHW cumulative intensity was not significantly different across periods. However, summer MHW cumulative intensity was different across Periods 1 and 3, and 2 and 3, with Period 3 representing the highest MHW intensity (Period 1: 1.2 ±

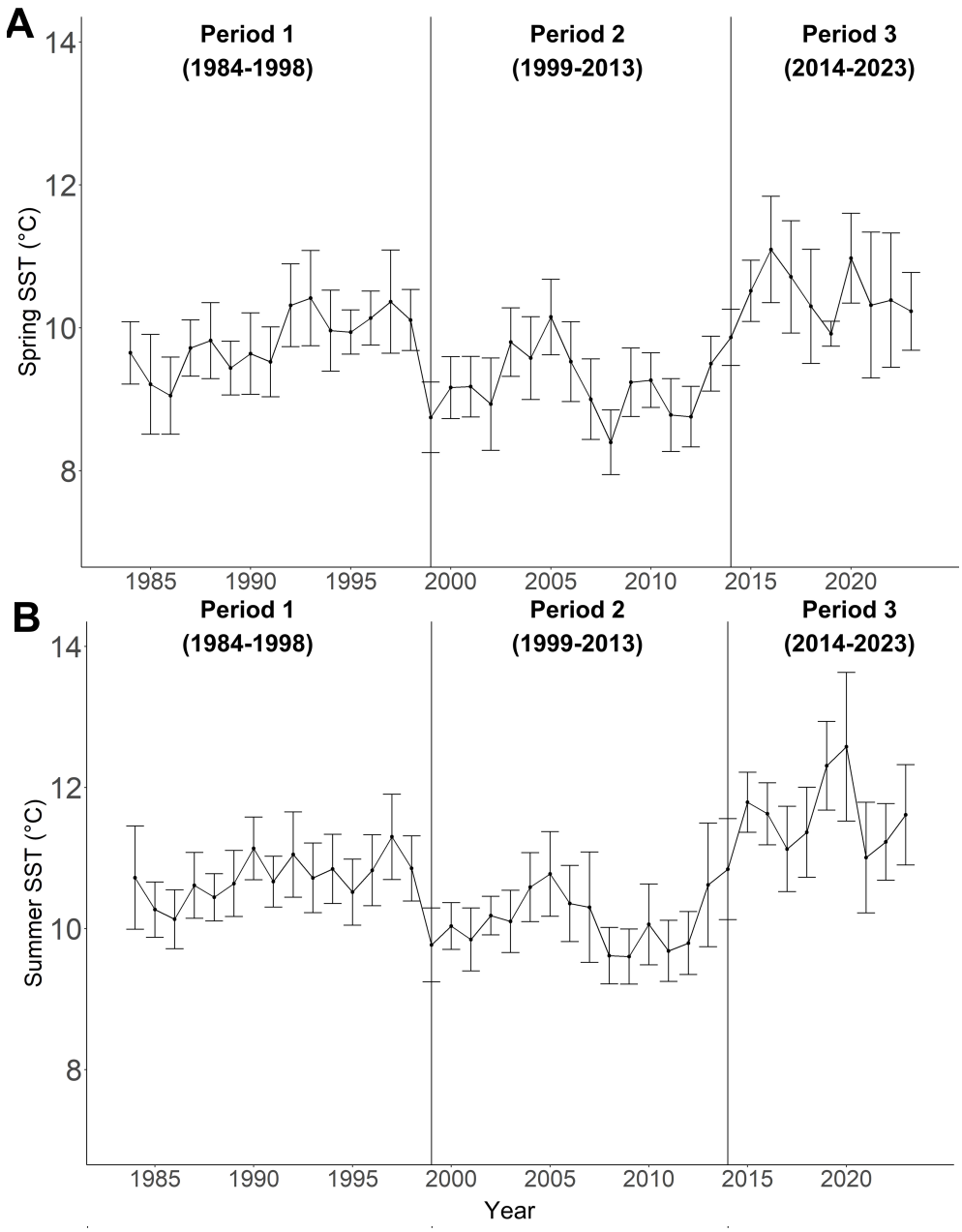

FIGURE 3
(A) Mean regional spring SST, and **(B)** mean regional summer SST from 1984 to 2023. All data was derived from the Pine Island Lighthouse daily SST climatology (1984 to 2023), with error bars representing the standard deviations. The vertical black lines depict the transitions between the climate periods.

54.32°C days, Period 2: 1.7 ± 6.21°C days, Period 3: 26.4 ± 106.84°C days) (Supplementary Figure S2, Table 3B). Note that Period 3 had a high standard deviation for cumulative summer MHW intensity because most days did not have MHWs, but the MHWs that did occur had high cumulative intensity (°C days).

On the global scale, Period 1 (1984 to 1998) generally showed positive PDO (mean Z-score ± SD: 0.617± 0.855) and ONI (0.203 ± 1.13) values, reaching the highest PDO (2.09) and the second highest ONI (2.20) of the time series in 1997 (Figure 5B). Interestingly, the lowest ONI (-1.84) in the time series was also documented within Period 1 in 1988. Period 2 (1999 to 2023) displayed mostly negative PDO (-0.425 ± 0.817) and ONI (-0.292 ± 1.13), although a positive PDO and ONI were documented from 2002 to 2007. When comparing differences in oscillations between Periods 1 and 2, PDO was significantly more negative in Period 2 than in Period 1, whereas there were no significant differences in

TABLE 3 Mann-Kendall's test results testing for significant increases, decreases, or lack thereof in environmental variables from 1984 to 2023, with cells colored in grey, and Kruskal-Wallis and Dunn's test results representing environmental differences between climate periods with cells colored in white (P1 = Period 1, P2 = Period 2, P3 = Period 3) at A) local, B) regional, and C) global scales.

	Testing for significant monotonic trends in each variable		Testing for significant differences between climate periods for each environmental variable				
Variable	Modified Mann-Kendall's Z-statistic (if p-value is significant, + = increasing trend, - = decreasing trend)	Modified Mann-Kendall's p-value	Kruskal-Wallis $\chi 2$	Kruskal-Wallis p-value	Dunn's test		
					Pair	*Z* statistic	Adjusted p-value (Benjamini-Hochberg method)
A: Local SST							
Malcolm Island (*Macrocystis* site)	**3.85**	**0.000121**	**9.18**	**0.0102**	P1-P2	1.76	0.0974
					P1-P3	**3.02**	**0.00744**
					P2-P3	1.66	0.0974
NR	0.0528	0.958	0.875	0.646	N/A	N/A	N/A
ABL	**2.96**	**0.00310**	**9.88**	**0.00716**	P1-P2	1.97	0.0988
					P1-P3	**3.14**	**0.00503**
					P2-P3	1.51	0.132
ABE	**2.36**	**0.0185**	**7.70**	**0.0213**	P1-P2	1.04	0.298
					P1-P3	**2.68**	**0.022**
					P2-P3	1.92	0.109
MIE	**2.66**	**0.00790**	4.81	0.0902	NA	NA	NA
PI	**2.06**	**0.0397**	5.13	0.0770	NA	NA	NA
BH	**3.48**	**0.000492**	**11.2**	**0.00362**	P1-P2	1.68	0.0937
					P1-P3	**3.35**	**0.00240**
					P2-P3	1.68	0.0937
WI	**3.75**	**0.000178**	**12.2**	**0.00228**	P1-P2	2.19	0.0569
					P1-P3	**3.43**	**0.00181**
					P2-P3	1.08	0.280
SLI	1.96	0.0501	**5.68**	**0.0584**	P1-P2	0.16	0.349
					P1-P3	2.26	0.0549
					P2-P3	2.18	0.260
B: Regional							
Regional spring SST	1.10	0.270	**22.4**	**1.39×10^{-5}**	**P1-P2**	**-2.58**	**1.51×10^{-2}**
					P1-P3	**2.43**	**1.51×10^{-2}**
					P2-P3	**4.68**	**8.59×10^{-6}**
Regional summer SST	1.76	0.315	**26.4**	**1.88×10^{-6}**	**P1-P2**	**-2.77**	**7.71×10^{-3}**
					P1-P3	**2.66**	**7.71×10^{-3}**
					P2-P3	**5.08**	**1.10×10^{-6}**
Cumulative pre-summer MHW	0.394	0.693	4.59	0.101	NA	NA	NA
Cumulative summer MHW	**3.13**	**0.00173**	15.90	0.000354	P1-P2	0.039	0.969
					P1-P3	**3.60**	**0.000931**
					P2-P3	**3.60**	**0.000931**
C: Global							
ONI	N/A	N/A	2.03	0.363	N/A	N/A	N/A
PDO	N/A	N/A	**8.03**	**0.0181**	**P1-P2**	**-2.57**	**0.0202**
					P1-P3	-1.93	0.106
					P2-P3	0.38	0.703

Bolded values represent statistical significance.

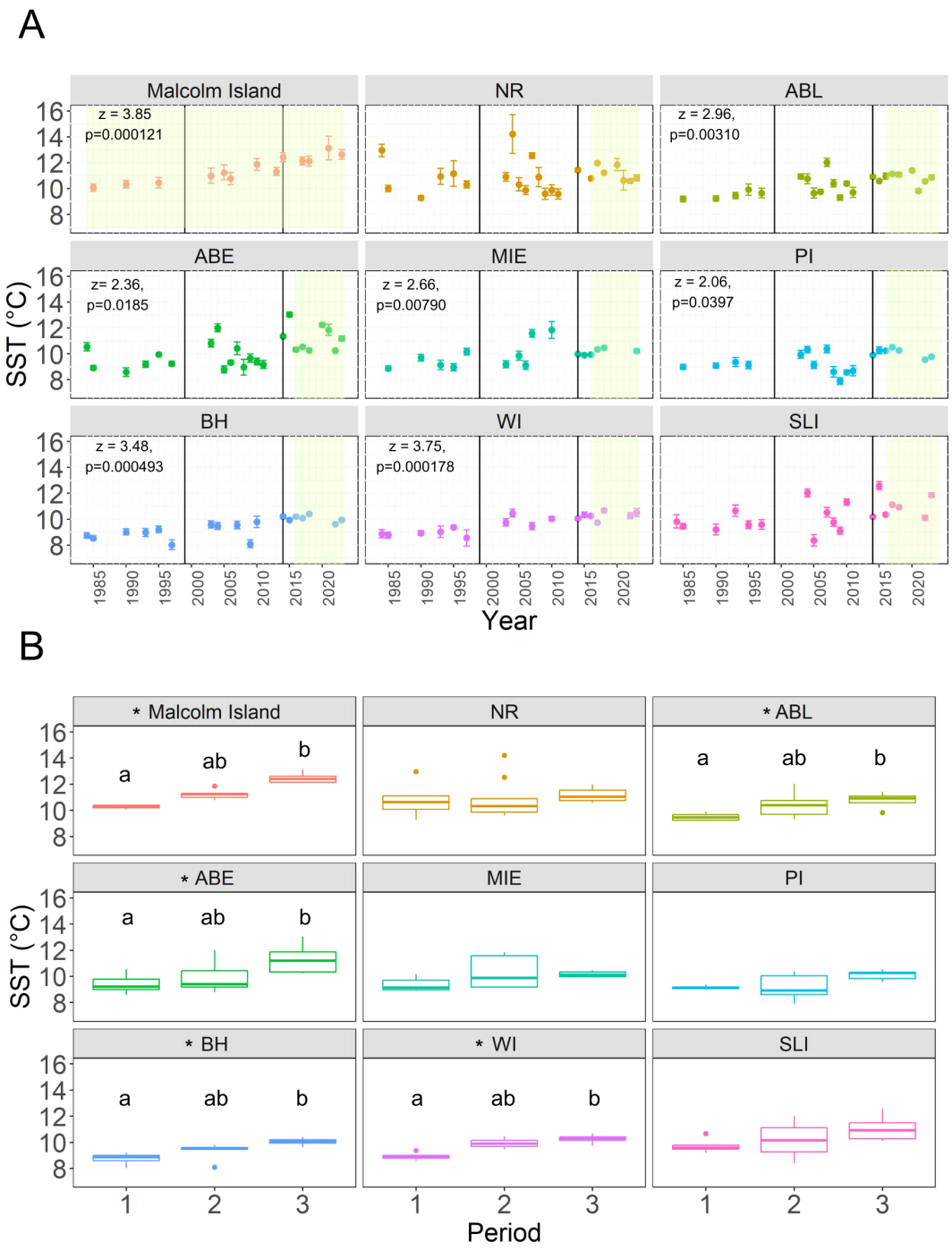

FIGURE 4
(A) Scatterplot showing the mean local summer SST for the *Macrocystis* site ("Malcolm Island") and each *Nereocystis* site (as denoted by the abbreviated site names) from 1984 to 2023, with the error bars around each point representing the standard deviation for each year. The vertical black lines in 1999 and 2014 represent the boundaries between climate periods. The modified Mann-Kendall's Z-statistic and p-value are reported in the top left corner for sites with significant monotonic trends. The green shaded areas of each site's panel represent the length of the kelp time series analyzed for each site. **(B)** The differences in mean local summer SST between each period. Sites with an asterisk (*) are sites with significant differences in local SST across periods. Different letters above each boxplot denote significant pairwise differences.

ONI (Figure 5B, Table 3C). Period 3 (2014 to 2023) started with positive ONI (0.180 ± 1.12) and PDO (-0.273 ± 1.09), with the highest ONI of the time series (2.21) documented in 2015. However, from 2020 onwards, both ONI and PDO shifted negative, with PDO reaching its lowest value of the time series (-1.91) in 2023, although ONI became positive again in 2023 (1.47). Ultimately, there were no significant differences in both ONI and PDO between Periods 1 and 3, and between Periods 2 and 3 (Table 3C).

3.2 Long-term (1984 to 2023) and short-term (2016 to 2023) kelp response to environmental changes

The maximum kelp area at the *Macrocystis* site (1984 to 2023) covered 4.84 million m^2. Percent kelp area ranged from 24.0% (absolute area: 1.15 million m^2) to 71.0% (3.44 million m^2), with a mean of 50.0% (2.46 million m^2) of the maximum kelp area. Further, we found a statistically significant increase in kelp area (Mann Kendall's τ=0.247, p=0.0300, Figure 6A) across all three climate periods. Among the climate periods, we observed statistically significant differences in kelp area between Periods 1 and 2 and between Periods 1 and 3, but not between Periods 2 and 3 (Figure 6A). Specifically, there was a slight increase in kelp area from 43.9 ± 9.34% in Period 1 to 53.8 ± 11.5% in Period 2, which remained high at 55.4 ± 10.4% in Period 3 (Figure 6B; Kruskal-Wallis $\chi2$ = 7.56, p=0.0228; Dunn's test: Period 1 vs Period 2: $\chi2$ = 2.35, p=0.0380; Period 1 vs Period 3, $\chi2$ = 2.35, p=0.0380, Period 2 vs Period 3, $\chi2$ = 0.348, p=0.727). Considering the kelp time series in its entirety, without division between climate periods, the results of the linear model showed no effects of 1-, 2-, or 3-year averages of spring and summer SST, pre-summer and summer cumulative MHW intensities, PDO, or ONI on kelp area, regardless of the combination of predictor variables used (Supplementary Table S4).

For the short-term time series, the maximum kelp areas across all *Nereocystis* sites ranged from 11,800 m^2 (BH) to 214,000 m^2 (MIE) (Figure 7). On a site level, mean percent kelp areas across all surveyed years ranged from 19.0 ± 30.2% (4,010 ± 6,360 m^2) at ABL to 58.5 ± 13.3% at PI (111,000 ± 25,100 m^2), with a total mean percent kelp area across all sites of 43.1 ± 19.3% (Figure 7) Most sites' mean kelp areas exhibited parametric behavior, except ABL, which had a left-skewed pattern caused by kelp loss in the years 2018, 2019, 2022, and 2023 (Figure 7). The eight *Nereocystis* sites also displayed variable temporal trends in kelp areas from 2016 to 2023. Six *Nereocystis* sites displayed no temporal trends (ABL, MIE, PI, BH, WI, SLI), one displayed a significantly decreasing trend (NR, modified Mann-Kendall's Z-statistic = -4.26, p=0.000203), and one displayed a significantly increasing trend (ABE, modified Mann Kendall's Z-statistic = 2.85, p=0.00443, Figure 7).

3.3 Spatial patterns of kelp persistence

The spatial analysis indicated that the *Macrocystis* site had 77.0% persistence, i.e., 77.0% of the maximum kelp area was present for more than 19 years out of the 38-year time series (Figure 8). The *Macrocystis* beds at the eastern part of the *Macrocystis* site were less spatially persistent than the western part (Figure 8). Five *Nereocystis* sites (NR, ABE, MIE, WI, SLI) had 20.6-33.8% persistence, i.e., area that was present for more than 4 years out of the 8-year time series (Figure 9). Sites PI and BH had larger proportions (53.1% and 53.6% respectively) of persistent kelp area, and ABL had no persistent kelp area (0.00% area). For both *Macrocystis* and *Nereocystis* sites, the persistent areas were mainly distributed in the center and inshore areas of each kelp bed (Figures 8-9).

4 Discussion

We found that kelp was both spatially and temporally persistent in the dynamic subregion of the Broughton Archipelago, with increases in the area occupied by *Macrocystis*. Specifically, we identified temporal trends in the kelp area and associated them with the changing environmental conditions using a long-term kelp change time series from 1984 to 2023 of the *Macrocystis* site and a short-term kelp change time series from 2016 to 2023 of the *Nereocystis* sites. We also identified spatial patterns of persistence by spatially combined kelp areas for each site.

4.1 Long-term (1984 to 2023) and short-term (2016 to 2023) kelp response to environmental changes

Overall, the kelp area in the Broughton Archipelago was mostly temporally persistent. Kelp percent area increased monotonically in the *Macrocystis* site from 1984 to 2023, specifically increasing by 9.90% in Period 2 and staying high throughout Period 3. The increase in kelp area at the *Macrocystis* site on the north shore of Malcolm Island corroborates reports from community members (SCFS, unpublished, 2023). This temporal increase indicated persistence in *Macrocystis* area from 1984 to 2023, which may be explained by the increase in local SST from ~10.0 to 13.0°C. This potentially represents a move towards more ideal environmental conditions for *Macrocystis*, which has an optimal thermal range from 12.0 to 17.0°C (Lüning and Neushul, 1978), although this range could vary among populations and life stages (e.g. spores, gametophytes, or sporophytes) (Muth et al., 2019; Hollarsmith et al., 2020; Le et al., 2022). For example, an increase from 9.5 to 12.9°C was experimentally associated with a ~5.00 µm increase in *Macrocystis* gametophyte germ-tube length (Le et al., 2022), and a 10.0 to 14.0°C increase to be associated with a ~2% increase in the relative growth rate of *Macrocystis* blades (Fernández et al., 2020). The local SST increases in the study area always remained below the upper thermal limits for *Macrocystis*, which lie around 18.0-25.0°C (Hay, 1990; Le et al., 2022; Ladah and Zertuche-González, 2007).

On the contrary, regional and global environmental conditions were not linked to significant changes in kelp area (based on the linear model results, Supplementary Table S4). This is likely as regional and global conditions occasionally diverged from the conditions kelps were facing locally in the nearshore environment (Brewer-Dalton et al., 2014; Lin and Bianucci, 2023). For example, the colder SST in Period 2 was only observed in the regional SST and inferred from the negative PDO, but not the local SST time series, which increased continuously throughout all three climate periods. Furthermore, occasional intense MHWs and higher local

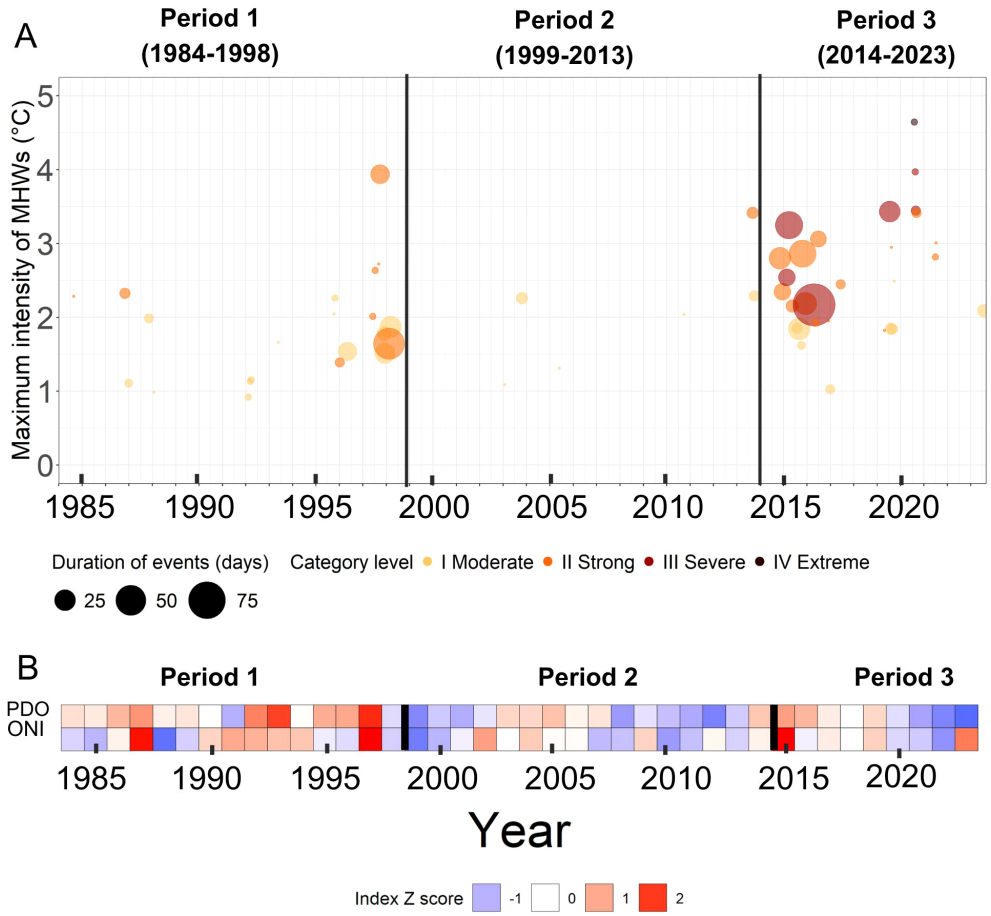

FIGURE 5
Regional and global conditions across the three climatic periods identified (Period 1, Period 2, and Period 3). For both panels, the black lines represent the transitions between climate periods. **(A)** MHWs and their associated duration and category level. The x-axis shows the date of each MHW's maximum intensity peak, and the y-axis shows the maximum intensity of each MHW. The size of each dot corresponds to the duration of each MHW. The MHW category corresponds to the multiples of the seasonal difference between the climatological mean and the climatological 90th percentile. The color of each MHW corresponds to its category level, with a darker color representing a higher category. **(B)** Z-score of mean spring and summer Pacific Decadal Oscillation (PDO) and Oceanic Niño Index (ONI) from 1984 to 2023.

SST were observed during and after 2020, despite a shift to more negative ONI and PDO during the same time. A similar disparity was found between local SST and global climatic oscillations in other parts of BC. For instance, local SST continuously increased after 2020 in the Salish Sea, despite climatic oscillations transitioning to negative phases (e.g. Amos et al., 2015; Mora-Soto et al., 2024a), suggesting that the local SST increase in the Broughton Archipelago may be linked to local oceanographic conditions and variation in coastal geomorphology (Brewer-Dalton et al., 2014; Lin and Bianucci, 2023). Despite mismatches in environmental conditions of different scales during certain years of the time series, generally speaking, Period 3 had higher local and regional SST, a higher frequency and magnitude of MHWs, and more positive PDO and ONI. Similar conditions observed in the Strait of Georgia and Barkley Sound resulted in a subsequent decrease in kelp area (Mora-Soto et al., 2024a; Starko et al, 2022). However, in the dynamic subregion of the Broughton Archipelago, both local and regional measurements of SST remained within *Macrocystis*' optimal thermal range during Period 3, and consequently, we did not observe decreases in the kelp area. This reinforces the observation that local temperature gradients can greatly influence kelp responses in the face of regional events such as MHWs (Starko et al., 2024b). It is unknown whether the climatic oscillations affected other environmental conditions not investigated in this study (e.g. nutrient availability) (Whitney, 2015; Bond et al., 2015), which may have impacted kelp physiology (Hollarsmith et al., 2022). Regardless, climatic oscillations did not directly relate to significant changes in the kelp area at the *Macrocystis* site.

Aside from environmental changes, there may be biotic conditions at play, such as a low abundance of sea urchins (Eisaguirre et al., 2020). Although not investigated in this study, Man et al. (in prep) found no sea urchins during a one-time sampling effort during the summer of 2023 at the *Macrocystis* site, suggesting that the absence or low abundance of sea urchins may have been conducive to kelp persistence at the *Macrocystis* site.

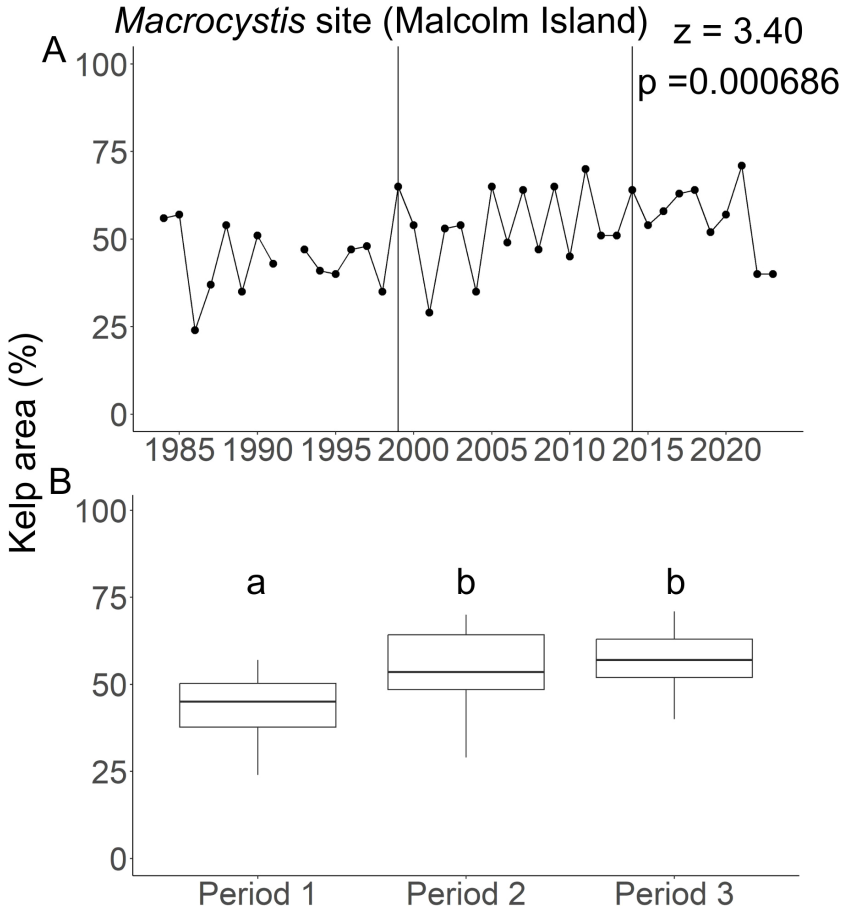

FIGURE 6
Kelp area changes in the *Macrocystis* site (Malcolm Island). **(A)** The temporal changes in the yearly kelp area from 1984 to 2023. Vertical lines in A) indicate the boundaries between periods. The Z-statistic represents the direction of monotonic change as determined by the modified Mann-Kendall's test, with negative values representing negative trends and positive value representing positive trends. The p represents the p-value. There is no data available for 1992. **(B)** Boxplots showing the differences in the median kelp area and their associated interquartile ranges among climate periods. Identical letters above the boxes represent no significant differences in median kelp area between the pair of periods as determined by the Kruskal-Wallis test, whereas different letters above the boxes represent significant differences in median kelp area between the respective periods.

Continuous time-series data about other environmental and biotic conditions could elucidate what specifically drove the increase in *Macrocystis* area in the study area.

Our observations of *Macrocystis* persistence in cooler waters corroborated patterns observed in cooler areas throughout the Northeast Pacific coast. For instance, centennial increases in the *Macrocystis* area were also observed in Southeast Alaska by Hollarsmith et al. (2024), which the authors attributed to various factors including temperature increases and the reintroduction of the sea otter, a keystone predator. Persistence in *Macrocystis* area was also observed in Cumshewa Inlet (Gendall et al., submitted), Ella Beach, BC (Mora-Soto et al., 2024a), and the outer coast of Washington (Pfister et al., 2018), where local summer SST increases (~10.0 to 14.0°C) over the past few decades were similar to those observed in the Broughton Archipelago and did not reach the upper thermal limits of *Macrocystis*. Similarly, these cooler, northern regions (BC and Washington) displayed *Macrocystis* persistence in response to the Blob of 2016. Conversely, the warmer southern regions (Central to Southern California, and Baja California Norte and Sur), which reached summer temperatures of ~17.0-24.0°C, experienced areal decreases to ~2-57% of their pre-Blob baseline (Mora-Soto et al., 2024b; Pfister et al., 2018; Cavanaugh et al., 2019; Bell et al., 2023).

Kelp persisted in most of the *Nereocystis* sites from 2016 to 2023, although some sites showed different trends in the kelp area. Specifically, ABL did not display a significant temporal trend, but exhibited kelp losses in four of the eight studied years, corroborating community anecdotes of kelp decrease in the area (SCFS, unpublished, 2023). Similarly, kelp also declined significantly at NR, confirming community reports of kelp decrease near Alder Bay and Green Island, which comprise the eastern areas of NR (Figure 9; SCFS, unpublished, 2023). An examination of Figure 9 revealed that the eastern areas of NR were indeed less spatially persistent. The observed increase in kelp area at ABE also reinforced local reports of a recent increase in kelp area after past decreases (SCFS, unpublished, 2023). Some of our results, however, contrasted with

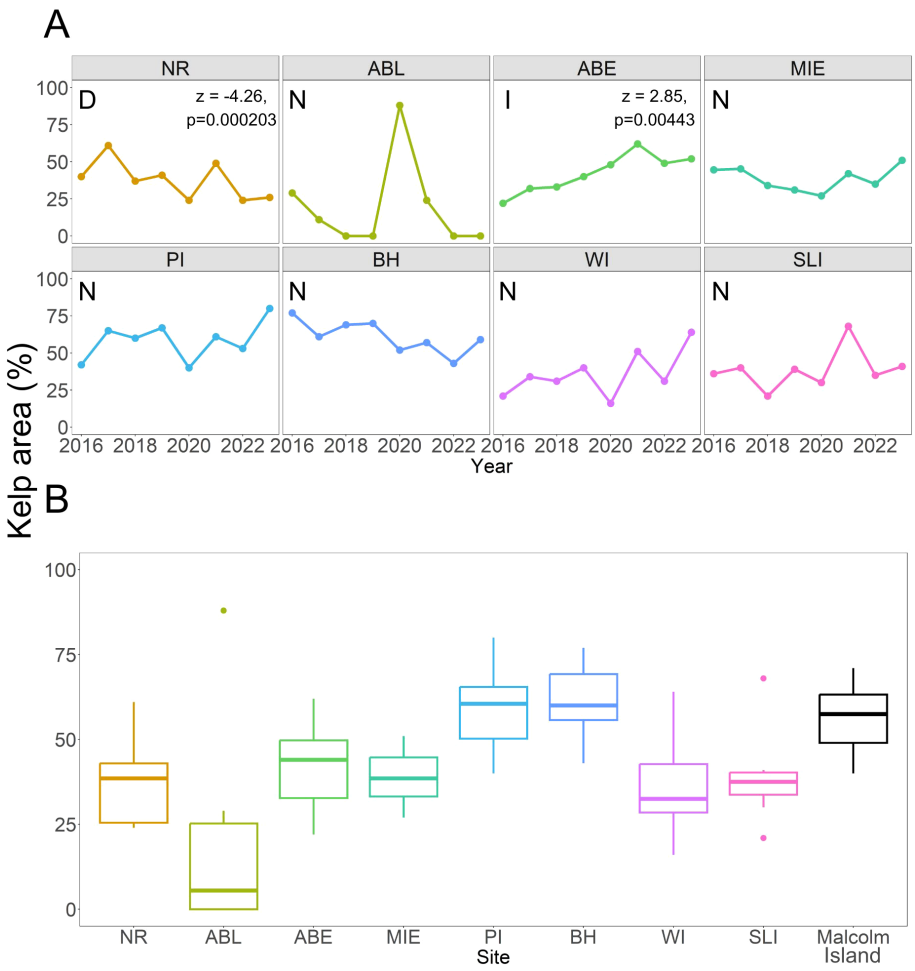

FIGURE 7
(A) Changes in percent kelp area in the 8 *Nereocystis* sites from 2016 to 2023. Sites with "N" under the site name are sites with no significant temporal trends, the site with "D" had a significantly decreasing trend, and the site with "I" had a significantly increasing trend, as per the modified Mann-Kendall test results. The significant test result is shown for the associated site. **(B)** Boxplot showing median kelp area and their associated interquartile ranges from 2016 to 2023 at each site. The mean percent kelp area for the *Macrocystis* site ("Malcolm Island") from 2016 to 2023 is also included for reference, although it is not part of the short-term time series.

some other community reports of kelp trends: e.g. a kelp increase at MIE after urchin harvesting began in that area, although the start date of urchin harvesting was not reported (Mountain, pers comm, 2023). Such discrepancies between the local community members' observations and our results may be linked to different study periods or time scales since they did not report the years where the changes in the kelp area were observed (SCFS, unpublished, 2023; Mountain, pers comm, 2023). Thus, it is possible that the changes identified by the local community were observed outside of the timeframe covered in this study between 2016 to 2023. Furthermore, short-term studies (<20 years) are less likely than long-term studies (>20 years) to capture patterns of kelp decrease due to kelp's high interannual variability and environmental conditions' multi-year or decadal dynamics (Wernberg et al., 2019). Therefore, it is also possible that our short-term time series was simply not long enough to detect the changes reported by local communities, or that *Nereocystis*' high interannual variability in canopy-forming area may have skewed community observations based on when the observations were made.

The observed overall kelp persistence in the *Nereocystis* sites may be partially explained by the local SST (~9.0-12.0°C), similar to the patterns observed in the *Macrocystis* site, Local SST increased at some of the *Nereocystis* sites but mostly remained below the upper thermal limits of *Nereocystis* (around 12.0-16.0°C for sporophytes, and 16.0-18.0°C for gametophytes, depending on the population) (Pontier et al., 2024; Korabik et al., 2023; Weigel et al., 2023). However, local SST may not be the only variable affecting kelp area changes, as kelp area only decreased at ABL and NR, despite local SST not increasing beyond 12.0°C between 2016 and 2023 at both sites. While examining the spatial patterns of kelp loss, we noted that the sites ABL and NR were close to each other and near the mouth of the Nimpkish River, which brings pulses of warmer water

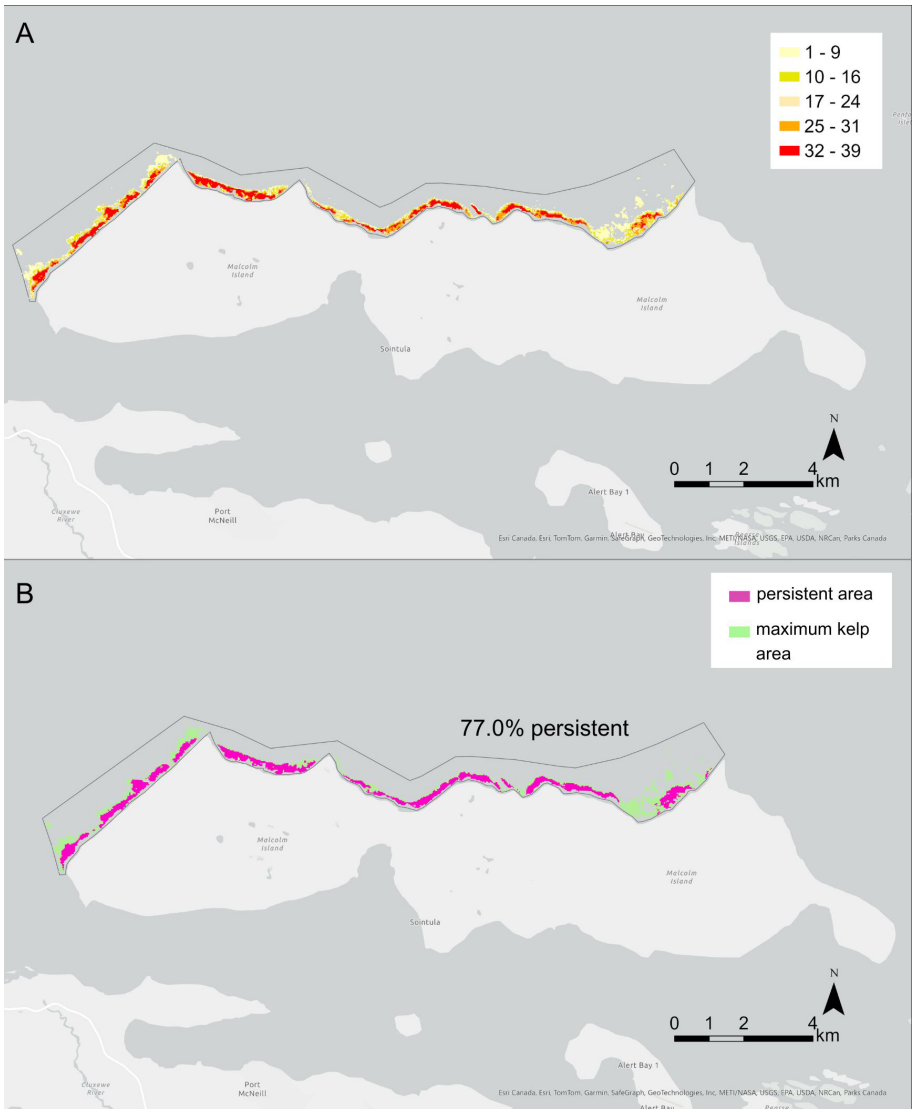

FIGURE 8
Maps showing the spatial patterns of kelp persistence at the *Macrocystis* site: the north shore of Malcolm Island. **(A)** shows the number of years of kelp presence out of the 39 years investigated, which was used to determine the areas of kelp persistence. The yellow-red scale indicates the number of years of kelp presence. **(B)** shows the persistent area in pink and the maximum kelp area in green. The total percentage area of the maximum kelp area that is persistent is indicated in **(B)** For both panels, the frame around the kelp beds shows the area considered for the analysis. Refer to Figure 1 for the location of the *Macrocystis* site.

above 20.0°C into the nearshore environment. This suggests the possibility that warmer freshwater pulses not captured from satellite-derived local SST and long-term regional SST averages may have affected kelp abundance (Figure 1, Barbosa & Man, personal communication, March 7, 2023). ABE, a site where the kelp area increased, did not have significantly different environmental conditions than the other six sites, which displayed no significant temporal change. Thus, the different temporal kelp trends in ABE, NR, and ABL may also be attributed to other environmental and/or biotic factors not researched in this study. One potentially important environmental factor not addressed here may be seasonal sediment outflows from the Nimpkish River, which may have increased the turbidity of the water, decreasing light availability at NR and ABL for kelps and affecting their growth. The phenomenon of river outflows limiting kelp growth has been observed in Southern Chilean Patagonia (Huovinen et al., 2020), however, further study is needed to test this hypothesis for these two sites. A potentially important biotic factor may be the understory kelps which can outcompete the more ruderal *Nereocystis* (Dayton et al., 1984; Springer et al., 2010), since a one-time underwater field inspection conducted by Man et al. (in prep) uncovered high understory kelp abundance at NR and ABL, which cannot easily be detected from satellite imagery (Cavanaugh et al., 2021). Similar

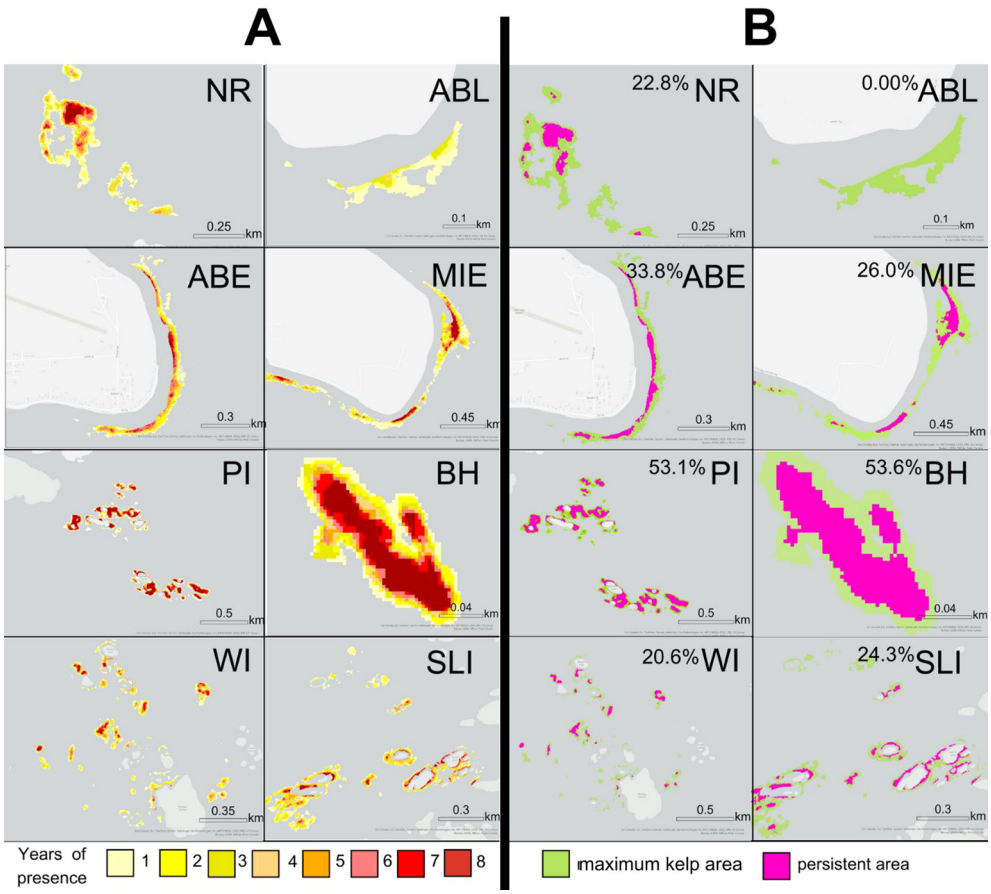

FIGURE 9
Maps showing the spatial patterns of kelp persistence at each *Nereocystis* site. **(A)** shows the number of years of kelp presence out of the eight years investigated, when higher resolution satellite images were available, which was used to determine the areas of kelp persistence. The yellow-red scale indicates the number of years of kelp presence. **(B)** shows the persistent area in pink and the maximum kelp area in green. The total percentage area of the maximum kelp area that is persistent is indicated in **(B)** Refer to Figure 1 for the location of each *Nereocystis* site.

to the *Macrocystis* site, regional and global environmental conditions did not appear to affect the overall kelp persistence in the *Nereocystis* sites, likely because these conditions differed from local SST conditions.

Kelp area in the *Nereocystis* sites remained mostly persistent during and after the Blob (Figure 7). It is important to note that the time series for the *Nereocystis* sites started at the end of the Blob (2016), lacking a pre-Blob baseline for the *Nereocystis* sites. Therefore, our results could mean that *Nereocystis* was either not affected by the Blob or was affected by the Blob and did not recover to possible higher pre-Blob abundances. This echoes findings of *Nereocystis* persistence after the Blob in Oregon (Hamilton et al., 2020) and in the southern Salish Sea (Mora-Soto et al., 2024a, 2024b), where SST remained cooler (~12.0-15.0°C). On the other hand, this contrasts with findings of *Nereocystis* trends in Northern California (McPherson et al., 2021; Cavanaugh et al., 2023; Bell et al., 2023), Southern Puget Sound (Berry et al., 2021), and the northern and central Salish Sea (Mora-Soto et al., 2024b; Starko et al., 2024a), where *Nereocystis* area declined after the Blob and showed limited recovery. The reasons for these kelp declines vary from higher SST (summer temperatures: ~13.0 to 20.0°C) to an increase in sea urchins after the loss of a keystone predator (sunflower sea stars) after the Blob (Hamilton et al., 2021), neither of which have been documented in the Broughton Archipelago.

Overall, we identified primarily persistent kelp forests, including *Macrocystis* and *Nereocystis* kelp areas, in the dynamic subregion of the Broughton Archipelago. As the documented SST trends remained within the favorable range for kelps throughout both time series, we cannot conclude if the kelps would be resilient to further SST increases (up to 20.0°C) in the study area, such as those observed SST increases in the northern Salish Sea, Southern Puget Sound, the sheltered parts of Barkley Sound, and in California. Regardless, the kelp forests have likely persisted for a long time in the study area, as all but two sites (BH and WI) were historically documented to have kelp present in the 1850s to 1950s based on records in the British Admiralty nautical charts (Figure 10; Costa et al., 2020). Note that this historical information only serves as a record of kelp presence, not kelp absence (Costa et al., 2020), thus, the lack of historical kelp documentation at BH does not necessarily mean that kelp was absent from the 1850s to the 1950s.

The likely centennial persistence of kelp suggests that the dynamic subregion of the Broughton Archipelago represents a climate refuge for kelp. Similar patterns of persistence can be expected and have been observed in other similar temperature regimes such as the more exposed areas of the Strait of Juan de Fuca (Mora-Soto et al., 2024a; Pfister et al., 2018) and Oregon (Hamilton et al., 2020), in the absence of other stressors such as high water turbidity and sea urchin abundance (Huovinen et al., 2020; Eisaguirre et al., 2020). It is important to consider that this observation of persistence in the dynamic subregion may not apply to other parts of the Broughton Archipelago, such as the fjord subregion, which have smaller, fringing kelp beds that are subject to significantly different environmental conditions (Man et al., in prep). Indeed, local community members have anecdotally noted decreases in kelp distribution and area in the fjord subregion, including near now-decommissioned open-net salmon farms (Mountain, pers comm, 2023). Future research can investigate kelp area changes in the fjord subregion using very-high-resolution satellite imagery (e.g. Worldview-2 at 0.46 m spatial resolution), which may be capable of accurately detecting the smaller, fringing kelp beds.

4.2 Spatial patterns of kelp persistence

Kelp beds of both species had similar spatial patterns of persistence, with the center and inshore areas of kelp beds being more persistent than the edges. This reinforces spatial patterns found in *Macrocystis* forests in Southern California (Young et al., 2016), and *Nereocystis* forests in Northern California (Arafeh-Dalmau et al., 2023), Oregon (Hamilton et al., 2020; Arafeh-Dalmau et al., 2023), and the outer coast of Washington (Arafeh-Dalmau et al., 2023). The spatial pattern of persistence may be associated with local variations in environmental and biotic factors, including current conditions, kelp dispersal, and sea urchin abundance (Jackson and Winant, 1983; Graham, 2003; Reeves et al., 2022). For instance, water current velocities are higher at the edges of the kelp bed than on the inside due to kelp plants' ability to buffer water currents (Jackson and Winant, 1983). Therefore, physical disturbances to kelps are more prone to happen at the kelp bed edges (Bekkby et al., 2019), potentially affecting its spatial persistence (e.g. Young et al., 2016). Currents may also play a role in kelp spore dispersal, with currents typically traveling further away at the kelp bed edge than in the interior, carrying zoospores away from the bed (Graham, 2003). In contrast, in the kelp forest interior, the drag from the high density of kelp sporophytes modifies current flow to primarily oscillate within the kelp bed, maintaining high levels of spore supply (Graham, 2003), and potentially contributing to the higher spatial persistence in the kelp bed interior. Biotic factors, such as increased urchin grazing at the edges of a kelp bed compared to the inside, may also cause lower kelp persistence at the edges (Reeves et al., 2022). However, it is unlikely that this is the situation at most of our study sites, as only some were documented to have abundant urchins (Man et al., in prep).

Beyond the potential influence of environmental and biotic drivers on the spatial patterns of persistence, the variable environmental conditions during the satellite imagery acquisition could have also affected the observed kelp area. Potential environmental conditions affecting the observed kelp area in the satellite images include the tidal height, which can submerge the edges of the kelp bed (short-term dataset tidal height: 0.716-2.50 m), and the currents that move kelps in different directions (Timmer et al., 2024). Timmer et al. (2024) found that kelp bed area can decrease by an average of 22.5% around the edges of the kelp bed per meter of tidal increase during low current speeds (<0.100 m/s) and 35.5% at high current speeds (>10.0 m/s). However, that study was conducted using drone imagery, thus the specific impacts of a tidal height increase on kelp bed edge submersion as detected from satellite imagery may slightly differ due to the difference in spatial resolution. We have reduced the influence of tidal height on detected kelp area by 1) aggregating images acquired under the different tidal heights for the long-term dataset and 2) testing and confirming with a linear mixed model the lack of a significant effect of tidal height on kelp area for the short-term dataset. No information on current speeds during the time of satellite imagery acquisition was available, however, according to the regional model by Foreman et al. (2009), tidal current speeds are generally high (~0.390 m/s) at the *Nereocystis* sites, thus it is possible that some kelp was submerged by the tidal currents. Nonetheless, the non-persistent areas in the short-term time series were all larger than 35.5% of the maximum kelp areas, thus it is unlikely that the spatial pattern of persistence can be entirely attributed to tidal height and tidal current speeds.

The proportion of persistent kelp area varied within the *Macrocystis* site. A visual assessment of the *Macrocystis* site showed that the western parts have more persistent kelp areas, whereas the eastern part had a smaller percentage of persistent kelp areas. Fieldwork conducted for Man et al. (in prep) and historical data from the BC Shorezone Mapping System[11] revealed submerged eelgrass beds interspersed between the *Macrocystis* at the eastern end of the north shore and homogenous *Macrocystis* patches at the western end. Thus, interspecific competition between *Macrocystis* and eelgrass may lead to smaller areas of persistence, a phenomenon that has been documented between other seaweed and seagrass species (Alexandre et al., 2017).

The kelp beds in the *Nereocystis* sites generally had lower proportions of spatially persistent area than in the *Macrocystis* site. ABL, the only *Nereocystis* site with years of kelp loss, was not spatially persistent, even in the center of its maximum kelp area. NR, the *Nereocystis* site with significantly decreasing kelp area, had 22.8% persistent area, with no persistent areas in the eastern part of the site. The sites that displayed no significant temporal changes, i.e., temporal persistence, had 20.6-53.6% spatially persistent areas; and the site where kelp was increasing (ABE) had a 33.8% spatially persistent area. It is important to note that for the *Nereocystis* sites, the threshold for kelp persistence was only 4 years out of the 8-year time series, much lower than that of the longer time series (19 out of 38 years), which may have led to the different percentages of

11 https://bcmca.ca/datafiles/individualfiles/bcmca_eco_vascplants_eelgrass_bioband_atlas.pdf

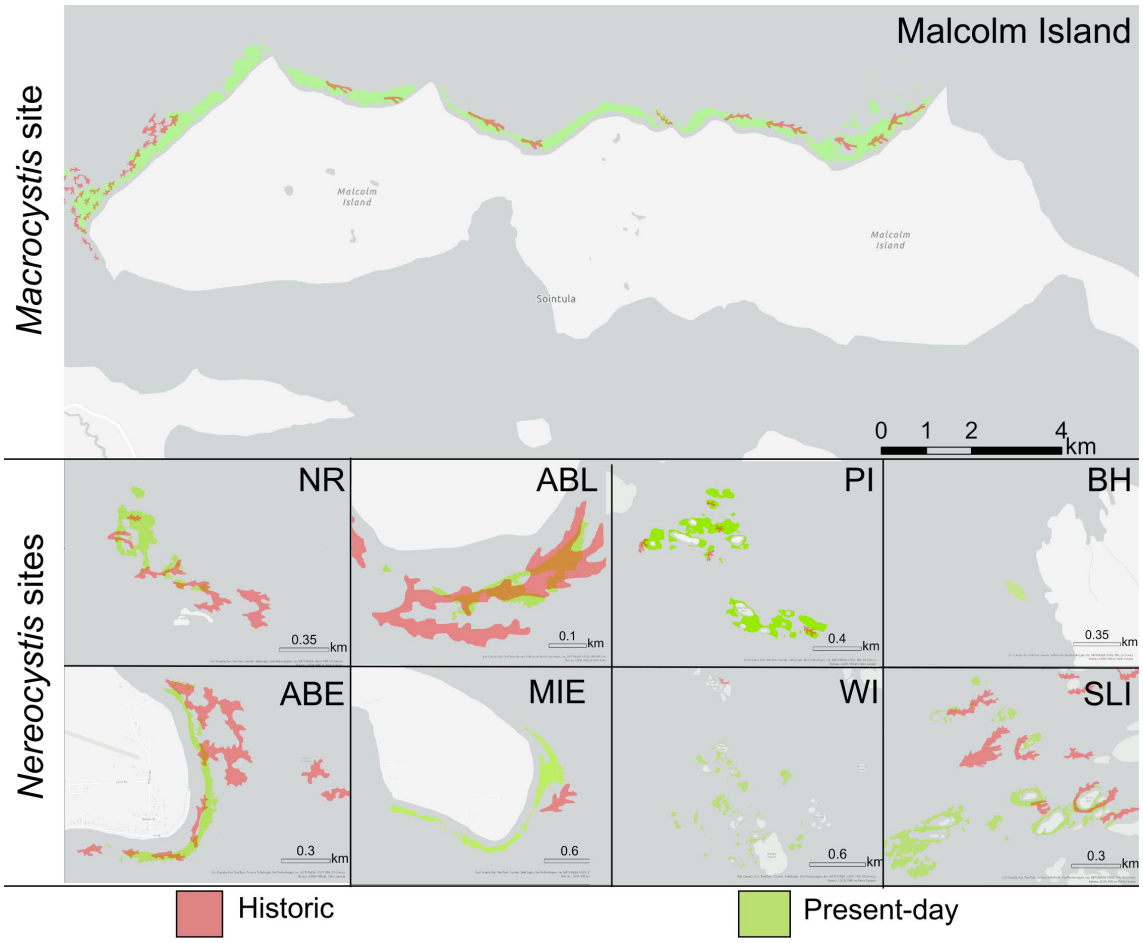

FIGURE 10
Map showing the location of historic kelp forests (1850s to 1950s) as documented in the British Admiralty nautical charts (red) and the maximum kelp area as derived from 'present-day' (*Macrocystis* site: aggregate from 1984 to 2023, 8 *Nereocystis* sites: aggregate from 2016 to 2023) satellite imagery (green). Note that the historic kelp polygons are only evidence of kelp presence, not kelp absence, and their shapes and sizes may not be related to the size of the actual kelp beds present during that time (Costa et al., 2020). Refer to Figure 1 for the location of each *Macrocystis* and *Nereocystis* site.

persistent area between the long-term and short-term datasets. However, the lower persistence levels in the *Nereocystis* sites, as compared to the *Macrocystis* sites, may also be partially explained by *Nereocystis'* ruderal quality and annual life history, which leads to higher interannual variability than other perennial kelp species, such as *Macrocystis* (Dayton et al., 1984; Springer et al., 2010). The phenomenon of *Nereocystis* having higher spatial variability than *Macrocystis* was also observed on the Washington coast (Pfister et al., 2018), which the study authors also attributed to *Nereocystis'* ruderal nature.

5 Conclusion

This study examined kelp forest responses to environmental changes in the dynamic subregion of the Broughton Archipelago across different spatial and temporal scales. Temporally, we documented overall kelp persistence in the dynamic subregion of the Broughton Archipelago, including areal increases from 1984 to 2023 in the *Macrocystis* site and primarily no significant change in kelp area at *Nereocystis* sites from 2016 to 2023. Increased local SST into the thermal optimum of *Macrocystis* was associated with increases in the *Macrocystis* area, whereas regional SST, MHWs, and climatic oscillations did not affect it. The *Nereocystis* area did not appear to be affected by environmental conditions at local, regional, and global scales, likely as temperatures remained within its thermal optimum. Spatially, we found that most sites had spatially persistent kelp, and areas in the center of a kelp bed were more likely to be persistent than the edges. The *Macrocystis* site had more spatially persistent areas than the *Nereocystis* sites.

In a broader context, our findings add to the understanding of kelp forest trends and patterns of persistence in the face of environmental changes in BC, the Northeast Pacific Ocean, and other temperate regions globally. The patterns observed in the dynamic subregion of the Broughton Archipelago reinforce findings that regional events such as MHWs may not negatively impact kelp populations if local conditions are favorable. Ultimately, by filling in the geographic gaps of kelp change, this study can inform marine spatial planning efforts for kelp conservation, management, and restoration.

Data availability statement

The raw data supporting the conclusions of this article will be made available by the authors, without undue reservation.

Author contributions

LM: Conceptualization, Data curation, Formal analysis, Investigation, Methodology, Project administration, Validation, Visualization, Writing – original draft, Writing – review & editing, Software. RB: Supervision, Writing – review & editing. LR: Data curation, Writing – review & editing, Resources, Funding acquisition, Investigation. LG: Conceptualization, Writing – review & editing, Project administration, Investigation. AW: Writing – review & editing. ND: Funding acquisition, Writing – review & editing, Project administration. UK: Funding acquisition, Writing – review & editing, Project administration. CN: Writing – review & editing. MC: Conceptualization, Funding acquisition, Project administration, Resources, Supervision, Writing – review & editing.

Funding

The author(s) declare that financial support was received for the research, authorship, and/or publication of this article. LM and ND acknowledge funding from the Broughton Aquaculture Transition Initiative. LM, LG, AW, and MC acknowledge funding from the Natural Sciences and Engineering Research Council of Canada Alliance grant awarded to MC (Ref. number: ALLRP 566735 - 21). RB. acknowledges funding from the Oceans Management Contribution Program (OMCP) of Fisheries and Oceans Canada (DFO) and Mitacs (Ref. number: IT40879) accelerate funding.

Acknowledgments

We express our gratitude to the Kwakwaka'wakw people on whose traditional territories we conducted this research. We would like to acknowledge the Broughton Aquaculture Transition Initiative field crew and staff for coordinating and conducting fieldwork with us, specifically: Andrew Wadhams, Jonah Johnson, Daniel Wadhams, Dennis Johnson, Jack Alfred, Joey Webber, Tre Alfred, Emily Wisden-Seaweed, Trish Alfred. We are grateful to Hereditary Chief Robert Mountain, for sharing his knowledge about kelp changes in your territories. We are thankful to Salmon Coast Field Station, particularly executive director Dr. Amy Kamarainen, for sharing information from the participatory mapping reports regarding kelp in the area. We would like to thank Dr. Alejandra Mora-Soto for providing code and advice for deriving sea-surface temperature from Landsat imagery and for calculating marine heatwave occurrences. We thank Dr. Tom Bell, for assistance with the Landsat kelp dataset. Finally, we thank Dr. Amanda Bates and Dr. Kylee Pawluk for providing feedback on a previous version of this manuscript.

Conflict of interest

Authors CN was employed by LGL Limited Environmental Research Associates.

The remaining authors declare that the research was conducted in the absence of any commercial or financial relationships that could be construed as a potential conflict of interest.

Generative AI statement

The author(s) declare that no Generative AI was used in the creation of this manuscript.

Publisher's note

Supplementary material

The Supplementary Material for this article can be found online at: https://www.frontiersin.org/articles/10.3389/fmars.2025.1537498/full#supplementary-material

References

Akaike, H. (1974). A new look at the statistical model identification. *IEEE Trans. Automatic Control* 19, 716–723. doi: 10.1109/TAC.1974.1100705

Alexandre, A., Baeta, A., Engelen, A. H., and Santos, R. (2017). Interactions between seagrasses and seaweeds during surge nitrogen acquisition determine interspecific competition. *Sci. Rep* 7, 13651. doi: 10.1038/s41598-017-13962-4

Amos, C. L., Martino, S., Sutherland, T. F., and Al Rashidi, T. (2015). Sea surface temperature trends in the coastal zone of British Columbia, Canada. *J. Coast. Res* 31, 434–446. doi: 10.2112/JCOASTRES-D-14-00114.1

Arafeh-Dalmau, N., Montaño-Moctezuma, G., Martinez, J. A., Beas-Luna, R., Schoeman, D. S., and Torres-Moye, G. (2019). Extreme marine heatwaves alter kelp forest community near its equatorward distribution limit. *Front. Mar. Sci* 6. doi: 10.3389/fmars.2019.00499

Arafeh-Dalmau, N., Olguín-Jacobson, C., Bell, T. W., Micheli, F., and Cavanaugh, K. C. (2023). Shortfalls in the protection of persistent bull kelp forests in the USA. *Biol. Conserv* 283, 110133. doi: 10.1016/j.biocon.2023.110133

Bates, D., Maechler, M., Bolker, B., Walker, S., Christensen, R. H. B., Singmann, H., et al. (2015). Package 'lme4'. *Convergence* 12, p.2. doi: 10.18637/jss.v067.i01

Beas-Luna, R., Micheli, F., Woodson, C. B., Carr, M., Malone, D., Torre, J., et al. (2020). Geographic variation in responses of kelp forest communities of the California Current to recent climatic changes. *Global Change Biol* 26, 6457–6473. doi: 10.1111/gcb.15273

Bekkby, T., Smit, C., Gundersen, H., Rinde, E., Steen, H., Tveiten, L., et al. (2019). The abundance of kelp is modified by the combined impact of depth, waves and currents. *Front. Mar. Sci* 6. doi: 10.3389/fmars.2019.00475

Bell, T. W., Allen, J. G., Cavanaugh, K. C., and Siegel, D. A. (2020). Three decades of variability in California's giant kelp forests from the Landsat satellites. *Remote Sens. Environ* 238, 110811. doi: 10.1016/j.rse.2018.06.039

Bell, T. W., Cavanaugh, K. C., Reed, D. C., and Siegel, D. A. (2015). Geographical variability in the controls of giant kelp biomass dynamics. *J. Biogeography* 42, 2010–2021. doi: 10.1111/jbi.12550

Bell, T. W., Cavanaugh, K. C., Saccomanno, V. R., Cavanaugh, K. C., Houskeeper, H. F., Eddy, N., et al. (2023). Kelpwatch: A new visualization and analysis tool to explore kelp canopy dynamics reveals variable response to and recovery from marine heatwaves. *PloS One* 18, e0271477. doi: 10.1371/journal.pone.0271477

Benjamini, Y., and Hochberg, Y. (1995). Controlling the false discovery rate: a practical and powerful approach to multiple testing. *J. R. Stat. Society: Ser. B (Methodological)* 57, 289–300. doi: 10.1111/j.2517-6161.1995.tb02031.x

Berry, H. D., Mumford, T. F., Christiaen, B., Dowty, P., Calloway, M., Ferrier, L., et al. (2021). Long-term changes in kelp forests in an inner basin of the Salish Sea. *PloS One* 16, e0229703. doi: 10.1371/journal.pone.0229703

Bond, N. A., Cronin, M. F., Freeland, H., and Mantua, N. (2015). Causes and impacts of the 2014 warm anomaly in the NE Pacific. *Geophysical Res. Lett* 42, 3414–3420. doi: 10.1002/2015gl063306

Brewer-Dalton, K., Page, F. H., Chandler, P., and Ratsimandresy, A. (2014). Oceanographic conditions of salmon farming areas with attention to those factors that may influence the biology and ecology of sea lice, *Lepeophtherius salmonis* and *Caligus* spp., and their control. *DFO Can. Sci. Advis. Sec. Res. Doc* 2014/048. vi + 47 p.

Burt, J. M., Tinker, M. T., Okamoto, D. K., Demes, K. W., Holmes, K., and Salomon, A. K. (2018). Sudden collapse of a mesopredator reveals its complementary role in mediating rocky reef regime shifts. *Proc. R. Soc. B: Biol. Sci* 285, 20180553. doi: 10.6084/m9.figshare.c.4161416.v2

Cavanaugh, K. C., Bell, T., Costa, M., Eddy, N. E., Gendall, L., Gleason, M. G., et al. (2021). A review of the opportunities and challenges for using remote sensing for management of surface-canopy forming kelps. *Front. Mar. Sci* 8. doi: 10.3389/fmars.2021.753531

Cavanaugh, K. C., Pawlak, C. C., Bell, T. W., and Saccomanno, V. R. (2023). CubeSats show persistence of bull kelp refugia amidst a regional collapse in California. *Remote Sens. Environ* 290, 113521. doi: 10.1016/j.rse.2023.113521

Cavanaugh, K. C., Reed, D. C., Bell, T. W., Castorani, M. C., and Du, L. R. (2019). Spatial variability in the resistance and resilience of giant kelp in southern and Baja California to a multiyear heatwave. *Front. Mar. Sci* 6, 413. doi: 10.3389/fmars.2019.00413

Cavanaugh, K. C., Siegel, D. A., Reed, D. C., and Dennison, P. E. (2011). Environmental controls of giant-kelp biomass in the Santa Barbara Channel, California. *Mar. Ecol. Prog. Ser* 429, 1–17. doi: 10.3354/meps09141

Cheng, L., von Schuckmann, K., Abraham, J. P., Trenberth, K. E., Mann, M. E., Zanna, L., et al. (2022). Past and future ocean warming. *Nat. Rev. Earth Environ* 3, 776–794. doi: 10.1038/s43017-022-00345-1

Connell, J. H., and Sousa, W. P. (1983). On the evidence needed to judge ecological stability or persistence. *Am. Nat* 121, 789–824. doi: 10.1086/284105

Costa, M., Le Baron, N., Tenhunen, K., Nephin, J., Willis, P., Mortimor, J. P., et al. (2020). Historical distribution of kelp forests on the coast of British Columbia: 1858–1956. *Appl. Geogr* 120, 102230. doi: 10.1016/j.apgeog.2020.102230

Davies, S. C., Gregr, E. J., Lessard, J., Bartier, P., and Wills, P. (2018). Coastal digital elevation models integrating ocean bathymetry and land topography for marine ecological analyses in Pacific Canadian waters. *Can. Tech. Rep. Fish. Aquat. Sci* 3321, vi + 38.

Dayton, P. K., Currie, V., Gerrodette, T., Keller, B. D., Rosenthal, R., and Tresca, D. V. (1984). Patch dynamics and stability of some California kelp communities. *Ecol. Monogr* 54, 253–289. doi: 10.2307/1942498

Di Lorenzo, E., and Mantua, N. (2016). Multi-year persistence of the 2014/15 North Pacific marine heatwave. *Nat. Climate Change* 6, 1042–1047. doi: 10.1038/nclimate3082

Di Lorenzo, E., Schneider, N., Cobb, K. M., Franks, P. J. S., Chhak, K., Miller, A. J., et al. (2008). North Pacific Gyre Oscillation links ocean climate and ecosystem change. *Geophysical Res. Lett* 35. doi: 10.1029/2007gl032838

Druehl, L. D. (1977). The distribution of *Macrocystis integrifolia* in British Columbia as related to environmental parameters. *Can. J. Bot* 56, 69–79. doi: 10.1139/b78-008

Dunn, O. J. (1964). Multiple comparisons using rank sums. *Technometrics* 6, 241–252. doi: 10.1080/00401706.1964.10490181

Eger, A. M., Marzinelli, E. M., Beas-Luna, R., Blain, C. O., Blamey, L. K., Byrnes, J. E., et al. (2023). The value of ecosystem services in global marine kelp forests. *Nat. Commun* 14, 1894. doi: 10.1038/s41467-023-37385-0

Eisaguirre, J. H., Eisaguirre, J. M., Davis, K., Carlson, P. M., Gaines, S. D., and Caselle, J. E. (2020). Trophic redundancy and predator size class structure drive differences in kelp forest ecosystem dynamics. *Ecology* 101, p.e02993. doi: 10.1002/ecy.2993

Fernández, P. A., Gaitán-Espitia, J. D., Leal, P. P., Schmid, M., Revill, A. T., and Hurd, C. L. (2020). Nitrogen sufficiency enhances thermal tolerance in habitat-forming kelp: implications for acclimation under thermal stress. *Sci. Rep* 10, 3186. doi: 10.1038/s41598-020-60104-4

Filbee-Dexter, K., Wernberg, T., Fredriksen, S., Norderhaug, K. M., and Pedersen, M. F. (2019). Arctic kelp forests: Diversity, resilience and future. *Global planetary Change* 172, 1–14. doi: 10.1016/j.gloplacha.2018.09.005

Foreman, M. G. G., Czajko, P., Stucchi, D. J., and Guo, M. (2009). A finite volume model simulation for the Broughton Archipelago, Canada. *Ocean Model* 30, 29–47. doi: 10.1016/j.ocemod.2009.05.009

Frölicher, T. L., Fischer, E. M., and Gruber, N. (2018). Marine heatwaves under global warming. *Nature*. 560 (7718), 360-364. doi: 10.1038/s41586-018-0383-9

Gendall, L., Schroeder, S. B., Wills, P., Hessing-Lewis, M., and Costa, M. (2023). A multi-satellite mapping framework for floating kelp forests. *Remote Sens* 15, 1276. doi: 10.3390/rs15051276

Gonzalez-Aragon, D., Rivadeneira, M. M., Lara, C., Torres, F. I., Vásquez, J. A., and Broitman, B. R. (2024). A species distribution model of the giant kelp *Macrocystis pyrifera*: worldwide changes and a focus on the Southeast Pacific. *Ecol. Evol* 14, e10901. doi: 10.1002/ece3.10901

Graham, M. H. (2003). Coupling propagule output to supply at the edge and interior of a giant kelp forest. *Ecology* 84, 1250–1264. doi: 10.1890/02-0245

Hadjimitsis, D. G., Clayton, C. R. I., and Retalis, A. (2004). On the darkest pixel atmospheric correction algorithm: a revised procedure applied over satellite remotely sensed images intended for environmental applications. In *Remote Sensing for Environmental Monitoring, GIS Applications, and Geology III* 5239, pp. 464-471. doi: 10.1117/12.511520

Haggarty, D., Gregr, E., Lessard, J., Fields, C., and Davies, S. (2020). Shallow substrate model (20m) of the Pacific Canadian coast. *Department Fisheries Oceans*. Available at: https://osdp-psdo.Canada.ca/dp/en/search/metadata/NRCAN-FGP-1-b100cf6c-7818-4748-9960-9eab2aa6a7a0 (Accessed August 5, 2024).

Hamed, K. H., and Rao, A. R. (1998). A modified Mann-Kendall trend test for autocorrelated data. *J. hydrology* 204, 182–196. doi: 10.1016/S0022-1694(97)00125-X

Hamilton, S. L., Bell, T. W., Watson, J. R., Grorud-Colvert, K., and Menge, B. A. (2020). Remote sensing: generation of long-term kelp bed data sets for evaluation of impacts of climatic variation. *Ecology*. 101 (7), e03031. doi: 10.1002/ecy.3031

Hamilton, S. L., Saccomanno, V. R., Heady, W. N., Gehman, A. L., Lonhart, S. I., Beas-Luna, R., et al. (2021). Disease-driven mass mortality event leads to widespread extirpation and variable recovery potential of a marine predator across the eastern Pacific. *Proc. R. Soc. B* 288, 20211195. doi: 10.1098/rspb.2021.1195

Hay, C. H. (1990). The distribution of Macrocystis (Phaeophyta: Laminariales) as a biological indicator of cool sea surface temperature, with special reference to New Zealand waters. *J. R. Soc. New Z* 20, 313–336. doi: 10.1080/03036758.1990.10426716

Hobday, A. J., Alexander, L. V., Perkins, S. E., Smale, D. A., Straub, S. C., Oliver, E. C. J., et al. (2016). A hierarchical approach to defining marine heatwaves. *Prog. Oceanography*. 141, 227-238. doi: 10.1016/j.pocean.2015.12.014

Hobday, A. J., Oliver, E. C., Gupta, A. S., Benthuysen, J. A., Burrows, M. T., Donat, M. G., et al. (2018). Categorizing and naming marine heatwaves. *Oceanography* 31, pp.162–pp.173. doi: 10.5670/oceanog.2018.205

Hollarsmith, J. A., Andrews, K., Naar, N., Starko, S., Calloway, M., Obaza, A., et al. (2022). Toward a conceptual framework for managing and conserving marine habitats: A case study of kelp forests in the Salish Sea. *Ecol. Evol* 12, e8510. doi: 10.1002/ece3.8510

Hollarsmith, J. A., Buschmann, A. H., Camus, C., and Grosholz, E. D. (2020). Varying reproductive success under ocean warming and acidification across giant kelp (*Macrocystis pyrifera*) populations. *J. Exp. Mar. Biol. Ecol* 522, 151247. doi: 10.1016/j.jembe.2019.151247

Hollarsmith, J. A., Cornett, J. C., Evenson, E., and Tugaw, A. (2024). A century of canopy kelp persistence and recovery in the Gulf of Alaska. *Ann. Bot* 133, 105–116. doi: 10.1093/aob/mcad149

Holling, C. S. (1973). Resilience and stability of ecological systems. *Annu. Rev. Ecology Evolution Systematics*. 4, 1-23. doi: 10.1146/annurev.es.04.110173.000245

Houskeeper, H.F., Rosenthal, I.S., Cavanaugh, K. C., Pawlak, C., Trouille, L., Byrnes, J.E., et al. (2022). Automated satellite remote sensing of giant kelp at the Falkland Islands (Islas Malvinas). *PLoS One*. 17 (1), p.e0257933.

Huovinen, P., Ramírez, J., Palacios, M., and Gómez, I. (2020). Satellite-derived mapping of kelp distribution and water optics in the glacier impacted Yendegaia Fjord (Beagle Channel, Southern Chilean Patagonia). *Sci. Total Environ* 703, 135531. doi: 10.1016/j.scitotenv.2019.135531

Jackson, G. A., and Winant, C. D. (1983). Effect of a kelp forest on coastal currents. *Continental Shelf Res* 2, 75–80. doi: 10.1016/0278-4343(83)90023-7

Jayathilake, D. R., and Costello, M. J. (2021). Version 2 of the world map of laminarian kelp benefits from more Arctic data and makes it the largest marine biome. *Biol. Conserv* 257, 109099. doi: 10.1016/j.biocon.2021.109099

Kendall, M. G. (1948). *Rank correlation methods* (London: Griffin).

Korabik, A. R., Winquist, T., Grosholz, E. D., and Hollarsmith, J. A. (2023). Examining the reproductive success of bull kelp (*Nereocystis luetkeana*, Phaeophyceae, Laminariales) in climate change conditions. *J. Phycology* 59, 989–1004. doi: 10.1111/jpy.13488

Krumhansl, K. A., Okamoto, D. K., Rassweiler, A., Novak, M., Bolton, J. J., Cavanaugh, K. C., et al. (2016). Global patterns of kelp forest change over the past half-century. *Proc. Natl. Acad. Sci* 113, 13785–13790. doi: 10.1073/pnas.1606102113

Kruskal, W. H., and Wallis, W. A. (1952). Use of ranks in one-criterion variance analysis. *J. Am. Stat. Assoc* 47, 583–621. doi: 10.1080/01621459.1952.10483441

Ladah, L. B., and Zertuche-González, J. A. (2007). Survival of microscopic stages of a perennial kelp (Macrocystis pyrifera) from the center and the southern extreme of its range in the Northern Hemisphere after exposure to simulated El Niño stress. *Mar. Biol* 152, pp.677–pp.686. doi: 10.1007/s00227-007-0723-z

Lamy, T., Koenigs, C., Holbrook, S. J., Miller, R. J., Stier, A. C., and Reed, D. C. (2020). Foundation species promote community stability by increasing diversity in a giant kelp forest. *Ecology* 101, e02987. doi: 10.1002/ecy.2987

Le, D. M., Desmond, M. J., Pritchard, D. W., and Hepburn, C. D. (2022). Effect of temperature on sporulation and spore development of giant kelp (*Macrocystis pyrifera*). *PloS One* 17, e0278268. doi: 10.1371/journal.pone.0278268

Levitus, S., Antonov, J. I., Boyer, T. P., and Stephens, C. (2000). Warming of the world ocean. *Science* 287, 2225–2229. doi: 10.1126/science.287.5461.2225

Lin, Y., and Bianucci, L. (2023). Seasonal variability of the ocean circulation in Queen Charlotte Strait, British Columbia. *Atmosphere-Ocean* 1–23 (1), 35-57. doi: 10.1080/07055900.2023.2184321

Lowman, H. E., Emery, K. A., Dugan, J. E., and Miller, R. J. (2022). Nutritional quality of giant kelp declines due to warming ocean temperatures. *Oikos* 2022 (7). doi: 10.1111/oik.08619

Lüning, K., and Neushul, M. (1978). Light and temperature demands for growth and reproduction of laminarian gametophytes in southern and central California. *Mar. Biol* 45, 297–309. doi: 10.1007/BF00391816

McPherson, M. L., Finger, D. J., Houskeeper, H. F., Bell, T. W., Carr, M. H., Rogers-Bennett, L., et al. (2021). Large-scale shift in the structure of a kelp forest ecosystem co-occurs with an epizootic and marine heatwave. *Commun. Biol* 4, 298. doi: 10.1038/s42003-021-02436-6

Mora-Soto, A., Palacios, M., Macaya, E. C., Gómez, I., Huovinen, P., Pérez-Matus, A., et al. (2020). A high-resolution global map of giant kelp (Macrocystis pyrifera) forests and intertidal green algae (Ulvophyceae) with Sentinel-2 imagery. *Remote Sens* 12, p.694. doi: 10.3390/rs12040694

Mora-Soto, A., Schroeder, S., Gendall, L., Wachmann, A., Narayan, G. R., Read, S., et al. (2024a). Kelp dynamics and environmental drivers in the southern Salish Sea, British Columbia, Canada. *Front. Mar. Sci* 11. doi: 10.3389/fmars.2024.1323448

Mora-Soto, A., Schroeder, S., Gendall, L., Wachmann, A., Narayan, G., Read, S., et al. (2024b). Back to the past: Long-term persistence of bull kelp forests in the Strait of Georgia, Salish Sea, Canada. *Front. Mar. Sci* 11. doi: 10.3389/fmars.2024.1446380

Muth, A. F., Graham, M. H., Lane, C. E., and Harley, C. D. (2019). Recruitment tolerance to increased temperature present across multiple kelp clades. *Ecology* 100 (3), e02594. doi: 10.1002/ecy.2594

Nijland, W., Reshitnyk, L., and Rubidge, E. (2019). Satellite remote sensing of canopy-forming kelp on a complex coastline: a novel procedure using the Landsat image archive. *Remote Sens. Environ* 220, 41–50. doi: 10.1016/j.rse.2018.10.032

Norel, M., Kałczyński, M., Pińskwar, I., Krawiec, K., and Kundzewicz, Z. W. (2021). Climate variability indices—a guided tour. *Geosciences* 11, 128. doi: 10.3390/geosciences11030128

Pfister, C. A., Berry, H. D., and Mumford, T. (2018). The dynamics of kelp forests in the Northeast Pacific Ocean and the relationship with environmental drivers. *J. Ecol* 106, 1520–1533. doi: 10.1111/1365-2745.12908

Pontier, O., Rhoades, O., Twist, B., Okamoto, D., and Hessing-Lewis, M. (2024). Bull kelp (Nereocystis luetkeana) growth rates as climate stress indicators for Canada's Pacific coast. *FACETS* 9, pp.1–pp19. doi: 10.1139/facets-2023-0237

Reed, D. C., Rassweiler, A. R., Miller, R. J., Page, H. M., and Holbrook, S. J. (2015). The value of a broad temporal and spatial perspective in understanding dynamics of kelp forest ecosystems. *Mar. Freshw. Res* 67, 14–24. doi: 10.1071/MF14158

Reed, D., Washburn, L., Rassweiler, A., Miller, R., Bell, T., and Harrer, S. (2016). Extreme warming challenges sentinel status of kelp forests as indicators of climate change. *Nat. Commun* 7, 13757. doi: 10.1038/ncomms13757

Reeves, S. E., Kriegisch, N., Johnson, C. R., and Ling, S. D. (2022). Kelp habitat fragmentation reduces resistance to overgrazing, invasion, and collapse to turf dominance. *J. Appl. Ecol* 59, 1619–1631. doi: 10.1111/1365-2664.14171

Roberts, D. A., Gardner, M., Church, R., Ustin, S., Scheer, G., and Green, R. O. (1998). Mapping chaparral in the Santa Monica Mountains using multiple endmember spectral mixture models. *Remote Sens. Environ* 65, pp.267–pp.279. doi: 10.1016/S0034-4257(98)00037-6

Salmon Coast Field Station (2023). *Sea lice on juvenile wild salmon in the Broughton Archipelago, British Columbia. 2023 report*. Available online at: https://salmoncoast.org/wp-content/uploads/2023/12/Salmon-Coast-Sea-Lice-Report-2023.pdf (Accessed August 5, 2024).

Schroeder, S. B., Boyer, L., Juanes, F., and Costa, M. (2020). Spatial and temporal persistence of nearshore kelp beds on the west coast of British Columbia, Canada using satellite remote sensing. *Remote Sens. Ecol. Conserv* 6, 327–343. doi: 10.1002/rse2.142

Schroeder, S. B., Dupont, C., Boyer, L., Juanes, F., and Costa, M. (2019). Passive remote sensing technology for mapping bull kelp (Nereocystis luetkeana): A review of techniques and regional case study. *Global Ecol. Conserv* 19, e00683. doi: 10.1016/j.gecco.2019.e00683

Shapiro, S. S., and Wilk, M. B. (1965). An analysis of variance test for normality (complete samples). *Biometrika* 52, 591–611. doi: 10.1093/biomet/52.3-4.591

Shugar, D. H., Walker, I. J., Lian, O. B., Eamer, J. B., Neudorf, C., McLaren, D., et al. (2014). Post-glacial sea-level change along the Pacific coast of North America. *Quaternary Sci. Rev* 97, pp.170–pp.192. doi: 10.1016/j.quascirev.2014.05.022

Smale, D. A. (2020). Impacts of ocean warming on kelp forest ecosystems. *New Phytol* 225, 1447–1454. doi: 10.1111/nph.16107

Smith, K. E., Aubin, M., Burrows, M. T., Filbee-Dexter, K., Hobday, A. J., Holbrook, N. J., et al. (2024). Global impacts of marine heatwaves on coastal foundation species. *Nat. Commun* 15, 5052. doi: 10.1038/s41467-024-49307-9

Springer, Y. P., Hays, C. G., Carr, M. H., and Mackey, M. R. (2010). Toward ecosystem-based management of marine macroalgae—The bull kelp, Nereocystis luetkeana. *Oceanography Mar. Biol* 48, p.1.

Starko, S., Neufeld, C. J., Gendall, L., Timmer, B., Campbell, L., Yakimishyn, J., et al. (2022). Microclimate predicts kelp forest extinction in the face of direct and indirect marine heatwave effects. *Ecol. Appl* 32, e2673. doi: 10.1002/eap.2673

Starko, S., Timmer, B., Reshitnyk, L., Csordas, M., McHenry, J., Schroeder, S., et al. (2024a). Local and regional variation in kelp loss and stability across coastal British Columbia. *Mar. Ecol. Prog. Ser* 733, 1–26. doi: 10.3354/meps14548

Starko, S., van der Mheen, M., Pessarrodona, A., Wood, G. V., Filbee-Dexter, K., Neufeld, C. J., et al. (2024b). Impacts of marine heatwaves in coastal ecosystems depend on local environmental conditions. *Global Change Biol* 30, p.e17469. doi: 10.1111/gcb.17469

Stekoll, M. S., Deysher, L., and Hess, M. (2006). A remote sensing approach to estimating harvestable kelp biomass. *J. Appl. Phycology* 1, 97–108. doi: 10.1007/s10811-006-9029-7

Sutherland, I. R. (1990). Kelp inventory 1989: The Vancouver Island and Malcolm Island shores of Queen Charlotte Strait, including a summary of historical inventory information for the area. *Br. Columbia Aquaculture Commercial Fisheries Branch Fisheries Dev. Rep. No. 36* 41.

Timmer, B., Reshitnyk, L. Y., Hessing-Lewis, M., Juanes, F., Gendall, L., and Costa, M. (2024). Capturing accurate kelp canopy extent: integrating tides, currents, and species-level morphology in kelp remote sensing. *Front. Environ. Sci* 12. doi: 10.3389/fenvs.2024.1338483

Traiger, S. B., and Konar, B. (2018). Mature and developing kelp bed community composition in a glacial estuary. *J. Exp. Mar. Biol. Ecol* 501, 26–35. doi: 10.1016/j.jembe.2017.12.016

Turner, N. J. (2001). "Coastal peoples and marine plants on the Northwest Coast," in *Proceedings of the international association of aquatic and marine science libraries and information centers* (Victoria, British Columbia).

Wachmann, A., Starko, S., Neufeld, C. J., and Costa, M. (2024). Validating landsat analysis ready data for nearshore sea surface temperature monitoring in the northeast pacific. *Remote Sens* 16, 920. doi: 10.3390/rs16050920

Watson, J., and Estes, J. A. (2011). Stability, resilience, and phase shifts in rocky subtidal communities along the west coast of Vancouver Island, Canada. *Ecol. Monogr* 81, 215–239. doi: 10.1890/10-0262.1

Weigel, B. L., Small, S. L., Berry, H., and Dethier, M. N. (2023). Effects of temperature and nutrients on microscopic stages of the bull kelp (Nereocystis luetkeana, Phaeophyceae). *J. Phycology*. 59 (5), 893-907. doi: 10.1111/jpy.13366

Wernberg, T., Krumhansl, K., Filbee-Dexter, K., and Pedersen, M. F. (2019). "Status and trends for the world's kelp forests," in *World seas: an environmental evaluation* (Cambridge: Academic Press), 57–78. doi: 10.1016/b978-0-12-805052-1.00003-6

Wernberg, T., Thomsen, M. S., Baum, J. K., Bishop, M. J., Bruno, J. F., Coleman, M. A., et al. (2024). Impacts of climate change on marine foundation species. *Annu. Rev. Mar. Sci* 16, 247–282. doi: 10.1146/annurev-marine-042023-093037

Whitney, F. A. (2015). Anomalous winter winds decrease 2014 transition zone productivity in the NE Pacific. *Geophysical Res. Lett* 42, 428–431. doi: 10.1002/2014GL062634

Young, M., Cavanaugh, K., Bell, T., Raimondi, P., Edwards, C. A., Drake, P. T., et al. (2016). Environmental controls on spatial patterns in the long-term persistence of giant kelp in central California. *Ecol. Monogr* 86, 45–60. doi: 10.1890/15-0267

Zhao, K., Wulder, M. A., Hu, T., Bright, R., Wu, Q., Qin, H., et al. (2019). Detecting change-point, trend, and seasonality in satellite time series data to track abrupt changes and nonlinear dynamics: A Bayesian ensemble algorithm. *Remote Sens. Environ* 232, 111181. doi: 10.1016/j.rse.2019.04.034

frontiers | Frontiers in Marine Science

TYPE Original Research
PUBLISHED 04 April 2025
DOI 10.3389/fmars.2025.1504701

OPEN ACCESS

EDITED BY
Christopher Edward Cornwall,
Victoria University of Wellington,
New Zealand

REVIEWED BY
François Thoral,
University of Waikato, New Zealand
Claire Butler,
University of Tasmania, Australia

*CORRESPONDENCE
Lianna Gendall
lianna.gendall@uwa.edu.au

RECEIVED 01 October 2024
ACCEPTED 18 February 2025
PUBLISHED 04 April 2025

CITATION
Gendall L, Hessing-Lewis M, Wachmann A, Schroeder S, Reshitnyk L, Crawford S, Lee LC, Guujaaw N and Costa M (2025) From archives to satellites: uncovering loss and resilience in the kelp forests of Haida Gwaii.
Front. Mar. Sci. 12:1504701.
doi: 10.3389/fmars.2025.1504701

From archives to satellites: uncovering loss and resilience in the kelp forests of Haida Gwaii

Lianna Gendall[1,2*], Margot Hessing-Lewis[3], Alena Wachmann[1], Sarah Schroeder[1], Luba Reshitnyk[3], Stuart Crawford[4], Lynn Chi Lee[5], Niisii Guujaaw[4] and Maycira Costa[1]

[1]Spectral Lab, Geography, University of Victoria, Victoria, BC, Canada, [2]The Oceans Institute, University of Western Australia, Crawley, WA, Australia, [3]Hakai Institute, Campbell River, BC, Canada, [4]Marine Planning Program, Council of the Haida Nation, Skidegate, BC, Canada, [5]Gwaii Haanas National Park Reserve, National Marine Conservation Area Reserve, and Haida Heritage Site, Skidegate, BC, Canada

Coastal foundation species such as kelps, corals, and seagrasses play vital roles in supporting marine biodiversity and ecosystem services globally, but are increasingly threatened by climate change. In particular, kelp forests are highly dynamic ecosystems experiencing natural fluctuations across seasons and climate cycles, e.g., El Niño Southern Oscillation, Pacific Decadal Oscillation. As climate change increases variability in these cycles and extreme events such as marine heatwaves become more frequent, long term data are essential to understand deviations from the norm and to better estimate trends of change. This study uses a century-long dataset to examine kelp forest responses to regional drivers in Haida Gwaii, British Columbia, by combining remote sensing data from 1973-2021 with a snapshot of kelp distribution derived from historical records from 1867-1945. We reveal complex patterns of change, with kelp losses and resilience varying at different spatial scales. Kelp forests that had likely persisted for over a century exhibited an overall declining trend of 5 $\pm$ 2% per decade starting in the 1970s. Throughout the time series kelp area was driven by multi-year impacts of the Pacific Decadal Oscillation, El Nino Southern Oscillation, sea surface temperature anomalies and marine heatwaves, such as the 1998 El Niño and the 2014-2016 marine heatwave known as the 'Blob'. In the warmest areas, kelp forests completely disappeared during the 1977 Pacific Decadal Oscillation shift. Cooler areas showed greater resilience, buffering the loss at the region wide scale, highlighting the importance of local gradients in understanding areas vulnerable to climate change. Lastly, local *in situ* surveys showed a lack of urchin barrens, and the presence of turf algae in the study region, further supporting the hypothesis that temperature, not herbivory, drove kelp forest loss in this region.

KEYWORDS

kelp forest canopy, El Niño, marine heatwave, resilience, persistence, scale-dependent responses, sea surface temperature, Pacific Decadal Oscillation (PDO)

Introduction

Coastal ecosystems, such as kelp forests, mangroves, and seagrass meadows, play pivotal roles in supporting global biodiversity by providing habitat, sequestering carbon, and delivering ecosystem goods and services (Wernberg et al., 2019; Cooley et al., 2022). However, the resilience of these ecosystems are threatened by climate change impacts (Krumhansl et al., 2016; Filbee-Dexter and Wernberg, 2018; Wernberg et al., 2019). Among these ecosystems, kelp forests, which cover nearly a third of the world's coastlines (Jayathilake and Costello, 2021), stand out as some of the planet's most productive ecosystems (Pessarrodona et al., 2022) but, despite their global significance, are the second most vulnerable coastal ecosystem to climate change after coral reefs (Cooley et al., 2022).

Climate change poses significant threats to kelp forests through both direct impacts of temperature and indirect effects primarily driven by altered species interactions (Wernberg et al., 2019). Direct impacts include rising sea surface temperatures (SST), storms and marine heatwaves (MHWs)—prolonged periods of anomalously warm water (Hobday et al., 2018). Increases in SST can reduce survival, growth and reproduction through physiological stress, while MHWs can cause sudden mortality by exceeding local temperature thesholds, even in populations far from range edges (Druehl, 1978; Arafeh-Dalmau et al., 2019; Rogers-Bennett and Catton, 2019; McPherson et al., 2021; Filbee-Dexter et al., 2022; Starko et al., 2022, 2024).

These temperature-driven effects manifest differently across geographic regions. At warm range edges, rising temperatures can drive kelp forest tropicalization either directly through temperature stress (Wernberg, 2021) or indirectly through the poleward expansion of tropical grazers (Vergés et al., 2016). In more temperate waters, the impacts of extreme events like MHWs and storms vary depending on local conditions (e.g., Mora-Soto et al., 2024a; Mora-Soto et al., 2024b; Starko et al., 2024). While storms can cause dislodgement through increasing wave height (Dayton and Tegner, 1984), waves may sometimes mitigate MHW impacts by increased mixing or reducing grazing (Hamilton et al., 2020; Starko et al., 2022).With the intensification of the El Niño cycle, MHWs and poor nutrient conditions are predicted to increase with the potential for the entire ocean to enter a permanent MHW state by 2100 (RCP 8.5 scenario; Oliver et al., 2019) likely having severe consequences for kelp forest across the world.

As a result of climate change, kelp forest distributions are already undergoing rapid transformations with significant differences in the scale and direction of change across the globe (Krumhansl et al., 2016). As predicted, these changes have led to significant kelp forest losses in some regions. In Western Australia, for example, approximately 100,000 ha of Ecklonia radiata forests were lost from the warm edge of its distribution during the 2011 marine heatwave (Wernberg, 2021), and in Southern Norway, approximately 780,000 ha of *Saccharina latissima* forests transitioned to turf reefs from increased warming and eutrophication (Filbee-Dexter et al., 2022). Alternatively, some places have shown stability despite climate change, like Southern Chile and the Falkland Islands, where stable SSTs maintain persistent *Macrocystis pyrifera* forests (Mora-Soto et al., 2021). In a few locations, kelp forests are even expanding, like South Africa's *Ecklonia maxima* forests (Bolton et al., 2012) or where sea ice has disappeared in the Canadian Arctic (Filbee-Dexter et al., 2019). These diverse patterns of change highlight the challenge of deciphering relationships between kelp forests and environmental drivers in a time of rapid global change.

Along the west coast of North America, kelps form large floating canopies that experience diverse environmental conditions, leading to complex patterns of change similar to global trends (Krumhansl et al., 2016). The overharvesting and extirpation of sea otters, key predators of herbivorous sea urchins, by the late 1800s, caused grazing-induced losses of kelp forests across North America (Watson and Estes, 2011). However, sea otter reintroductions along the northwest coast of Vancouver Island (Watson and Estes, 2011), and the expansion of remnant populations in central California (Nicholson et al., 2024), have supported kelp forest recovery in a small portion of sea otters' historical range. More recently, an unprecedented mass of warm water formed in the northeastern Pacific in 2014, compounded by a strong El Niño in 2015-2016, leading to the large-scale MHW event known as 'The Blob' (Di Lorenzo and Mantua, 2016). This led to severe kelp forest declines in Baja California (Arafeh-Dalmau et al., 2019) and the transition of kelp forests to urchin barrens in Northern California, exacerbated by the seastar wasting disease epidemic, where the loss of the seastar *Pycnopodia helianthoides* led to an increase in urchin herbivory (Rogers-Bennett and Catton, 2019). Conversely, during the same 2014-2016 'Blob' MHW, kelp forests remained stable in Southern California and Oregon (Reed et al., 2016; Hamilton et al., 2020). In British Columbia (BC), Canada, research on kelp forests trends remains sparse, with most studies relying on localized *in situ* surveys or short time series (Sutherland et al., 2008; Watson and Estes, 2011; Schroeder et al., 2019; Starko et al., 2022, 2024). Notably, only a few studies include continuous time series exceeding five years (Mora-Soto et al., 2024a, 2024b; Starko et al., 2024). This limited scope leaves significant knowledge gaps in understanding the complex patterns of change along most of BC's intricate coastline, highlighting the need for longer series to disentangle natural variability from long-term trends.

In this study, we investigate environmental heterogeneity and geographic scale within a region of BC's complex coastline to understand the variability in kelp forest responses to regional climate drivers, such as the Pacific Decadal Oscillation (PDO), El Niño Southern Oscillation (ENSO), North Pacific Gyre Oscillation (NPGO), SST anomalies, and MHW metrics. To achieve this, we compiled a long-term dataset of floating kelp forest canopy area from the Cumshewa Inlet and Gray Bay region (Figure 1), located within the Haida Gwaii archipelago, Canada, where local indigenous communities have observed recent declines (HMTK Participants et al., 2011; MaPP, 2021). Specifically, we assessed long-term changes in kelp forest distribution by comparing historical data (1867-1945) with satellite imagery (1973 to 2021). Using the satellite imagery time series (1973 to 2021; Table 1), we then quantified kelp forest trends and environmental drivers of change at regional (800 km^2), subregional (five distinct areas), and local (1 km segments) scales. Based on the observed increases in climate disturbances in this region, we hypothesized that greater environmental heterogeneity at the regional scale would confer higher resilience. Specifically, we expected less drastic declines and more recovery after climatic events, like El Niño and MHW events, at the regional scale. In contrast, we expected more variable responses at

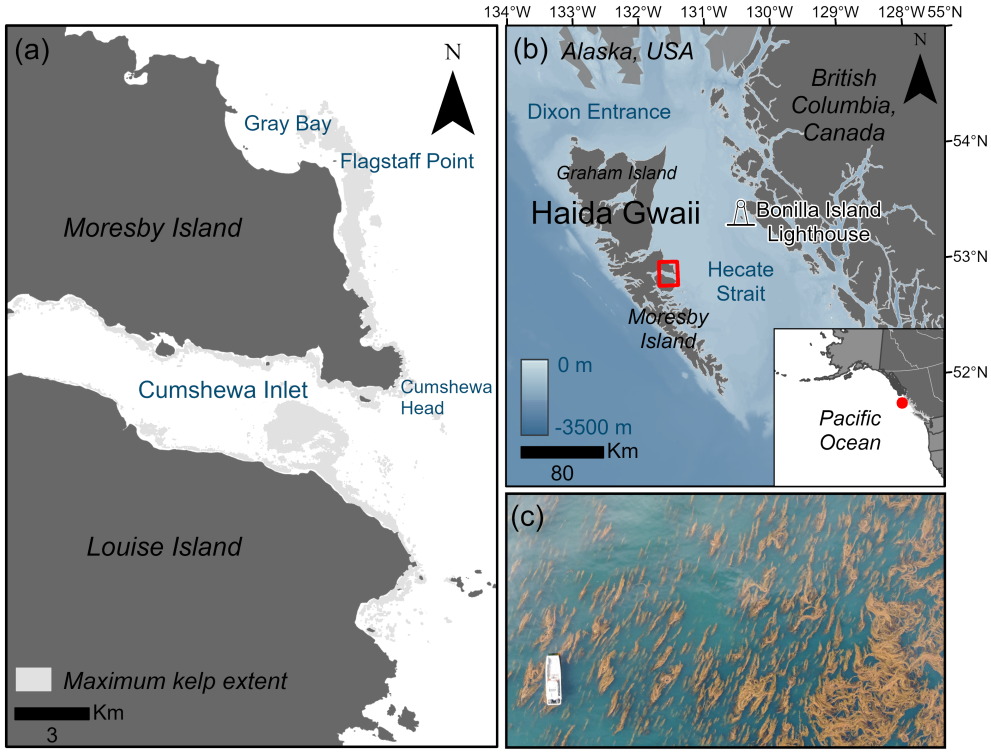

FIGURE 1
(a) Map of the study region where the maximum kelp area across the complete time series (1973-2021) is shown in gray. **(b)** Map of the Haida Gwaii archipelago and study region shown in red in relation to the mainland coast of British Columbia and Alaska, showing bathymetry in meters (m) below chart datum and the location of the Bonilla Island Lighthouse, the location of the *in situ* SST data. **(c)** Image showing an example of the size and density of giant kelp (*Macrocystis*) forests found within the study region in relation to a 10 m research vessel.

the local and sub-regional scales, where outcomes would likely depend on each area's position along local environmental gradients, such as SST, fetch, wind and tidal current.

Methods

Study region

Haida Gwaii is a remote archipelago located off Canada's mainland Pacific coast (Figure 1) and the recognized Aboriginal title lands of the Haida Nation (Haida Nation and Canada, 2024a, 2024b). The archipelago is characterized by cool, nutrient-rich marine environments which support extensive *Nereocystis luetkeana* and *Macrocystis pyrifera* (Lindstrom, 2023;syn. *Macrocystis tenuifolia*) kelp forests (HMTK Participants et al., 2011; Lee et al., 2021). The boundaries of the study region were defined to include the Hl̲kinul ChiiG̲as.sgii SG̲aagiidaay Protection Management Zone designated in the Haida Gwaii Marine Plan (MaPP, 2015) to protect an extensive kelp forest. Our study region of 800 km² on the northeast coast of Moresby Island (Figure 1) spans a sea surface temperature gradient of ~3°C and a strong exposure (fetch, wind and tidal current) gradient, allowing us to represent a wide range of conditions while minimizing the impact of confounding variables when comparing across vast distances. Sea otters were extirpated from Haida Gwaii during the maritime fur trade (1785-1840) and have not yet returned (Lee et al., 2021). This region is characterized by dense, large *Macrocystis* forests throughout (Figure 1c), with smaller dense patches of *Nereocystis* forests around Cumshewa Head (Figure 1a). These kelp forests are detectable from medium- to high-resolution satellites allowing us to monitor kelp forest change back to the 1970s (Gendall et al., 2023). Haida people note the importance of the Cumshewa and Flagstaff areas within the study region as crucial ecological and cultural areas for *Macrocystis* harvest for the herring-roe-on-kelp fishery (in Haida: k'aaw), however, have observed kelp declines in the early 2000s (HMTK Participants et al., 2011; MaPP, 2021) highlighting the need for increased monitoring and management (MaPP, 2015).

Kelp canopy area time series

The time series comprises two components: (i) a historical snapshot of century-old kelp presence recorded in British Admiralty charts, and (ii) kelp canopy area derived from satellite imagery collected from 1973 to 2021. The British Admiralty charts data were created between 1867 and 1945 (hereafter historical kelp; Costa et al., 2020). Charts with scales ranging from 1:6,080 to 1:500,000 were scanned, georeferenced, and manually digitized to capture hand-drawn kelp features. In cases where overlapping kelp features were present on multiple charts, in the same region, the highest-resolution charts were prioritized. Each kelp feature was assigned a reliability category based on the depth of the seafloor

TABLE 1 Summary of medium- to high resolution archived satellite imagery used to build the time series of kelp canopy area where the resolution refers to the spatial resolution of the multispectral imagery, inputs refer to band and band indices (NDVI: Normalized Difference Vegetation Index, GNDVI: NDVI with green instead of red, RE: red-edge, NIR: near-infrared) used in the object-based image classification and global accuracy refers to the measure of global accuracy attained in the validation of the classification.

Sensor	Resolution	Years	Inputs	Source	Global Accuracy
Landsat 1-3	60 m resampled from 80 m	1973-74 1976-77	NDVI Green Red NIR	Freely Available from United States Geological Survey (USGS)	–
Landsat 4-5	30 m	1982 1984-86 1988-92	NDVI Green Red NIR	Freely Available from United States Geological Survey (USGS)	89%
Landsat 7	30 m	2001-02	NDVI Green Red NIR	Freely Available from United States Geological Survey (USGS)	–
Spot 2-4	20 m	2006 2008 2011	NDVI Green Red NIR	Available to researchers through the Centre national d'études spatiales (CNES)	–
Spot 5-7	10 m	2005-06 2009 2016	NDVI Green Red NIR	SPOT 7 imagery was purchase from Apollo Imaging Corp.	93%
Geoeye-1	1.84 m	2017	G-NDVI Green Red NIR	Private data sharing agreement	89%
Quickbird-2	2.62 m	2008 2013	GNDVI Green Red NIR	Private data sharing agreement	92%
Worldview-2	1.84 m	2013	RE/Yellow Green Red NIR	Private data sharing agreement	91%
Rapideye	5 m	2010-12 2014-15	RE/Green Green Red RedEdge NIR	Available to researchers through Planet Labs Inc	88%
Planetscope	3.7 m	2017-2021	NIR/ Green Green Red NIR	Available to researchers through Planet Labs Inc	94%
Aerial Imagery	0.5 m	2007	Red/Green Green Blue	Private data sharing agreement	88%

below the feature, with all features within the study region classified as 'Very High' reliability due to their occurrence in depths shallower than 40 m. These charts, originally designed to map potential navigational risks for mariners, provide only a snapshot of kelp presence and should not be used to infer absences, as not all kelp forests may have been mapped. As such, the historical kelp distribution (Costa et al., 2020) was visually compared with the kelp distribution derived from the satellite imagery time series and was not included in any statistical analyses.

To construct a satellite imagery time series (1973-2021) of floating kelp forest canopy area (hereafter kelp area), we adopted the methodological framework outlined in Gendall et al. (2023). This framework includes: 1) imagery compilation and assessment, 2) imagery preprocessing, 3) classification, and 4) validation (see Supplementary Methods for detailed description of each step). To collect and assess the imagery, we compiled a dataset of archived remote sensing imagery from 1973 to 2021, with resolutions ranging from high (0.5 m) to medium (60 m; Table 1). Images were selected

based on criteria (Supplementary Table S1, see Supplementary Methods) controlling for cloud cover, tidal conditions (Supplementary Figure S1), haze, waves, glint, and acquisition month (Schroeder et al., 2019; Cavanaugh et al., 2021; Gendall et al., 2023). The final image dataset consisted of 52 suitable images spanning 48 years. Imagery preprocessing included geometric corrections, atmospheric corrections, masking of land, deepwater and soft substrate (Gendall et al., 2023). Steep sloping bathymetry result in a narrow band of depths that are habitable to kelp before becoming too deep, limiting the extent of kelp forests to thin, fringing strips close to shore making detection difficult from medium-resolution satellites (Gendall et al., 2023). To mitigate uncertainties related to mapping small kelp forest canopies at varying resolutions, we excluded these areas of steep sloping bathymetry, exceeding 11.4%, from the analysis (Gendall et al., 2023). However, these steep sloping nearshore areas that were removed only accounted for 0.01% of the overall kelp area in the study region (Gendall et al., 2023).

To improve the detectability of kelp from non-kelp features in the imagery, we generated band indices/ratios specific to kelp (Table 1; Supplementary Table S2), which were linearly enhanced and integrated with the original bands for input into the classification process. Satellite imagery was classified utilizing eCognition Developer Software (Trimble Germany, 2011) with enhanced indices/ratios and bands as inputs. The classification results were validated by cross-referencing with available field and historical data (Gendall et al., 2023; Supplementary Table S3). When considering all sensors included in the validation, the overall global accuracy ranged between 88% and 94% (Table 1; Supplementary Table S3), where most errors were associated with sparse, fringing, or partially submerged kelp canopy (Gendall et al., 2023).

Scale of analyses

Regional

At the regional scale of analysis, we investigated the total kelp area of the entire study region through time and examined the relationship with regional drivers, including the PDO, ENSO, NPGO, SST anomalies, and MHW metrics. Since the dominant kelp in the region is *Macrocystis*, a perennial species, the annual averages, or sums in the case of MHW metrics, for the year preceding the month when most images were acquired were used. As most of images were acquired in July, annual measures were therefore calculated as the conditions experienced between August of the previous year and July of the sampling year (hereafter referred to as year and denoted by the year the image was acquired).

Annual averages of PDO (Huang et al., 2017), NPGO (Di Lorenzo et al., 2008), and ENSO (NOAA, 2015) were calculated from monthly data spanning 1969 to 2021. Annual SST anomalies (°C) and MHW metrics were calculated using daily *in situ* SST measures from the Bonilla Island lighthouse station (53°29'34.5" N; 130°38'17.0" W, Figure 1, Chandler, 2010). Bonilla Island lighthouse, located approximately 80 km from the study region, is the nearest site with continuous SST data dating back to the 1960s. Both MHW metrics and SST anomalies were calculated using a 55-year climatology starting in 1966. SST anomalies were calculated as the annual average temperature (°C) deviations above or below the time series climatological average. MHW metrics were calculated using the heatwaveR package in R (Schlegel and Smit, 2018), where a MHW was defined as a period of at least five consecutive days during which SST exceed the 90th percentile of the climatological average (Hobday et al., 2016). MHW days were calculated as the sum of the total number of days classified as a MHW in a given year. MHW cumulative intensity was calculated as the sum of daily temperature anomalies (°C) exceeding the climatological threshold, accumulated over the duration of all MHW events within a given year. While satellite-derived SST data, such as the Optimum Interpolation Sea Surface Temperature (OISST; Huang et al., 2021), are available for the study region, they do not cover the full temporal duration of the time series. A comparison of MHW metrics from Bonilla lighthouse and OISST data from the study region, revealed strong correlations for both MHW days ($r = 0.90$, $df = 39$, $p<0.001$) and MHW cumulative intensity ($r = 0.85$, $df = 39$, $p<0.001$; Supplementary Figure S2). Therefore, Bonilla lighthouse data were deemed suitable to represent MHW conditions within the study region.

To statistically compare kelp with regional drivers, annual kelp area was normalized as the percentage of the maximum kelp area observed through time and linear regressions were employed to assess temporal trends and relationships with regional drivers at multi-year scales. We examined the influence of previous years' conditions by considering one-, two-, and three-year metrics of regional drivers. The regional drivers exhibited some level of correlation (Supplementary Table S4), in which ENSO, PDO, SST anomalies and MHW metrics displayed positive correlations, and the NPGO showed an inverse correlation. Across all climate variables, SST anomalies showed a warming trend of 0.62°C between 1973 and 2021 (Supplementary Table S5). We assessed model residuals for normality (Faraway, 2004), and selected the best models based on the Akaike Information Criteria adjusted for a small sample size (AICc, Hurvich and Tsai, 1993). Univariate relationships between each regional driver and kelp area were tested, followed by the creation of multivariate models incorporating significant variables. Since most regional drivers were correlated (Supplementary Table S4) and largely represent temperature, we did not include non-significant predictors or test for interactions unlikely to exist. This approach simplifies analyses, reduces overfitting, and focuses on the most important drivers of kelp forest area (Anderson and Burnham, 2002; Coelho et al., 2019). All statistical analyses were conducted using R Studio (R Core Team, 2021) with the lme package (Bates et al., 2015).

Subregions

Subregions were defined by clustering areas together with similar local environmental conditions of SST, fetch, wind and tidal currents. Landsat Analysis Ready Data (ARD) Surface Temperature (ST) from Landsat 5, 7, and 8 thermal sensors were used to quantify local SST conditions, as they offer the highest resolution SST data currently available (30 m; Dwyer et al., 2018; Wachmann et al., 2024). Local SST climatology was derived from all available cloud-free Landsat ARD ST images from July or August between 1984 to 2021 (1988, 1989, 2007, 2009 to 2011, 2014, 2015, and 2017) as clouds greatly increase the inaccuracy of SST measurements (Wachmann et al., 2024). As a proxy for exposure, fetch was estimated at 50 m intervals along the coastline and refers

to the sum of fetch (max = 200 km), which is calculated by summing the distance to the nearest land mass at every 5° bearing around points on the shoreline (Gregr et al., 2019). Local wind conditions were represented using a raster of mean wind power density (W/m^2, 250 m resolution) at 10 m above sea level sourced from the Global Wind Atlas (Davis et al., 2023) and tidal currents were represented by root mean square average tidal speed (m/s) obtained from the BC Marine Conservation Analysis Marine Atlas (BCMCA, 2011).

We divided the entire study region into segments, each approximately 1 km in shoreline length, following the methodology outlined by Berry et al. (2003; Supplementary Figure S3, See Supplementary Methods) from the shoreline to the 20 m bathymetry limit using a bathymetry dataset from the Canadian Hydrographic Service (Davies et al., 2019). All local environmental conditions of SST, fetch, wind, tidal currents and depth were averaged per 1 km segment. We then employed a spatially constrained cluster analysis (k nearest neighbors = 4) in ArcMap (ESRI, 2018) to group 1 km segments into subregions based on local conditions excluding depth. To prevent statistical redundancies and the overweighting of correlated variables in the spatially constrained cluster analysis (Ketchen and Shook, 1996), we removed correlated drivers using Spearman rank-order correlations.

Similarly to the regional scale assessment, we normalized the timeseries of kelp area as a percentage of the maximum kelp area for each subregion and used linear regressions to show trends through time and relationships with regional drivers of PDO, ENSO, NPGO, SST anomalies, MHW days and MHW cumulative intensity. We defined 'resilience' at both the regional and subregional scale as areas that were variable but experienced no declining trends. In other words, we describe resilience as areas that exhibited resistance, ability to persist through disturbance, and/or recovery, the ability to bounce back following a disturbance (as defined by Holling, 1973) but did not specifically separate and quantify resistance and recovery.

Local

At the local scale, a kelp persistence analysis (Schroeder et al., 2019) was performed on the 1 km segments (Supplementary Figure S3). Persistence was quantified as the percentage of years kelp was present in a segment across the entire time series, with 100% indicating continuous presence, lower values indicating reduced persistence, and 0% indicating a complete absence of kelp from a given segment. To better understand how local environmental conditions influence persistence, we examined the relationships between persistence and local conditions of SST, fetch, wind, tidal current and depth using linear regressions.

In August 2021, we conducted field surveys to investigate factors influencing kelp forest dynamics that could not be captured through remote sensing data, and to lend insight into the patterns of change documented in the time series analyses. In particular, we used photo-quadrats and a remotely operated vehicle (ROV) to quantify substrate type, urchin presence, and understory seaweed composition in areas where kelp had disappeared, persisted or was never present. Photoquadrats consisted of a goPro Hero 7 affixed to a tripod mounted on a $1m^2$ quadrat. Both the photo-quadrats and the QYSEA Fifish V6 ROV were deployed from a boat at points across the study region. To ensure we spanned a gradient of no kelp to persistent kelp forests, we first used a stratified random sampling approach to create points in the northern part (Gray Bay and Flagstaff subregions) of the study region and opportunistically haphazardly added points in the field to increase sample size. To provide a comparison between persistent kelp forests in the northern and southern subregions we were able to sample eight points within the Cumshewa West subregion. However due to logistical constrainst were unable to sample within the Cumshewa East and Mathers Creek subregions.

A single representative frame was used from the ROV footage to avoid issues of spatial auto-correlation, issues of video quality in high current areas, and to make the ROV footage comparable with the photoquadrat data. The combined photoquadrat (n = 44) and ROV data (n = 4), resulted in a total sample size of 48. We identified urchin abundance, dominant substrate types, and dominant understory seaweeds present in ImageJ software (Schneider et al., 2012). Substrate types were classified into five categories: sand (0.06-2 mm grain size diameter), granule (2-4 mm), pebble (4-64 mm), cobble (64-256 mm), and boulder (0.25-3 m; Greene et al., 1999). Understory algae were categorized into three dominant functional groups: turf (short benthic algae), branched (*Desmerestia* sp.), and kelp (large brown algae in the order Laminariales).

Results

Regional variability of kelp area over the last century

The historical distribution of kelp from approximately a century ago (1867-1945; Figure 2a) closely mirrored the distribution of the maximum kelp area observed in satellite imagery from 1973 (8.18 km^2; Figure 2b). However, since the historical kelp distribution was represented as artistic, hand-drawn features on maps, direct comparisons of kelp area were not possible.

Our satellite imagery analysis revealed a regional declining trend of 5 ± 2% (± SE) per decade between 1973 and 2021 ($p<0.05$, $R^2 = 0.11$, df = 1,33), with significant variability driven by regional drivers like the ENSO, PDO, SST anomalies and MHW metrics (Figure 3; Table 2). Warmer conditions coincided with lower kelp area, with environmental factors explaining up to 29% of the variance in kelp area (Table 2; Supplementary Table S6). Our best models identified the ENSO (one-year averages), SST anomalies (one-year to two year averages) and MHW metrics (MHW days and MHW cumulative intensity, one- to two-year sums) as equally good predictors ($\Delta AICc < 2$) of regional kelp area (Table 2; Supplementary Table S6).

The time series exhibited periodic losses and recoveries with kelp area initially declining by 75% between 1973 and 1977 (Figures 2b, c, 3a) coinciding with the PDO phase shift (Figure 3b). This PDO phase shift was marked by an annual average SST anomaly of 0.26°C and a 10 day MHW in may of 1977 (Figures 3b–d). Subsequent fluctuations were tied to major El Niño events (e.g., 1983, 1998) and the 2014-2016 'Blob' MHW. In

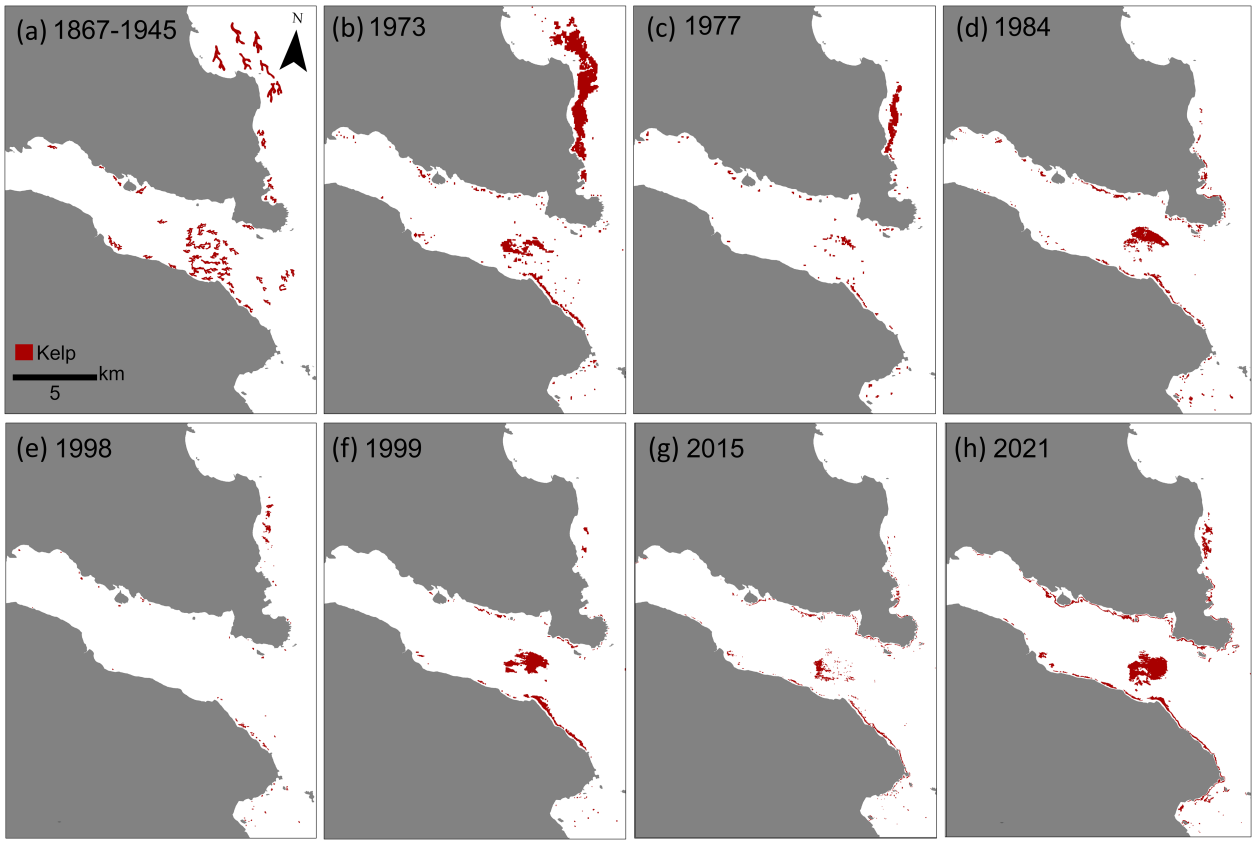

FIGURE 2
(a) Map of the historic distribution of kelp canopy derived from British Nautical charts. **(b-h)** Maps of kelp canopies derived from satellite imagery from notable years.

1998, one of the strongest El Niño events on record occurred, with SST of 1.23°C above average, a total of 193 MHW days and a MHW cumulative intensity of 348.67°C (Figures 3b–d). This event aligned with the time series minima, where only 5% of the kelp area (0.43 km^2) remained (Figure 2e), however recovered to 33% by 1999 (Figure 2f).

In the study region, the 2014-2016 'Blob' MHW had minimal impacts on regional SST in 2014, but led to SST anomaly of 0.92°C with a total of 179 MHW days in 2015, and in 2016 a SST anomaly of 0.91°C with a total of 114 MHW days (Figures 3b–d). This event corresponded with the second and third lowest kelp areas at 13% and 17% in 2015 and 2016, respectively (Figures 2g, 3a). Following the 'Blob', SST remained above average for the duration of the study period (2016-2021), however, not as extreme, allowing kelp forests to recover to 48% by 2021 (Figures 2h, 3a).

Subregional spatially explicit responses

We employed a spatially constrained cluster analysis to group local 1 km segments into subregions based on fetch, local SST, wind, and tidal current. Fetch, wind, and tidal current exhibited high correlations (fetch and wind r = 0.78, fetch and tidal current r = 0.86, wind and tidal current r = 0.80, df = 237, p<0.001). Consequently, only fetch and SST were included in the cluster analysis. The pseudo-F-statistic analysis (Milligan and Cooper, 1985) defined five as the number of optimal subregions (pseudo-f-statistic: 4 groups = 272.92, 5 groups = 303.61, 6 groups = 279.9233; Supplementary Table S7). Gray Bay (subregion 1) and Flagstaff (subregion 2) were characterized by warm SSTs and moderate fetch, wind and current speeds (Figure 4a; Supplementary Table S7). Cumshewa East and West (subregions 3 and 4, respectively) were characterized by cooler SST, however, Cumshewa West had lower fetch, wind and tidal current (i.e. was more sheltered) than Cumshewa East. Mathers Creek (subregion 5) was characterized by warmer SSTs and low fetch, wind and current speeds.

Five subregions exhibited varying responses to climatic events, largely driven by differences in SST. Warmer more exposed subregions like Gray Bay and Flagstaff experienced drastic declines, with complete kelp loss in Gray Bay after 1977 (Figures 4a, b). Flagstaff showed a long-term decline of 9 ± 2% per decade (p<0.001, R^2 = 0.34, df = 1,33), with minimal recovery after the loss in the late 1970s (Figures 2c, d, 4c). Three-year SST averages best explained the variation (42 %) in the Flagstaff subregion (Table 2; Supplementary Table S8). By the early 21st century, approximately 90% of the original kelp area in the Flagstaff subregion had disappeared (Figure 4c).

In contrast, the cooler Cumshewa East and Cumshewa West subregions displayed resilience, with no significant long-term

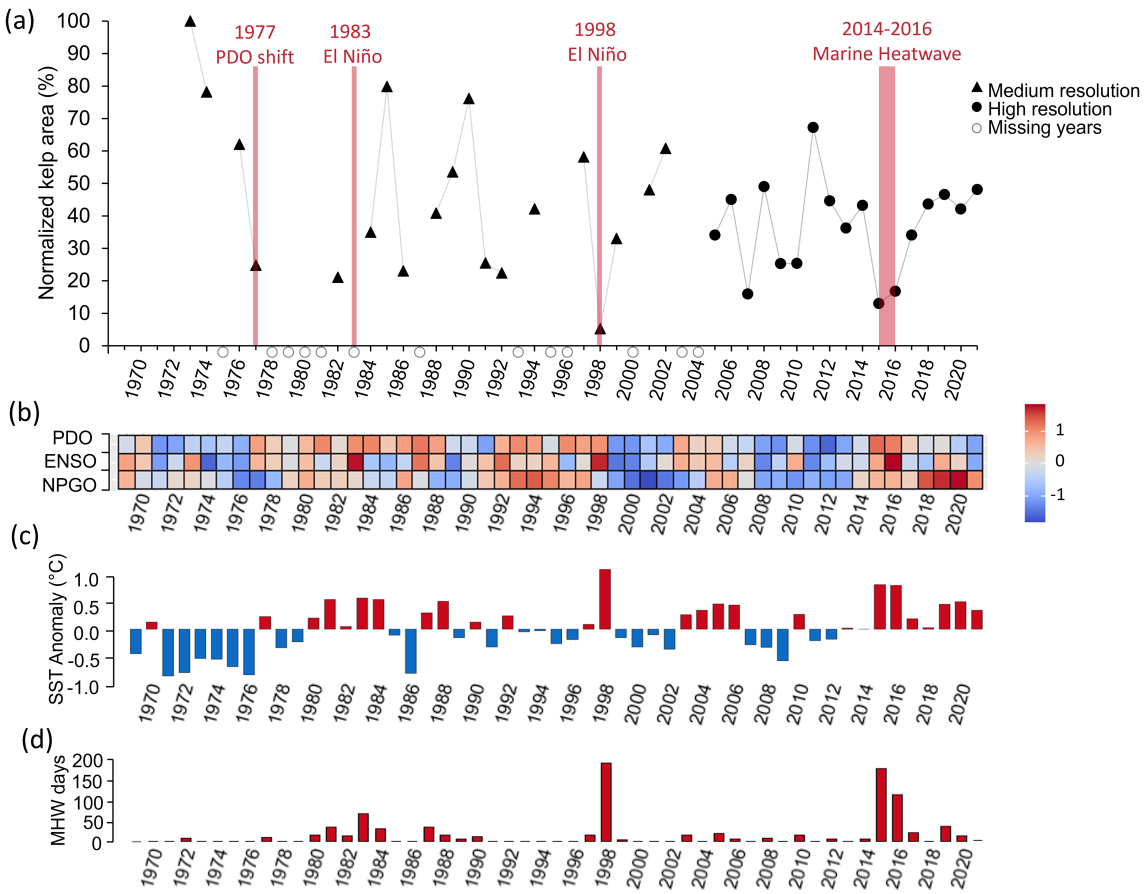

FIGURE 3
(a) Time series of normalized kelp area from 1973 to 2021 with major events displayed in red **(b)** Annual z-scores of climate indices, Pacific Decadal Oscillation (PDO), El Niño Southern Oscillation (ENSO), and North Pacific Gyre Oscillation (NPGO; inverted scale), such that positive values represent warm conditions (red) and negative values (blue) represent cool conditions. **(c)** Annual SST anomalies calculated using a 55-year historical average starting in 1966, where bars represent either positive (red) or negative (blue) anomalies in degrees Celsius above or below the time series average. **(d)** Annual sum of marine heatwave days calculated as number of days above the 90th percentile of the climatological average.

declining trends (Figures 4a, d, e). Kelp area in both subregions still fluctuated with environmental conditions, with ENSO (one-year and two-year averages) and MHW metrics (MHW days and MHW cumulative intensity, one- to three-year sums) explaining up to 25% (Cumshewa East) and 34% (Cumshewa West) of variation in kelp area (Table 2; Supplementary Tables S9, S10). However, unlike the northern subregions, these cooler subregions demonstrated a greater capacity for recovery following events, such as the 1977 PDO shift, the 1983 El Niño, and the 1998 El Niño (Figures 4d, e). Kelp area declined drastically during the 2014-2016 MHW in both subregions, however,

TABLE 2 Lowest AICc value of linear regressions of normalized kelp area by regional driver for the regional and subregional scale of analysis (p value < 0.5 *, <0.01**, <0.001***).

Scale of analysis	Best Predictor Model	Regression Coefficient	R^2	AICc	df
Region	ENSO (One-year average) + SST (Two-year average)	-10.48* -14.99**	0.2987	308.2649	2,33
Flagstaff (2)	SST (three-year average)	-36.56***	0.4179	300.9599	1,33
Cumshewa East (3)	ENSO (two-year average)	-21.29***	0.2080	316.7684	1,32
Cumshewa West (4)	ENSO (one-year average)	-19.78***	0.3209	318.9754	1,33
Mathers Creek (5)	PDO (one-year average)	-15.25***	0.2145	331.7842	1,33

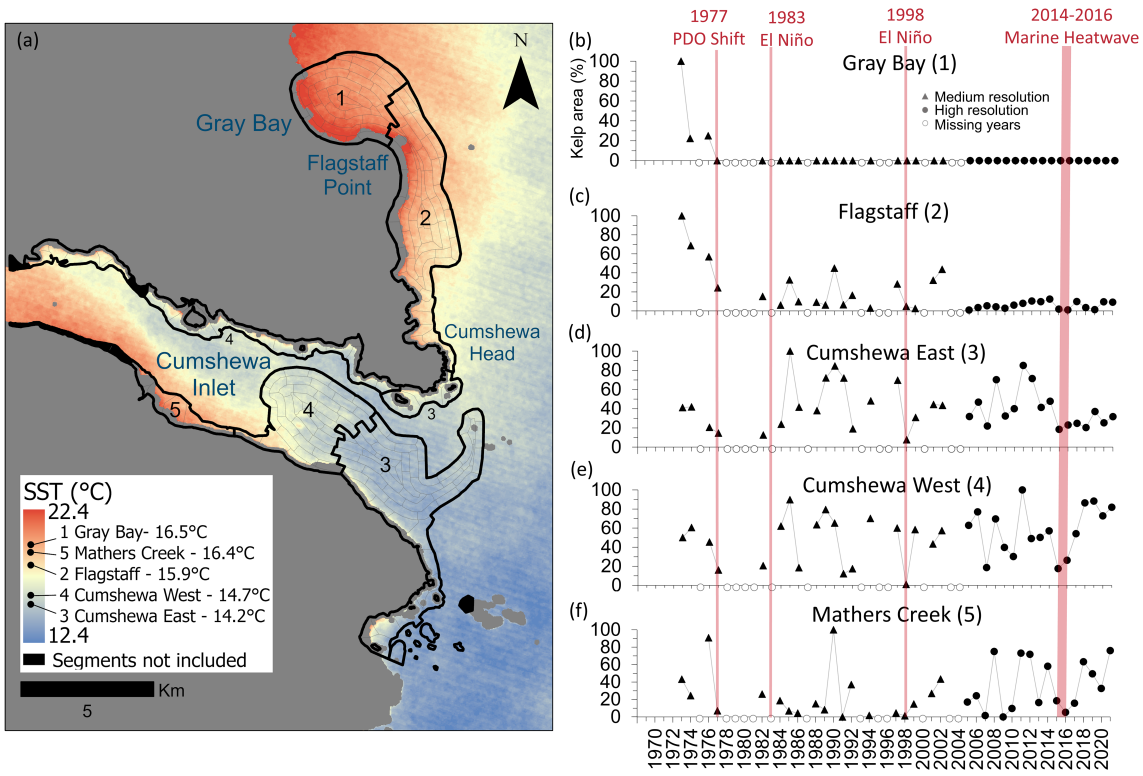

FIGURE 4
(a) Map of subregions derived from the environmental cluster analysis showing the local SST climatology across the region and average temperature experienced in each subregion derived from the Landsat satellite thermal band. **(b-f)** Time series of normalized kelp area from 1973 to 2021 for each subregion with major events displayed in red.

Cumshewa West rebounded to approximately 77% (2017-2021), while Cumshewa East only reached 28% (Figures 4d, e).

The Mathers Creek subregion, despite being geographically warmer like Flagstaff and Gray Bay subregions, exhibited resilience similar to Cumshewa East and Cumshewa West (Figures 4a, f). In the Mathers Creek subregion, the PDO (one-year averages) and ENSO (one- and two-year averages) explained up to 24% of the variation in kelp area (Table 2; Supplementary Table S11). This subregion supported the lowest proportion of kelp area (maximum of 0.21 km^2 in 1990; Figure 4f), which was largely located around the mouth of Mathers Creek in the cooler portion of the subregion.

Local responses to environmental gradients

At the local scale, variability of kelp persistence was significantly explained by local conditions of SST, wind, tidal current and depth where less wind, shallower depths and lower tidal currents coincided with higher persistence (Supplementary Table S12). Specifically, our best model included SST, wind and depth, which explained 41% of variation in kelp persistence (Supplementary Table S12). In Gray Bay, shallow water segments (2-5 m depth) experienced the warmest SST and exhibited no kelp persistence (0%; Figure 5a). Segments further offshore in Gray Bay showed low persistence (3-5%) and coincided with areas where kelp forests had entirely disappeared during the late 1970s PDO shift. In the Flagstaff subregion, kelp canopy persistence closely mirrored the SST gradient, where the warmer northern segments displayed low persistence (3-31%) with no recovery, and cooler southern segments demonstrated high persistence (67-95%), regularly recovering after climate events when cross referenced with the time series. In the more resilient subregions, the more sheltered nearshore segments in Cumshewa East (3), Cumshewa West (4), and Mathers Creek (5) maintained persistent kelp forests. Further offshore within the shallower mid-channel areas of Cumshewa East (3) and Cumshewa West (4), a core kelp area known as Fairbairn Shoals remained persistent throughout the time series.

Where kelp was lost, field surveys suggested the habitat transitioned to turf-dominated reefs rather than urchin barrens. In particular, we observed only five individual urchins within the study region (n = 48), and in subregions Gray Bay and Flagstaff, where kelp was lost, the understory community was predominantly composed of short turf seaweeds and branched brown algae such as *Desmarestia* spp. on subtrate primarily composed of a mix of granule and cobble (Figures 5b, c). In the Flagstaff subregion, only one site where kelp was lost supported an understory kelp community; this site was closest to the remaining kelp forests. In contrast, where kelp canopy persisted, an abundant understory of

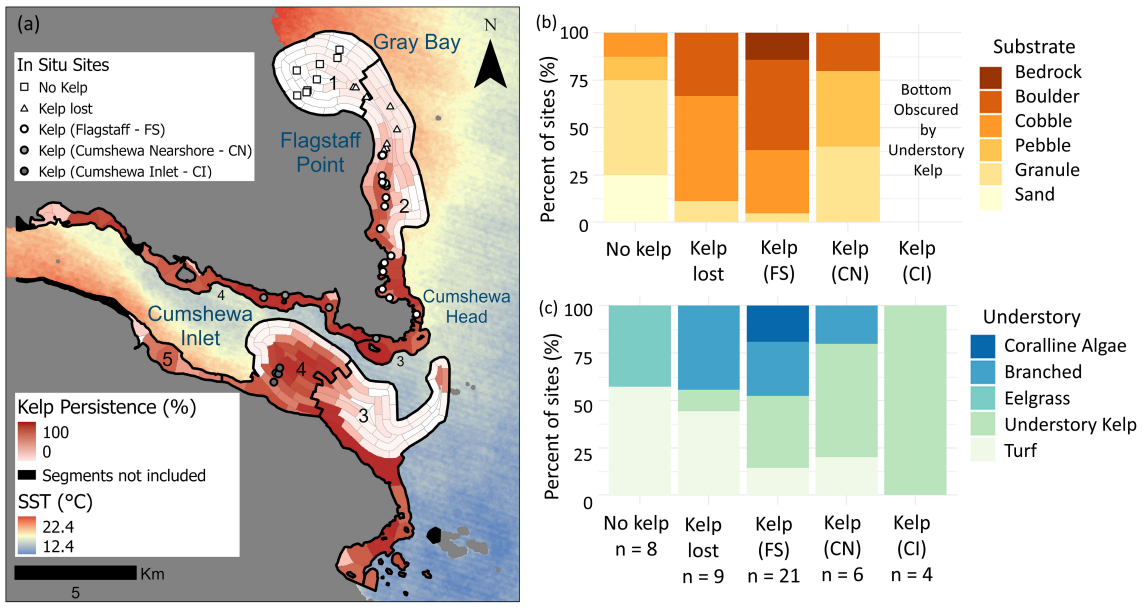

FIGURE 5
(a) Locations of in situ survey sites overlaid over a map of the local persistence metric. **(b, c)** Stacked bar plots showing **(b)** the percent of substrate classes and **(c)** dominant understory algae classes documented in areas of no kelp, kelp loss and kelp persistence.

kelp species were found on a variety of substrate types from pebble to boulders and bedrock (Figures 5b, c).

Discussion

Climate change poses multifaceted threats, driving rapid shifts in kelp forest distributions, with some regions experiencing severe reductions, while others have remained stable or even expanded, complicating efforts to identify and disentangle drivers operating across spatial and temporal scales (e.g., Cavanaugh et al., 2011; Krumhansl et al., 2016; Pfister et al., 2018; Hamilton et al., 2020; Starko et al., 2022; Mora-Soto et al., 2024a). Using remote sensing (1973-2021) and historical data (1867-1945) from Haida Gwaii, we found that the kelp forest distribution in the early 1970s closely matched historical distribution, suggesting century-long stability prior to the significant declines observed in the late 1970s in the study region. In the satellite time series, kelp area fluctuated with regional drivers at one-, two- and three- year averages showing multi-year impacts where warmer conditions corresponding with reduced kelp area. While we observed a long-term declining trend at the regional scale, this decline was less severe than the declines observed in the warmest areas of the local and subregional scales, supporting the initial hypothesis that greater environmental heterogeneity confers higher resilience at broader spatial scales. Local and subregional kelp dynamics exhibited more variable trends, supporting the second hypothesis that the response to regional drivers is primarily determined by positioning along local gradients such as SST. Moreover, *in situ* observations supported that temperature, not urchin grazing, was the primary driver of loss and resilience in this study region.

Regional drivers and change across a century

The inclusion of historical data and medium resolution satellites revealed substantial kelp forest losses that would have gone undetected using only high-resolution satellite imagery. Specifically, we discovered a major episodic decline in the 1970s of kelp forests that had likely persisted for over a century – a finding that emerged only through our analysis of pre-1984 data sources, including nautical charts (1867-1945) and early Landsat imagery. The creation of long-term time series are crucial, as shorter time series (< 20 years) can mask important patterns in kelp forest resilience due to high interannual variability (Bell et al., 2020; Wernberg et al., 2019). While most remote sensing of kelp canopy on the Pacific Coast of North America focuses on 30 m Landsat imagery from 1984 onwards (e.g., Cavanaugh et al., 2011; Bell et al., 2020; Hamilton et al., 2020), researchers have successfully integrated diverse historical records to establish long-term baselines. Examples include the use of early 20th century kelp census data in Washington (Pfister et al., 2018), historical surveys from unpublished theses and aerial photography dating to the 1930s in South Australia (Carnell and Keough, 2019), Darwin's observations on the *Voyage of the Beagle* in Southern Chile (Mora-Soto et al., 2021), and nineteenth-century nautical charts in the Salish Sea (Mora-Soto et al., 2024b) – the latter revealing similar patterns of kelp loss in warmer regions. This underscores how incorporating historical data sources, despite their varying quality, resolution and methodologies, is essential for establishing accurate pre-industrial ecological baselines and understanding the true magnitude of changes that may otherwise be obscured by recent data alone.

Our findings emphasize that regional drivers, such as the PDO, ENSO, SST anomalies, and MHW metrics, are critical in explaining kelp forest dynamics, with impacts extending beyond immediate SST stress, with multi-year metrics explaining more variation in kelp area than single-year averages. Many studies corroborate that these regional drivers at multiple scales, from MHW metrics to large scale climate cycles like the PDO and ENSO, impact kelp forest conditions, where warm conditions are detrimental to kelp forests (e.g., Cavanaugh et al., 2011; Bell et al., 2020; Arafeh-Dalmau et al., 2019; Wernberg et al., 2019; McPherson et al., 2021; Wernberg, 2021). The extended multi-year impacts likely result from complete mortality of whole kelp plants rather than surface die back, as mortality reduces the reproductive capacity of the remaining kelp forest even after favorable conditions return (Cavanaugh et al., 2011; Pfister et al., 2018; Schroeder et al., 2019; Starko et al., 2022).

Regional drivers not only influence SST but also interact with other oceanic conditions exacerbating not only changes in kelp forests but the ecosystem as a whole. For instance, the significant kelp declines in the 1970s coincided with the 1977 PDO shift, which brought warmer SSTs, a deepening of the thermocline, low nutrient availability and increased ocean stratification across the North Pacific (McGowan et al., 2003; Parnell et al., 2010). This shift triggered a cascade of declines in other coastal systems, particularly in California such as reduced plankton biomass, larval fish abundance, fisheries landings, and similarly, *Macrocystis* biomass (McGowan et al., 2003; Parnell et al., 2010). Notably, the documented loss of kelp forests in this study predates the widespread coral reef declines attributed to the 1983 El Niño (Oliver et al., 2009) challenging the notion that kelp forests are not sensitive indicators of broader climate change impacts (Reed et al., 2016).

Spatially explicit responses across scales

Local heterogeneity in factors like SST can either ameliorate or exacerbate the responses of foundation species like kelp forests to regional drivers, leading to complex patterns of decline and resilience (Russell and Connell, 2012; Starko et al., 2022). In our study region, cooler areas, like Cumshewa East and West, contribute to this resilience, as kelp forests there exhibited a stronger ability to endure and recover after adverse regional conditions. This spatial pattern of temperature-dependant responses has been documented elsewhere on the Pacific Coast, with losses concentrated in warmer areas during the 2014-2016 'Blob' MHW in Barkley Sound (Starko et al., 2022) and the southern Salish Sea (Mora-Soto et al., 2024a). The complex coastline of British Columbia and Alaska creates high environmental heterogeneity (Starko et al., 2019; Cavanaugh et al., 2021), making it crucial to consider local factors such as temperature, wave exposure, and trophic dynamics (e.g., Watson and Estes, 2011; Rogers-Bennett and Catton, 2019; McPherson et al., 2021; Starko et al., 2022, 2024) to understand kelp forest variability and accurately forecast species responses to climate change moving forward (Russell and Connell, 2012).

In addition to temperature, local patterns of exposure, wind and current can either ameliorate or exacerbate the response of kelp forest to regional drivers. In more exposed locations, storms can tear up large swaths of kelp forests like the intense storms during the 1983 El Niño in Point Loma, California, that led to a loss of 560 ha of kelp forests (Dayton and Tegner, 1984). Recent work shows that storm tracks have intensified on the coast of BC from the 1960s onwards (Abeysirigunawardena, 2010) and with the significant negative relationship between kelp persistence and wind in the study region, storms could have compounded or caused some of the loss or variation not explained by regional or local drivers in this study.

In situ evidence of temperature-driven loss

Multiple lines of evidence, the lack of urchins, and presence of turf reefs, in our 2021 field survey suggest that temperature, rather than herbivory, likely drove kelp forest declines in the study region. Despite the presence of urchin barrens (HMTK Participants et al., 2011; Lee et al., 2021), and the absence of sea otters since the late 1800s (Lee et al., 2021) in Haida Gwaii, our field survey found no urchin barrens and very few individual urchins in areas of kelp loss and persistence. The absence of urchin barrens is particularly notable as they are known to persist for years to decades due to urchins' ability to slow metabolic activity when food resources are scarce (Spindel et al., 2021). Additionally, the patchy mix of unconsolidated substrate – consisting of sand, pebbles, cobbles and boulders, is known to dissuade urchins from foraging (Laur et al., 1986) and may limit the distribution of urchins across the study region. Notably, in Gray Bay, where kelp was never present, both turf and eelgrass dominated shallow areas on sand and pebbles. This distribution pattern aligns with known habitat requirements, as canopy forming kelp require larger hard substratum such as cobbles, boulders or bedrock to provide secure attachment points (Druehl, 1978; Gregr et al., 2019; Starko et al., 2022), suggesting that substrate type likely plays a key role in determining kelp forest distribution across the region. Additionally, in areas where kelp disappeared, we found predominantly turf and branched algae (*Desmarestia* spp.) – a transition pattern commonly observed from temperature driven kelp losses in other regions of the globe, such as Western Australia (Wernberg, 2021), Atlantic Canada, France and Denmark (Filbee-Dexter and Wernberg, 2018). While our conclusion about herbivore impacts in this system is supported by two lines of evidence, our single time-point highlights the need for further research to fully understand trophic dynamics in this ecosystem.

Methodological considerations, and limitations

The regional and local drivers included in this study did not account for all variation observed in kelp area and persistence. Variability in other potential drivers, such as nutrients (e.g.,

Zimmerman and Kremer, 1986), light availability (e.g., Deysher and Dean, 1986), salinity (e.g., Druehl, 1978) and local stressors from human activities like pollution or overharvesting, are known to impact kelp forests (e.g., Foster and Schiel, 2010; Pfister et al., 2018), but data were unavailable for the region. Warmer SST often coincides with lower nutrients and salinity (Druehl, 1978), which generally slows kelp growth, weakens tissue and diminishes reproduction (Zimmerman and Kremer, 1986). As such, nutrients likely play an important role alongside SST in regulating kelp dynamics but were unavailable in this region. Although light data were unavailable, the significant relationship we found between depth and kelp persistence likely reflects the influence of light availability, as light attenuation increases with water column depth (Timmer et al., 2022).

While coastal development, point-source pollution and overharvesting can drive kelp declines (Foster and Schiel, 2010; Pfister et al., 2018), anthropogenic stressors are likely minimal in Haida Gwaii given its small population (< 5000 people) and minimal development (Statistics Canada, 2017) when compared to densely populated coastal areas with observed kelp declines like in Washington or South Australia (Krumhansl et al., 2016; Pfister et al., 2018). Although *Macrocystis* kelp was historically harvested for the herring-roe-on-kelp commercial fisheries in the Flagstaff subregion, BC's strict harvest limits leave the majority of the kelp plants intact minimizing harvest impacts. While turbidity related to logging runoff on Haida Gwaii (Klein et al., 2012) could impact kelp, the persistence of healthy kelp forests at the mouth of Mathers Creek—the region's only river—suggests minimal impacts from both turbidity and reduced salinity. Instead, the river's outflow may actually buffer SST impacts as evidenced by the retention of kelp forests in the Mathers Creek subregion despite losses in the similarly warm Flagstaff and Gray Bay subregions.

Previous work suggests that interannual changes in kelp area up to 7% could potentially arise from errors associated with measuring kelp area at different spatial resolutions (Gendall et al., 2023). While measurement uncertainty is an inherent challenge in remote sensing of kelp forests, the magnitude of kelp decline we observed far exceeds the potential error threshold identified by Gendall et al. (2023). Additionally, our focus on long-term trends and persistence over multiple decades helps mitigate the influence of such errors on our overall findings (Magurran et al., 2010). This approach to analyzing temporal patterns is sound as it emphasizes directional changes over long time scales rather than year-to-year fluctuations that might be influenced by artifacts or uncertainties in remote sensing measurements. Additionally, our use of multiple temporal metrics—including both area changes at the regional and subregional scale and persistence patterns at the local scale—provide complementary lines of evidence that strengthen our confidence in the patterns of kelp forest change herein.

Conclusion

This century-long analysis of kelp forests in Hada Gwaii elucidates the complex interplay between climate change and kelp forest dynamics operating across multiple spatial scales. Our analysis showed that kelp forests that likely remained stable for over a century began showing significant declines in the 1970s, with a regional loss of 5 ± 2% per decade. These responses varied across spatial scales. With local environmental conditions – particulary SST – playing an important role in determining outcomes. Warmer areas experienced complete kelp loss following the 1977 PDO shift, while, cooler areas exhibited greater resilience and the capacity to recover from large-scale climatic events, such as el Niño and MHW events. The absence of urchin barrens and presence of turf-dominated reefs in areas of kelp loss suggest that temperature, rather than herbivory, was the primary driver of decline in this study region. These findings offer valuable insights for the integration of historical data and the consideration of scale-dependent responses when assessing climate change impacts on coastal ecosystems. Continued monitoring and conservation efforts remain essential to ensure the persistence and resilience of these vital coastal ecosystems.

Data availability statement

The datasets presented in this study can be found in online repositories. The names of the repository/repositories and accession number(s) can be found below: https://github.com/liannagendall/HaidaGwaii_Kelp and https://doi.org/10.5281/zenodo.14984911.

Author contributions

LG: Conceptualization, Data curation, Formal analysis, Funding acquisition, Investigation, Methodology, Project administration, Resources, Software, Supervision, Validation, Visualization, Writing – original draft, Writing – review & editing. MH-L: Conceptualization, Funding acquisition, Methodology, Resources, Supervision, Writing – review & editing. AW: Data curation, Formal analysis, Methodology, Writing – review & editing. SS: Conceptualization, Methodology, Writing – review & editing. LR: Conceptualization, Methodology, Writing – review & editing. SC: Conceptualization, Methodology, Resources, Writing – review & editing. LL: Conceptualization, Methodology, Resources, Writing – review & editing. NG: Conceptualization, Resources, Writing – review & editing. MC: Conceptualization, Data curation, Formal analysis, Funding acquisition, Methodology, Project administration, Resources, Software, Supervision, Validation, Writing – review & editing.

Funding

The author(s) declare that financial support was received for the research and/or publication of this article. This research was supported through a Natural Sciences and Engineering Research Council of Canada (NSERC) Alliance grant (Ref. number: ALLRP 566735 - 21) and NSERC Discovery grant awarded to MC. LG was

also supported during this research through a MITACS Accelerate internship with the Hakai Institute.

Acknowledgments

We thank the Hakai Institute for partially funding this work, as well as the Canadian Hydrographic Service, Transport Canada, the Department of Fisheries and Oceans Canada (in particular Joanne Lessard), Environment and Climate Change Canada, and ShoreZone, for providing satellite data and ground-truth data. A special thanks to Parks Canada and the Council of the Haida Nation for assistance with field equipment on Haida Gwaii.

Conflict of interest

The authors declare that the research was conducted in the absence of any commercial or financial relationships that could be construed as a potential conflict of interest.

Generative AI statement

The author(s) declare that no Generative AI was used in the creation of this manuscript.

Publisher's note

Supplementary material

The Supplementary Material for this article can be found online at: https://www.frontiersin.org/articles/10.3389/fmars.2025.1504701/full#supplementary-material

References

Abeysirigunawardena, D. S. (2010).Climate variability and change impacts on coastal environmental variables in British Columbia, Canada. Available online at: https://dspace.library.uvic.ca/handle/1828/2664 (Accessed November 06, 2023).

Anderson, D. R., and Burnham, K. P. (2002). Avoiding pitfalls when using information-theoretic methods. *J. Wildl. Manage.* 66, 912. doi: 10.2307/3803155

Arafeh-Dalmau, N., Montaño-Moctezuma, G., Martínez, J. A., Beas-Luna, R., Schoeman, D. S., and Torres-Moye, G. (2019). Extreme marine heatwaves alter kelp forest community near its equatorward distribution limit. *Front. Mar. Sci.* 6. doi: 10.3389/fmars.2019.00499

Bates, D., Mächler, M., Bolker, B., and Walker, S. (2015). *Lme4: Linear mixed-effects models using "Eigen" and S4 (R package version 1.1-21)*. Available online at: https://CRAN.R-project.org/package=lme4 (Accessed March 27, 2022).

BCMCA (2011). *Marine Atlas of Pacific Canada: a product of the British Columbia Marine Conservation Analysis (BCMCA)* (Vancouver, BC, Canada: British Columbia Marine Conservation Analysis).

Bell, T. W., Allen, J. G., Cavanaugh, K. C., and Siegel, D. A. (2020). Three decades of variability in California's giant kelp forests from the Landsat satellites. *Remote Sens. Environ.* 238, 110811. doi: 10.1016/j.rse.2018.06.039

Berry, H. D., Sewell, A. T., Wyllie-Echeverria, S., Reeves, B. R., Mumford, T. F., Skalski, J. R., et al. (2003). *Puget Sound Submerged Vegetation Monitoring Project: 2000 - 2002 Monitoring Report* (Olympia, WA: Washington State Department of Resources), Vol. 170.

Bolton, J., Anderson, R., Smit, A., and Rothman, M. (2012). South african kelp moving eastwards: the discovery of ecklonia maxima (Osbeck) papenfuss at de hoop nature reserve on the south coast of south africa. *Afr. J. Mar. Sci.* 34, 1. doi: 10.2989/1814232X.2012.675125

Carnell, P. E., and Keough, M. J. (2019). Reconstructing historical marine populations reveals major decline of a kelp forest ecosystem in Australia. *Estuaries Coasts* 42, 765–778. doi: 10.1007/s12237-019-00525-1

Cavanaugh, K. C., Bell, T., Costa, M., Eddy, N. E., Gendall, L., Gleason, M. G., et al. (2021). A review of the opportunities and challenges for using remote sensing for management of surface-canopy forming kelps. *Front. Mar. Sci.* 8. doi: 10.3389/fmars.2021.753531

Cavanaugh, K., Siegel, D., Reed, D., and Dennison, P. (2011). Environmental controls of giant-kelp biomass in the Santa Barbara Channel, California. *Mar. Ecol. Prog. Ser.* 429, 1–17. doi: 10.3354/meps09141

Chandler, P. C. (2014). Sea surface temperature and salinity trends observed at lighthouses and weather buoys in British Columbia, 2013. In: R. I. Perry (Ed). *State of the physical, biological and selected fishery resources of Pacific Canadian marine ecosystems in 2013. Can. Tech. Rep. Fish. Aquat. Sci.*, 3102. Available online at: https://www.researchgate.net/profile/Tyson-Carswell/publication/304380333_Costa_M_Carswell_T_Sweeting_R_Young_E_2014_Spatial-temporal_phytoplankton_bloom_initiation_in_the_Strait_of_Georgia_derived_from_MODIS_imagery_2002-2013_In_RI_Perry_Ed_State_of_the_physical_biological/links/576d75ec08ae0b3a3b75528f/Costa-M-Carswell-T-Sweeting-R-Young-E-2014-Spatial-temporal-phytoplankton-bloom-initiation-in-the-Strait-of-Georgia-derived-from-MODIS-imagery-2002-2013-In-RI-Perry-Ed-State-of-the-physical-b.pdf (Accessed May 20, 2024).

Coelho, M. T. P., Diniz-Filho, J. A., and Rangel, T. F. (2019). A parsimonious view of the parsimony principle in ecology and evolution. *Ecography* 42, 968–976. doi: 10.1111/ecog.04228

Cooley, S., Schoeman, D., Bopp, L., Byod, P., Donner, S., Ito, S., et al. (2022). *Ocean and coastal ecosystems and their services*. (Cambridge, United Kingdom: Cambridge University Press). doi: 10.1017/9781009325844

Costa, M., Le Baron, N., Tenhunen, K., Nephin, J., Willis, P., Mortimor, J. P., et al. (2020). Historical distribution of kelp forests on the coast of British Columbia: 1858–1956. *Appl. Geogr.* 120, 102230. doi: 10.1016/j.apgeog.2020.102230

Davies, S. C., Gregr, E. J., Lessard, J., Bartier, P., and Wills, P. (2019). *Coastal digital elevation models integrating ocean bathymetry and land topography for marine ecological analyses in Pacific Canadian waters* (Ottawa, ON, Canada: Fisheries and Oceans Canada). Available online at: http://epe.lac-bac.gc.ca/100/201/301/weekly_acquisitions_list-ef/2019/19-43/publications.gc.ca/collections/collection_2019/mpo-dfo/Fs97-6-3321-eng.pdf (Accessed August 27, 2020).

Davis, N. N., Badger, J., Hahmann, A. N., Hansen, B. O., Mortensen, N. G., Kelly, M., et al. (2023). The global wind atlas: A high-resolution dataset of climatologies and associated web-based application. *Bull. Am. Meteorol. Soc.* 104, E1507–E1525. doi: 10.1175/BAMS-D-21-0075.1

Dayton, P. K., and Tegner, M. J. (1984). Catastrophic storms, El Nino, and patch stability in a southern California kelp community. *Science* 224, 283–285. doi: 10.1126/science.224.4646.283

Deysher, L. E., and Dean, T. A. (1986). Interactive effects of light and temperature on sporophyte production in the giant kelp Macrocystis pyrifera. *Mar. Biol.* 93, 17–20. doi: 10.1007/BF00428650

Di Lorenzo, E., and Mantua, N. (2016). Multi-year persistence of the 2014/15 North Pacific marine heatwave. *Nat. Clim. Change* 6, 1042–1047. doi: 10.1038/nclimate3082

Di Lorenzo, E., Schneider, N., Cobb, K. M., Franks, P. J. S., Chhak, K., Miller, A. J., et al. (2008). North Pacific Gyre Oscillation links ocean climate and ecosystem change. *Geophys. Res. Lett.* 35, L08607. doi: 10.1029/2007GL032838

Druehl, L. D. (1978). The distribution of *Macrocystis integrifolia* in British Columbia as related to environmental parameters. *Can. J. Bot.* 56, 69–79. doi: 10.1139/b78-007

Dwyer, J. L., Roy, D. P., Sauer, B., Jenkerson, C. B., Zhang, H. K., and Lymburner, L. (2018). Analysis ready data: enabling analysis of the landsat archive. *Remote Sens.* 10, 1363. doi: 10.3390/rs10091363

ESRI (Environmental Systems Research Institute) (2018). *ArcMap (10.7)*.

Faraway, J. J. (2004). *Linear Models with R* (Boca Raton, Florida: Chapman and Hall/CRC).

Filbee-Dexter, K., Wernberg, T., Fredriksen, S., Norderhaug, K. M., and Pedersen, M. F. (2019). Arctic kelp forests: Diversity, resilience and future. *Glob. Planet. Change.* 172, 1–14. doi: 10.1016/j.gloplacha.2018.09.005

Filbee-Dexter, K., and Wernberg, T. (2018). Rise of turfs: A new battlefront for globally declining kelp forests. *BioScience* 68, 64–76. doi: 10.1093/biosci/bix147

Filbee-Dexter, K., Wernberg, T., Barreiro, R., Coleman, M. A., de Bettignies, T., Feehan, C. J., et al. (2022). Leveraging the blue economy to transform marine forest restoration. *J. Phycol.* 58, 198–207. doi: 10.1111/jpy.13239

Foster, M. S., and Schiel, D. R. (2010). Loss of predators and the collapse of southern California kelp forests (?): Alternatives, explanations and generalizations. *J. Exp. Mar. Biol. Ecol.* 393, 59–70. doi: 10.1016/j.jembe.2010.07.002

Gendall, L., Schroeder, S. B., Wills, P., Hessing-Lewis, M., and Costa, M. (2023). A multi-satellite mapping framework for floating kelp forests. *Remote Sens.* 15, 1276. doi: 10.3390/rs15051276

Greene, H. G., Yoklavich, M. M., Starr, R. M., O'Connell, V. M., Wakefield, W. W., Sullivan, D. E., et al. (1999). A classification scheme for deep seafloor habitats. *Oceanol. Acta* 22, 663–678. doi: 10.1016/S0399-1784(00)88957-4

Gregr, E. J., Palacios, D. M., Thompson, A., and Chan, K. M. A. (2019). Why less complexity produces better forecasts: an independent data evaluation of kelp habitat models. *Ecography* 42, 428–443. doi: 10.1111/ecog.03470

Haida Marine Traditional Knowledge (HMTK), , Council of the Haida Nation, and Haida Oceans Technical Team, Winbourne, J. (2011). *Haida Marine Traditional Knowledge Volume III* (Skidegate, BC, Canada: Council of the Haida Nation).

Haida Nation and Canada (2024a). *Chiixuujin / Chaaw Kaawgaa Big Tide (Low Water) Haida Title Lands Agreement*. Available online at: https://www.haidanation.ca/wp-content/uploads/2024/12/CHIIXUUJIN-CHAAW-KAAWGAA-BIG-TIDE-LOW-WATER-SIGNED-IN-COUNTERPART-2024-12-04.pdf (Accessed December 3, 2024).

Haida Nation and Canada (2024b). *Gaayhllxid/ Giihlagalgang "Rising Tide" Haida Title Lands Agreement*. Available online at: https://www.haidanation.ca/wp-content/uploads/2024/04/GG-Haida-Title-Lands-Agreement-April-6-2024.pdf (Accessed December 3, 2024).

Hamilton, S. L., Bell, T. W., Watson, J. R., Grorud-Colvert, K. A., and Menge, B. A. (2020). Remote sensing: generation of long-term kelp bed data sets for evaluation of impacts of climatic variation. *Ecology* 101, e03031. doi: 10.1002/ecy.3031

Hobday, A. J., Alexander, L. V., Perkins, S. E., Smale, D. A., Straub, S. C., Oliver, E. C. J., et al. (2016). A hierarchical approach to defining marine heatwaves. *Prog. Oceanogr.* 141, 227–238. doi: 10.1016/j.pocean.2015.12.014

Hobday, A., Oliver, E., Sen Gupta, A., Benthuysen, J., Burrows, M., Donat, M., et al. (2018). Categorizing and naming marine heatwaves. *Oceanog* 31, 162–173. doi: 10.5670/oceanog.2018.205

Holling, C. S. (1973). Resilience and stability of ecological systems. *Annu. Rev. Ecol. System.* 4, 1–23. doi: 10.1146/annurev.es.04.110173.000245

Huang, B., Liu, C., Banzon, V., Freeman, E., Graham, G., Hankins, B., et al. (2021). *Improvements of the Daily Optimum Interpolation Sea Surface Temperature (DOISST) Version 2.1*. doi: 10.1175/JCLI-D-20-0166.1

Huang, B., Thorne, P. W., Banzon, V. F., Boyer, T., Chepurin, G., Lawimore, J. H., et al. (2017). *PDO from NOAA Extended Reconstructed Sea Surface Temperature (ERSST), Version 5*. doi: 10.7289/V5T72FNM

Hurvich, C. M., and Tsai, C.-L. (1993). A corrected akaike information criterion for vector autoregressive model selection. *J. Time Ser. Anal.* 14, 271–279. doi: 10.1111/j.1467-9892.1993.tb00144.x

Jayathilake, D. R. M., and Costello, M. J. (2021). Version 2 of the world map of laminarian kelp benefits from more Arctic data and makes it the largest marine biome. *Biol. Conserv.* 257, 109099. doi: 10.1016/j.biocon.2021.109099

Ketchen, D. J., and Shook, C. L. (1996). The application of cluster analysis in strategic management research: an analysis and critique. *Strat. Manage. J.* 17, 441–458. doi: 10.1002/(SICI)1097-0266(199606)17:6<441::AID-SMJ819>3.0.CO;2-G

Klein, R. D., Lewis, J., and Buffleben, M. S. (2012). Logging and turbidity in the coastal watersheds of northern California. *Geomorphology* 139–140, 136–144. doi: 10.1016/j.geomorph.2011.10.011

Krumhansl, K. A., Okamoto, D. K., Rassweiler, A., Novak, M., Bolton, J. J., Cavanaugh, K. C., et al. (2016). Global patterns of kelp forest change over the past half-century. *Proc. Natl. Acad. Sci. U.S.A.* 113, 13785–13790. doi: 10.1073/pnas.1606102113

Laur, D. R., Ebeling, A. W., and Reed, D. C. (1986). Experimental evaluations of substrate types as barriers to sea urchin (Strongylocentrotus spp.) movement. *Mar. Biol.* 93, 209–215. doi: 10.1007/BF00508258

Lee, L. C., Daniel McNeill, G., Ridings, P., Featherstone, M., Okamoto, D. K., Spindel, N. B., et al. (2021). Chiixuu tll iinasdll: indigenous ethics and values lead to ecological restoration for people and place in gwaii haanas. *Ecol. Rest.* 39, 45–51. doi: 10.3368/er.39.1-2.45

Lindstrom, S. C. (2023). A reinstated species name for north-eastern Pacific Macrocystis (Laminariaceae, Phaeophyceae). *Notulae Algarum* 290. Available at: https://www.notulaealgarum.com/2023/documents/Notulae%20Algarum%20No.%20290.pdf (Accessed May 20, 2024).

Magurran, A. E., Baillie, S. R., Buckland, S. T., Dick, J. M., Elston, D. A., Scott, E. M., et al. (2010). Long-term datasets in biodiversity research and monitoring: assessing change in ecological communities through time. *Trends Ecol. Evol.* 25, 574–582. doi: 10.1016/j.tree.2010.06.016

Marine Plan Partnership for the North Pacific Coast (MaPP) (2015). *Haida Gwaii Marine Plan*.

Marine Plan Partnership for the North Pacific Coast (MaPP) (2021). *Regional Kelp Monitoring on the North Pacific Coast: A Community -Based Monitoring Initiative to Inform Ecosystem-Based Management*. Available online at: https://storymaps.arcgis.com/stories/78945b1d95ec4b9fab5142670088174f (Accessed April 25, 2024).

McGowan, J. A., Bograd, S. J., Lynn, R. J., and Miller, A. J. (2003). The biological response to the 1977 regime shift in the California Current. *Deep Sea Res. Part II: Topical Stud. Oceanogr.* 50, 2567–2582. doi: 10.1016/S0967-0645(03)00135-8

McPherson, M. L., Finger, D. J. I., Houskeeper, H. F., Bell, T. W., Carr, M. H., Rogers-Bennett, L., et al. (2021). Large-scale shift in the structure of a kelp forest ecosystem co-occurs with an epizootic and marine heatwave. *Commun. Biol.* 4, 298. doi: 10.1038/s42003-021-01827-6

Milligan, G. W., and Cooper, M. C. (1985). An examination of procedures for determining the number of clusters in a data set. *Psychometrika.* 50, 2. doi: 1 0.1007/BF02294245

Mora-Soto, A., Capsey, A., Friedlander, A. M., Palacios, M., Brewin, P. E., Golding, N., et al. (2021). One of the least disturbed marine coastal ecosystems on Earth: Spatial and temporal persistence of Darwin's sub-Antarctic giant kelp forests. *J. Biogeogr.* 48, 2562–2577. doi: 10.1111/jbi.14221

Mora-Soto, A., Schroeder, S., Gendall, L., Wachmann, A., Narayan, G. R., Read, S., et al. (2024a). Kelp dynamics and environmental drivers in the southern Salish Sea, British Columbia, Canada. *Front. Mar. Sci.* 11. doi: 10.3389/fmars.2024.1323448

Mora-Soto, A., Schroeder, S., Gendall, L., Wachmann, A., Narayan, G., Read, S., et al. (2024b). Back to the past: long-term persistence of bull kelp forests in the Strait of Georgia, Salish Sea, Canada. *Front. Mar. Sci.* 11. doi: 10.3389/fmars.2024.1446380

Nicholson, T. E., McClenachan, L., Tanaka, K. R., and Houtan, K. S. V. (2024). Sea otter recovery buffers century-scale declines in California kelp forests. *PloS Climate* 3, e0000290. doi: 10.1371/journal.pclm.0000290

NOAA Center for Weather and Climate Prediction and Climate Prediction Center (2015). *El Nino Suthern Oscillation (ENSO)*. Available online at: https://origin.cpc.ncep.noaa.gov/products/analysis_monitoring/ensostuff/ONI_v5.php (Accessed March 05, 2022).

Oliver, J. K., Berkelmans, R., and Eakin, C. M. (2009). "Coral Bleaching in Space and Time," in *Coral Bleaching: Patterns, Processes, Causes and Consequences*. Eds. M. J. H. van Oppen and J. M. Lough (Springer, Berlin, Heidelberg), 21–39. doi: 10.1007/978-3-540-69775-6_3

Oliver, E. C. J., Burrows, M. T., Donat, M. G., Sen Gupta, A., Alexander, L. V., Perkins-Kirkpatrick, S. E., et al. (2019). Projected marine heatwaves in the 21st century and the potential for ecological impact. *Front. Mar. Sci.* 6. doi: 10.3389/fmars.2019.00734

Parnell, P. E., Miller, E. F., Cody, C. E. L., Dayton, P. K., Carter, M. L., and Stebbinsd, T. D. (2010). The response of giant kelp (Macrocystis pyrifera) in southern California to low-frequency climate forcing. *Limnol. Oceanogr.* 55, 2686–2702. doi: 10.4319/lo.2010.55.6.2686

Pessarrodona, A., Assis, J., Filbee-Dexter, K., Burrows, M. T., Gattuso, J.-P., Duarte, C. M., et al. (2022). Global seaweed productivity. *Sci. Adv.* 8, eabn2465. doi: 10.1126/sciadv.abn2465

Pfister, C. A., Berry, H. D., and Mumford, T. (2018). The dynamics of Kelp Forests in the Northeast Pacific Ocean and the relationship with environmental drivers. *J. Ecol.* 106, 1520–1533. doi: 10.1111/1365-2745.12908

R Core Team (2021). *R: A language and environment for statistical computing (Version 4.1.2)*. Available online at: https://www.R-project.org/ (Accessed November 06, 2023).

Reed, D., Washburn, L., Rassweiler, A., Miller, R., Bell, T., and Harrer, S. (2016). Extreme warming challenges sentinel status of kelp forests as indicators of climate change. *Nat. Commun.* 7, 13757. doi: 10.1038/ncomms13757

Rogers-Bennett, L., and Catton, C. A. (2019). Marine heat wave and multiple stressors tip bull kelp forest to sea urchin barrens. *Sci. Rep.* 9, 15050. doi: 10.1038/s41598-019-51114-y

Russell, B. D., and Connell, S. D. (2012). Origins and consequences of global and local stressors: incorporating climatic and non-climatic phenomena that buffer or accelerate ecological change. *Mar. Biol.* 159, 2633–2639. doi: 10.1007/s00227-011-1863-8

Schlegel, R. W., and Smit, A. J. (2018). heatwaveR: A central algorithm for the detection of heatwaves and cold-spells. *J. Open Source Softw.* 3, 821. doi: 10.21105/joss.00821

Schneider, C. A., Rasband, W. S., and Eliceiri, K. W. (2012). NIH Image to ImageJ: 25 years of image analysis. *Nat. Methods* 9, 671–675. doi: 10.1038/nmeth.2089

Schroeder, S. B., Boyer, L., Juanes, F., and Costa, M. (2019). Spatial and temporal persistence of nearshore kelp beds on the west coast of British Columbia, Canada using satellite remote sensing. *Remote Sens. Ecol. Conserv.* 6, 327–343. doi: 10.1002/rse2.142

Spindel, N. B., Lee, L. C., and Okamoto, D. K. (2021). Metabolic depression in sea urchin barrens associated with food deprivation. *Ecology* 102, 1–5. doi: 10.1002/ecy.v102.11

Starko, S., Bailey, L. A., Creviston, E., James, K. A., Warren, A., Brophyid, M. K., et al. (2019). Environmental heterogeneity mediates scale- dependent declines in kelp diversity on intertidal rocky shores. *PloS One* 14, e0213191. doi: 10.1371/journal.pone.0213191

Starko, S., Neufeld, C. J., Gendall, L., Timmer, B., Campbell, L., Yakimishyn, J., et al. (2022). Microclimate predicts kelp forest extinction in the face of direct and indirect marine heatwave effects. *Ecol. Appl.*, e2673. doi: 10.1002/eap.2673

Starko, S., Timmer, B., Reshitnyk, L., Csordas, M., McHenry, J., Schroeder, S., et al. (2024). Local and regional variation in kelp loss and stability across coastal British Columbia. *Mar. Ecol. Prog. Ser.* 733, 1–26. doi: 10.3354/meps14548

Statistics Canada (2017). *Focus on Geography Series 2016 Census* (Ottawa, Ontario: Statistics Canada).

Sutherland, I. R., Karpouzi, V., Mamoser, M., and Carswell, B. (2008). *Kelp inventory 2007 : Areas of the British Columbia Central Coast from Hakai Passage to the Bardswell Group* (Victoria, BC, Canada: Oceans and Marine Fisheries Branch, B.C., Ministry of Environment, Fisheries and Oceans Canada B.C., Ministry of Agriculture and Lands and Heiltsuk Tribal Council).

Timmer, B., Reshitnyk, L. Y., Hessing-Lewis, M., Juanes, F., and Costa, M. (2022). Comparing the use of red-edge and near-infrared wavelength ranges for detecting submerged kelp canopy. *Remote Sens.* 14, 2241. doi: 10.3390/rs14092241

Trimble Germany (2011). *eCognition Developer (8.64).* (Munich, German: Trimble Inc.).

Vergés, A., Doropoulos, C., Malcolm, H. A., Skye, M., Garcia-Pizá, M., Marzinelli, E. M., et al. (2016). Long-term empirical evidence of ocean warming leading to tropicalization of fish communities, increased herbivory, and loss of kelp. *Proc. Natl. Acad. Sci. U.S.A.* 113, 13791–13796. doi: 10.1073/pnas.1610725113

Wachmann, A., Starko, S., Neufeld, C. J., and Costa, M. (2024). Validating landsat analysis ready data for nearshore sea surface temperature monitoring in the northeast pacific. *Remote Sens.* 16, 920. doi: 10.3390/rs16050920

Watson, J., and Estes, J. A. (2011). Stability, resilience, and phase shifts in rocky subtidal communities along the west coast of Vancouver Island, Canada. *Ecol. Monogr.* 81, 215–239. doi: 10.1890/10-0262.1

Wernberg, T. (2021). "Marine Heatwave Drives Collapse of Kelp Forests in Western Australia," in *Ecosystem Collapse and Climate Change*. Eds. J. G. Canadell and R. B. Jackson (Springer International Publishing, Cham), 325–343. doi: 10.1007/978-3-030-71330-0_12

Wernberg, T., Krumhansl, K., Filbee-Dexter, K., and Pedersen, M. F. (2019). "Chapter 3 - Status and Trends for the World's Kelp Forests," in *World Seas: an Environmental Evaluation*, *2nd ed.*, vol. 57–78 . Ed. C. Sheppard (Academic Press, Cambridge, MA, USA). doi: 10.1016/B978-0-12-805052-1.00003-6

Zimmerman, R., and Kremer, J. (1986). *In situ* growth and chemical composition of the giant kelp, Macrocystis pyrifera: response to temporal changes in ambient nutrient availability. *Mar. Ecol. Prog. Ser.* 27, 277–285. doi: 10.3354/meps027277

Frontiers in Marine Science

Explores ocean-based solutions for emerging global challenges

The third most-cited marine and freshwater biology journal, advancing our understanding of marine systems and addressing global challenges including overfishing, pollution, and climate change.

Discover the latest Research Topics

See more →

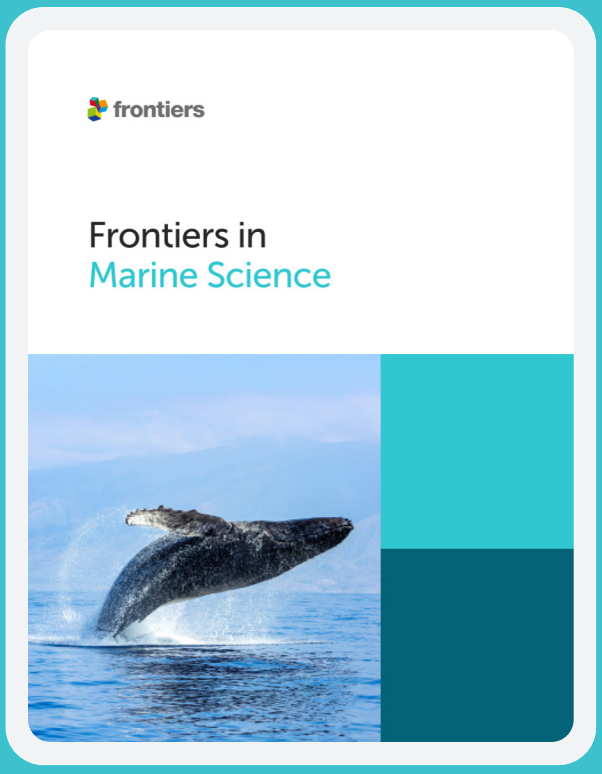

Frontiers

Avenue du Tribunal-Fédéral 34
1005 Lausanne, Switzerland
frontiersin.org

Contact us

+41 (0)21 510 17 00
frontiersin.org/about/contact